

Appendix G3. Concept Design Seismic Site Response Analysis (Final Draft)

1. Introduction and Purpose

This Technical Memorandum (TM) was initially prepared to document supported details for the Delta Conveyance Project (Project) Engineering Project Reports, (DCA 2022a, 2022b). At that time of submittal in 2022, the Delta Conveyance Authority (DCA) prepared two Engineering Project Reports, one report for the Central Corridor and Eastern Corridor and another report for the Bethany Reservoir Alternative. In December 2023, the Environmental Impact Report (EIR) (DCA, 2023) was released and stated that the Bethany Reservoir Alternative would be the selected Project and renamed it as the Bethany Reservoir Alignment. The Bethany Reservoir Alignment and the Delta Conveyance Project can be interchanged as the selected Project.

In September 2024, this TM was prepared to describe the selected Project. No technical changes and recommendations are presented since the Final Draft Submittal in 2023. It should be noted that the term "Central Corridor" is no longer a part of the Project and the terms "Eastern Corridor" or "East Corridor" should be here on interpreted as part of the Bethany Reservoir Alignment only from Intake C-E-3 down to Lower Roberts Island Tunnel Launch Shaft. It also should be noted that some references to the Central and/or Eastern Corridors remain in the TM to provide a greater extent of background information for portions of the Delta between the intakes and Clifton Court Forebay which also influence design considerations for the Project. This includes Attachments 1 and 2 that present the development of reference ground motions at key facility locations along the Central and Eastern Corridors as well as the Bethany Reservoir Alignment.

1.1 Purpose

This Technical Memorandum (TM) was prepared to summarize the procedures and results of the conceptual design phase seismic site response analyses performed at nine (9) of the selected Delta Conveyance facility sites located along the Bethany Reservoir Alignment. The results of these analyses, in terms of site ground motions and associated site amplifications, are presented and compared to those developed previously using published site amplification relationships. Design Peak Ground Accelerations (PGAs) at the ground surface were also developed for use in liquefaction analyses and corresponding estimation of required ground improvement.

1.2 Introduction

One-dimensional (1-D) seismic site response analyses were performed at nine (9) sites along the selected Delta Conveyance Project (Project) Bethany Reservoir Alignment. These analyses were conducted to obtain site- or facility-specific earthquake ground motions at the ground surface for conceptual liquefaction evaluations at intake, tunnel shaft, pumping plant, and other structure sites.

Input to the 1-D analyses included time histories for horizontal ground motions at a reference depth, where the reference depth is defined by a corresponding shear wave velocity (V_s) for each site. This TM discusses the idealized soil profiles and dynamic soil properties used in the site response analyses at each of these nine (9) Project sites, the assumptions and approaches within the site response models, as well as the results of the site-specific analyses and recommended design PGA values at the ground surface. Comparison with the PGA values at the ground surface previously estimated using the non-site-

specific published relationship (Kishida et al., 2009) used in the previous liquefaction analyses is also presented. Refer to the Conceptual Engineering Report (CER) Appendix G2 *Liquefaction and Ground Improvement Analysis* for more information on liquefaction and ground improvements.

1.3 Organization

This TM will follow the structure given below:

- Introduction and Purpose
- Subsurface Data
- One-Dimensional Site Response Analysis
- Recommended Design Peak Ground Accelerations at Ground Surface
- Summary
- References
- Attachment 1 - Development of Conceptual Seismic Design Ground Motions at Reference Depths
- Attachment 2 - Development of Design and Maximum Considered Earthquake (MCER) for Bethany Reservoir Pumping Plant
- Attachment 3 - DEEPSOIL Model Calibrations
- Attachment 4 - Development of Spectrally-Matched Time Histories

2. Subsurface Data

Various historic soil boring logs, cone penetration test (CPT) soundings, and well completion reports were reviewed to develop the idealized soil profile used for analysis at each site. At locations where no reliable geotechnical data were available, data from historic explorations at other locations with similar ground conditions were used. The idealized soil profiles used for the current analyses, and hence the recommendations presented herein, are subject to change during future design phases when additional investigations are completed.

2.1 Available Subsurface Investigations

At the time of these analyses, subsurface soil investigations completed near the facility sites included twenty-six (26) CPT soundings with shear wave velocity (V_s) measurements, complemented by forty-nine (49) soil borings and nine (9) well completion reports. Soil borings and CPT soundings completed as part of the California WaterFix and Delta Habitat Conservation and Conveyance Program were also reviewed where available. Figure 1 shows the approximate locations of these soil investigations and the respective Project facility locations.

2.2 Soil Profiles

Data from the available soil investigations were reviewed and used to develop idealized soil profiles at each facility site. Shear wave velocity (V_s) measurements from CPTs and soil borings were generally available to a depth of 100 feet below the existing ground surface (bgs) and were used at all the sites, except at the Bethany Reservoir Pumping Plant, where V_s had to be estimated from corrected blow counts. The measured V_s values at each site location were used to assign V_s values to the soil layers

within the idealized soil profile for analysis. The idealized soil profiles and assigned soil dynamic properties for each of the nine (9) sites are discussed in Section 5 below.

Based on the available data, the idealized soil profiles generally consist of alternating layers of coarse- to fine-grained sediments, with V_s values ranging from 500 feet per second (ft/s) to 1,200 ft/s. Thin surficial layers of organic rich soils (peats), with V_s as low as 400 ft/s, were encountered overlying high-plasticity clays at some of the sites.

2.3 Groundwater

Groundwater depths observed during drilling near the selected facility sites ranged from 5 to 40 feet bgs.

3. One-Dimensional Site Response Analysis

Table 1 summarizes the facility sites along the Project at which the 1-D site response analyses were performed. The development of Maximum Design Earthquake (MDE) and Maximum Considered Earthquake (MCE) response spectra at the reference depths are detailed in Attachments 1 and 2, respectively. The last column of the table lists the V_s values, and their corresponding elevations, assigned to the half-space in the site response model. The V_s values are the time-averaged shear-wave velocities (in the top 30 m) used to develop the reference ground motions (see Attachment 1). The half-space elevations were determined from the top elevations of the Modesto or Riverbank Formations (see Table 1 of Attachment 1 for more information), adjusted using the measured V_s profile at each site. All analyses were performed for the MDE or MCE depending on the nature of the planned facility, as defined in the CER Appendix G1 *Concept Seismic Design and Geohazard Criteria*.

Note that the Bethany Reservoir Discharge Structure overlies rock, and therefore, no site response analysis was performed at this site.

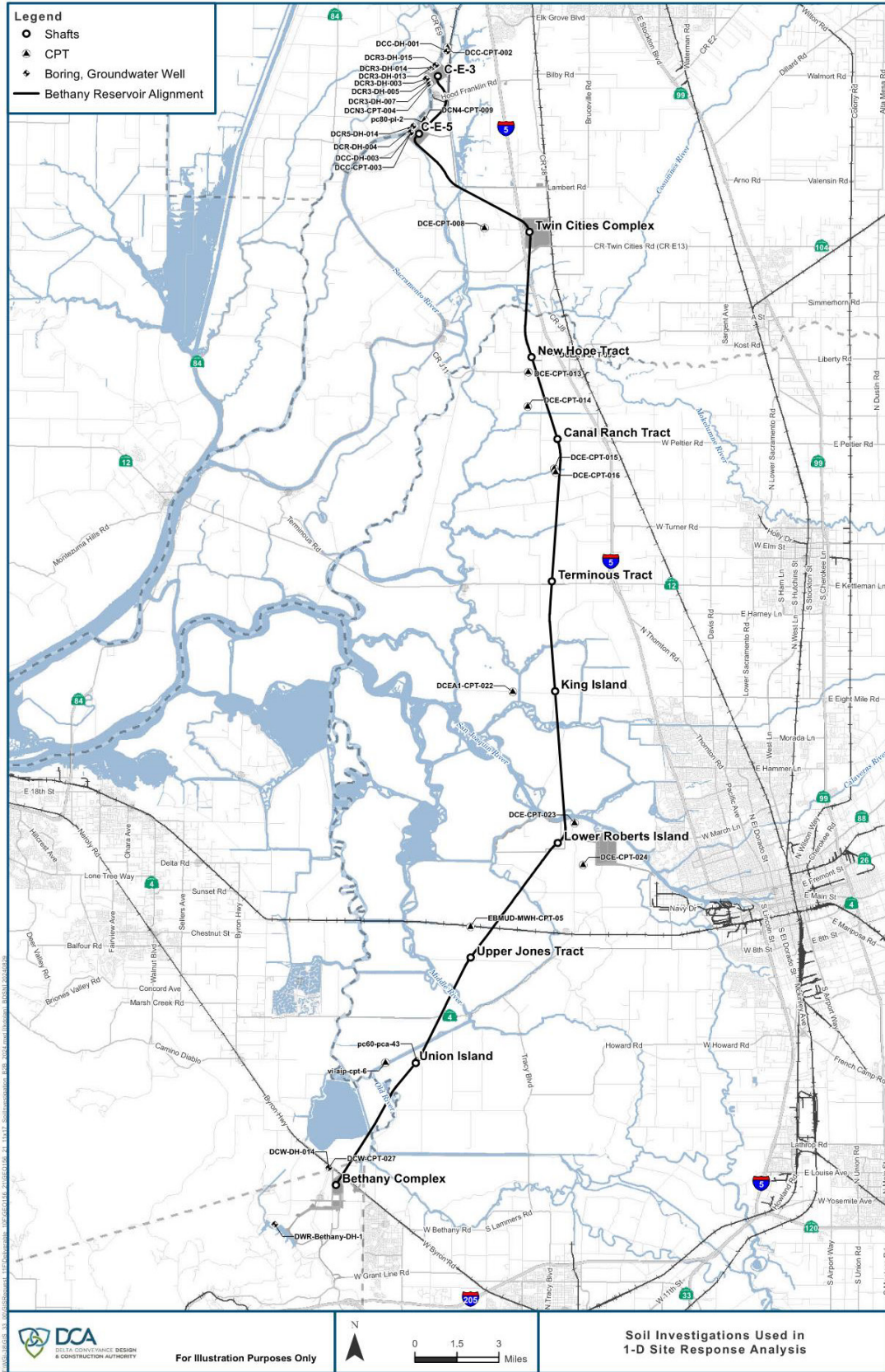


Figure 1. Locations of selected facilities and soil investigations used in 1-D Site Response Analysis

Table 1. Input/Reference Motions at Selected Facility Sites

Facility	Facility Type	MDE Ground Motions (unless noted)	V _s Half-Space ^[a] (ft/s) [elevation (ft)]
Bethany Reservoir Pumping Plant	Pumping Plant	2019 CBC – MCE ^[b]	1,100 [6]
Canal Ranch Tract	Shaft	Envelope of 2,475-year probabilistic and 84 th -percentile deterministic	1,200 [-40]
Intake No 3	Intake	Envelope of 975-year probabilistic and 84 th -percentile deterministic	1,200 [-70]
Intake No 5	Intake	Envelope of 975-year probabilistic and 84 th -percentile deterministic	1,300 [-35]
King Island	Shaft	Envelope of 2,475-year probabilistic and 84 th -percentile deterministic	1,212 [-73]
Lower Roberts Island	Shaft	Envelope of 2,475-year probabilistic and 84 th -percentile deterministic	800 [-28]
New Hope Tract	Shaft	Envelope of 2,475-year probabilistic and 84 th -percentile deterministic	1,104 [-46]
Twin Cities Road	Shaft	Envelope of 2,475-year probabilistic and 84 th -percentile deterministic	1,104 [-39]
Union Island	Shaft	Envelope of 2,475-year probabilistic and 84 th -percentile deterministic	1,100 [-80]

^[a] See Tables 2 through 10 and Figures 2 through 10 for locations/depths of half-space. □

^[b] See Attachment 2 for the development of MCE response spectra.

Ft/s = feet per second, MDE = maximum design earthquake, CBC = California Building Code, MCE = maximum considered earthquake

3.1 Soil Model Used for Site Response Analysis

The computer program DEEPSOIL (Version 7.0, 2021) was used for the 1-D non-linear site response analysis. The soil’s responses under seismic loadings were modeled using the nonlinear, total-stress, pressure-dependent Modified Kondner Zelasko (MKZ) unloading-reloading formulation with Non-Masing Hysteretic model (Phillips and Hashash, 2009). The soil’s model parameters were fitted/calibrated using the normalized G/G_{max} and damping versus shear strain curves proposed by Darendali (2001) and plasticity indexes and unit weights of the soils. Attachment 3 presents the results of these calibrations.

The idealized soil profiles used for analyses at the selected nine (9) facility sites are illustrated in Figures 2 through 10 and are summarized in Tables 2 through 10. The approximate location of selected tunnel shafts are shown in grey in each profile, and the approximate groundwater elevation is shown in blue dashed line on each profile. The soils below the elevation where the reference ground motions were inputted was modeled as half-space and assigned a V_s value as listed in the last column of Table 1. As mentioned above, the depth of the half-space was chosen as a depth to top of the Modesto or Riverbank Formations, adjusted to where the measured V_s value approximately matches the V_s value of reference ground motions. The thicknesses of the soil layers in the DEEPSOIL model were selected to allow propagation of waves of up to 50 Hz.

Table 2. Idealized Soil Profile and Parameters at Bethany Reservoir Pumping Plant Site

Layer #	Top Elevation ^[a] (ft)	Thickness (ft)	Soil Type ^[b]	γ_t (pcf)	OCR	PI	Vs (ft/s)
1	46	3	SC	115	not applicable	not applicable	525
2	43	6	SM	115	not applicable	not applicable	500
3	37	5	CL	115	1	20	525
4	32	10	SM	120	not applicable	not applicable	575
5	22	16	(CL)s	120	1	16	950
Half-Space	6	not applicable	not applicable	120	not applicable	not applicable	1,100

[a] NAVD88

[b] Unified Soil Classification System (USCS)

ft = feet; ft/s = feet per second; γ_t = total unit weight; pcf = pounds per cubic foot; OCR = over-consolidation ratio; PI = plasticity index

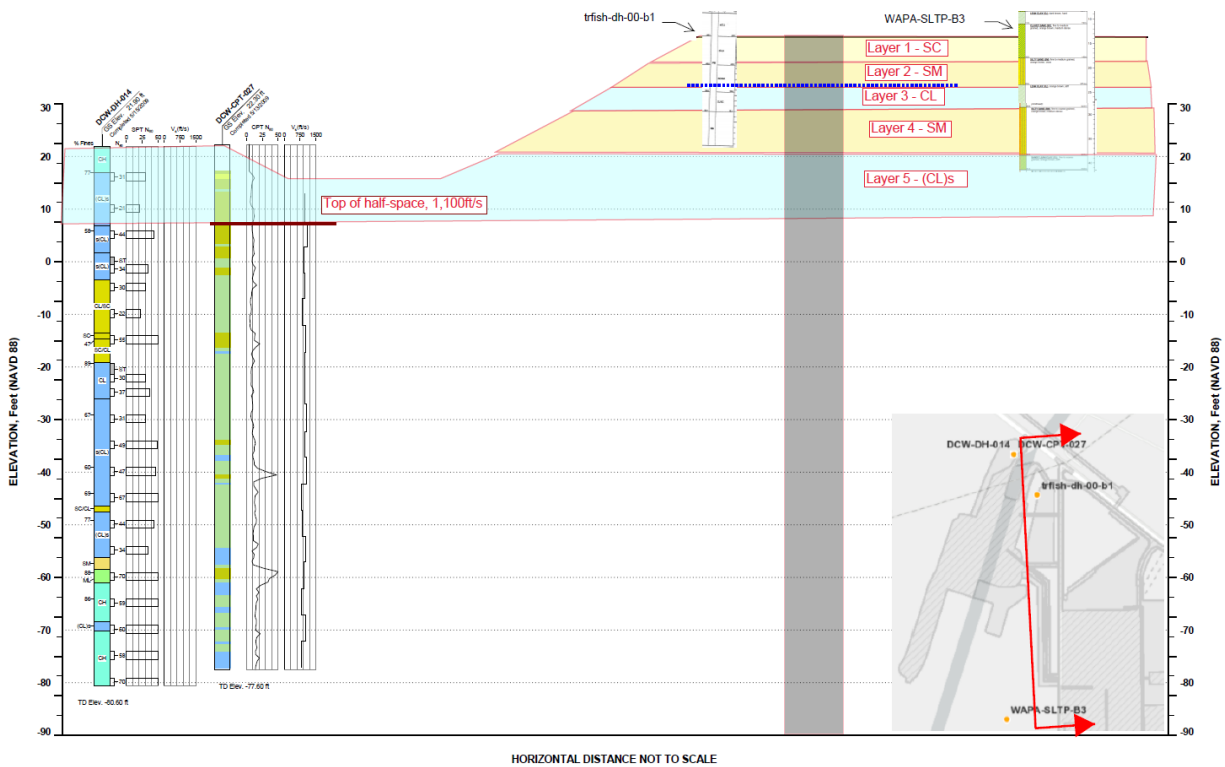


Figure 2. Idealized Soil Profile at Bethany Reservoir Pumping Plant Site

(Profile is oriented north-south and faces east; tunnel invert at approximate El. -164 feet, not shown)

Table 3. Idealized Soil Profile and Parameters at Canal Ranch Tract Facility Site

Layer #	Top Elevation ^[a] (ft)	Thickness (ft)	Soil Type ^[b]	γ_t (pcf)	OCR	PI	Vs (ft/s)
1 ^[a]	not applicable	5	SP	123	not applicable	not applicable	900
1 ^[b]	-5	5	SP	123	not applicable	not applicable	900
2	-10	11	CL	125	1	15	1,000
3	-21	7	SC	125	not applicable	not applicable	900
4	-28	12	SM	125	not applicable	not applicable	1,100
Half-Space	-40	not applicable	not applicable	130	not applicable	not applicable	1,200

[a] NAVD88

[b] Unified Soil Classification System (USCS)

ft = feet; ft/s = feet per second; γ_t = total unit weight; pcf = pounds per cubic foot; OCR = over-consolidation ratio; PI = plasticity index

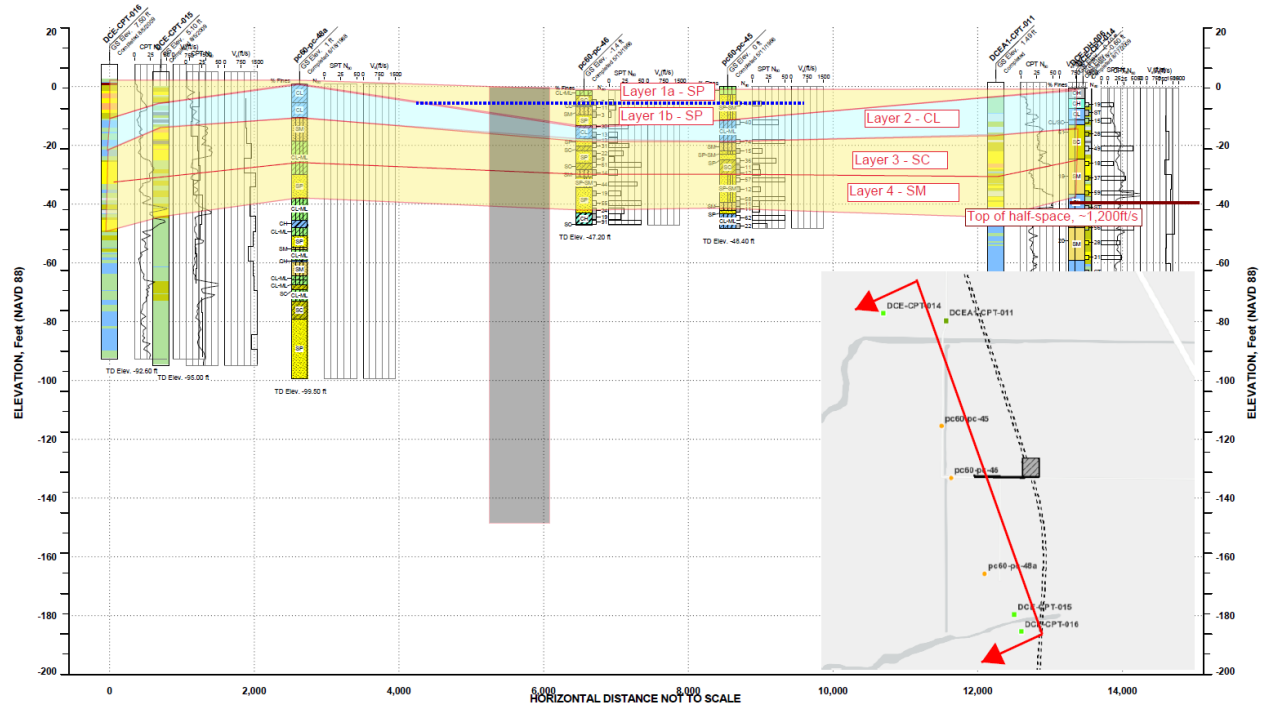


Figure 3. Idealized Soil Profile at Canal Ranch Tract Facility Site

(Profile is oriented northwest-southeast and faces southwest; tunnel invert at approximate El. -149 feet)

Table 4. Idealized Soil Profile and Parameters at Intake 3 Site

Layer #	Top Elevation ^[a] (ft)	Thickness (ft)	Soil Type ^[a]	γ_t (pcf)	OCR	PI	Vs (ft/s)
1a	15	7	CL/ML	115	1	12	450
1b	8	16	CL/ML	115	1	12	450
2	-8	12	SM	120	not applicable	not applicable	650
3	-20	10	SM	120	not applicable	not applicable	750
4	-30	8	CL	120	1	12	800
5	-38	7	CL/ML	120	1	12	700
6	-45	10	SP-SM	125	not applicable	not applicable	750
7	-55	15	CL	130	1.5	12	1,000
Half-space	-70	not applicable	not applicable	not applicable	not applicable	not applicable	1,200

[a] NAVD88

[b] Unified Soil Classification System (USCS)

ft = feet; ft/s = feet per second; γ_t = total unit weight; pcf = pounds per cubic foot; OCR = over-consolidation ratio; PI = plasticity index

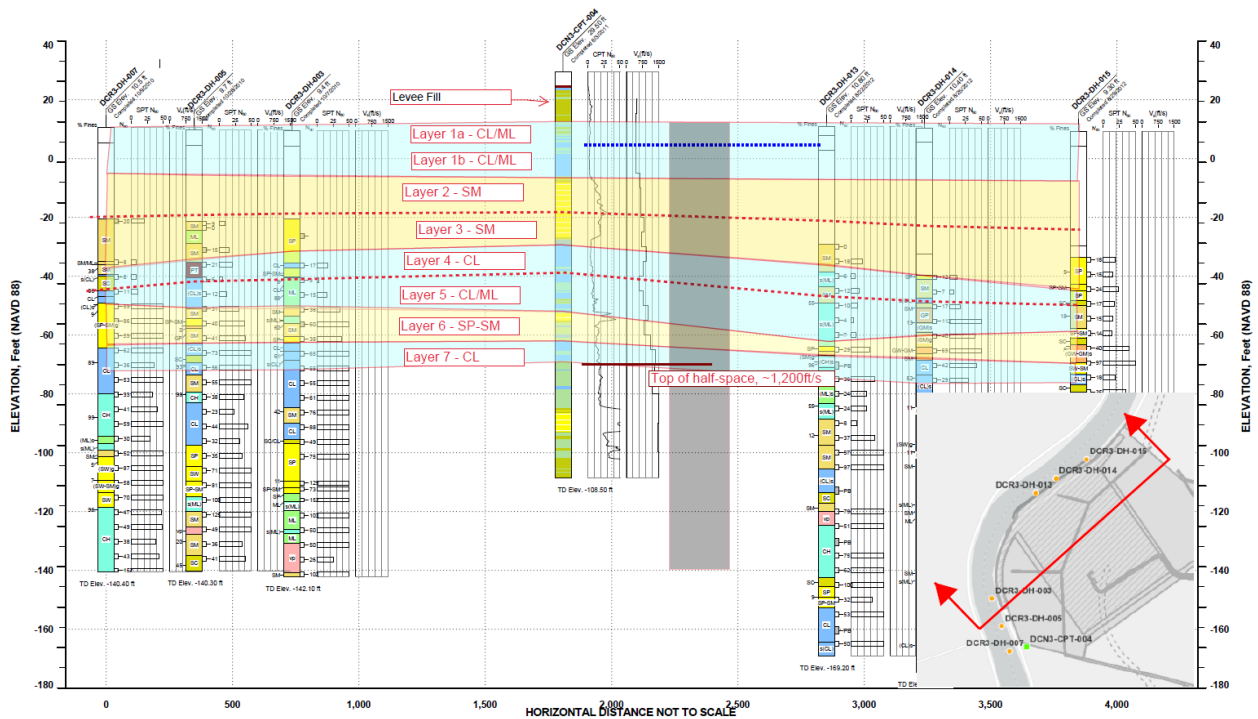


Figure 4. Idealized Soil Profile at Intake 3 Site

(Profile is oriented northeast-southwest and faces northwest; tunnel invert at approximate El. -140 feet)

Table 5. Idealized Soil Profile and Parameters at Intake 5 Site

Layer #	Top Elevation ^[a] (ft)	Thickness (ft)	Soil Type ^[b]	γ_t (pcf)	OCR	PI	Vs (ft/s)
1	10	10	(CL)s	115	1	12	520
2	0	10	SP	120	not applicable	not applicable	600
3	-10	10	SP	120	not applicable	not applicable	750
4	-20	15	SM	120	not applicable	not applicable	1,000
Half-Space	-35	not applicable	not applicable	125	not applicable	not applicable	1,300

[a] NAVD88

[b] Unified Soil Classification System (USCS)

ft = feet; ft/s = feet per second; γ_t = total unit weight; pcf = pounds per cubic foot; OCR = over-consolidation ratio; PI = plasticity index

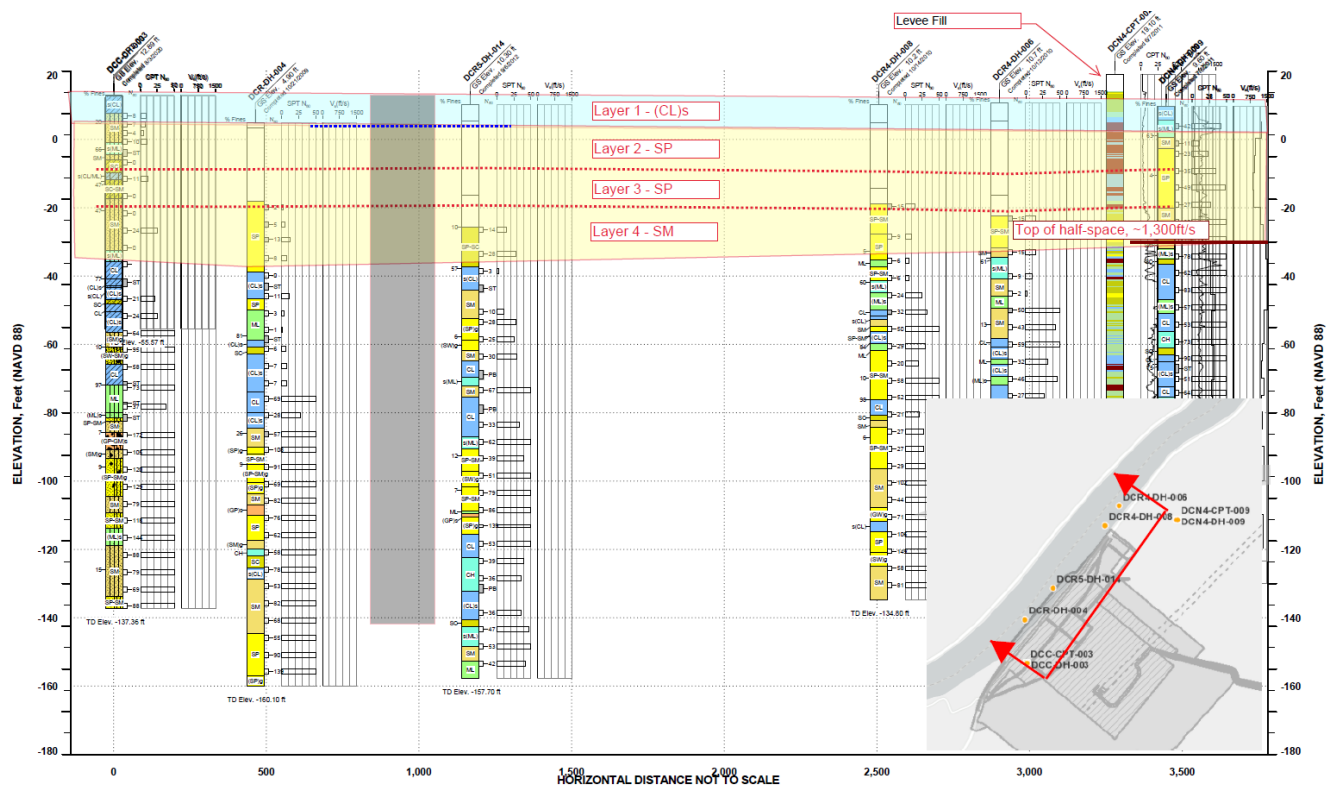


Figure 5. Idealized Soil Profile at Intake 5 Site

(Profile is oriented northeast-southwest and faces northwest; tunnel invert at approximate El. -142 feet)

Table 6. Idealized Soil Profile and Parameters at King Island Facility Site

Layer #	Top Elevation ^[a] (ft)	Thickness (ft)	Soil Type ^[b]	γ_t (pcf)	OCR	PI	Vs (ft/s)
1	-4	7	PT	60	1	40	400
2	-11	22	CL/ML	115	1	15	950
3	-33	16	SP-SM	115	not applicable	not applicable	1,100
4	-49	10	CL/ML	100	1	15	750
5	-59	8	SM	110	not applicable	not applicable	850
6	-67	6	CL/ML	120	1	15	700
Half-space	-73	not applicable	not applicable	125	not applicable	not applicable	1,212

[a] NAVD88

[b] Unified Soil Classification System (USCS)

ft = feet; ft/s = feet per second; γ_t = total unit weight; pcf = pounds per cubic foot; OCR = over-consolidation ratio; PI = plasticity index

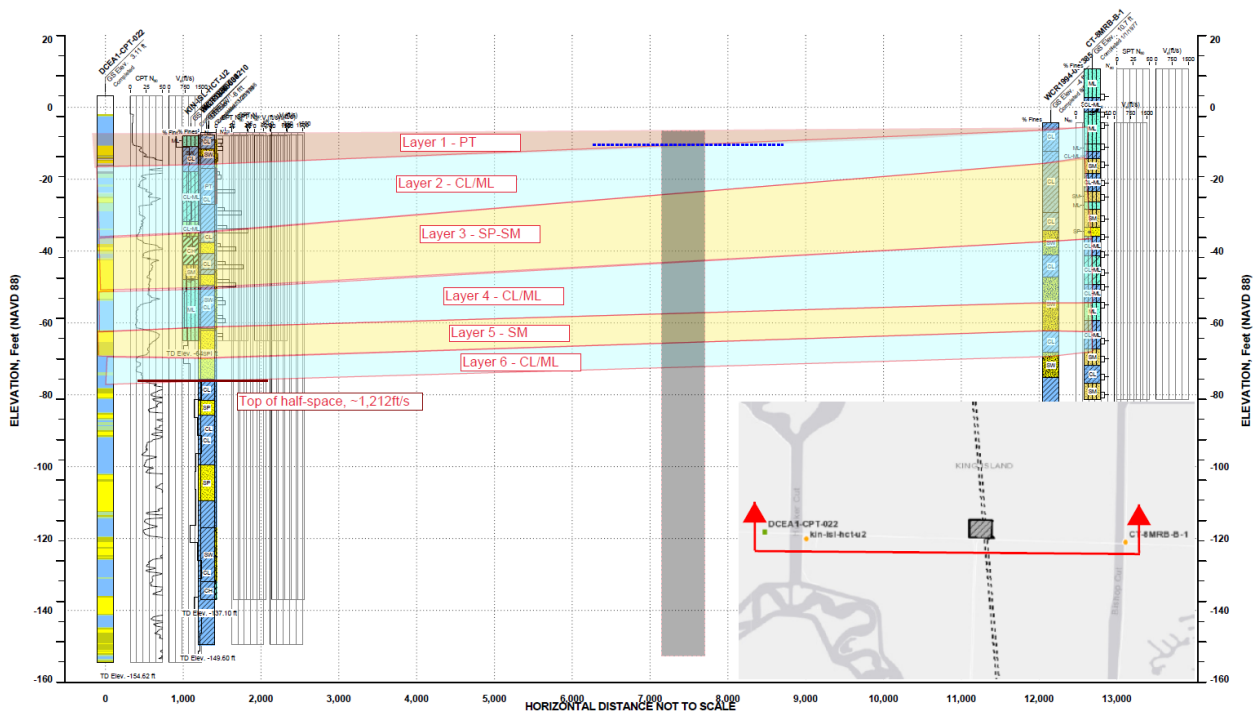


Figure 6. Idealized Soil Profile at King Island Facility Site

(Profile is oriented east-west and faces north; tunnel invert at approximate El. -154 feet)

Table 7. Idealized Soil Profile and Parameters at Lower Roberts Island Facility Site

Layer #	Top Elevation ^[a] (ft)	Thickness (ft)	Soil Type ^[b]	γ_t (pcf)	OCR	PI	Vs (ft/s)
1	2	7	CL	110	1	15	500
2	-5	7	PT	60	1	40	400
3	-12	16	SP-SM	115	not applicable	not applicable	500
Half-Space	-28	not applicable	not applicable	120	not applicable	not applicable	800

[a] NAVD88

[b] Unified Soil Classification System (USCS)

ft = feet; ft/s = feet per second; γ_t = total unit weight; pcf = pounds per cubic foot; OCR = over-consolidation ratio; PI = plasticity index

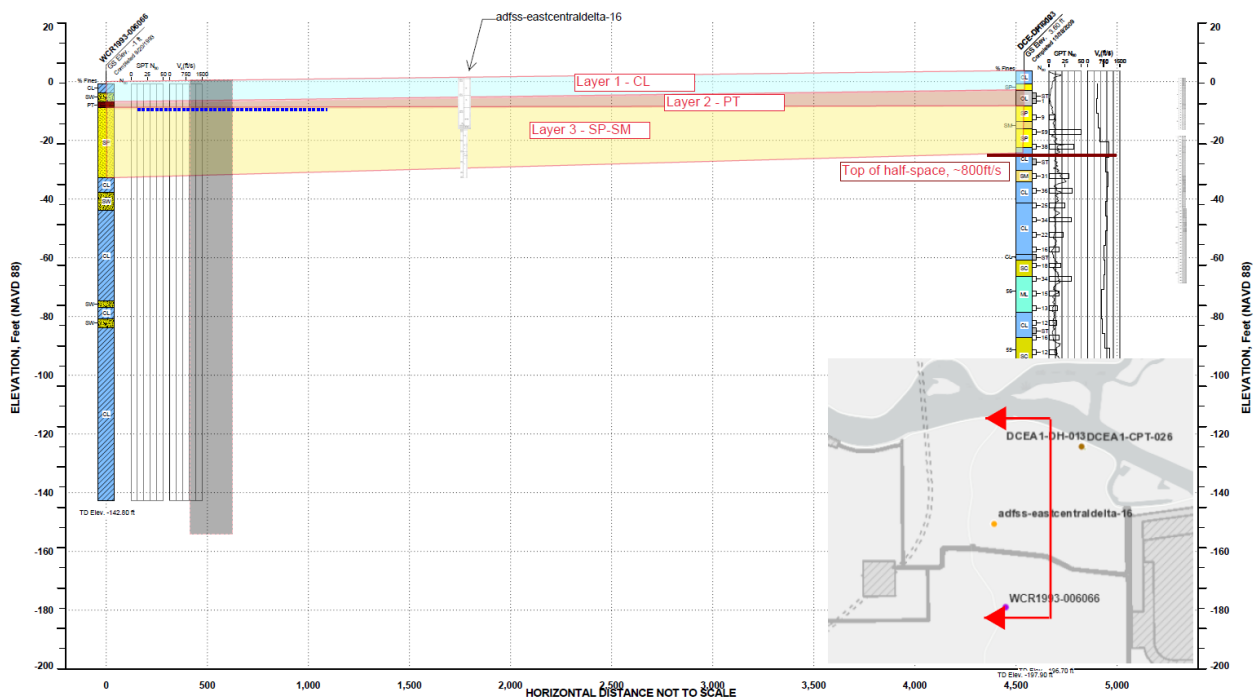


Figure 7. Idealized Soil Profile at Lower Roberts Island Facility Site

(Profile is oriented north-south and faces west; tunnel invert at approximate El. -156 feet)

Table 8. Idealized Soil Profile and Parameters at New Hope Tract Facility Site

Layer #	Top Elevation ^[a] (ft)	Thickness (ft)	Soil Type ^[a]	γ_t (pcf)	OCR	PI	Vs (ft/s)
1a	6	10	CL	120	1	15	720
1b	-4	4	CL	120	1	15	720
2	-8	4	ML	125	not applicable	not applicable	675
3	-12	10	SP	125	not applicable	not applicable	600
4	-22	10	SC	125	1.5	not applicable	750
5	-32	14	CL	125	1.5	25	1,000
Half-Space	-46	not applicable	not applicable	130	not applicable	not applicable	1,104

[a] NAVD88

[b] Unified Soil Classification System (USCS)

ft = feet; ft/s = feet per second; γ_t = total unit weight; pcf = pounds per cubic foot; OCR = over-consolidation ratio; PI = plasticity index

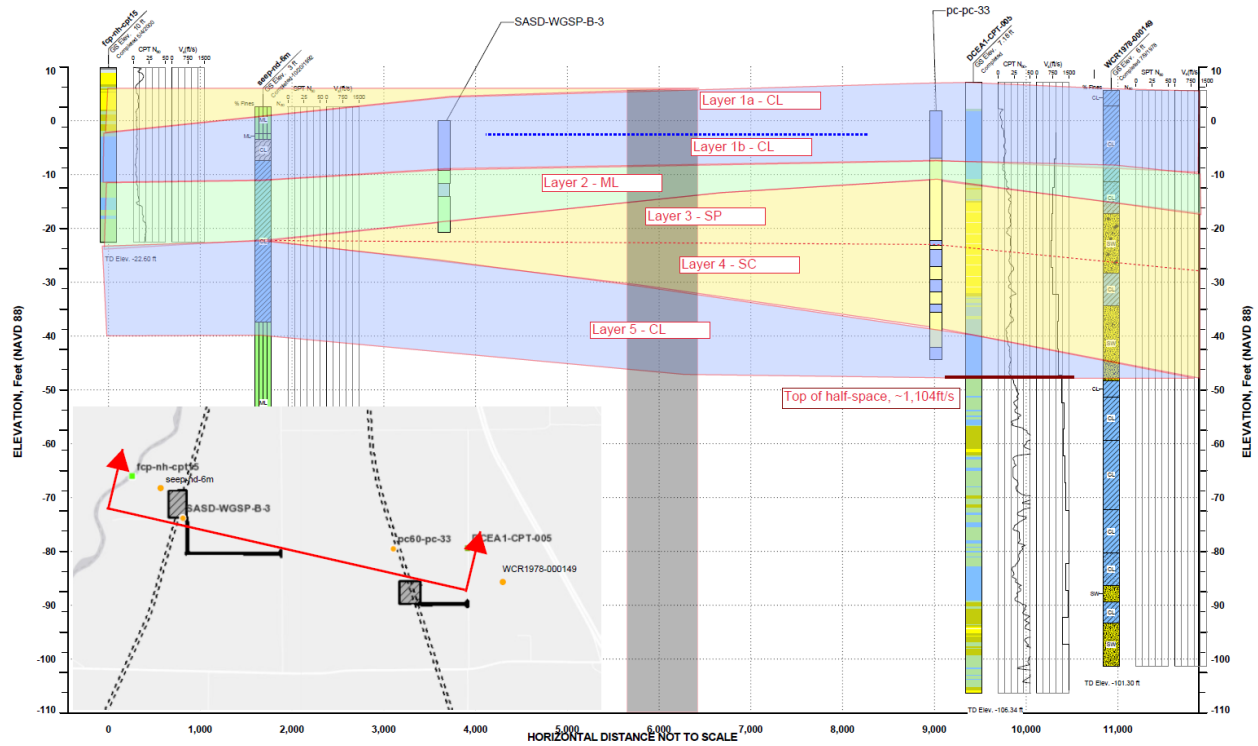


Figure 8. Idealized Soil Profile at New Hope Tract Facility Site

(Profile is oriented east-west and faces north. The representative shaft location is shown in grey in the profile, as this profile spans facilities for the Central and Eastern Corridors; tunnel invert at approximate El. -148 feet for the Central Corridor and El. -147 for the Eastern Corridor, not shown)

Table 9. Idealized Soil Profile and Parameters at Twin Cities Road Facility Site

Layer #	Top Elevation ^[a] (ft)	Thickness (ft)	Soil Type ^[b]	γ_t (pcf)	OCR	PI	Vs (ft/s)
1	6	7	ML/CL	115	1	15	1,050
2	-1	6	SP-SM	120	not applicable	not applicable	1,050
3	-7	3	SM	120	not applicable	not applicable	1,150
4	-10	9	ML/CL	120	1	15	1,250
5	-19	5	SC	120	not applicable		1,300
6	-24	10	CL	120	1.5	21	900
7	-34	5	SP	120	not applicable	not applicable	1,100
Half-Space	-39	not applicable	not applicable	130	not applicable	not applicable	1,104

[a] NAVD88

[b] Unified Soil Classification System (USCS)

ft = feet; ft/s = feet per second; γ_t = total unit weight; pcf = pounds per cubic foot; OCR = over-consolidation ratio; PI = plasticity index

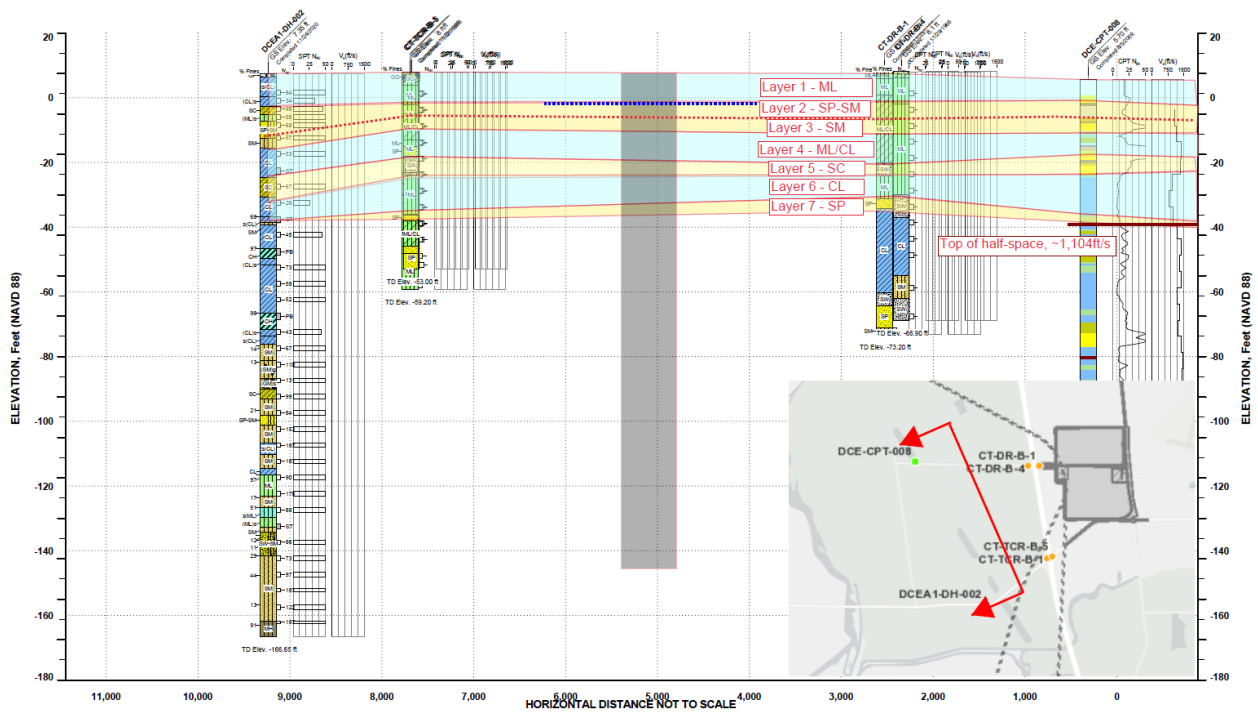


Figure 9. Idealized Soil Profile at Twin Cities Road Facility Site

(Profile is oriented northwest-southeast and faces southwest; tunnel invert at approximate El. -146 feet for the Central Corridor and El. -145 for the Eastern Corridor)

Table 10. Idealized Soil Profile and Parameters at Union Island Facility Site

Layer #	Top Elevation ^[a] (ft)	Thickness (ft)	Soil Type ^[b]	γ_t (pcf)	OCR	PI	Vs (ft/s)
1	-3	5	PT	60	1	40	400
2a	-8	7	SP-SM	120	not applicable	not applicable	450
2b	-15	8	SP-SM	120	not applicable	not applicable	450
3	-23	16	CH	120	1	33	550
4	-39	9	SP-SM	120	not applicable	not applicable	650
5	-48	10	CH	120	1.5	41	600
6	-58	4	(CL)s	125	1.5	8	625
7	-62	9	CH	125	1.5	39	700
8	-71	9	SC-SM	125	not applicable	not applicable	900
Half-Space	-80	not applicable	not applicable	130	not applicable	not applicable	1,100

[a] NAVD88

[b] Unified Soil Classification System (USCS)

ft = feet; ft/s = feet per second; γ_t = total unit weight; pcf = pounds per cubic foot; OCR = over-consolidation ratio; PI = plasticity index

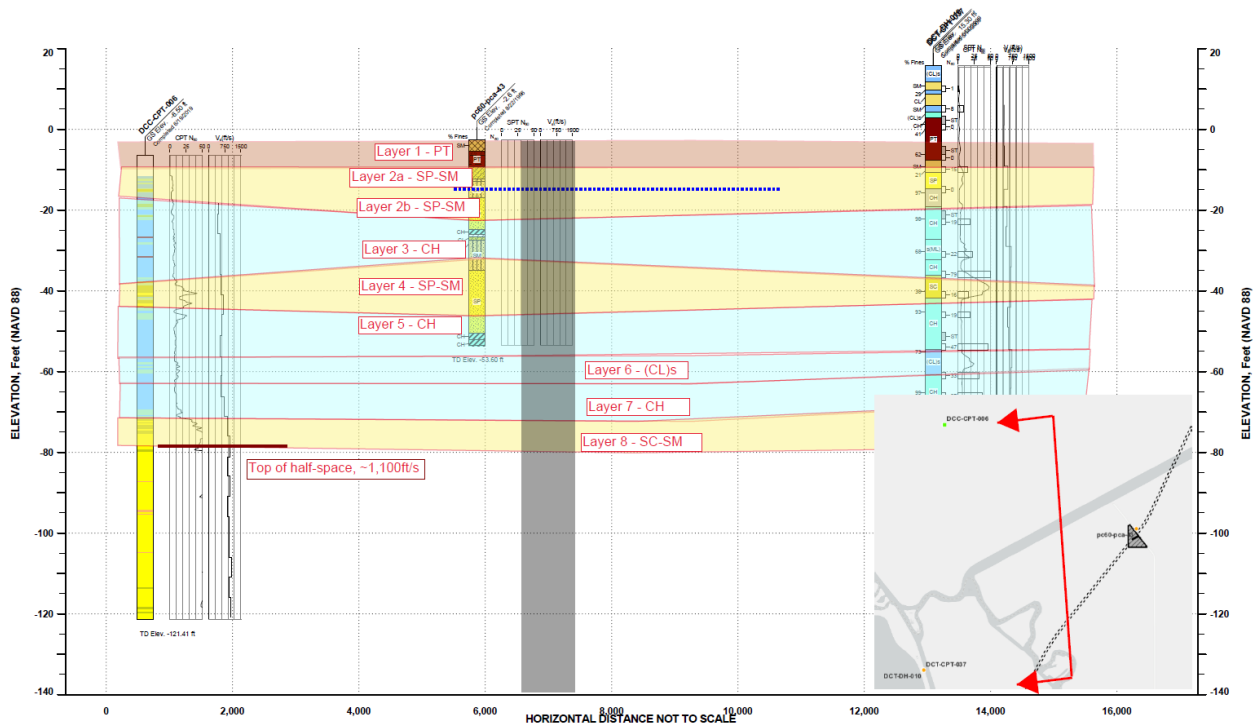


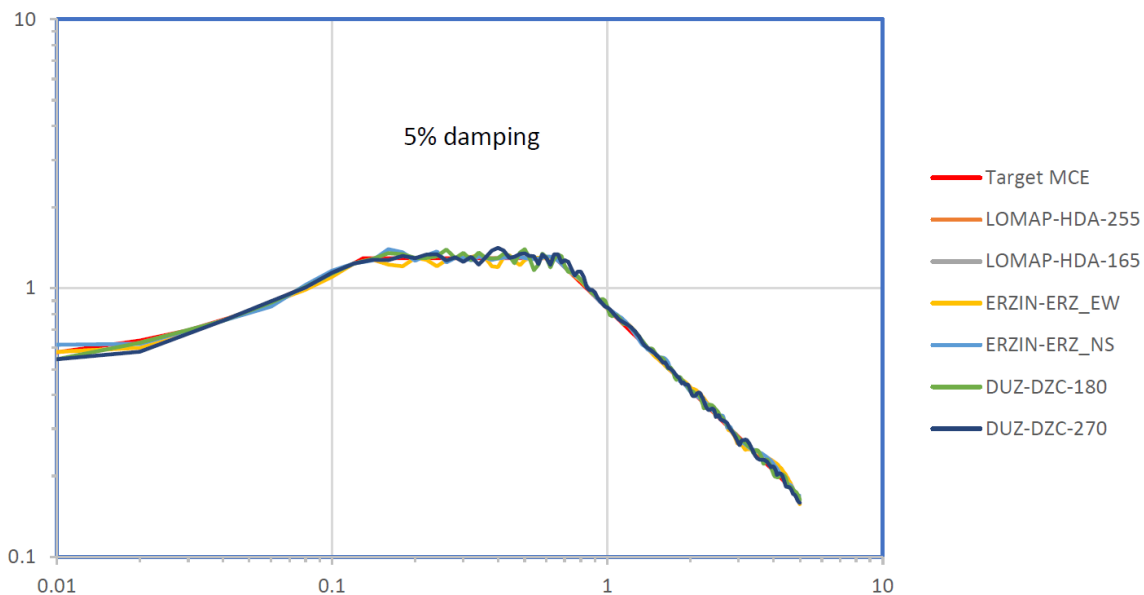
Figure 10. Idealized Soil Profile at Union Island Facility Site

(Profile is oriented north-south and faces west; tunnel invert at approximate El. -161 feet, not shown)

3.2 Input Earthquake Ground Motions

Two orthogonal horizontal components of earthquake time histories recorded during three (3) past earthquakes were used as inputs for site response analysis at each of the facility sites. The selected earthquake time histories recorded during past earthquakes (seed time histories) were spectrally-modified to better match the MDE/MCE response spectrum at each facility site using the time-domain procedure proposed by Al Atik and Abrahamson (2010). Lettis Consultants International (LCI) selected seed time histories for horizontal ground motions and spectrally modified these motions at four (4) facility sites along the Project (see Attachment 1), which were then used by performing additional spectral modifications to match the target design spectra for the remaining five (5) facility sites (see Attachment 4 for the development of input ground motions at these 5 sites).

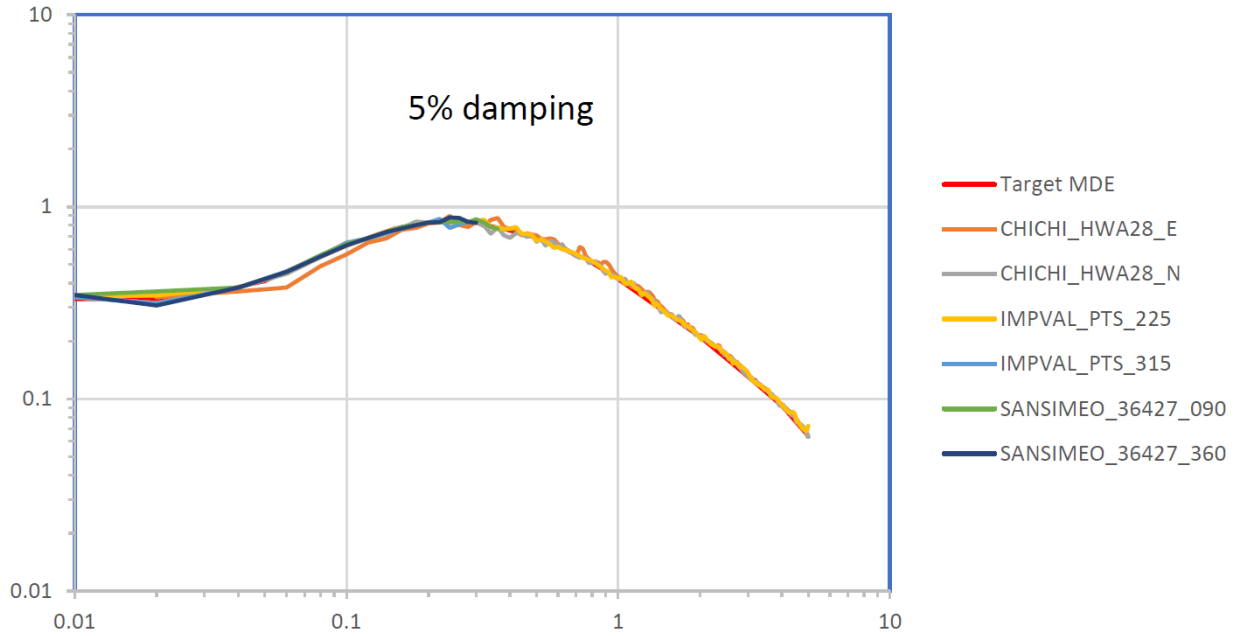
Response spectra for 5% damping were developed, as this is the standard damping value adopted by ground motion models and codes. Spectral values for other dampings can be developed from these spectra during future design phases, as required. Response spectra calculated from the spectrally-modified time histories are compared with the MDE/MCE spectra at the nine (9) facilities sites on Figures 11 through 19. As can be seen from these figures, the averages of the six (6) time histories at each facility site match reasonably well to the MDE/MCE spectra.



Notes

LOMAP-HDA = 1989 Loma Prieta Earthquake, recorded at Hollister Dif. Array (225/165 deg horizontal component)
ERZIN-ERZ = 1992 Erzican, Turkey Earthquake, recorded at Erzincan (east-west/north-south horizontal component)
DUZ-DZC = 1999 Duzce, Turkey Earthquake, recorded at Duzce (180/270 deg horizontal component)

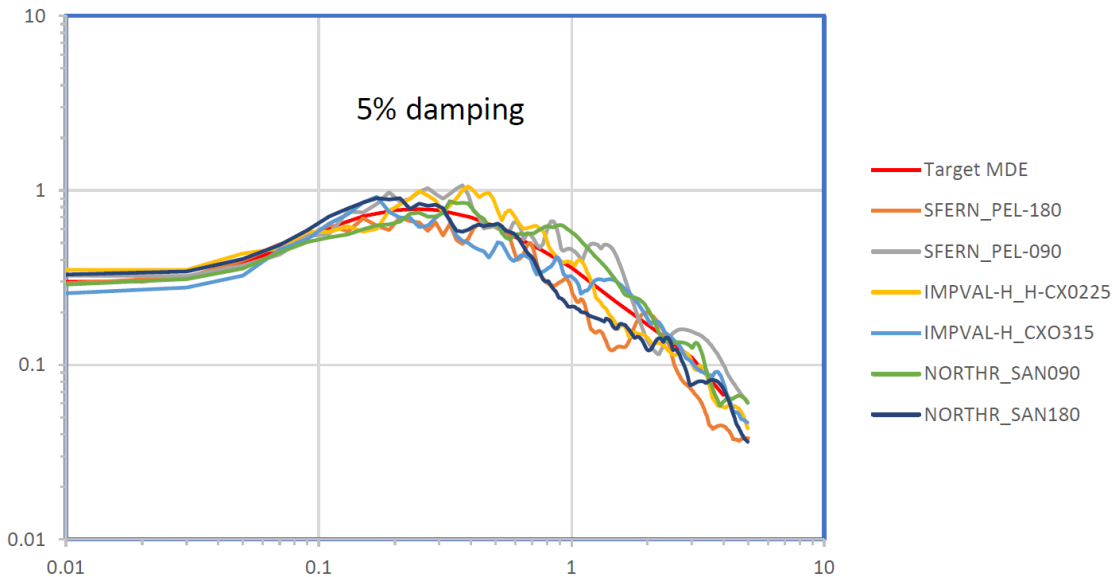
Figure 11. Comparison of Response Spectra at the Bethany Reservoir Pumping Plant Facility Site (MCE)



Notes

CHICHI_HWA28 = 1999 Chi-Chi, Taiwan Earthquake, recorded at HWA028 (east/north horizontal component)
 IMPVAL_PTS = 1979 Imperial Valley-06 Earthquake, recorded at Parachute Test Site (225/315 deg horizontal component)
 SANSIMEO_36427 = 2003 San Simeon Earthquake, recorded at Point Buchon – Los Osos (90/360 deg horizontal component)

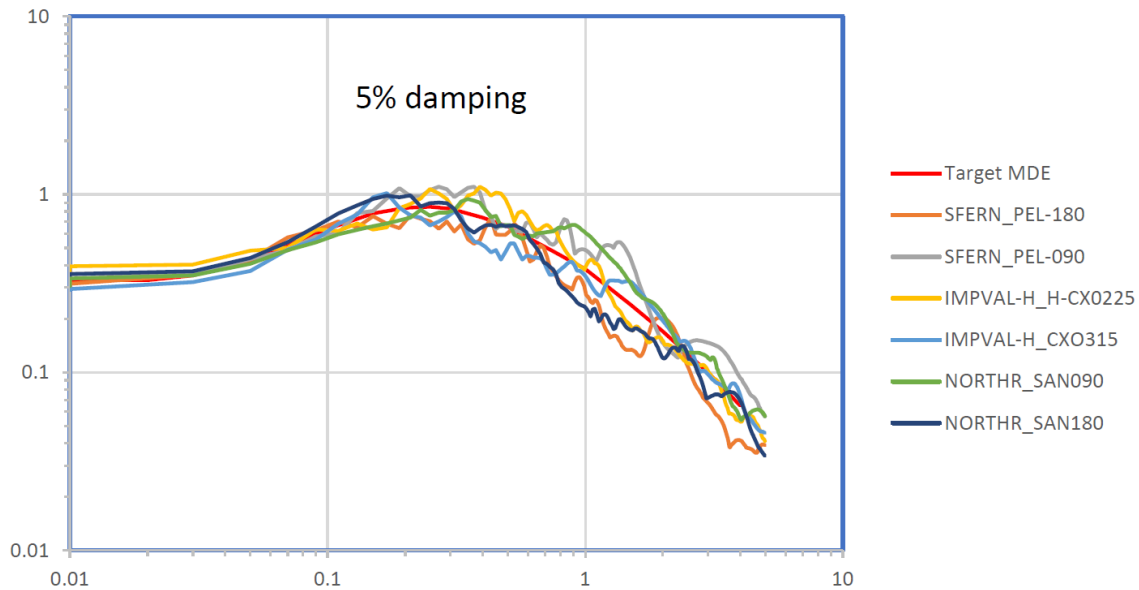
Figure 12. Comparison of Response Spectra at the Canal Ranch Tract Facility Site (MDE)



Notes

SFERN_PEL = 1971 San Fernando Earthquake, recorded at LA-Hollywood Stor FF (90/180 deg horizontal component)
 IMPVAL-H_CXO = 1979 Imperial Valley-06 Earthquake, recorded at Calexico Fire Stn. (225/315 deg horizontal component)
 NORTHR_SAN: 1994 Northridge Earthquake, recorded at Sandberg – Bal Mtn. (90/180 deg horizontal component)

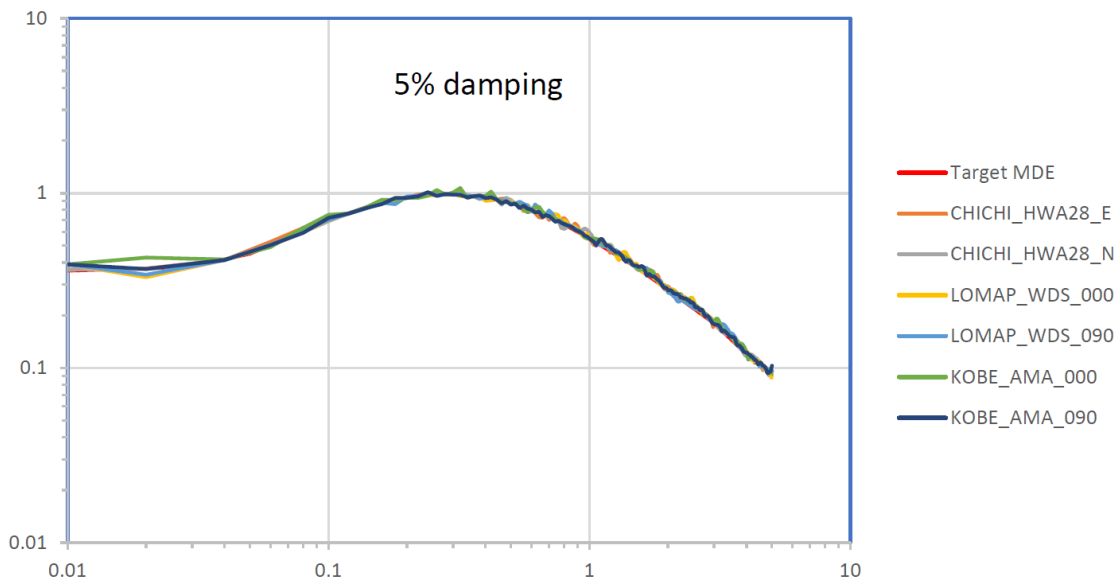
Figure 13. Comparison of Response Spectra at the Intake 3 Facility Site (MDE)



Notes

SFERN_PEL = 1971 San Fernando Earthquake, recorded at LA-Hollywood Stor FF (90/180 deg horizontal component)
 IMPVAL-H_CXO = 1979 Imperial Valley-06 Earthquake, recorded at Calexico Fire Stn. (225/315 deg horizontal component)
 NORTHR_SAN: 1994 Northridge Earthquake, recorded at Sandberg – Bal Mtn. (90/180 deg horizontal component)

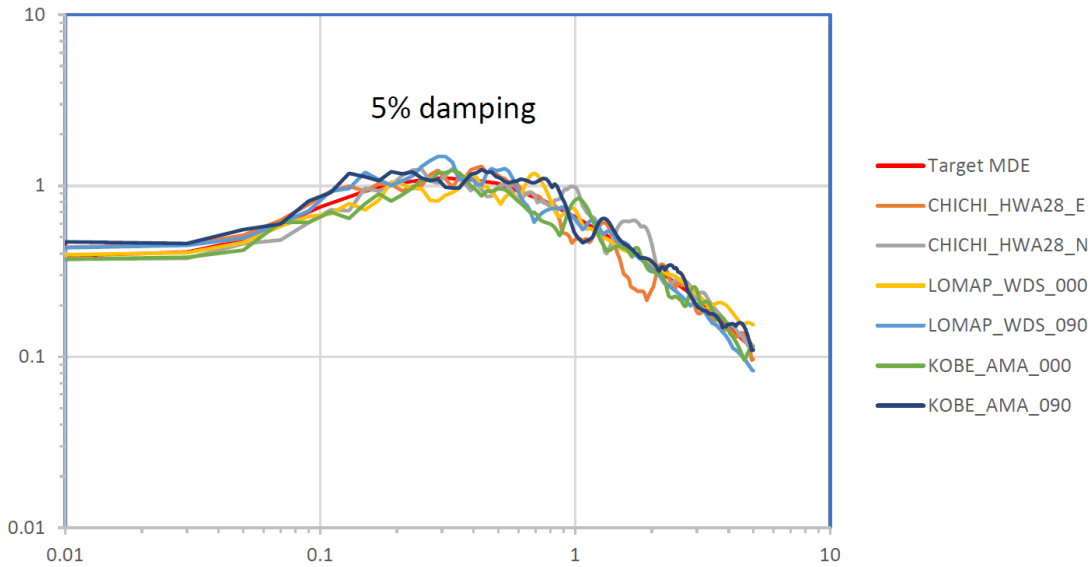
Figure 14. Comparison of Response Spectra at the Intake 5 Facility Site (MDE)



Notes

CHICHI_HWA28 = 1999 Chi-Chi, Taiwan earthquake, recorded at HWA 028 (east/west horizontal component)
 LOMAP_WDS = 1989 Loma Prieta Earthquake, recorded at Woodside, (00/90 deg horizontal component)
 KOBE_AMA = 1995 Kobe, Japan Earthquake, recorded at Amagasaki (0/90 degree horizontal component)

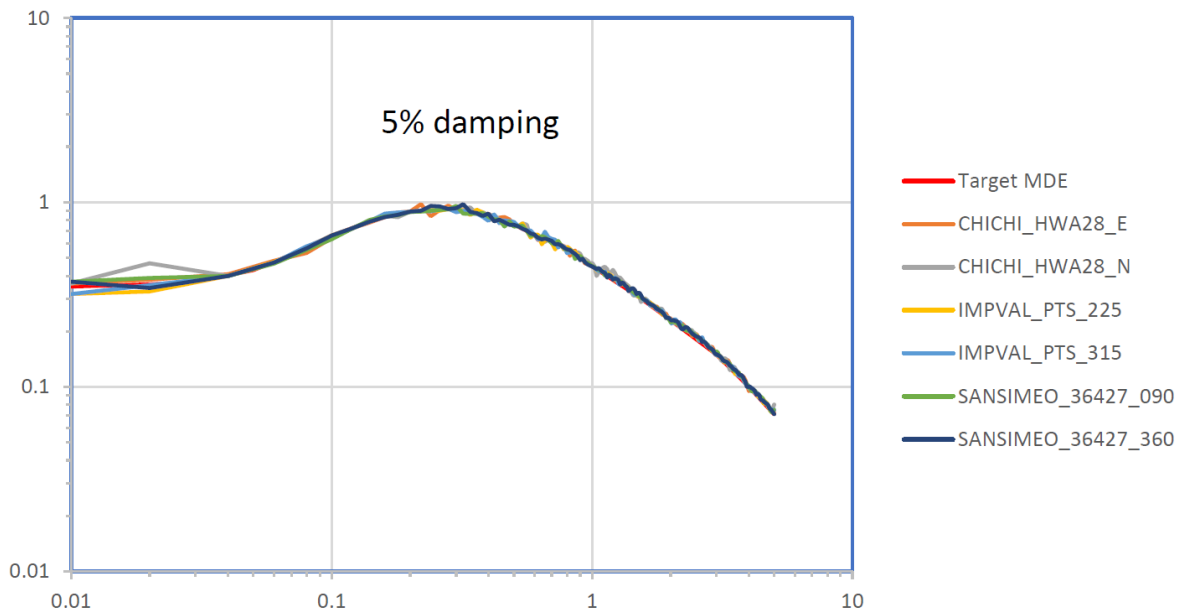
Figure 15. Comparison of Response Spectra at the King Island Facility Site (MDE)



Notes

CHICHI_HWA28 = 1999 Chi-Chi, Taiwan earthquake, recorded at HWA 028 (east/west horizontal component)
 LOMAP_WDS = 1989 Loma Prieta Earthquake, recorded at Woodside, (00/90 deg horizontal component)
 KOBE_AMA = 1995 Kobe, Japan Earthquake, recorded at Amagasaki (0/90 degree horizontal component)

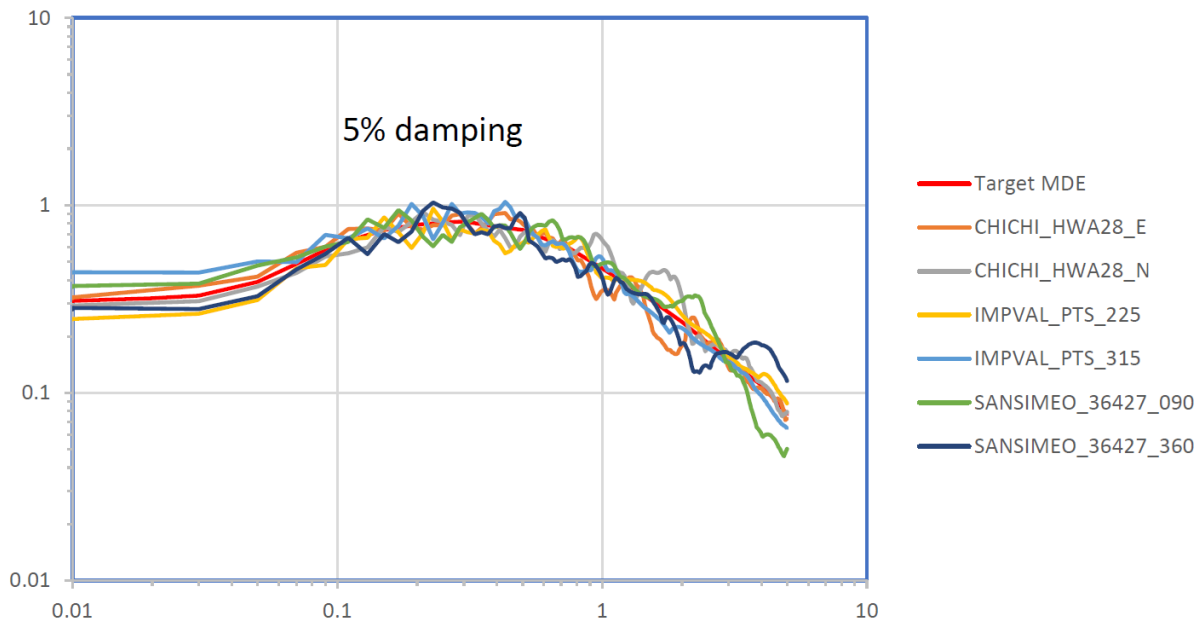
Figure 16. Comparison of Response Spectra at the Lower Roberts Island Facility Site (MDE)



Notes

CHICHI_HWA28 = 1999 Chi-Chi, Taiwan Earthquake, recorded at HWA028 (east/north horizontal component)
 IMPVAL_PTS = 1979 Imperial Valley-06 Earthquake, recorded at Parachute Test Site (225/315 deg horizontal component)
 SANSIMEO_36427 = 2003 San Simeon Earthquake, recorded at Point Buchon – Los Osos (90/360 deg horizontal component)

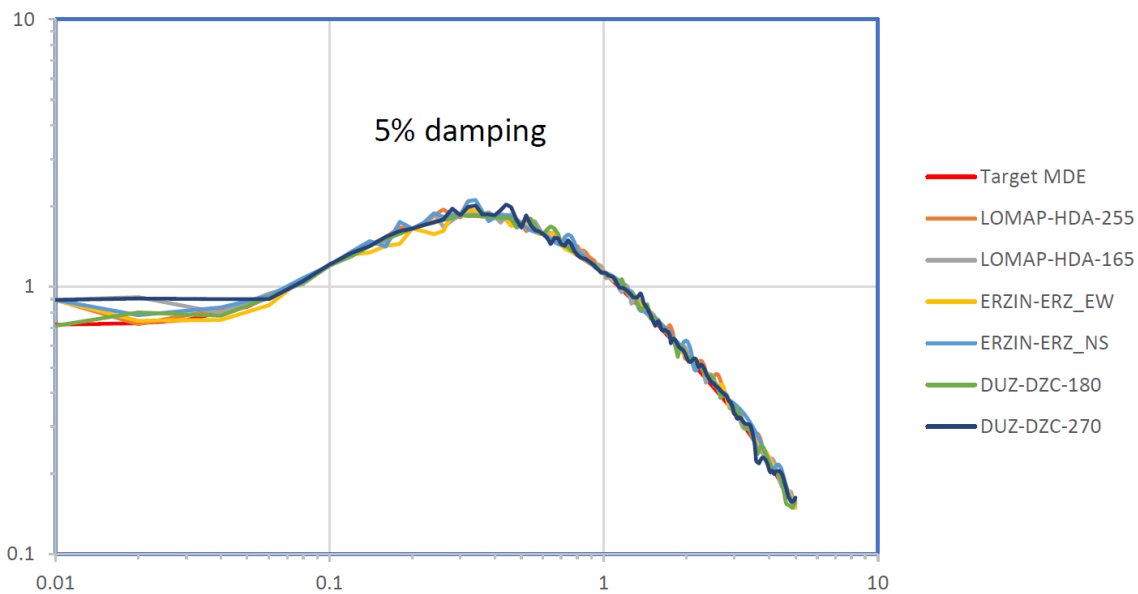
Figure 17. Comparison Response Spectra at the New Hope Tract Facility Site (MDE)



Notes

CHICHI_HWA28 = 1999 Chi-Chi, Taiwan Earthquake, recorded at HWA028 (east/north horizontal component)
 IMPVAL_PTS = 1979 Imperial Valley-06 Earthquake, recorded at Parachute Test Site (225/315 deg horizontal component)
 SANSIMEO_36427 = 2003 San Simeon Earthquake, recorded at Point Buchon – Los Osos (90/360 deg horizontal component)

Figure 18. Comparison of Response Spectra at the Twin Cities Road Facility Site (MDE)



Notes

LOMAP-HDA = 1989 Loma Prieta Earthquake, recorded at Hollister Dif. Array (225/165 deg horizontal component)
 ERZIN-ERZ = 1992 Erzican, Turkey Earthquake, recorded at Erzincan (east-west/north-south horizontal component)
 DUZ-DZC = 1999 Duzce, Turkey Earthquake, recorded at Duzce (180/270 deg horizontal component)

Figure 19. Comparison of Response Spectra at the Union Island Facility Site (MDE)

3.3 Results of 1-D Site Response Analysis

The spectrally-modified earthquake time histories described above were input at the top of the half-space at each of the facility sites and propagated upward through the idealized soil profile using the program DEEPSOIL to obtain site-specific earthquake ground motions at the ground surface. At each site facility, the response spectral values calculated at the ground surface were divided by the corresponding spectral values of input ground motion to produce site amplification factors as a function of vibratory period. These site amplification factors were then averaged at each facility to produce period-dependent averaged amplification factors at each site, including the amplification factor for PGA.

Table 11 presents the ranges of PGA values and computed site amplifications at the nine (9) facility sites, as well as the amplification factors that were used in the initial liquefaction analyses that utilized Kishida et. al (2009) (CER Appendix G2). As shown in the table, the site amplification factors assigned to the sites in the initial liquefaction analyses are generally larger than the values calculated in the current site response analyses. It should be noted that the amplification factors estimated using the published correlations as presented in Kishida et al. (2009) include the amplifications through levee embankments (i.e., they represent the ground motions at levee crests). The Kishida et al. (2009) amplification factors were also developed using the equivalent-linear soil model, which can't adequately capture the non-linear soil behaviors where large shear strains (> 1%) are expected during shaking.

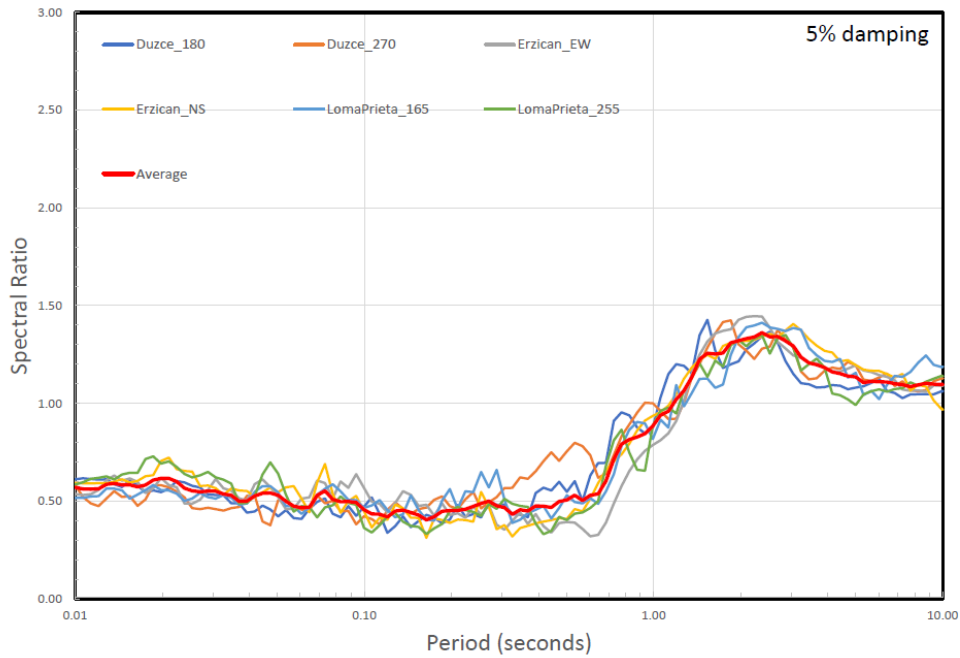
Figures 20 through 28 show the plots of the calculated and average site spectral amplifications as a function of period for the nine (9) facility sites.

Table 11. Calculated Ground Surface PGAs and Amplification Factors at Selected Facility Sites

Facility	Peak Ground Accelerations (%g) Range of Input PGAs	Peak Ground Accelerations (%g) Range of Calculated Ground Surface PGAs	Average Site Amplification Factor	Initial Site Amplification Factor ^[a]
Bethany Reservoir Pumping Plant	0.37 - 0.49	0.29 - 0.33	0.57	0.61
Canal Ranch Tract	0.28 – 0.36	0.31 – 0.35	1.02	1.00
Intake No 3	0.26 – 0.40	0.19 – 0.24	0.67	1.00
Intake No 5	0.32 – 0.40	0.27 – 0.37	0.88	1.00
King Island	0.34 – 0.49	0.25 – 0.36	0.75	1.00
Lower Roberts Island	0.36 – 0.57	0.2 – 0.24	0.52	1.00
New Hope Tract	0.32 – 0.51	0.23 – 0.33	0.66	1.00
Twin Cities Road	0.25 – 0.44	0.28 – 0.41	0.92	1.00
Union Island	0.69 – 0.92	0.24 – 0.32	0.37	0.72

^[a] Prior site amplification factors from Kishida et al. (2009) as presented in CER Appendix G2.

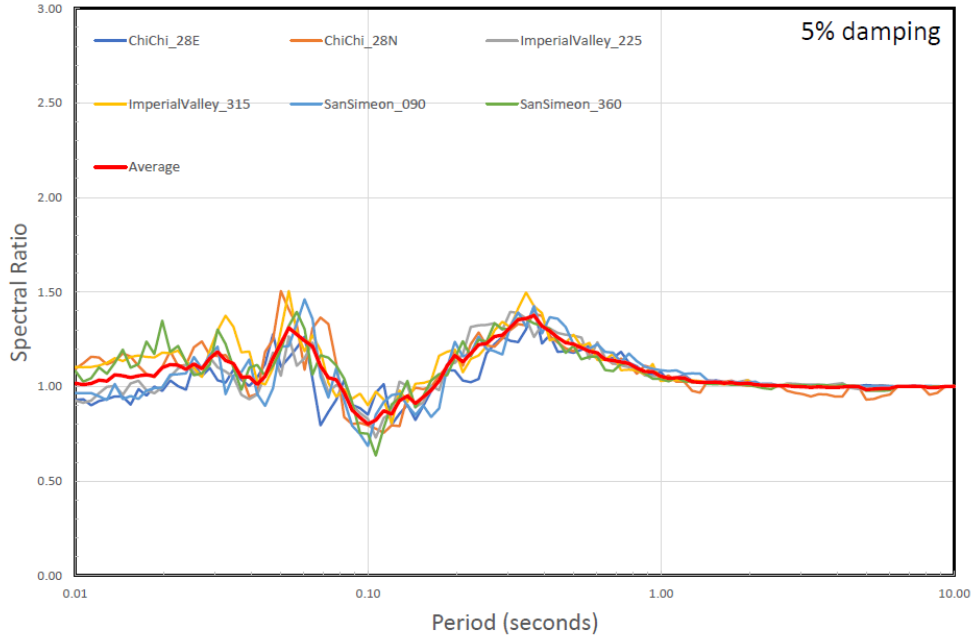
%g = acceleration, percent of gravity



Notes

See previous figures for earthquake definitions

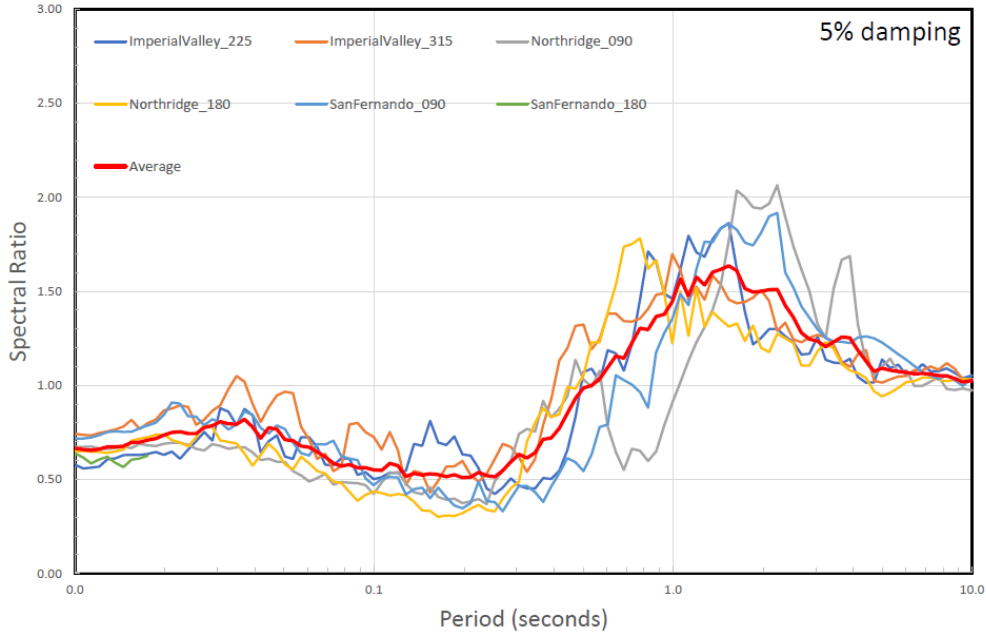
Figure 20. Site Spectral Amplifications Ratio Vs. Period at Bethany Reservoir Pumping Plant Site



Notes

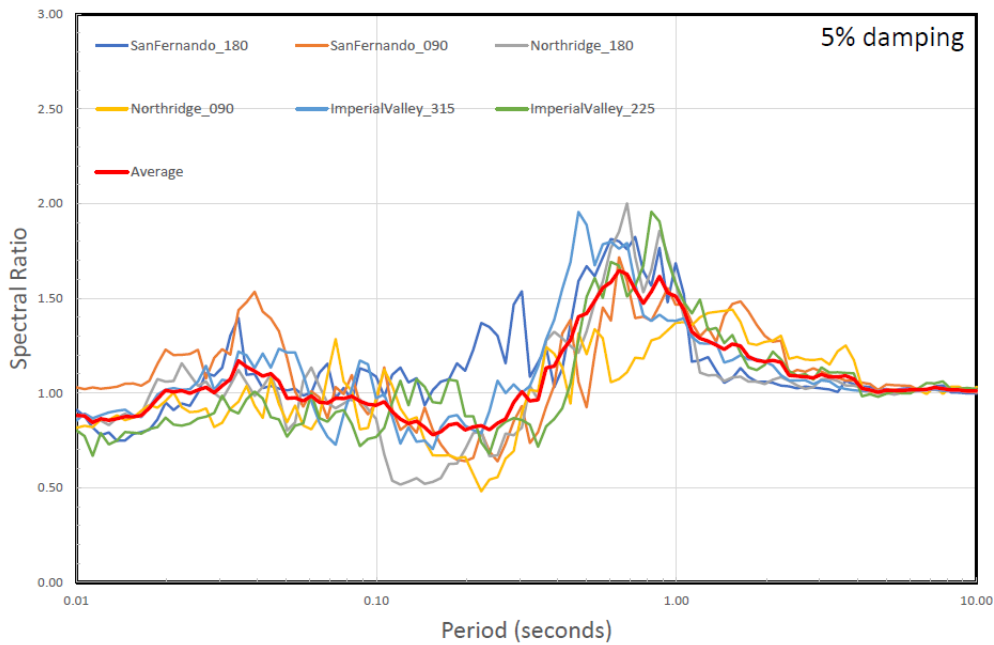
See previous figures for earthquake definitions

Figure 21. Site Spectral Amplifications Ratio Vs. Period at the Canal Ranch Tract Facility Site



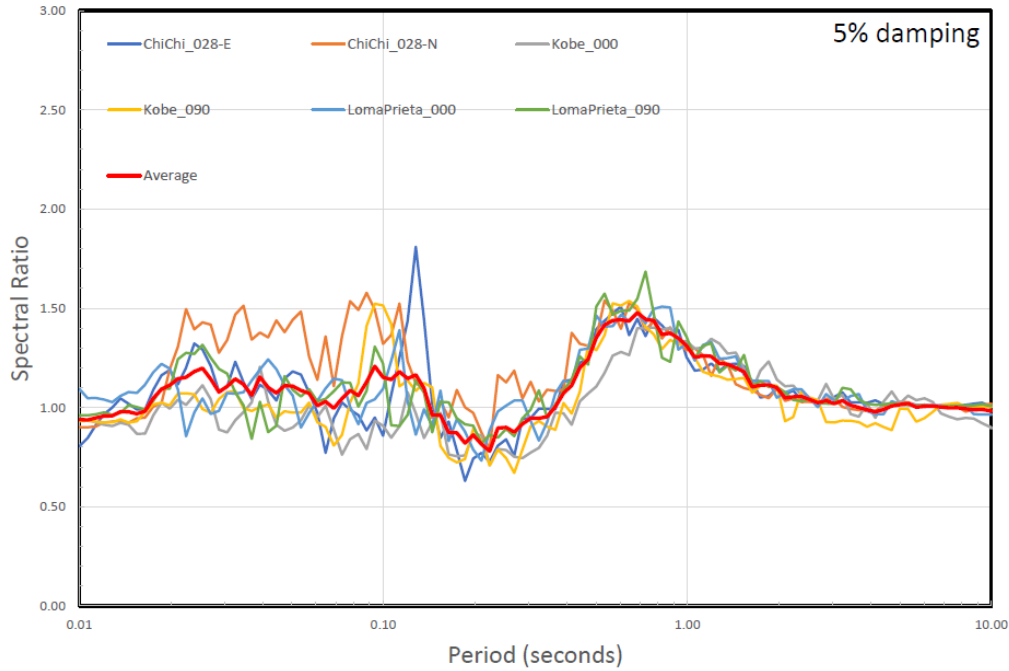
Notes
See previous figures for earthquake definitions

Figure 22. Site Spectral Amplifications Ratio Vs. Period at the Intake 3 Facility Site



Notes
See previous figures for earthquake definitions

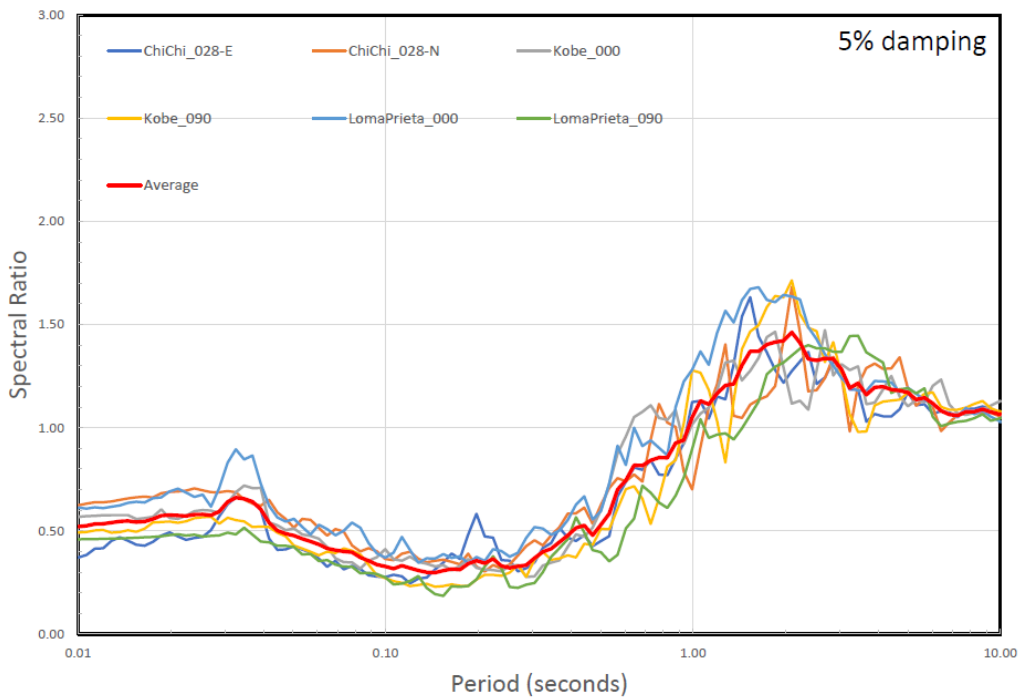
Figure 23. Site Spectral Amplifications Ratio Vs. Period at the Intake 5 Facility Site



Notes

See previous figures for earthquake definitions

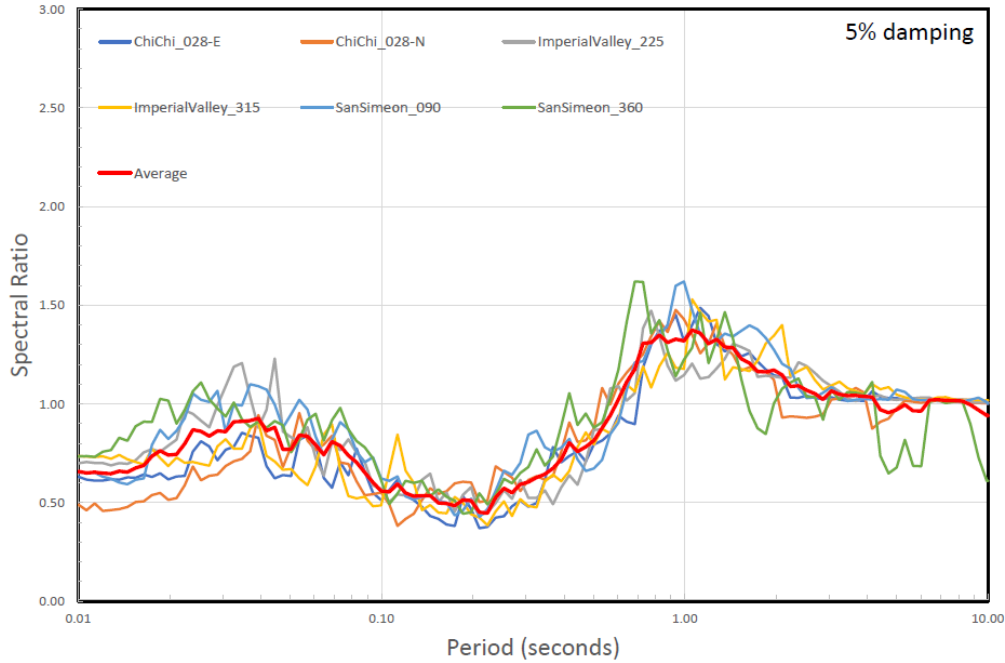
Figure 24. Site Spectral Amplification Vs. Period at the King Island Facility Site



Notes

See previous figures for earthquake definitions

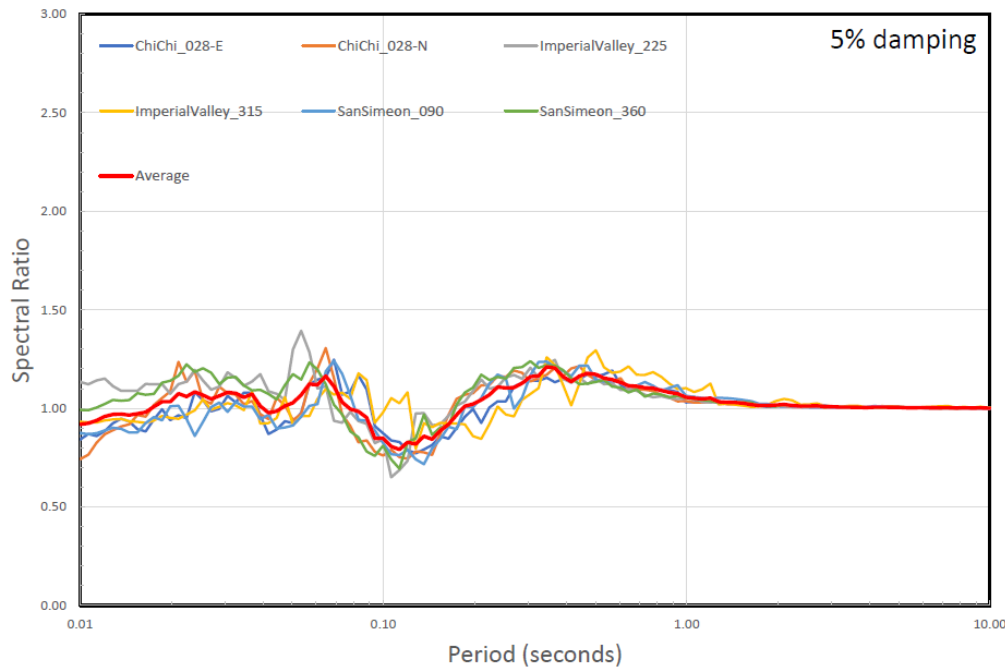
Figure 25. Site Spectral Amplifications Ratio Vs. Period at the Lower Roberts Island Facility Site



Notes

See previous figures for earthquake definitions

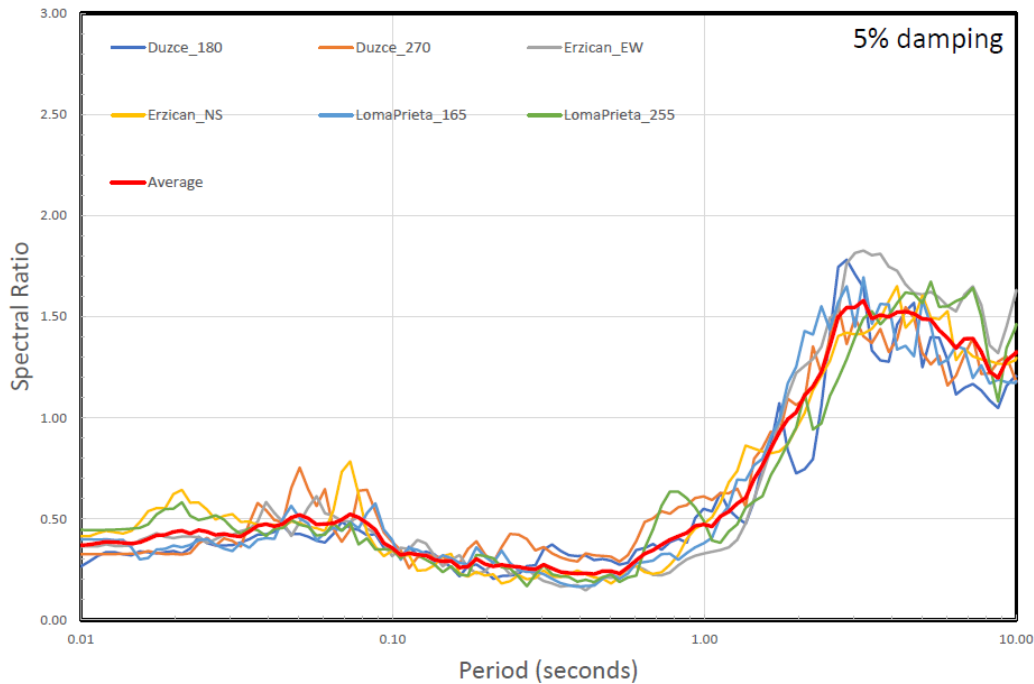
Figure 26. Site Spectral Amplifications Ratio Vs. Period at the New Hope Tract Facility Site



Notes

See previous figures for earthquake definitions

Figure 27. Site Spectral Amplifications Ratio Vs. Period at the Twin Cities Road Facility Site



Notes
See previous figures for earthquake definitions

Figure 28. Site Spectral Amplifications Ratio Vs. Period at the Union Island Facility Site

4. Recommended Ground Surface Peak Ground Accelerations for Liquefaction Analysis

Based on the results of 1-D site response analyses discussed above, the recommended ground surface PGA values for liquefaction potential assessments at the nine (9) facility sites are summarized in Table 12 below. These recommended PGA values are for the MDE/MCE ground motions. The table also compares the PGA values obtained from the current site response analysis (the recommended values) to the PGA values used in the previous liquefaction analysis (CER Appendix G2). It should be noted that the PGA values used in the previous liquefaction analysis were estimated using the published relationships for Delta levee site amplifications proposed by Kishida et al. (2009).

Table 12. Recommended Ground Surface Peak Ground Acceleration Values for Liquefaction Analysis

Facility	Seismic Design Basis (CER Appendix G1)	PGAs Used in Previous Analysis ^[a]	Recommended PGAs Obtained from 1-D Site Response Analysis
Bethany Pumping Plant	MCE	0.62	0.33
Canal Ranch Tract	MDE	0.35	0.34
Discharge Structure	MDE	N/A	N/A
Intake No 3	MDE	0.31	0.20
Intake No 5	MDE	0.31	0.29
King Island	MDE	0.35	0.27
Lower Roberts Island	MDE	0.50	0.20

Facility	Seismic Design Basis (CER Appendix G1)	PGAs Used in Previous Analysis ^[a]	Recommended PGAs Obtained from 1-D Site Response Analysis
New Hope Tract	MDE	0.34	0.23
Twin Cities Road	MDE	0.33	0.29
Union Island	MDE	0.52	0.20

^[a] As presented in CER Appendix G2.

Notes

MDE = Maximum Design Earthquake

MCE = Maximum Considered Earthquake, as defined in ASCE 7-16 and 2019 CBC

5. Summary

This Technical Memorandum presents the results of the conceptual design phase 1-D seismic site response analyses performed for nine (9) facility sites along the selected Project. The analyses were performed using available historic soil and groundwater data, and hence, the results and recommendations presented herein are subject to change when additional soil and groundwater data become available during future design phases of the Project.

The site response analyses were conducted for the MDE/MCE ground motions using the non-linear, total-stress, soil models. No analysis was performed for the OBE and temporary during-construction ground motions, as the current analysis is intended to support a feasibility/conceptual study, and MDE/MCE ground motions will likely be the controlling ground motions for liquefaction and the required mitigation.

The results of the site response analyses were used to refine the recommended PGA values, at the ground surface, used in liquefaction potential analyses at selected facility locations along the selected Bethany Reservoir Alignment. Reductions in PGA values of 3 to 61% from the values used in the previous liquefaction analysis were estimated.

6. References

Al Atik and Abrahamson, N. 2010. An Improved Method for Nonstationary Spectral Matching. *Earthquake Spectra*, Vol 26, p. 601-617.

California Department of Water Resources (DWR). 2019. Atlas GIS database of soil boring and CPT logs. Provided to DCA on July 26.

California Department of Water Resources (DWR). 2021. Online System for Well Completion Reports viewed through SGMA Data viewer. Data for Well Completion Reports 02N06W36_442595 and WCR1996-002369. Accessed March 22. <https://data.cnra.ca.gov/dataset/well-completion-reports>.

California Department of Water Resources (DWR). 2023. *Delta Conveyance Project Final Environmental Impact Report*. SCH# 2020010227. December 2023.

Delta Conveyance Design and Construction Authority (DCA). 2022a. Delta Conveyance Final Draft Engineering Project Report, Central and Eastern Options. May 2022.

Delta Conveyance Design and Construction Authority (DCA). 2022b. Delta Conveyance Final Draft Engineering Project Report. Bethany Reservoir Alternative. May 2022.

DEEPSOIL, Version 7.0. Nonlinear And Equivalent Linear Seismic Site Response of One-Dimensional Soil Columns. Department of Civil and Environmental Engineering, University of Illinois at Urbana-Champaign. November, 2020.

Kishida, T., R. Boulanger, N. Abrahamson, D. Driller, and T. Wehling. 2009. "Site Effects for the Sacramento-San Joaquin Delta." Earthquake Spectra. Vol. 25. No. 2. pp. 301–322. Earthquake Engineering Research Institute.

Phillips, C. and Hashash, Y.M. 2009. Damping Formulation for Nonlinear 1D Site Response Analyses. Soil Dynamics and Earthquake Engineering, 29(7), 1143-1158.

Attachment 1

Development of Conceptual Seismic Design Ground Motions at Reference Depths

Seismic Hazard Analyses and Development of Conceptual Seismic Design Ground Motions for the Delta Conveyance^[a]

Delta Conveyance Probabilistic and Deterministic Ground Motions for Bethany Alternative Sites

Delta Conveyance Probabilistic and Deterministic Ground Motions for Union Island Shaft

Notes:

^[a] This report was initially prepared by the Lettis Consultants International, Inc. in September 2021. At that time, the Central and Eastern Corridor were still being considered as options for the Project. Now that the selected Project was chosen to be the Bethany Reservoir Alignment, it should be noted that the term "Central Corridor" is no longer a part of the Project and the terms "Eastern Corridor" or "East Corridor" should be here on interpreted as part of the Bethany Reservoir Alignment only from Intake C-E-3 down to Lower Roberts Island Tunnel Launch Shaft.

Final Report, Rev. 2
Seismic Hazard Analyses and Development of Conceptual
Seismic Design Ground Motions for the Delta Conveyance



Prepared for:
Delta Conveyance Design and Construction Authority

Prepared by:
Ivan Wong, Patricia Thomas, Arash Zandieh,
Nora Lewandowski, Sarah Smith, and Jeff Unruh
Lettis Consultants International, Inc. (LCI)

1 September 2021

TABLE OF CONTENTS

1.0	INTRODUCTION	1
1.1	Scope of Work	1
1.2	Acknowledgements.....	1
2.0	SEISMIC SOURCE MODEL	2
2.1	MWD Model.....	2
2.2	Background Seismicity	6
3.0	SITE CHARACTERIZATION	8
4.0	SEISMIC HAZARD ANALYSES	9
4.1	PSHA.....	9
4.1.1	PSHA Methodology and Inputs.....	9
4.1.1.1	Seismic Source Model.....	9
4.1.1.2	Ground Motion Models	10
4.1.2	Results.....	11
4.2	DSHA.....	13
4.3	Design Response Spectra	13
5.0	DEVELOPMENT OF TIME HISTORIES	15
5.1	Approach to Spectral Matching	15
5.2	Spectrally-Matched Time Histories.....	16
6.0	REFERENCES	18

LIST OF TABLES

Table 1.	Locations and Site Conditions of Hazard Sites
Table 2.	Summary of Probabilistic Ground Motions
Table 3.	Seismic Source Contributions to PGA and 1.0 Sec Horizontal SA
Table 4.	Magnitude and Distance Deaggregation
Table 5.	Mean Uniform Hazard Spectra
Table 6.	DSHA Input Parameters
Table 7.	Controlling Deterministic Response Spectra
Table 8.	Maximum Design Earthquake (MDE) Spectra

Table 9. Operational Basis Earthquake (OBE) Spectra

Table 10. Properties of Time Histories

Table 11. Time Histories AI and Duration Targets

LIST OF FIGURES

Figure 1. Historical Seismicity in the Project Region 1781 to September 2019

Figure 2. Quaternary Faults in the San Francisco Bay Region

Figure 3. Active Faults in the Delta Region

Figure 4. Seismic Hazard Curves for Peak Horizontal Acceleration for Intake No. 3

Figure 5. Seismic Hazard Curves for 1.0 Sec Horizontal Spectral Acceleration for Intake No. 3

Figure 6. Seismic Hazard Curves for Peak Horizontal Acceleration for Intake No. 5

Figure 7. Seismic Hazard Curves for 1.0 Sec Horizontal Spectral Acceleration for Intake No. 5

Figure 8. Seismic Hazard Curves for Peak Horizontal Acceleration for Twin Cities

Figure 9. Seismic Hazard Curves for 1.0 Sec Horizontal Spectral Acceleration for Twin Cities

Figure 10. Seismic Hazard Curves for Peak Horizontal Acceleration for New Hope

Figure 11. Seismic Hazard Curves for 1.0 Sec Horizontal Spectral Acceleration for New Hope

Figure 12. Seismic Hazard Curves for Peak Horizontal Acceleration for Canal Ranch

Figure 13. Seismic Hazard Curves for 1.0 Sec Horizontal Spectral Acceleration for Canal Ranch

Figure 14. Seismic Hazard Curves for Peak Horizontal Acceleration for Bouldin

Figure 15. Seismic Hazard Curves for 1.0 Sec Horizontal Spectral Acceleration for Bouldin

Figure 16. Seismic Hazard Curves for Peak Horizontal Acceleration for King Island

Figure 17. Seismic Hazard Curves for 1.0 Sec Horizontal Spectral Acceleration for King Island

Figure 18. Seismic Hazard Curves for Peak Horizontal Acceleration for Lower Roberts

Figure 19. Seismic Hazard Curves for 1.0 Sec Horizontal Spectral Acceleration for Lower Roberts

Figure 20. Seismic Hazard Curves for Peak Horizontal Acceleration for Bacon

Figure 21. Seismic Hazard Curves for 1.0 Sec Horizontal Spectral Acceleration for Bacon

Figure 22. Seismic Hazard Curves for Peak Horizontal Acceleration for Southern Forebay North

Figure 23. Seismic Hazard Curves for 1.0 Sec Horizontal Spectral Acceleration for Southern Forebay North

Figure 24. Seismic Hazard Curves for Peak Horizontal Acceleration for Southern Forebay South

Figure 25. Seismic Hazard Curves for 1.0 Sec Horizontal Spectral Acceleration for Southern Forebay South

Figure 26. Seismic Hazard Curves for Peak Horizontal Acceleration for Jones Connection

Figure 27. Seismic Hazard Curves for 1.0 Sec Horizontal Spectral Acceleration for Jones Connection

Figure 28. Seismic Source Contributions for Mean Peak Horizontal Acceleration Hazard for Intake No. 3

Figure 29. Seismic Source Fractional Contributions for Mean Peak Horizontal Acceleration Hazard for Intake No. 3

Figure 30. Seismic Source Contributions for Mean Peak Horizontal Acceleration Hazard for Intake No. 5

Figure 31. Seismic Source Fractional Contributions for Mean Peak Horizontal Acceleration Hazard for Intake No. 5

Figure 32. Seismic Source Contributions for Mean Peak Horizontal Acceleration Hazard for Twin Cities

Figure 33. Seismic Source Fractional Contributions for Mean Peak Horizontal Acceleration Hazard for Twin Cities

Figure 34. Seismic Source Contributions for Mean Peak Horizontal Acceleration Hazard for New Hope

Figure 35. Seismic Source Fractional Contributions for Mean Peak Horizontal Acceleration Hazard for New Hope

Figure 36. Seismic Source Contributions for Mean Peak Horizontal Acceleration Hazard for Canal Ranch

Figure 37. Seismic Source Fractional Contributions for Mean Peak Horizontal Acceleration Hazard for Canal Ranch

Figure 38. Seismic Source Contributions for Mean Peak Horizontal Acceleration Hazard for Bouldin

Figure 39. Seismic Source Fractional Contributions for Mean Peak Horizontal Acceleration Hazard for Bouldin

Figure 40. Seismic Source Contributions for Mean Peak Horizontal Acceleration Hazard for King Island

Figure 41. Seismic Source Fractional Contributions for Mean Peak Horizontal Acceleration Hazard for King Island

Figure 42. Seismic Source Contributions for Mean Peak Horizontal Acceleration Hazard for Lower Roberts

Figure 43. Seismic Source Fractional Contributions for Mean Peak Horizontal Acceleration Hazard for Lower Roberts

Figure 44. Seismic Source Contributions for Mean Peak Horizontal Acceleration Hazard for Bacon

Figure 45. Seismic Source Fractional Contributions for Mean Peak Horizontal Acceleration Hazard for Bacon

Figure 46. Seismic Source Contributions for Mean Peak Horizontal Acceleration Hazard for Southern Forebay North

Figure 47. Seismic Source Fractional Contributions for Mean Peak Horizontal Acceleration Hazard for Southern Forebay North

Figure 48. Seismic Source Contributions for Mean Peak Horizontal Acceleration Hazard for Southern Forebay South

Figure 49. Seismic Source Fractional Contributions for Mean Peak Horizontal Acceleration Hazard for Southern Forebay South

Figure 50. Seismic Source Contributions for Mean Peak Horizontal Acceleration Hazard for Jones Connection

Figure 51. Seismic Source Fractional Contributions for Mean Peak Horizontal Acceleration Hazard for Jones Connection

Figure 52. Seismic Source Contributions for Mean 1.0 Sec Horizontal Spectral Acceleration Hazard for Intake No. 3

Figure 53. Seismic Source Fractional Contributions for Mean 1.0 Sec Horizontal Spectral Acceleration Hazard for Intake No. 3

Figure 54. Seismic Source Contributions for Mean 1.0 Sec Horizontal Spectral Acceleration Hazard for Intake No.5

Figure 55. Seismic Source Fractional Contributions for Mean 1.0 Sec Horizontal Spectral Acceleration Hazard for Intake No.5

Figure 56. Seismic Source Contributions for Mean 1.0 Sec Horizontal Spectral Acceleration Hazard for Twin Cities

Figure 57. Seismic Source Fractional Contributions for Mean 1.0 Sec Horizontal Spectral Acceleration Hazard for Twin Cities

Figure 58. Seismic Source Contributions for Mean 1.0 Sec Horizontal Spectral Acceleration Hazard for New Hope

Figure 59. Seismic Source Fractional Contributions for Mean 1.0 Sec Horizontal Spectral Acceleration Hazard for New Hope

Figure 60. Seismic Source Contributions for Mean 1.0 Sec Horizontal Spectral Acceleration Hazard for Canal Ranch

Figure 61. Seismic Source Fractional Contributions for Mean 1.0 Sec Horizontal Spectral Acceleration Hazard for Canal Ranch

Figure 62. Seismic Source Contributions for Mean 1.0 Sec Horizontal Spectral Acceleration Hazard for Bouldin

Figure 63. Seismic Source Fractional Contributions for Mean 1.0 Sec Horizontal Spectral Acceleration Hazard for Bouldin

Figure 64. Seismic Source Contributions for Mean 1.0 Sec Horizontal Spectral Acceleration Hazard for King Island

Figure 65. Seismic Source Fractional Contributions for Mean 1.0 Sec Horizontal Spectral Acceleration Hazard for King Island

Figure 66. Seismic Source Contributions for Mean 1.0 Sec Horizontal Spectral Acceleration Hazard for Lower Roberts

Figure 67. Seismic Source Fractional Contributions for Mean 1.0 Sec Horizontal Spectral Acceleration Hazard for Lower Roberts

Figure 68. Seismic Source Contributions for Mean 1.0 Sec Horizontal Spectral Acceleration Hazard for Bacon

Figure 69. Seismic Source Fractional Contributions for Mean 1.0 Sec Horizontal Spectral Acceleration Hazard for Bacon

Figure 70. Seismic Source Contributions for Mean 1.0 Sec Horizontal Spectral Acceleration Hazard for Southern Forebay North

Figure 71. Seismic Source Fractional Contributions for Mean 1.0 Sec Horizontal Spectral Acceleration Hazard for Southern Forebay North

Figure 72. Seismic Source Contributions for Mean 1.0 Sec Horizontal Spectral Acceleration Hazard for Southern Forebay South

Figure 73. Seismic Source Fractional Contributions for Mean 1.0 Sec Horizontal Spectral Acceleration Hazard for Southern Forebay South

Figure 74. Seismic Source Contributions for Mean 1.0 Sec Horizontal Spectral Acceleration Hazard for Jones Connection

Figure 75. Seismic Source Fractional Contributions for Mean 1.0 Sec Horizontal Spectral Acceleration Hazard for Jones Connection

Figure 76. Magnitude and Distance Contributions to the Mean Peak Horizontal Hazard at 475 and 2,475-Year Return Periods for Intake No. 3

Figure 77. Magnitude and Distance Contributions to the Mean Peak Horizontal Hazard at 475 and 2,475-Year Return Periods for Intake No.5

Figure 78. Magnitude and Distance Contributions to the Mean Peak Horizontal Hazard at 475 and 2,475-Year Return Periods for Twin Cities

Figure 79. Magnitude and Distance Contributions to the Mean Peak Horizontal Hazard at 475 and 2,475-Year Return Periods for New Hope

Figure 80. Magnitude and Distance Contributions to the Mean Peak Horizontal Hazard at 475 and 2,475-Year Return Periods for Canal Ranch

Figure 81. Magnitude and Distance Contributions to the Mean Peak Horizontal Hazard at 475 and 2,475-Year Return Periods for Bouldin

Figure 82. Magnitude and Distance Contributions to the Mean Peak Horizontal Hazard at 475 and 2,475-Year Return Periods for King Island

Figure 83. Magnitude and Distance Contributions to the Mean Peak Horizontal Hazard at 475 and 2,475-Year Return Periods for Lower Roberts

Figure 84. Magnitude and Distance Contributions to the Mean Peak Horizontal Hazard at 475 and 2,475-Year Return Periods for Bacon

Figure 85. Magnitude and Distance Contributions to the Mean Peak Horizontal Hazard at 475 and 2,475-Year Return Periods for Southern Forebay North

Figure 86. Magnitude and Distance Contributions to the Mean Peak Horizontal Hazard at 475 and 2,475-Year Return Periods for Southern Forebay South

Figure 87. Magnitude and Distance Contributions to the Mean Peak Horizontal Hazard at 475 and 2,475-Year Return Periods for Jones Connection

Figure 88. Magnitude and Distance Contributions to the Mean 1.0 Sec Spectral Hazard at 475 and 2,475-Year Return Periods for Intake No. 3

Figure 89. Magnitude and Distance Contributions to the Mean 1.0 Sec Spectral Hazard at 475 and 2,475-Year Return Periods for Intake No.5

Figure 90. Magnitude and Distance Contributions to the Mean 1.0 Sec Spectral Hazard at 475 and 2,475-Year Return Periods for Twin Cities

Figure 91. Magnitude and Distance Contributions to the Mean 1.0 Sec Spectral Hazard at 475 and 2,475-Year Return Periods for New Hope

Figure 92. Magnitude and Distance Contributions to the Mean 1.0 Sec Spectral Hazard at 475 and 2,475-Year Return Periods for Canal Ranch

Figure 93. Magnitude and Distance Contributions to the Mean 1.0 Sec Spectral Hazard at 475 and 2,475-Year Return Periods for Bouldin

Figure 94. Magnitude and Distance Contributions to the Mean 1.0 Sec Spectral Hazard at 475 and 2,475-Year Return Periods for King Island

Figure 95. Magnitude and Distance Contributions to the Mean 1.0 Sec Spectral Hazard at 475 and 2,475-Year Return Periods for Lower Roberts

Figure 96. Magnitude and Distance Contributions to the Mean 1.0 Sec Spectral Hazard at 475 and 2,475-Year Return Periods for Bacon

Figure 97. Magnitude and Distance Contributions to the Mean 1.0 Sec Spectral Hazard at 475 and 2,475-Year Return Periods for Southern Forebay North

Figure 98. Magnitude and Distance Contributions to the Mean 1.0 Sec Spectral Hazard at 475 and 2,475-Year Return Periods for Southern Forebay South

Figure 99. Magnitude and Distance Contributions to the Mean 1.0 Sec Spectral Hazard at 475 and 2,475-Year Return Periods for Jones Connection

Figure 100. Mean Uniform Hazard Spectra at 144-Year Return Period

Figure 101. Mean Uniform Hazard Spectra at 200-Year Return Period

Figure 102. Mean Uniform Hazard Spectra at 475-Year Return Period

Figure 103. Mean Uniform Hazard Spectra at 975-Year Return Period

Figure 104. Mean Uniform Hazard Spectra at 2,475-Year Return Period

Figure 105. 84th Percentile Deterministic Spectra for Intake No. 3

Figure 106. Comparison of UHS and Enveloped Deterministic Spectra for Intake No. 3

Figure 107. 84th Percentile Deterministic Spectra for Intake No.5

Figure 108. Comparison of UHS and Enveloped Deterministic Spectra for Intake No.5

Figure 109. 84th Percentile Deterministic Spectra for Twin Cities

Figure 110. Comparison of UHS and Enveloped Deterministic Spectra for Twin Cities

Figure 111. 84th Percentile Deterministic Spectra for New Hope

Figure 112. Comparison of UHS and Enveloped Deterministic Spectra for New Hope

Figure 113. 84th Percentile Deterministic Spectra for Canal Ranch

Figure 114. Comparison of UHS and Enveloped Deterministic Spectra for Canal Ranch

- Figure 115. 84th Percentile Deterministic Spectra for Bouldin
- Figure 116. Comparison of UHS and Enveloped Deterministic Spectra for Bouldin
- Figure 117. 84th Percentile Deterministic Spectra for King Island
- Figure 118. Comparison of UHS and Enveloped Deterministic Spectra for King Island
- Figure 119. 84th Percentile Deterministic Spectra for Lower Roberts
- Figure 120. Comparison of UHS and Enveloped Deterministic Spectra for Lower Roberts
- Figure 121. 84th Percentile Deterministic Spectra for Bacon
- Figure 122. Comparison of UHS and Enveloped Deterministic Spectra for Bacon
- Figure 123. 84th Percentile Deterministic Spectra for Southern Forebay North
- Figure 124. Comparison of UHS and Enveloped Deterministic Spectra for Southern Forebay North
- Figure 125. 84th Percentile Deterministic Spectra for Southern Forebay South
- Figure 126. Comparison of UHS and Enveloped Deterministic Spectra for Southern Forebay South
- Figure 127. 84th Percentile Deterministic Spectra for Jones Connection
- Figure 128. Comparison of UHS and Enveloped Deterministic Spectra for Jones Connection
- Figure 129. MDE Response Spectrum for Intake No. 3
- Figure 130. MDE Response Spectrum for Intake No. 5
- Figure 131. MDE Response Spectrum for Twin Cities
- Figure 132. MDE Response Spectra for New Hope
- Figure 133. MDE Response Spectra for Canal Ranch
- Figure 134. MDE Response Spectrum for Bouldin
- Figure 135. MDE Response Spectra for King Island
- Figure 136. MDE Response Spectrum for Lower Roberts
- Figure 137. MDE Response Spectra for Bacon
- Figure 138. MDE Response Spectrum for Southern Forebay North
- Figure 139. MDE Response Spectra for Southern Forebay South
- Figure 140. MDE Response Spectra for Jones Connection
- Figure 141. Response Spectra for MDE Time Histories for Intake No. 3, RSN 68
- Figure 142. Spectral Matches for MDE Time Histories for Intake No. 3, RSN 68
- Figure 143. Time History Spectrally-Matched to MDE for Intake No. 3, RSN 68 (H1)
- Figure 144. Time History Spectrally-Matched to MDE for Intake No. 3, RSN 68 (H2)
- Figure 145. Response Spectra for MDE Time Histories for Intake No. 3, RSN 162

- Figure 146. Spectral Matches for MDE Time Histories for Intake No. 3, RSN 162
- Figure 147. Time History Spectrally-Matched to MDE for Intake No. 3, RSN 162 (H1)
- Figure 148. Time History Spectrally-Matched to MDE for Intake No. 3, RSN 162 (H2)
- Figure 149. Response Spectra for MDE Time Histories for Intake No. 3, RSN 1074
- Figure 150. Spectral Matches for MDE Time Histories for Intake No. 3, RSN 1074
- Figure 151. Time History Spectrally-Matched to MDE for Intake No. 3, RSN 1074 (H1)
- Figure 152. Time History Spectrally-Matched to MDE for Intake No. 3, RSN 1074 (H2)
- Figure 153. Response Spectra for MDE Time Histories for Intake No. 5, RSN 68
- Figure 154. Spectral Matches for MDE Time Histories for Intake No. 5, RSN 68
- Figure 155. Time History Spectrally-Matched to MDE for Intake No. 5, RSN 68 (H1)
- Figure 156. Time History Spectrally-Matched to MDE for Intake No. 5, RSN 68 (H2)
- Figure 157. Response Spectra for MDE Time Histories for Intake No. 5, RSN 162
- Figure 158. Spectral Matches for MDE Time Histories for Intake No. 5, RSN 162
- Figure 159. Time History Spectrally-Matched to MDE for Intake No. 5, RSN 162 (H1)
- Figure 160. Time History Spectrally-Matched to MDE for Intake No. 5, RSN 162 (H2)
- Figure 161. Response Spectra for MDE Time Histories for Intake No. 5, RSN 1074
- Figure 162. Spectral Matches for MDE Time Histories for Intake No. 5, RSN 1074
- Figure 163. Time History Spectrally-Matched to MDE for Intake No. 5, RSN 1074 (H1)
- Figure 164. Time History Spectrally-Matched to MDE for Intake No. 5, RSN 1074 (H2)
- Figure 165. Response Spectra for MDE Time Histories for Bouldin, RSN 68
- Figure 166. Spectral Matches for MDE Time Histories for Bouldin, RSN 68
- Figure 167. Time History Spectrally-Matched to MDE for Bouldin, RSN 68 (H1)
- Figure 168. Time History Spectrally-Matched to MDE for Bouldin, RSN 68 (H2)
- Figure 169. Response Spectra for MDE Time Histories for Bouldin, RSN 174
- Figure 170. Spectral Matches for MDE Time Histories for Bouldin, RSN 174
- Figure 171. Time History Spectrally-Matched to MDE for Bouldin, RSN 174 (H1)
- Figure 172. Time History Spectrally-Matched to MDE for Bouldin, RSN 174 (H2)
- Figure 173. Response Spectra for MDE Time Histories for Bouldin, RSN 4031
- Figure 174. Spectral Matches for MDE Time Histories for Bouldin, RSN 4031
- Figure 175. Time History Spectrally-Matched to MDE for Bouldin, RSN 4031 (H1)
- Figure 176. Time History Spectrally-Matched to MDE for Bouldin, RSN 4031 (H2)

- Figure 177. Response Spectra for MDE Time Histories for Twin Cities, RSN 187
- Figure 178. Spectral Matches for MDE Time Histories for Twin Cities, RSN 187
- Figure 179. Time History Spectrally-Matched to MDE for Twin Cities, RSN 187 (H1)
- Figure 180. Time History Spectrally-Matched to MDE for Twin Cities, RSN 187 (H2)
- Figure 181. Response Spectra for MDE Time Histories for Twin Cities, RSN 1277
- Figure 182. Spectral Matches for MDE Time Histories for Twin Cities, RSN 1277
- Figure 183. Time History Spectrally-Matched to MDE for Twin Cities, RSN 1277 (H1)
- Figure 184. Time History Spectrally-Matched to MDE for Twin Cities, RSN 1277 (H2)
- Figure 185. Response Spectra for MDE Time Histories for Twin Cities, RSN 4009
- Figure 186. Spectral Matches for MDE Time Histories for Twin Cities, RSN 4009
- Figure 187. Time History Spectrally-Matched to MDE for Twin Cities, RSN 4009 (H1)
- Figure 188. Time History Spectrally-Matched to MDE for Twin Cities, RSN 4009 (H2)
- Figure 189. Response Spectra for MDE Time Histories for Lower Roberts, RSN 812
- Figure 190. Spectral Matches for MDE Time Histories for Lower Roberts, RSN 812
- Figure 191. Time History Spectrally-Matched to MDE for Lower Roberts, RSN 812 (H1)
- Figure 192. Time History Spectrally-Matched to MDE for Lower Roberts, RSN 812 (H2)
- Figure 193. Response Spectra for MDE Time Histories for Lower Roberts, RSN 1101
- Figure 194. Spectral Matches for MDE Time Histories for Lower Roberts, RSN 1101
- Figure 195. Time History Spectrally-Matched to MDE for Lower Roberts, RSN 1101 (H1)
- Figure 196. Time History Spectrally-Matched to MDE for Lower Roberts, RSN 1101 (H2)
- Figure 197. Response Spectra for MDE Time Histories for Lower Roberts, RSN 1277
- Figure 198. Spectral Matches for MDE Time Histories for Lower Roberts, RSN 1277
- Figure 199. Time History Spectrally-Matched to MDE for Lower Roberts, RSN 1277 (H1)
- Figure 200. Time History Spectrally-Matched to MDE for Lower Roberts, RSN 1277(H2)
- Figure 201. Response Spectra for MDE Time Histories for Southern Forebay North, RSN 778
- Figure 202. Spectral Matches for MDE Time Histories for Southern Forebay North, RSN 778
- Figure 203. Time History Spectrally-Matched to MDE for Southern Forebay North, RSN 778 (H1)
- Figure 204. Time History Spectrally-Matched to MDE for Southern Forebay North, RSN 778 (H2)
- Figure 205. Response Spectra for MDE Time Histories for Southern Forebay North, RSN 821
- Figure 206. Spectral Matches for MDE Time Histories for Southern Forebay North, RSN 821
- Figure 207. Time History Spectrally-Matched to MDE for Southern Forebay North, RSN 821 (H1)

Figure 208. Time History Spectrally-Matched to MDE for Southern Forebay North, RSN 821 (H2)

Figure 209. Response Spectra for MDE Time Histories for Southern Forebay North, RSN 1605

Figure 210. Spectral Matches for MDE Time Histories for Southern Forebay North, RSN 1605

Figure 211. Time History Spectrally-Matched to MDE for Southern Forebay North, RSN 1605 (H1)

Figure 212. Time History Spectrally-Matched to MDE for Southern Forebay North, RSN 4031 (H2)

1.0 Introduction

The Sacramento-San Joaquin Delta is particularly susceptible to damage in a large earthquake due to the vulnerability of the levees which protect cities, farms, and infrastructure. The Delta is located adjacent to the seismically-active San Andreas fault system and is also subject to strong ground shaking from numerous other seismic sources in central California (Figures 1 and 2). At the request of the Delta Conveyance and Construction Office (DCA), site-specific seismic hazard analyses have been performed at 12 sites along two proposed alignments of the Delta Conveyance Project (Table 1; Figure 3). Conceptual seismic design ground motions including acceleration response spectra and time histories were developed in accordance with the draft guidance *Conceptual-Level Seismic Design and Geohazard Evaluation Criteria* prepared for DCA (2021). This included the Maximum Design Earthquake (MDE) and Operational Basis Earthquake (OBE) ground motions for specific structures and facilities at selected sites. Note Figures 1 and 2 also show a third alternative alignment called the Bethany alignment. The conceptual seismic design ground motions for the Bethany Reservoir shaft, Union Island shaft, and pumping plant are reported in a memorandum dated 1 September 2021 by Thomas *et al.* (2021) and for the Union Island shaft (expanded results) in a memorandum also dated 1 September 2021 by Thomas and Wong (2021).

Both probabilistic seismic hazard analyses (PSHA) and deterministic seismic hazard analyses (DSHA) were performed for the 12 sites. This study leverages off an earlier seismic hazard evaluation for Metropolitan Water District's (MWD) Emergency Freshwater Pathway also located in the Delta (Wong *et al.*, 2021).

1.1 Scope of Work

In this study, we evaluated the seismic hazards along two proposed alignments of the Delta Conveyance and developed conceptual seismic design ground motions (Figure 3). Both probabilistic and deterministic ground motion estimates were made for the 12 sites along the two alignments at the top of the soil below any existing peat, muck, and basin deposits. This datum corresponded with the top of either the Modesto or Riverbank Formations as shown in Table 1. The PSHA was performed using a logic tree approach to address the epistemic uncertainties in input parameters and models. An updated seismic source model used in the MWD study and originally developed as part of DWR's Delta Risk Management Strategy (DRMS) Project and the Next Generation of Attenuation (NGA)-West2 ground motion models (GMMs) were used in the hazard analyses. A DSHA was also performed considering the most significant deterministic seismic sources to the alignments.

1.2 Acknowledgements

This study was sponsored by DCA. Our thanks to Andrew Finney and Dario Rosidi for project support and to Lanka Ilankatharan for his review of this report. Our appreciation to Claire Unruh and Whitney Newcomb for assistance in the preparation of this report.

2.0 Seismic Source Model

In this section, the seismic source model used in these analyses was adapted from the MWD Emergency Freshwater Pathway Project (Wong *et al.*, 2021) as described below. The approach to characterizing the background seismicity also implemented for the MWD Project is also discussed.

2.1 MWD Seismic Source Model

The MWD seismic source model is an updated version of the source model used in the DRMS study (URS/Benjamin & Associates, 2008). As described in URS/Benjamin & Associates (2008), the DRMS PSHA incorporated fault-source characterizations developed by the USGS Working Group on Northern California Earthquake Potential (WGNCEP, 1996), the USGS Working Group on California Earthquake Probabilities (WGCEP, 2003) and the California Geological Survey's seismic source model used in the USGS National Hazard Maps (Cao *et al.*, 2003). The majority of these fault sources are relatively well-studied faults in the greater San Francisco Bay region. The characterizations of the fault sources were updated as appropriate for the DRMS study to reflect then-current research. The DRMS model also incorporated new characterizations of potential seismic sources in the Delta and along the western margin of the Central Valley (URS/Benjamin & Associates, 2008).

Since completion of the DRMS study in the late 2000's, a new comprehensive statewide seismic hazard evaluation (UCERF3; Field *et al.*, 2013) has been performed that uses an updated seismic source model and new analytical approaches. In addition to revising the geometries and activity rates of major faults in the San Francisco Bay region, the UCERF3 analysis allows for greater linkage of faults during modeled ruptures than was considered for DRMS and previous statewide seismic hazard models, and thus incorporates the possibility of very large, infrequent, multi-segment fault ruptures in the hazard evaluation.

The seismic source model for the current investigation includes the fault sources used in the PSHA for the DRMS study. As appropriate, the geometry of some of the fault sources, and other parameters such as seismogenic crustal thickness and slip rate, have been modified from the DRMS model to incorporate new data and interpretations, some of which are included in the UCERF3 source model (Field *et al.*, 2013). In the DRMS study, time-dependent recurrence for the major faults of the San Andreas fault system taken from WGCEP (2003) was included. In this study, the Bay Area faults were treated in a time-independent manner. Significant local fault sources are summarized below. The following discussion is adopted from Wong *et al.* (2021).

West Tracy Fault The West Tracy fault is a northwest-striking, southwest-dipping blind reverse or reverse-oblique fault along the southwestern margin of the Delta region that was originally identified during exploration for natural gas (Sterling, 1992). The trace of the fault passes beneath the southwestern part of Clifton Court Forebay (Sterling, 1992; Unruh and Krug, 2007; Fugro Consultants, 2011; Figures 2 and 3). The DRMS source model assigned a range of weighted slip rates from 0.07 to 0.5 mm/yr to the West Tracy fault (weighted average 0.27 mm/yr), and earthquake magnitudes of $M 6.5 \pm 0.25$ (see Table 1 in URS/Benjamin & Associates, 2008).

Geologic investigations and research conducted since the DRMS study have developed additional data in support of late Quaternary activity of the West Tracy fault, and have revised the long-term average dip-slip rate to about 0.3 ± 0.1 mm/yr (Unruh and Hitchcock, 2015). For this study, we adopt a range of slip rate values between 0.2 to 0.6 mm/yr (weighted average 0.4 mm/yr) to encompass uncertainty in the timing of deformation and the potential for a component of strike-slip displacement on the fault.

Analysis of LiDAR and remote sensing data suggest that the fault may branch into two splays northwest of Clifton Court Forebay (Unruh and Hitchcock, 2015); the revised fault trace for this PSHA includes two options for the northern termination of the fault to model this geometry (Figure 3). The range of modeled earthquake magnitudes was also revised to **M** 6.25 to 6.75 to reflect current interpretations of the fault dip and crustal thickness in this region.

Midland Fault The Midland fault is an approximately north- to northwest-striking blind reverse or reverse-oblique fault that borders the western margin of the central Delta region, and dips west and southwest beneath the Montezuma Hills north of the Sacramento River at the latitude of Rio Vista (Figures 2 and 3). The southern end of the fault is located near the town of Byron in the southwestern Delta. Although some studies show the Midland fault extending over 100 km north into the southwestern Sacramento Valley (e.g., Jennings *et al.*, 2010), experts in the oil and gas industry interpret the northern termination of the fault at about the latitude of the northern Montezuma Hills (DOGGR, 1982; Krug *et al.*, 1992).

Based on subsurface mapping of the Midland fault for oil and gas exploration, the southern 27 km reach of the fault is characterized as a single fault trace or narrow, discrete fault zone (DOGGR, 1982). At about the latitude of the southern Montezuma Hills, the fault is interpreted to branch into multiple splays, and in the vicinity of Lindsay Slough the main trace of the fault steps or bends sharply to the west and assumes a more northwesterly strike (DOGGR, 1982). Krug *et al.*, (1992) interpreted the northern Midland fault to break up into a series of right-stepping *en echelon* splays.

Based on these south-to-north variations in the subsurface geometry, the DRMS study modeled the southern 27 km of the Midland fault as a discrete fault source (i.e., the “Southern Midland fault”). The less well-documented right-stepping northern splays of the Midland fault (as interpreted by Krug *et al.*, 1992) were captured in an areal source zone (“Northern Midland fault zone”), which was extended north to the latitude of the towns of Davis and Winters to capture buried faults associated with numerous gas fields between the Delta and southwestern Sacramento Valley. The DRMS model assumed similar activity rates for the Southern Midland fault and structures in the Northern Midland areal zone, and assigned a range of weighted slip rates from 0.1 to 1.0 mm/yr to both sources (weighted average 0.5 mm/yr; URS/Benjamin & Associates, 2008).

New work on the Midland fault since the DRMS study has developed the following data and observations:

- 1) A detailed subsurface trace of the Midland fault, compiled from analysis of individual gas field maps published by DOGGR (1982), documents that the northwest-striking, southwest-dipping fault terminates northward in the vicinity of Lindsay Slough bordering the northern Montezuma hills. Total length of the fault is approximately 62 km (Table 2-1).

- 2) The long-term average slip rate on the southern part of the Midland fault has been revised in light of new information on uplift and folding of the basal Miocene unconformity in the hanging wall of the fault (Unruh *et al.*, 2016). For a range of dip values from 45° to 75°, Unruh *et al.* (2016) estimated that the long-term average reverse slip rate on the southern reach of the Midland fault ranges between 0.03 to 0.13 mm/yr. We adopt a broader range in weighted slip rates for this current study (0.02 to 0.2 mm/yr; weighted average 0.08 mm/yr) to incorporate additional uncertainty in the timing of deformation, and to account for the possibility that there is a component of lateral (strike-slip) motion on the fault that is not recorded in the vertical separation documented by Unruh *et al.* (2016).
- 3) Buried fault structures associated with gas fields north of Lindsay Slough typically dip northeast (DOGGR, 1982), opposite the southwest dip direction of the northern part of the Midland fault, and thus they are not likely to be a simple northern continuation of the Midland fault as assumed in the DRMS definition of the Northern Midland fault areal source zone.
- 4) Late Cenozoic activity of the southern reach the Midland fault is associated with uplift of the Montezuma Hills (Unruh *et al.*, 2016), which is a prominent Quaternary landform along the central-western margin of the Delta with maximum summit elevations of about 75 m above the surrounding lowlands. No comparable landforms are associated with the northern part of the Midland fault or other buried faults beneath gas fields north of the Montezuma hills. If neotectonic topography can be considered a first-order proxy for slip rate, then the slip rates of faults in the Northern Midland fault areal zone are significantly lower than that of the southern part of the Midland fault.

Based on these observations, the DRMS characterization of the Midland fault was updated. The trace of the Midland fault is revised to extend approximately from Byron to the vicinity of Lindsay Slough, for a total length of about 62 km (Figures 2 and 3). The revised trace of the Midland fault includes the 27-km-long “Southern Midland fault” in the DRMS model, as well as the more complex northern splays of the fault previously incorporated in the southern part of the “Northern Midland” areal zone. Empirical relations between earthquake magnitude and source dimensions suggest that rupture of the entire 62-km length of the Midland fault could produce a **M** 7.1 event. Although we cannot preclude this as a possibility, we believe that the pattern of late Cenozoic uplift along the fault as reflected in topography of the Montezuma Hills is not consistent with frequent ruptures of the entire subsurface fault trace. Specifically, the maximum topographic uplift of the hills, as well as maximum structural relief on the basal Miocene unconformity (Unruh *et al.*, 2016), is associated with the southern part of the Midland fault, and the topographic and structural relief of the hills both decrease northward, which implies a south-to-north gradient in slip rate if movement on the Midland fault is primarily responsible for uplift of the Montezuma Hills. Consequently, we have developed two alternative rupture models for the Midland fault:

- (1) Full 62 km rupture of the fault in **M** 7.1 events. We assigned a low weight (0.05) to this model; and
- (2) Floating ruptures of **M** 6.5 ± 0.25 along the entire 62 km length of the fault, but with a higher cumulative slip rate on the southern 31 km of the fault so that larger events are modeled to occur more frequently there (the northern 31 km is modeled to have 50% of the slip rate of the southern 31 km). This

model (weight 0.95) captures key elements of the DRMS characterization, is consistent with observations indicating that greater late Cenozoic uplift has occurred on the southern part of the fault, and also allows for infrequent larger events to occur north of the “Southern Midland fault” to reflect detailed information on the subsurface fault trace (DOGGR, 1982).

Based on the compilation of DOGGR (1982) gas field data, as well as the absence of neotectonic topography at gas fields in the Delta region north of the Montezuma Hills, we conclude that there is no compelling justification for distinguishing the “Northern Midland zone” as a discrete areal source. We thus have eliminated the Northern Midland areal zone for this study and now assign this area to the general background source zone.

In this study, the seismic source model includes a scenario in which the West Tracy fault and Midland fault rupture together in a single earthquake. This scenario is consistent with assumptions of the statewide UCERF3 model that allow for infrequent large earthquakes to rupture multiple faults in a single event. Although the West Tracy and Midland faults both are part of the Coast Range Sierra Boundary zone (CRSBZ) of Wong and Ely (1983) and Wong *et al.* (1988), and the northern end of the West Tracy fault is nearly coincident with the southern end of the Midland fault, the two faults have distinctly different strikes and possibly different slip rates (Unruh *et al.*, 2016; Unruh and Hitchcock, 2015), which suggests there may be significant behavioral differences between them that mitigate against a joint rupture.

At present there is very little data bearing on the timing, magnitude and frequency of earthquakes on the West Tracy and Midland faults to provide a robust assessment of the likelihood of a combined rupture. Unruh and Hitchcock (2015) interpreted geomorphic and borehole data from the northern end of the West Tracy fault between Clifton Court forebay and Byron as evidence for either two late Quaternary events, including one in the Holocene, that produced about 1.5 m of vertical separation during each event; or a single 3 m late Quaternary event. A 1.5 m displacement is consistent at the upper bound for full rupture of the 30-km-long West Tracy fault, whereas a single 3 m event is better explained by an earthquake that ruptured both the West Tracy fault and at least part of the Midland fault. Data constraining slip per event on the Southern Midland fault are very uncertain, but variations in the thickness of Holocene peat, and variations in the elevation of the base of peat across the fault, can be questionably interpreted to document 1 to 4 m of displacement in the Holocene (Unruh *et al.*, 2016). If the interpreted displacement occurred in a single event, and if it produced up to 4 m of vertical separation on the base of the peat, then the earthquake probably ruptured more than the 30 km length of the Southern Midland fault, thus possibly included part or all of the West Tracy fault.

To summarize, although available information is permissive of a combined rupture on the two faults, we note that the data are very uncertain, and we judge the likelihood of a combined rupture to be low given the different geometries of the faults and their likely different slip rates. We thus assign a weight of 0.2 to the combined rupture scenario in the seismic source model. Additional data on the magnitude and timing of events on both the West Tracy and Midland faults are required to rigorously evaluate the combined rupture hypothesis.

Montezuma Hills Source Zone The DRMS study defined an areal source zone west of the Midland fault to encompass the possibility that potentially seismogenic blind faults are present and responsible for uplift and northeast tilting of the surface of the Montezuma Hills during the Quaternary (Figure 3). Given the uncertainty about the origin of the hills, the DRMS source model assigned a $P(a) 0.5$ to the possibility that presently unknown seismogenic faults, independent of the Midland fault, are present beneath the Montezuma Hills. The DRMS model adopted a range of slip rates from 0.05 to 0.5 mm/yr (weighted average 0.27 mm/yr) for the Montezuma Hills source zone, with the assumption that the activity rate of faults beneath the hills is likely to be similar to the Midland fault. For this study, we have revised the range of slip rates for the Montezuma Hills source zone downward to be the same as the revised rates for the Midland fault (0.02 to 0.2 mm/yr; weighted average 0.08 mm/yr).

The DRMS model assumed that the preferred orientations of potentially seismogenic faults beneath the Montezuma hills strike approximately north-south, sub-parallel to the southern part of the Midland fault. Exploration for oil and gas has documented that the Montezuma Hills are underlain by a system of early Tertiary west-northwest-east-southeast-striking normal faults (Krug *et al.*, 1992). Consequently, we have revised the preferred orientation of potential fault sources beneath the hills for this study to be sub-parallel to the buried structural fabric.

Thornton Arch Source Zone The DRMS study defined an areal zone in the northwestern Delta region to encompass the possibility that a buried structure associated with the Thornton and West Thornton gas fields may be a potential seismic source. The motivation for assuming that an active fault may be present is the observation that the Mokelumne River does not continue along a straight course across the Delta from the point where it exits the western Sierran foothills, but rather it appears to be deflected to the north in an anomalous loop north and west of the town of Thornton, approximately around the gas fields (URS/JBA, 2008). The DRMS study assigned a low probability of activity ($P[a]$ of 0.2) to the Thornton Arch areal source, and it adopted a range of maximum magnitudes with a weighted mean of **M** 6.25. No new information bearing on the seismic potential of the Thornton Arch zone has been published since DRMS, and we did not update or re-evaluate this source for the MWD study.

2.2 Background Seismicity

The background seismicity rates were updated for MWD. To account for the hazard from background (floating or random) earthquakes that are not associated with known or mapped faults, regional seismic source zones are used in the PSHA. In most of the western U.S., the maximum magnitude of earthquakes not associated with known faults usually ranges from **M** 6 to 6.5. Repeated events larger than these magnitudes generally produce recognizable fault-or-fold related features at the earth's surface (e.g., dePolo, 1994). Examples of background earthquakes are the 1986 **M** 5.7 Mt. Lewis and 31 October 2007 **M** 5.4 Alum Rock earthquakes, both of which occurred east of San Jose and resulted in no discernable surface rupture.

Background earthquakes occur on crustal faults that exhibit no surficial expression (buried faults) or are unmapped due to inadequate studies. In this study, we model the hazard from background earthquakes through two seismic source zones, the Coast Ranges Zone and the Central Valley Zone (Figure 1). The two

seismic source zones are delineated based on similar seismotectonic characteristics such as style(s) of faulting, seismogenic thickness, estimated maximum earthquake magnitude (for earthquakes not occurring on the fault sources within that seismic source zone), and historic and instrumental seismicity rate. Hazard for each seismic source zone is modeled through two different implementations: (1) a “gridded” model, in which locations of past seismicity are assumed to be likely locations of future seismicity (stationarity; captured by smoothing the catalog seismicity and having spatially variable rates defined over a grid of points); and (2) a “uniform” model, in which earthquakes are assumed to occur randomly and uniformly within each zone. For both models, the nucleation depth of the background earthquakes is modeled to occur uniformly from the bottom of the seismogenic crust to 2 km depth. The maximum depths of the seismogenic crust are generally consistent with the characterizations of the crustal faults within each zone and are based on the depth distribution of catalog seismicity.

The recurrence parameters for the source zones were developed using the historical seismicity record for the period of 1781 through July 2018, spanning almost 238 years. The magnitudes of all events were converted to a uniform M . In order to account for bias due to rounding of magnitude values (Felzer, 2008), values of N^* were calculated for each event in the catalog, where N^* is defined by the uncertainty in the magnitude for the event, σ , and an assumed b-value for the source zone:

$$N^* = e^{-(b \ln(10))^2 \sigma^2}$$

A b-value of 0.8, which is the b-value calculated by Felzer (2008) for the declustered catalog for the entire state of California, was used for all calculations of N^* . The catalog was declustered using the Gardner and Knopoff (1974) algorithm to remove foreshocks and aftershocks. Additionally, fault-related crustal earthquakes were removed to avoid double-counting the resulting hazard. The completeness intervals for the catalog in each seismic source zone were estimated based on settlement history, seismographic installation dates, and by using Stepp (1972) plot analyses.

In this analysis, we considered the discrete five-point sampling method of Miller and Rice (1983) to model a M_{\max} range of M 6.75 ± 0.25 for both of the seismic source zones. We estimated recurrence for the background earthquakes for both the gridded seismicity model and uniform model. In both cases, recurrence parameters (b-values and rates) were calculated using the program ABSMOOTH (LCI proprietary software; EPRI/DOE/NRC, 2012). To incorporate uncertainty into the hazard analysis, we implemented eight realizations (which include eight b-values and corresponding rates) generated by ABSMOOTH, with equal weight applied to each realization.

We assign weights of [0.7] and [0.3] to the use of the gridded and uniform seismicity, respectively. Recent seismicity may be considered more likely representative of seismicity occurring in the next 100 years. However, given the relatively short 238-year-long and incomplete historical record, the possibility exists that the catalog is not representative of the long-term record of seismicity.

3.0 Site Characterization

As stated earlier, the reference datum where the hazard was estimated at the 12 sites was the top of either the Modesto or Riverbank Formations. The time-averaged shear-wave velocity (V_s) in the top 30 m (V_{s30}) was assigned to each site by DCA as shown in Table 1. The V_{s30} computed for the 12 sites ranged from a relatively soft soil condition of V_{s30} 240 m/sec to moderately firm soil of V_s 370 m/sec.

It is assumed that the deep V_s structure in the Delta beneath the 12 sites is similar to the average V_s profiles that are implicit in the NGA-West2 GMMs such that their use adequately captures the site amplification of the deeper structure within the Delta. This assumption will need to be tested.

The depths to the basin terms $Z_{1.0}$ and $Z_{2.5}$ in the NGA-West2 GMMs (Section 4.1.1.2) were adopted from the USGS 3D Geologic and Seismic Velocity Models of the San Francisco Bay region (USGS version 08.3.0). For the 12 sites, $Z_{1.0}$ was 0.7 km and $Z_{2.5}$ ranged from 3.5 to 4.0 km.

4.0 Seismic Hazard Analyses

The PSHA and DSHA are described below.

4.1 PSHA

The methodology, inputs, and results of the PSHA are described below.

4.1.1 PSHA Methodology and Inputs

The PSHA approach used in this study is based on the model developed principally by Cornell (1968). The seismic hazard is expressed in terms of the probabilities of exceeding peak and spectral accelerations is computed by combining the following three probability distributions for all seismic sources: (1) probability distribution of earthquake magnitude in time (earthquake recurrence); (2) probability distribution of distance from the earthquake rupture area to the site given magnitude (geometry); and (3) probability distribution of peak and spectral accelerations given magnitude and distance (attenuation). Logic trees are used to address epistemic uncertainty in the seismic source characterization and ground motion prediction models. Hazard curves are computed at 21 spectral periods between 0.01 (PGA) and 10 sec. The hazard is deaggregated to show contributions by magnitude and distance. Calculations were made using the computer program HAZ45.2 developed by Dr. Norman Abrahamson, and which has been validated using the test cases in two Pacific Earthquake Engineering Research (PEER) Center-sponsored validation projects (Thomas *et al.*, 2010; Hale *et al.*, 2018).

Based on our seismic source model for the San Francisco Bay region including the Delta and the 2014 NGA-West2 GMMs, we calculated site-specific probabilistic ground motions at 12 hazard locations along the two alignments (Figure 3).

4.1.1.1 Seismic Source Model

Seismic source characterization is concerned with three fundamental elements: (1) the identification, location, and geometry of significant sources of earthquakes; (2) the maximum size of the earthquakes associated with these sources; and (3) the rate at which the earthquakes occur. The MWD seismic source model used in this study includes crustal faults capable of generating large-magnitude, surface rupturing earthquakes, and areal source zones, which accounts for background crustal seismicity that cannot be attributed to identified faults explicitly included in the seismic source model (Section 2). Seismic sources are modeled in the hazard analysis in terms of geometry and earthquake recurrence.

The geometric source parameters for faults include fault location, segmentation model, dip, and thickness of the seismogenic zone. The recurrence parameters include recurrence model, recurrence rate (slip rate or average recurrence interval for the maximum event), slope of the recurrence curve (*b*-value), and maximum magnitude. Clearly, the geometry and recurrence are not totally independent. For example, if a fault is modeled with several small segments instead of large segments, the maximum magnitude is lower, and a given slip rate requires many more small earthquakes to accommodate a cumulative seismic

moment. For areal source zones, only the areas, maximum magnitude, and recurrence parameters (based on the historical earthquake record) need to be defined.

Uncertainties in the seismic source parameters as described below, which were sometimes large, were incorporated into the PSHA using a logic tree approach. In this procedure, values of the source parameters are represented by the branches of logic trees with weights that define the distribution of values. In general, three values for each parameter were weighted and used in the analysis. Statistical analyses by Keefer and Bodily (1983) indicate that a three-point distribution of 5th, 50th, and 95th percentiles weighted 0.185, 0.63, and 0.185 (rounded to 0.2, 0.6, and 0.2), respectively, is the best discrete approximation of a continuous distribution. Alternatively, they found that the 10th, 50th, and 90th percentiles weighted 0.3, 0.4, and 0.3, respectively, can be used when limited available data make it difficult to determine the extreme tails (i.e., the 5th and 95th percentiles) of a distribution. Note that the weights associated with the percentiles are not equivalent to probabilities for these values, but rather are weights assigned to define the distribution. We generally applied these guidelines in developing distributions for seismic source parameters with continuous distributions (e.g., M_{max} , fault dip, slip rate or recurrence) unless the available data suggested otherwise. Estimating the 5th, 95th, or even 50th percentiles is typically challenging and involves subjective judgment given limited available data.

4.1.1.2 Ground Motion Models

To estimate the ground motions for crustal earthquakes in the PSHA and DSHA, we have used GMMs appropriate for tectonically active crustal regions. The models, developed as part of the NGA-West2 Project sponsored by PEER Center Lifelines Program, were published in 2014. The NGA-West2 models by Chiou and Youngs (2014), Campbell and Bozorgnia (2014), Abrahamson *et al.* (2014), and Boore *et al.* (2014) were equally weighted in both the PSHA and DSHA. The model of Idriss (2014) was not used due to the fact that the site conditions were all outside the range of applicability of the Idriss (2014) model.

Baltay and Boatwright (2015) analyzed the ground motions that recorded the 2014 M 6.0 South Napa earthquake using the data compiled and reported by ShakeMap. They compared the recorded data with four of the NGA-West2 GMMs: Abrahamson *et al.* (2014), Boore *et al.* (2014), Campbell and Bozorgnia (2014), and Chiou and Youngs (2014), as well as the model of Graizer and Kalkan (2015). At high frequencies (i.e., PGA), they found that the data within 20 km was very consistent with the GMMs and a stress drop of about 50 bars. This stress drop is consistent with the median value for California earthquakes (Baltay and Boatwright, 2015). At all other frequencies, they found that the GMMs over-predicted the data suggesting that the attenuation in the Napa and Delta region is stronger than the average attenuation in California (Baltay and Boatwright, 2015).

Erdem *et al.* (2019) evaluated 14 additional Bay area earthquakes ($M > 4$) to assess whether the same attenuation effects observed in the 2014 South Napa earthquake are also present in the Delta and surrounding region. They restricted the dataset to PGA and peak ground velocity (PGV) and for stations where the raypaths crossed through the Delta. They compared these data with the Boore *et al.* (2014) GMM and calculated adjustment factors. In general, they found that the Boore *et al.* (2014) model also over-predicted the observed peak ground motions indicating that the attenuation in the Delta is greater

than what is implied by the GMM. They concluded that a depth-dependent attenuation model for the Delta would improve ground motion estimates and that a regional GMM would reduce the peak ground motions in the Delta from Bay area earthquakes.

In the MWD study, we compared the available strong motion data with 14 earthquakes ($M \geq 4.0$) that have occurred within 100 km of the center of the Delta since 1980 (Wong *et al.*, 2021). Only six of the earthquakes in our data set were evaluated by Erdem *et al.* (2019) because they restricted their dataset to only include earthquakes whose raypaths traversed the Delta. We did not restrict our dataset to just raypaths through the Delta and we evaluated both PGA and 1.0 s spectral acceleration (SA).

Although few in number, the data recorded by Delta stations do not appear to be significantly lower than other non-Delta stations for most of the 14 earthquakes evaluated in this study (Wong *et al.*, 2021). It is not surprising that GMMs cannot predict the ground motions for all earthquakes. The variability observed in actual data attests to the complexities in seismic source, path, and site effects that cannot be accounted for by these simple models. Overall, based on these comparisons, we did not see a compelling reason to not use or adjust the NGA-West2 GMMs in the PSHA based on the observations of the 14 crustal earthquakes.

The hazard in the Delta comes from seismic sources located at a larger range of azimuths (generally northwest to southwest) and so the bias observed in the strong motion data in the 2014 South Napa earthquake is potentially accounted for in the aleatory uncertainty in the GMMs. As noted in a few earthquakes (Wong *et al.*, 2021), the NGA-West2 GMMs under-predict the recorded ground motions. It is possible that a non-ergodic adjustment to the GMMs could be made to account for possible stronger attenuation in the Delta if that is the cause of the over-prediction observed in the 2014 earthquake, but evaluating that was beyond the scope of this study. In an ongoing analysis, a similar result was reached by UCLA/DWR (Jon Stewart, UCLA, personal communication, June 2020).

As noted by Al Atik and Youngs (2014), the development of the NGA-West2 models was a collaborative effort with many interactions and exchanges of ideas among the developers and the developers indicated that an additional epistemic uncertainty needs to be incorporated into the median ground motions in order to more fully represent an appropriate level of epistemic uncertainty. Hence, for each of the four NGA-West2 models an additional epistemic uncertainty on the median ground motion was included. The three-point distribution and model of Al Atik and Youngs (2014) was applied. The model is a function of magnitude, style of faulting, and spectral period.

The aleatory variability in the four NGA-West2 models in this analysis is generally a function of period, magnitude, and V_{s30} . Details of the individual aleatory variability models can be found in Abrahamson *et al.* (2014), Boore *et al.* (2014), Chiou and Youngs (2014), and Campbell and Bozorgnia (2014). Note that the aleatory variability in the NGA-West2 models represent ergodic sigma, which includes site-to-site variability. When site response analysis is performed and variability in the site amplification is included, then there is some double-counting of site aleatory variability. The use of single-station sigma or fully non-ergodic GMMs in the hazard analysis would eliminate this conservatism. Non-ergodic GMMs for California along with the required hazard code modifications are currently being developed (Norm Abrahamson, personal communication, June 2020). When these models are available, comparisons can

be made to verify the distance attenuation in the NGA-West2 GMM for the Delta, as well as reduce the double-counting of site variability.

Rupture directivity was not included in the DSHA or PSHA. The sites along the alignment are not expected to see significant directivity effects as they are not located in the near-field of any large, strike-slip faults. The southern end of the alignment, lies within 4 km of the Midland fault and crosses the West Tracy fault, both of which are reverse or reverse-oblique faults. There is currently no consensus on directivity effects from reverse faulting events, with large variations in currently available models. In addition, there is likely some directivity effects accommodated in the aleatory variability associated with the NGA-West2 GMMs.

4.1.2 Results

The results of the PSHA are presented in terms of ground motion as a function of annual exceedance frequency (AEF). AEF is the reciprocal of the average return period. Note that hazard results presented in this section are for the reference site conditions as shown in Table 1. Results are presented for the twelve sites in order from north to south. PGA and 1.0 sec SA hazard curves for all twelve sites are shown on Figure 4 to 27.

Figure 4 shows the mean, median (50th percentile), 5th, 15th, 85th, and 95th percentile PGA hazard curves for Intake No. 3. The range of uncertainty between the 5th and 95th percentile (fractiles) is a factor of 1.6 at a return period of 2,475 years. These fractiles indicate the range of epistemic uncertainty about the mean hazard. The 1.0 sec horizontal spectral acceleration (SA) hazard curves for Intake No. 3 are shown on Figure 5 showing a factor of 1.9 at a return period of 2,475 years. Fractile ranges for the other eleven sites are similar (Figures 6 to 27). Table 2 lists the mean and 5th to 95th percentile PGA and 1.0 sec SA values for all 12 sites and return periods of 144, 200, 475, 975 and 2,475 years.

The contributions of the various seismic sources to the mean PGA hazard are shown in Figures 28 to 51 for the twelve sites as hazard curves and fractional contribution plots. Seismic sources that contribute at least 5 percent to the hazard over the return period range of 144 to 2,475 years are identified on these figures. Figures 28 and 29 show for Intake No. 3, the PGA hazard is controlled by the Central Valley seismic source zone (background seismicity) at return periods longer than about 300 years. The source contributions to the PGA hazard are very similar at Intake No. 5 (Figures 30 and 31). At Twin Cities, which lies farther to the east than Intakes No.3 and No.5, the PGA hazard is dominated by the Central Valley seismic source zone for all return periods (Figures 32 and 33). Relative contributions from the faults to the west are lower at Twin Cities than at Intakes No.3 and No.5 due to the increased distance (Figure 1). At New Hope and Canal Ranch, the PGA hazard is also dominated by the Central Valley seismic source zone, with some small contributions from Mt. Diablo, Hayward, and San Andreas faults for return periods less than 2,475 years (Figures 34 to 37).

At Bouldin in the central area of the alignments, the PGA hazard is controlled by the Mt. Diablo fault at return periods of less than 8,000 years (Figures 38 and 39). The PGA hazard at King Island is controlled by the Mt. Diablo fault, at return periods shorter than 2,000 years and the Central Valley seismic source zone at longer periods because the site is farther east than Bouldin (Figures 1, 40, and 41). The PGA hazard at

Lower Roberts is largely controlled by the Mt. Diablo fault (Figures 42 and 43). The PGA hazard at the Bacon site, which is located along the central alignment (Figure 1), is also controlled by the Mt. Diablo fault for all return periods and has secondary contributions from the West Tracy-Midland faults (Figures 44 and 45).

At the southern end of the alignment, the PGA hazard at Southern Forebay North, Southern Forebay South, and Jones Connection is controlled by the Mt. Diablo fault at all return periods even though these sites are close to the West Tracy-Midland fault (Figures 1, 46 to 51), which has a much lower slip rate.

At 1.0 sec SA, the controlling sources change (Figures 52 to 75). At the northern four sites (Intake No.3, Intake No.5, Twin Cities and New Hope), the San Andreas fault system dominates, contributing 20 percent or more at all return periods (Figures 52 to and 61). The San Andreas fault is a major contributor to the 1.0 sec SA due to its ability to generate relatively frequent large magnitude events.

In the central portion of the alignment, the San Andreas fault remains a significant contributor, but there is increased contribution from Mt. Diablo, Calaveras and Hayward faults. At the Bouldin, King Island and Lower Roberts sites, the San Andreas fault is the largest contributor to the 1.0 sec SA hazard (Figures 62 to 67). At the Bacon site, the Mt. Diablo fault controls the 1.0 sec SA hazard with the San Andres, Hayward and Calaveras faults as secondary contributors (Figures 68 and 69).

At the southern end of the alignment, the Mt. Diablo fault contributes the largest to the 1.0 sec SA hazard, but there is also contribution from the Greenville, Hayward, Calaveras, San Andreas, West Tracy-Midland and Midway-Black Butte faults (Figures 70 to 75). The relative contribution of these sources at Southern Forebay North (Figures 70 and 71) and Southern Forebay South (Figures 72 and 73) are similar, with increased contribution form Greenville and Midway-Black Butte faults at the Jones Connection site (Figures 74 and 75).

Table 3 summarizes the significant seismic sources and their percent contributions at PGA and 1.0 sec SA hazard (> 10%) for the suite of return periods from 144 to 2,475 years.

The hazard can also be deaggregated in terms of the joint magnitude-distance-epsilon probability conditional on the ground motion parameter (PGA or SA exceeding a specific value). Epsilon is the difference between the logarithm of the ground motion amplitude and the mean logarithm of ground motion (for that M and D) measured in units of standard deviation (σ). Thus, positive epsilons indicate larger-than-average ground motions. By deaggregating the PGA and 1.0 sec SA hazard by magnitude, distance, and epsilon bins, we can illustrate the contributions by events at various periods. Figure 76 shows the deaggregation at the return periods of 475 and 2,475 years for PGA at Intake No. 3. The contributions to the hazard are coming from a wide range of M and D reflecting contribution from several seismic sources (Figures 28 and 29). The magnitude and distance contributions are quite similar at the Intake No.5, Twin Cities, New Hope and Canal Ranch sites (Figures 77 to 80). At Bouldin, King Island and Lower Roberts, most of the PGA hazard is centered at about **M** 7.0 and at 30 to 50 km (Figures 81 to 83). At the Bacon site, the PGA hazard is mainly from event of **M** 6.6 to **M** 7.2 within 40 km (Figure 84). For the southernmost sites Southern Forebay North, Southern Forebay South and Jones Connection, events of **M**

6.6 to **M** 7.2 within 30 km dominate the PGA hazard (Figures 85 to 87).

The 1.0 sec SA hazard deaggregation is shown in Figures 88 to 99. These figures clearly show the large contribution to the 1.0 sec SA hazard from larger magnitude and more distant faults than for the PGA hazard. At most sites, the 1.0 sec SA hazard show bimodal or trimodal behavior with contribution from faults at various distances (e.g., Figure 95). The large peak at about 100 km and **M** 8 is the San Andreas fault. For the sites at the southern portion of the alignment (Bacon, Southern Forebays North and South, and Jones Connection), the 1.0 sec SA hazard deaggregation shows a majority of the contribution from a smaller range of magnitudes and distances (Figures 96 to 99), where faults within about 40 to 50 km dominate the hazard.

Based on the magnitude and distance deaggregated results, the controlling earthquakes as defined by the mean magnitude (\bar{M}) and modal magnitude (M^*), and mean distance (\bar{D}) and modal distance (D^*) can be calculated. Table 4 lists the \bar{M} , M^* , \bar{D} , and D^* for the five return periods (144, 200, 475, 975, and 2,475 years) and for PGA and 1.0 sec horizontal SA. These results are used for selecting seed time histories in developing the MDE time histories (Section 5).

Uniform Hazard Spectra (UHS) at a 144-year return period for all 12 sites are shown in Figure 100. A UHS depicts the ground motions at all spectral periods with the same annual exceedance frequency or return period. Similarly, Figures 101 to 104, compare the UHS for the 12 sites for return periods of 200, 475, 975 and 2,475 years, respectively. At 2,475 year return period, the hazard is highest at Southern Forebay North and South except at spectral periods less than 0.5 sec (Figure 104). Jones Connection which is in the hanging wall of the West Tracy fault has lower hazard at 0.5 sec and greater because of its higher V_s 30 of 340 m/sec. The lowest hazard is at the northern end of the alignments (Figures 100 to 104). Hazard generally increases east to west and north to south along the alignments due to proximity to the major active faults in the San Francisco Bay Area and faults along the western edge of the Delta. The UHS are tabulated in Table 5.

4.2 DSHA

We have calculated deterministic median, 69th, 84th, and 95th percentile acceleration response spectra for the significant faults at all 12 sites and compared the spectra with the UHS at the five return periods of interest. The same four NGA-West2 GMMs used in the PSHA were used in the DSHA. Inputs for these scenarios are provided in Table 6.

Figure 105 shows the 84th percentile 5%-damped response spectra for the three significant deterministic earthquakes at Intake No. 3 including a **M** 6.6 on the Midland fault, a **M** 6.9 on the Pittsburg-Kirby Hills fault zone, and a **M** 8.0 on the northern San Andreas fault (Table 6). The Midland fault is the controlling deterministic fault except at spectral periods of more than 3.5 sec. An envelope of the Midland and San Andreas fault response spectra, which is the enveloped deterministic spectrum, is also shown on Figure 105. Figure 106 shows a comparison of the enveloped median, 69th, 84th, and 95th percentile deterministic spectra with the UHS. The 2,475 year return period UHS is larger than the enveloped 84th percent deterministic spectrum (Figure 106). Figures 107 to 114 show the deterministic spectra and the

comparisons of the deterministic spectra with the UHS for the Intake No.5, Twin Cities, New Hope and Canal Ranch sites. The Midland fault scenario gives the largest deterministic ground motions at these sites because of the fault's proximity to the sites (Figures 107, 109, 111, and 113). At the Intake No.5, New Hope and Canal Ranch sites, the 84th percentile deterministic spectrum is generally similar to the 2,475-year UHS (Figure 108, 112 and 114), while at the Twin Cities site the 2,475-year return period UHS is larger than the 84th percentile deterministic spectrum (Figure 110).

At Bouldin, deterministic ground motions were computed for more earthquake scenarios because the site is closer to the faults relative to the sites in the northern portion of the alignment (Figure 3 and Table 6). The controlling deterministic fault at Bouldin is the Midland fault because it is near the site (Figures 3 and 115). The 84th percentile spectrum for the Midland fault is higher than the 2,475-year return period UHS (Figure 116). At King Island, the Midland fault scenario controls the enveloped deterministic spectrum at spectral periods less than 4 sec, while the San Andreas fault scenario controls at longer spectral periods (Figure 117). The resulting enveloped 84th percentile deterministic spectrum for King Island is slightly lower than the 2,475-year return period UHS (Figure 118). The pattern is similar at Lower Roberts (Figures 119 and 120). At Bacon, the Midland fault scenario controls the enveloped deterministic spectrum for all spectral periods less than 8 sec, with the San Andreas fault scenario controlling at longer periods (Figure 121). The resulting enveloped 84th percentile deterministic spectrum for Bacon is larger than the 2,475-year return period UHS except at spectral periods greater than about 6 sec (Figure 122).

For the sites at the southern end of the alignment (Southern Forebays North and South and Jones Connection), it is not surprising the West Tracy fault is the controlling deterministic fault because these sites are located within 3 km of the fault (Figures 3, 123, 125, and 127). The 84th percentile spectrum for the West Tracy fault is significantly larger than the 2,475 year return period UHS at most spectral periods for these three sites (Figures 124, 126, and 128). Table 7 shows the enveloped median, 69th, 84th, and 95th percentile deterministic spectra for each significant deterministic earthquake for all 12 sites.

4.3 Design Response Spectra

MDE ground motions were computed for all 12 sites based on the categorization of the structures at the site and the Delta Conveyance seismic design criteria (DCA, 2021). The MDE for the Intakes (No.3 and No.5) is defined as the envelope of the 84th percentile deterministic spectrum and the 975-year UHS. For the permanent shafts (Twin Cities, New Hope, Canal Ranch, Bouldin, King Island, Lower Roberts, Bacon, and Southern Forebays North and South), MDE are defined as the envelope of the 84th percentile deterministic spectrum and the 2,475-year UHS. The MDE for Southern Forebay North is also appropriate for the embankment dam. For the canals and gates conveyance facilities at Jones Connection, the MDE is defined as the 975-year UHS. The MDE spectra are listed in Table 8.

Figures 129 to 140 illustrate the development of the MDE spectra. MDE spectra for Intakes No. 3 and 5 are shown on Figures 129 and 130, respectively. In both cases, the 84th percentile enveloped deterministic spectrum is generally the higher spectrum (Figures 129 and 130). At the Twin Cities site, the MDE is the 2,475-year return period UHS (Figure 131). At both the New Hope and Canal Ranch sites, the 2,475-year UHS and 84th percentile deterministic spectrum are similar, with the 2,475-year UHS controlling the MDE

at moderate and longer spectral periods (> 0.5 sec) and the 84th percentile deterministic spectra controlling at shorter spectral periods (Figures 132 and 133). At Bouldin, the MDE is the 84th percentile enveloped deterministic spectrum (Figure 134). At the King Island and Lower Roberts sites, the MDE is equal to the 2,475-year UHS for all spectral periods (Figures 135 and 136). At the Bacon site, the 84th percentile deterministic spectrum controls the MDE at spectral periods less than 6 sec (Figure 137). For the shafts at the Southern Forebays North and South, the MDE is controlled by the 84th percentile deterministic spectrum, which is significantly larger than the 2,475-year UHS (Figures 138 and 139). Note that this MDE also applies to an embankment at the Southern Forebay North site, as the 84th percentile enveloped deterministic spectrum is larger than both the 975 and 2,475-year return period UHS and the Delta Conveyance seismic design criteria for embankments (DCA, 2021) is the envelope of the 84th percentile deterministic spectrum and the 975-year UHS.

OBE spectra, defined as the 475-year UHS, were also computed for all 12 sites (Figure 102 and Table 9).

5.0 Development of Time Histories

A total of three sets each of horizontal-component MDE time histories were developed for the intakes, shafts, and embankment dam at six selected sites: Intake No.3, Intake No.5, Bouldin, Twin Cities, Lower Roberts, and Southern Forebay North.. The procedure proposed by Lilhanand and Tseng (1988), as modified by Al Atik and Abrahamson (2010), and contained in the computer program RSPMatch09 was used to perform the spectral matching. The approach used to select and match time histories is described in Section 5.1 and the resulting matched time histories are presented in Section 5.2.

5.1 Approach to Spectral Matching

Recorded time histories that are used as input for spectral matching are referred to as “seed” records. Seed records were selected from the NGA-West2 database (Ancheta *et al.*, 2013) so that the geometric mean spectra for each pair of horizontal seed records have a scaled spectral shape similar to the MDE target spectrum. If the MDE spectrum is primarily an UHS then the seed time history should correspond to the magnitudes and distances similar to those that dominate the hazard at the return period of the target spectrum, as determined from the deaggregation discussed in Section 4.1.2 and shown in Table 4. If the MDE is primarily the controlling deterministic earthquake, then that the deterministic scenario magnitude and distance is the basis for selecting seed time histories. At both the Twin Cities and Lower Roberts sites, there is significant contribution to the hazard from the distant San Andreas fault, as well as from more moderate magnitude events from closer regional seismic source, and so seeds were selected to represent both of these scenarios.

A similar spectral shape minimizes the changes required by the spectral matching program and improves the overall quality of the matched record (Grant *et al.*, 2008). Therefore, the NGA-West2 database is searched for potential seed records that have a low mean-squared error between the scaled geometric mean spectrum and target (geometric mean) spectrum. Relatively small scale factors are preferred (between 0.5 and 3.5), and a small window around seismological characteristics is expanded until a sufficient number of seed records can be identified.

Time-domain approaches to spectral matching, such as the one taken in *RSPMatch2009*, are preferable to frequency-domain approaches because the resulting adjustments to the time history are more localized in time (Lilhanand and Tseng, 1988); the matched acceleration, velocity, and displacement time histories more closely resemble those of the seed record (Lilhanand and Tseng, 1988); and because frequency-domain approaches can cause large changes to the overall energy content of the time history (Naeim and Lew, 1995).

Within any spectral matching procedure, a response spectrum must be defined as the target to which the seed records are spectrally matched. In the procedure used here, a unique target response spectrum was developed for each seed time history horizontal component, H1 and H2, in a manner that conserves the correlation between H1 and H2 spectral ordinates as well as the natural peaks and valleys in each spectrum. This is in contrast to using a single, smooth spectrum for all horizontal component records, as

often is the case when spectral matching is performed. Maintaining the H1 to H2 correlation and peaks and valleys in the individual horizontal time histories ensures that the natural variability is not removed.

For each pair of horizontal components (H1 and H2), individual target spectra were computed as follows:

$$H1_{\text{target}} = \frac{H1_{\text{Seed}}}{\text{Geomean}(H1,H2)_{\text{seed}}} * \text{MDE Spectrum}(\text{geomean})$$

$$H2_{\text{target}} = \frac{H2_{\text{Seed}}}{\text{Geomean}(H1,H2)_{\text{seed}}} * \text{MDE Spectrum}(\text{geomean})$$

where $H1_{\text{target}}$ is the target response spectrum of the H1 component (similar for H2), $H1_{\text{seed}}$ is the scaled seed response spectrum of the H1 component (similar for H2), $\text{Geomean}_{\text{seed}}$ is the geometric mean for the scaled seed time history pair H1, H2, and MDE spectrum (geomean), which is a RotD50 spectrum.

5.2 Spectrally-Matched Time Histories

Figures 141 to 212 show the spectral matching process and the resulting time histories for the MDE spectra at the six sites. For example, the top panel in Figure 141 shows the spectra of the seed time histories (H1, H2 and geometric mean), which in this case are the Los Angeles Hollywood Storage records from the 1971 **M** 6.6 San Fernando, California earthquake scaled to minimize the difference between the scaled geometric mean spectrum and the target spectrum. This scaling shows how the spectral shapes of the seed time histories compared to the target MDE spectrum. The bottom panel in Figure 141 shows the spectra of the matched time histories, their geomean, and the target spectrum. The spectral matching was done over the entire period range of 0.01 to 10.0 sec and the geomean shows a good match to the target. Figure 142 shows the individual component matched, target, and scaled response spectra. Figures 143 and 144 show the resulting acceleration, velocity, and displacement time histories. Also shown on Figures 143 and 144 are Husid plots. Husid plots which illustrate the increase in energy (normalized Arias intensity) with time (see following discussion).

Table 10 list the properties of the seed and matched time histories, which include PGA, peak ground velocity (PGV), and peak ground displacement (PGD), as well as Arias intensities and 5-95% durations. In developing the time histories, attention was paid to both Arias intensity and 5-95% duration appropriate for the magnitude and distance of the deterministic or controlling earthquake. The seed time histories (Table 10) were selected based on the similarity of spectral shape to the target spectrum along with mean magnitude and mean distance from the deaggregation. Duration and Arias intensity were also considered.

Arias intensity is a ground motion parameter defined by Arias (1970) as the integral of the square of acceleration over the duration of a time series record, as follows:

$$I_a = \frac{\pi}{2g} \int_0^{\infty} a(t)^2 dt$$

where I_a is Arias intensity, $a(t)$ is acceleration, and g is the acceleration of gravity. Studies have shown that I_a correlates well with the damage potential of earthquakes (Travasarou *et al.*, 2003). The target geometric mean I_a for the horizontal time histories, computed using the models of Watson-Lamprey and Abrahamson (2006), and Abrahamson *et al.* (2016) are provided in Table 11a. Note that these models are for the geometric mean of two horizontal components. The I_a of the matched horizontal time histories are also provided in Table 11a. The average of the geometric mean generally falls within the \pm one sigma range.

Duration of a strong ground motion is related to the time required for release of accumulated strain energy by rupture along the fault and generally increases with magnitude of the earthquake. Trifunac and Brady (1975) defined significant duration as the time interval between the points at which 5% and 95% of the total energy (I_a) has been recorded. The target durations for the time histories were calculated using the models of Abrahamson and Silva (1996) and Kempton and Stewart (2006) and are provided in Table 11b. The durations of the spectrally-matched horizontal time histories have durations are also provided in Table 11b. The matched time histories have durations that generally fall within the ± 1 sigma range of the predicted target duration (Table 11b).

6.0 References

- Abrahamson, N.A. and Silva, W.J., 1996, Empirical ground motion models: Report to Brookhaven National Laboratory.
- Abrahamson, N.A., Silva, W.J., and Kamai, R., 2014, Summary of the ASK14 ground-motion relation for active crustal regions: *Earthquake Spectra*, v. 30, p. 1025-1055.
- Abrahamson, C., Hao-Jun, M.S. and Yang, B., 2016, Ground-motion prediction equations for arias intensity consistent with the NGA-West2 ground-motion Models: PEER Report No. 2016/05, Pacific Earthquake Engineering Research Center, University of California, Berkeley, 42 p.
- Al Atik, L. and Abrahamson, N., 2010, An improved method for nonstationary spectral matching: *Earthquake Spectra*, v. 26, p. 601-617.
- Al Atik, L. and Youngs, R., 2014, Epistemic uncertainty for NGA-West2 models: *Earthquake Spectra*, v. 30, p. 1301-1318.
- Ancheta, T. D., R. B. Darragh, J. P. Stewart, E. Seyhan, W. J. Silva, B. S. J. Chiou, K. E. Woodell, R. W. Graves, A. R. Kottke, D. M. Boore, T. Kishida, and J. L. Donahue. 2013, PEER NGA-West2 Database: PEER Report No. 2013/03, Pacific Earthquake Engineering Research Center, University of California, Berkeley.
- Arias, A., 1970, A measure of earthquake intensity: *Seismic Design for Nuclear Power Plants*, R.J. Hansen, ed., MIT Press, Cambridge, Massachusetts, pp.438-483.
- Baltay, A.S. and Boatwright, J., 2015, Ground-motion observations of the 2014 South Napa earthquake: *Seismological Research Letters*, v. 86, p. 1-6.
- Boore, D.M., Stewart, J.P., Seyhan, E., and Atkinson, G.M., 2014, NGA-West2 equations for predicting PGA, PGV, and 5%-damped PSA for shallow crustal earthquakes: *Earthquake Spectra*, v. 30, p. 1057-1085.
- Campbell, K.W. and Bozorgnia, Y., 2014, NGA-West2 ground motion model for the average horizontal components of PGA, PGV, and 5%-damped linear acceleration response spectra: *Earthquake Spectra*, v. 30, p. 1087-1115.
- Cao, T., Bryant, W.A, Rowshandel, B., Branum, D., and Wills, C.J., 2003, The revised 2002 California probabilistic seismic hazard maps, June 2003: California Geological Survey, http://www.consrv.ca.gov/CGS/rghm/psha/fault_parameters/pdf/2002_CA_Hazard_Maps.pdf.
- Chiou, B-S.J. and Youngs, R.R., 2014, Update of the Chiou and Youngs NGA ground motion model for average horizontal component of peak ground motion and response spectra: *Earthquake Spectra*, v. 30, p. 1117-1153.
- Cornell, C.A., 1968, Engineering seismic risk analysis: *Bulletin of the Seismological Society of America*, v. 58, p. 1583-1606.
- DCA (Delta Conveyance Design and Construction Authority), 2021, Conceptual-Level Seismic Design Criteria, prepared for DWR/Delta Conveyance Office, 26 p.

dePolo, C. M., 1994, The maximum background earthquake for the Basin and Range Province, western North America: *Bulletin of the Seismological Society of America*, v. 84, p. 466-472.

Division of Oil, Gas and Geothermal Resources (DOGGR), 1982, California Oil and Gas Fields, Volume III – Northern California; Contour maps, cross sections and data sheets: California Department of Conservation, 330 p. (available from <http://repository.usgin.org/category/place-keywords/california>; last accessed 3/4/19)

EPRI/DOE/NRC, 2012, Technical Report: Central and Eastern United States Seismic Source Characterization for Nuclear Facilities.

Erdem, J.E., Boatwright, J. and Fletcher, J.B., 2019, Ground-motion attenuation in the Sacramento-San Joaquin Delta, California, South Napa earthquake: *Bulletin of the Seismological Society of America*, v. 109, p. 1025-1035.

Felzer, K.R., 2008, Calculating California seismicity rates: U.S. Geological Survey Open-File Report 2007-1437-I, 41 p.

Field, E.H., Biasi, G.P., Bird, P., Dawson, T.E., Felzer, K.R., Jackson, D.D., Johnson, K.M., Jordan, T.H., Madden, C., Michael, A.J., Milner, K.R., Page, M.T., Parsons, T., Powers, P.M., Shaw, B.E., Thatcher, W.R., Weldon, R.J., II, and Zeng, Y., 2013, Uniform California earthquake rupture forecast, version 3 (UCERF3); the time-independent model: U.S. Geological Survey Open-File Report 2013-1165.

Fugro Consultants, Inc., 2011, Reprocessing and Interpretation of Seismic Reflection Data, Clifton Court Forebay: letter report submitted to California Department of Water Resources, Project Geology Section, 18 p. plus tables and figures.

Gardner, J.K., and Knopoff, L., 1974, Is the sequence of earthquakes in southern California, with aftershocks removed, Poissonian?: *Bulletin of the Seismological Society of America*, v. 64, p. 1363–1367.

Graizer, V. and Kalkan, E., 2015, Update of the Graizer-Kalkan ground-motion prediction equations for shallow crustal continental earthquakes: U.S. Geological Survey Open-File Report OF-2015-1009, p. 98.

Grant, D. N., Greening, P. D., Taylor, M. L., and Ghosh, B., 2008, Seed record selection for spectral matching with RSPMatch2005: 14th World Conference on Earthquake Engineering, Beijing, China.

Hale, C., Abrahamson, N. and Bozorgnia, Y., 2018, Probabilistic seismic hazard analysis code verification: Pacific Earthquake Engineering Research Center, College of Engineering, University of California, Berkeley, PEER Report 2018/03, 105 p.

Idriss, I.M., 2014, An NGA-West2 empirical model estimating the horizontal spectral values generated by shallow crustal earthquakes: *Earthquake Spectra*, v. 30, p. 1155-1177.

Jennings, C.W., Gutierrez, C., Bryant, W., Saucedo, G., and Wills, C., 2010, Geologic Map of California: California Geological Survey, 1:750,000 scale (online map version at <https://www.arcgis.com/home/webmap/viewer.html?webmap=2a718c86c96e41e298410c8b58515812>; last accessed 3/20/19).

- Keefer, D.I. and Bodily, S.E., 1983, Three-point approximations for continuous random variables: *Management Science*, v. 26, p. 595-609.
- Kempton, J.J. and Stewart, J.P., 2006, Prediction equations for significant duration of earthquake ground motions considering site and near-source effects: *Earthquake Spectra*, v. 22, p. 985-1013.
- Krug, E.H., Cherven, V.B., Hatten, C.W., and Roth, J.C., 1992, Subsurface structure in the Montezuma Hills, southwestern Sacramento basin: in Cherven, V.B., and Edmondson, W.F., eds., *Structural Geology of the Sacramento Basin*: v. MP-41, Annual Meeting, Pacific Section, Society of Economic Paleontologists and Mineralogists, p. 41-60.
- Lilhanand, K. and Tseng, W. S., 1988, Development and application of realistic earthquake time histories compatible with multiple-damping design spectra: *Proceedings of the 9th World Conference on Earthquake Engineering*, Tokyo, Japan.
- Miller, A.C., and Rice, T.R., 1983, Discrete approximations of probability distributions: *Management Science*, v. 29, p. 352-362.
- Naeim, F., and Lew, M., 1995, On the use of design spectrum compatible time histories: *Earthquake Spectra*, v. 11, p. 111-127.
- Silva, W.J., Abrahamson, N.A., Toro, G., and Constantino, C., 1997, Description and validation of the stochastic ground motion model: unpublished report prepared for the Brookhaven National Laboratory.
- Stepp, J.C., 1972, Analysis of completeness of the earthquake sample in the Puget Sound area and its effect on statistical estimates of earthquake hazard: *Proceedings of the International Conference on Microzonation*, v. 2, 897-910.
- Sterling, R., 1992, Intersection of the Stockton and Vernalis faults, southern Sacramento Valley, California, in Chevron, V.B., and Edmondson, W.F., eds, *Structural Geology of the Sacramento Basin: American Association of Petroleum Geologists Miscellaneous Publication 41*, Pacific Section, p. 143-151.
- Thomas, P.A., Wong, I.G., and Abrahamson, N., 2010, Verification of probabilistic seismic hazard analysis software programs: Pacific Earthquake Engineering Research Center, College of Engineering, University of California, Berkeley, PEER Report 2010/106, 173 p.
- Thomas, P., Smith, S., and Wong, I., 2021, Data transmittal – Delta Conveyance probabilistic and deterministic ground motions for Bethany Alternative sites, memorandum of transmittal to Andrew Finney and Dario Rosidi prepared by Lettis Consultants International dated 1 September 2021.
- Thomas, P. and Wong, I., 2021, Data transmittal – Delta Conveyance probabilistic and deterministic ground motions for Union Island shaft, memorandum of transmittal to Andrew Finney and Dario Rosidi prepared by Lettis Consultants International dated 1 September 2021.
- Travasarou, T., Bray, J.D., and Abrahamson, N.A., 2003, Empirical attenuation relationship for Arias intensity: *Earthquake Engineering and Structural Dynamics*, v. 32, p. 1133-1155.
- Trifunac, M. D. and Brady, A.G., 1975, On the correlation of seismic intensity scales with the peaks of recorded strong ground motion: *Bulletin of the Seismological Society of America*, v. 65, p. 139-162.

Unruh, J.R., and Hitchcock, C.S., 2015, Detailed Mapping and Analysis of Fold Deformation Above the West Tracy Fault, Southern San Joaquin-Sacramento Delta, Northern California: Collaborative Research with Lettis Consultants International and InfraTerra: Final Technical Report submitted to the U.S. Geological Survey National Earthquake Hazards Reduction Program award number G14AP00069, 32 p. plus figures and plates.

Unruh, J., and Krug, K., 2007, Assessment and Documentation of Transpressional Structures, Northeastern Diablo Range, for the Quaternary Fault Map Database: Collaborative Research with William Lettis & Associates, Inc., and the U.S. Geological Survey: Final Technical Report for U.S. Geological Survey National Earthquake Hazard Reduction Program (NEHRP), Award No. 05HQGR0054, 45 p.

Unruh, J.R., Hitchcock, C.S., Hector, S., and Blake, K., 2016, Characterization of the Southern Midland Fault in the Sacramento-San Joaquin Delta, in Anderson, R. and Ferriz, H., eds., Applied Geology in California: Association of Engineering Geologists, Start Pub Co., p. 757-775.

URS Corporation, 2012, Update of the Probabilistic and Deterministic Seismic Hazard Analyses of Success Dam, California, unpublished report submitted to U.S. Army Corps of Engineers.

URS Corporation/Jack R. Benjamin & Associates, 2008, Delta Risk Management Strategy (DRMS) Phase 1, Topic Area: Seismology: Final Technical Memorandum submitted to the California Department of Water Resources, 5 December 2008, 32 p. plus tables and figures.

Watson-Lamprey, J. and Abrahamson, N., 2006, Selection of ground motion time series and limits on scaling: Soil Dynamics and Earthquake Engineering, v. 26, p. 477-482.

Wong, I.G., and Ely, R.W., 1983, Historical seismicity and tectonics of the Coast Ranges-Sierran Block boundary: implications to the 1983 Coalinga earthquakes, in Bennet, J., and Sherburne, R., eds., The 1983 Coalinga, California Earthquakes: California Division of Mines and Geology Special Publication 66, p. 89-104.

Wong, I., Ely, R., and Kollman, A.C., 1988, Contemporary seismicity and tectonics along the northern and central Coast Ranges-Sierran Block boundary zone, California: Journal of Geophysical Research, v. 93, 7813-7833.

Wong, I., Thomas, P., Lewandowski, N., Unruh, J., Darragh, R., and Silva, W., 2021, Seismic hazard analyses of the Metropolitan Water District Emergency Freshwater Pathway, California: Earthquake Spectra.

Working Group for California Earthquake Probabilities (WGCEP), 2003, Earthquake probabilities in the San Francisco Bay area: 2002-2031: U.S. Geological Survey Open-File Report 03-214.

Working Group on Northern California Earthquake Potential (WGNCEP), 1996, Database of potential sources for earthquakes larger than magnitude 6 in northern California: U.S. Geological Survey Open-File Report 96-705, 40 p. plus figures.

Tables

Table 1. Locations and Site Conditions of Hazard Sites

	HAZARD SITE	INTAKE 3	INTAKE 5	TWIN CITIES	NEW HOPE (CENTRAL) ¹	BOULDIN (CENTRAL)	CANAL RANCH (EASTERN)	KING ISLAND (EASTERN) ¹	BACON (CENTRAL)	LOWER ROBERTS (EASTERN)	SOUTHERN FOREBAY NORTH ¹	SOUTHERN FOREBAY SOUTH	JONES CONNECTION
	Latitude	-121.516599	-121.529043	-121.455147	-121.478803	-121.532003	-121.444275	-121.433822	-121.547715	-121.433233	-121.590859	-121.596853	-121.603262
	Longitude	38.378252	38.347752	38.298196	38.240012	38.099805	38.187717	38.059199	37.95776	37.982619	37.871603	37.844726	37.820825
	V _{s30} ²	1,200 ft/sec (370 m/sec)	1,300 ft/sec (400 m/sec)	1,104 ft/sec (340 m/sec)	1,104 ft/sec (340 m/sec)	960 ft/sec (290 m/sec)	1,212 ft/sec (370 m/sec)	959 ft/sec (290 m/sec)	800 ft/sec (240 m/sec)	811 ft/sec (250 m/sec)	800 ft/sec (240 m/sec)	850 ft/sec (260 m/sec)	1100 ft/sec (340 m/sec)
Top Elevation (NAVD88) (ft)	10	Basin Deposits V _s = 600 ft/s											Basin Deposits V _s = 700 ft/s
	0		Basin Deposits V _s = 600 ft/s							Basin Deposits 450			
	-10		Modesto Fm. V _s = 900 ft/s	Modesto Fm. V _s = 900 ft/s	Peat and Muck V _s = 200 ft/s	Modesto Fm. V _s = 1,100 ft/s	Peat and Muck V _s = 400 ft/s	Basin Deposits V _s = 500 ft/s	Peat and Muck V _s = 500 ft/s				
	-20		Basin Deposits V _s = 600 ft/s							Basin Deposits V _s = 600 ft/s	Basin Deposits V _s = 650 ft/s	Basin Deposits V _s = 700 ft/s	
	-30												
	-40												
	-50		Riverbank Fm. V _s = 1,300 ft/s	Riverbank Fm. V _s = 1,300 ft/s	Modesto Fm. V _s = 800 ft/s	Modesto Fm. V _s = 900 ft/s	Modesto Fm. V _s = 750 ft/s	Basin Deposits V _s = 600 ft/s	Basin Deposits V _s = 650 ft/s	Basin Deposits V _s = 700 ft/s			
	-60												
	-70		Riverbank Fm. V _s = 1,200 ft/s	Riverbank Fm. V _s = 1,300 ft/s	Riverbank Fm. V _s = 1,300 ft/s	Riverbank Fm. V _s = 1,300 ft/s	Riverbank Fm. V _s = 1,300 ft/s	Modesto Fm. V _s = 800 ft/s	Modesto Fm. V _s = 800 ft/s	Modesto Fm. V _s = 800 ft/s	Modesto Fm. V _s = 850 ft/s	Modesto Fm. V _s = 1,100 ft/s	
	-80												
	-90												
-100													
-110									Riverbank Fm. V _s = 1,200 ft/s				

¹ Assumed shear-wave velocities (V_s) based on geologic mapping and correlations with SPT results

² V_{s30} computed for top of Modesto Fm, except at Intake No.3 and Intake No.5 where V_{s30} computed at top of Riverbank Fm.

Table 2. Summary of Probabilistic Ground Motions

(a) Peak Horizontal Ground Acceleration (g)

	INTAKE No. 3	INTAKE No. 5	TWIN CITIES	NEW HOPE	CANAL RANCH	BOULDIN	KING ISLAND	LOWER ROBERTS	BACON	SOUTHERN FOREBAY NORTH	SOUTHERN FOREBAY SOUTH	JONES CONNECTION
144-Year Return Period												
Mean	0.12	0.12	0.12	0.13	0.12	0.16	0.15	0.17	0.20	0.24	0.25	0.25
5th-95th Percentiles	0.1 - 0.12	0.09 - 0.11	0.1 - 0.13	0.1 - 0.13	0.1 - 0.12	0.13 - 0.18	0.12 - 0.17	0.13 - 0.2	0.16 - 0.24	0.19 - 0.28	0.19 - 0.27	0.19 - 0.23
200-Year Return Period												
Mean	0.14	0.14	0.14	0.15	0.14	0.18	0.17	0.19	0.23	0.27	0.28	0.29
5th-95th Percentiles	0.11 - 0.13	0.11 - 0.13	0.11 - 0.14	0.12 - 0.15	0.11 - 0.14	0.15 - 0.2	0.13 - 0.19	0.15 - 0.23	0.18 - 0.27	0.21 - 0.32	0.22 - 0.32	0.22 - 0.27
475-Year Return Period												
Mean	0.19	0.18	0.19	0.20	0.19	0.25	0.23	0.25	0.30	0.37	0.39	0.41
5th-95th Percentiles	0.15 - 0.18	0.14 - 0.17	0.15 - 0.19	0.16 - 0.2	0.15 - 0.19	0.19 - 0.27	0.18 - 0.25	0.19 - 0.31	0.24 - 0.37	0.28 - 0.45	0.3 - 0.45	0.32 - 0.39
975-Year Return Period												
Mean	0.23	0.23	0.23	0.25	0.24	0.31	0.28	0.31	0.37	0.46	0.50	0.54
5th-95th Percentiles	0.18 - 0.23	0.18 - 0.21	0.18 - 0.24	0.19 - 0.25	0.18 - 0.23	0.24 - 0.34	0.22 - 0.32	0.24 - 0.38	0.29 - 0.48	0.35 - 0.58	0.38 - 0.59	0.41 - 0.53
2,475-Year Return Period												
Mean	0.30	0.30	0.31	0.32	0.31	0.40	0.36	0.39	0.48	0.60	0.65	0.72
5th-95th Percentiles	0.24 - 0.29	0.23 - 0.28	0.24 - 0.31	0.25 - 0.33	0.24 - 0.31	0.3 - 0.45	0.27 - 0.41	0.3 - 0.5	0.37 - 0.63	0.45 - 0.79	0.49 - 0.82	0.54 - 0.74

(b) 1.0 Sec Horizontal Spectral Acceleration (g)

	INTAKE No. 3	INTAKE No. 5	TWIN CITIES	NEW HOPE	CANAL RANCH	BOULDIN	KING ISLAND	LOWER ROBERTS	BACON	SOUTHERN FOREBAY NORTH	SOUTHERN FOREBAY SOUTH	JONES CONNECTION
144-Year Return Period												
Mean	0.16	0.14	0.17	0.17	0.16	0.23	0.21	0.25	0.30	0.35	0.35	0.29
5th-95th Percentiles	0.15 - 0.21	0.15 - 0.18	0.15 - 0.23	0.16 - 0.22	0.15 - 0.2	0.2 - 0.28	0.18 - 0.26	0.2 - 0.31	0.25 - 0.37	0.3 - 0.43	0.31 - 0.43	0.32 - 0.36
200-Year Return Period												
Mean	0.19	0.16	0.20	0.20	0.18	0.26	0.24	0.29	0.35	0.41	0.40	0.34
5th-95th Percentiles	0.17 - 0.24	0.16 - 0.21	0.17 - 0.26	0.18 - 0.25	0.17 - 0.22	0.23 - 0.32	0.21 - 0.3	0.23 - 0.36	0.28 - 0.42	0.33 - 0.5	0.35 - 0.5	0.37 - 0.43
475-Year Return Period												
Mean	0.26	0.23	0.27	0.27	0.25	0.35	0.33	0.40	0.48	0.57	0.58	0.51
5th-95th Percentiles	0.22 - 0.34	0.22 - 0.29	0.23 - 0.36	0.24 - 0.34	0.23 - 0.31	0.3 - 0.44	0.28 - 0.41	0.3 - 0.49	0.37 - 0.59	0.46 - 0.71	0.49 - 0.72	0.52 - 0.64
975-Year Return Period												
Mean	0.33	0.29	0.35	0.34	0.31	0.45	0.42	0.50	0.61	0.75	0.77	0.69
5th-95th Percentiles	0.28 - 0.43	0.28 - 0.37	0.28 - 0.45	0.3 - 0.43	0.29 - 0.4	0.37 - 0.56	0.34 - 0.52	0.37 - 0.62	0.46 - 0.75	0.57 - 0.93	0.62 - 0.95	0.67 - 0.86
2,475-Year Return Period												
Mean	0.43	0.38	0.46	0.45	0.42	0.60	0.55	0.66	0.82	1.03	1.07	0.98
5th-95th Percentiles	0.37 - 0.56	0.37 - 0.49	0.38 - 0.6	0.4 - 0.57	0.38 - 0.53	0.49 - 0.74	0.44 - 0.69	0.48 - 0.82	0.59 - 1.01	0.74 - 1.27	0.81 - 1.33	0.89 - 1.23

Table 3. Seismic Source Contributions at PGA and 1.0 Sec SA for 2,475-Year Return Period

(a) Peak Horizontal Ground Acceleration

RETURN PERIOD	INTAKE NO. 3	INTAKE NO. 5	TWIN CITIES	NEW HOPE	CANAL RANCH	BOULDIN	KING ISLAND	LOWER ROBERTS	BACON	SOUTHERN FOREBAY NORTH	SOUTHERN FOREBAY SOUTH	JONES CONNECTION
144 YEARS	15% CRSB North 11% Central Valley Background Seismicity 11% Berryessa-Green Valley 10% Hayward 10% San Andreas	14% CRSB North 11% Berryessa-Green Valley 10% Central Valley Background Seismicity 10% Hayward 10% San Andreas	11% Central Valley Background Seismicity 10% CRSB North 10% Hayward 10% San Andreas	11% Hayward 11% Mt. Diablo 10% Central Valley Background Seismicity 10% San Andreas	12% Mt. Diablo 11% Hayward 10% Central Valley Background Seismicity 10% San Andreas	16% Mt. Diablo 10% Hayward	15% Mt. Diablo 10% Hayward 10% Calaveras 10% San Andreas	17% Mt. Diablo 11% Calaveras	21% Mt. Diablo 10% Calaveras	25% Mt. Diablo 12% Greenville 11% Calaveras	25% Mt. Diablo 13% Greenville 11% Calaveras	25% Mt. Diablo 15% Greenville 11% Calaveras 11% Midway-Black Butte
200 YEARS	15% CRSB North 12% Central Valley Background Seismicity 11% Berryessa-Green Valley	14% CRSB North 12% Central Valley Background Seismicity 10% Berryessa-Green Valley	13% Central Valley Background Seismicity 10% CRSB North 10% Hayward 10% San Andreas 10% Mt. Diablo	11% Mt. Diablo 11% Central Valley Background Seismicity 10% Hayward 10% San Andreas	12% Mt. Diablo 11% Central Valley Background Seismicity 10% Hayward 10% San Andreas	17% Mt. Diablo 10% Hayward	16% Mt. Diablo	18% Mt. Diablo 10% Calaveras	23% Mt. Diablo	27% Mt. Diablo 10% Calaveras 13% Greenville	27% Mt. Diablo 14% Greenville 10% Calaveras 10% Midway-Black Butte	27% Mt. Diablo 16% Greenville 13% Midway-Black Butte
475 YEARS	18% Central Valley Background Seismicity 16% CRSB North 10% Berryessa-Green Valley	17% Central Valley Background Seismicity 15% CRSB North	18% Central Valley Background Seismicity 10% CRSB North 10% Mt. Diablo	16% Central Valley Background Seismicity 12% Mt. Diablo	16% Central Valley Background Seismicity 13% Mt. Diablo	18% Mt. Diablo 10% Central Valley Background Seismicity	18% Mt. Diablo 13% Central Valley Background Seismicity	20% Mt. Diablo 10% Central Valley Background Seismicity	26% Mt. Diablo 12% West Tracy-Midland	32% Mt. Diablo 13% Greenville 10% West Tracy-Midland	32% Mt. Diablo 14% Greenville 12% Midway-Black Butte 11% West Tracy-Midland	31% Mt. Diablo 17% Greenville 16% Midway-Black Butte 10% West Tracy-Midland
975 YEARS	24% Central Valley Background Seismicity 16% CRSB North	22% Central Valley Background Seismicity 15% CRSB North 10% Pittsburg-Kirby Hills	24% Central Valley Background Seismicity 10% CRSB North	21% Central Valley Background Seismicity 11% Mt. Diablo	21% Central Valley Background Seismicity 13% Mt. Diablo	19% Mt. Diablo 13% Central Valley Background Seismicity 11% West Tracy-Midland	19% Mt. Diablo 16% Central Valley Background Seismicity	22% Mt. Diablo 13% Central Valley Background Seismicity	28% Mt. Diablo 16% West Tracy-Midland	35% Mt. Diablo 14% West Tracy-Midland 13% Greenville 10% Midway-Black Butte	35% Mt. Diablo 15% West Tracy-Midland 14% Greenville 13% Midway-Black Butte	33% Mt. Diablo 18% Midway-Black Butte 16% Greenville 14% West Tracy-Midland
2,475 YEARS	34% Central Valley Background Seismicity 15% CRSB North	32% Central Valley Background Seismicity 13% CRSB North 12% Pittsburg-Kirby Hills	34% Central Valley Background Seismicity	28% Central Valley Background Seismicity 10% Mt. Diablo	29% Central Valley Background Seismicity 12% Mt. Diablo	18% Mt. Diablo 17% Central Valley Background Seismicity 15% West Tracy-Midland	22% Central Valley Background Seismicity 19% Mt. Diablo	24% Mt. Diablo 17% Central Valley Background Seismicity	30% Mt. Diablo 21% West Tracy-Midland	38% Mt. Diablo 19% West Tracy-Midland 11% Greenville 10% Midway-Black Butte	36% Mt. Diablo 20% West Tracy-Midland 13% Midway-Black Butte 12% Greenville	34% Mt. Diablo 20% West Tracy-Midland 19% Midway-Black Butte 14% Greenville

Note: Seismic sources that contribute 10 percent or greater to the PGA hazard are listed.

(b) 1.0 Sec Spectral Acceleration

RETURN PERIOD	INTAKE NO. 3	INTAKE NO. 5	TWIN CITIES	NEW HOPE	CANAL RANCH	BOULDIN	KING ISLAND	LOWER ROBERTS	BACON	SOUTHERN FOREBAY NORTH	SOUTHERN FOREBAY SOUTH	JONES CONNECTION
144 YEARS	21% San Andreas 13% Hayward 10% Berryessa-Green Valley	20% San Andreas 13% Hayward 10% Berryessa-Green Valley	21% San Andreas 13% Hayward	20% San Andreas 13% Hayward	20% San Andreas 13% Hayward	18% San Andreas 13% Hayward 11% Mt. Diablo	19% San Andreas 13% Hayward 11% Calaveras 10% Mt. Diablo	18% San Andreas 13% Calaveras 12% Hayward 12% Mt. Diablo	15% San Andreas 15% Mt. Diablo 12% Calaveras 12% Hayward	19% Mt. Diablo 13% Calaveras 12% San Andreas 11% Hayward 10% Greenville 10% Midway-Black Butte	19% Mt. Diablo 13% Calaveras 11% San Andreas 11% Greenville 10% Hayward	20% Mt. Diablo 13% Calaveras 12% Greenville 10% Hayward 10% San Andreas
200 YEARS	21% San Andreas 13% Hayward 10% Berryessa-Green Valley	20% San Andreas 13% Hayward 10% Berryessa-Green Valley	21% San Andreas 13% Hayward	20% San Andreas 13% Hayward	20% San Andreas 13% Hayward	18% San Andreas 13% Hayward 12% Mt. Diablo	19% San Andreas 13% Hayward 11% Mt. Diablo 11% Calaveras	18% San Andreas 13% Mt. Diablo 12% Calaveras 12% Hayward	16% Mt. Diablo 15% San Andreas 11% Calaveras 11% Hayward	21% Mt. Diablo 12% San Andreas 12% Calaveras 10% Hayward 11% Greenville	21% Mt. Diablo 12% Calaveras 12% Greenville 11% San Andreas	22% Mt. Diablo 11% Calaveras 14% Greenville 10% Midway-Black Butte
475 YEARS	22% San Andreas 13% Hayward 10% Berryessa-Green Valley 10% CRSB North	21% San Andreas 13% Hayward	22% San Andreas 13% Hayward	21% San Andreas 13% Hayward	21% San Andreas 13% Hayward	18% San Andreas 12% Hayward 13% Mt. Diablo	19% San Andreas 13% Mt. Diablo 12% Hayward	18% San Andreas 15% Mt. Diablo 11% Hayward	20% Mt. Diablo 14% San Andreas 10% Hayward	26% Mt. Diablo 12% Greenville	26% Mt. Diablo 14% Greenville 12% Calaveras 11% Midway-Black Butte	27% Mt. Diablo 16% Greenville 14% Midway-Black Butte
975 YEARS	23% San Andreas 12% Hayward 10% CRSB North	22% San Andreas 12% Hayward	23% San Andreas 12% Hayward	22% San Andreas 12% Hayward	22% San Andreas 12% Hayward	18% San Andreas 14% Mt. Diablo 11% Hayward	20% San Andreas 14% Mt. Diablo 11% Hayward	18% San Andreas 16% Mt. Diablo 10% Hayward	22% Mt. Diablo 13% San Andreas	29% Mt. Diablo 13% Greenville 11% West Tracy-Midland	29% Mt. Diablo 14% Greenville 12% Midway-Black Butte 12% West Tracy-Midland	29% Mt. Diablo 17% Greenville 17% Midway-Black Butte 11% West Tracy-Midland
2,475 YEARS	24% San Andreas 11% Hayward 10% CRSB North	24% San Andreas 11% Hayward	25% San Andreas 11% Hayward	23% San Andreas 11% Hayward	23% San Andreas 11% Hayward	18% San Andreas 14% Mt. Diablo 11% West Tracy-Midland 10% Hayward	21% San Andreas 15% Mt. Diablo 10% Hayward	18% San Andreas 18% Mt. Diablo	24% Mt. Diablo 12% San Andreas	32% Mt. Diablo 17% West Tracy-Midland 13% Greenville	32% Mt. Diablo 18% West Tracy-Midland 14% Greenville 13% Midway-Black Butte	31% Mt. Diablo 19% Midway-Black Butte 17% West Tracy-Midland 16% Greenville

Note: Seismic sources that contribute 10 percent or greater to the PGA hazard are listed.

Table 4. Magnitude and Distance Deaggregation

PERIOD (SEC)	INTAKE NO. 3		INTAKE NO. 5		TWIN CITIES		NEW HOPE		CANAL RANCH		BOULDIN		KING ISLAND		LOWER ROBERTS		BACON		SOUTHERN FOREBAY NORTH		SOUTHERN FOREBAY SOUTH		JONES CONNECTION		
	PGA	1.0 Sec SA	PGA	1.0 Sec SA	PGA	1.0 Sec SA	PGA	1.0 Sec SA	PGA	1.0 Sec SA	PGA	1.0 Sec SA	PGA	1.0 Sec SA	PGA	1.0 Sec SA	PGA	1.0 Sec SA	PGA	1.0 Sec SA	PGA	1.0 Sec SA	PGA	1.0 Sec SA	
144-YEAR RETURN PERIOD																									
Modal M	6.3	7.1	6.7	7.1	6.7	7.7	6.7	6.7	6.7	6.7	6.5	6.5	6.5	7.1	6.7	6.7	6.7	6.7	6.7	6.7	6.7	6.7	6.7	6.7	6.7
Modal R_{RUP} (km)	45	85	55	85	65	118	55	55	55	55	35	35	45	75	35	35	25	25	18	18	18	18	13	13	
Mean M	6.7	7.0	6.7	6.9	6.7	7.0	6.7	6.9	6.7	6.9	6.6	6.9	6.6	6.9	6.6	6.9	6.6	6.8	6.5	6.8	6.5	6.8	6.5	6.7	
Mean R_{RUP} (km)	67.7	88.4	65.6	86.1	69.2	89.5	64.8	83.9	64.6	83.9	53.0	68.9	58.0	75.4	52.8	69.1	42.2	55.7	31.9	42.9	28.8	39.2	25.7	35.3	
200-YEAR RETURN PERIOD																									
Modal M	6.3	7.9	6.7	7.1	6.9	7.7	6.7	6.7	6.7	6.7	6.5	6.5	6.5	6.7	6.7	6.7	6.7	6.7	6.7	6.7	6.7	6.7	6.7	6.7	
Modal R_{RUP} (km)	45	118	55	85	65	118	55	55	55	55	35	35	45	45	35	35	25	25	18	18	18	18	13	13	
Mean M	6.7	7.0	6.6	7.0	6.7	7.0	6.6	6.9	6.6	6.9	6.6	6.9	6.6	6.9	6.6	6.9	6.6	6.8	6.6	6.8	6.5	6.8	6.5	6.8	
Mean R_{RUP} (km)	65.7	87.1	63.5	84.8	67.1	88.2	62.6	82.4	62.5	82.5	51.0	67.1	56.1	73.8	50.8	67.4	40.1	53.7	29.6	40.2	26.5	36.3	23.2	32.2	
475-YEAR RETURN PERIOD																									
Modal M	6.3	7.9	6.5	7.9	6.9	7.9	6.7	6.7	6.7	6.9	6.5	6.7	6.5	6.7	6.7	6.7	6.7	6.7	6.7	6.7	6.7	6.7	6.7	6.7	
Modal R_{RUP} (km)	45	118	35	118	65	118	55	55	55	55	35	35	45	45	35	35	25	25	18	18	18	18	13	13	
Mean M	6.6	7.0	6.6	7.0	6.6	7.0	6.6	7.0	6.6	7.0	6.6	6.9	6.6	7.0	6.6	6.9	6.6	6.9	6.6	6.8	6.5	6.8	6.5	6.8	
Mean R_{RUP} (km)	60.2	84.2	8.0	81.7	61.0	85.2	56.7	78.8	56.4	78.9	45.7	63.1	51.5	70.2	45.9	63.3	35.3	48.6	24.8	33.9	21.6	29.6	18.3	2.2	
975-YEAR RETURN PERIOD																									
Modal M	6.3	7.9	6.5	7.9	6.5	7.9	6.7	6.7	6.7	8.1	6.5	6.7	6.7	6.7	6.7	6.7	6.7	6.7	6.7	6.9	6.7	6.7	6.7	6.7	
Modal R_{RUP} (km)	45	118	35	118	45	118	55	55	55	105	35	35	45	45	35	35	25	25	18	18	18	18	13	13	
Mean M	6.5	7.1	6.5	7.0	6.5	7.1	6.5	7.0	6.9	7.0	6.6	6.9	6.6	7.0	6.6	6.9	6.6	6.9	6.6	6.8	6.5	6.8	6.6	6.8	
Mean R_{RUP} (km)	55.1	82.2	53.1	79.5	55.3	82.8	51.1	75.9	50.6	76.1	41.6	59.9	47.1	67.7	42.5	60.5	32.0	45.0	21.7	29.6	18.6	25.1	15.6	20.9	
2,475-YEAR RETURN PERIOD																									
Modal M	6.3	7.9	6.5	7.9	6.5	7.9	6.7	6.7	6.9	8.1	6.5	6.7	6.7	6.7	6.7	6.7	6.7	6.7	6.7	6.9	6.7	6.7	6.7	6.7	
Modal R_{RUP} (km)	45	118	35	118	45	118	55	55	55	105	35	35	45	45	35	35	25	25	18	18	18	18	13	13	
Mean M	6.4	7.1	6.4	7.1	6.4	7.1	6.4	7.0	6.4	7.0	6.5	6.9	6.5	7.0	6.6	7.0	6.6	6.9	6.6	6.8	6.6	6.8	6.6	6.8	
Mean R_{RUP} (km)	48.0	79.5	46.0	76.8	46.8	79.3	42.7	71.4	42.0	71.9	36.2	56.0	42.1	64.8	38.4	57.4	28.4	40.8	18.7	24.9	15.8	20.5	13.3	16.7	

Table 5. Mean Uniform Hazard Spectra

(a) Intake No. 3

PERIOD (SEC)	144-YEAR RETURN PERIOD, SA (g)	200-YEAR RETURN PERIOD, SA (g)	475-YEAR RETURN PERIOD, SA (g)	975-YEAR RETURN PERIOD, SA (g)	2,475-YEAR RETURN PERIOD, SA (g)
0.01	0.12	0.14	0.19	0.23	0.30
0.03	0.13	0.15	0.20	0.25	0.33
0.05	0.15	0.17	0.24	0.30	0.39
0.075	0.20	0.22	0.31	0.39	0.51
0.10	0.24	0.27	0.37	0.47	0.62
0.15	0.29	0.33	0.44	0.56	0.74
0.20	0.31	0.35	0.47	0.59	0.78
0.25	0.31	0.35	0.48	0.60	0.79
0.30	0.31	0.35	0.48	0.60	0.79
0.40	0.29	0.33	0.45	0.56	0.74
0.50	0.27	0.31	0.42	0.53	0.70
0.60	0.24	0.28	0.38	0.48	0.63
0.75	0.21	0.24	0.33	0.42	0.56
1.0	0.16	0.19	0.26	0.33	0.43
1.5	0.11	0.13	0.18	0.23	0.30
2.0	0.072	0.090	0.13	0.17	0.22
3.0	0.039	0.047	0.075	0.11	0.14
4.0	0.027	0.031	0.047	0.067	0.10
5.0	0.020	0.023	0.034	0.047	0.070
7.5	0.013	0.015	0.022	0.029	0.042
10.0	0.009	0.011	0.015	0.020	0.029

(b) Intake No. 5

PERIOD (SEC)	144-YEAR RETURN PERIOD, SA (g)	200-YEAR RETURN PERIOD, SA (g)	475-YEAR RETURN PERIOD, SA (g)	975-YEAR RETURN PERIOD, SA (g)	2,475-YEAR RETURN PERIOD, SA (g)
0.01	0.12	0.14	0.18	0.23	0.30
0.03	0.13	0.14	0.20	0.25	0.32
0.05	0.15	0.17	0.24	0.30	0.39
0.075	0.20	0.22	0.30	0.39	0.51
0.10	0.23	0.27	0.36	0.46	0.61
0.15	0.28	0.32	0.43	0.55	0.73
0.20	0.30	0.34	0.46	0.58	0.76
0.25	0.30	0.34	0.46	0.58	0.76
0.30	0.30	0.33	0.45	0.57	0.75
0.40	0.27	0.31	0.42	0.52	0.69
0.50	0.25	0.28	0.38	0.48	0.63
0.60	0.22	0.25	0.34	0.43	0.57
0.75	0.19	0.21	0.29	0.37	0.49
1.0	0.14	0.16	0.23	0.29	0.38
1.5	0.094	0.11	0.15	0.19	0.26
2.0	0.058	0.071	0.11	0.14	0.19
3.0	0.033	0.039	0.061	0.087	0.12
4.0	0.023	0.027	0.040	0.054	0.082
5.0	0.018	0.021	0.029	0.039	0.058
7.5	0.012	0.014	0.019	0.025	0.036
10.0	0.008	0.010	0.014	0.018	0.026

(c) Twin Cities

PERIOD (SEC)	144-YEAR RETURN PERIOD, SA (g)	200-YEAR RETURN PERIOD, SA (g)	475-YEAR RETURN PERIOD, SA (g)	975-YEAR RETURN PERIOD, SA (g)	2,475-YEAR RETURN PERIOD, SA (g)
0.01	0.12	0.14	0.19	0.23	0.31
0.03	0.13	0.15	0.20	0.25	0.33
0.05	0.15	0.17	0.24	0.30	0.39
0.075	0.20	0.22	0.30	0.38	0.51
0.10	0.24	0.27	0.37	0.46	0.62
0.15	0.29	0.33	0.45	0.56	0.74
0.20	0.32	0.36	0.48	0.60	0.79
0.25	0.32	0.37	0.49	0.62	0.81
0.30	0.33	0.37	0.50	0.62	0.82
0.40	0.31	0.35	0.47	0.59	0.77
0.50	0.29	0.33	0.44	0.56	0.74
0.60	0.26	0.29	0.40	0.50	0.67
0.75	0.23	0.26	0.35	0.45	0.59
1.0	0.17	0.20	0.27	0.35	0.46
1.5	0.12	0.14	0.19	0.24	0.32
2.0	0.081	0.10	0.14	0.18	0.24
3.0	0.043	0.052	0.084	0.11	0.15
4.0	0.029	0.034	0.052	0.073	0.11
5.0	0.022	0.025	0.037	0.051	0.077
7.5	0.014	0.016	0.023	0.031	0.046
10.0	0.010	0.011	0.016	0.022	0.031

(d) New Hope

PERIOD (SEC)	144-YEAR RETURN PERIOD, SA (g)	200-YEAR RETURN PERIOD, SA (g)	475-YEAR RETURN PERIOD, SA (g)	975-YEAR RETURN PERIOD, SA (g)	2,475-YEAR RETURN PERIOD, SA (g)
0.01	0.13	0.15	0.20	0.25	0.32
0.03	0.14	0.16	0.21	0.26	0.34
0.05	0.16	0.18	0.25	0.31	0.41
0.075	0.21	0.24	0.32	0.40	0.54
0.10	0.25	0.28	0.39	0.49	0.65
0.15	0.31	0.35	0.47	0.59	0.78
0.20	0.33	0.37	0.51	0.63	0.83
0.25	0.34	0.38	0.52	0.65	0.85
0.30	0.34	0.38	0.52	0.65	0.85
0.40	0.31	0.35	0.48	0.60	0.80
0.50	0.29	0.33	0.45	0.56	0.75
0.60	0.26	0.30	0.40	0.51	0.67
0.75	0.22	0.26	0.35	0.44	0.59
1.0	0.17	0.20	0.27	0.34	0.45
1.5	0.11	0.13	0.18	0.23	0.31
2.0	0.075	0.094	0.13	0.17	0.23
3.0	0.040	0.048	0.077	0.11	0.15
4.0	0.027	0.032	0.048	0.067	0.10
5.0	0.021	0.024	0.035	0.047	0.071
7.5	0.013	0.015	0.022	0.029	0.043
10.0	0.010	0.011	0.016	0.021	0.030

(e) Canal Ranch

PERIOD (SEC)	144-YEAR RETURN PERIOD, SA (g)	200-YEAR RETURN PERIOD, SA (g)	475-YEAR RETURN PERIOD, SA (g)	975-YEAR RETURN PERIOD, SA (g)	2,475-YEAR RETURN PERIOD, SA (g)
0.01	0.12	0.14	0.19	0.24	0.31
0.03	0.13	0.15	0.20	0.25	0.33
0.05	0.16	0.18	0.24	0.31	0.41
0.075	0.20	0.23	0.31	0.40	0.53
0.10	0.24	0.28	0.38	0.48	0.63
0.15	0.30	0.33	0.45	0.57	0.75
0.20	0.32	0.36	0.48	0.61	0.80
0.25	0.32	0.36	0.49	0.61	0.81
0.30	0.32	0.36	0.48	0.61	0.80
0.40	0.29	0.33	0.45	0.56	0.75
0.50	0.27	0.30	0.41	0.52	0.69
0.60	0.24	0.27	0.37	0.46	0.62
0.75	0.21	0.23	0.32	0.40	0.54
1.0	0.16	0.18	0.25	0.31	0.42
1.5	0.11	0.12	0.17	0.21	0.28
2.0	0.066	0.081	0.12	0.15	0.21
3.0	0.037	0.043	0.068	0.10	0.13
4.0	0.025	0.029	0.043	0.060	0.092
5.0	0.019	0.022	0.032	0.043	0.064
7.5	0.013	0.014	0.020	0.027	0.039
10.0	0.009	0.011	0.015	0.019	0.028

(f) Bouldin

PERIOD (SEC)	144-YEAR RETURN PERIOD, SA (g)	200-YEAR RETURN PERIOD, SA (g)	475-YEAR RETURN PERIOD, SA (g)	975-YEAR RETURN PERIOD, SA (g)	2,475-YEAR RETURN PERIOD, SA (g)
0.01	0.16	0.18	0.25	0.31	0.40
0.03	0.17	0.19	0.26	0.32	0.42
0.05	0.20	0.23	0.30	0.38	0.49
0.075	0.26	0.29	0.39	0.49	0.64
0.10	0.31	0.35	0.47	0.59	0.77
0.15	0.39	0.44	0.59	0.73	0.94
0.20	0.42	0.48	0.64	0.80	1.03
0.25	0.44	0.49	0.66	0.82	1.07
0.30	0.44	0.50	0.66	0.83	1.08
0.40	0.41	0.46	0.63	0.78	1.03
0.50	0.38	0.43	0.58	0.73	0.97
0.60	0.34	0.39	0.52	0.66	0.87
0.75	0.29	0.33	0.46	0.58	0.76
1.0	0.23	0.26	0.35	0.45	0.60
1.5	0.15	0.17	0.24	0.31	0.41
2.0	0.11	0.12	0.17	0.22	0.30
3.0	0.056	0.069	0.11	0.14	0.19
4.0	0.035	0.042	0.066	0.10	0.13
5.0	0.026	0.030	0.045	0.063	0.10
7.5	0.016	0.018	0.027	0.036	0.054
10.0	0.011	0.013	0.018	0.024	0.036

(g) King Island

PERIOD (SEC)	144-YEAR RETURN PERIOD, SA (g)	200-YEAR RETURN PERIOD, SA (g)	475-YEAR RETURN PERIOD, SA (g)	975-YEAR RETURN PERIOD, SA (g)	2,475-YEAR RETURN PERIOD, SA (g)
0.01	0.15	0.17	0.23	0.28	0.36
0.03	0.16	0.18	0.24	0.29	0.38
0.05	0.18	0.21	0.28	0.34	0.45
0.075	0.23	0.27	0.36	0.44	0.58
0.10	0.29	0.32	0.43	0.54	0.70
0.15	0.36	0.40	0.54	0.67	0.86
0.20	0.39	0.44	0.59	0.73	0.94
0.25	0.41	0.46	0.61	0.76	0.98
0.30	0.41	0.46	0.61	0.76	0.99
0.40	0.38	0.43	0.58	0.72	0.94
0.50	0.35	0.40	0.54	0.68	0.89
0.60	0.32	0.36	0.49	0.61	0.80
0.75	0.28	0.31	0.42	0.53	0.70
1.0	0.21	0.24	0.33	0.42	0.55
1.5	0.14	0.16	0.23	0.29	0.38
2.0	0.10	0.12	0.16	0.21	0.28
3.0	0.052	0.063	0.10	0.13	0.18
4.0	0.033	0.039	0.061	0.088	0.12
5.0	0.024	0.028	0.042	0.059	0.091
7.5	0.015	0.018	0.026	0.035	0.052
10.0	0.011	0.012	0.018	0.024	0.035

(h) Lower Roberts

PERIOD (SEC)	PERIOD (SEC)	144-YEAR RETURN PERIOD, SA (g)	200-YEAR RETURN PERIOD, SA (g)	475-YEAR RETURN PERIOD, SA (g)	975-YEAR RETURN PERIOD, SA (g)
0.01	0.17	0.19	0.25	0.31	0.39
0.03	0.17	0.19	0.26	0.32	0.41
0.05	0.20	0.23	0.30	0.37	0.48
0.075	0.26	0.29	0.38	0.48	0.62
0.10	0.31	0.35	0.47	0.59	0.75
0.15	0.40	0.45	0.59	0.73	0.93
0.20	0.44	0.50	0.66	0.81	1.03
0.25	0.46	0.52	0.69	0.85	1.08
0.30	0.47	0.53	0.70	0.86	1.11
0.40	0.44	0.50	0.67	0.83	1.08
0.50	0.42	0.47	0.63	0.79	1.03
0.60	0.37	0.42	0.57	0.71	0.93
0.75	0.32	0.37	0.50	0.63	0.82
1.0	0.25	0.29	0.40	0.50	0.66
1.5	0.17	0.20	0.27	0.35	0.46
2.0	0.12	0.14	0.20	0.26	0.34
3.0	0.068	0.084	0.12	0.16	0.22
4.0	0.041	0.049	0.079	0.11	0.15
5.0	0.029	0.034	0.052	0.074	0.11
7.5	0.017	0.020	0.030	0.041	0.062
10.0	0.012	0.014	0.020	0.027	0.040

(i) Bacon

PERIOD (SEC)	144-YEAR RETURN PERIOD, SA (g)	200-YEAR RETURN PERIOD, SA (g)	475-YEAR RETURN PERIOD, SA (g)	975-YEAR RETURN PERIOD, SA (g)	2,475-YEAR RETURN PERIOD, SA (g)
0.01	0.20	0.23	0.30	0.37	0.48
0.03	0.21	0.23	0.31	0.39	0.50
0.05	0.24	0.27	0.36	0.45	0.57
0.075	0.30	0.34	0.46	0.57	0.74
0.10	0.37	0.42	0.57	0.70	0.90
0.15	0.47	0.53	0.71	0.87	1.11
0.20	0.53	0.59	0.78	0.97	1.23
0.25	0.55	0.62	0.82	1.02	1.30
0.30	0.56	0.63	0.84	1.05	1.34
0.40	0.53	0.60	0.81	1.02	1.32
0.50	0.50	0.56	0.76	0.96	1.25
0.60	0.44	0.50	0.68	0.86	1.14
0.75	0.38	0.44	0.60	0.76	1.01
1.0	0.30	0.35	0.48	0.61	0.82
1.5	0.21	0.24	0.33	0.42	0.57
2.0	0.15	0.17	0.24	0.31	0.42
3.0	0.087	0.11	0.15	0.19	0.26
4.0	0.050	0.061	0.10	0.13	0.18
5.0	0.034	0.040	0.064	0.094	0.13
7.5	0.019	0.023	0.034	0.047	0.073
10.0	0.013	0.015	0.022	0.030	0.045

(j) Southern Forebay North

PERIOD (SEC)	144-YEAR RETURN PERIOD, SA (g)	200-YEAR RETURN PERIOD, SA (g)	475-YEAR RETURN PERIOD, SA (g)	975-YEAR RETURN PERIOD, SA (g)	2,475-YEAR RETURN PERIOD, SA (g)
0.01	0.24	0.27	0.37	0.46	0.60
0.03	0.25	0.28	0.38	0.47	0.62
0.05	0.28	0.32	0.43	0.54	0.70
0.075	0.36	0.41	0.55	0.69	0.89
0.10	0.44	0.50	0.67	0.83	1.08
0.15	0.55	0.62	0.83	1.03	1.32
0.20	0.61	0.69	0.92	1.14	1.45
0.25	0.64	0.72	0.97	1.20	1.54
0.30	0.65	0.74	1.00	1.25	1.62
0.40	0.61	0.70	0.97	1.22	1.61
0.50	0.57	0.66	0.91	1.16	1.54
0.60	0.51	0.59	0.82	1.05	1.40
0.75	0.44	0.51	0.72	0.93	1.25
1.0	0.35	0.41	0.57	0.75	1.03
1.5	0.24	0.28	0.39	0.52	0.72
2.0	0.17	0.20	0.29	0.38	0.53
3.0	0.11	0.12	0.18	0.23	0.32
4.0	0.060	0.075	0.12	0.16	0.22
5.0	0.040	0.048	0.079	0.11	0.16
7.5	0.021	0.025	0.038	0.054	0.085
10.0	0.014	0.016	0.024	0.033	0.049

(k) Southern Forebay South

PERIOD (SEC)	144-YEAR RETURN PERIOD, SA (g)	200-YEAR RETURN PERIOD, SA (g)	475-YEAR RETURN PERIOD, SA (g)	975-YEAR RETURN PERIOD, SA (g)	2,475-YEAR RETURN PERIOD, SA (g)
0.01	0.25	0.28	0.39	0.50	0.65
0.03	0.26	0.30	0.41	0.51	0.67
0.05	0.30	0.34	0.46	0.59	0.77
0.075	0.38	0.43	0.59	0.74	0.98
0.10	0.46	0.52	0.71	0.90	1.18
0.15	0.58	0.65	0.88	1.10	1.42
0.20	0.63	0.72	0.98	1.21	1.56
0.25	0.66	0.75	1.02	1.28	1.66
0.30	0.66	0.76	1.04	1.32	1.73
0.40	0.62	0.71	1.00	1.28	1.71
0.50	0.58	0.66	0.94	1.21	1.63
0.60	0.51	0.59	0.84	1.09	1.48
0.75	0.44	0.51	0.73	0.96	1.31
1.0	0.35	0.40	0.58	0.77	1.07
1.5	0.23	0.27	0.39	0.52	0.73
2.0	0.17	0.19	0.29	0.38	0.53
3.0	0.10	0.12	0.17	0.23	0.32
4.0	0.058	0.072	0.12	0.15	0.21
5.0	0.038	0.046	0.077	0.11	0.15
7.5	0.021	0.024	0.037	0.052	0.082
10.0	0.014	0.016	0.023	0.031	0.047

(I) Jones Connection

PERIOD (SEC)	144-YEAR RETURN PERIOD, SA (g)	200-YEAR RETURN PERIOD, SA (g)	475-YEAR RETURN PERIOD, SA (g)	975-YEAR RETURN PERIOD, SA (g)	2,475-YEAR RETURN PERIOD, SA (g)
0.01	0.25	0.29	0.41	0.54	0.72
0.03	0.27	0.31	0.44	0.57	0.76
0.05	0.31	0.36	0.52	0.67	0.90
0.075	0.40	0.46	0.66	0.85	1.14
0.10	0.48	0.56	0.79	1.02	1.36
0.15	0.59	0.68	0.95	1.22	1.61
0.20	0.63	0.73	1.03	1.32	1.76
0.25	0.64	0.74	1.05	1.36	1.83
0.30	0.63	0.73	1.05	1.36	1.86
0.40	0.57	0.66	0.97	1.27	1.76
0.50	0.52	0.60	0.88	1.17	1.63
0.60	0.45	0.53	0.78	1.04	1.45
0.75	0.39	0.45	0.66	0.89	1.26
1.0	0.29	0.34	0.51	0.69	0.98
1.5	0.19	0.22	0.33	0.44	0.63
2.0	0.13	0.16	0.23	0.31	0.44
3.0	0.073	0.092	0.14	0.19	0.26
4.0	0.044	0.054	0.091	0.12	0.17
5.0	0.031	0.037	0.059	0.086	0.13
7.5	0.017	0.020	0.030	0.041	0.063
10.0	0.012	0.014	0.019	0.026	0.038

**Table 6. DSHA Input Parameters
(a) Intake No. 3**

INPUT PARAMETER	INPUT PARAMETER DEFINITION	MIDLAND	PITTSBURG- KIRBY HILLS	SAN ANDREAS
<i>M</i>	Moment magnitude	6.6	6.9	8.0
<i>R_{RUP}</i>	Closest distance to coseismic rupture (km)	20.5	39.3	113.8
<i>R_{JB}</i>	Closest distance to surface projection of coseismic rupture (km)	20.5	39.3	113.8
<i>R_X</i>	Horizontal distance from top of rupture measured perpendicular to fault strike (km)	-20.5	39.3	113.8
<i>R_{y0}</i>	The horizontal distance off the end of the rupture measured parallel to strike (km)	0	0	0
<i>U</i>	Unspecified-mechanism factor: 1 for unspecified; 0 otherwise	0	0	0
<i>F_{RV}</i>	Reverse-faulting factor: 0 for strike slip, normal, normal-oblique; 1 for reverse, reverse-oblique and thrust	1	0	0
<i>F_N</i>	Normal-faulting factor: 0 for strike slip, reverse, reverse-oblique, thrust and normal-oblique; 1 for normal	0	0	0
<i>F_{HW}</i>	Hanging-wall factor: 1 for site on down-dip side of top of rupture; 0 otherwise	0	0	0
<i>Z_{TOR}</i>	Depth to top of coseismic rupture (km)	1	0	0
<i>Dip</i>	Average dip of rupture plane (degrees)	70	80	90
<i>V_{S30}</i>	The average shear-wave velocity (m/s) over a subsurface depth of 30 m	370	370	370
<i>F_{Measured}</i>	0 = inferred, 1 = measured	0	0	0
<i>Z_{HYP}</i>	Hypocentral depth from the earthquake	Default	Default	Default
<i>Z_{1.0}</i>	Depth to Vs=1 km/sec	0.7	0.7	0.7
<i>Z_{2.5}</i>	Depth to Vs=2.5 km/sec	3.5	3.5	3.5
<i>W</i>	Fault rupture width (km)	14.9	20.3	13
<i>Region</i>	Specific Regions considered in the models	California	California	California

(b) Intake No. 5

INPUT PARAMETER	INPUT PARAMETER DEFINITION	MIDLAND	PITTSBURG-KIRBY HILLS	SAN ANDREAS
<i>M</i>	Moment magnitude	6.6	6.9	8.0
<i>R_{RUP}</i>	Closest distance to coseismic rupture (km)	18.1	37.0	111.3
<i>R_{JB}</i>	Closest distance to surface projection of coseismic rupture (km)	18.1	37.0	111.3
<i>R_X</i>	Horizontal distance from top of rupture measured perpendicular to fault strike (km)	-18.1	37.0	111.3
<i>R_{y0}</i>	The horizontal distance off the end of the rupture measured parallel to strike (km)	0	0	0
<i>U</i>	Unspecified-mechanism factor: 1 for unspecified; 0 otherwise	0	0	0
<i>F_{RV}</i>	Reverse-faulting factor: 0 for strike slip, normal, normal-oblique; 1 for reverse, reverse-oblique and thrust	1	0	0
<i>F_N</i>	Normal-faulting factor: 0 for strike slip, reverse, reverse-oblique, thrust and normal-oblique; 1 for normal	0	0	0
<i>F_{HW}</i>	Hanging-wall factor: 1 for site on down-dip side of top of rupture; 0 otherwise	0	0	0
<i>Z_{TOR}</i>	Depth to top of coseismic rupture (km)	1	0	0
<i>Dip</i>	Average dip of rupture plane (degrees)	70	80	90
<i>V_{S30}</i>	The average shear-wave velocity (m/s) over a subsurface depth of 30 m	400	400	400
<i>F_{Measured}</i>	0 = inferred, 1 = measured	0	0	0
<i>Z_{HYP}</i>	Hypocentral depth from the earthquake	Default	Default	Default
<i>Z_{1.0}</i>	Depth to Vs=1 km/sec	0.7	0.7	0.7
<i>Z_{2.5}</i>	Depth to Vs=2.5 km/sec	3.5	3.5	3.5
<i>W</i>	Fault rupture width (km)	14.9	20.3	13
<i>Region</i>	Specific Regions considered in the models	California	California	California

(c) Twin Cities

INPUT PARAMETER	INPUT PARAMETER DEFINITION	MIDLAND	PITTSBURG-KIRBY HILLS	SAN ANDREAS
<i>M</i>	Moment magnitude	6.6	6.9	8.0
<i>R_{RUP}</i>	Closest distance to coseismic rupture (km)	21.8	42.0	114.4
<i>R_{JB}</i>	Closest distance to surface projection of coseismic rupture (km)	21.8	42.0	114.4
<i>R_X</i>	Horizontal distance from top of rupture measured perpendicular to fault strike (km)	-21.8	42.0	114.4
<i>R_{y0}</i>	The horizontal distance off the end of the rupture measured parallel to strike (km)	0	0	0
<i>U</i>	Unspecified-mechanism factor: 1 for unspecified; 0 otherwise	0	0	0
<i>F_{RV}</i>	Reverse-faulting factor: 0 for strike slip, normal, normal-oblique; 1 for reverse, reverse-oblique and thrust	1	0	0
<i>F_N</i>	Normal-faulting factor: 0 for strike slip, reverse, reverse-oblique, thrust and normal-oblique; 1 for normal	0	0	0
<i>F_{HW}</i>	Hanging-wall factor: 1 for site on down-dip side of top of rupture; 0 otherwise	0	0	0
<i>Z_{TOR}</i>	Depth to top of coseismic rupture (km)	1	0	0
<i>Dip</i>	Average dip of rupture plane (degrees)	70	80	90
<i>V_{S30}</i>	The average shear-wave velocity (m/s) over a subsurface depth of 30 m	340	340	340
<i>F_{Measured}</i>	0 = inferred, 1 = measured	0	0	0
<i>Z_{HYP}</i>	Hypocentral depth from the earthquake	Default	Default	Default
<i>Z_{1.0}</i>	Depth to Vs=1 km/sec	0.7	0.7	0.7
<i>Z_{2.5}</i>	Depth to Vs=2.5 km/sec	3.5	3.5	3.5
<i>W</i>	Fault rupture width (km)	14.9	20.3	13
<i>Region</i>	Specific Regions considered in the models	California	California	California

(d) New Hope

INPUT PARAMETER	INPUT PARAMETER DEFINITION	MIDLAND	PITTSBURG-KIRBY HILLS	SAN ANDREAS
<i>M</i>	Moment magnitude	6.6	6.9	8.0
<i>R_{RUP}</i>	Closest distance to coseismic rupture (km)	17.4	39.2	109.0
<i>R_{JB}</i>	Closest distance to surface projection of coseismic rupture (km)	17.4	39.2	109.0
<i>R_X</i>	Horizontal distance from top of rupture measured perpendicular to fault strike (km)	-17.4	39.2	109.0
<i>R_{y0}</i>	The horizontal distance off the end of the rupture measured parallel to strike (km)	0	0	0
<i>U</i>	Unspecified-mechanism factor: 1 for unspecified; 0 otherwise	0	0	0
<i>F_{RV}</i>	Reverse-faulting factor: 0 for strike slip, normal, normal-oblique; 1 for reverse, reverse-oblique and thrust	1	0	0
<i>F_N</i>	Normal-faulting factor: 0 for strike slip, reverse, reverse-oblique, thrust and normal-oblique; 1 for normal	0	0	0
<i>F_{HW}</i>	Hanging-wall factor: 1 for site on down-dip side of top of rupture; 0 otherwise	0	0	0
<i>Z_{TOR}</i>	Depth to top of coseismic rupture (km)	1	0	0
<i>Dip</i>	Average dip of rupture plane (degrees)	70	80	90
<i>V_{S30}</i>	The average shear-wave velocity (m/s) over a subsurface depth of 30 m	340	340	340
<i>F_{Measured}</i>	0 = inferred, 1 = measured	0	0	0
<i>Z_{HYP}</i>	Hypocentral depth from the earthquake	Default	Default	Default
<i>Z_{1.0}</i>	Depth to Vs=1 km/sec	0.7	0.7	0.7
<i>Z_{2.5}</i>	Depth to Vs=2.5 km/sec	4.0	4.0	4.0
<i>W</i>	Fault rupture width (km)	14.9	20.3	13
<i>Region</i>	Specific Regions considered in the models	California	California	California

(e) Canal Ranch

INPUT PARAMETER	INPUT PARAMETER DEFINITION	MIDLAND	WEST TRACY	SAN ANDREAS
<i>M</i>	Moment magnitude	6.6	6.9	8.0
<i>R_{RUP}</i>	Closest distance to coseismic rupture (km)	18.7	39.4	107.9
<i>R_{JB}</i>	Closest distance to surface projection of coseismic rupture (km)	18.7	39.4	107.9
<i>R_X</i>	Horizontal distance from top of rupture measured perpendicular to fault strike (km)	-18.7	39.4	107.9
<i>R_{Y0}</i>	The horizontal distance off the end of the rupture measured parallel to strike (km)	0	NA (Footwall)	0
<i>U</i>	Unspecified-mechanism factor: 1 for unspecified; 0 otherwise	0	0	0
<i>F_{RV}</i>	Reverse-faulting factor: 0 for strike slip, normal, normal-oblique; 1 for reverse, reverse-oblique and thrust	1	1	0
<i>F_N</i>	Normal-faulting factor: 0 for strike slip, reverse, reverse-oblique, thrust and normal-oblique; 1 for normal	0	0	0
<i>F_{HW}</i>	Hanging-wall factor: 1 for site on down-dip side of top of rupture; 0 otherwise	0	0	0
<i>Z_{TOR}</i>	Depth to top of coseismic rupture (km)	1	0	0
<i>Dip</i>	Average dip of rupture plane (degrees)	70	70	90
<i>V_{S30}</i>	The average shear-wave velocity (m/s) over a subsurface depth of 30 m	370	370	370
<i>F_{Measured}</i>	0 = inferred, 1 = measured	0	0	0
<i>Z_{HYP}</i>	Hypocentral depth from the earthquake	Default	Default	Default
<i>Z_{1.0}</i>	Depth to Vs=1 km/sec	0.7	0.7	0.7
<i>Z_{2.5}</i>	Depth to Vs=2.5 km/sec	3.5	3.5	3.5
<i>W</i>	Fault rupture width (km)	14.9	20.3	13
<i>Region</i>	Specific Regions considered in the models	California	California	California

(f) Bouldin

INPUT PARAMETER	INPUT PARAMETER DEFINITION	MIDLAND	WEST TRACY	GREENVILLE	MT. DIABLO (ZTOR = 1 KM)	MT. DIABLO (ZTOR = 5 KM)	SAN ANDREAS
<i>M</i>	Moment magnitude	6.6	6.9	7.0	7.0	7.0	8.0
<i>R_{RUP}</i>	Closest distance to coseismic rupture (km)	9.3	27.5	38.1	37.2	37.7	109.0
<i>R_{JB}</i>	Closest distance to surface projection of coseismic rupture (km)	9.3	27.5	38.1	33.4	34.0	109.0
<i>R_X</i>	Horizontal distance from top of rupture measured perpendicular to fault strike (km)	-9.3	-27.5	38.1	48.4	45.0	109.0
<i>R_{YD}</i>	The horizontal distance off the end of the rupture measured parallel to strike (km)	0	NA (Footwall)	NA (Vertical SS)	0	0	0
<i>U</i>	Unspecified-mechanism factor: 1 for unspecified; 0 otherwise	0	0	0	0	0	0
<i>F_{RV}</i>	Reverse-faulting factor: 0 for strike slip, normal, normal-oblique; 1 for reverse, reverse-oblique and thrust	1	1	0	1	1	0
<i>F_N</i>	Normal-faulting factor: 0 for strike slip, reverse, reverse-oblique, thrust and normal-oblique; 1 for normal	0	0	0	0	0	0
<i>F_{HW}</i>	Hanging-wall factor: 1 for site on down-dip side of top of rupture; 0 otherwise	0	0	0	1	1	0
<i>Z_{TOR}</i>	Depth to top of coseismic rupture (km)	1	0	0	1	1	0
<i>Dip</i>	Average dip of rupture plane (degrees)	70	70	90	45	45	90
<i>V_{S30}</i>	The average shear-wave velocity (m/s) over a subsurface depth of 30 m	290	290	290	290	290	290
<i>F_{Measured}</i>	0 = inferred, 1 = measured	0	0	0	0	0	0
<i>Z_{HYP}</i>	Hypocentral depth from the earthquake	Default	Default	Default	Default	Default	Default
<i>Z_{1.0}</i>	Depth to Vs=1 km/sec	0.7	0.7	0.7	0.7	0.7	0.7
<i>Z_{2.5}</i>	Depth to Vs=2.5 km/sec	4.0	4.0	4.0	4.0	4.0	3.5
<i>W</i>	Fault rupture width (km)	14.9	20.3	15.0	21.2	15.6	13
<i>Region</i>	Specific Regions considered in the models	California	California	California	California	California	California

(g) King Island

INPUT PARAMETER	INPUT PARAMETER DEFINITION	MIDLAND	WEST TRACY	GREENVILLE	MT. DIABLO (ZTOR = 1 KM)	MT. DIABLO (ZTOR = 5 KM)	ORESTIMBA (ZTOR = 1 KM)	ORESTIMBA (ZTOR = 3 KM)	SAN ANDREAS
M	Moment magnitude	6.6	6.9	7.0	7.0	7.0	7.1	7.1	8.0
R_{RUP}	Closest distance to coseismic rupture (km)	17.3	27.6	41.3	39.4	39.5	46.6	47.2	100.9
R_{JB}	Closest distance to surface projection of coseismic rupture (km)	17.3	27.6	41.3	35.9	36.1	46.6	47.1	100.9
R_X	Horizontal distance from top of rupture measured perpendicular to fault strike (km)	-17.3	-27.6	41.3	50.9	47.1	NA (Footwall)	NA (Footwall)	100.9
R_{Y0}	The horizontal distance off the end of the rupture measured parallel to strike (km)	0	0	0	0	0	NA (Footwall)	NA (Footwall)	0
U	Unspecified-mechanism factor: 1 for unspecified; 0 otherwise	0	0	0	0	0	0	0	0
F_{RV}	Reverse-faulting factor: 0 for strike slip, normal, normal-oblique; 1 for reverse, reverse-oblique and thrust	1	1	0	1	1	1	1	0
F_N	Normal-faulting factor: 0 for strike slip, reverse, reverse-oblique, thrust and normal-oblique; 1 for normal	0	0	0	0	0	0	0	0
F_{HW}	Hanging-wall factor: 1 for site on down-dip side of top of rupture; 0 otherwise	0	0	0	1	1	0	0	0
Z_{TOR}	Depth to top of coseismic rupture (km)	1	0	0	1	5	1	3	0
Dip	Average dip of rupture plane (degrees)	70	70	90	45	45	45	45	90
V_{S30}	The average shear-wave velocity (m/s) over a subsurface depth of 30 m	290	290	290	290	290	290	290	290
F_{Measured}	0 = inferred, 1 = measured	0	0	0	0	0	0	0	0
Z_{HYP}	Hypocentral depth from the earthquake	Default	Default	Default	Default	Default	Default	Default	Default
Z_{1.0}	Depth to Vs=1 km/sec	0.7	0.7	0.7	0.7	0.7	0.7	0.7	0.7
Z_{2.5}	Depth to Vs=2.5 km/sec	4.0	4.0	4.0	4.0	4.0	4.0	4.0	3.5
W	Fault rupture width (km)	14.9	20.3	15.0	21.2	15.6	19.8	14.1	13
Region	Specific Regions considered in the models	CA	CA	CA	CA	CA	CA	CA	CA

(h) Lower Roberts

INPUT PARAMETER	INPUT PARAMETER DEFINITION	MIDLAND	WEST TRACY	GREENVILLE	Mt. DIABLO (ZTOR = 1 KM)	Mt. DIABLO (ZTOR = 5 KM)	ORESTIMBA (ZTOR = 1 KM)	ORESTIMBA (ZTOR = 3 KM)	SAN ANDREAS
M	Moment magnitude	6.6	6.9	7.0	7.0	7.0	7.1	7.1	8.0
R_{RUP}	Closest distance to coseismic rupture (km)	16.0	21.0	36.5	33.9	34.2	39.5	40.1	96.0
R_{JB}	Closest distance to surface projection of coseismic rupture (km)	16.0	21.0	36.5	29.9	30.2	39.5	40.0	96.0
R_X	Horizontal distance from top of rupture measured perpendicular to fault strike (km)	-16.0	-21.0	36.5	44.9	41.2	NA (Footwall)	NA (Footwall)	96.0
R_{yo}	The horizontal distance off the end of the rupture measured parallel to strike (km)	0	0	0	0	0	NA (Footwall)	NA (Footwall)	0
U	Unspecified-mechanism factor: 1 for unspecified; 0 otherwise	0	0	0	0	0	0	0	0
F_{RV}	Reverse-faulting factor: 0 for strike slip, normal, normal-oblique; 1 for reverse, reverse-oblique and thrust	1	1	0	1	1	1	1	0
F_N	Normal-faulting factor: 0 for strike slip, reverse, reverse-oblique, thrust and normal-oblique; 1 for normal	0	0	0	0	0	0	0	0
F_{HW}	Hanging-wall factor: 1 for site on down-dip side of top of rupture; 0 otherwise	0	0	0	1	1	0	0	0
Z_{TOR}	Depth to top of coseismic rupture (km)	1	0	0	1	5	1	3	0
Dip	Average dip of rupture plane (degrees)	70	70	90	45	45	45	45	90
V_{S30}	The average shear-wave velocity (m/s) over a subsurface depth of 30 m	250	250	250	250	250	250	250	250
F_{Measured}	0 = inferred, 1 = measured	0	0	0	0	0	0	0	0
Z_{HYP}	Hypocentral depth from the earthquake	Default	Default	Default	Default	Default	Default	Default	Default
Z_{1.0}	Depth to Vs=1 km/sec	0.7	0.7	0.7	0.7	0.7	0.7	0.7	0.7
Z_{2.5}	Depth to Vs=2.5 km/sec	4.0	4.0	4.0	4.0	4.0	4.0	4.0	3.5
W	Fault rupture width (km)	14.9	20.3	15.0	21.2	15.6	19.8	14.1	13
Region	Specific Regions considered in the models	CA	CA	CA	CA	CA	CA	CA	CA

(i) Bacon

INPUT PARAMETER	INPUT PARAMETER DEFINITION	MIDLAND	WEST TRACY	GREENVILLE	MT. DIABLO (ZTOR = 1 KM)	MT. DIABLO (ZTOR = 5 KM)	SAN ANDREAS
M	Moment magnitude	6.6	6.9	7.0	7.0	7.0	8.0
R_{RUP}	Closest distance to coseismic rupture (km)	5.8	12.6	26.6	26.4	26.5	86.4
R_{JB}	Closest distance to surface projection of coseismic rupture (km)	5.8	12.6	26.6	20.9	21.0	86.4
R_X	Horizontal distance from top of rupture measured perpendicular to fault strike (km)	-5.8	-12.6	26.6	35.9	32.0	86.4
R_{yo}	The horizontal distance off the end of the rupture measured parallel to strike (km)	0	0	0	0	0	0
U	Unspecified-mechanism factor: 1 for unspecified; 0 otherwise	0	0	0	0	0	0
F_{RV}	Reverse-faulting factor: 0 for strike slip, normal, normal-oblique; 1 for reverse, reverse-oblique and thrust	1	1	0	1	1	0
F_N	Normal-faulting factor: 0 for strike slip, reverse, reverse-oblique, thrust and normal-oblique; 1 for normal	0	0	0	0	0	0
F_{HW}	Hanging-wall factor: 1 for site on down-dip side of top of rupture; 0 otherwise	0	0	0	1	1	0
Z_{TOR}	Depth to top of coseismic rupture (km)	1	0	0	1	5	0
Dip	Average dip of rupture plane (degrees)	70	70	90	45	45	90
V_{S30}	The average shear-wave velocity (m/s) over a subsurface depth of 30 m	240	240	240	240	240	240
F_{Measured}	0 = inferred, 1 = measured	0	0	0	0	0	0
Z_{HYP}	Hypocentral depth from the earthquake	Default	Default	Default	Default	Default	Default
Z_{1.0}	Depth to Vs=1 km/sec	0.7	0.7	0.7	0.7	0.7	0.7
Z_{2.5}	Depth to Vs=2.5 km/sec	4.0	4.0	4.0	4.0	4.0	3.5
W	Fault rupture width (km)	14.9	20.3	15.0	21.2	15.6	13
Region	Specific Regions considered in the models	California	California	California	California	California	California

(j) Southern Forebay North

INPUT PARAMETER	INPUT PARAMETER DEFINITION	WEST TRACY	SAN ANDREAS
<i>M</i>	Moment magnitude	6.9	8.0
<i>R_{RUP}</i>	Closest distance to coseismic rupture (km)	2.8	77.5
<i>R_{JB}</i>	Closest distance to surface projection of coseismic rupture (km)	2.8	77.5
<i>R_X</i>	Horizontal distance from top of rupture measured perpendicular to fault strike (km)	-2.8	77.5
<i>R_{y0}</i>	The horizontal distance off the end of the rupture measured parallel to strike (km)	0	0
<i>U</i>	Unspecified-mechanism factor: 1 for unspecified; 0 otherwise	0	0
<i>F_{RV}</i>	Reverse-faulting factor: 0 for strike slip, normal, normal-oblique; 1 for reverse, reverse-oblique and thrust	1	0
<i>F_N</i>	Normal-faulting factor: 0 for strike slip, reverse, reverse-oblique, thrust and normal-oblique; 1 for normal	0	0
<i>F_{HW}</i>	Hanging-wall factor: 1 for site on down-dip side of top of rupture; 0 otherwise	0	0
<i>Z_{TOR}</i>	Depth to top of coseismic rupture (km)	0	0
<i>Dip</i>	Average dip of rupture plane (degrees)	70	90
<i>V_{S30}</i>	The average shear-wave velocity (m/s) over a subsurface depth of 30 m	240	240
<i>F_{Measured}</i>	0 = inferred, 1 = measured	0	0
<i>Z_{HYP}</i>	Hypocentral depth from the earthquake	Default	Default
<i>Z_{1.0}</i>	Depth to Vs=1 km/sec	0.7	0.7
<i>Z_{2.5}</i>	Depth to Vs=2.5 km/sec	4.0	3.5
<i>W</i>	Fault rupture width (km)	20.3	13
<i>Region</i>	Specific Regions considered in the models	California	California

(k) Southern Forebay South

INPUT PARAMETER	INPUT PARAMETER DEFINITION	WEST TRACY	SAN ANDREAS
<i>M</i>	Moment magnitude	6.9	8.0
<i>R_{RUP}</i>	Closest distance to coseismic rupture (km)	0.21	75.3
<i>R_{JB}</i>	Closest distance to surface projection of coseismic rupture (km)	0.21	75.3
<i>R_X</i>	Horizontal distance from top of rupture measured perpendicular to fault strike (km)	-0.21	75.3
<i>R_{Y0}</i>	The horizontal distance off the end of the rupture measured parallel to strike (km)	0	0
<i>U</i>	Unspecified-mechanism factor: 1 for unspecified; 0 otherwise	0	0
<i>F_{RV}</i>	Reverse-faulting factor: 0 for strike slip, normal, normal-oblique; 1 for reverse, reverse-oblique and thrust	1	0
<i>F_N</i>	Normal-faulting factor: 0 for strike slip, reverse, reverse-oblique, thrust and normal-oblique; 1 for normal	0	0
<i>F_{HW}</i>	Hanging-wall factor: 1 for site on down-dip side of top of rupture; 0 otherwise	0	0
<i>Z_{TOR}</i>	Depth to top of coseismic rupture (km)	0	0
<i>Dip</i>	Average dip of rupture plane (degrees)	70	90
<i>V_{S30}</i>	The average shear-wave velocity (m/s) over a subsurface depth of 30 m	260	260
<i>F_{Measured}</i>	0 = inferred, 1 = measured	0	0
<i>Z_{HYP}</i>	Hypocentral depth from the earthquake	Default	Default
<i>Z_{1.0}</i>	Depth to Vs=1 km/sec	0.7	0.7
<i>Z_{2.5}</i>	Depth to Vs=2.5 km/sec	4.0	3.5
<i>W</i>	Fault rupture width (km)	20.3	13
<i>Region</i>	Specific Regions considered in the models	California	California

(I) Jones Connection

INPUT PARAMETER	INPUT PARAMETER DEFINITION	WEST TRACY	SAN ANDREAS
<i>M</i>	Moment magnitude	6.9	8.0
<i>R_{RUP}</i>	Closest distance to coseismic rupture (km)	2.0	73.2
<i>R_{JB}</i>	Closest distance to surface projection of coseismic rupture (km)	0.0	73.2
<i>R_X</i>	Horizontal distance from top of rupture measured perpendicular to fault strike (km)	2.1	73.2
<i>R_{y0}</i>	The horizontal distance off the end of the rupture measured parallel to strike (km)	0	0
<i>U</i>	Unspecified-mechanism factor: 1 for unspecified; 0 otherwise	0	0
<i>F_{RV}</i>	Reverse-faulting factor: 0 for strike slip, normal, normal-oblique; 1 for reverse, reverse-oblique and thrust	1	0
<i>F_N</i>	Normal-faulting factor: 0 for strike slip, reverse, reverse-oblique, thrust and normal-oblique; 1 for normal	0	0
<i>F_{HW}</i>	Hanging-wall factor: 1 for site on down-dip side of top of rupture; 0 otherwise	1	0
<i>Z_{TOR}</i>	Depth to top of coseismic rupture (km)	0	0
<i>Dip</i>	Average dip of rupture plane (degrees)	70	90
<i>V_{S30}</i>	The average shear-wave velocity (m/s) over a subsurface depth of 30 m	340	340
<i>F_{Measured}</i>	0 = inferred, 1 = measured	0	0
<i>Z_{HYP}</i>	Hypocentral depth from the earthquake	Default	Default
<i>Z_{1.0}</i>	Depth to Vs=1 km/sec	0.7	0.7
<i>Z_{2.5}</i>	Depth to Vs=2.5 km/sec	4.0	3.5
<i>W</i>	Fault rupture width (km)	20.3	13
<i>Region</i>	Specific Regions considered in the models	California	California

**Table 7. DSHA Results
 (a) Intake No. 3**

PERIOD (SEC)	MIDLAND				SAN ANDREAS				ENVELOPE			
	MEDIAN (g)	69 TH PERCENTILE (g)	84 TH PERCENTILE (g)	95 TH PERCENTILE (g)	MEDIAN (g)	69 TH PERCENTILE (g)	84 TH PERCENTILE (g)	95 TH PERCENTILE (g)	MEDIAN (g)	69 TH PERCENTILE (g)	84 TH PERCENTILE (g)	95 TH PERCENTILE (g)
0.01	0.17	0.23	0.30	0.44	0.069	0.093	0.12	0.18	0.17	0.23	0.30	0.44
0.02	0.17	0.23	0.30	0.44	0.069	0.092	0.12	0.18	0.17	0.23	0.30	0.44
0.03	0.18	0.24	0.32	0.47	0.071	0.10	0.13	0.19	0.18	0.24	0.32	0.47
0.05	0.21	0.28	0.38	0.56	0.076	0.10	0.14	0.22	0.21	0.28	0.38	0.56
0.075	0.26	0.35	0.48	0.71	0.086	0.12	0.17	0.25	0.26	0.35	0.48	0.71
0.10	0.31	0.42	0.58	0.86	0.10	0.13	0.19	0.29	0.31	0.42	0.58	0.86
0.15	0.39	0.53	0.71	1.05	0.11	0.16	0.21	0.33	0.39	0.53	0.71	1.05
0.20	0.42	0.57	0.77	1.14	0.13	0.17	0.24	0.36	0.42	0.57	0.77	1.14
0.25	0.42	0.57	0.78	1.16	0.14	0.20	0.27	0.40	0.42	0.57	0.78	1.16
0.30	0.41	0.56	0.77	1.15	0.16	0.21	0.30	0.44	0.41	0.56	0.77	1.15
0.40	0.37	0.50	0.70	1.05	0.16	0.21	0.30	0.45	0.37	0.50	0.70	1.05
0.50	0.32	0.45	0.62	0.95	0.15	0.21	0.29	0.45	0.32	0.45	0.62	0.95
0.75	0.23	0.32	0.46	0.71	0.12	0.18	0.25	0.40	0.23	0.32	0.46	0.71
1.0	0.18	0.25	0.36	0.56	0.10	0.14	0.20	0.32	0.18	0.25	0.36	0.56
1.5	0.11	0.16	0.23	0.36	0.076	0.11	0.16	0.25	0.11	0.16	0.23	0.36
2.0	0.079	0.11	0.16	0.25	0.059	0.084	0.12	0.19	0.079	0.11	0.16	0.25
3.0	0.046	0.066	0.094	0.15	0.042	0.060	0.086	0.14	0.046	0.066	0.094	0.15
4.0	0.030	0.042	0.060	0.095	0.033	0.047	0.066	0.10	0.033	0.047	0.066	0.10
5.0	0.020	0.029	0.041	0.064	0.026	0.036	0.052	0.082	0.026	0.036	0.052	0.082
7.5	0.009	0.013	0.019	0.030	0.017	0.024	0.034	0.053	0.017	0.024	0.034	0.053
10.0	0.005	0.007	0.010	0.016	0.010	0.015	0.021	0.032	0.010	0.015	0.021	0.032

(b) Intake No. 5

PERIOD (SEC)	MIDLAND				SAN ANDREAS				ENVELOPE			
	MEDIAN (g)	69 TH PERCENTILE (g)	84 TH PERCENTILE (g)	95 TH PERCENTILE (g)	MEDIAN (g)	69 TH PERCENTILE (g)	84 TH PERCENTILE (g)	95 TH PERCENTILE (g)	MEDIAN (g)	69 TH PERCENTILE (g)	84 TH PERCENTILE (g)	95 TH PERCENTILE (g)
0.01	0.19	0.25	0.33	0.48	0.073	0.10	0.13	0.19	0.19	0.25	0.33	0.48
0.02	0.19	0.25	0.33	0.48	0.072	0.10	0.13	0.19	0.19	0.25	0.33	0.48
0.03	0.20	0.26	0.35	0.51	0.074	0.10	0.13	0.20	0.20	0.26	0.35	0.51
0.05	0.23	0.31	0.42	0.62	0.081	0.11	0.15	0.23	0.23	0.31	0.42	0.62
0.075	0.29	0.39	0.54	0.80	0.094	0.13	0.18	0.27	0.29	0.39	0.54	0.80
0.10	0.34	0.47	0.64	0.96	0.11	0.15	0.20	0.31	0.34	0.47	0.64	0.96
0.15	0.43	0.58	0.78	1.16	0.13	0.17	0.24	0.36	0.43	0.58	0.78	1.16
0.20	0.46	0.62	0.84	1.25	0.14	0.19	0.27	0.40	0.46	0.62	0.84	1.25
0.25	0.46	0.62	0.85	1.26	0.15	0.21	0.29	0.43	0.46	0.62	0.85	1.26
0.30	0.44	0.61	0.83	1.25	0.16	0.22	0.30	0.46	0.44	0.61	0.83	1.25
0.40	0.39	0.54	0.74	1.13	0.16	0.22	0.30	0.45	0.39	0.54	0.74	1.13
0.50	0.34	0.47	0.66	1.01	0.15	0.21	0.29	0.44	0.34	0.47	0.66	1.01
0.75	0.24	0.34	0.48	0.76	0.12	0.17	0.24	0.38	0.24	0.34	0.48	0.76
1.0	0.19	0.27	0.38	0.60	0.10	0.14	0.20	0.31	0.19	0.27	0.38	0.60
1.5	0.12	0.17	0.24	0.38	0.073	0.10	0.15	0.24	0.12	0.17	0.24	0.38
2.0	0.083	0.12	0.17	0.27	0.057	0.082	0.12	0.19	0.083	0.12	0.17	0.27
3.0	0.049	0.070	0.10	0.16	0.042	0.059	0.085	0.13	0.049	0.07	0.10	0.16
4.0	0.032	0.045	0.064	0.10	0.032	0.046	0.065	0.10	0.032	0.046	0.065	0.10
5.0	0.021	0.031	0.043	0.069	0.025	0.036	0.050	0.079	0.025	0.036	0.050	0.079
7.5	0.010	0.014	0.020	0.032	0.016	0.023	0.032	0.050	0.016	0.023	0.032	0.050
10.0	0.005	0.008	0.011	0.017	0.010	0.014	0.020	0.031	0.010	0.014	0.020	0.031

(c) Twin Cities

PERIOD (SEC)	MIDLAND				SAN ANDREAS				ENVELOPE			
	MEDIAN (g)	69 TH PERCENTILE (g)	84 TH PERCENTILE (g)	95 TH PERCENTILE (g)	MEDIAN (g)	69 TH PERCENTILE (g)	84 TH PERCENTILE (g)	95 TH PERCENTILE (g)	MEDIAN (g)	69 TH PERCENTILE (g)	84 TH PERCENTILE (g)	95 TH PERCENTILE (g)
0.01	0.16	0.22	0.29	0.42	0.07	0.10	0.13	0.20	0.16	0.22	0.29	0.42
0.02	0.16	0.22	0.29	0.42	0.07	0.10	0.13	0.19	0.16	0.22	0.29	0.42
0.03	0.17	0.23	0.30	0.44	0.07	0.10	0.14	0.20	0.17	0.23	0.30	0.44
0.05	0.20	0.26	0.36	0.52	0.08	0.11	0.15	0.23	0.20	0.26	0.36	0.52
0.075	0.25	0.33	0.45	0.67	0.09	0.13	0.18	0.27	0.25	0.33	0.45	0.67
0.10	0.30	0.40	0.55	0.81	0.11	0.15	0.20	0.31	0.30	0.40	0.55	0.81
0.15	0.37	0.50	0.68	1.00	0.13	0.18	0.24	0.37	0.37	0.50	0.68	1.00
0.20	0.41	0.55	0.74	1.09	0.15	0.20	0.28	0.41	0.41	0.55	0.74	1.09
0.25	0.41	0.56	0.76	1.12	0.16	0.22	0.30	0.46	0.41	0.56	0.76	1.12
0.30	0.41	0.55	0.75	1.12	0.17	0.24	0.32	0.49	0.41	0.55	0.75	1.12
0.40	0.36	0.50	0.69	1.04	0.17	0.24	0.33	0.50	0.36	0.50	0.69	1.04
0.50	0.32	0.45	0.62	0.95	0.16	0.23	0.32	0.49	0.32	0.45	0.62	0.95
0.75	0.23	0.32	0.46	0.72	0.13	0.19	0.27	0.42	0.23	0.32	0.46	0.72
1.0	0.18	0.25	0.36	0.56	0.11	0.15	0.22	0.34	0.18	0.25	0.36	0.56
1.5	0.11	0.16	0.23	0.37	0.082	0.12	0.17	0.26	0.11	0.16	0.23	0.37
2.0	0.080	0.11	0.16	0.26	0.064	0.092	0.13	0.21	0.080	0.11	0.16	0.26
3.0	0.047	0.067	0.10	0.15	0.046	0.066	0.094	0.15	0.047	0.067	0.10	0.15
4.0	0.030	0.043	0.061	0.10	0.036	0.051	0.072	0.11	0.036	0.051	0.072	0.11
5.0	0.020	0.029	0.041	0.065	0.027	0.039	0.055	0.087	0.027	0.039	0.055	0.087
7.5	0.009	0.013	0.019	0.030	0.017	0.024	0.035	0.054	0.017	0.024	0.035	0.054
10.0	0.005	0.007	0.010	0.016	0.011	0.015	0.022	0.033	0.011	0.015	0.022	0.033

¹ Midland fault scenario is largest deterministic ground motions at all spectral periods.

(d) New Hope

PERIOD (SEC)	MIDLAND				SAN ANDREAS				ENVELOPE			
	MEDIAN (g)	69 TH PERCENTILE (g)	84 TH PERCENTILE (g)	95 TH PERCENTILE (g)	MEDIAN (g)	69 TH PERCENTILE (g)	84 TH PERCENTILE (g)	95 TH PERCENTILE (g)	MEDIAN (g)	69 TH PERCENTILE (g)	84 TH PERCENTILE (g)	95 TH PERCENTILE (g)
0.01	0.20	0.26	0.34	0.47	0.080	0.11	0.14	0.21	0.20	0.27	0.35	0.51
0.02	0.20	0.26	0.34	0.47	0.079	0.11	0.14	0.21	0.20	0.27	0.36	0.51
0.03	0.21	0.27	0.35	0.49	0.080	0.11	0.15	0.21	0.21	0.28	0.37	0.54
0.05	0.24	0.31	0.41	0.58	0.087	0.12	0.16	0.24	0.24	0.32	0.43	0.63
0.075	0.30	0.39	0.52	0.74	0.10	0.14	0.19	0.29	0.30	0.40	0.54	0.80
0.10	0.36	0.47	0.62	0.89	0.12	0.16	0.22	0.33	0.36	0.49	0.66	0.97
0.15	0.45	0.59	0.77	1.10	0.14	0.19	0.26	0.40	0.45	0.61	0.82	1.20
0.20	0.49	0.65	0.85	1.20	0.16	0.22	0.30	0.44	0.49	0.66	0.89	1.31
0.25	0.50	0.66	0.87	1.23	0.17	0.24	0.33	0.49	0.50	0.68	0.92	1.35
0.30	0.50	0.66	0.87	1.24	0.18	0.25	0.35	0.52	0.50	0.67	0.92	1.36
0.40	0.45	0.60	0.80	1.16	0.18	0.25	0.35	0.53	0.45	0.61	0.84	1.27
0.50	0.40	0.53	0.72	1.05	0.17	0.24	0.34	0.52	0.40	0.55	0.76	1.17
0.75	0.29	0.39	0.53	0.80	0.14	0.20	0.28	0.44	0.29	0.40	0.57	0.89
1.0	0.22	0.30	0.42	0.63	0.11	0.16	0.23	0.36	0.22	0.32	0.45	0.71
1.5	0.14	0.20	0.27	0.41	0.087	0.12	0.18	0.28	0.14	0.20	0.29	0.46
2.0	0.10	0.14	0.19	0.29	0.068	0.10	0.14	0.22	0.10	0.14	0.20	0.32
3.0	0.059	0.081	0.11	0.17	0.049	0.070	0.10	0.16	0.059	0.084	0.12	0.19
4.0	0.038	0.052	0.071	0.11	0.038	0.053	0.076	0.12	0.038	0.053	0.076	0.12
5.0	0.025	0.035	0.048	0.072	0.029	0.041	0.058	0.092	0.029	0.041	0.058	0.092
7.5	0.012	0.016	0.022	0.033	0.018	0.026	0.037	0.057	0.018	0.026	0.037	0.057
10.0	0.006	0.009	0.012	0.017	0.011	0.016	0.023	0.035	0.011	0.016	0.023	0.035

(e) Canal Ranch

PERIOD (SEC)	MIDLAND				SAN ANDREAS				ENVELOPE			
	MEDIAN (g)	69 TH PERCENTILE (g)	84 TH PERCENTILE (g)	95 TH PERCENTILE (g)	MEDIAN (g)	69 TH PERCENTILE (g)	84 TH PERCENTILE (g)	95 TH PERCENTILE (g)	MEDIAN (g)	69 TH PERCENTILE (g)	84 TH PERCENTILE (g)	95 TH PERCENTILE (g)
0.01	0.18	0.25	0.33	0.47	0.078	0.10	0.14	0.20	0.18	0.25	0.33	0.47
0.02	0.18	0.25	0.33	0.48	0.077	0.10	0.14	0.20	0.18	0.25	0.33	0.48
0.03	0.19	0.26	0.35	0.50	0.079	0.11	0.14	0.21	0.19	0.26	0.35	0.50
0.05	0.22	0.30	0.41	0.60	0.086	0.12	0.16	0.24	0.22	0.30	0.41	0.60
0.075	0.28	0.38	0.52	0.77	0.10	0.14	0.19	0.29	0.28	0.38	0.52	0.77
0.10	0.34	0.46	0.62	0.93	0.11	0.16	0.22	0.33	0.34	0.46	0.62	0.93
0.15	0.42	0.57	0.77	1.13	0.14	0.19	0.26	0.39	0.42	0.57	0.77	1.13
0.20	0.45	0.61	0.83	1.22	0.15	0.21	0.29	0.43	0.45	0.61	0.83	1.22
0.25	0.46	0.62	0.84	1.25	0.17	0.23	0.31	0.47	0.46	0.62	0.84	1.25
0.30	0.45	0.61	0.83	1.24	0.17	0.24	0.33	0.50	0.45	0.61	0.83	1.24
0.40	0.40	0.55	0.75	1.14	0.17	0.24	0.33	0.50	0.40	0.55	0.75	1.14
0.50	0.35	0.48	0.67	1.03	0.16	0.23	0.32	0.48	0.35	0.48	0.67	1.03
0.75	0.25	0.35	0.50	0.78	0.13	0.19	0.26	0.41	0.25	0.35	0.50	0.78
1.0	0.19	0.27	0.39	0.61	0.11	0.15	0.21	0.34	0.19	0.27	0.39	0.61
1.5	0.12	0.17	0.25	0.39	0.080	0.11	0.16	0.26	0.12	0.17	0.25	0.39
2.0	0.086	0.12	0.18	0.28	0.063	0.089	0.13	0.20	0.086	0.12	0.18	0.28
3.0	0.050	0.072	0.10	0.16	0.045	0.064	0.092	0.15	0.050	0.072	0.10	0.16
4.0	0.032	0.046	0.066	0.10	0.035	0.049	0.070	0.11	0.035	0.049	0.070	0.11
5.0	0.022	0.031	0.045	0.070	0.027	0.038	0.054	0.086	0.027	0.038	0.054	0.086
7.5	0.010	0.014	0.021	0.032	0.017	0.024	0.034	0.054	0.017	0.024	0.034	0.054
10.0	0.006	0.008	0.011	0.017	0.011	0.015	0.021	0.033	0.011	0.015	0.021	0.033

(f) Bouldin

PERIOD (SEC)	MIDLAND				SAN ANDREAS				ENVELOPE			
	MEDIAN (g)	69 TH PERCENTILE (g)	84 TH PERCENTILE (g)	95 TH PERCENTILE (g)	MEDIAN (g)	69 TH PERCENTILE (g)	84 TH PERCENTILE (g)	95 TH PERCENTILE (g)	MEDIAN (g)	69 TH PERCENTILE (g)	84 TH PERCENTILE (g)	95 TH PERCENTILE (g)
0.01	0.32	0.41	0.54	0.77	0.084	0.11	0.15	0.22	0.32	0.41	0.54	0.77
0.02	0.32	0.41	0.54	0.77	0.083	0.11	0.15	0.22	0.32	0.41	0.54	0.77
0.03	0.32	0.42	0.55	0.79	0.084	0.11	0.15	0.22	0.32	0.42	0.55	0.79
0.05	0.35	0.47	0.62	0.88	0.090	0.12	0.16	0.24	0.35	0.47	0.62	0.88
0.075	0.43	0.57	0.76	1.09	0.10	0.14	0.19	0.29	0.43	0.57	0.76	1.09
0.10	0.51	0.68	0.90	1.30	0.12	0.17	0.23	0.34	0.51	0.68	0.90	1.30
0.15	0.65	0.85	1.12	1.60	0.15	0.20	0.28	0.41	0.65	0.85	1.12	1.60
0.20	0.73	0.96	1.26	1.79	0.17	0.23	0.32	0.47	0.73	0.96	1.26	1.79
0.25	0.77	1.02	1.35	1.93	0.19	0.26	0.35	0.52	0.77	1.02	1.35	1.93
0.30	0.78	1.05	1.40	2.02	0.20	0.28	0.38	0.56	0.78	1.05	1.40	2.02
0.40	0.74	1.00	1.35	2.00	0.20	0.28	0.38	0.58	0.74	1.00	1.35	2.00
0.50	0.67	0.92	1.27	1.91	0.20	0.27	0.38	0.58	0.67	0.92	1.27	1.91
0.75	0.51	0.71	1.00	1.54	0.16	0.23	0.32	0.50	0.51	0.71	1.00	1.54
1.0	0.41	0.57	0.81	1.27	0.13	0.19	0.26	0.41	0.41	0.57	0.81	1.27
1.5	0.27	0.38	0.54	0.85	0.10	0.14	0.20	0.32	0.27	0.38	0.54	0.85
2.0	0.19	0.27	0.39	0.61	0.078	0.11	0.16	0.25	0.19	0.27	0.39	0.61
3.0	0.11	0.16	0.23	0.36	0.056	0.080	0.11	0.18	0.11	0.16	0.23	0.36
4.0	0.071	0.10	0.14	0.23	0.043	0.061	0.086	0.14	0.071	0.10	0.14	0.23
5.0	0.047	0.067	0.10	0.15	0.033	0.046	0.066	0.10	0.047	0.067	0.10	0.15
7.5	0.021	0.029	0.042	0.066	0.020	0.029	0.041	0.064	0.021	0.029	0.042	0.066
10.0	0.011	0.016	0.022	0.034	0.012	0.018	0.025	0.039	0.012	0.018	0.025	0.039

(g) King Island

PERIOD (SEC)	MIDLAND				SAN ANDREAS				ENVELOPE			
	MEDIAN (g)	69 TH PERCENTILE (g)	84 TH PERCENTILE (g)	95 TH PERCENTILE (g)	MEDIAN (g)	69 TH PERCENTILE (g)	84 TH PERCENTILE (g)	95 TH PERCENTILE (g)	MEDIAN (g)	69 TH PERCENTILE (g)	84 TH PERCENTILE (g)	95 TH PERCENTILE (g)
0.01	0.21	0.36	0.27	0.51	0.092	0.16	0.12	0.24	0.21	0.36	0.27	0.51
0.02	0.21	0.36	0.27	0.52	0.091	0.16	0.12	0.23	0.21	0.36	0.27	0.52
0.03	0.21	0.37	0.28	0.53	0.091	0.16	0.12	0.24	0.21	0.37	0.28	0.53
0.05	0.24	0.42	0.32	0.61	0.10	0.18	0.13	0.27	0.24	0.42	0.32	0.61
0.075	0.29	0.53	0.39	0.77	0.11	0.21	0.16	0.32	0.29	0.53	0.39	0.77
0.10	0.36	0.64	0.48	0.93	0.13	0.25	0.18	0.38	0.36	0.64	0.48	0.93
0.15	0.45	0.80	0.60	1.16	0.16	0.30	0.22	0.45	0.45	0.80	0.60	1.16
0.20	0.51	0.89	0.67	1.29	0.19	0.35	0.25	0.51	0.51	0.89	0.67	1.29
0.25	0.53	0.94	0.70	1.36	0.21	0.38	0.28	0.57	0.53	0.94	0.70	1.36
0.30	0.53	0.95	0.71	1.40	0.22	0.41	0.30	0.61	0.53	0.95	0.71	1.40
0.40	0.48	0.90	0.66	1.34	0.22	0.41	0.30	0.62	0.48	0.90	0.66	1.34
0.50	0.43	0.82	0.60	1.25	0.21	0.40	0.29	0.62	0.43	0.82	0.60	1.25
0.75	0.32	0.63	0.45	0.97	0.17	0.34	0.24	0.53	0.32	0.63	0.45	0.97
1.0	0.25	0.50	0.35	0.79	0.14	0.28	0.20	0.44	0.25	0.50	0.35	0.79
1.5	0.16	0.33	0.23	0.52	0.11	0.21	0.15	0.34	0.16	0.33	0.23	0.52
2.0	0.12	0.23	0.16	0.37	0.083	0.17	0.12	0.27	0.12	0.23	0.16	0.37
3.0	0.067	0.14	0.10	0.22	0.059	0.12	0.085	0.19	0.067	0.14	0.10	0.22
4.0	0.043	0.087	0.061	0.14	0.045	0.091	0.064	0.14	0.045	0.091	0.064	0.14
5.0	0.029	0.058	0.041	0.092	0.035	0.070	0.049	0.11	0.035	0.070	0.049	0.11
7.5	0.013	0.026	0.018	0.041	0.021	0.043	0.030	0.067	0.021	0.043	0.030	0.067
10.0	0.007	0.014	0.010	0.021	0.013	0.026	0.018	0.041	0.013	0.026	0.018	0.041

(h) Lower Roberts

PERIOD (SEC)	MIDLAND				WEST TRACY				SAN ANDREAS				ENVELOPE			
	MEDIAN (g)	69 TH PERC. (g)	84 TH PERC. (g)	95 TH PERC. (g)	MEDIAN (g)	69 TH PERC. (g)	84 TH PERC. (g)	95 TH PERC. (g)	MEDIAN (g)	69 TH PERC. (g)	84 TH PERC. (g)	95 TH PERC. (g)	MEDIAN (g)	69 TH PERC. (g)	84 TH PERC. (g)	95 TH PERC. (g)
0.01	0.22	0.29	0.38	0.53	0.20	0.26	0.35	0.49	0.10	0.13	0.18	0.25	0.22	0.29	0.38	0.53
0.02	0.22	0.29	0.38	0.53	0.20	0.26	0.34	0.49	0.10	0.13	0.18	0.25	0.22	0.29	0.38	0.53
0.03	0.22	0.29	0.38	0.54	0.20	0.27	0.35	0.50	0.10	0.13	0.18	0.26	0.22	0.29	0.38	0.54
0.05	0.24	0.32	0.43	0.61	0.22	0.29	0.39	0.56	0.11	0.14	0.19	0.28	0.24	0.32	0.43	0.61
0.075	0.30	0.40	0.53	0.76	0.27	0.36	0.48	0.70	0.12	0.17	0.23	0.34	0.30	0.40	0.53	0.76
0.10	0.37	0.48	0.64	0.93	0.33	0.44	0.59	0.85	0.14	0.20	0.27	0.40	0.37	0.48	0.64	0.93
0.15	0.47	0.62	0.82	1.16	0.42	0.56	0.74	1.06	0.18	0.24	0.33	0.49	0.47	0.62	0.82	1.16
0.20	0.53	0.70	0.92	1.30	0.48	0.64	0.84	1.19	0.21	0.28	0.38	0.55	0.53	0.70	0.92	1.30
0.25	0.57	0.74	0.98	1.39	0.51	0.68	0.89	1.28	0.24	0.32	0.42	0.62	0.57	0.74	0.98	1.39
0.30	0.57	0.76	1.01	1.46	0.52	0.70	0.93	1.34	0.25	0.34	0.46	0.67	0.57	0.76	1.01	1.46
0.40	0.54	0.73	0.98	1.44	0.50	0.67	0.90	1.33	0.25	0.34	0.47	0.69	0.54	0.73	0.98	1.44
0.50	0.49	0.67	0.91	1.36	0.46	0.62	0.85	1.26	0.24	0.33	0.46	0.69	0.49	0.67	0.91	1.36
0.75	0.37	0.51	0.71	1.09	0.35	0.48	0.67	1.03	0.20	0.28	0.39	0.60	0.37	0.51	0.71	1.09
1.0	0.29	0.41	0.58	0.91	0.28	0.39	0.55	0.86	0.16	0.23	0.32	0.51	0.29	0.41	0.58	0.91
1.5	0.20	0.28	0.40	0.62	0.19	0.27	0.39	0.61	0.12	0.18	0.25	0.40	0.20	0.28	0.40	0.62
2.0	0.14	0.20	0.29	0.45	0.14	0.20	0.29	0.45	0.10	0.14	0.20	0.31	0.14	0.20	0.29	0.45
3.0	0.083	0.12	0.17	0.27	0.087	0.12	0.18	0.28	0.070	0.10	0.14	0.23	0.087	0.12	0.18	0.28
4.0	0.052	0.075	0.11	0.17	0.058	0.082	0.12	0.18	0.053	0.076	0.11	0.17	0.058	0.082	0.12	0.18
5.0	0.035	0.050	0.071	0.11	0.040	0.056	0.080	0.13	0.040	0.058	0.082	0.13	0.040	0.058	0.082	0.13
7.5	0.015	0.022	0.031	0.049	0.019	0.027	0.038	0.059	0.024	0.035	0.049	0.077	0.024	0.035	0.049	0.077
10.0	0.008	0.011	0.016	0.025	0.010	0.014	0.020	0.031	0.015	0.021	0.029	0.046	0.015	0.021	0.029	0.046

Perc. = Percentile

(i) Bacon

PERIOD (SEC)	MIDLAND				SAN ANDREAS				ENVELOPE			
	MEDIAN (g)	69 TH PERCENTILE (g)	84 TH PERCENTILE (g)	95 TH PERCENTILE (g)	MEDIAN (g)	69 TH PERCENTILE (g)	84 TH PERCENTILE (g)	95 TH PERCENTILE (g)	MEDIAN (g)	69 TH PERCENTILE (g)	84 TH PERCENTILE (g)	95 TH PERCENTILE (g)
0.01	0.38	0.49	0.63	0.87	0.11	0.15	0.20	0.28	0.38	0.49	0.63	0.87
0.02	0.38	0.49	0.63	0.88	0.11	0.15	0.20	0.28	0.38	0.49	0.63	0.88
0.03	0.38	0.49	0.63	0.88	0.11	0.15	0.20	0.28	0.38	0.49	0.63	0.88
0.05	0.40	0.52	0.68	0.95	0.12	0.16	0.21	0.31	0.40	0.52	0.68	0.95
0.075	0.47	0.62	0.81	1.14	0.14	0.19	0.25	0.37	0.47	0.62	0.81	1.14
0.10	0.56	0.73	0.96	1.35	0.16	0.22	0.30	0.44	0.56	0.73	0.96	1.35
0.15	0.70	0.91	1.18	1.63	0.20	0.28	0.37	0.54	0.70	0.91	1.18	1.63
0.20	0.81	1.04	1.33	1.83	0.24	0.32	0.42	0.62	0.81	1.04	1.33	1.83
0.25	0.89	1.14	1.47	2.03	0.27	0.35	0.47	0.69	0.89	1.14	1.47	2.03
0.30	0.93	1.21	1.58	2.21	0.28	0.38	0.51	0.75	0.93	1.21	1.58	2.21
0.40	0.92	1.22	1.62	2.33	0.28	0.38	0.52	0.77	0.92	1.22	1.62	2.33
0.50	0.87	1.17	1.57	2.30	0.27	0.37	0.51	0.77	0.87	1.17	1.57	2.30
0.75	0.70	0.96	1.32	1.99	0.22	0.31	0.43	0.66	0.70	0.96	1.32	1.99
1.0	0.58	0.82	1.14	1.76	0.18	0.26	0.36	0.56	0.58	0.82	1.14	1.76
1.5	0.41	0.57	0.81	1.27	0.14	0.20	0.28	0.44	0.41	0.57	0.81	1.27
2.0	0.30	0.42	0.60	0.95	0.11	0.16	0.22	0.35	0.30	0.42	0.60	0.95
3.0	0.18	0.25	0.36	0.57	0.079	0.11	0.16	0.25	0.18	0.25	0.36	0.57
4.0	0.11	0.16	0.22	0.35	0.060	0.085	0.12	0.19	0.11	0.16	0.22	0.35
5.0	0.072	0.10	0.15	0.23	0.045	0.064	0.091	0.14	0.072	0.10	0.15	0.23
7.5	0.030	0.043	0.061	0.10	0.027	0.038	0.054	0.085	0.030	0.043	0.061	0.10
10.0	0.016	0.023	0.032	0.050	0.016	0.023	0.032	0.050	0.016	0.023	0.032	0.050

(j) Southern Forebay North

PERIOD (SEC)	WEST TRACY ¹			
	MEDIAN (g)	69 TH PERCENTILE (g)	84 TH PERCENTILE (g)	95 TH PERCENTILE (g)
0.01	0.47	0.60	0.77	1.06
0.02	0.47	0.60	0.77	1.06
0.03	0.46	0.60	0.77	1.06
0.05	0.49	0.63	0.81	1.13
0.075	0.56	0.73	0.95	1.34
0.10	0.65	0.85	1.11	1.55
0.15	0.81	1.04	1.33	1.85
0.20	0.92	1.18	1.51	2.07
0.25	1.03	1.32	1.69	2.33
0.30	1.12	1.44	1.86	2.59
0.40	1.14	1.51	1.98	2.82
0.50	1.11	1.48	1.98	2.86
0.75	0.94	1.29	1.76	2.64
1.0	0.82	1.14	1.58	2.42
1.5	0.60	0.84	1.19	1.85
2.0	0.45	0.64	0.91	1.44
3.0	0.29	0.41	0.58	0.92
4.0	0.18	0.26	0.37	0.58
5.0	0.12	0.18	0.25	0.39
7.5	0.054	0.076	0.11	0.17
10.0	0.029	0.041	0.057	0.090

¹West Tracy fault scenario is largest deterministic ground motions at all spectral periods.

(k) Southern Forebay South

PERIOD (SEC)	WEST TRACY ¹			
	MEDIAN (g)	69 TH PERCENTILE (g)	84 TH PERCENTILE (g)	95 TH PERCENTILE (g)
0.01	0.54	0.69	0.89	1.23
0.02	0.54	0.70	0.89	1.24
0.03	0.54	0.69	0.89	1.24
0.05	0.57	0.74	0.95	1.34
0.075	0.65	0.85	1.11	1.57
0.10	0.76	0.98	1.28	1.81
0.15	0.92	1.19	1.54	2.14
0.20	1.05	1.35	1.73	2.39
0.25	1.18	1.51	1.95	2.70
0.30	1.27	1.65	2.14	3.00
0.40	1.30	1.72	2.28	3.27
0.50	1.26	1.69	2.27	3.31
0.75	1.07	1.47	2.02	3.05
1.0	0.92	1.28	1.79	2.76
1.5	0.66	0.93	1.31	2.05
2.0	0.49	0.70	0.99	1.56
3.0	0.31	0.44	0.63	0.99
4.0	0.20	0.28	0.40	0.63
5.0	0.13	0.19	0.27	0.42
7.5	0.058	0.082	0.116	0.18
10.0	0.031	0.044	0.062	0.10

¹West Tracy fault scenario is largest deterministic ground motions at all spectral periods.

(I) Jones Connection

PERIOD (SEC)	WEST TRACY ¹			
	MEDIAN (g)	69 TH PERCENTILE (g)	84 TH PERCENTILE (g)	95 TH PERCENTILE (g)
0.01	0.61	0.79	1.03	1.46
0.02	0.61	0.80	1.05	1.47
0.03	0.63	0.82	1.07	1.52
0.05	0.69	0.91	1.20	1.70
0.075	0.81	1.08	1.43	2.05
0.10	0.94	1.25	1.65	2.37
0.15	1.14	1.50	1.98	2.81
0.20	1.29	1.69	2.21	3.14
0.25	1.39	1.84	2.43	3.47
0.30	1.46	1.95	2.61	3.78
0.40	1.43	1.95	2.65	3.93
0.50	1.33	1.84	2.53	3.83
0.75	1.06	1.49	2.09	3.24
1.0	0.85	1.20	1.70	2.67
1.5	0.56	0.79	1.13	1.77
2.0	0.39	0.55	0.79	1.25
3.0	0.23	0.33	0.47	0.75
4.0	0.15	0.21	0.30	0.47
5.0	0.10	0.14	0.20	0.32
7.5	0.044	0.06	0.089	0.14
10.0	0.025	0.035	0.049	0.077

¹West Tracy fault scenario is largest deterministic ground motions at all spectral periods.

Table 8. Maximum Design Earthquake (MDE) Spectra

PERIOD (SEC)	INTAKE No. 3 (g)	INTAKE No. 5 (g)	TWIN CITIES (g)	NEW HOPE (g)	CANAL RANCH (g)	BOULDIN (g)	KING ISLAND (g)	LOWER ROBERTS (g)	BACON (g)	SOUTHERN FOREBAY NORTH (g)	SOUTHERN FOREBAY SOUTH (g)	JONES CONNECTION (g)
0.01	0.30	0.33	0.31	0.35	0.33	0.54	0.36	0.39	0.63	0.77	0.89	0.54
0.02	0.30	0.33	0.32	0.36	0.33	0.54	0.37	0.40	0.63	0.77	0.89	0.55
0.03	0.32	0.35	0.33	0.37	0.35	0.55	0.38	0.41	0.63	0.77	0.89	0.57
0.05	0.38	0.42	0.39	0.43	0.41	0.62	0.45	0.48	0.68	0.81	0.95	0.67
0.075	0.48	0.54	0.51	0.54	0.53	0.76	0.58	0.62	0.81	0.95	1.11	0.85
0.10	0.58	0.64	0.62	0.66	0.63	0.90	0.70	0.75	0.96	1.11	1.28	1.02
0.15	0.71	0.78	0.74	0.82	0.77	1.12	0.86	0.93	1.18	1.33	1.54	1.22
0.20	0.77	0.84	0.79	0.89	0.83	1.26	0.94	1.03	1.33	1.51	1.73	1.32
0.25	0.78	0.85	0.81	0.92	0.84	1.35	0.98	1.08	1.47	1.69	1.95	1.36
0.30	0.77	0.83	0.82	0.92	0.83	1.40	0.99	1.11	1.58	1.86	2.14	1.36
0.40	0.70	0.74	0.77	0.84	0.75	1.35	0.94	1.08	1.62	1.98	2.28	1.27
0.50	0.62	0.66	0.74	0.76	0.69	1.27	0.89	1.03	1.57	1.98	2.27	1.17
0.60	0.54	0.57	0.67	0.67	0.62	1.14	0.80	0.93	1.45	1.88	2.15	1.04
0.75	0.46	0.48	0.59	0.59	0.54	1.00	0.70	0.82	1.32	1.76	2.02	0.89
1.0	0.36	0.38	0.46	0.45	0.42	0.81	0.55	0.66	1.14	1.58	1.79	0.69
1.5	0.23	0.24	0.32	0.31	0.28	0.54	0.38	0.46	0.81	1.19	1.31	0.44
2.0	0.17	0.17	0.24	0.23	0.21	0.39	0.28	0.34	0.60	0.91	0.99	0.31
3.0	0.11	0.10	0.15	0.15	0.13	0.23	0.18	0.22	0.36	0.58	0.63	0.19
4.0	0.067	0.064	0.11	0.10	0.092	0.14	0.12	0.1	0.22	0.37	0.40	0.12
5.0	0.047	0.043	0.077	0.071	0.064	0.098	0.091	0.11	0.15	0.25	0.27	0.086
7.5	0.029	0.025	0.046	0.043	0.039	0.054	0.052	0.062	0.073	0.11	0.12	0.041
10.0	0.020	0.018	0.031	0.030	0.028	0.036	0.035	0.040	0.045	0.057	0.062	0.047

Table 9. Operational Basis Earthquake (OBE) Spectra

PERIOD (SEC)	INTAKE No. 3 (g)	INTAKE No. 5 (g)	TWIN CITIES (g)	NEW HOPE (g)	CANAL RANCH (g)	BOULDIN (g)	KING ISLAND (g)	LOWER ROBERTS (g)	BACON (g)	SOUTHERN FOREBAY NORTH (g)	SOUTHERN FOREBAY SOUTH (g)	JONES CONNECTION (g)
0.01	0.19	0.18	0.19	0.20	0.19	0.25	0.23	0.25	0.30	0.37	0.39	0.41
0.02	0.19	0.19	0.19	0.20	0.20	0.25	0.23	0.26	0.31	0.37	0.40	0.43
0.03	0.20	0.20	0.20	0.21	0.20	0.26	0.24	0.26	0.31	0.38	0.41	0.44
0.05	0.24	0.24	0.24	0.25	0.24	0.30	0.28	0.30	0.36	0.43	0.46	0.52
0.075	0.31	0.30	0.30	0.32	0.31	0.39	0.36	0.38	0.46	0.55	0.59	0.66
0.10	0.37	0.36	0.37	0.39	0.38	0.47	0.43	0.47	0.57	0.67	0.71	0.79
0.15	0.44	0.43	0.45	0.47	0.45	0.59	0.54	0.59	0.71	0.83	0.88	0.95
0.20	0.47	0.46	0.48	0.51	0.48	0.64	0.59	0.66	0.78	0.92	0.98	1.03
0.25	0.48	0.46	0.49	0.52	0.49	0.66	0.61	0.69	0.82	0.97	1.02	1.05
0.30	0.48	0.45	0.50	0.52	0.48	0.66	0.61	0.70	0.84	1.00	1.04	1.05
0.40	0.45	0.42	0.47	0.48	0.45	0.63	0.58	0.67	0.81	0.97	1.00	0.97
0.50	0.42	0.38	0.44	0.45	0.41	0.58	0.54	0.63	0.76	0.91	0.94	0.88
0.60	0.38	0.34	0.40	0.40	0.37	0.52	0.49	0.57	0.68	0.82	0.84	0.78
0.75	0.33	0.29	0.35	0.35	0.32	0.46	0.42	0.50	0.60	0.72	0.73	0.66
1.0	0.26	0.23	0.27	0.27	0.25	0.35	0.33	0.40	0.48	0.57	0.58	0.51
1.5	0.18	0.15	0.19	0.18	0.17	0.24	0.23	0.27	0.33	0.39	0.39	0.33
2.0	0.13	0.11	0.14	0.13	0.12	0.17	0.16	0.20	0.24	0.29	0.29	0.23
3.0	0.075	0.061	0.084	0.077	0.068	0.109	0.10	0.124	0.15	0.176	0.17	0.14
4.0	0.047	0.040	0.052	0.048	0.043	0.066	0.061	0.079	0.10	0.118	0.12	0.091
5.0	0.034	0.029	0.037	0.035	0.032	0.045	0.042	0.052	0.064	0.079	0.077	0.059
7.5	0.022	0.019	0.023	0.022	0.020	0.027	0.026	0.030	0.034	0.038	0.037	0.030
10.0	0.015	0.014	0.016	0.016	0.015	0.018	0.018	0.020	0.022	0.024	0.023	0.023

Table 10. Properties of Time Histories

(a) Intake No. 3

SEED TIME HISTORIES												
RSN	Year	Earthquake Name	Station Name	Comp	Mag	ClstD (km)	VS30 (m/s)	PGA (g)	PGV (cm/s)	PGD (cm)	AI (m/sec)	5-95% Dur (sec)
68	1971	San Fernando	LA - Hollywood Stor FF	090	6.6	22.8	316	0.22	21.8	15.9	0.67	13.2
68	1971	San Fernando	LA - Hollywood Stor FF	180	6.6	22.8	316	0.19	17.0	12.9	0.45	13.5
162	1979	Imperial Valley-06	Calexico Fire Station	225	6.5	10.5	231	0.28	22.5	9.9	0.86	11.0
162	1979	Imperial Valley-06	Calexico Fire Station	315	6.5	10.5	231	0.20	18.7	15.9	0.75	14.8
1074	1994	Northridge-01	Sandberg - Bald Mtn	090	6.7	41.6	421	0.09	12.2	4.8	0.15	14.1
1074	1994	Northridge-01	Sandberg - Bald Mtn	180	6.7	41.6	421	0.10	8.9	4.7	0.10	15.9
SPECTRALLY-MATCHED TIME HISTORIES												
RSN	Year	Earthquake Name	Station Name	Comp	Mag	ClstD (km)	VS30 (m/s)	PGA (g)	PGV (cm/s)	PGD (cm)	AI (m/sec)	5-95% Dur (sec)
68	1971	San Fernando	LA - Hollywood Stor FF	090	6.6	22.8	316	0.32	31.6	29.2	1.56	12.4
68	1971	San Fernando	LA - Hollywood Stor FF	180	6.6	22.8	316	0.27	26.1	23.1	1.07	13.4
162	1979	Imperial Valley-06	Calexico Fire Station	225	6.5	10.5	231	0.34	34.2	15.2	1.76	11.0
162	1979	Imperial Valley-06	Calexico Fire Station	315	6.5	10.5	231	0.26	34.2	26.1	1.33	15.5
1074	1994	Northridge-01	Sandberg - Bald Mtn	090	6.7	41.6	421	0.29	41.6	16.2	1.27	16.8
1074	1994	Northridge-01	Sandberg - Bald Mtn	180	6.7	41.6	421	0.33	22.5	21.0	0.87	18.7

(b) Intake No. 5

SEED TIME HISTORIES												
RSN	Year	Earthquake Name	Station Name	Comp	Mag	ClstD (km)	VS30 (m/s)	PGA (g)	PGV (cm/s)	PGD (cm)	AI (m/sec)	5-95% Dur (sec)
68	1971	San Fernando	LA - Hollywood Stor FF	090	6.6	22.8	316	0.22	21.8	15.9	0.67	13.2
68	1971	San Fernando	LA - Hollywood Stor FF	180	6.6	22.8	316	0.19	17.0	12.9	0.45	13.5
162	1979	Imperial Valley-06	Calexico Fire Station	225	6.5	10.5	231	0.28	22.5	9.9	0.86	11.0
162	1979	Imperial Valley-06	Calexico Fire Station	315	6.5	10.5	231	0.20	18.7	15.9	0.75	14.8
1074	1994	Northridge-01	Sandberg - Bald Mtn	090	6.7	41.6	421	0.09	12.2	4.8	0.15	14.1
1074	1994	Northridge-01	Sandberg - Bald Mtn	180	6.7	41.6	421	0.10	8.9	4.7	0.10	15.9
SPECTRALLY-MATCHED TIME HISTORIES												
RSN	Year	Earthquake Name	Station Name	Comp	Mag	ClstD (km)	VS30 (m/s)	PGA (g)	PGV (cm/s)	PGD (cm)	AI (m/sec)	5-95% Dur (sec)
68	1971	San Fernando	LA - Hollywood Stor FF	090	6.6	22.8	316	0.35	31.0	24.3	1.87	12.4
68	1971	San Fernando	LA - Hollywood Stor FF	180	6.6	22.8	316	0.30	27.0	18.7	1.16	14.0
162	1979	Imperial Valley-06	Calexico Fire Station	225	6.5	10.5	231	0.37	34.9	12.6	2.02	11.0
162	1979	Imperial Valley-06	Calexico Fire Station	315	6.5	10.5	231	0.29	32.3	21.7	1.57	14.6
1074	1994	Northridge-01	Sandberg - Bald Mtn	090	6.7	41.6	421	0.31	43.6	14.0	1.46	17.3
1074	1994	Northridge-01	Sandberg - Bald Mtn	180	6.7	41.6	421	0.35	22.0	19.0	1.06	18.1

(c) Bouldin

SEED TIME HISTORIES												
RSN	Year	Earthquake Name	Station Name	Comp	Mag	ClstD (km)	VS30 (m/s)	PGA (g)	PGV (cm/s)	PGD (cm)	AI (m/sec)	5-95% Dur (sec)
68	1971	San Fernando	LA - Hollywood Stor FF	090	6.6	22.8	316	0.22	21.8	15.9	0.67	13.2
68	1971	San Fernando	LA - Hollywood Stor FF	180	6.6	22.8	316	0.19	17.0	12.9	0.45	13.5
174	1979	Imperial Valley-06	El Centro Array #11	140	6.5	12.6	196	0.37	36.0	25.1	2.00	9.0
174	1979	Imperial Valley-06	El Centro Array #11	230	6.5	12.6	196	0.38	44.6	21.4	1.63	7.9
4031	2003	San Simeon, CA	Templeton - 1-story Hospital	90	6.5	6.2	411	0.44	38.9	14.7	1.63	8.9
4031	2003	San Simeon, CA	Templeton - 1-story Hospital	360	6.5	6.2	411	0.48	23.0	11.4	1.88	9.1
SPECTRALLY-MATCHED TIME HISTORIES												
RSN	Year	Earthquake Name	Station Name	Comp	Mag	ClstD (km)	VS30 (m/s)	PGA (g)	PGV (cm/s)	PGD (cm)	AI (m/sec)	5-95% Dur (sec)
68	1971	San Fernando	LA - Hollywood Stor FF	090	6.6	22.8	316	0.57	87.5	55.9	6.36	8.5
68	1971	San Fernando	LA - Hollywood Stor FF	180	6.6	22.8	316	0.49	50.4	45.5	3.85	12.5
174	1979	Imperial Valley-06	El Centro Array #11	140	6.5	12.6	196	0.52	63.4	33.0	4.66	10.9
174	1979	Imperial Valley-06	El Centro Array #11	230	6.5	12.6	196	0.51	75.5	30.0	4.00	9.3
4031	2003	San Simeon, CA	Templeton - 1-story Hospital	90	6.5	6.2	411	0.53	95.3	37.8	4.57	9.8
4031	2003	San Simeon, CA	Templeton - 1-story Hospital	360	6.5	6.2	411	0.61	66.1	26.9	4.89	11.5

(d) Twin Cities

SEED TIME HISTORIES												
RSN	Year	Earthquake Name	Station Name	Comp	Mag	ClstD (km)	VS30 (m/s)	PGA (g)	PGV (cm/s)	PGD (cm)	AI (m/sec)	5-95% Dur (sec)
187	1979	Imperial Valley-06	Parachute Test Site	225	6.5	12.7	349	0.11	18.3	14.2	0.21	18.6
187	1979	Imperial Valley-06	Parachute Test Site	315	6.5	12.7	349	0.21	17.7	12.2	0.22	16.9
1277	1999	Chi-Chi, Taiwan	HWA028	E	7.6	53.8	407	0.10	14.8	21.3	0.22	35.3
1277	1999	Chi-Chi, Taiwan	HWA028	N	7.6	53.8	407	0.09	14.9	12.5	0.27	30.2
4009	2003	San Simeon, CA	Point Buchon - Los Osos	090	6.5	31.9	486	0.09	12.2	6.9	0.10	18.5
4009	2003	San Simeon, CA	Point Buchon - Los Osos	360	6.5	31.9	486	0.06	14.3	7.4	0.08	18.3
SPECTRALLY-MATCHED TIME HISTORIES												
RSN	Year	Earthquake Name	Station Name	Comp	Mag	ClstD (km)	VS30 (m/s)	PGA (g)	PGV (cm/s)	PGD (cm)	AI (m/sec)	5-95% Dur (sec)
187	1979	Imperial Valley-06	Parachute Test Site	225	6.5	12.7	349	0.25	47.6	31.1	1.77	15.5
187	1979	Imperial Valley-06	Parachute Test Site	315	6.5	12.7	349	0.44	41.4	28.4	1.65	14.0
1277	1999	Chi-Chi, Taiwan	HWA028	E	7.6	53.8	407	0.32	46.0	68.9	2.05	32.8
1277	1999	Chi-Chi, Taiwan	HWA028	N	7.6	53.8	407	0.29	35.7	39.7	2.07	26.0
4009	2003	San Simeon, CA	Point Buchon - Los Osos	90	6.5	31.9	486	0.37	46.3	37.8	2.07	18.4
4009	2003	San Simeon, CA	Point Buchon - Los Osos	360	6.5	31.9	486	0.28	52.2	28.6	1.86	16.2

(d) Lower Roberts

SEED TIME HISTORIES												
RSN	Year	Earthquake Name	Station Name	Comp	Mag	ClstD (km)	VS30 (m/s)	PGA (g)	PGV (cm/s)	PGD (cm)	AI (m/sec)	5-95% Dur (sec)
812	1989	Loma Prieta	Woodside	000	6.9	34.1	454	0.08	14.0	9.3	0.11	16.8
812	1989	Loma Prieta	Woodside	090	6.9	34.1	454	0.08	17.9	12.0	0.13	15.6
1101	1995	Kobe, Japan	Amagasaki	000	6.9	11.3	256	0.28	33.6	26.7	1.70	19.3
1101	1995	Kobe, Japan	Amagasaki	090	6.9	11.3	256	0.33	44.9	27.9	1.95	19.4
1277	1999	Chi-Chi, Taiwan	HWA028	E	7.6	53.8	407	0.10	14.8	21.3	0.22	35.3
1277	1999	Chi-Chi, Taiwan	HWA028	N	7.6	53.8	407	0.09	14.9	12.5	0.27	30.2
SPECTRALLY-MATCHED TIME HISTORIES												
RSN	Year	Earthquake Name	Station Name	Comp	Mag	ClstD (km)	VS30 (m/s)	PGA (g)	PGV (cm/s)	PGD (cm)	AI (m/sec)	5-95% Dur (sec)
812	1989	Loma Prieta	Woodside	000	6.9	34.1	454	0.38	53.7	35.6	2.73	18.3
812	1989	Loma Prieta	Woodside	090	6.9	34.1	454	0.43	76.9	53.3	2.65	13.2
1101	1995	Kobe, Japan	Amagasaki	000	6.9	11.3	256	0.37	51.2	37.7	2.53	20.2
1101	1995	Kobe, Japan	Amagasaki	090	6.9	11.3	256	0.46	60.6	41.5	2.91	22.7
1277	1999	Chi-Chi, Taiwan	HWA028	E	7.6	53.8	407	0.43	65.8	93.3	3.85	33.1
1277	1999	Chi-Chi, Taiwan	HWA028	N	7.6	53.8	407	0.37	51.1	49.4	3.51	24.4

(e) Southern Forebay North

SEED TIME HISTORIES												
RSN	Year	Earthquake Name	Station Name	Comp	Mag	ClstD (km)	VS30 (m/s)	PGA (g)	PGV (cm/s)	PGD (cm)	AI (m/sec)	5-95% Dur (sec)
778	1989	Loma Prieta	Hollister Differential Array	165	6.9	24.8	216	0.27	44.3	19.7	0.81	12.6
778	1989	Loma Prieta	Hollister Differential Array	255	6.9	24.8	216	0.28	35.8	14.6	1.04	13.3
821	1992	Erzican, Turkey	Erzincan	NS	6.7	4.4	352	0.39	107.2	32.0	1.52	8.4
821	1992	Erzican, Turkey	Erzincan	EW	6.7	4.4	352	0.50	78.2	28.0	1.79	7.4
1605	1999	Duzce, Turkey	Duzce	180	7.1	6.6	282	0.40	71.2	49.6	2.70	11.1
1605	1999	Duzce, Turkey	Duzce	270	7.1	6.6	282	0.51	84.3	47.9	2.93	10.9
SPECTRALLY-MATCHED TIME HISTORIES												
RSN	Year	Earthquake Name	Station Name	Comp	Mag	ClstD (km)	VS30 (m/s)	PGA (g)	PGV (cm/s)	PGD (cm)	AI (m/sec)	5-95% Dur (sec)
778	1989	Loma Prieta	Hollister Differential Array	165	6.9	24.8	216	0.74	159.2	94.1	9.38	13.4
778	1989	Loma Prieta	Hollister Differential Array	255	6.9	24.8	216	0.83	128.5	56.8	10.33	16.4
821	1992	Erzican, Turkey	Erzincan	NS	6.7	4.4	352	0.74	246.5	94.6	8.45	8.8
821	1992	Erzican, Turkey	Erzincan	EW	6.7	4.4	352	0.86	180.3	76.8	8.26	7.4
1605	1999	Duzce, Turkey	Duzce	180	7.1	6.6	282	0.63	136.2	69.5	9.99	10.8
1605	1999	Duzce, Turkey	Duzce	270	7.1	6.6	282	0.78	171.4	91.9	13.37	10.3

Table 11. Target Arias Intensities and Durations for Time Histories

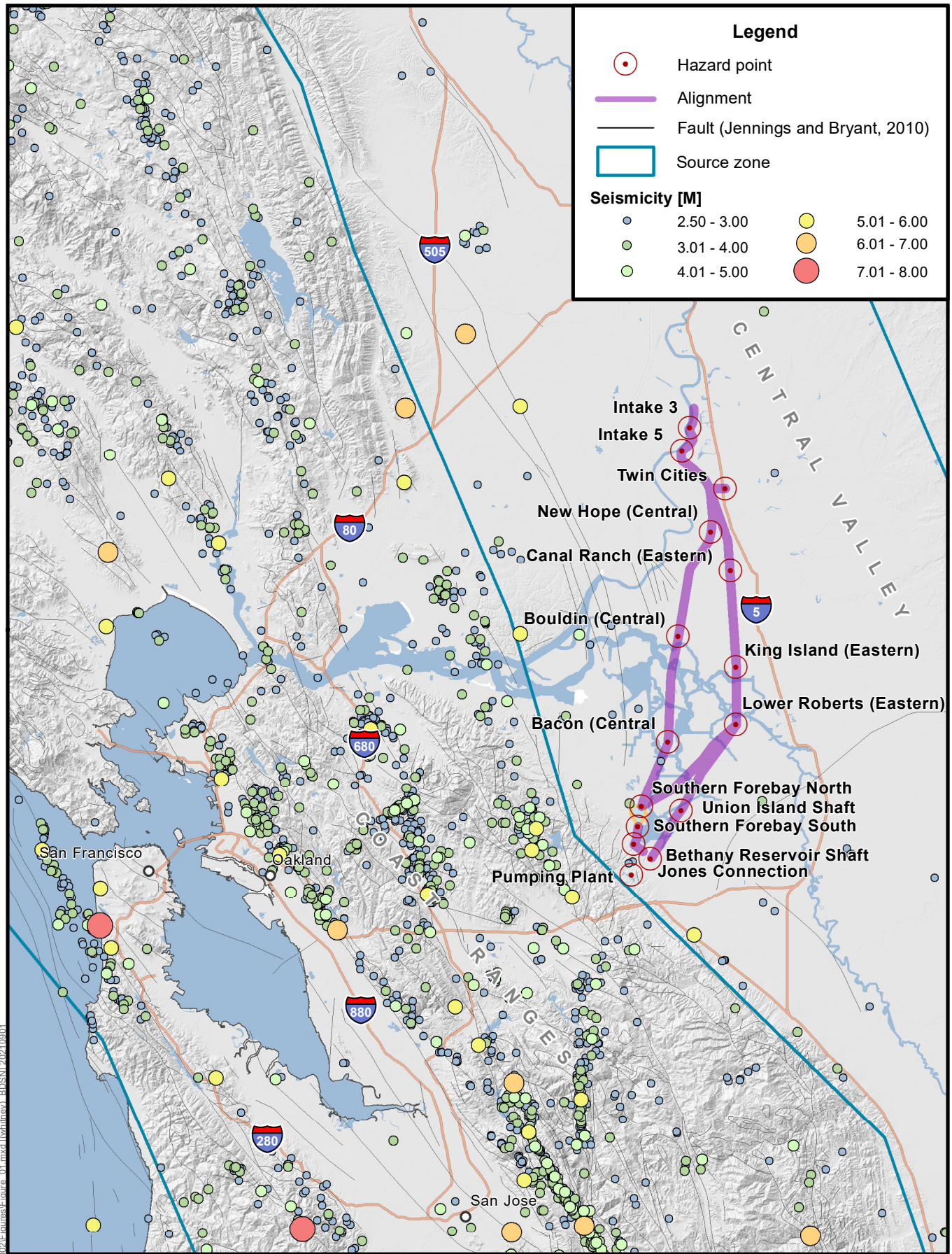
(a) Arias Intensities

TARGET ARIAS INTENSITY MODEL	TARGET			SPECTRALLY-MATCHED TIME HISTORIES	
	Median	-1 sigma	+1 sigma	Average	Range
Intake No.3					
Watson-Lamprey and Abrahamson (2006)	1.1	0.8	1.5	1.3	1.1 – 1.5
Abrahamson et al. (2016)	1.1	0.7	1.6		
Intake No. 5					
Watson-Lamprey and Abrahamson (2006)	1.2	0.9	1.7	1.5	1.2 – 1.8
Abrahamson et al. (2016)	1.2	0.8	1.8		
Twin Cities, M 6.6 Seeds					
Watson-Lamprey and Abrahamson (2006)	1.1	0.8	1.6	1.8	1.7 – 2.0
Abrahamson et al. (2016)	1.2	0.8	1.8		
Twin Cities, M 7.7 Seed					
Watson-Lamprey and Abrahamson (2006)	1.8	1.3	2.5	2.1	2.1
Abrahamson et al. (2016)	2.1	1.4	3.1		
Bouldin					
Watson-Lamprey and Abrahamson (2006)	3.4	2.4	4.7	4.7	4.3 – 4.9
Abrahamson et al. (2016)	3.3	2.3	4.9		
Lower Roberts, M 6.8 Seeds					
Watson-Lamprey and Abrahamson (2006)	2.2	1.5	3.0	2.7	2.7
Abrahamson et al. (2016)	2.2	1.5	3.3		
Lower Roberts, M 7.6 Seed					
Watson-Lamprey and Abrahamson (2006)	2.9	2.1	4.1	3.7	3.7
Abrahamson et al. (2016)	3.3	2.3	4.9		
Southern Forebay North					
Watson-Lamprey and Abrahamson (2006)	8.4	6.0	11.8	9.9	8.4 – 11.6
Abrahamson et al. (2016)	8.0	5.5	11.8		

(b) Durations

TARGET DURATION MODEL	TARGET			SPECTRALLY-MATCHED TIME HISTORIES	
	Median	-1 sigma	+1 sigma	Average	Range
Intake No.3					
Silva et al. (1997)	13.3	8.1	21.7	14.6	11.0 – 18.7
Kempton and Stewart (2006)	13.6	8.8	21.2		
Intake No. 5					
Silva et al. (1997)	12.9	7.9	21.2	14.6	11.0 – 18.1
Kempton and Stewart (2006)	12.8	8.2	19.9		
Twin Cities, M 6.6 Seeds					
Silva et al. (1997)	18.2	11.1	29.8	16.0	14.0 – 18.4
Kempton and Stewart (2006)	18.8	12.1	29.2		
Twin Cities, M 7.7 Seed					
Silva et al. (1997)	45.7	27.9	74.8	29.4	26.0 – 32.8
Kempton and Stewart (2006)	46.3	29.8	71.9		
Bouldin					
Silva et al. (1997)	11.7	7.2	19.2	10.4	8.5 – 12.5
Kempton and Stewart (2006)	10.5	6.7	16.3		
Lower Roberts, M 6.8 Seeds					
Silva et al. (1997)	19.2	11.7	31.4	18.6	13.2 – 22.7
Kempton and Stewart (2006)	20.1	12.9	31.2		
Lower Roberts, M 7.6 Seed					
Silva et al. (1997)	40.0	24.5	65.5	28.8	24.4 – 33.1
Kempton and Stewart (2006)	40.9	26.4	63.6		
Southern Forebay North					
Silva et al. (1997)	14.7	9.0	24.0	11.2	7.4 – 16.4
Kempton and Stewart (2006)	11.1	7.2	17.3		

Figures



Legend

- Hazard point
- Alignment
- Fault (Jennings and Bryant, 2010)
- Source zone

Seismicity [M]

● 2.50 - 3.00	● 5.01 - 6.00
● 3.01 - 4.00	● 6.01 - 7.00
● 4.01 - 5.00	● 7.01 - 8.00

Figure 1
Historical Seismicity in the
Project Region 1781 to
September 2019

 **DCA**
 DELTA CONVEYANCE DESIGN
 & CONSTRUCTION AUTHORITY

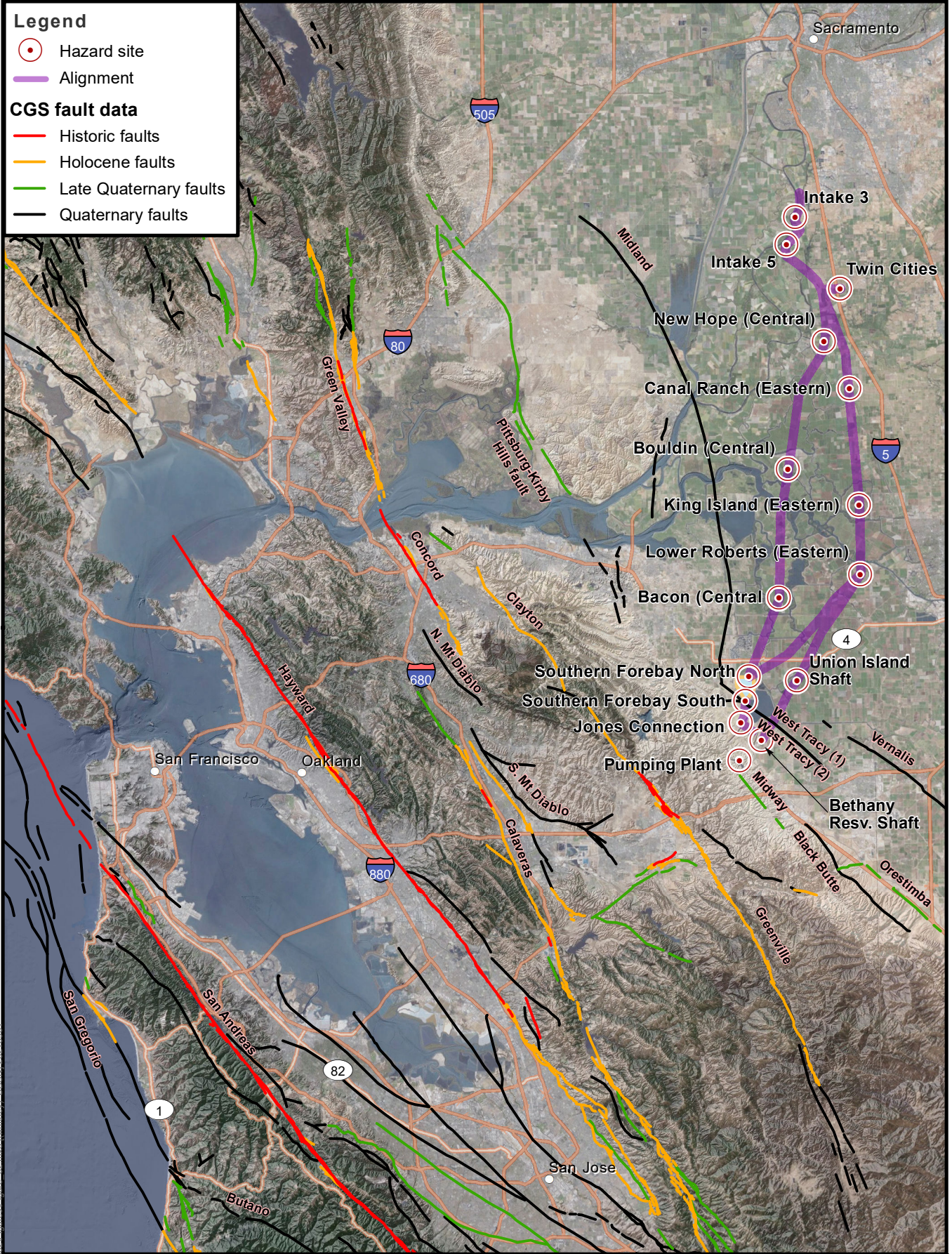
**For Illustration
 Purposes Only**

N

0 5 10 15 Miles

Data Source: DCA, NSHMP (2014), USGS (2018)

S:\18102\Figures\18102_002\Figures\Figure_01.mxd (vwhitnev) BDSN1 2021.0801



S:\18102\Figures\18102_002\Figures\Figure_02.mxd (AutoInexp)_RDSN\2024.0804

DCA
DELTA CONVEYANCE DESIGN
& CONSTRUCTION AUTHORITY

**For Illustration
Purposes Only**

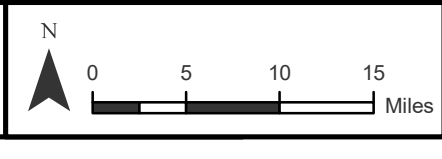



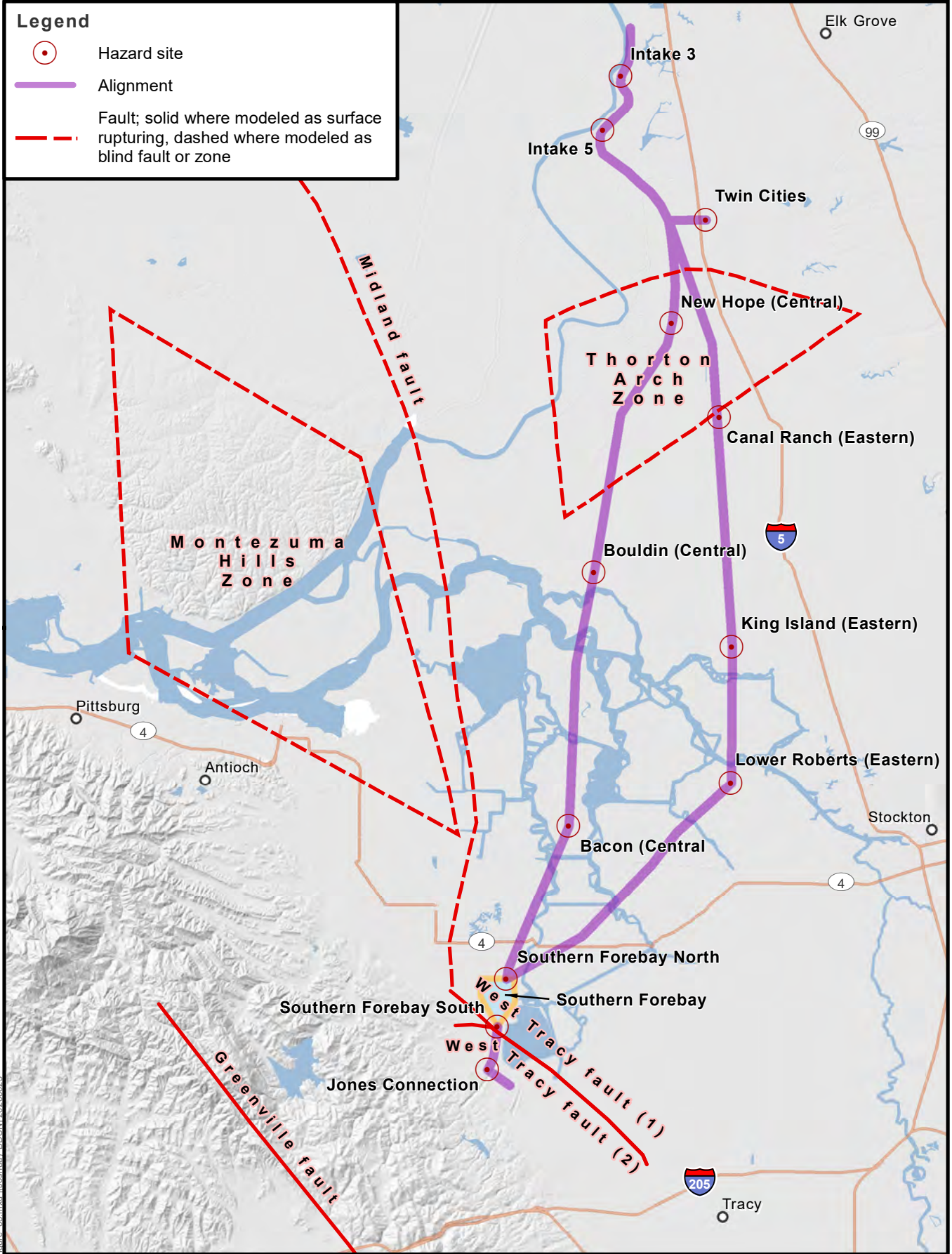


Figure 2
**Quaternary Faults in the
San Francisco Bay Region**

Data Source: DCA, CGS (2005)

Legend

-  Hazard site
-  Alignment
-  Fault; solid where modeled as surface rupturing, dashed where modeled as blind fault or zone

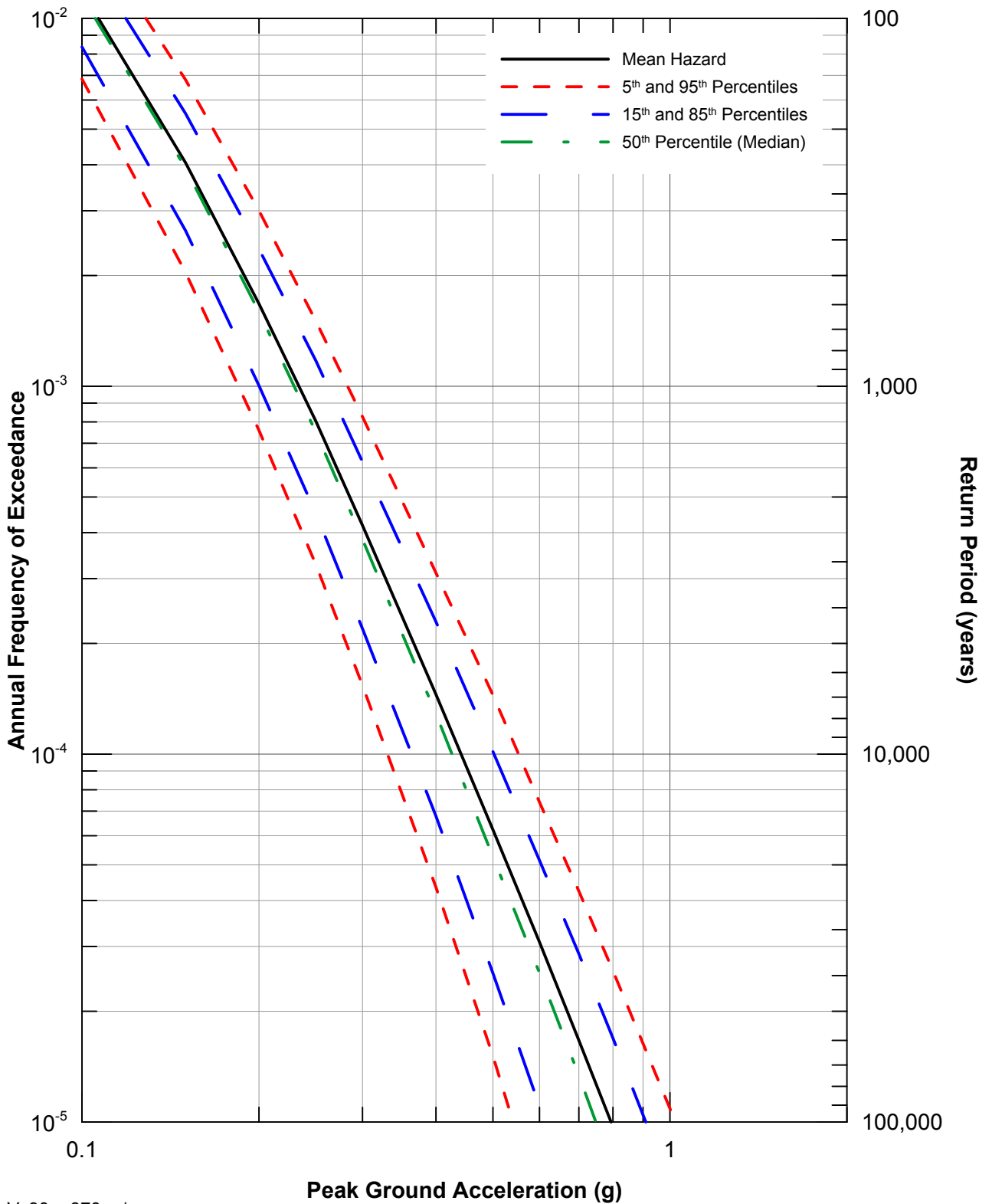


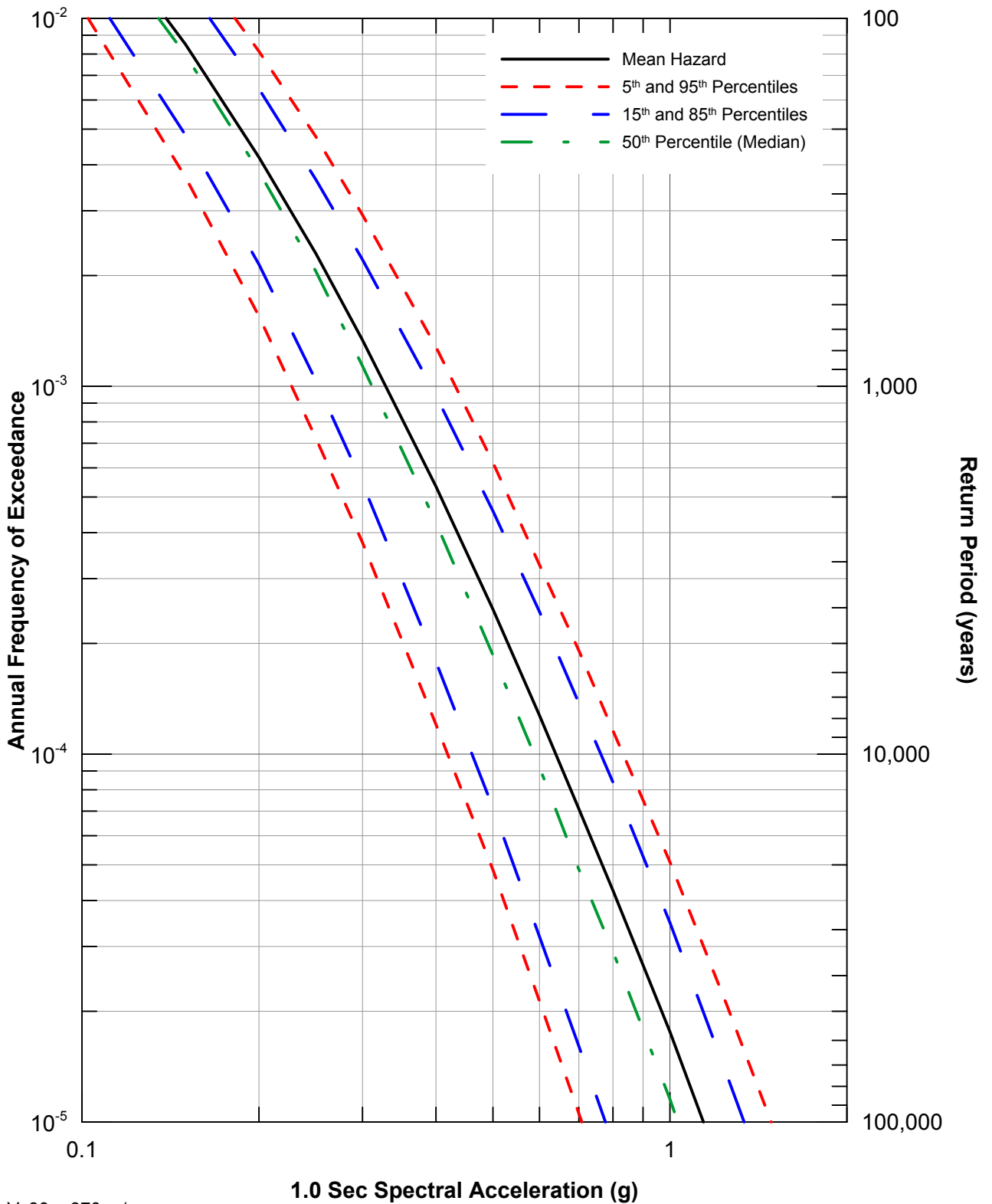
For Illustration
Purposes Only

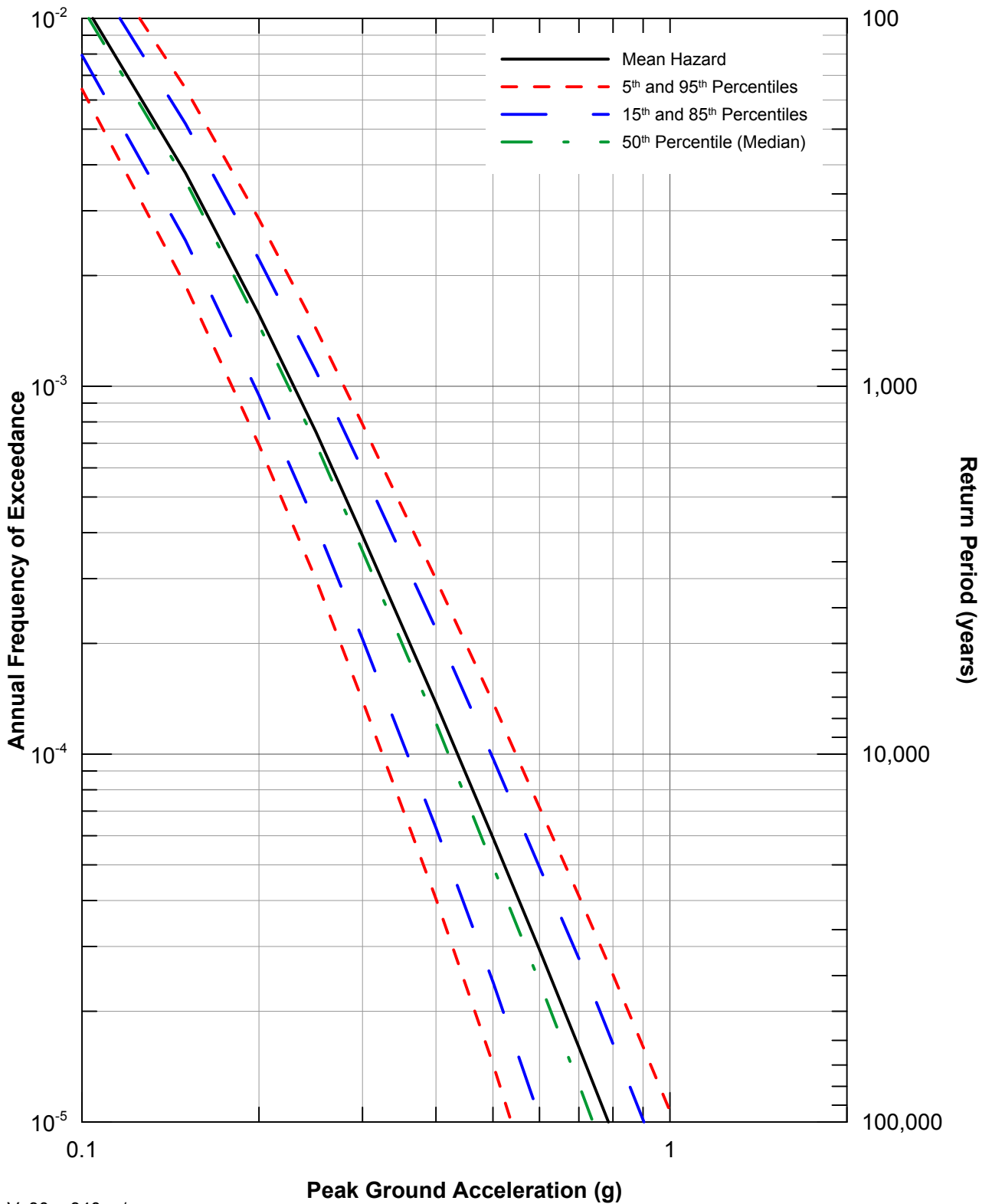


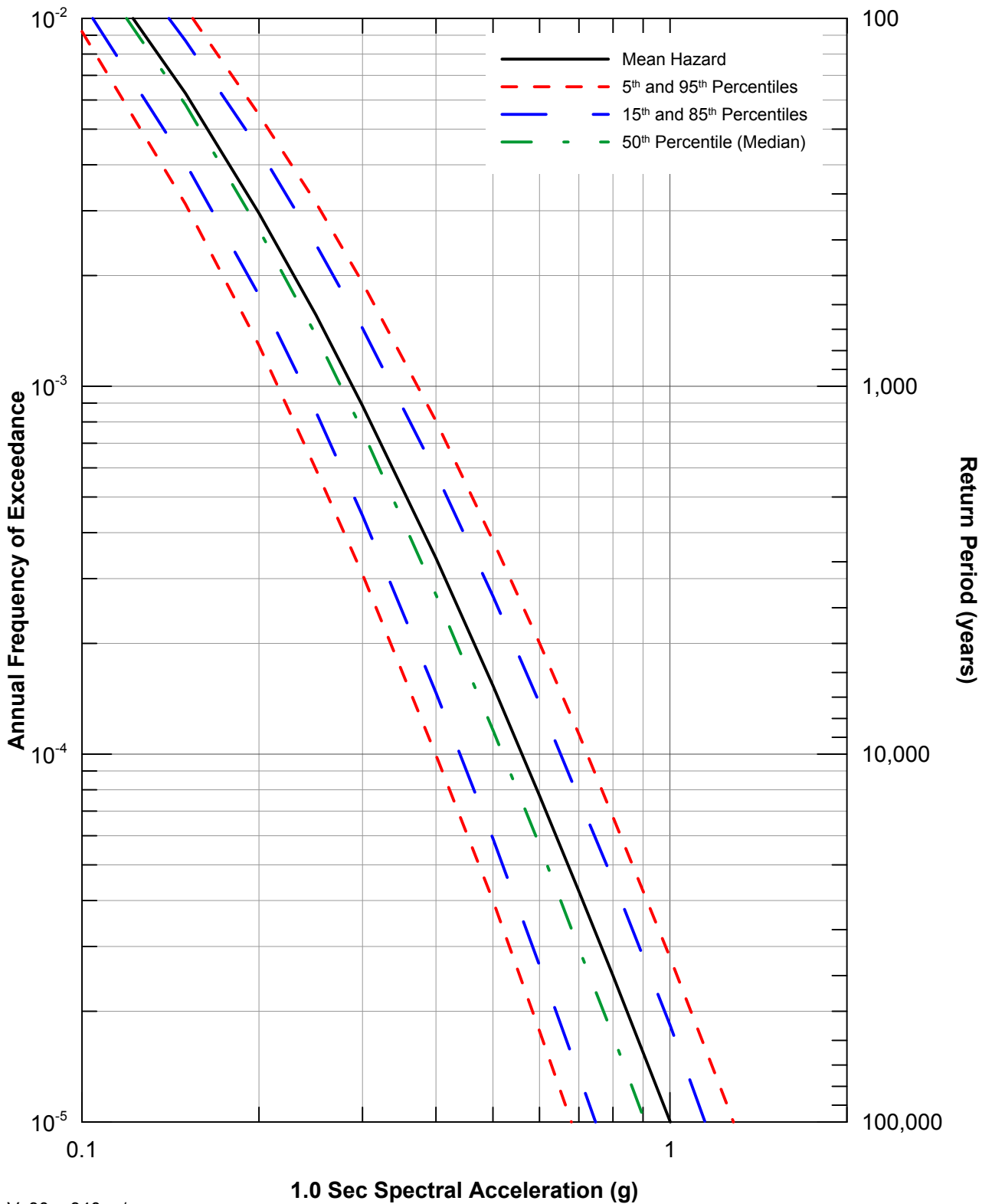
Figure 3
Active Faults in the
Delta Region

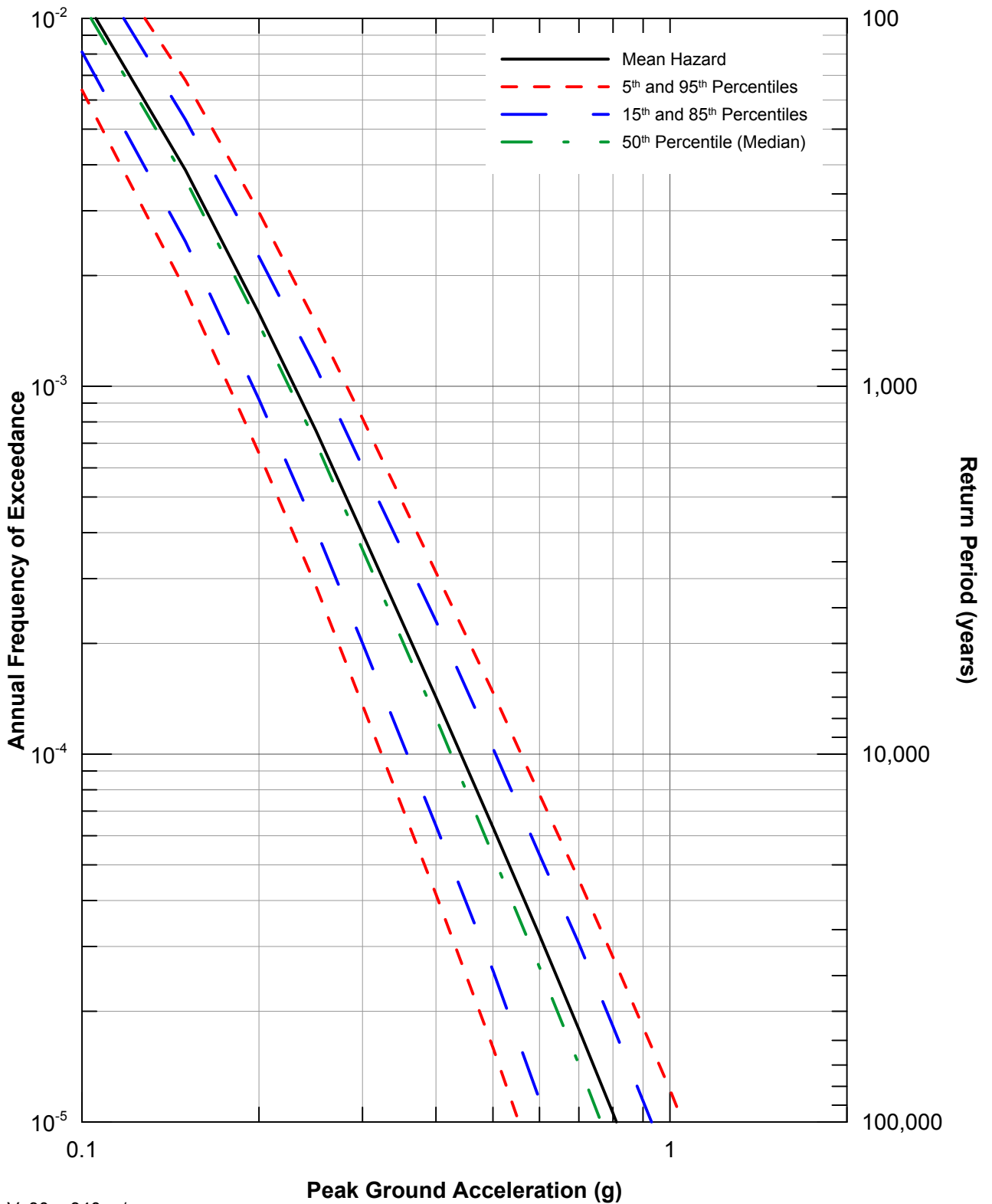
S:\1802\Figures\DCA\Figure_03.mxd (Joshua) 1_BDSN1 20200825

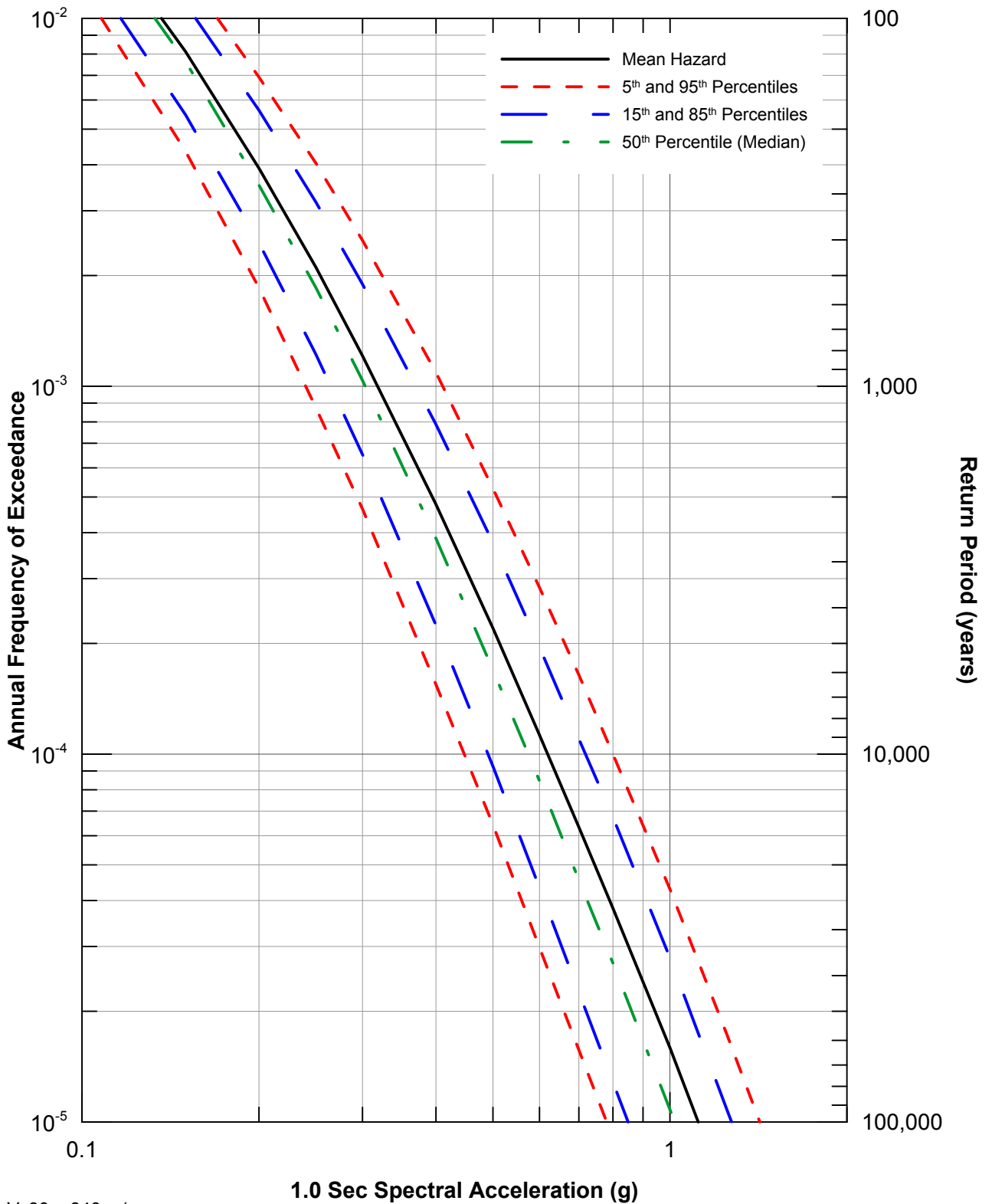


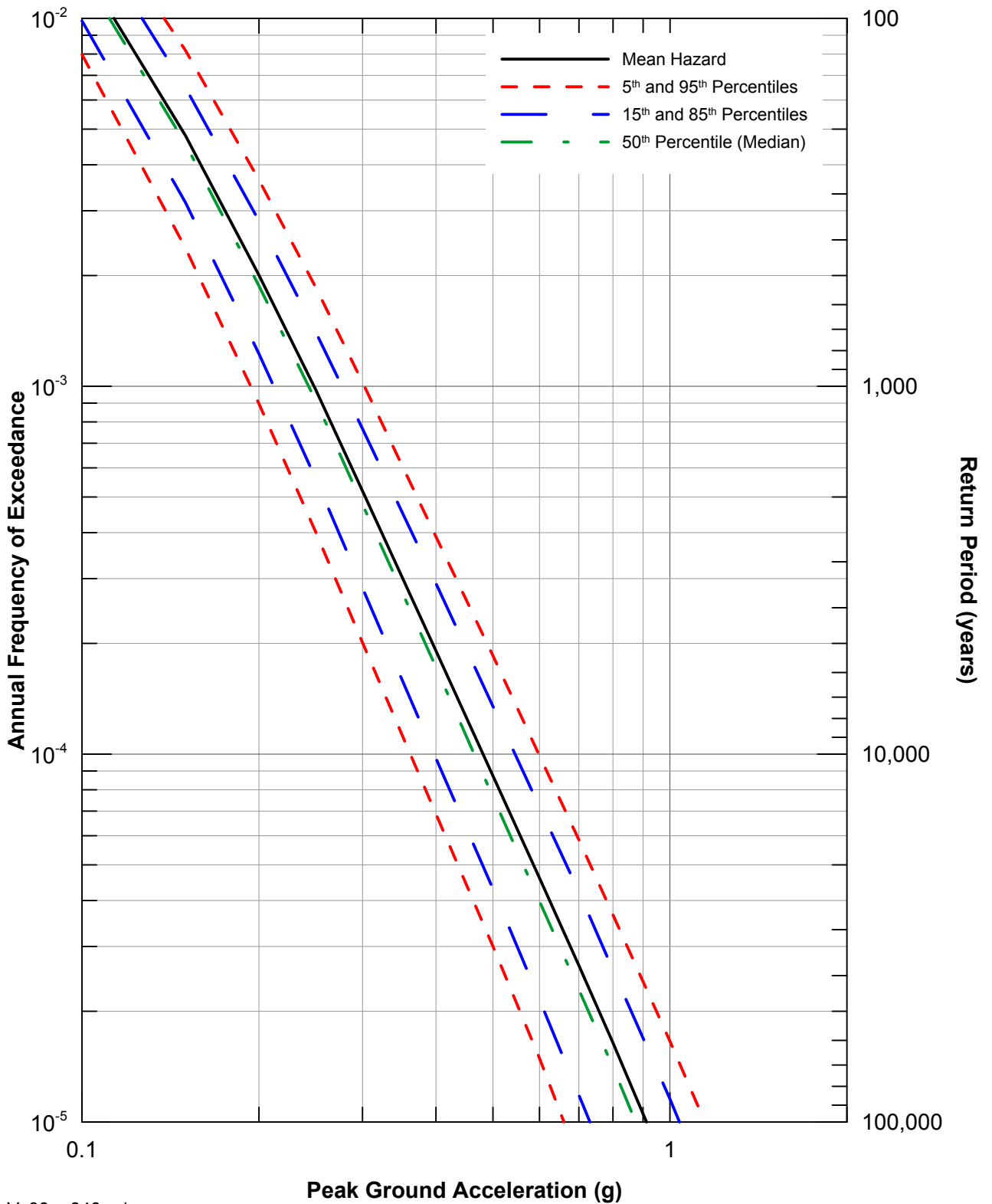


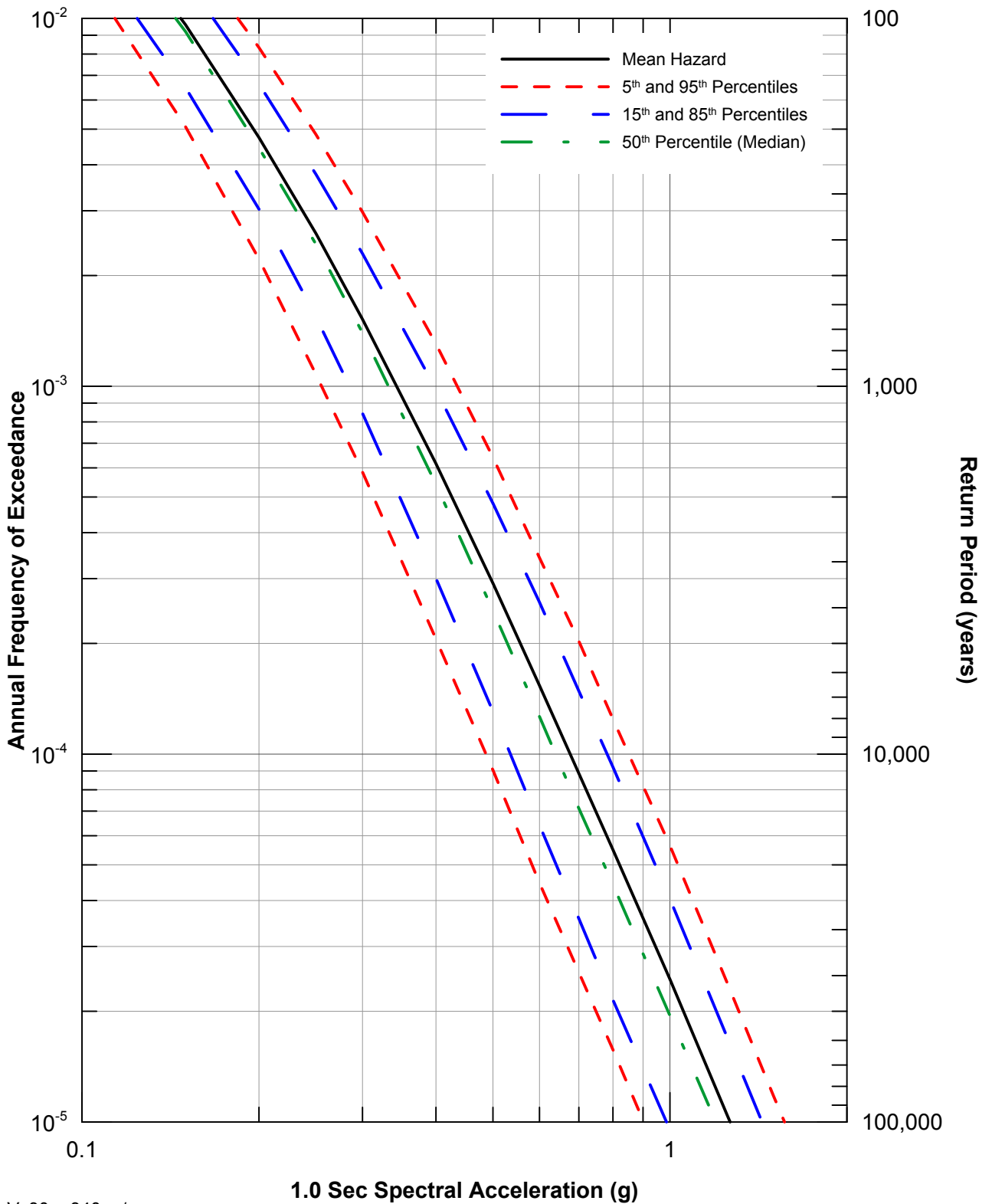


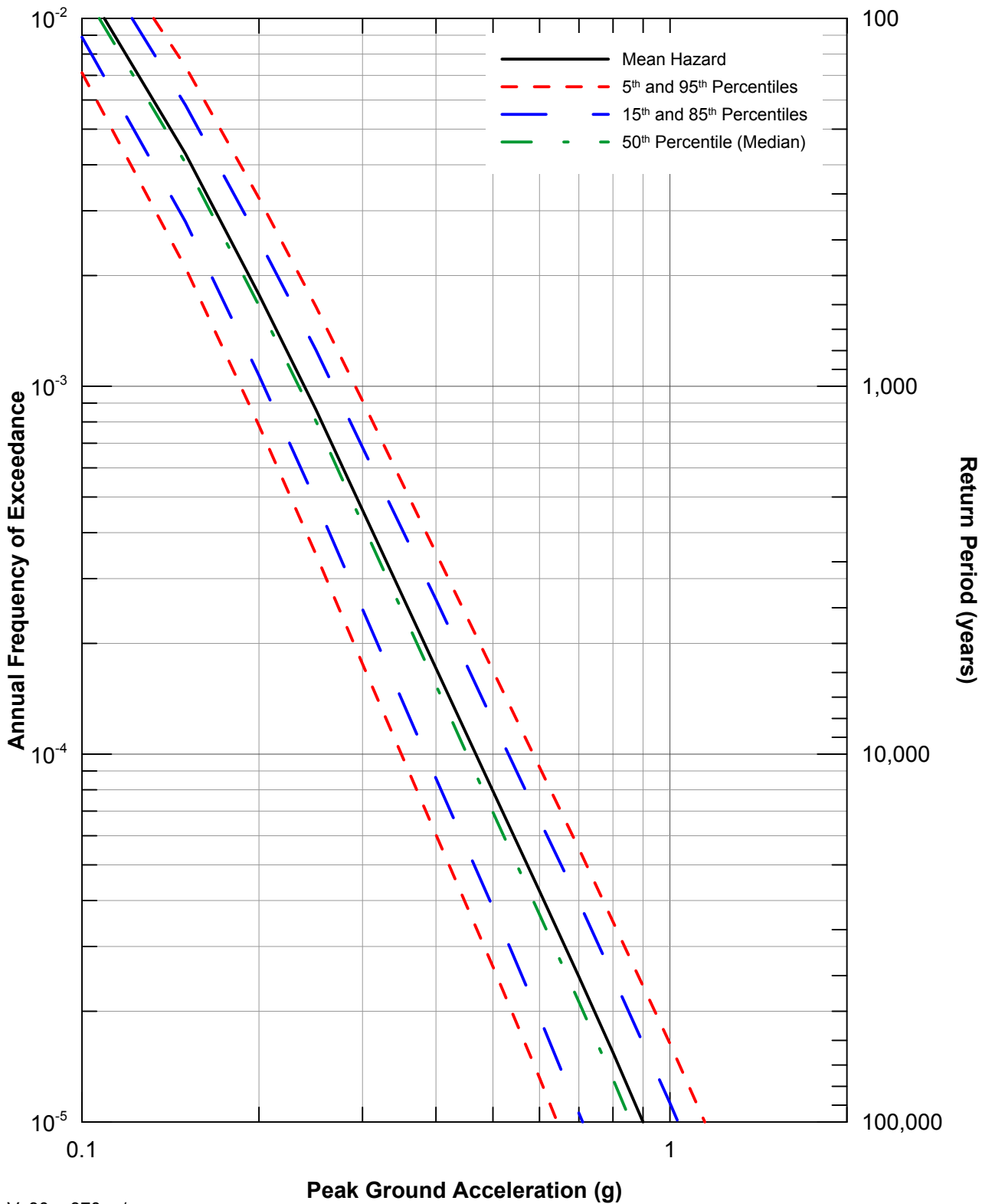


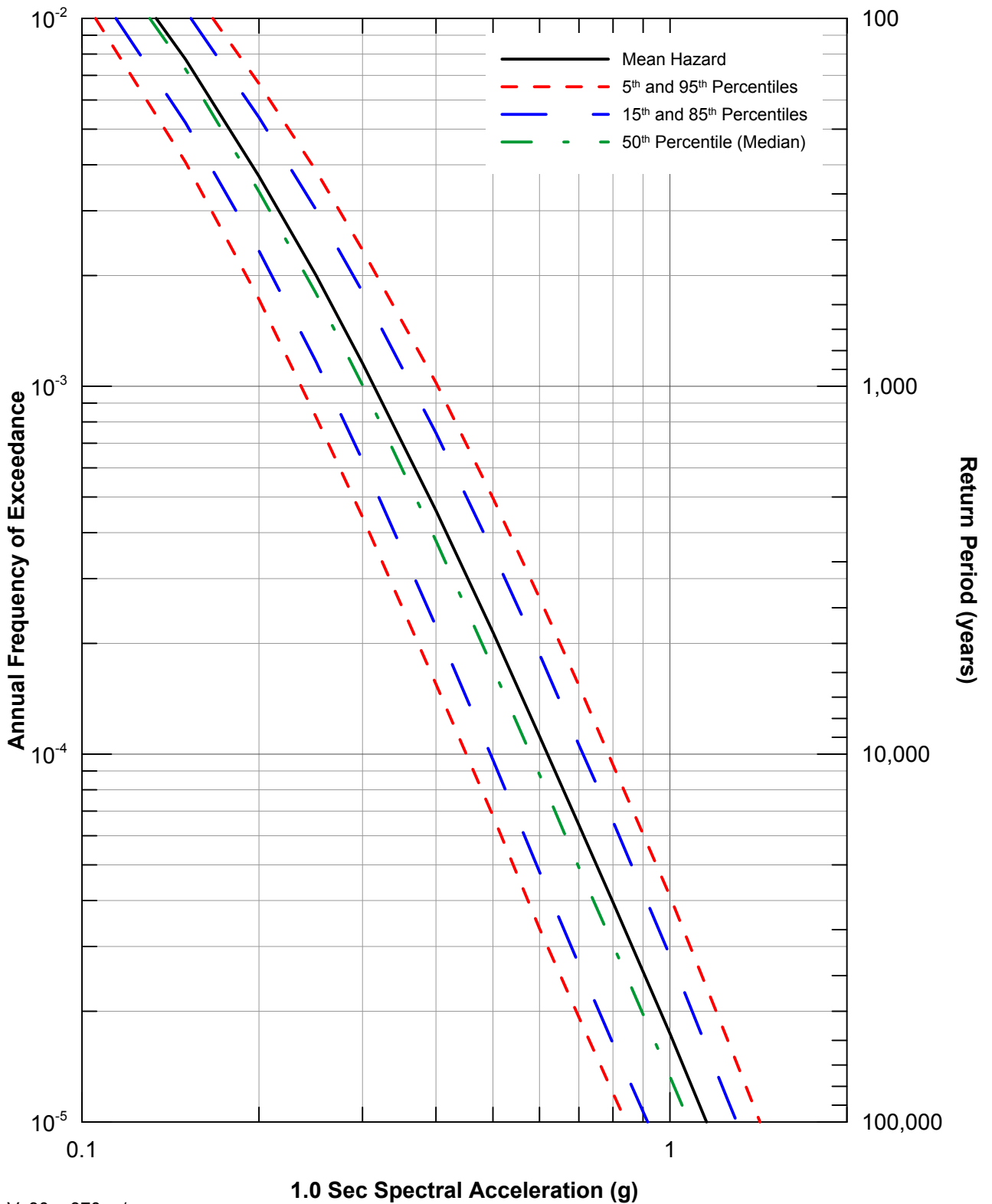


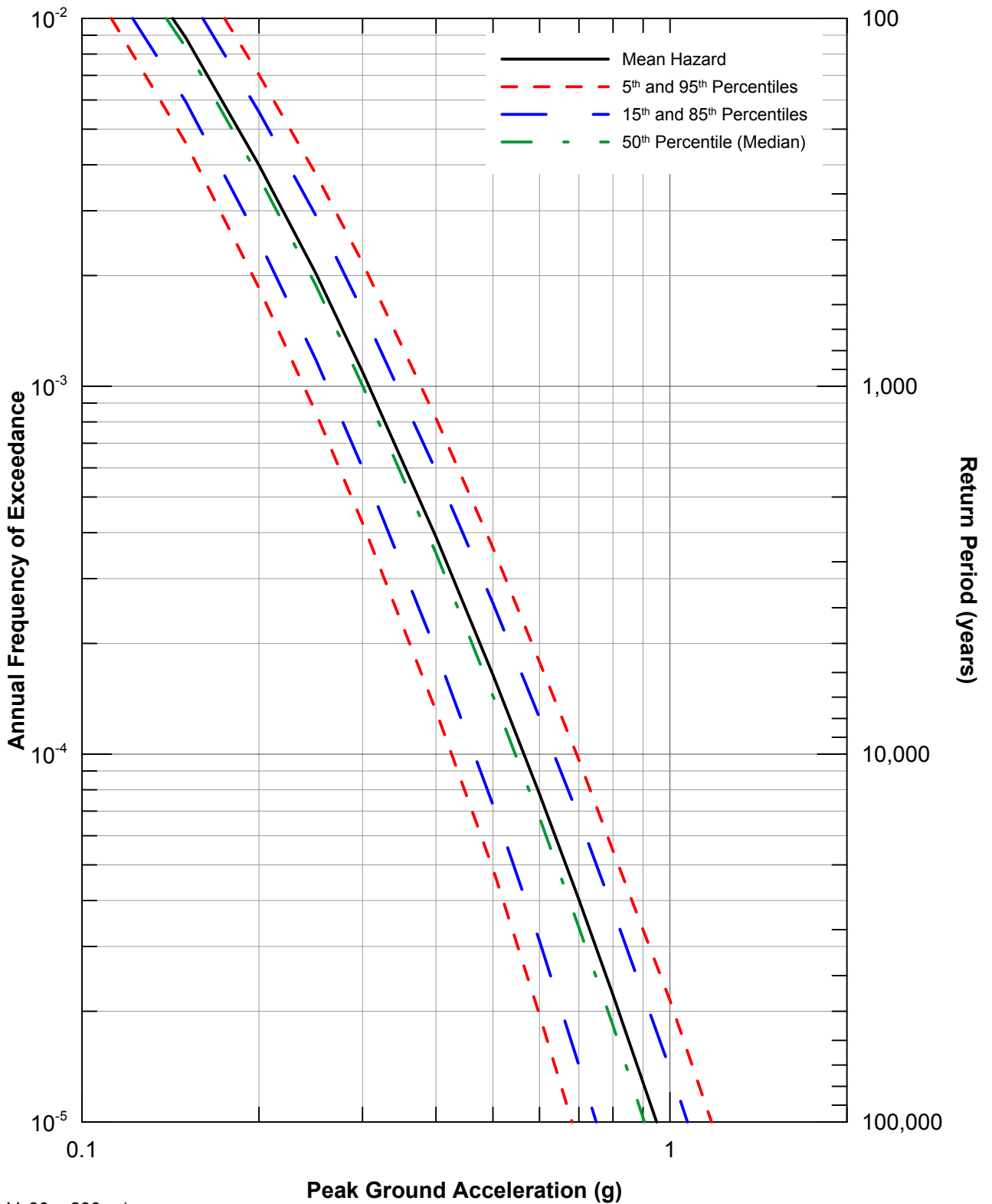


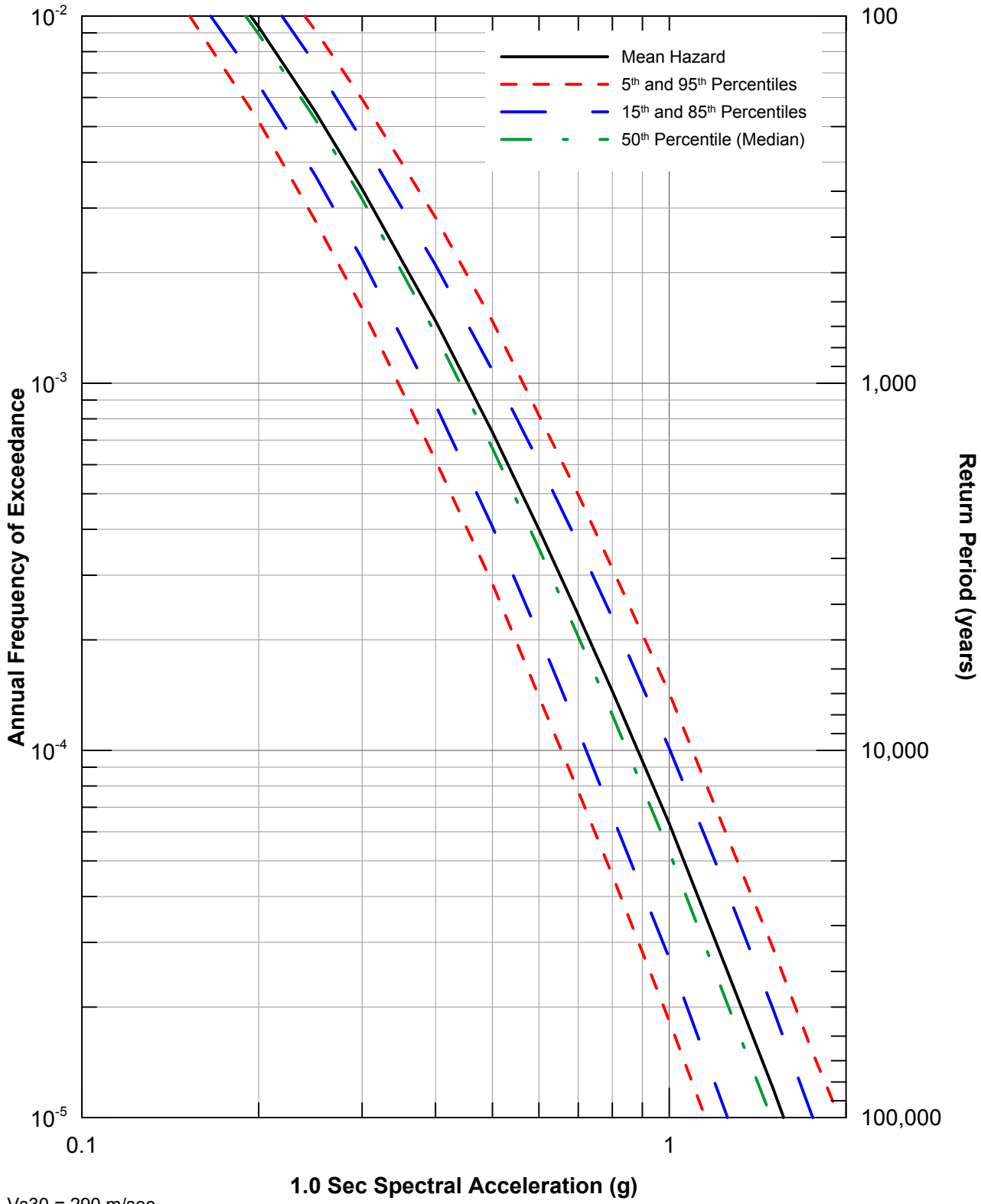


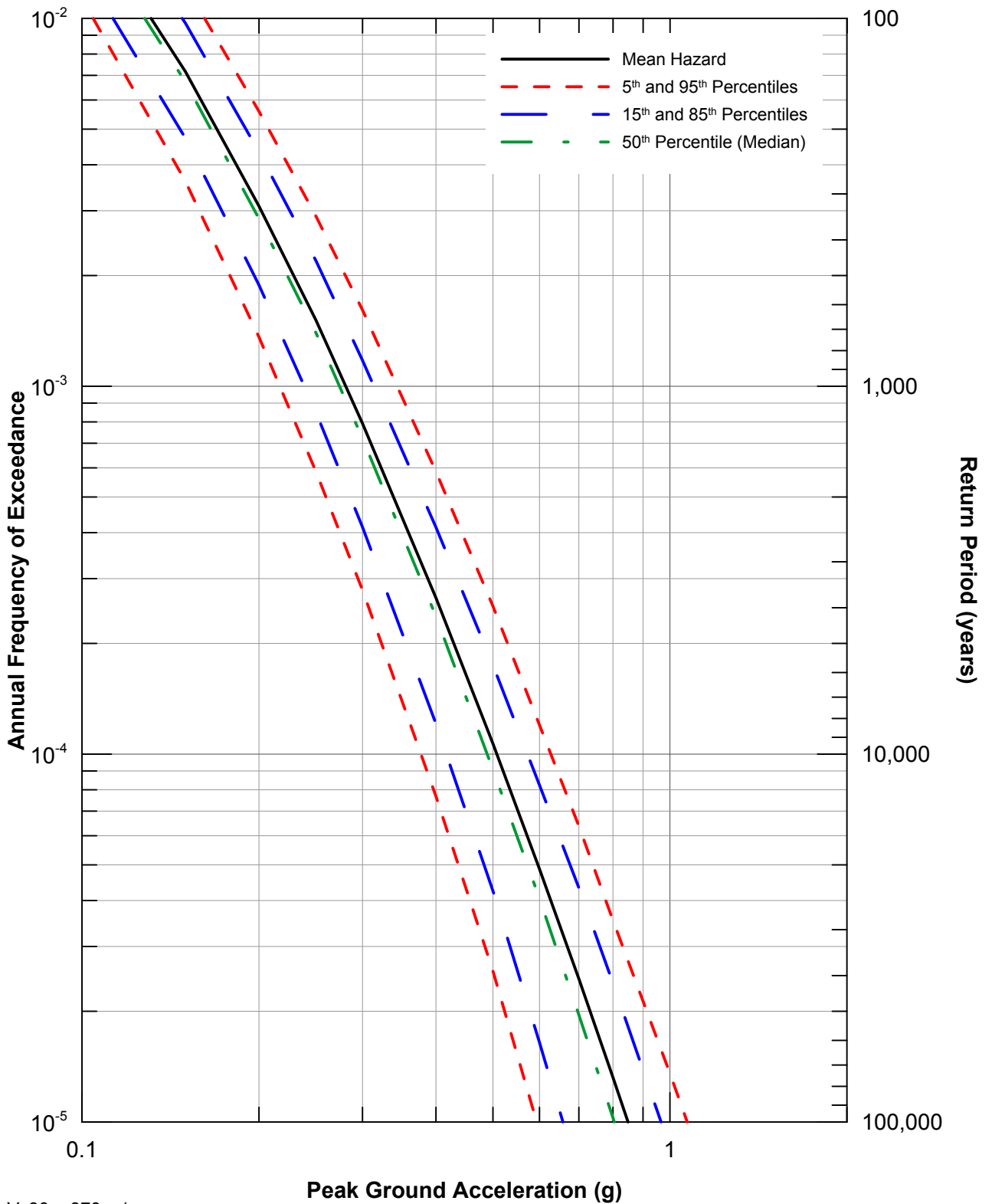


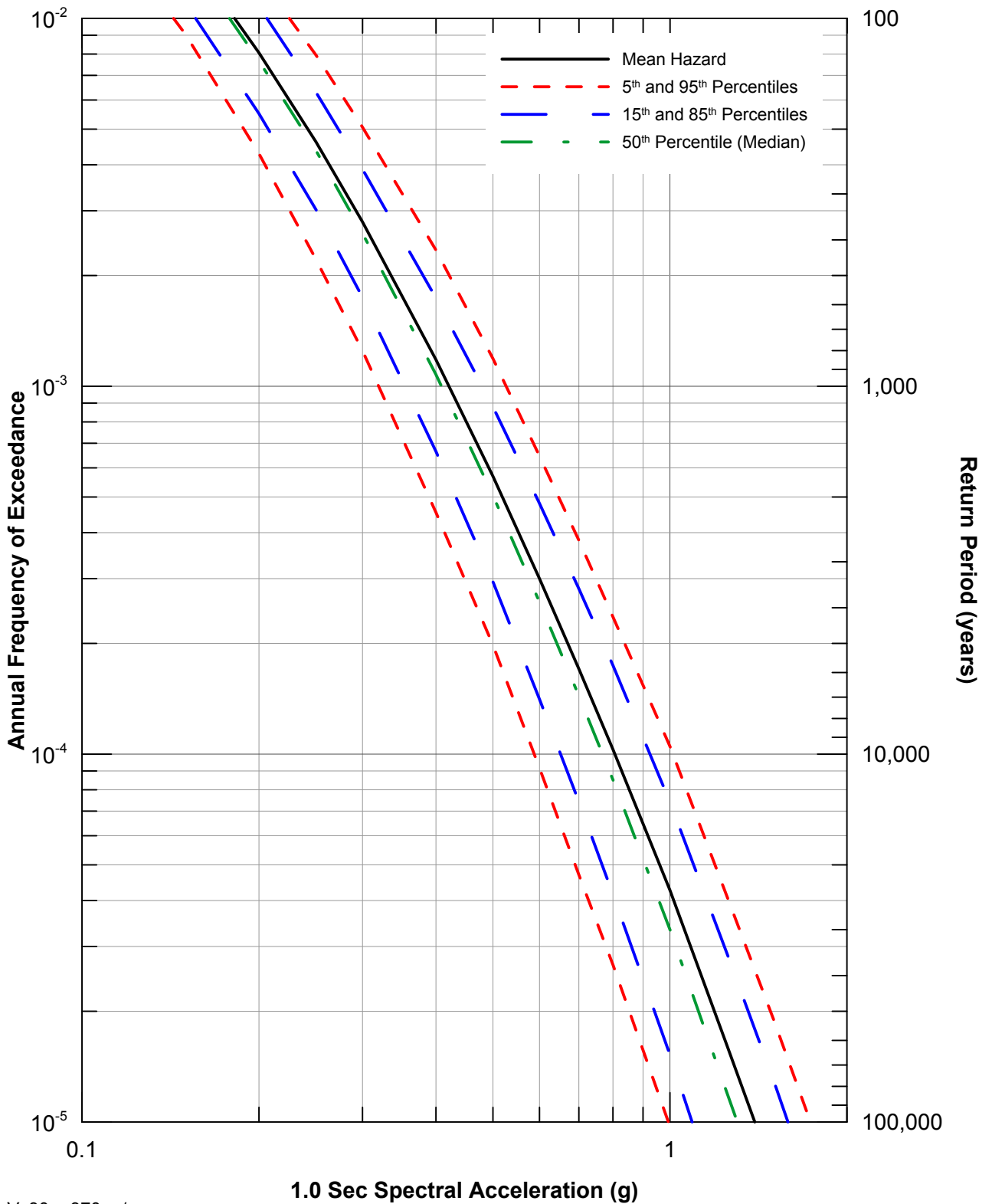


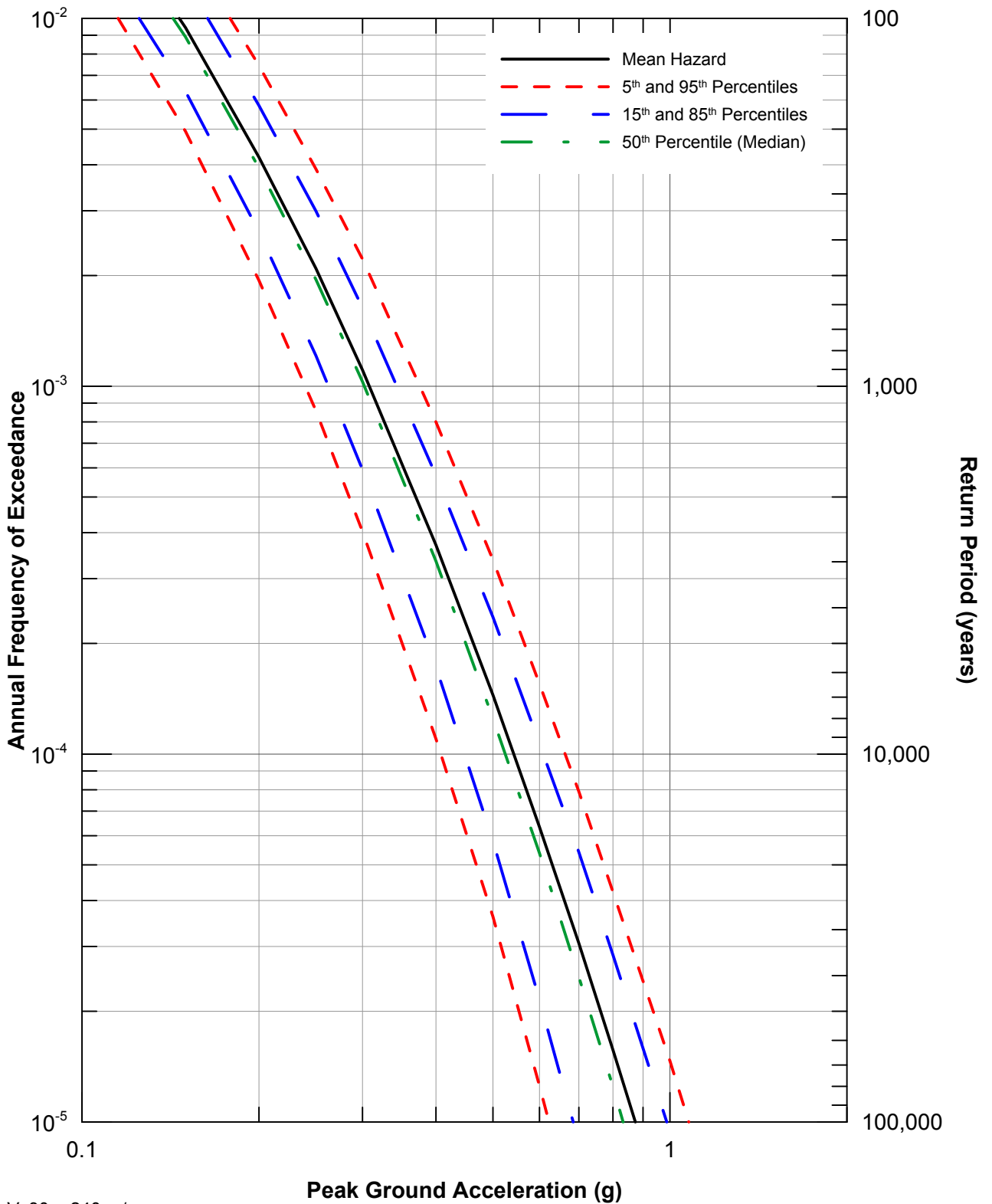


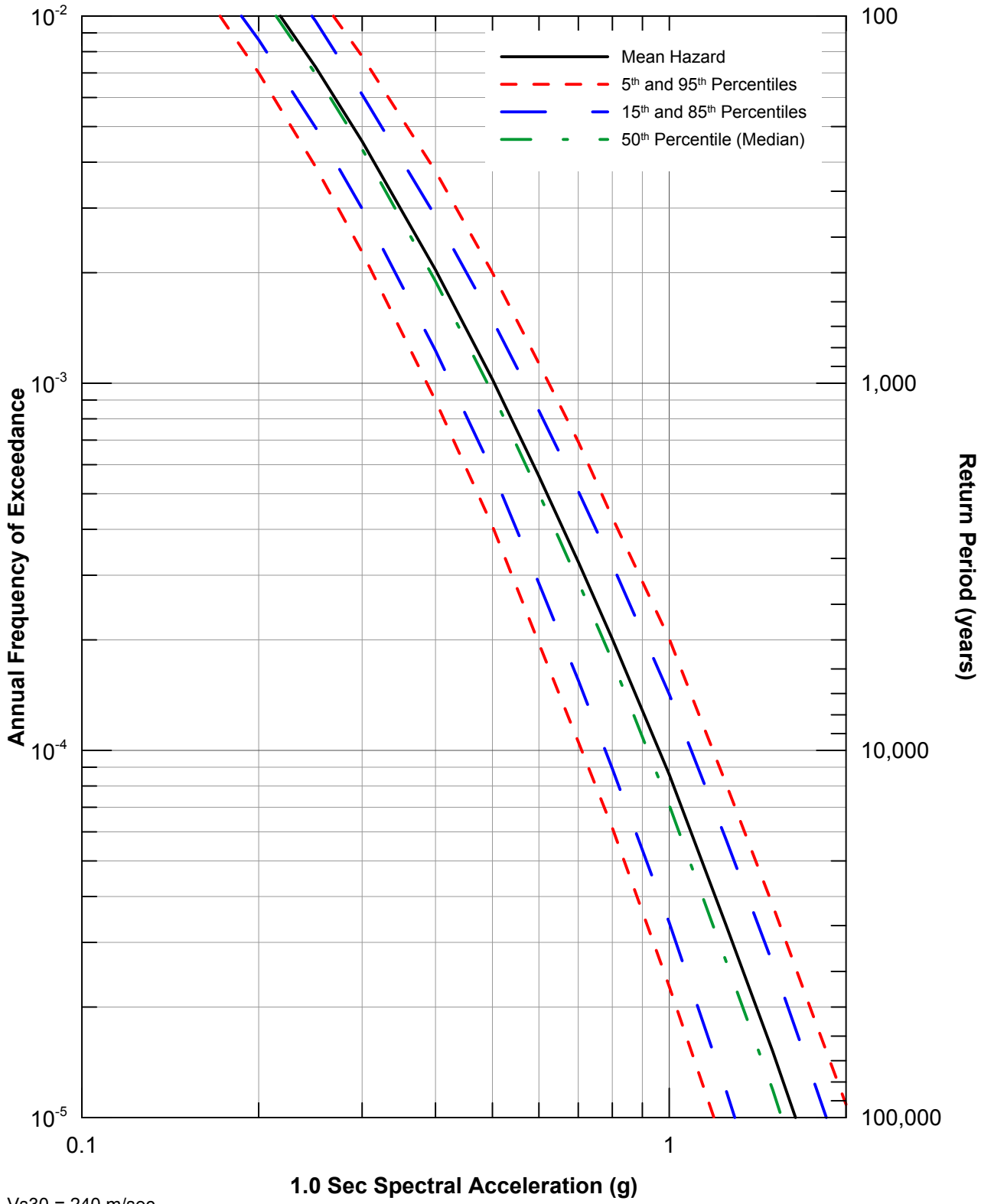


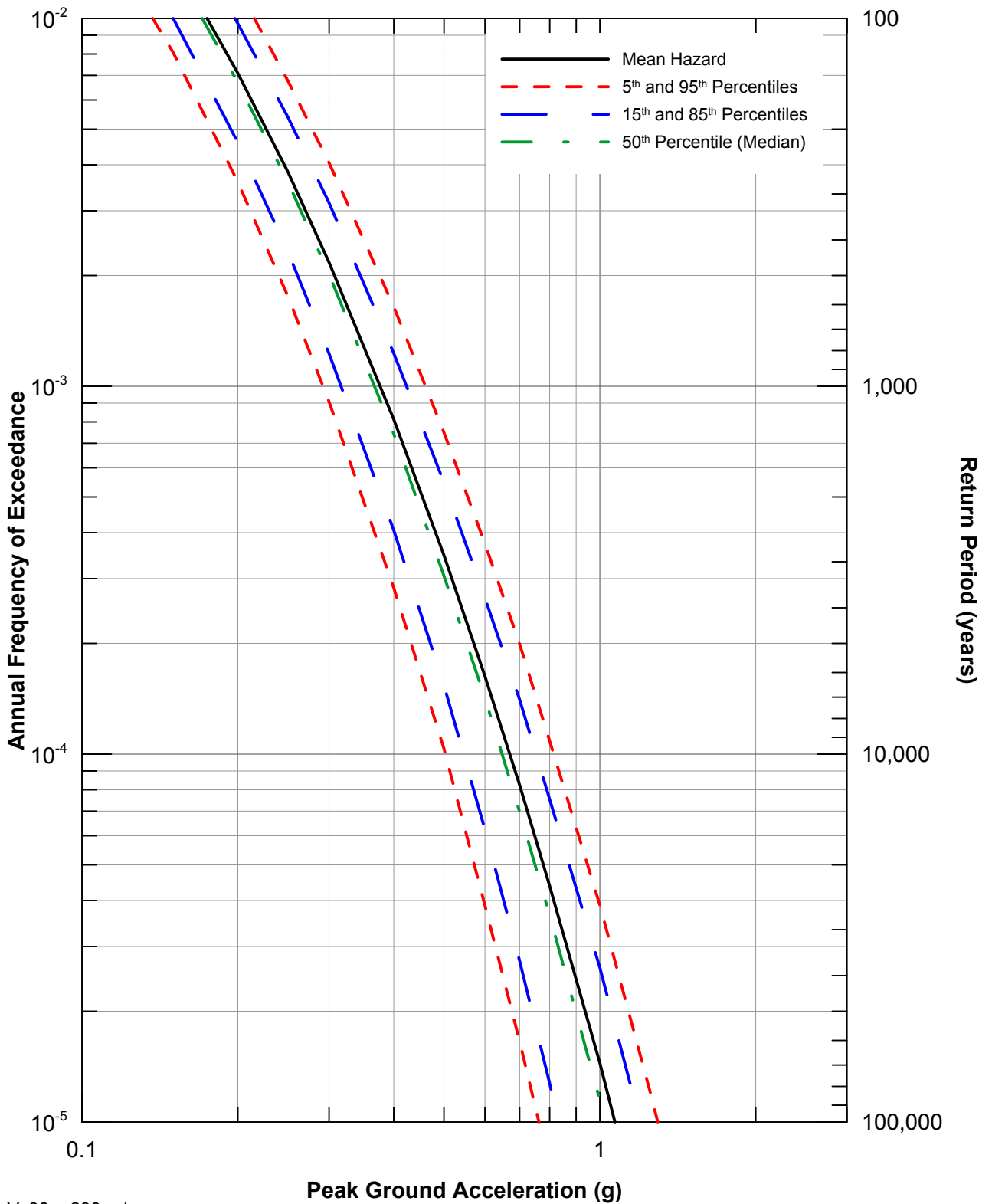


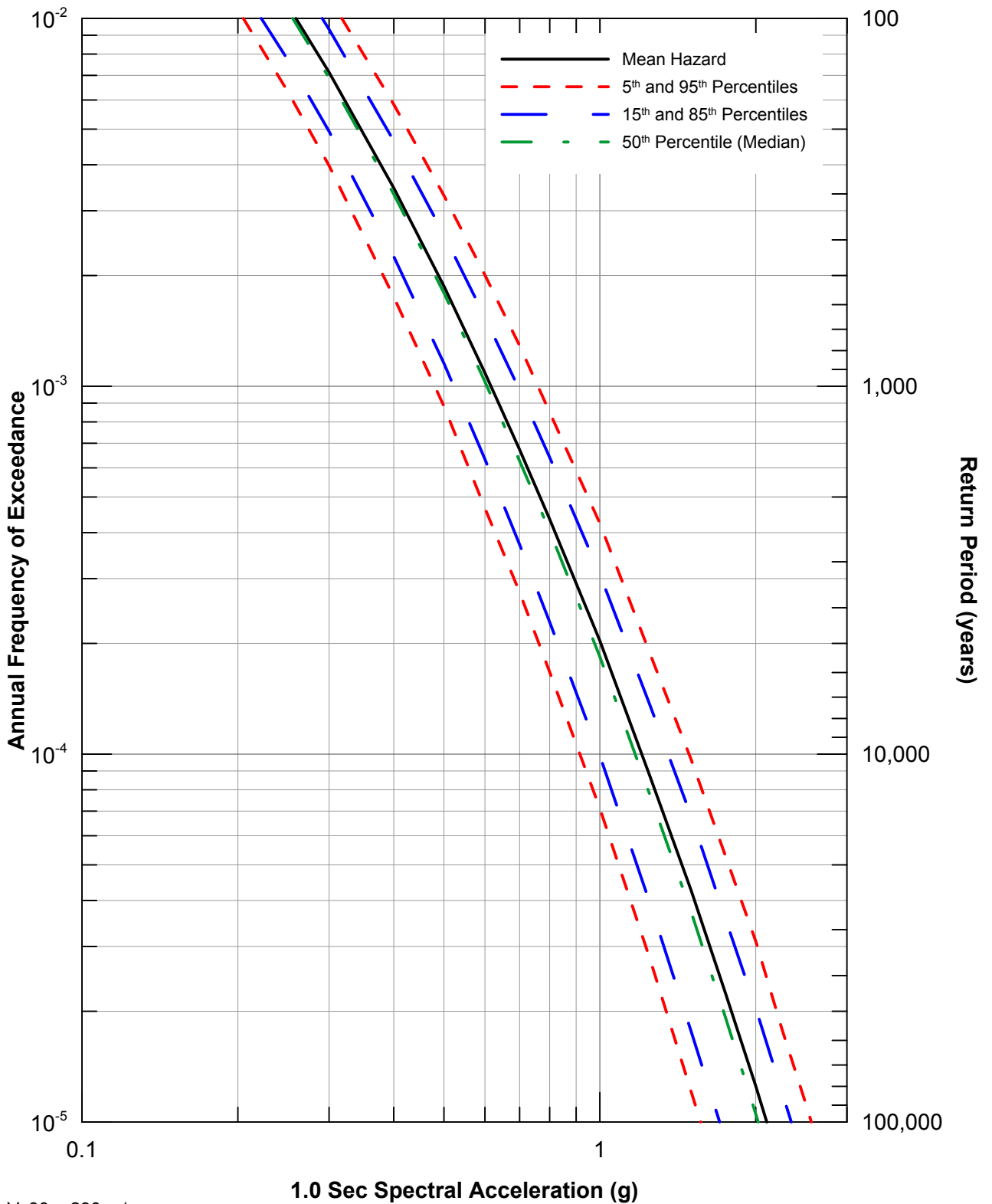


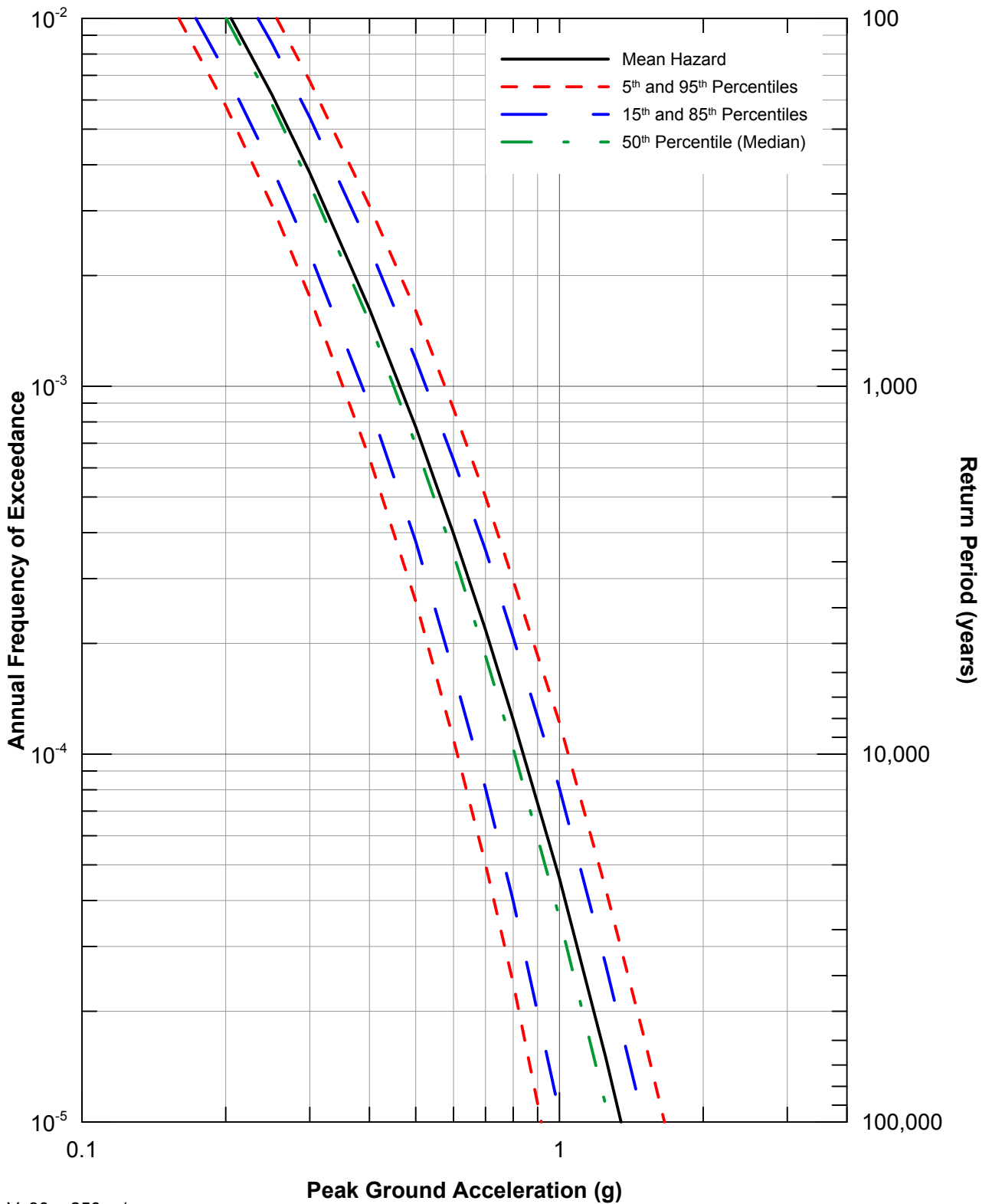


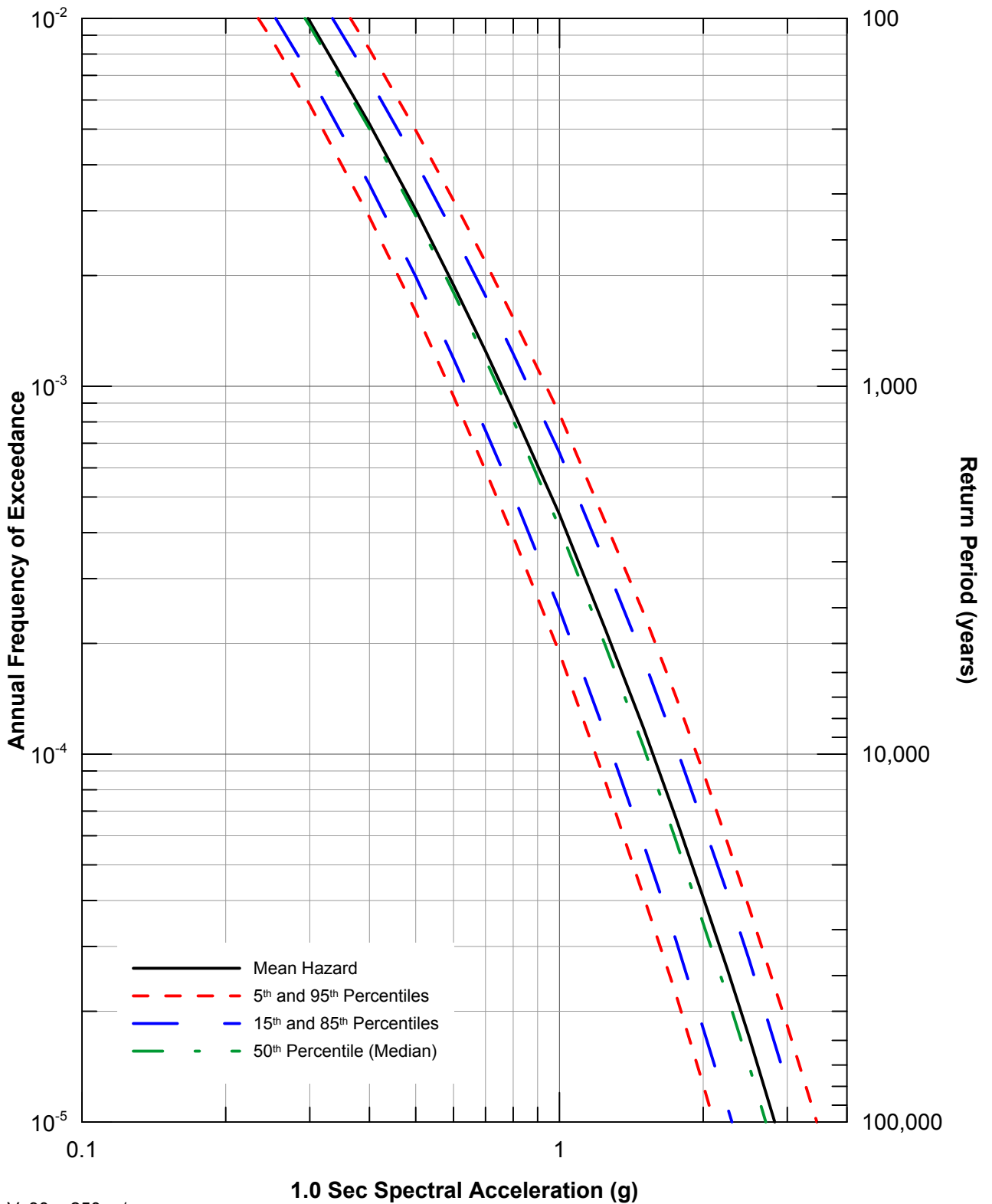


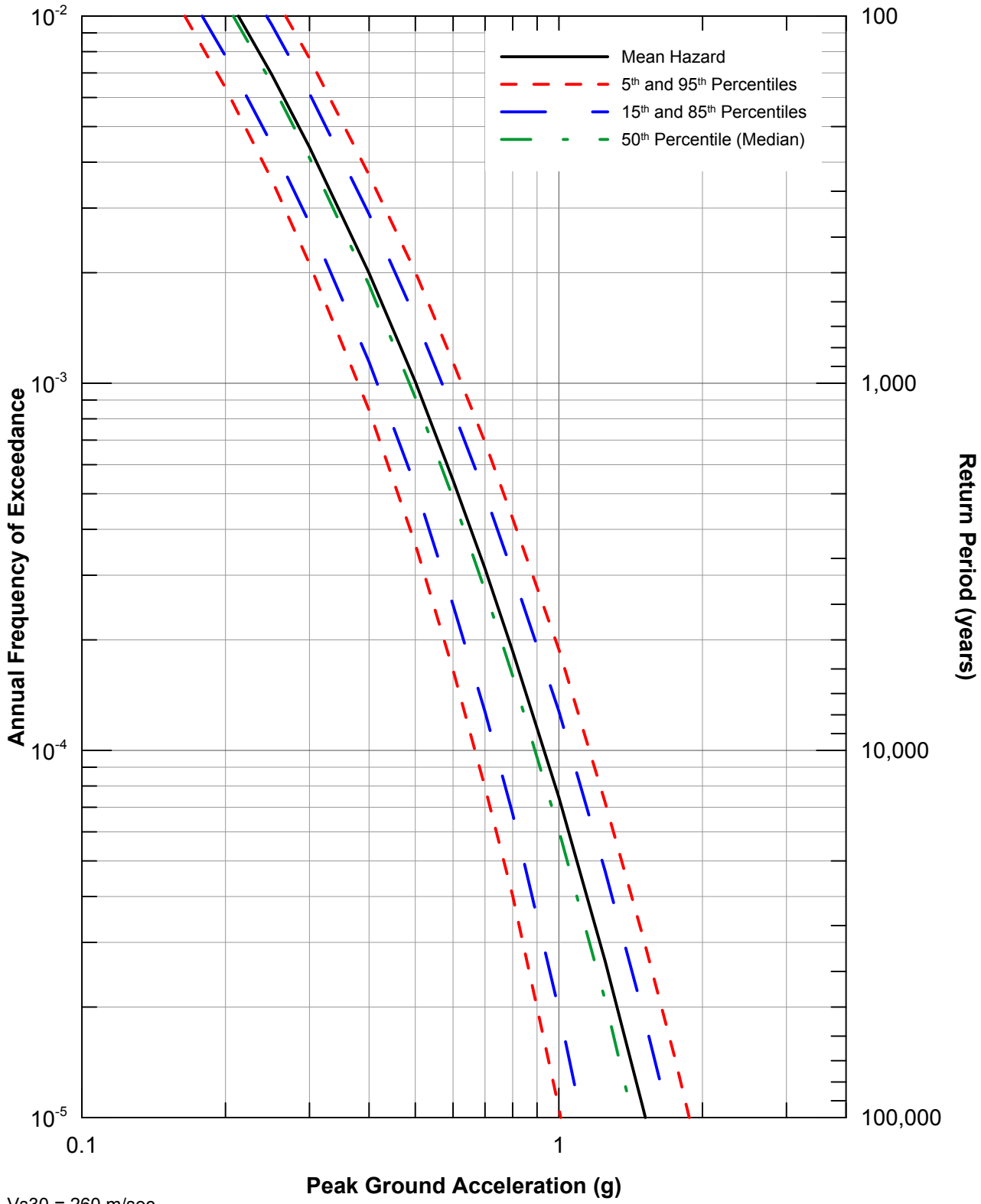


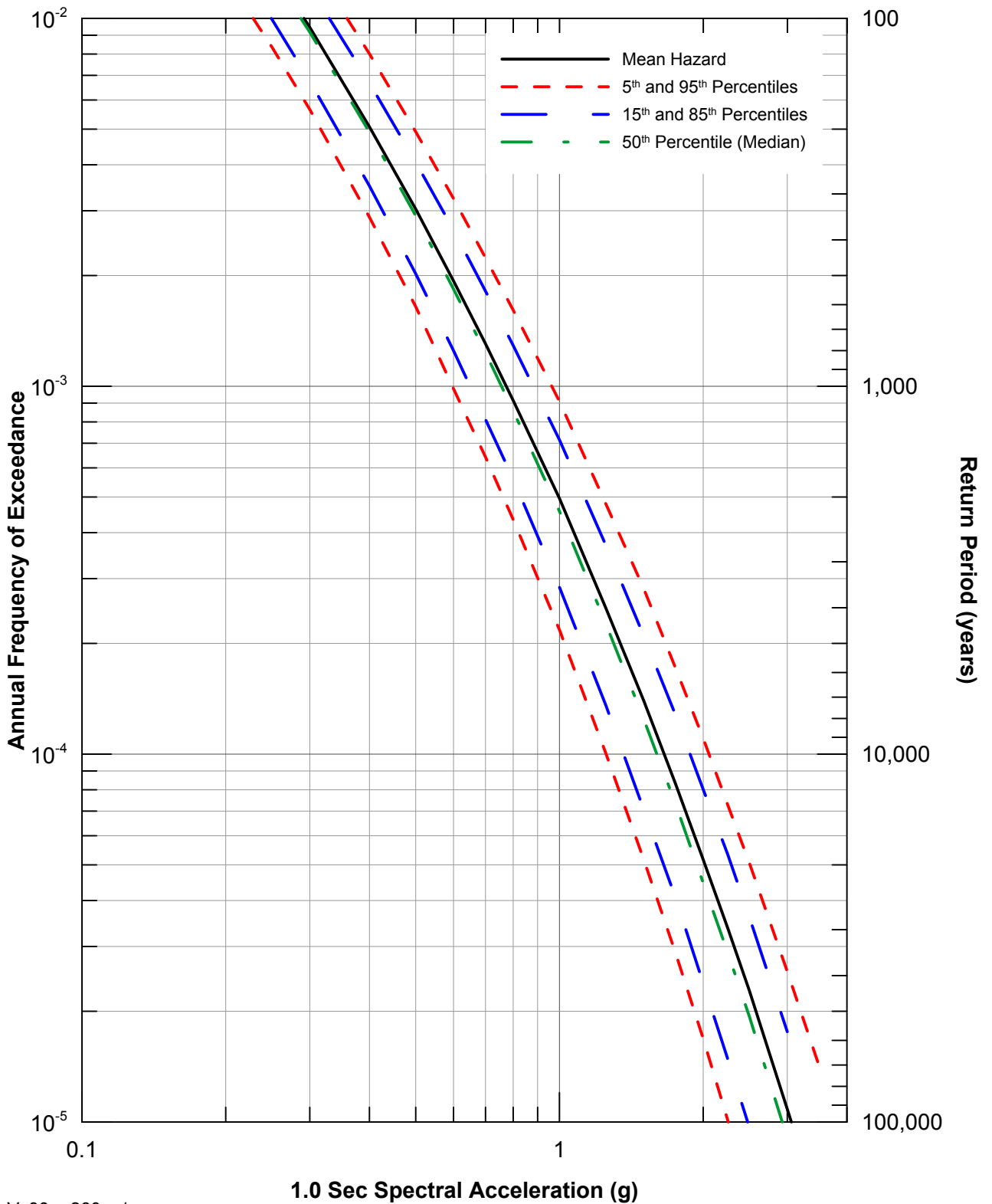


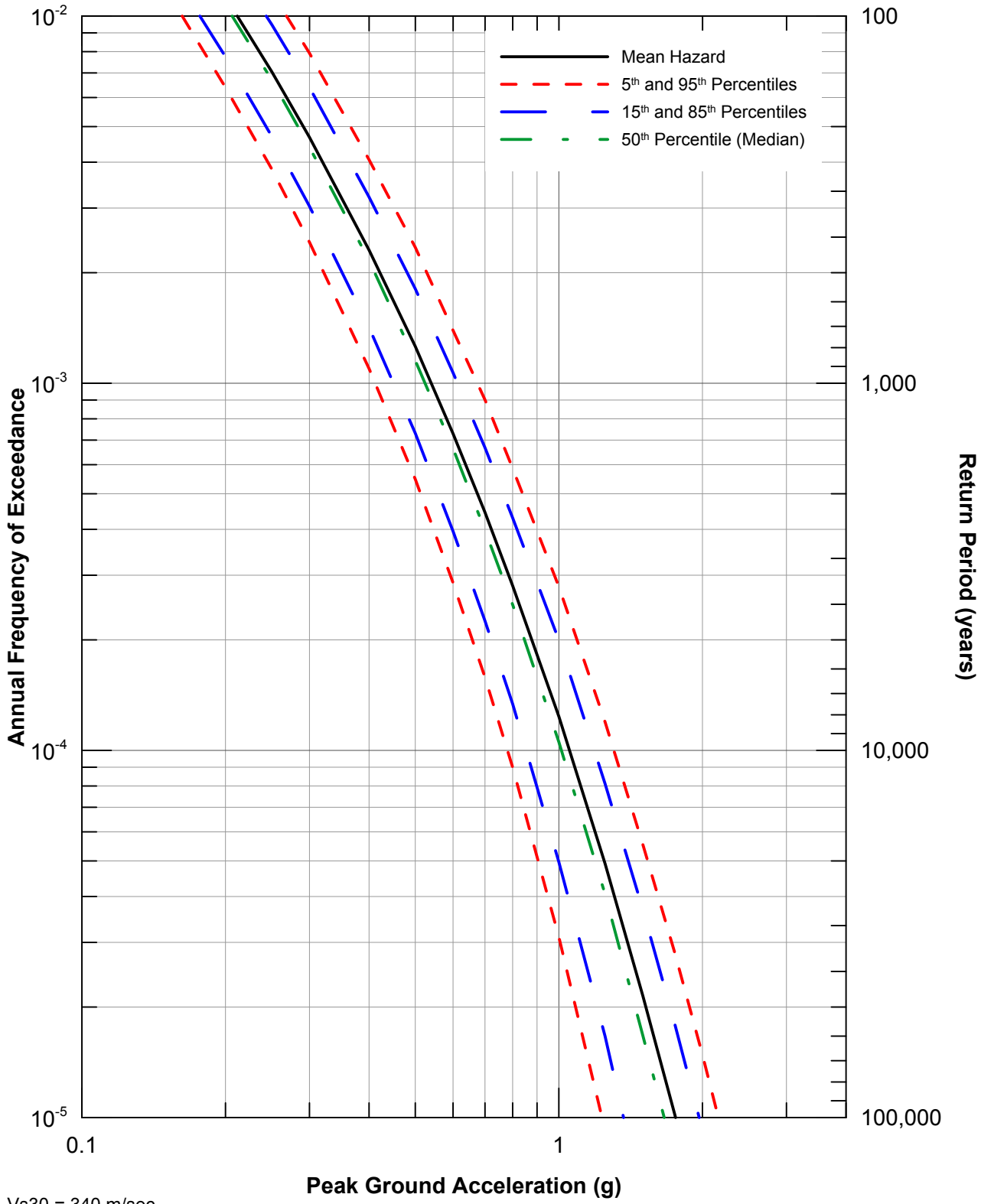


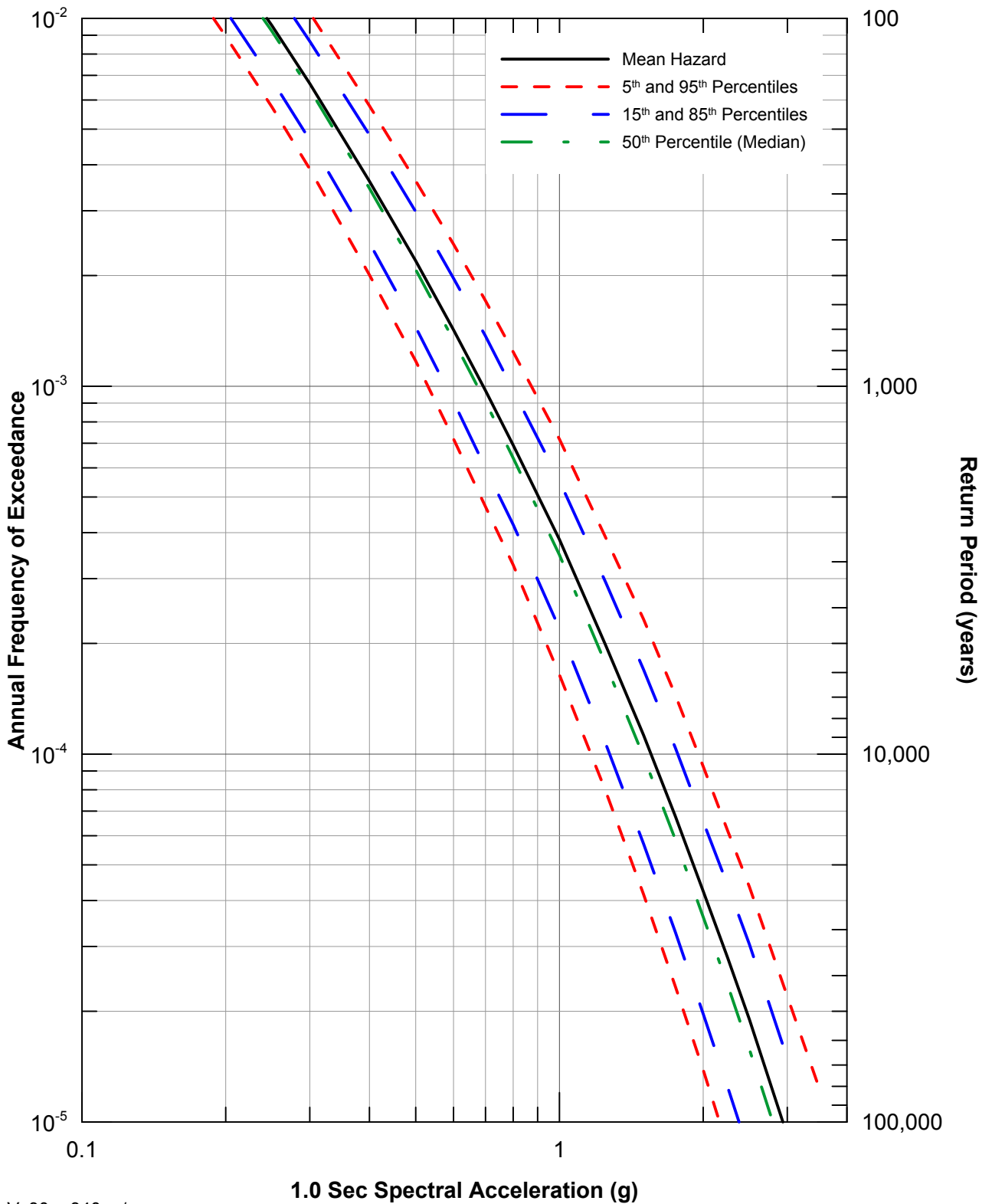


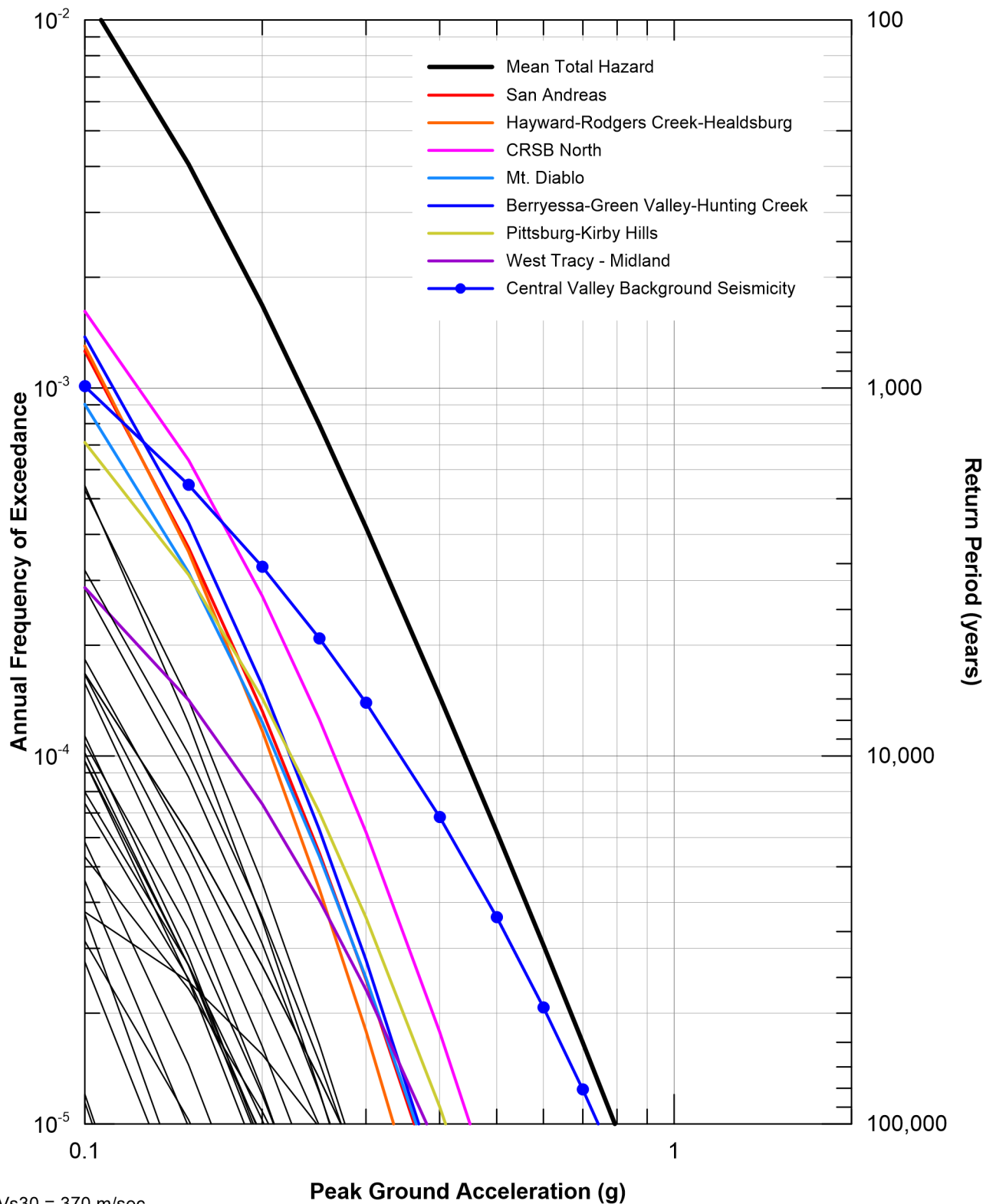










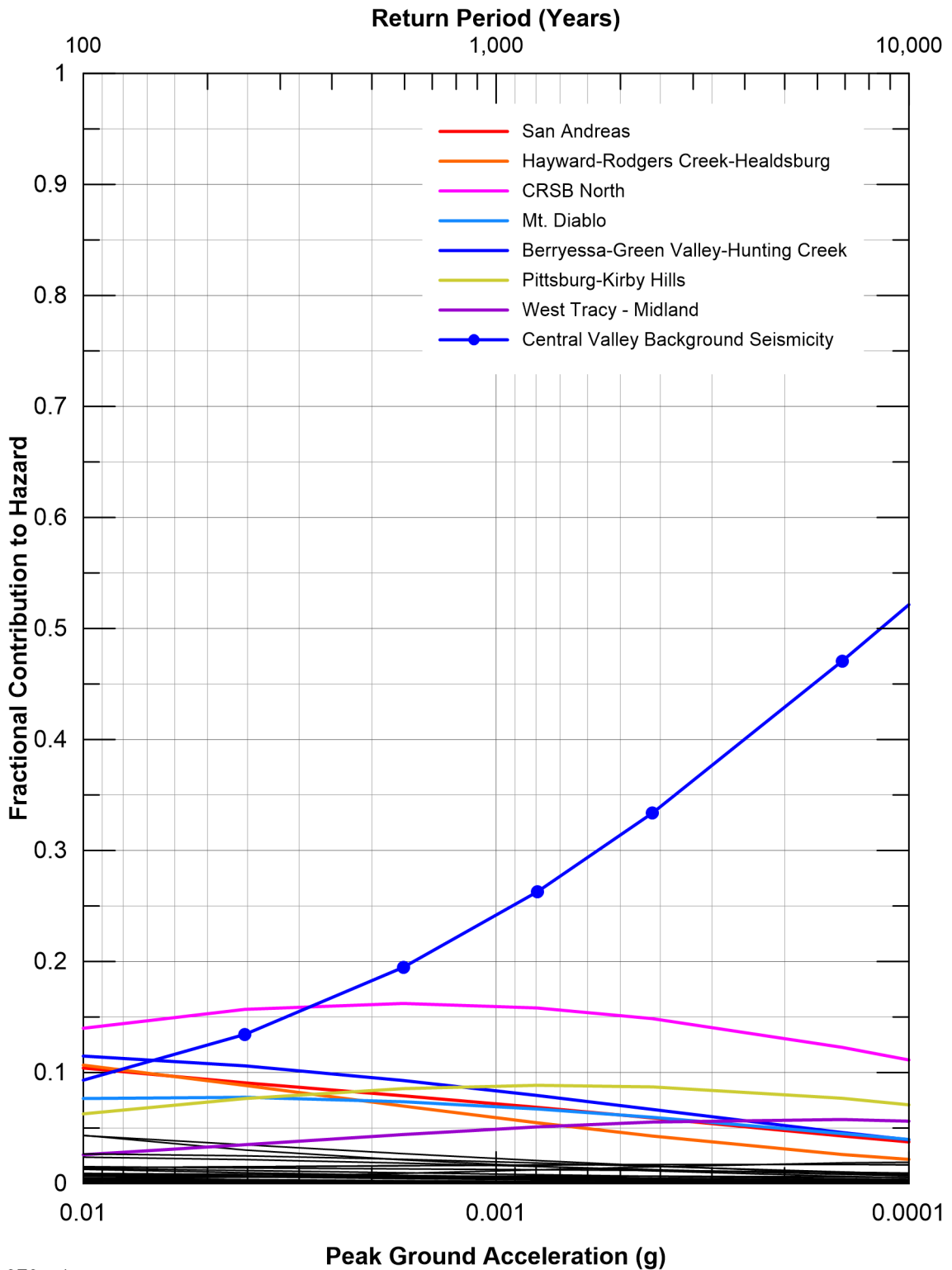


Vs30 = 370 m/sec
 Sources contributing 5% or more in
 144 to 2,475-year return period range listed.
 Other less significant sources shown in black
 not listed.



For Illustration
 Purposes Only

Figure 28
 Seismic Source Contributions
 for Mean Peak Horizontal Acceleration
 Hazard for Intake No. 3

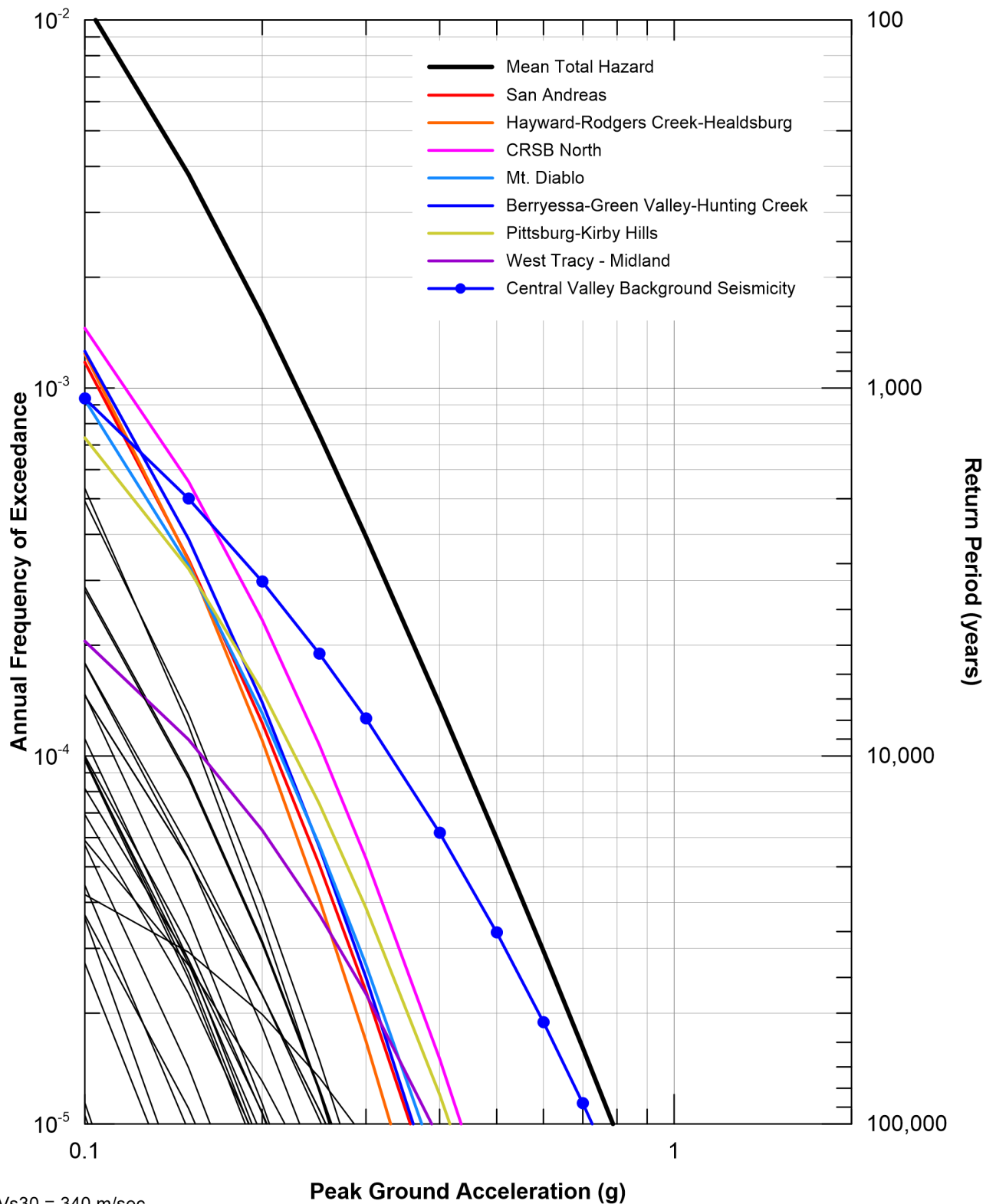


Vs30 = 370 m/sec
 Sources contributing 5% or more in
 144 to 2,475-year return period range listed.
 Other less significant sources shown in black
 not listed.



For Illustration
Purposes Only

Figure 29
 Seismic Source Fractional Contributions
 for Mean Peak Horizontal Acceleration
 Hazard for Intake No. 3

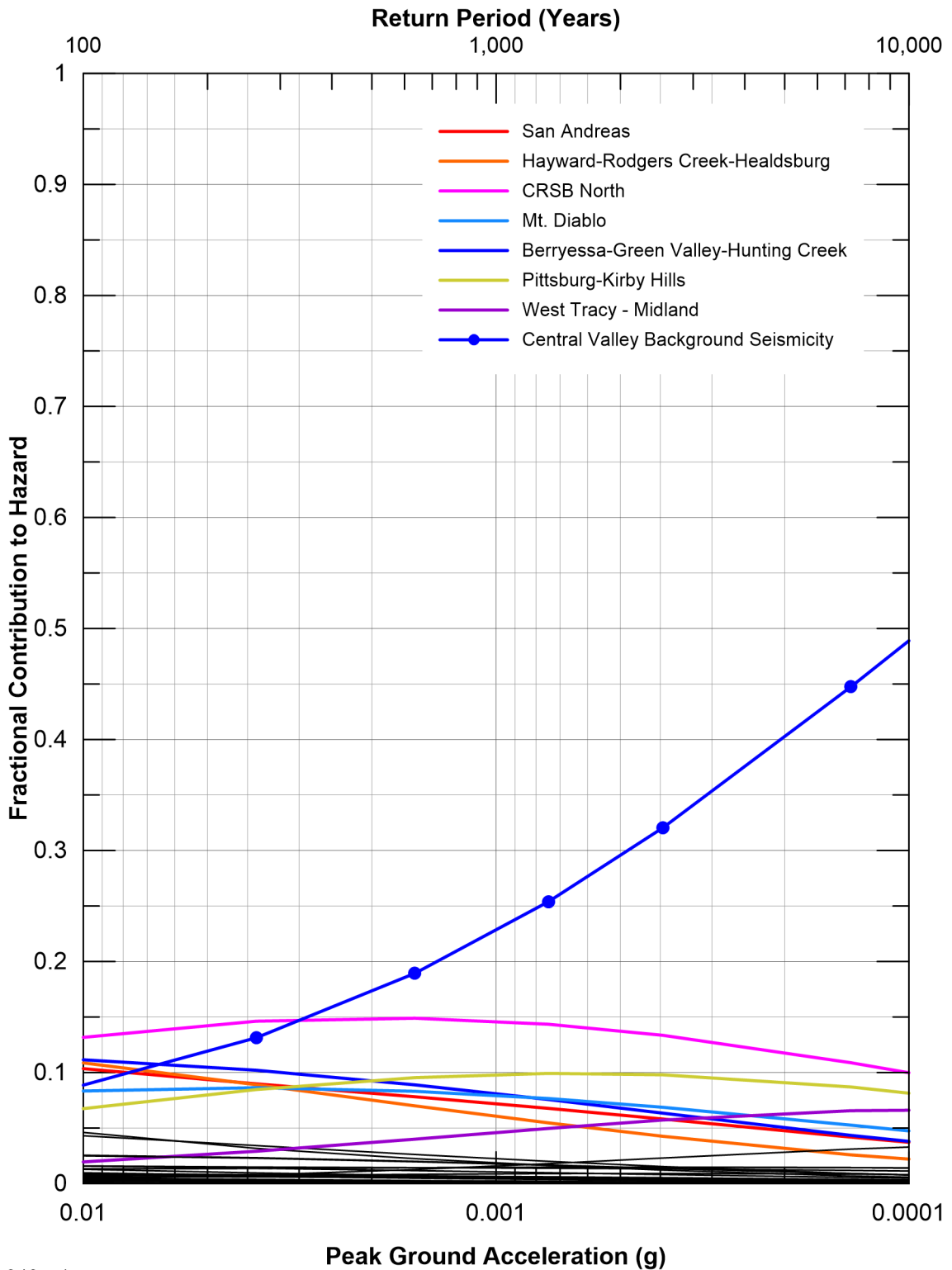


Vs30 = 340 m/sec
 Sources contributing 5% or more in
 144 to 2,475-year return period range listed.
 Other less significant sources shown in black
 not listed.



For Illustration
 Purposes Only

Figure 30
 Seismic Source Contributions
 for Mean Peak Horizontal Acceleration
 Hazard for Intake No. 5

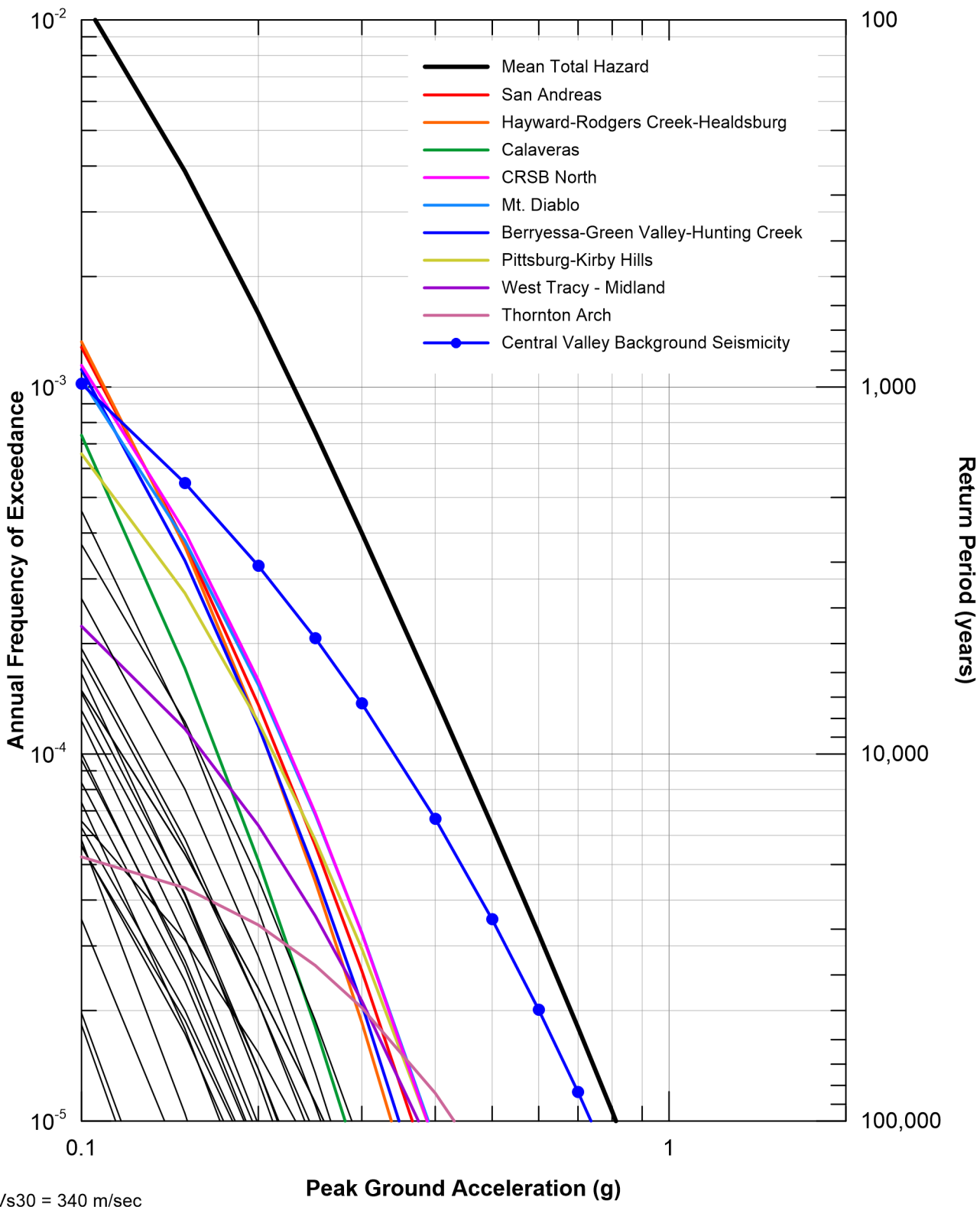


Vs30 = 340 m/sec
 Sources contributing 5% or more in
 144 to 2,475-year return period range listed.
 Other less significant sources shown in black
 not listed.



For Illustration
 Purposes Only

Figure 31
 Seismic Source Fractional Contributions
 for Mean Peak Horizontal Acceleration
 Hazard for Intake No. 5

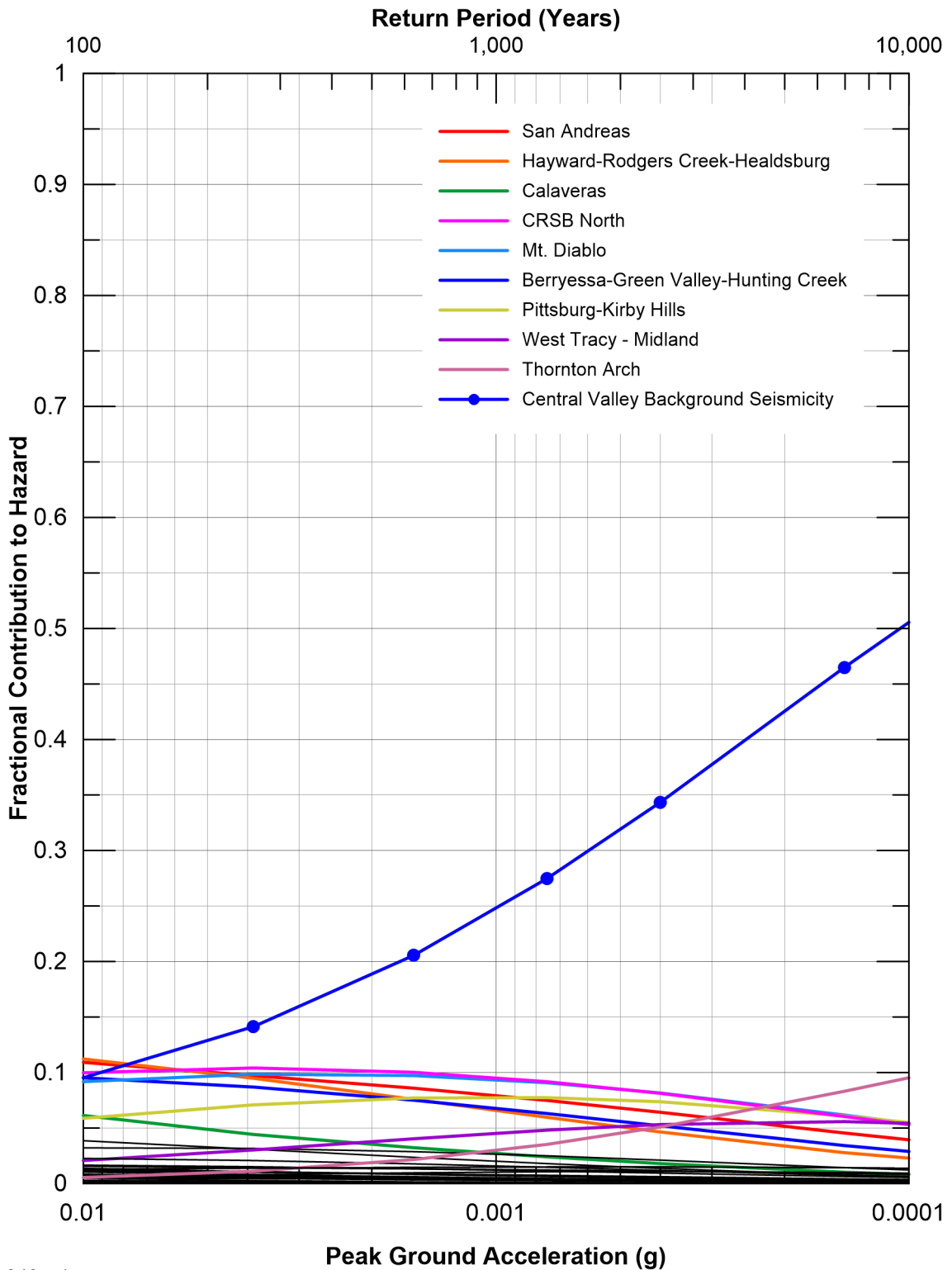


Vs30 = 340 m/sec
 Sources contributing 5% or more in
 144 to 2,475-year return period range listed.
 Other less significant sources shown in black
 not listed.



For Illustration
 Purposes Only

Figure 32
 Seismic Source Contributions
 for Mean Peak Horizontal Acceleration
 Hazard for Twin Cities

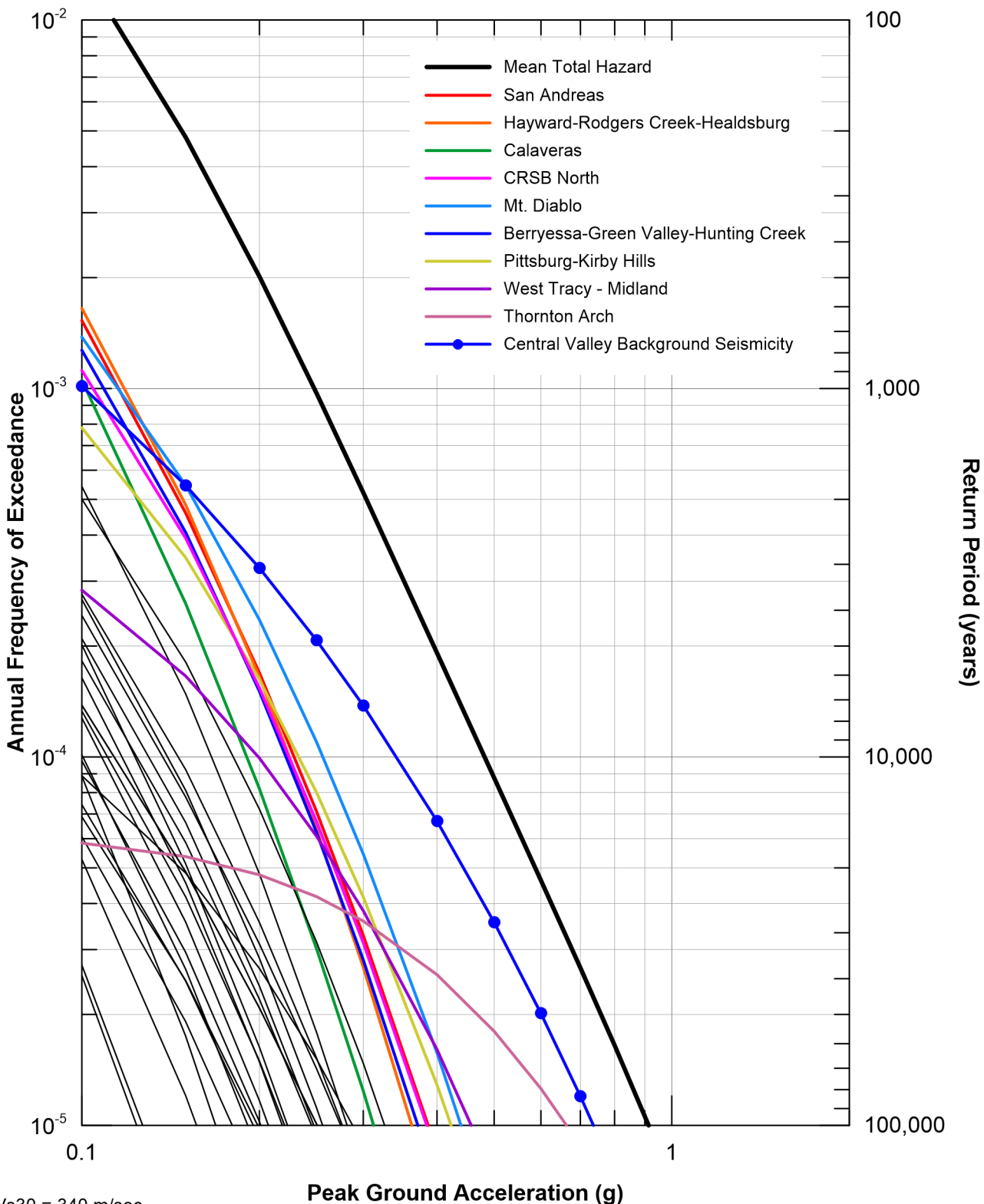


Vs30 = 340 m/sec
 Sources contributing 5% or more in
 144 to 2,475-year return period range listed.
 Other less significant sources shown in black
 not listed.



For Illustration
 Purposes Only

Figure 33
 Seismic Source Fractional Contributions
 for Mean Peak Horizontal Acceleration
 Hazard for Twin Cities

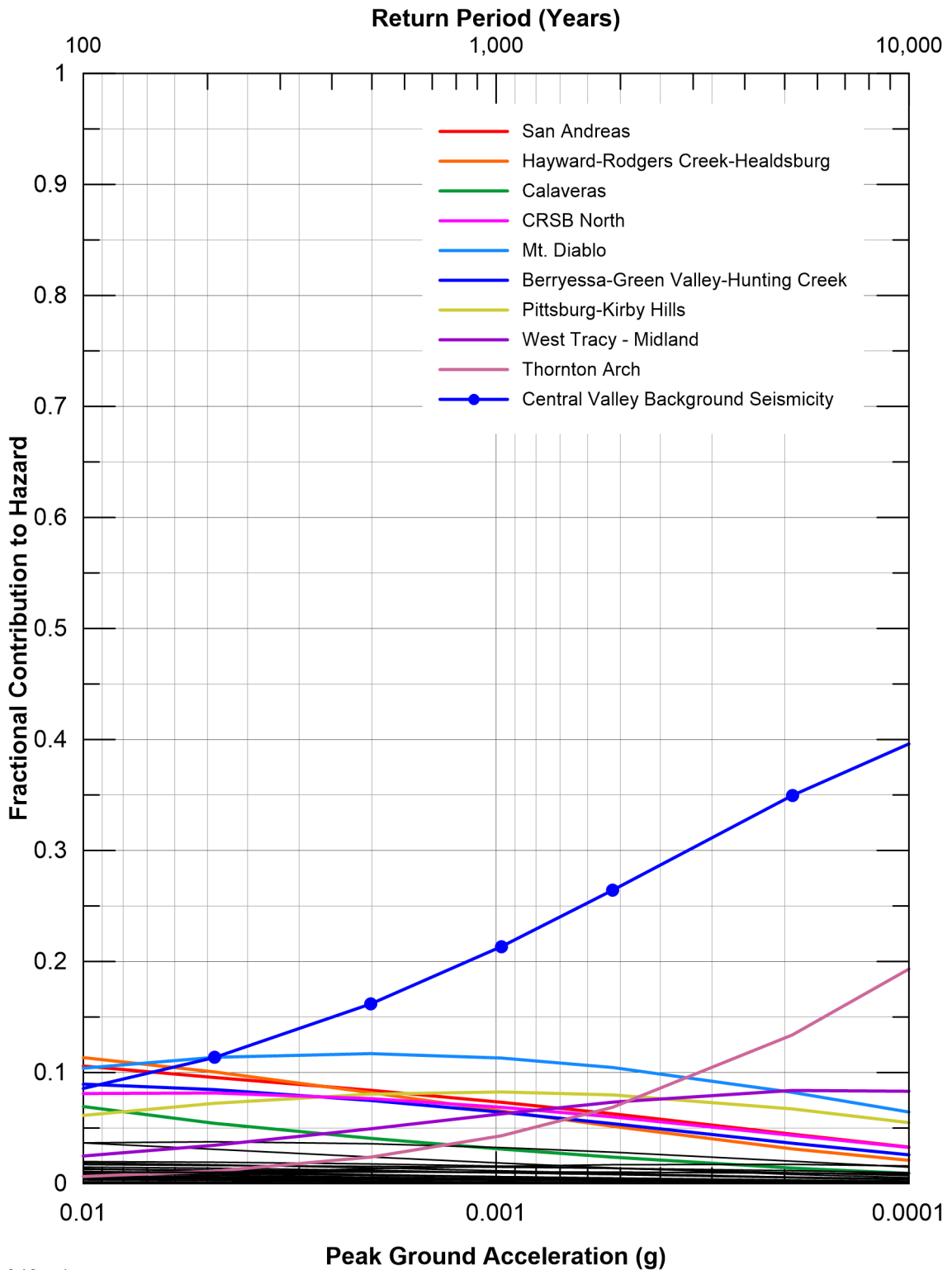


Vs30 = 340 m/sec
 Sources contributing 5% or more in
 144 to 2,475-year return period range listed.
 Other less significant sources shown in black
 not listed.



For Illustration
 Purposes Only

Figure 34
 Seismic Source Contributions
 for Mean Peak Horizontal Acceleration
 Hazard for New Hope

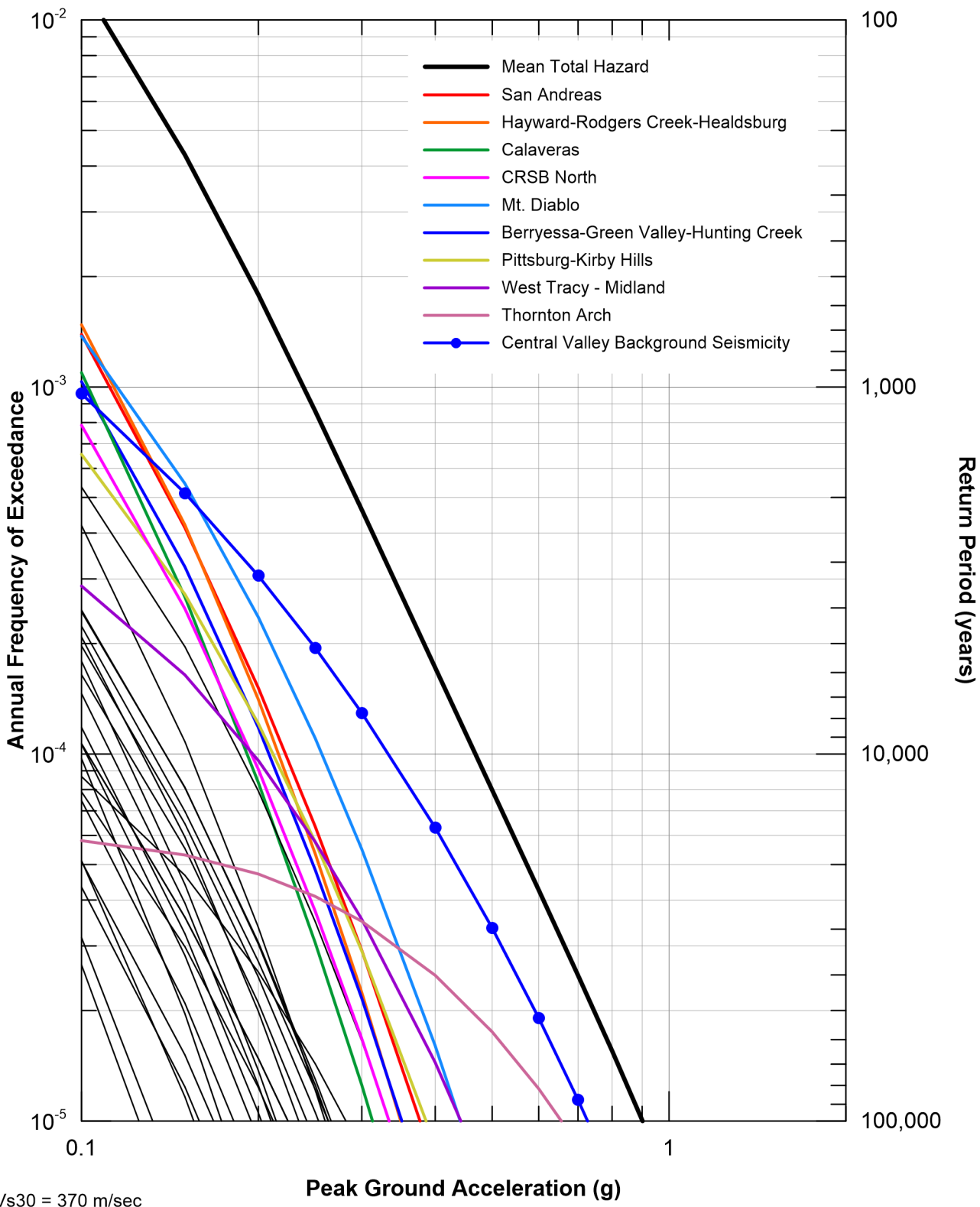


Vs30 = 340 m/sec
 Sources contributing 5% or more in
 144 to 2,475-year return period range listed.
 Other less significant sources shown in black
 not listed.



For Illustration
 Purposes Only

Figure 35
 Seismic Source Fractional Contributions
 for Mean Peak Horizontal Acceleration
 Hazard for New Hope

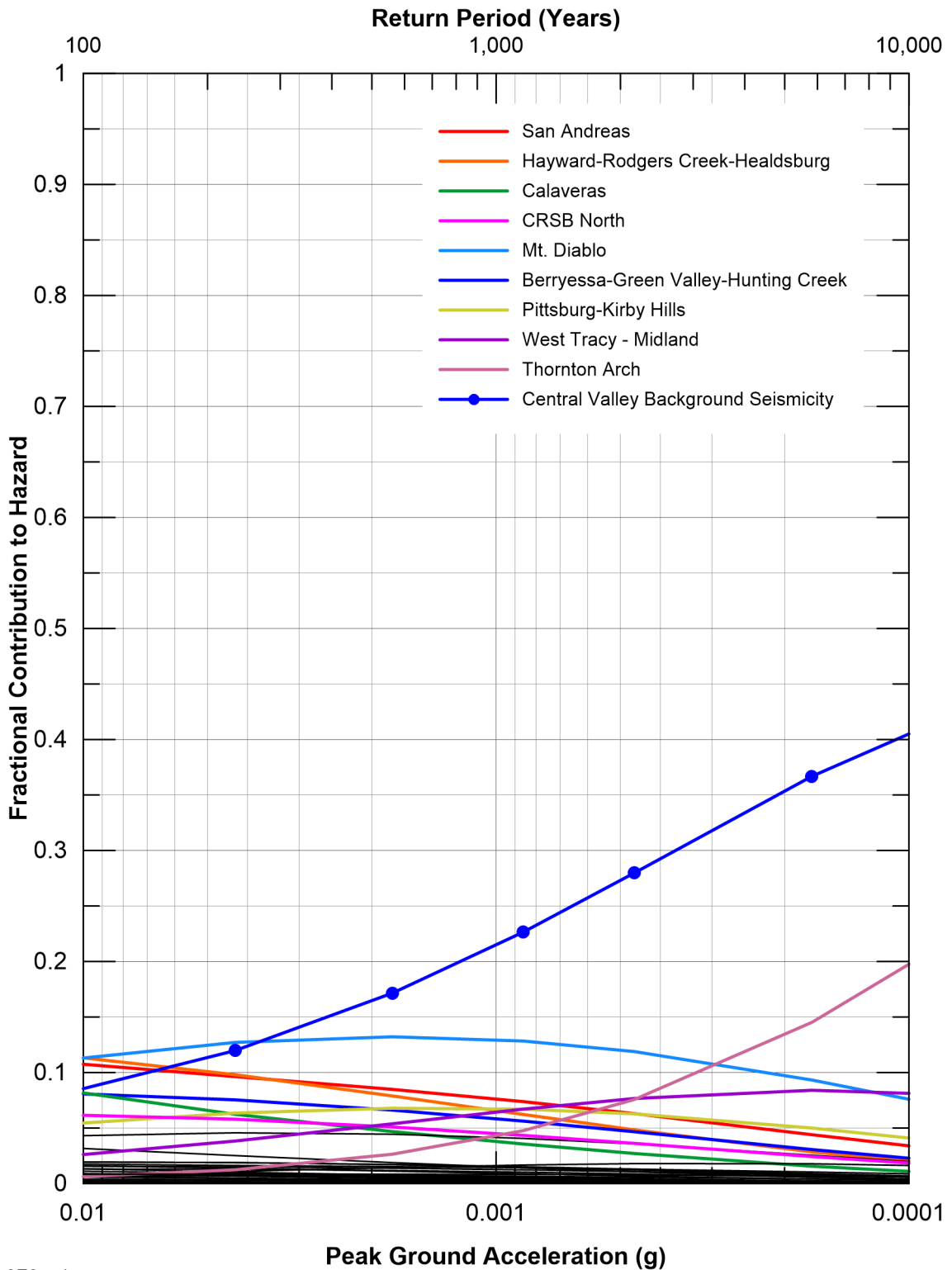


Vs30 = 370 m/sec
 Sources contributing 5% or more in
 144 to 2,475-year return period range listed.
 Other less significant sources shown in black
 not listed.



For Illustration
 Purposes Only

Figure 36
 Seismic Source Contributions
 for Mean Peak Horizontal Acceleration
 Hazard for Canal Ranch

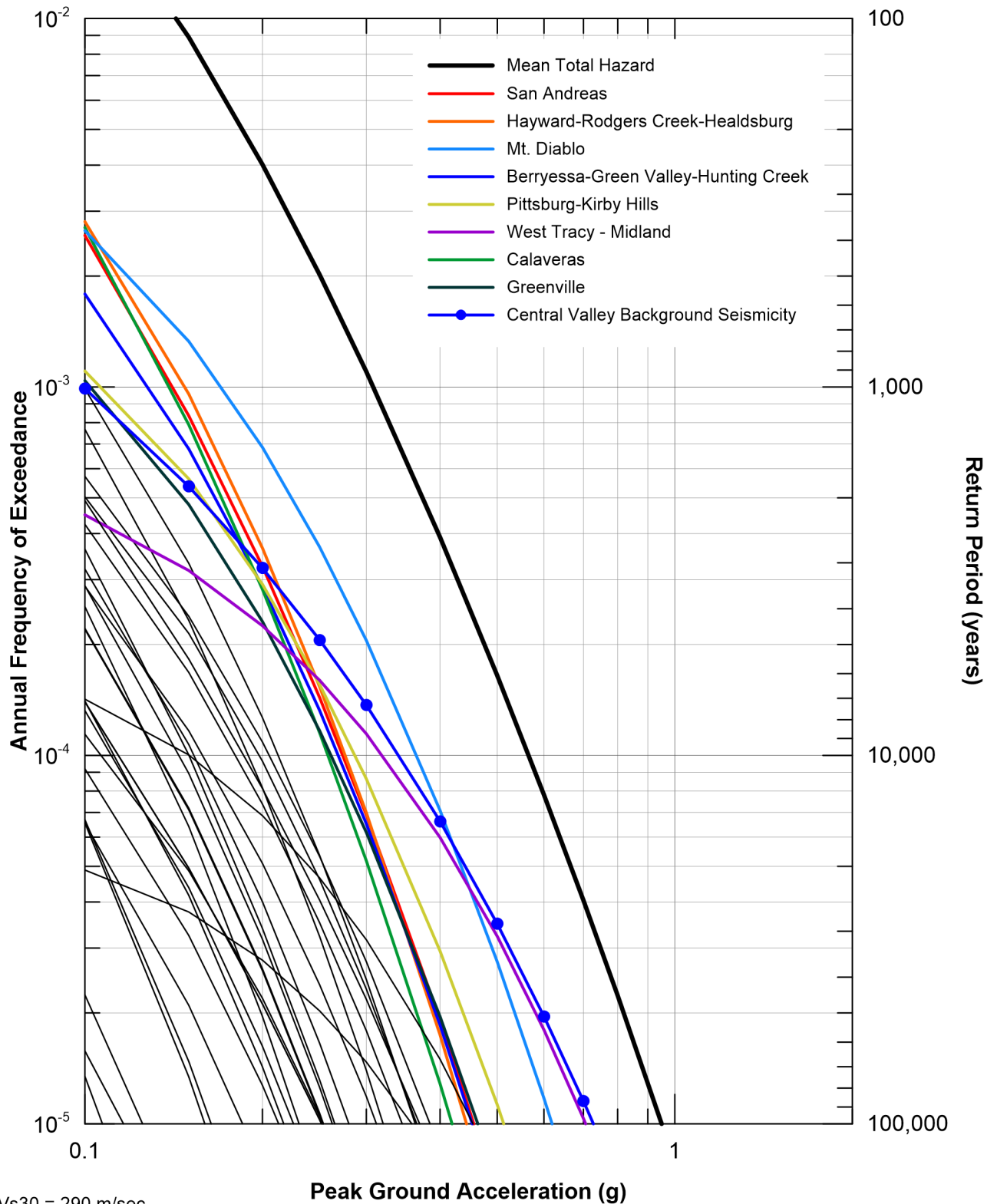


Vs30 = 370 m/sec
 Sources contributing 5% or more in
 144 to 2,475-year return period range listed.
 Other less significant sources shown in black
 not listed.



For Illustration
 Purposes Only

Figure 37
 Seismic Source Fractional Contributions
 for Mean Peak Horizontal Acceleration
 Hazard for Canal Ranch

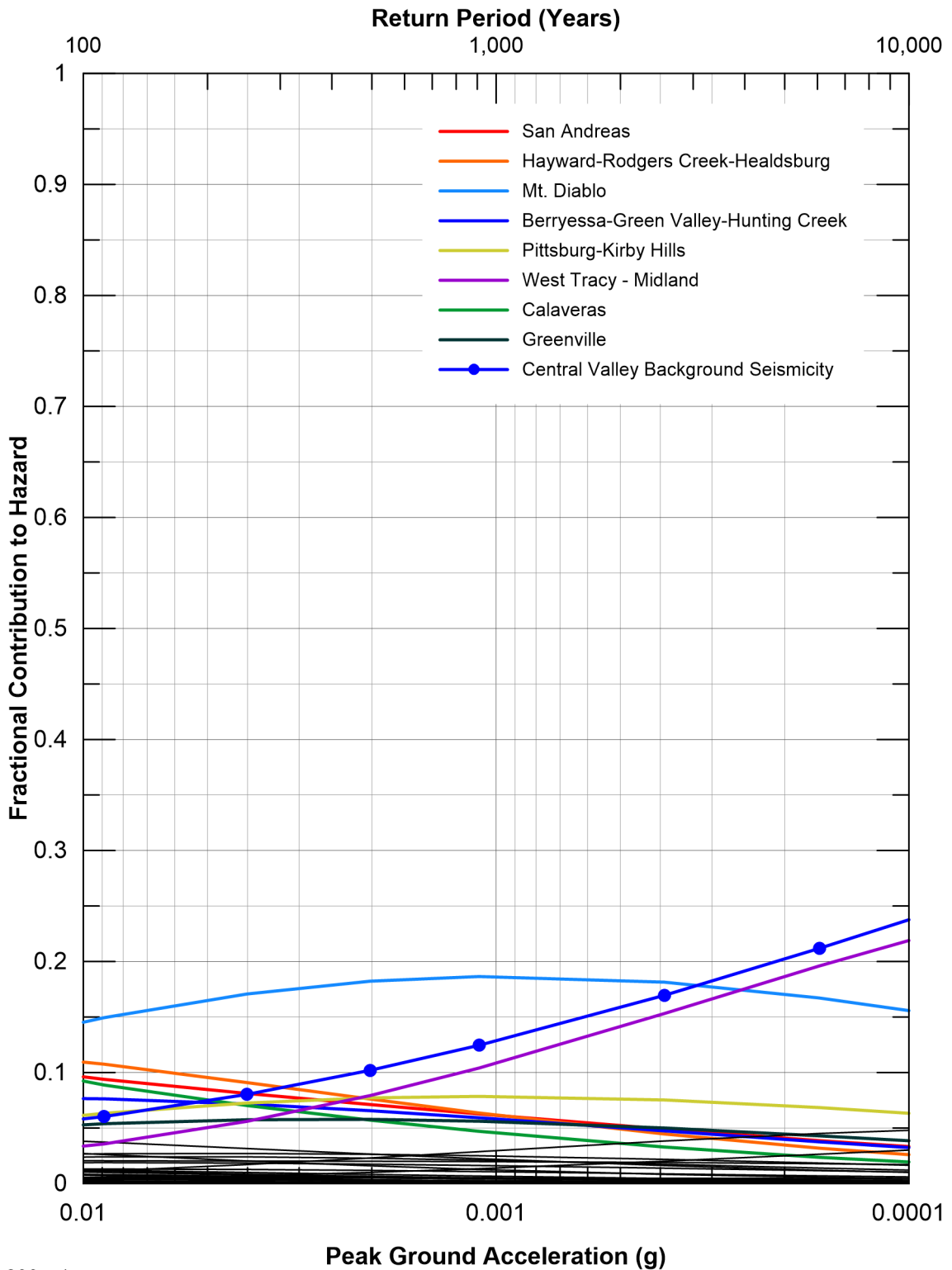


Vs30 = 290 m/sec
 Sources contributing 5% or more in
 144 to 2,475-year return period range listed.
 Other less significant sources shown in black
 not listed.



For Illustration
 Purposes Only

Figure 38
 Seismic Source Contributions
 for Mean Peak Horizontal Acceleration
 Hazard for Bouldin

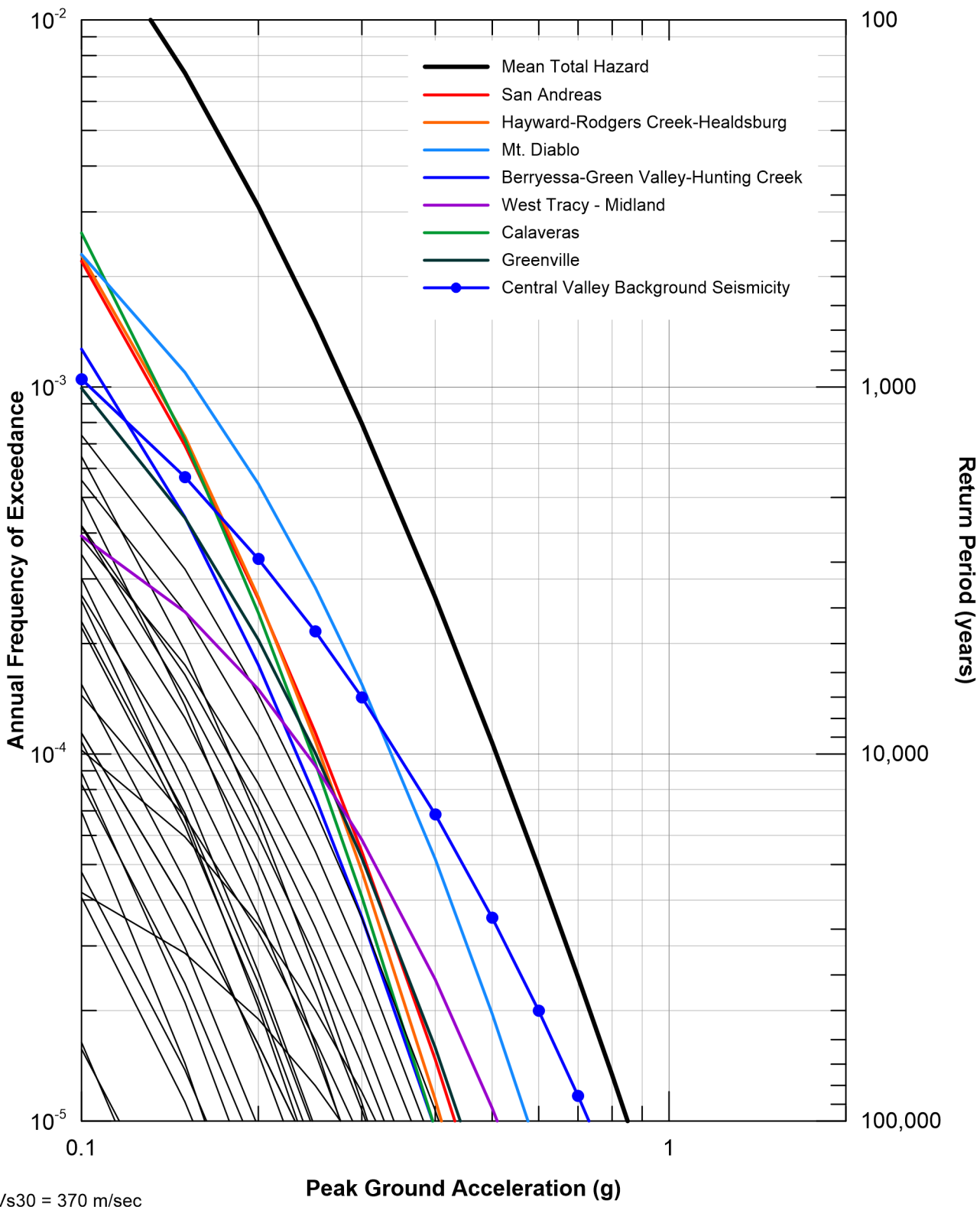


Vs30 = 290 m/sec
 Sources contributing 5% or more in
 144 to 2,475-year return period range listed.
 Other less significant sources shown in black
 not listed.



For Illustration
 Purposes Only

Figure 39
 Seismic Source Fractional Contributions
 for Mean Peak Horizontal Acceleration
 Hazard for Bouldin

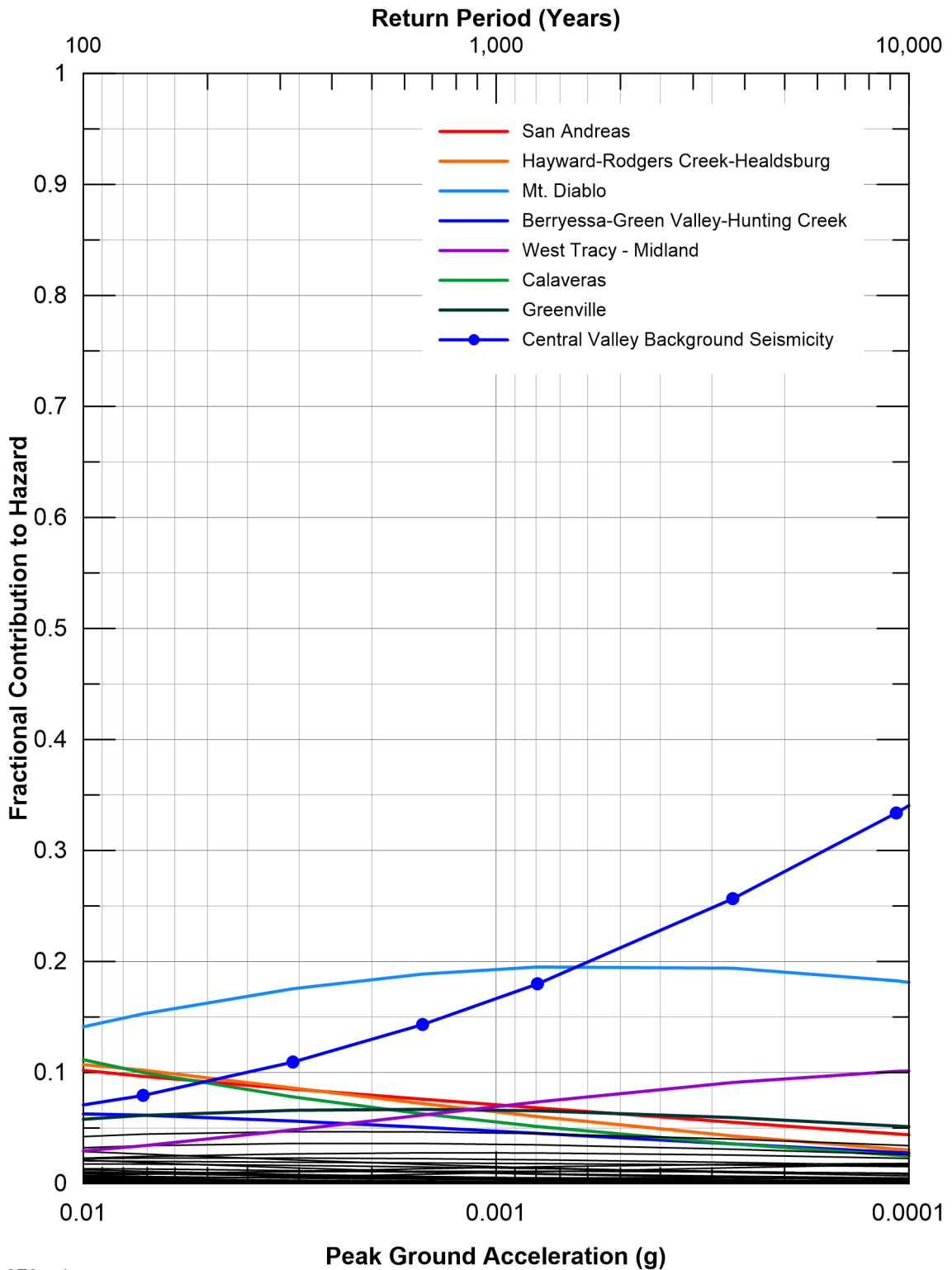


Vs30 = 370 m/sec
 Sources contributing 5% or more in
 144 to 2,475-year return period range listed.
 Other less significant sources shown in black
 not listed.



For Illustration
Purposes Only

Figure 40
 Seismic Source Contributions
 for Mean Peak Horizontal Acceleration
 Hazard for King Island

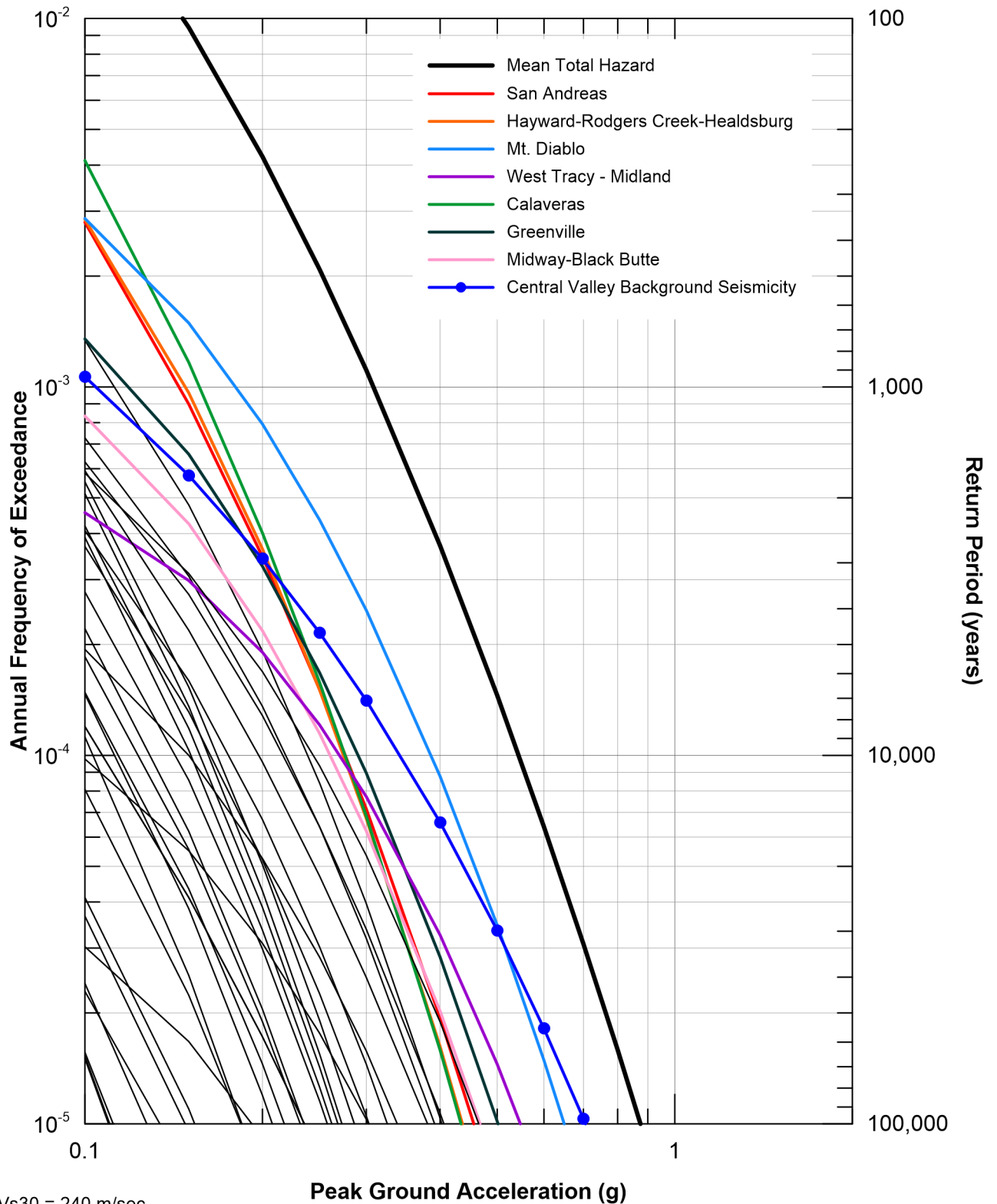


Vs30 = 370 m/sec
 Sources contributing 5% or more in
 144 to 2,475-year return period range listed.
 Other less significant sources shown in black
 not listed.



For Illustration
 Purposes Only

Figure 41
 Seismic Source Fractional Contributions
 for Mean Peak Horizontal Acceleration
 Hazard for King Island

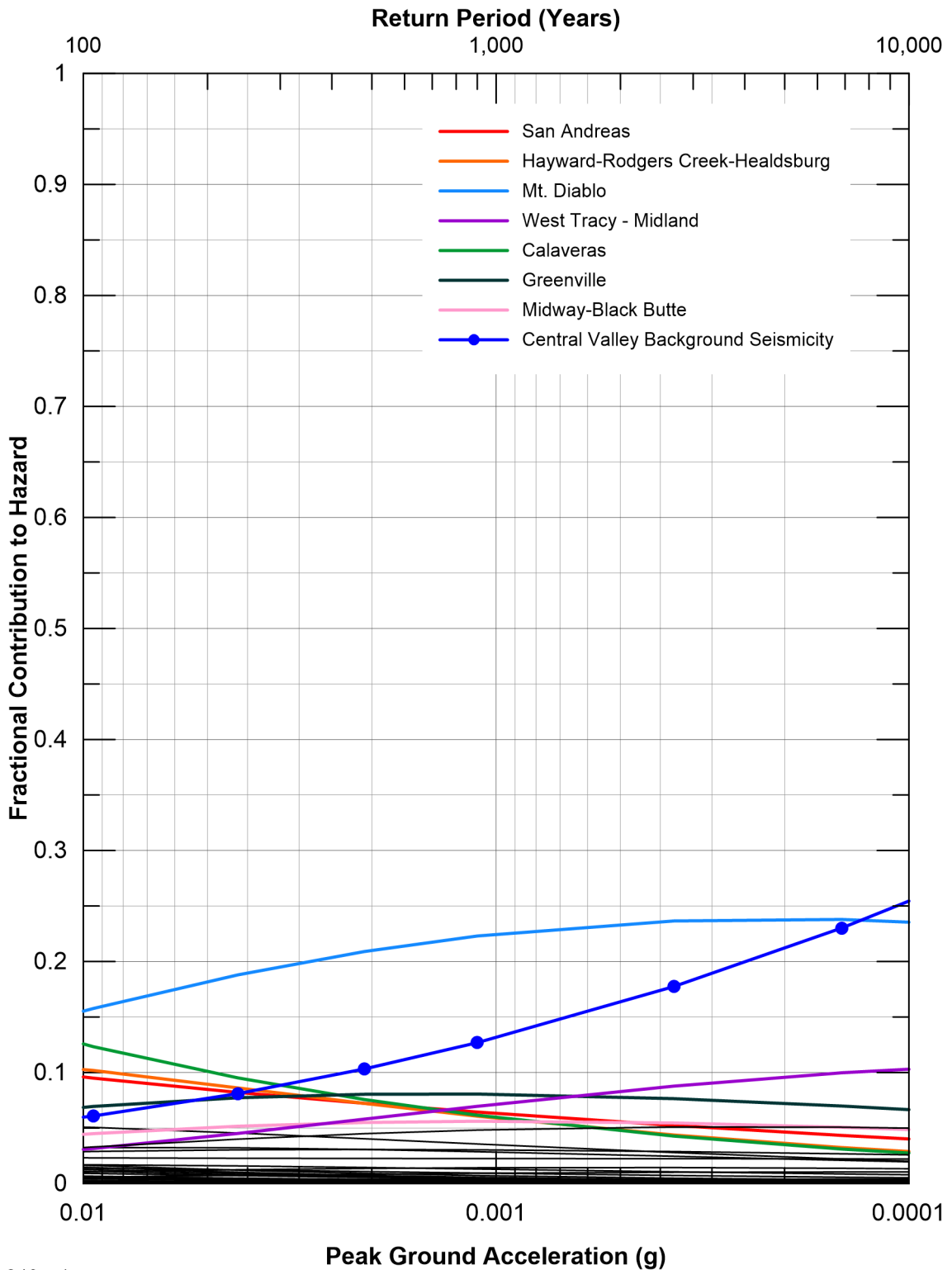


Vs30 = 240 m/sec
 Sources contributing 5% or more in
 144 to 2,475-year return period range listed.
 Other less significant sources shown in black
 not listed.



For Illustration
 Purposes Only

Figure 42
 Seismic Source Contributions
 for Mean Peak Horizontal Acceleration
 Hazard for Lower Roberts

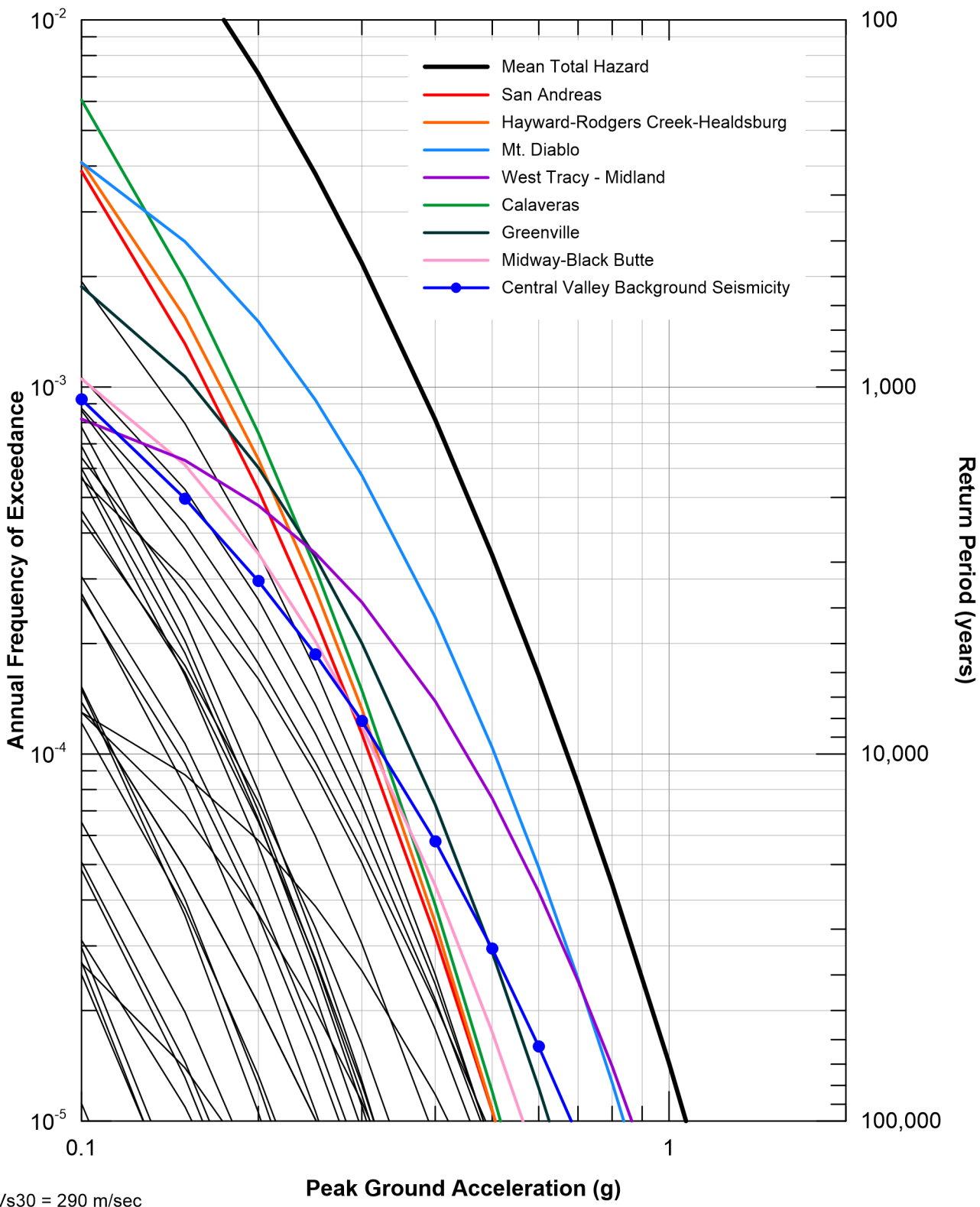


Vs30 = 240 m/sec
 Sources contributing 5% or more in
 144 to 2,475-year return period range listed.
 Other less significant sources shown in black
 not listed.



For Illustration
 Purposes Only

Figure 43
 Seismic Source Fractional Contributions
 for Mean Peak Horizontal Acceleration
 Hazard for Lower Roberts

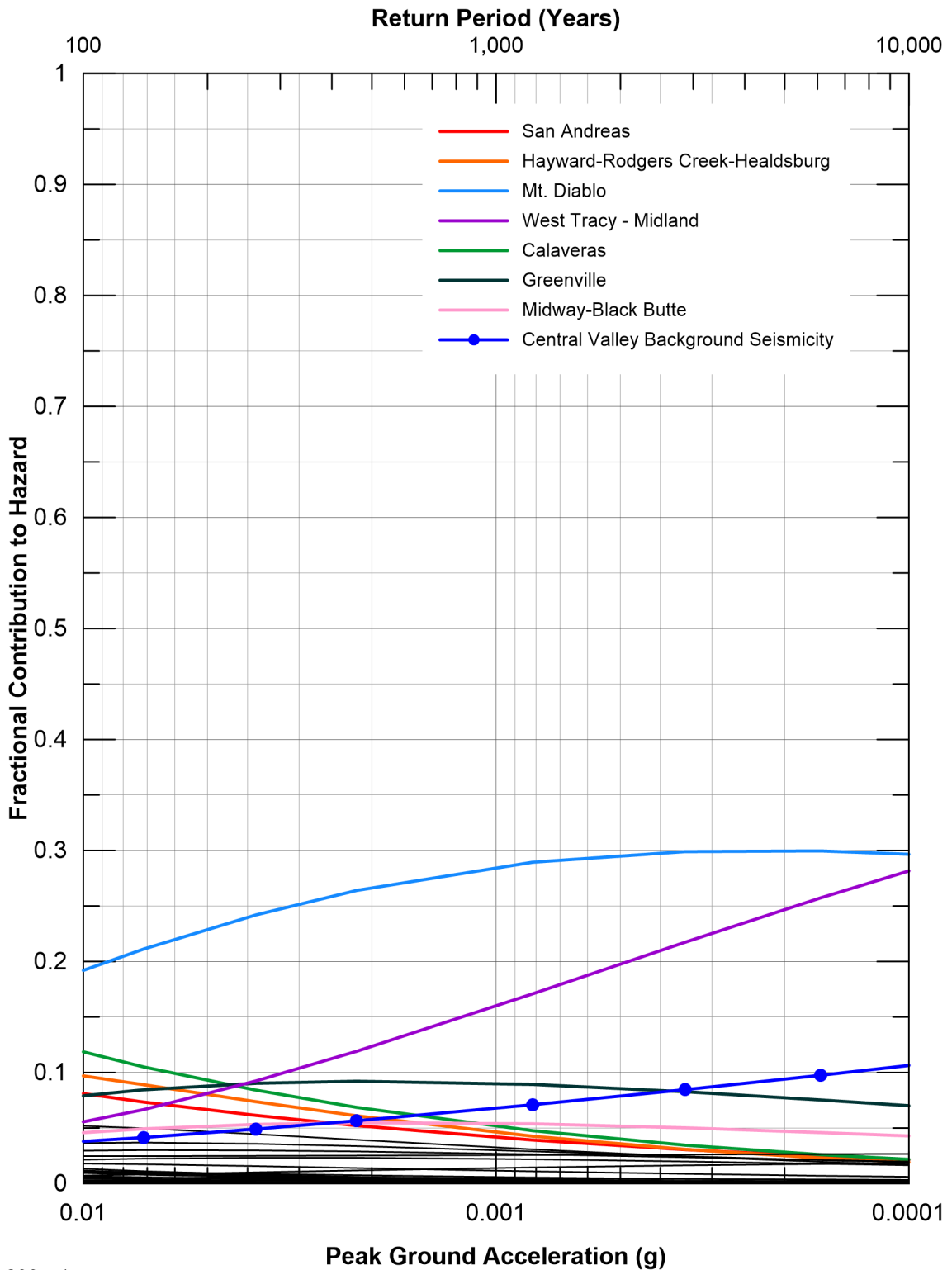


Vs30 = 290 m/sec
 Sources contributing 5% or more in
 144 to 2,475-year return period range listed.
 Other less significant sources shown in black
 not listed.



For Illustration
 Purposes Only

Figure 44
 Seismic Source Contributions
 for Mean Peak Horizontal Acceleration
 Hazard for Bacon

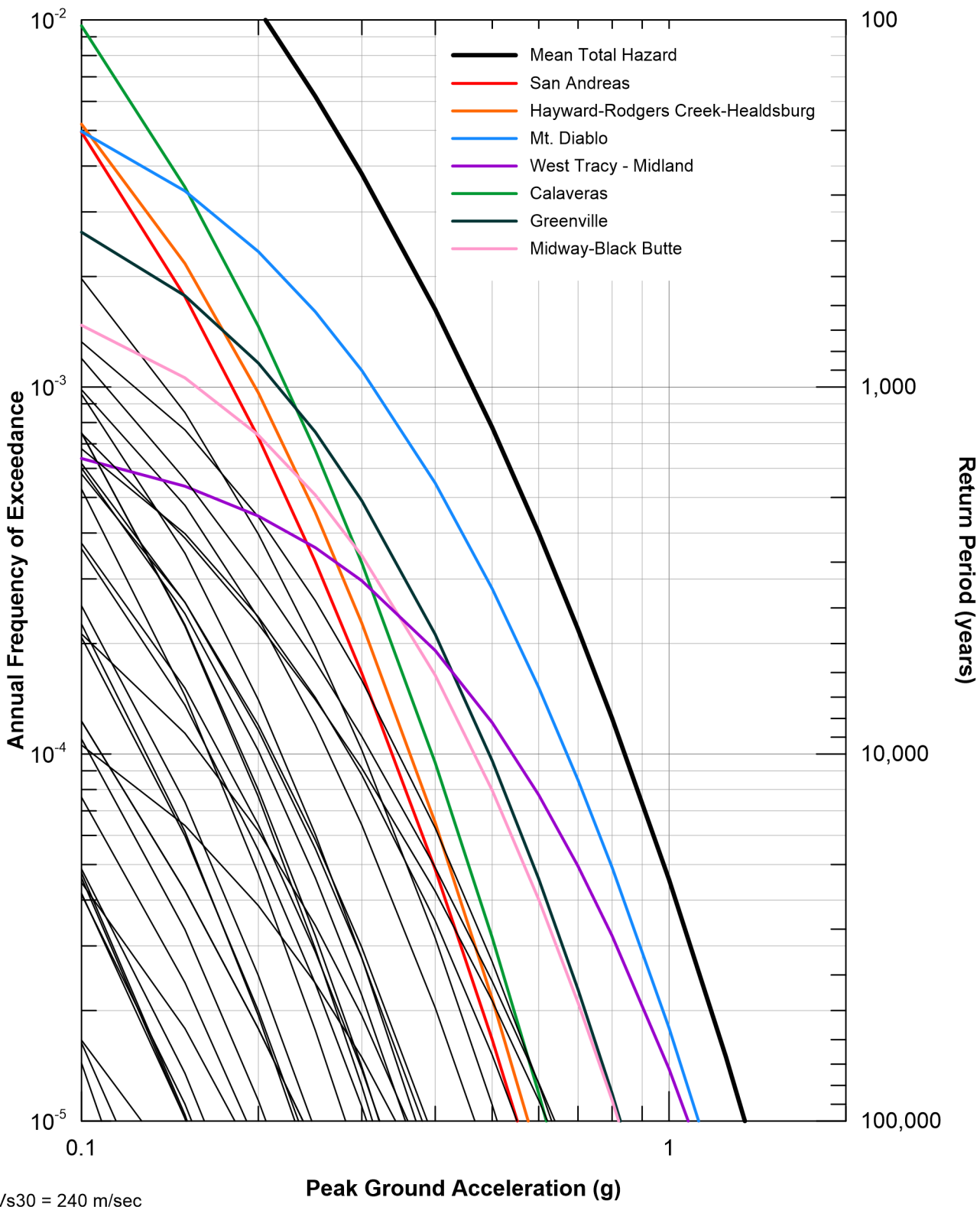


Vs30 = 290 m/sec
 Sources contributing 5% or more in
 144 to 2,475-year return period range listed.
 Other less significant sources shown in black
 not listed.



For Illustration
 Purposes Only

Figure 45
 Seismic Source Fractional Contributions
 for Mean Peak Horizontal Acceleration
 Hazard for Bacon

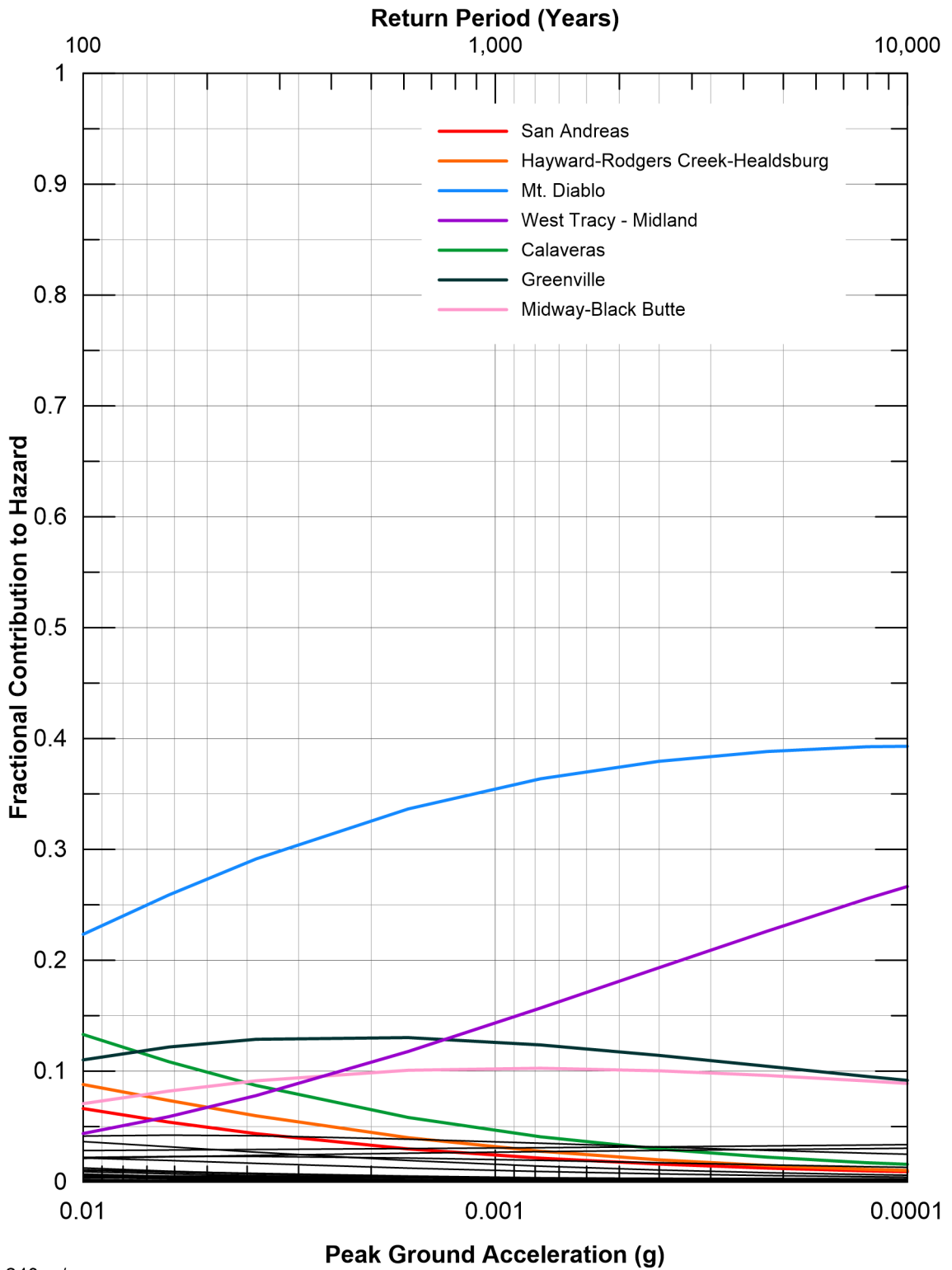


Vs30 = 240 m/sec
 Sources contributing 5% or more in
 144 to 2,475-year return period range listed.
 Other less significant sources shown in black
 not listed.



For Illustration
Purposes Only

Figure 46
 Seismic Source Contributions
 for Mean Peak Horizontal Acceleration
 Hazard for Southern Forebay North

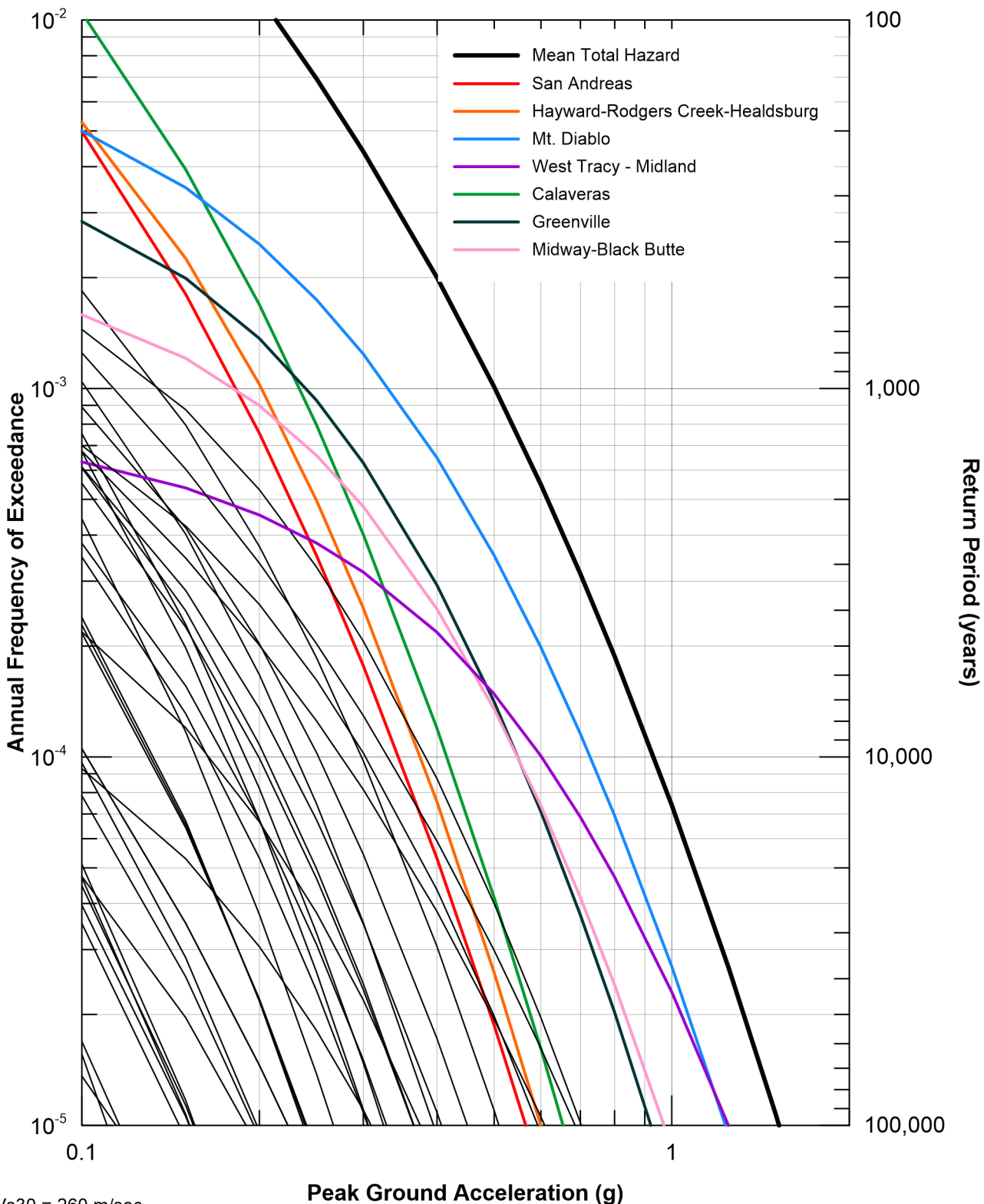


Vs30 = 240 m/sec
 Sources contributing 5% or more in
 144 to 2,475-year return period range listed.
 Other less significant sources shown in black
 not listed.



For Illustration
 Purposes Only

Figure 47
 Seismic Source Fractional Contributions
 for Mean Peak Horizontal Acceleration
 Hazard for Southern Forebay North

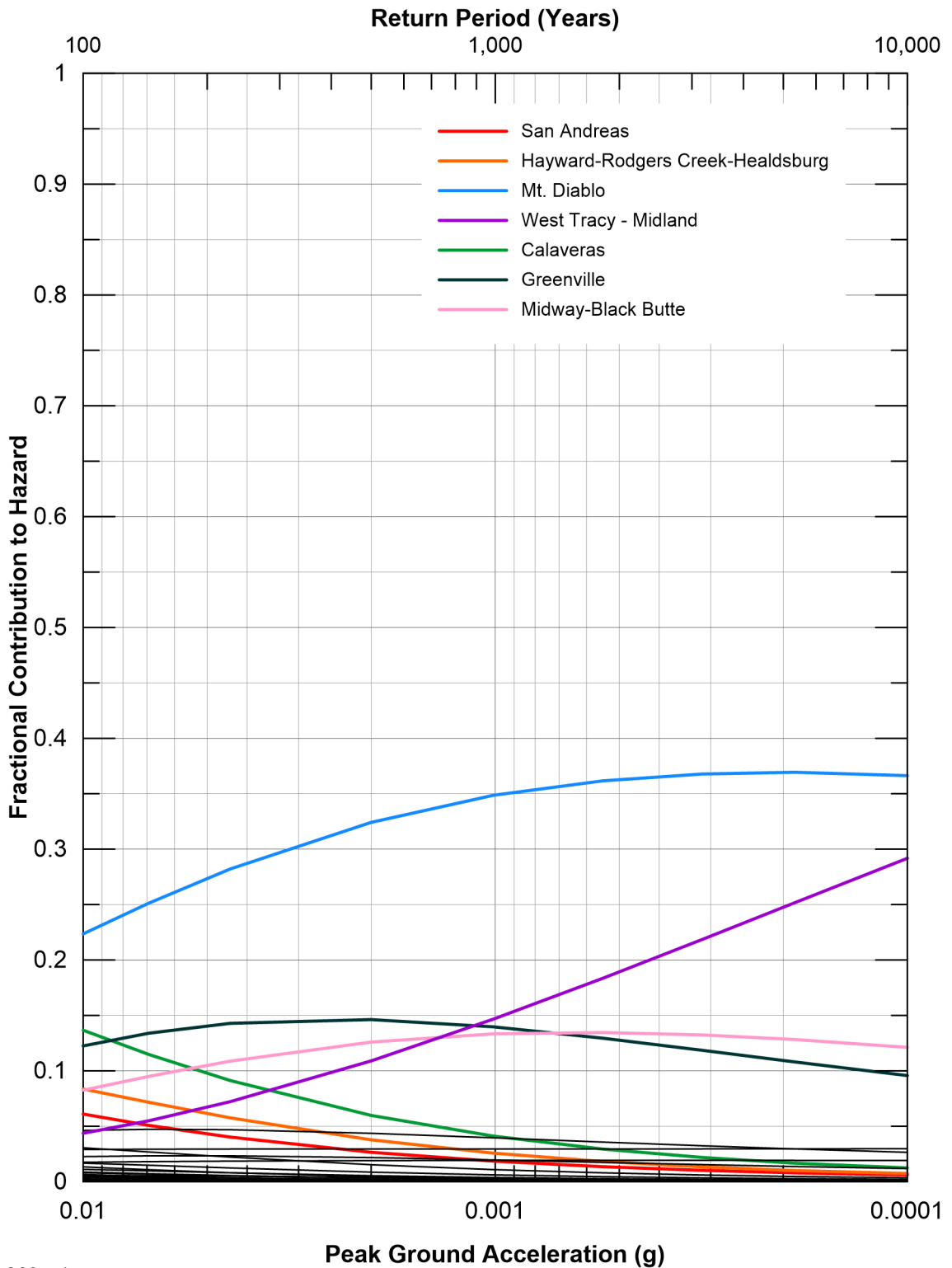


Vs30 = 260 m/sec
 Sources contributing 5% or more in
 144 to 2,475-year return period range listed.
 Other less significant sources shown in black
 not listed.



For Illustration
Purposes Only

Figure 48
 Seismic Source Contributions
 for Mean Peak Horizontal Acceleration
 Hazard for Southern Forebay South

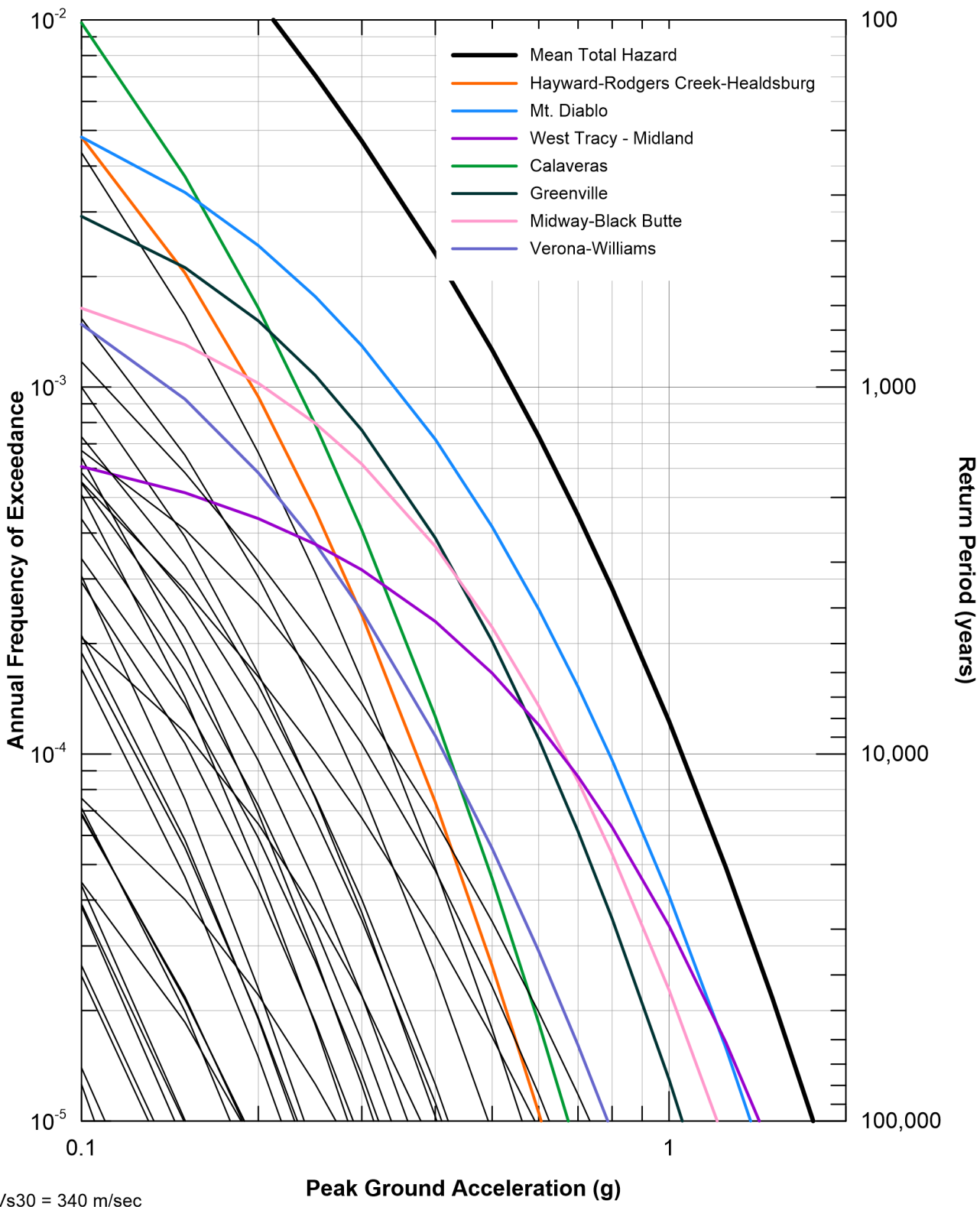


Vs30 = 260 m/sec
 Sources contributing 5% or more in
 144 to 2,475-year return period range listed.
 Other less significant sources shown in black
 not listed.



For Illustration
 Purposes Only

Figure 49
 Seismic Source Fractional Contributions
 for Mean Peak Horizontal Acceleration
 Hazard for Southern Forebay South

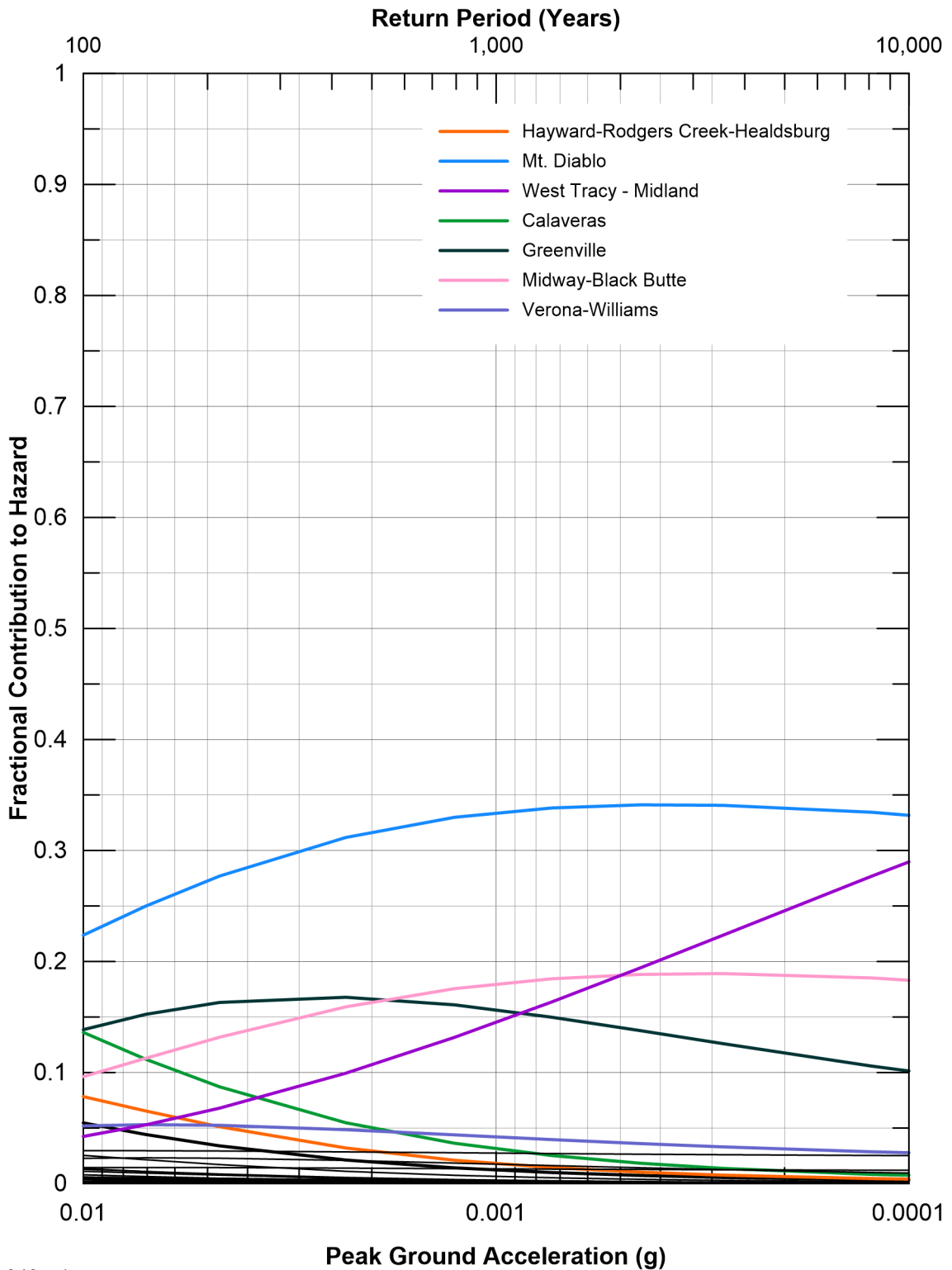


Vs30 = 340 m/sec
 Sources contributing 5% or more in
 144 to 2,475-year return period range listed.
 Other less significant sources shown in black
 not listed.



For Illustration
Purposes Only

Figure 50
 Seismic Source Contributions
 for Mean Peak Horizontal Acceleration
 Hazard for Jones Connection

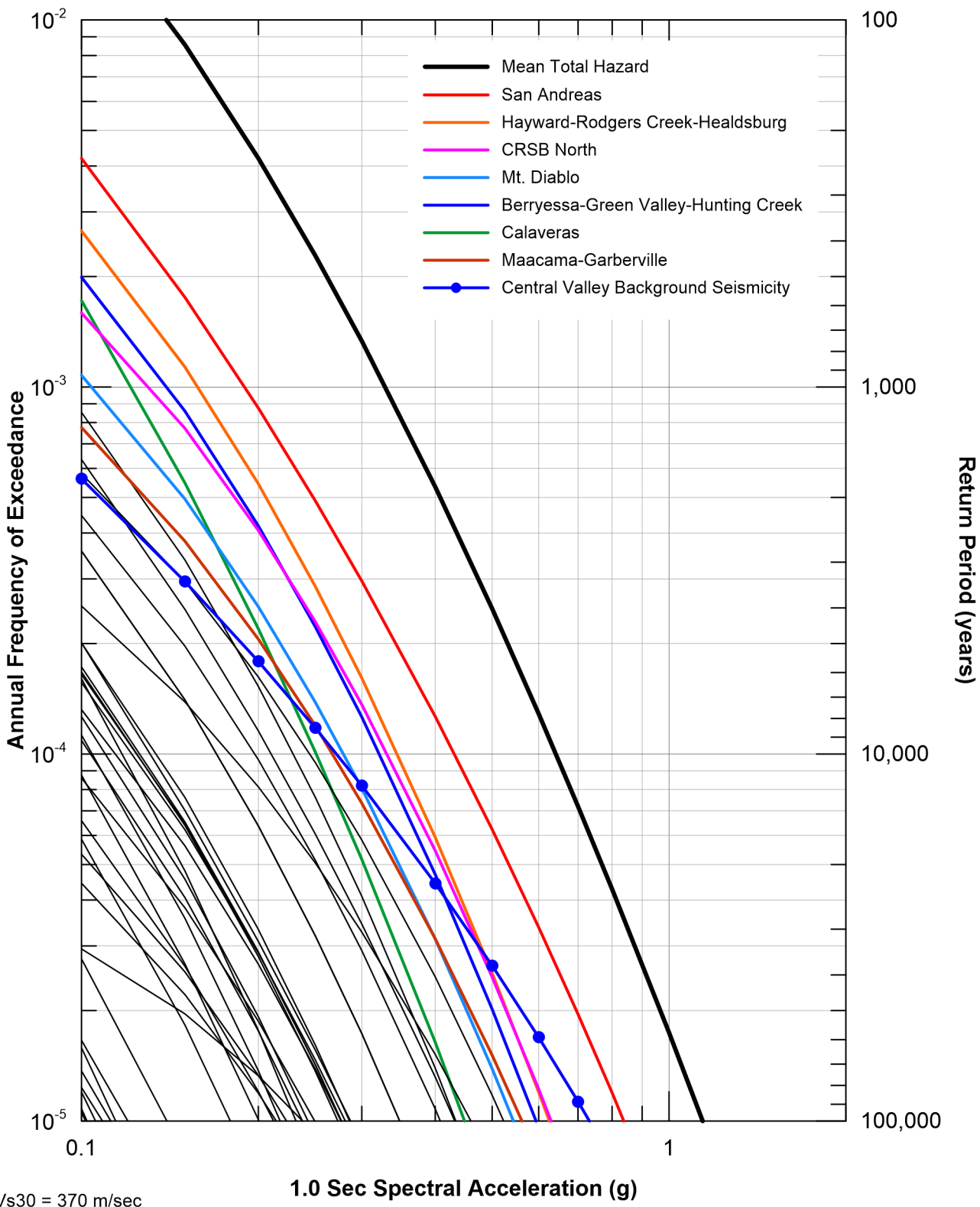


Vs30 = 340 m/sec
 Sources contributing 5% or more in
 144 to 2,475-year return period range listed.
 Other less significant sources shown in black
 not listed.



For Illustration
 Purposes Only

Figure 51
 Seismic Source Fractional Contributions
 for Mean Peak Horizontal Acceleration
 Hazard for Jones Connection

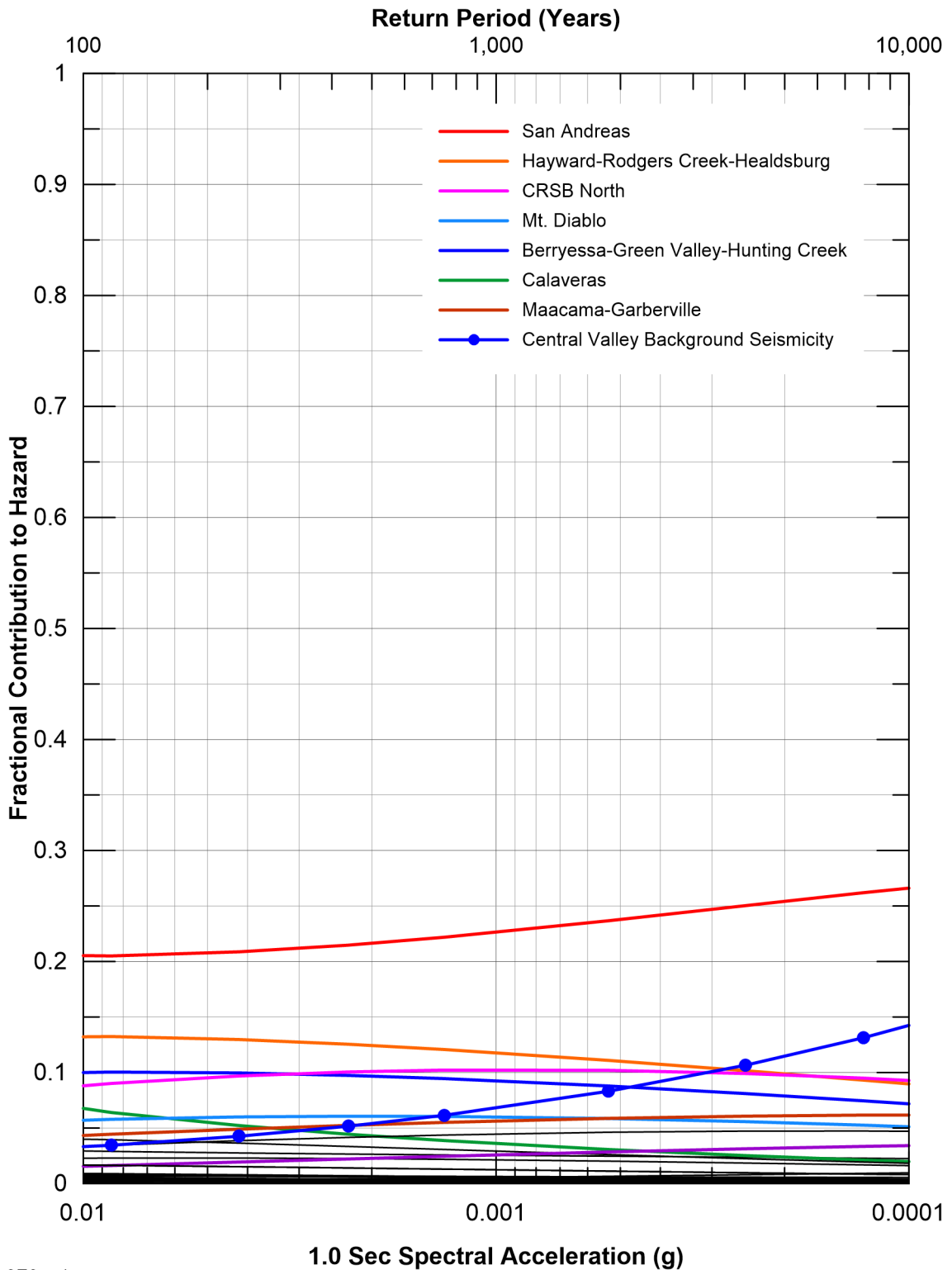


Vs30 = 370 m/sec
 Sources contributing 5% or more in
 144 to 2,475-year return period range listed.
 Other less significant sources shown in black
 not listed.



For Illustration
 Purposes Only

Figure 52
 Seismic Source Contributions
 for Mean 1.0 Sec Horizontal Spectral
 Acceleration Hazard for Intake No. 3

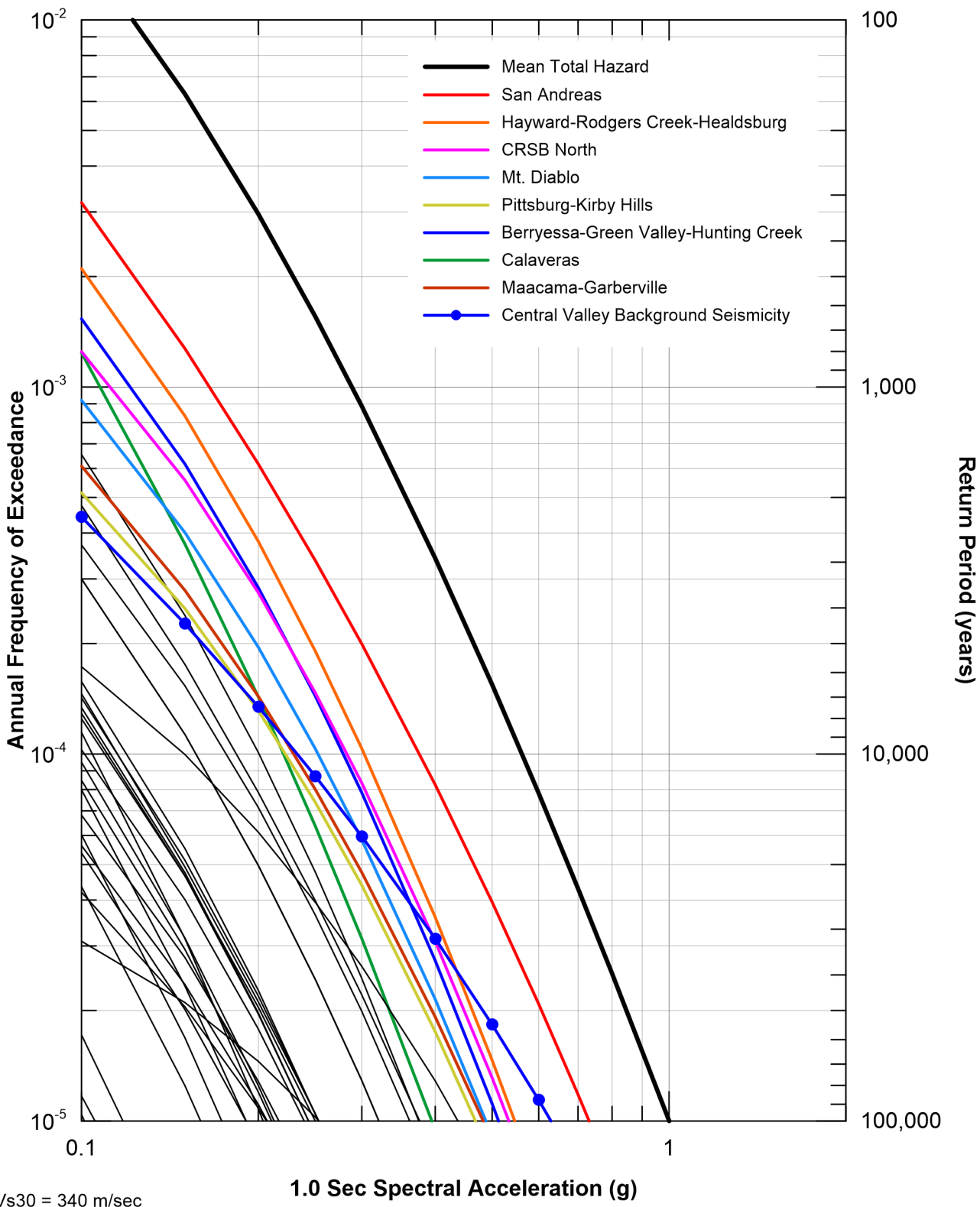


Vs30 = 370 m/sec
 Sources contributing 5% or more in
 144 to 2,475-year return period range listed.
 Other less significant sources shown in black
 not listed.



For Illustration
 Purposes Only

Figure 53
 Seismic Source Fractional Contributions
 for Mean 1.0 Sec Horizontal Spectral
 Acceleration Hazard for Intake No. 3

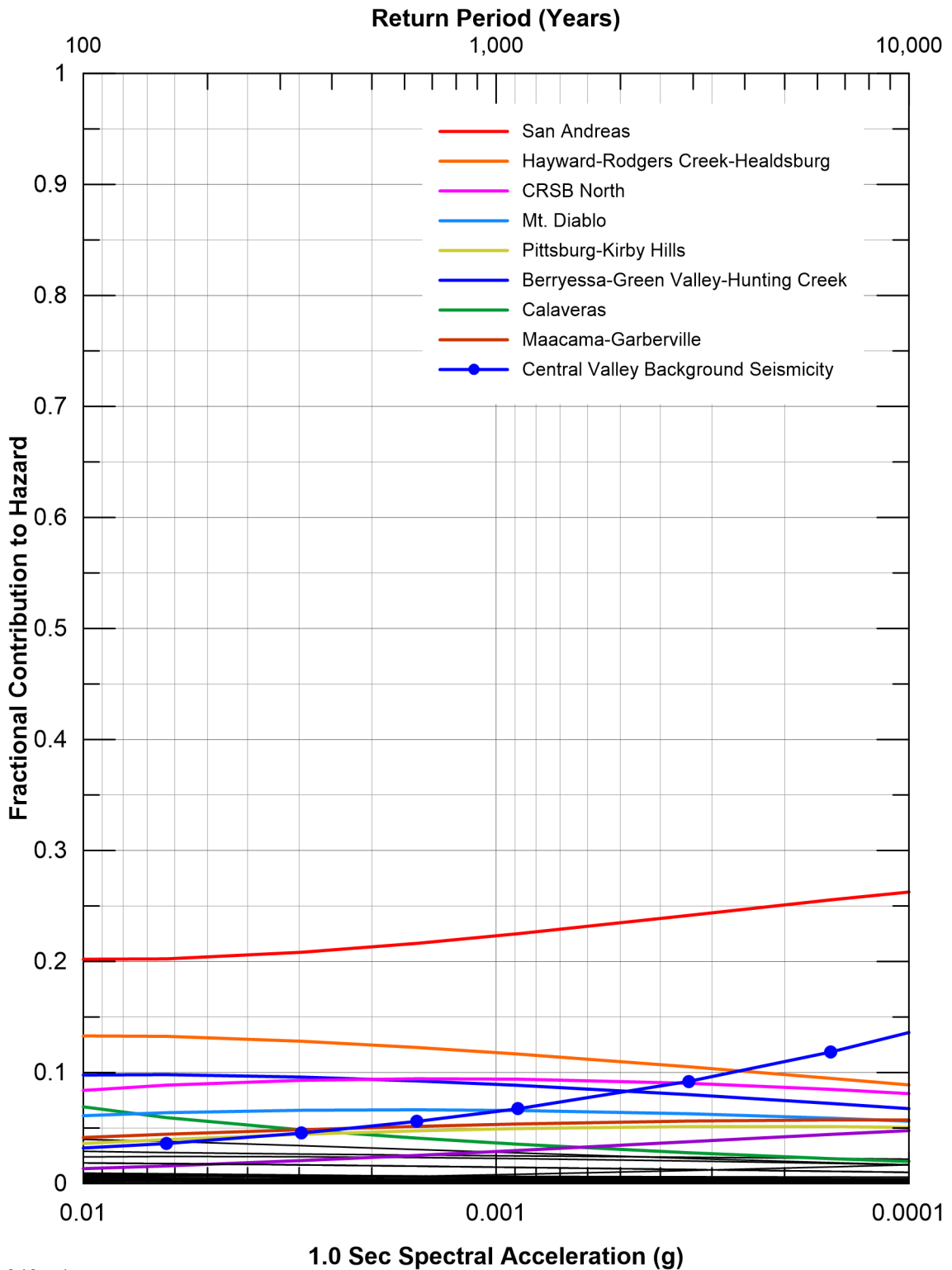


Vs30 = 340 m/sec
 Sources contributing 5% or more in
 144 to 2,475-year return period range listed.
 Other less significant sources shown in black
 not listed.



For Illustration
 Purposes Only

Figure 54
 Seismic Source Contributions
 for Mean 1.0 Sec Horizontal Spectral
 Acceleration Hazard for Intake No. 5

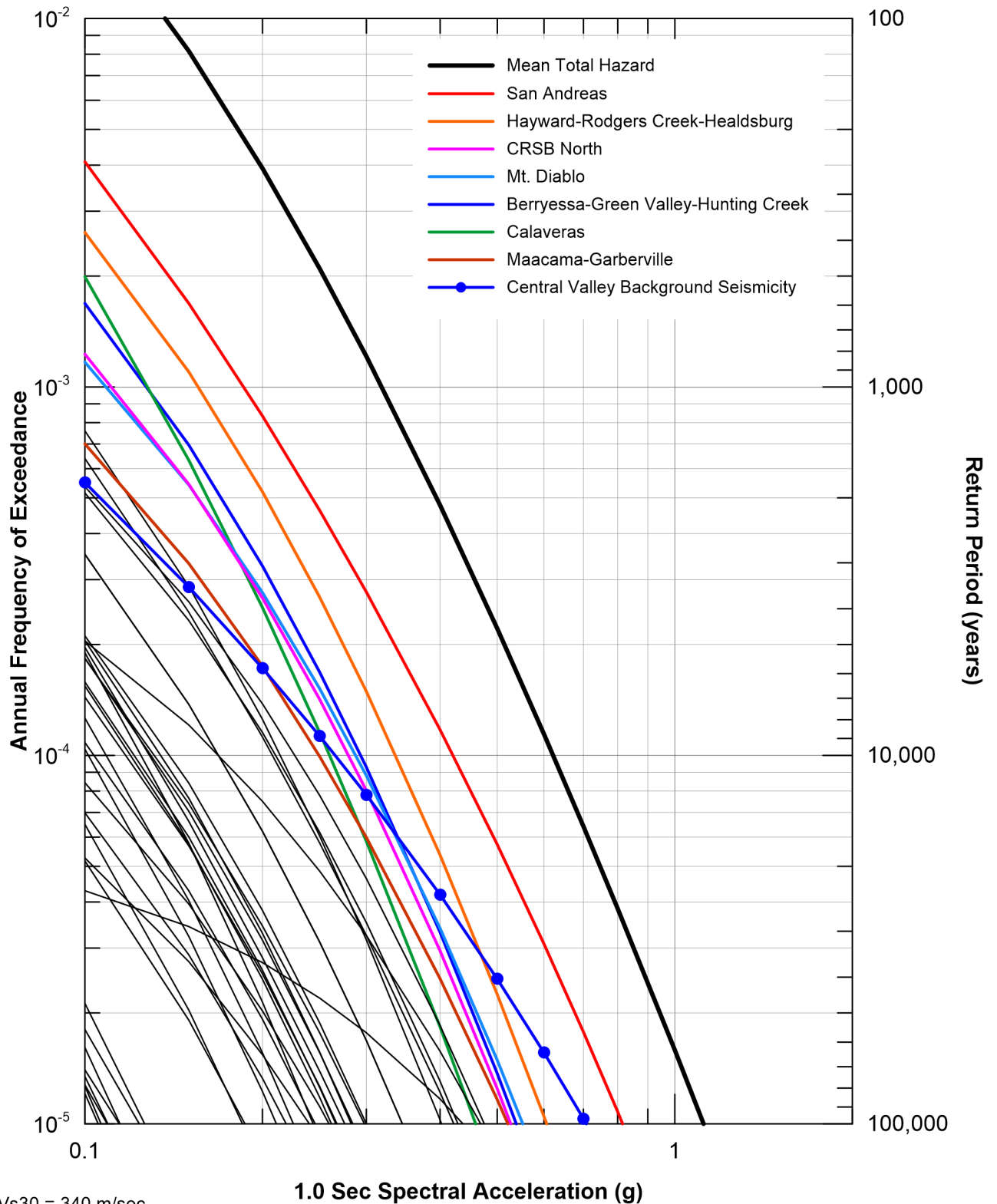


Vs30 = 340 m/sec
 Sources contributing 5% or more in
 144 to 2,475-year return period range listed.
 Other less significant sources shown in black
 not listed.



For Illustration
 Purposes Only

Figure 55
 Seismic Source Fractional Contributions
 for Mean 1.0 Sec Horizontal Spectral
 Acceleration Hazard for Intake No. 5

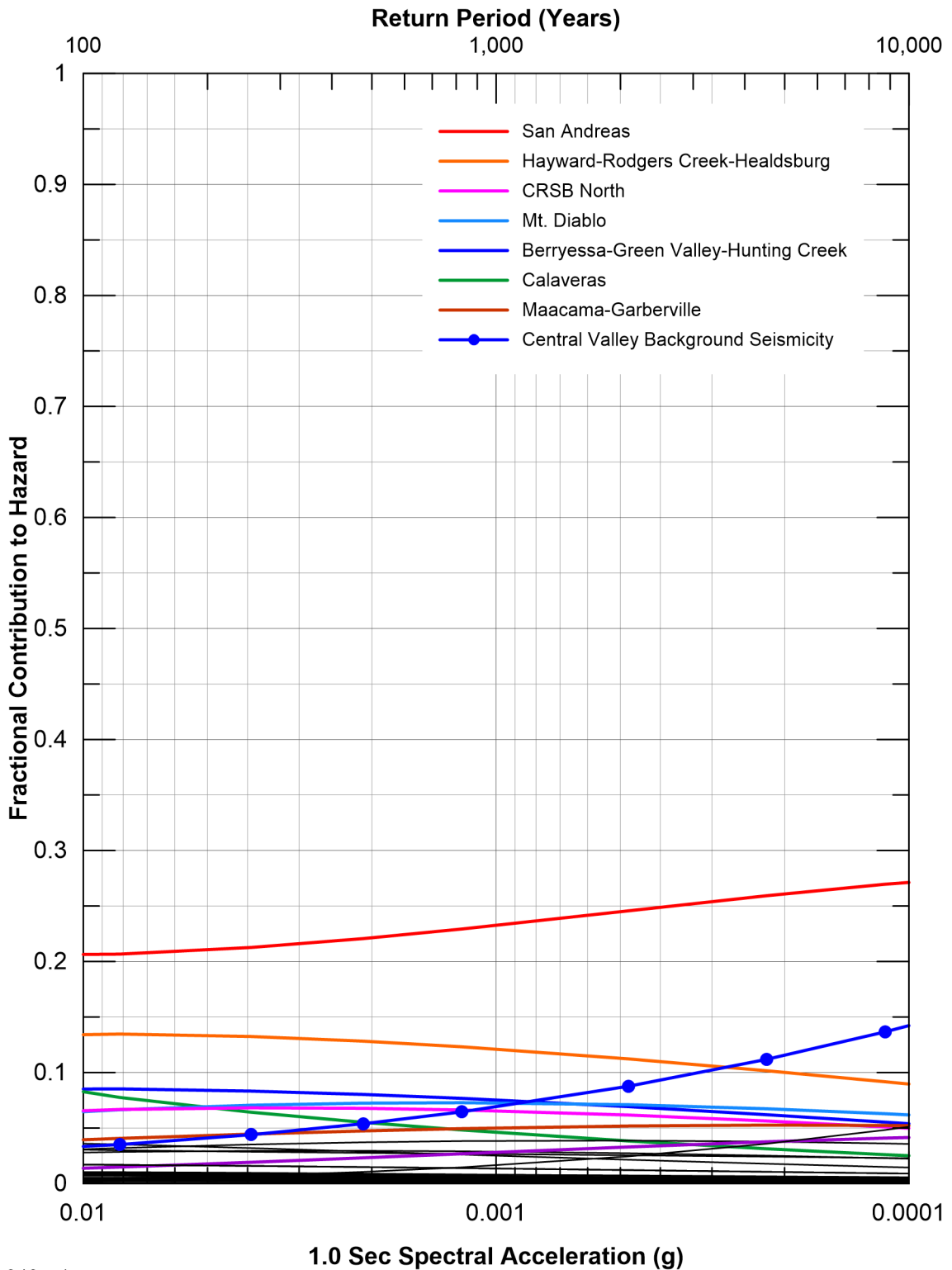


Vs30 = 340 m/sec
 Sources contributing 5% or more in
 144 to 2,475-year return period range listed.
 Other less significant sources shown in black
 not listed.



For Illustration
 Purposes Only

Figure 56
 Seismic Source Contributions
 for Mean 1.0 Sec Horizontal Spectral
 Acceleration Hazard for Twin Cities

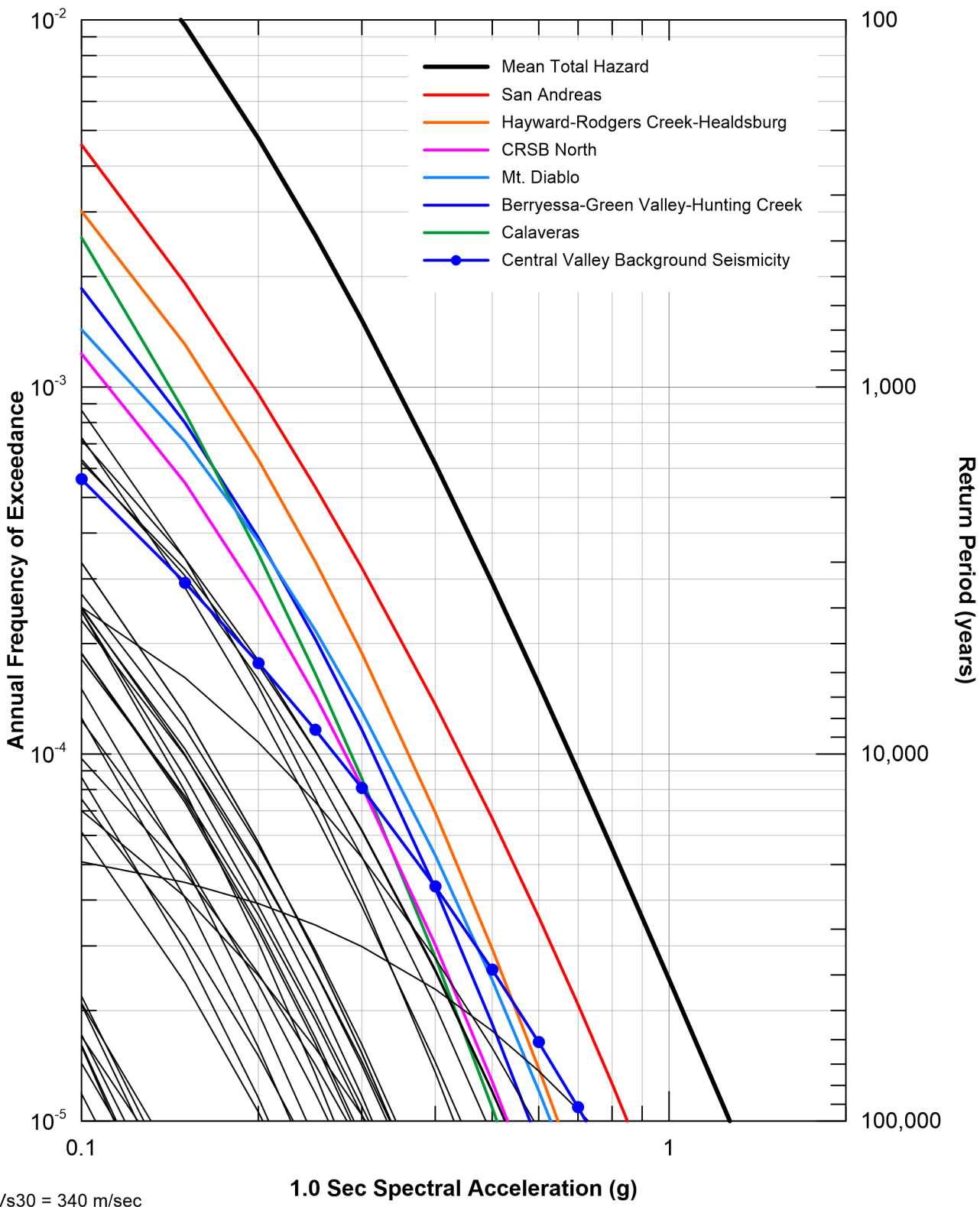


Vs30 = 340 m/sec
 Sources contributing 5% or more in
 144 to 2,475-year return period range listed.
 Other less significant sources shown in black
 not listed.



For Illustration
Purposes Only

Figure 57
 Seismic Source Fractional Contributions
 for Mean 1.0 Sec Horizontal Spectral
 Acceleration Hazard for Twin Cities

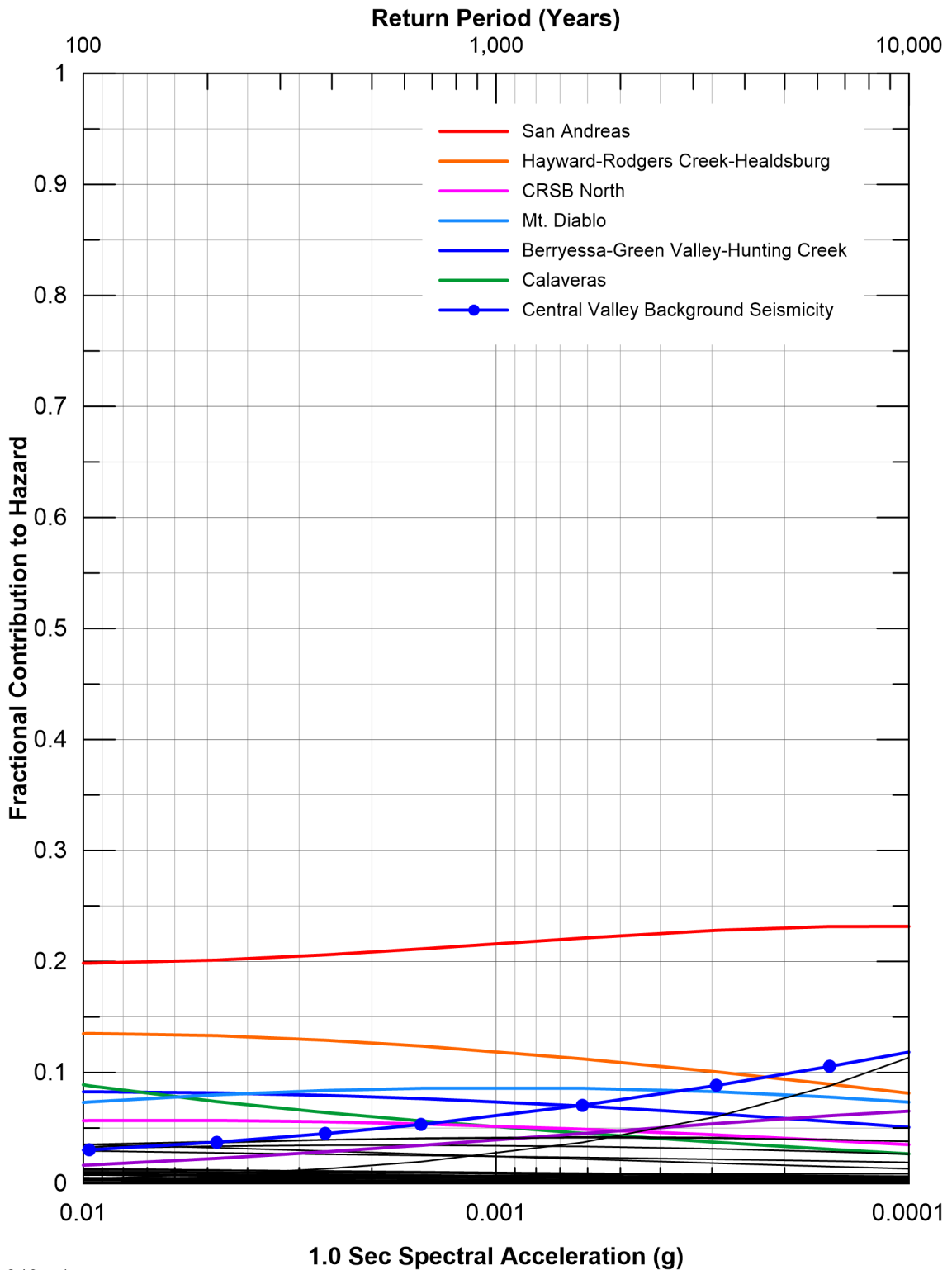


Vs30 = 340 m/sec
 Sources contributing 5% or more in
 144 to 2,475-year return period range listed.
 Other less significant sources shown in black
 not listed.



For Illustration
 Purposes Only

Figure 58
 Seismic Source Contributions
 for Mean 1.0 Sec Horizontal Spectral
 Acceleration Hazard for New Hope

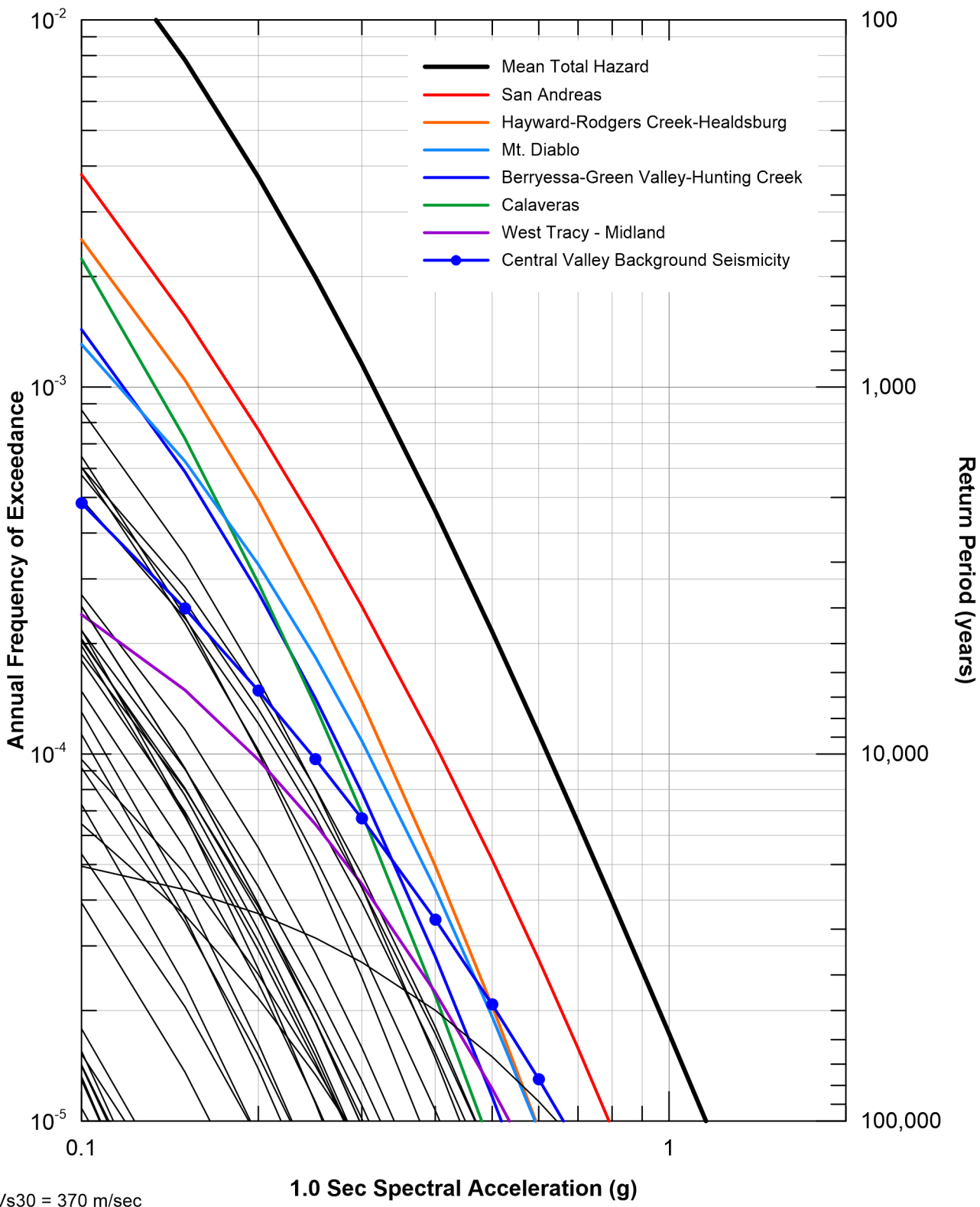


Vs30 = 340 m/sec
 Sources contributing 5% or more in
 144 to 2,475-year return period range listed.
 Other less significant sources shown in black
 not listed.



For Illustration
 Purposes Only

Figure 59
 Seismic Source Fractional Contributions
 for Mean 1.0 Sec Horizontal Spectral
 Acceleration Hazard for New Hope

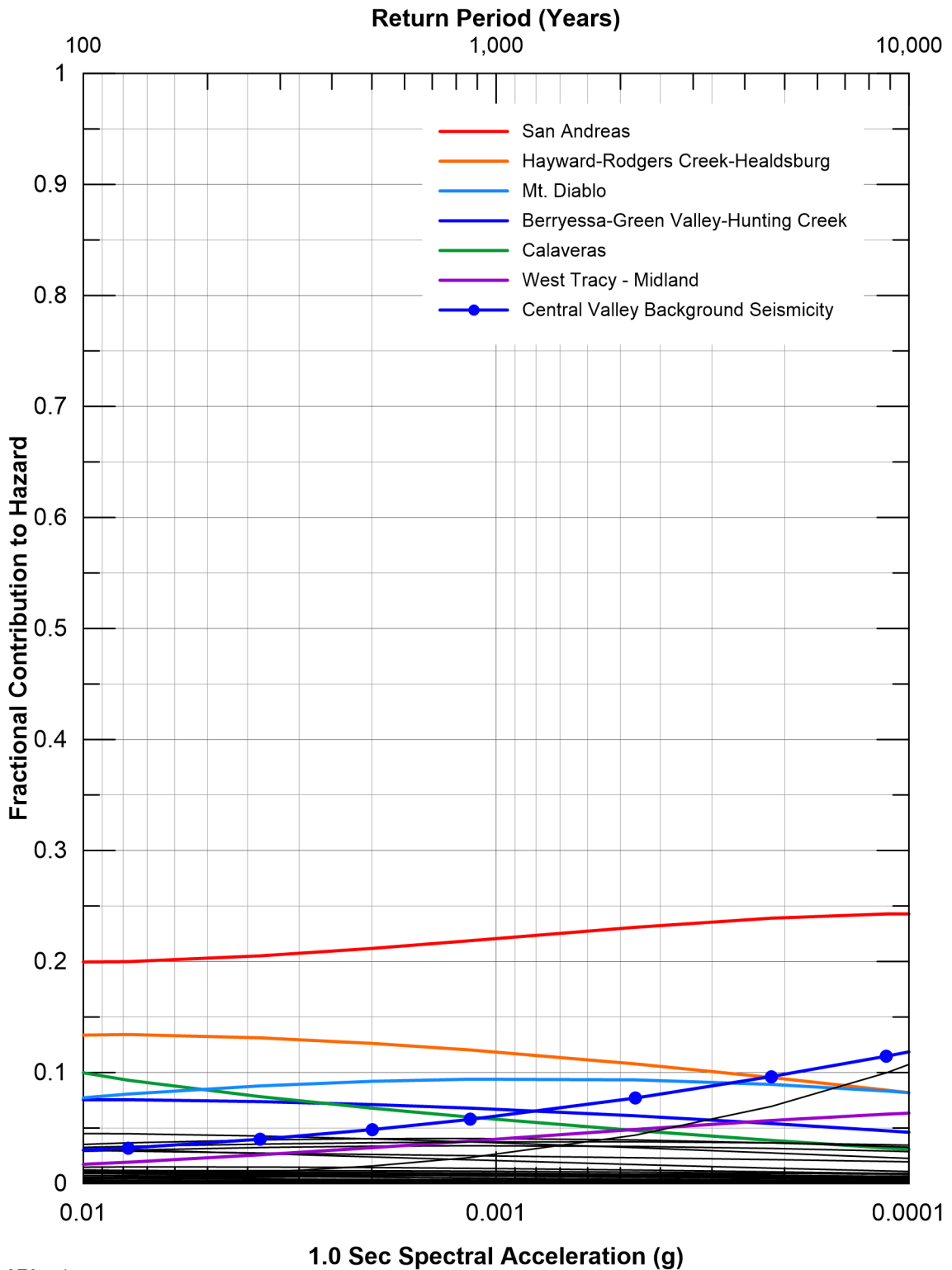


Vs30 = 370 m/sec
 Sources contributing 5% or more in
 144 to 2,475-year return period range listed.
 Other less significant sources shown in black
 not listed.



For Illustration
Purposes Only

Figure 60
 Seismic Source Contributions
 for Mean 1.0 Sec Horizontal Spectral
 Acceleration Hazard for Canal Ranch

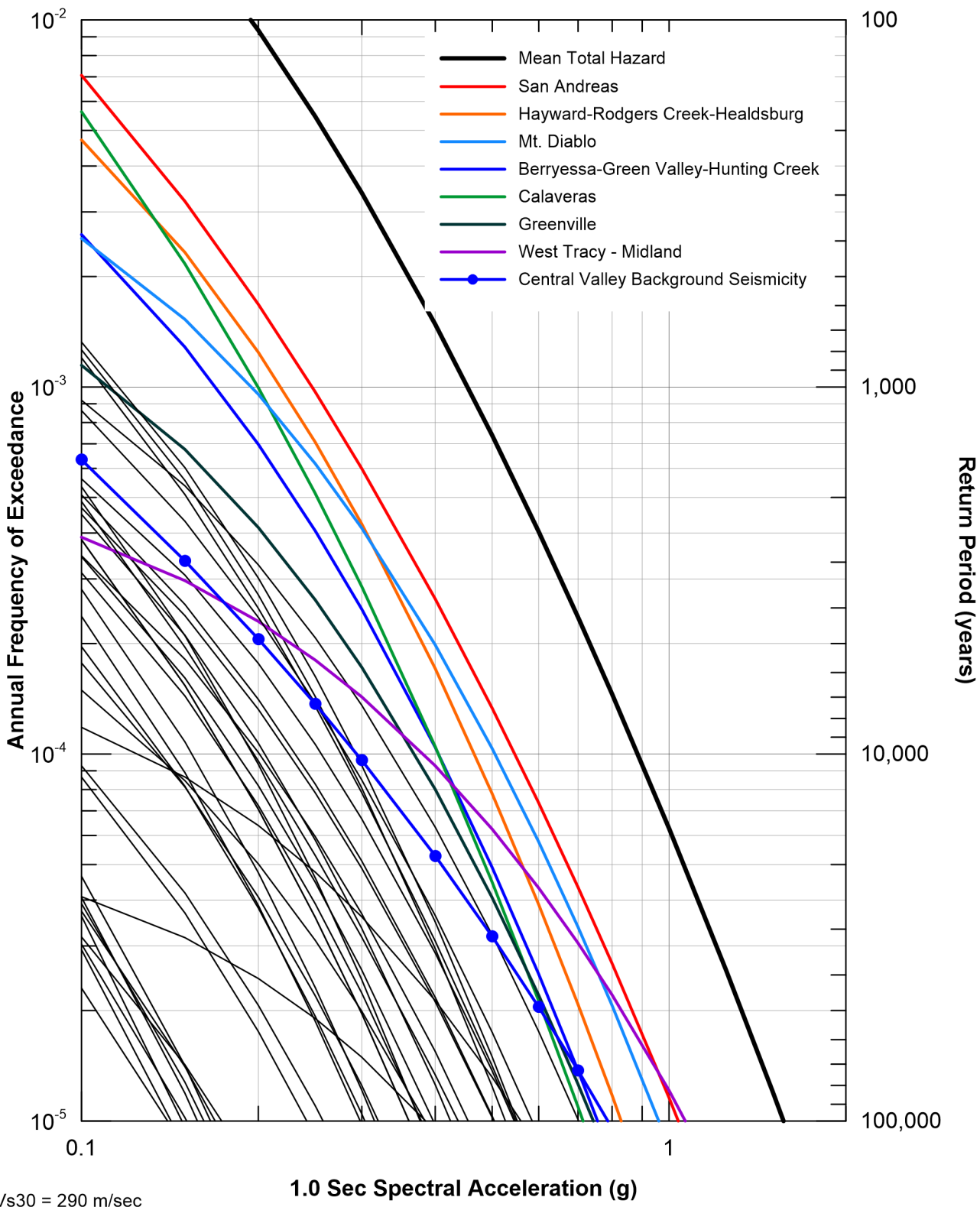


Vs30 = 370 m/sec
 Sources contributing 5% or more in
 144 to 2,475-year return period range listed.
 Other less significant sources shown in black
 not listed.



For Illustration
 Purposes Only

Figure 61
 Seismic Source Fractional Contributions
 for Mean 1.0 Sec Horizontal Spectral
 Acceleration Hazard for Canal Ranch

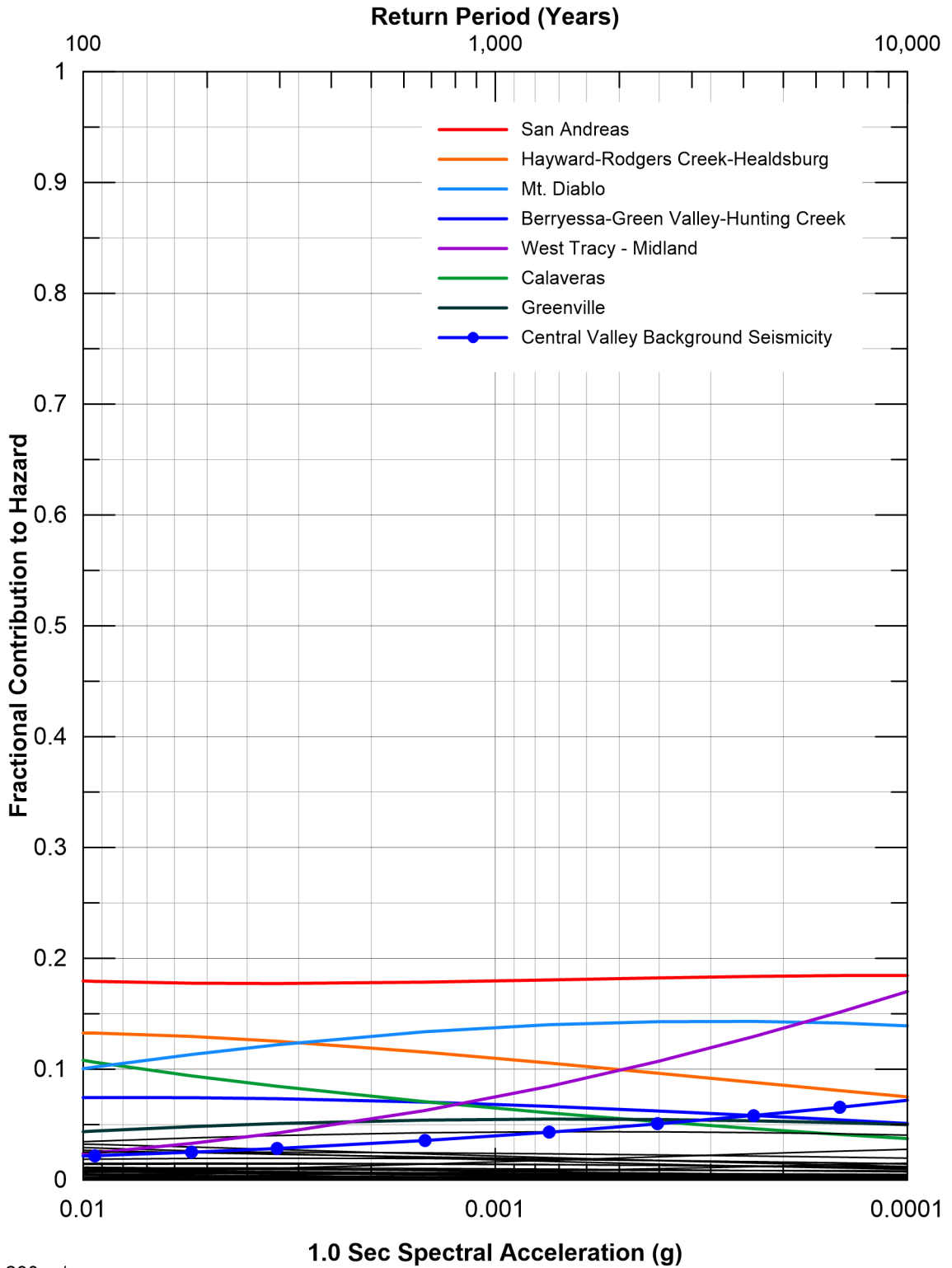


Vs30 = 290 m/sec
 Sources contributing 5% or more in
 144 to 2,475-year return period range listed.
 Other less significant sources shown in black
 not listed.

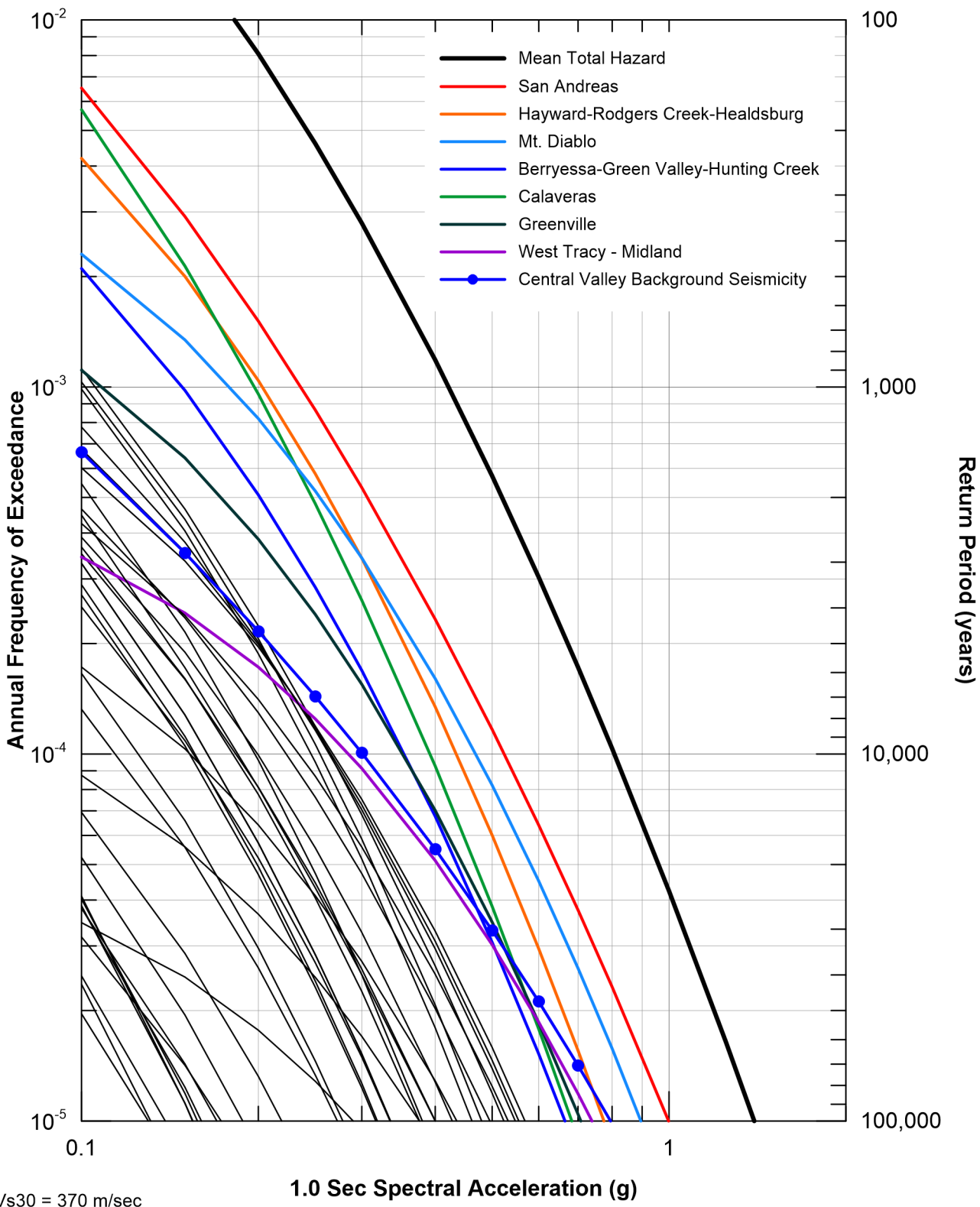


For Illustration
Purposes Only

Figure 62
 Seismic Source Contributions
 for Mean 1.0 Sec Horizontal Spectral
 Acceleration Hazard for Bouldin



Vs30 = 290 m/sec
 Sources contributing 5% or more in
 144 to 2,475-year return period range listed.
 Other less significant sources shown in black
 not listed.

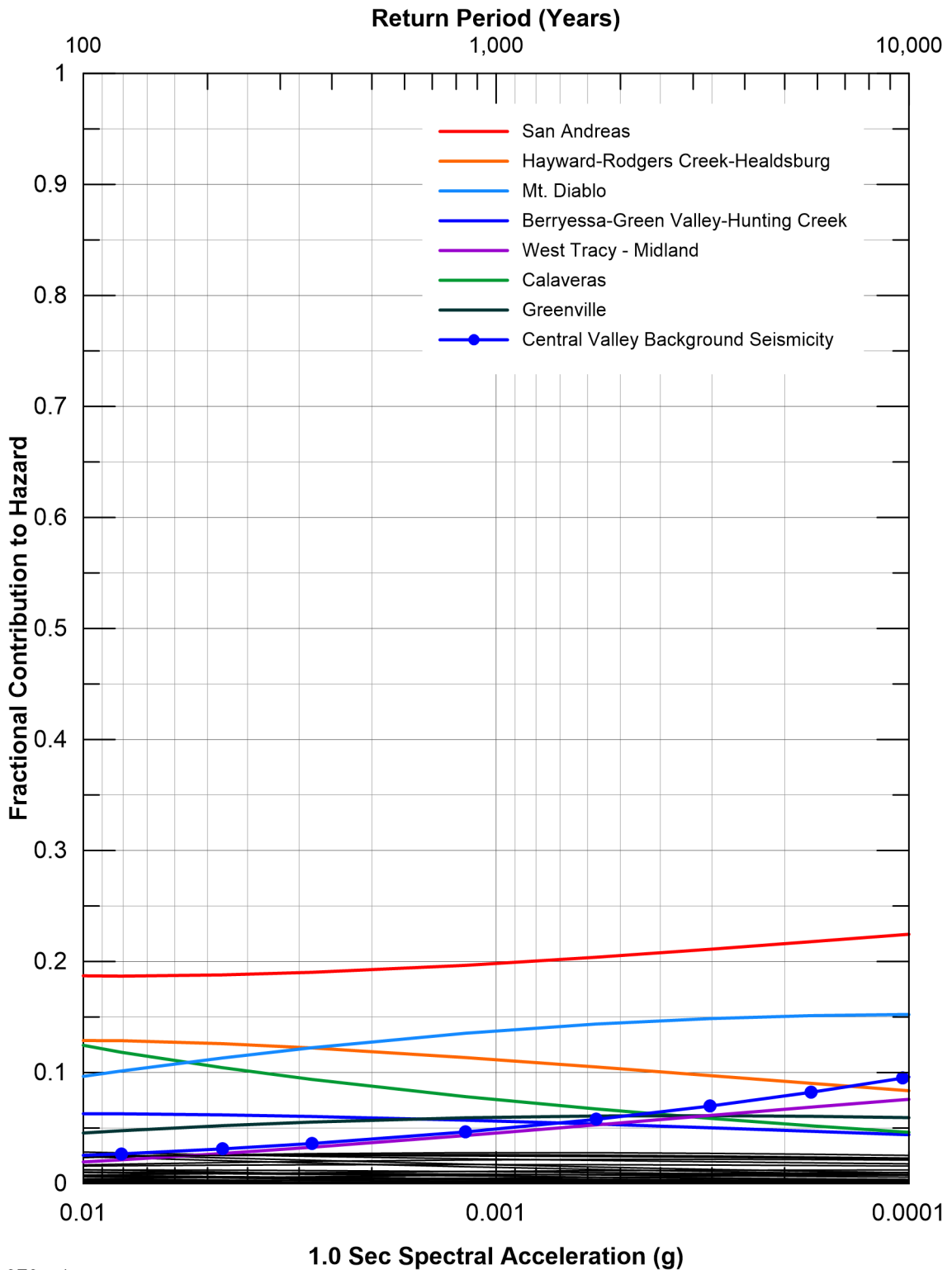


Vs30 = 370 m/sec
 Sources contributing 5% or more in
 144 to 2,475-year return period range listed.
 Other less significant sources shown in black
 not listed.



For Illustration
 Purposes Only

Figure 64
 Seismic Source Contributions
 for Mean 1.0 Sec Horizontal Spectral
 Acceleration Hazard for King Island

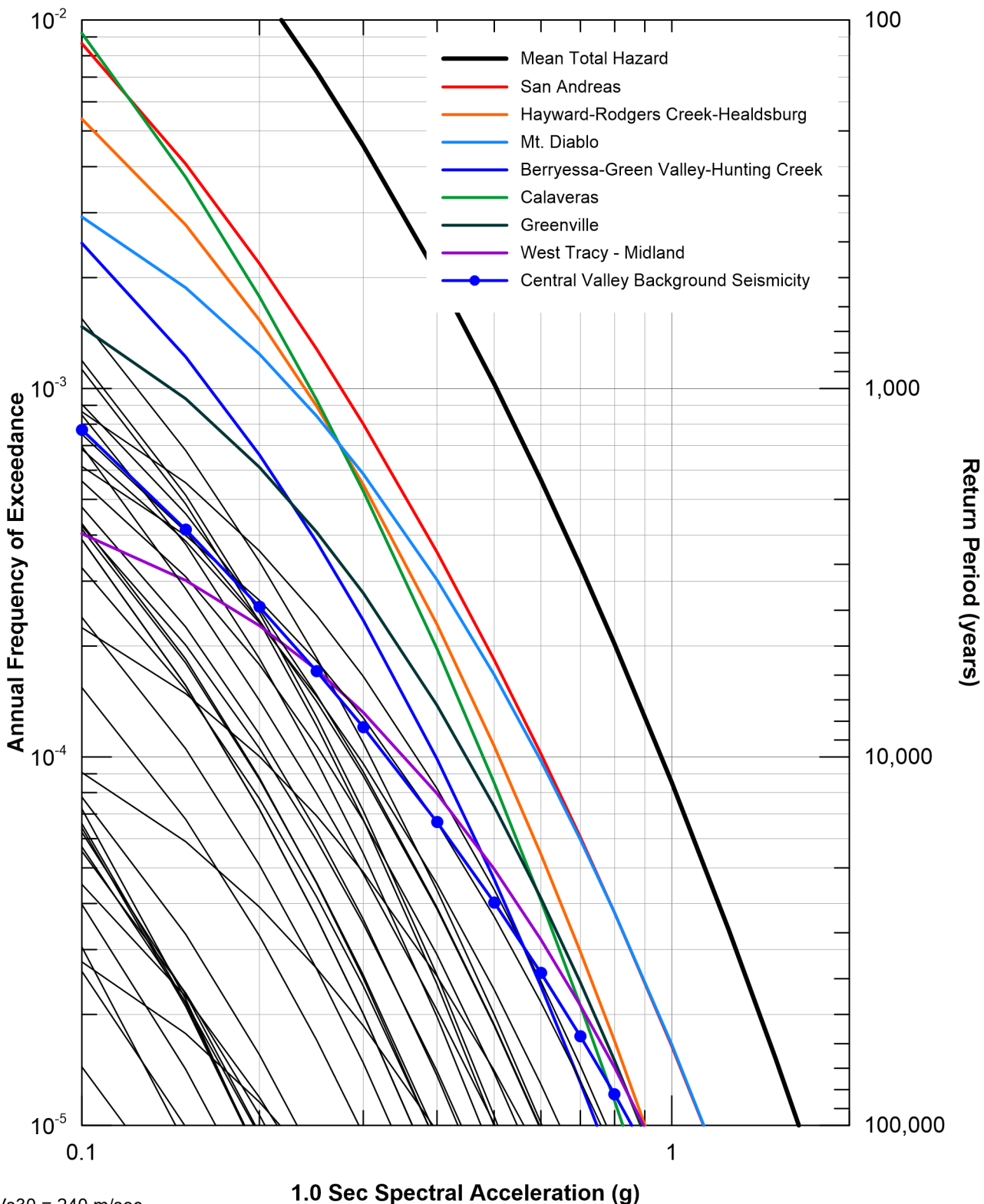


Vs30 = 370 m/sec
 Sources contributing 5% or more in
 144 to 2,475-year return period range listed.
 Other less significant sources shown in black
 not listed.



For Illustration
 Purposes Only

Figure 65
 Seismic Source Fractional Contributions
 for Mean 1.0 Sec Horizontal Spectral
 Acceleration Hazard for King Island

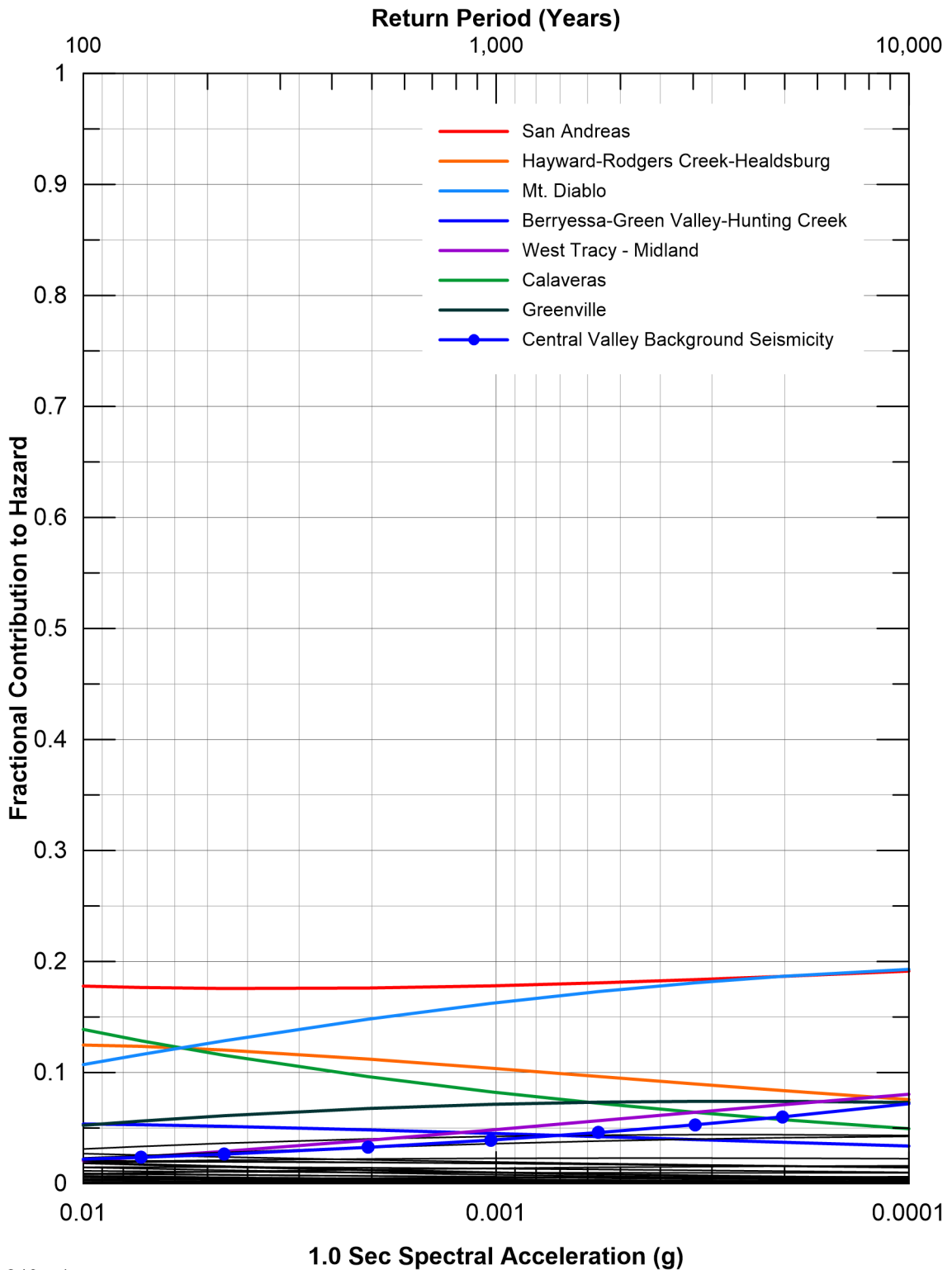


Vs30 = 240 m/sec
 Sources contributing 5% or more in
 144 to 2,475-year return period range listed.
 Other less significant sources shown in black
 not listed.



For Illustration
 Purposes Only

Figure 66
 Seismic Source Contributions
 for Mean 1.0 Sec Horizontal Spectral
 Acceleration Hazard for Lower Roberts

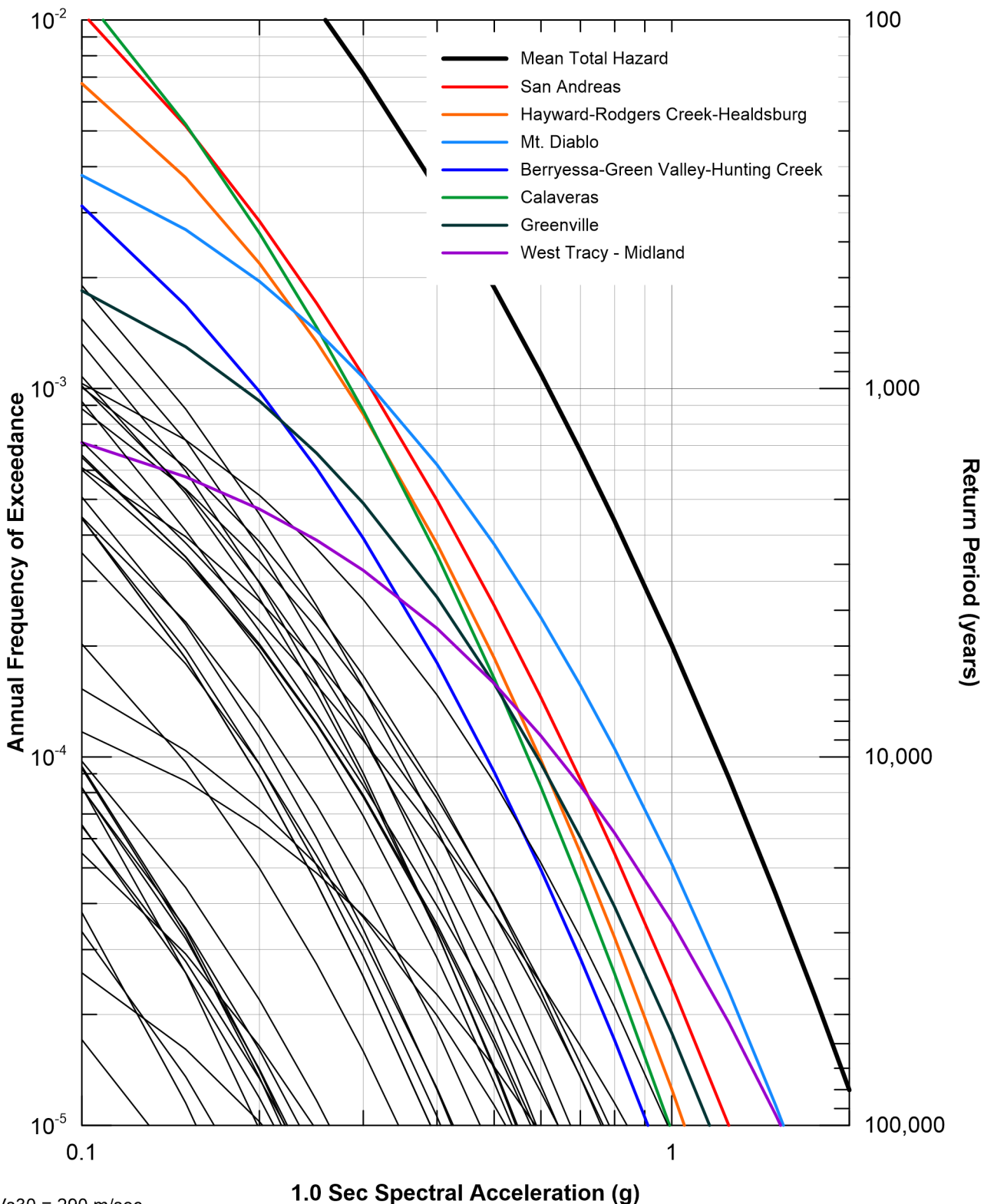


Vs30 = 240 m/sec
 Sources contributing 5% or more in
 144 to 2,475-year return period range listed.
 Other less significant sources shown in black
 not listed.



For Illustration
 Purposes Only

Figure 67
 Seismic Source Fractional Contributions
 for Mean 1.0 Sec Horizontal Spectral
 Acceleration Hazard for Lower Roberts

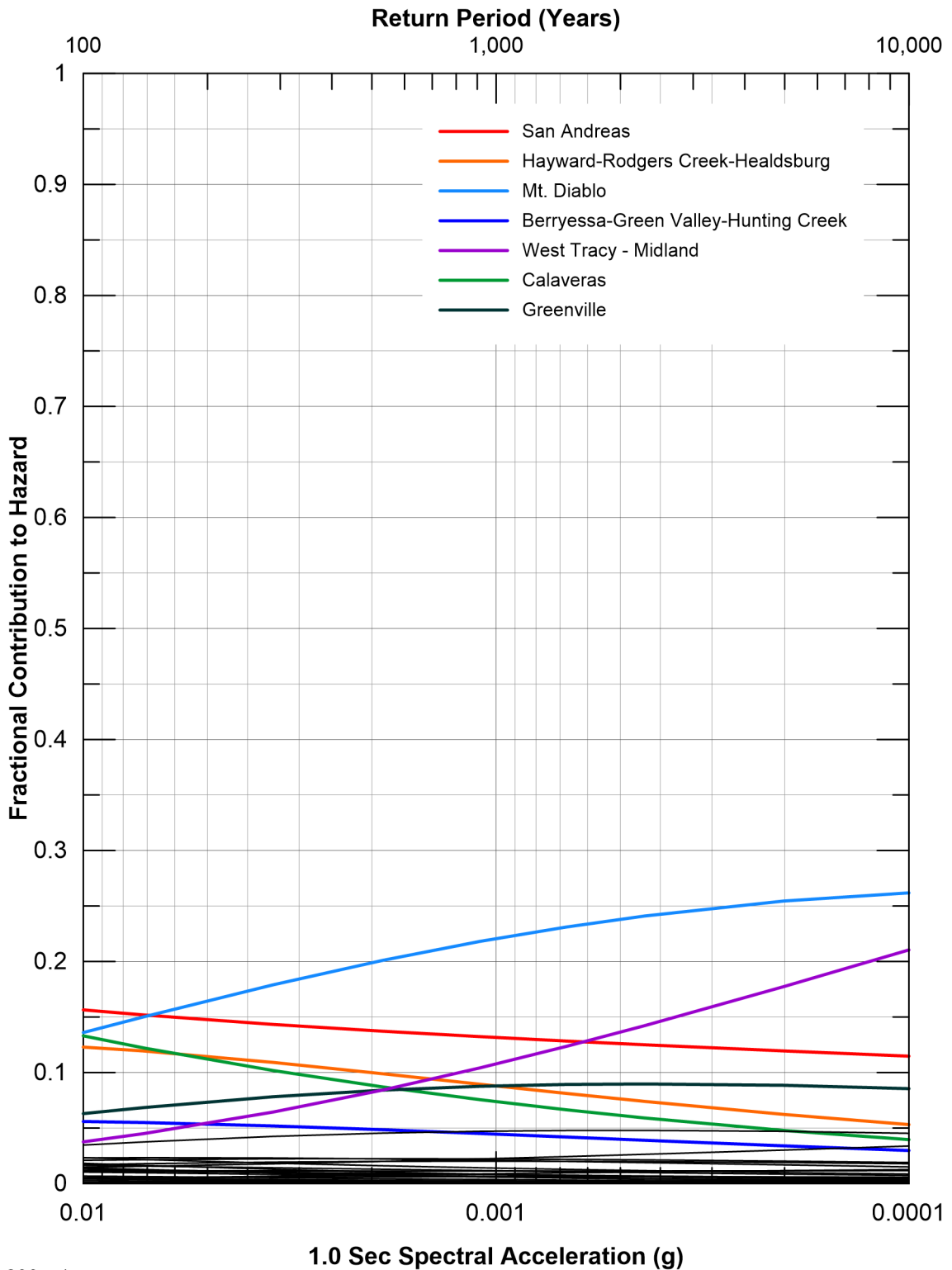


$V_{s30} = 290 \text{ m/sec}$
 Sources contributing 5% or more in
 144 to 2,475-year return period range listed.
 Other less significant sources shown in black
 not listed.



For Illustration
 Purposes Only

Figure 68
 Seismic Source Contributions
 for Mean 1.0 Sec Horizontal Spectral
 Acceleration Hazard for Bacon

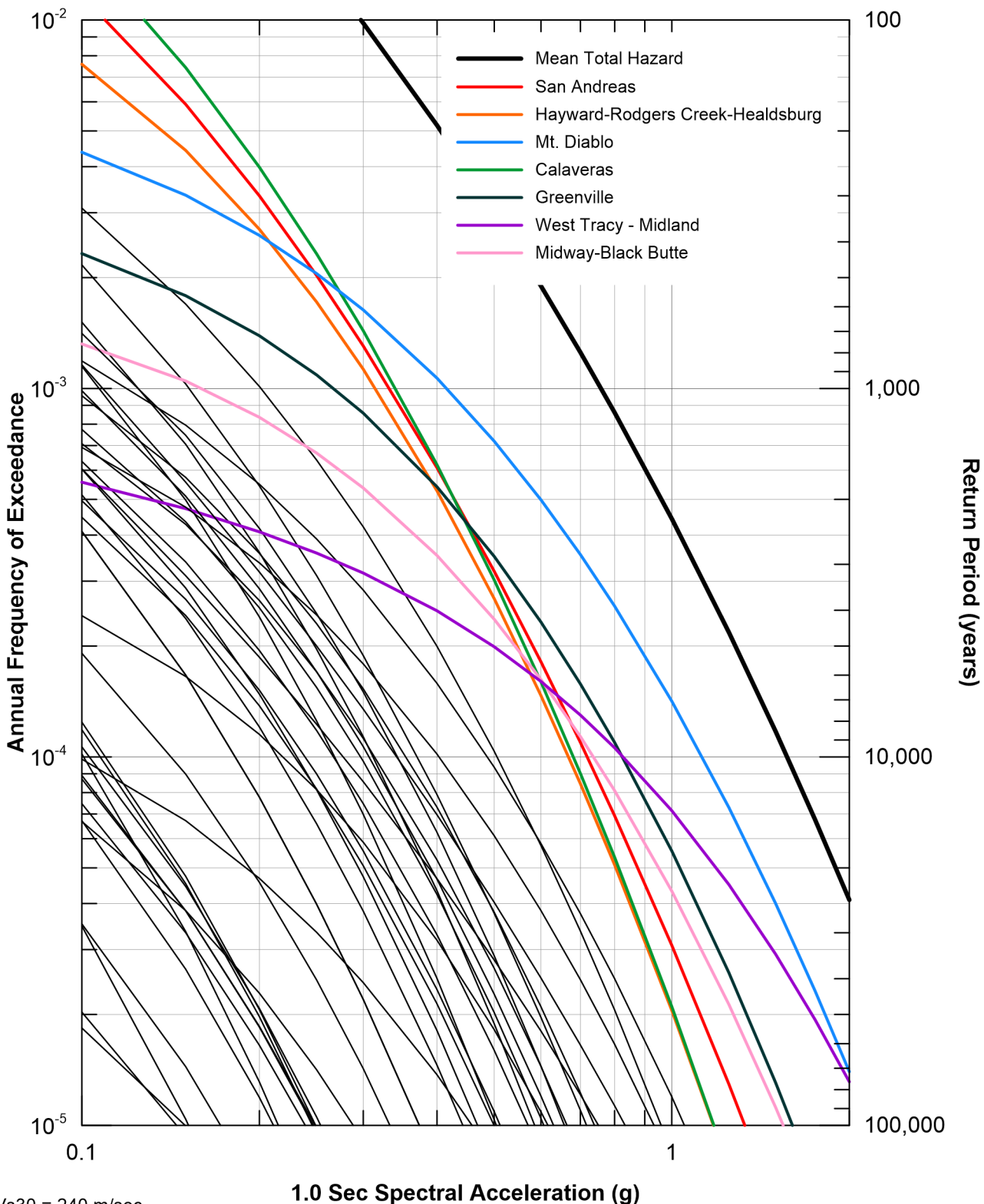


Vs30 = 290 m/sec
 Sources contributing 5% or more in
 144 to 2,475-year return period range listed.
 Other less significant sources shown in black
 not listed.



For Illustration
 Purposes Only

Figure 69
 Seismic Source Fractional Contributions
 for Mean 1.0 Sec Horizontal Spectral
 Acceleration Hazard for Bacon

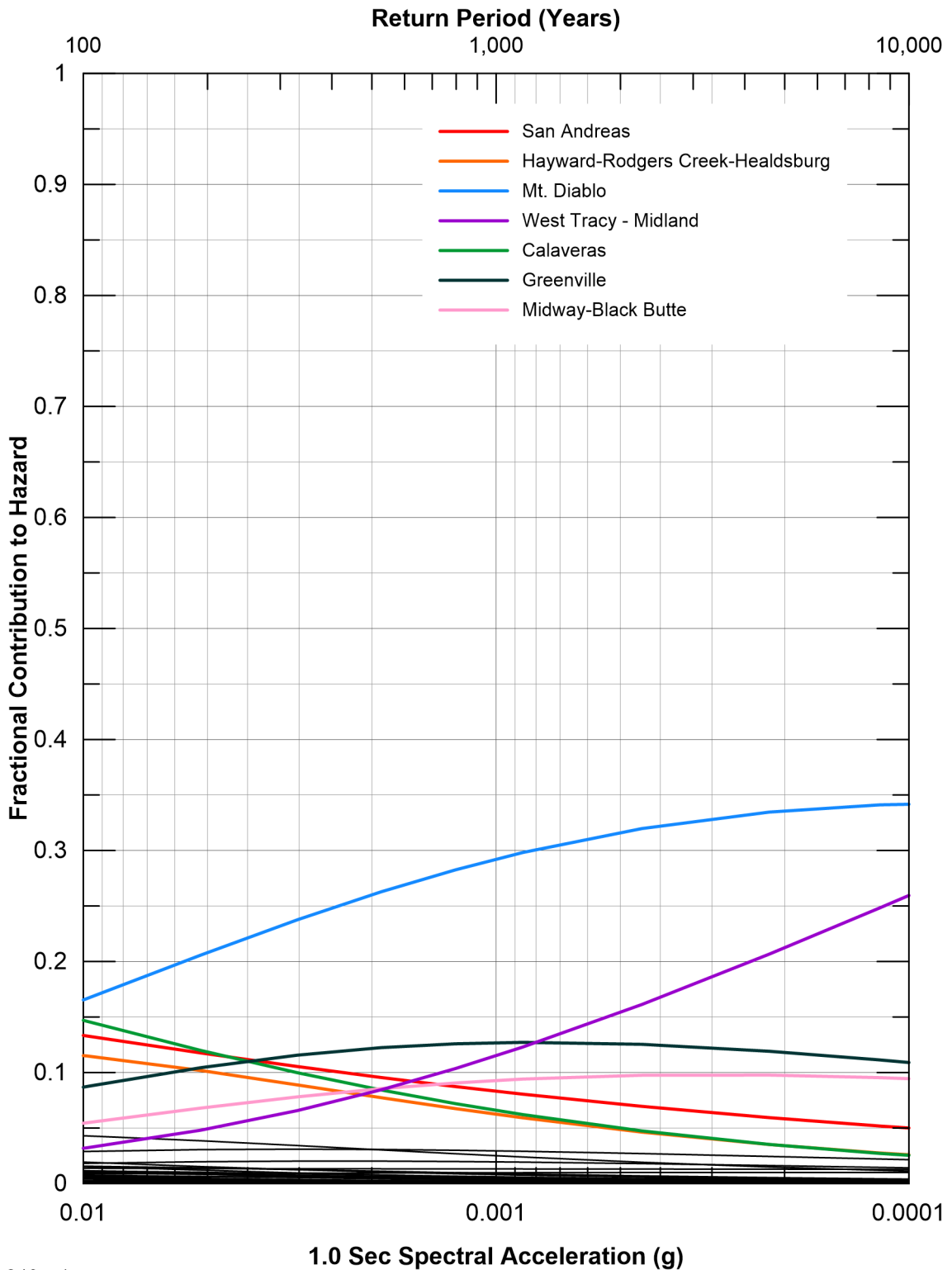


Vs30 = 240 m/sec
 Sources contributing 5% or more in
 144 to 2,475-year return period range listed.
 Other less significant sources shown in black
 not listed.



For Illustration
 Purposes Only

Figure 70
 Seismic Source Contributions for Mean
 1.0 Sec Horizontal Spectral Acceleration
 Hazard for Southern Forebay North

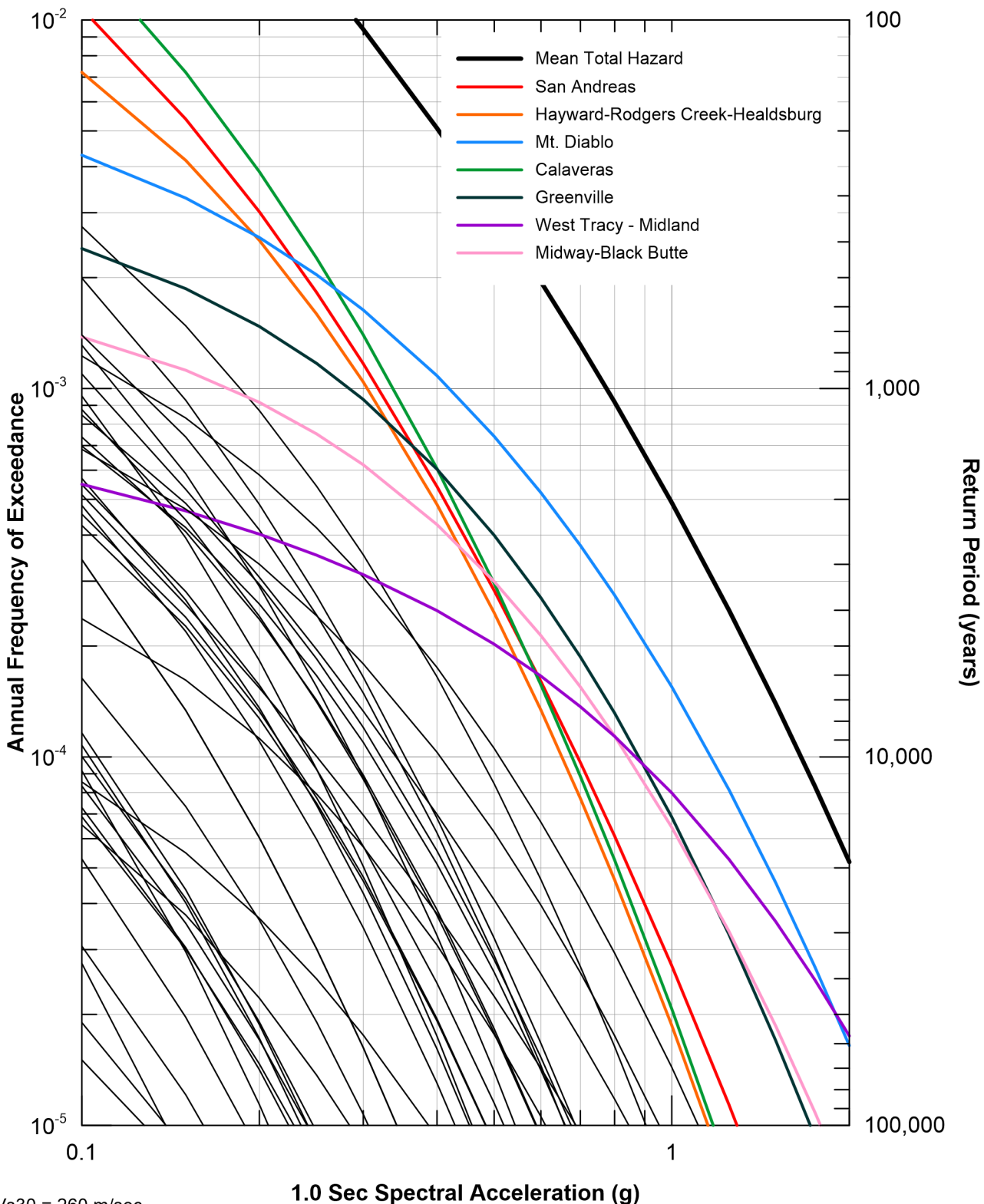


Vs30 = 240 m/sec
 Sources contributing 5% or more in
 144 to 2,475-year return period range listed.
 Other less significant sources shown in black
 not listed.



For Illustration
 Purposes Only

Figure 71
 Seismic Source Fractional Contributions
 for Mean 1.0 Sec Horizontal Spectral
 Acceleration Hazard for
 Southern Forebay North

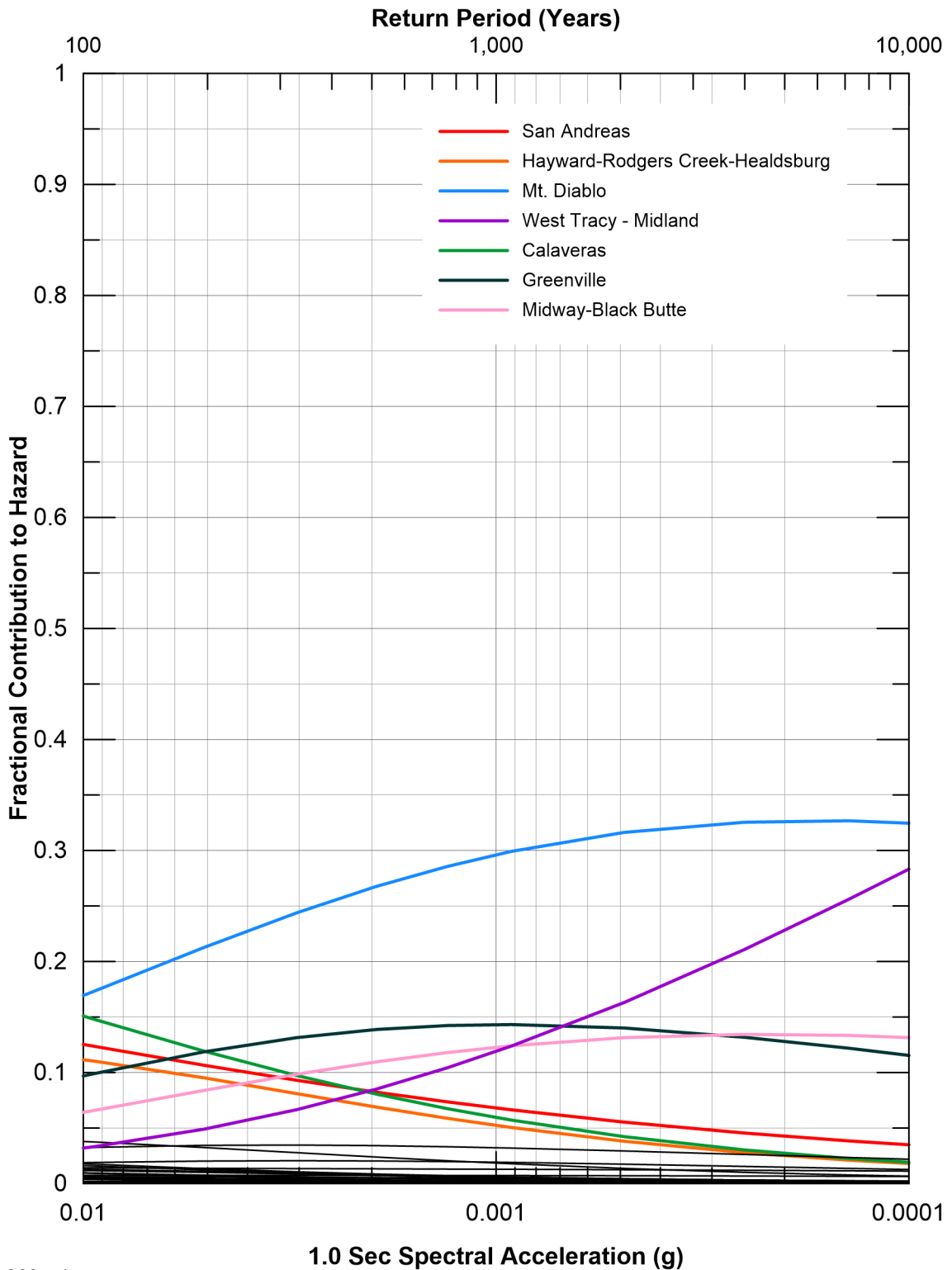


Vs30 = 260 m/sec
 Sources contributing 5% or more in
 144 to 2,475-year return period range listed.
 Other less significant sources shown in black
 not listed.



For Illustration
 Purposes Only

Figure 72
 Seismic Source Contributions for Mean
 1.0 Sec Horizontal Spectral Acceleration
 Hazard for Southern Forebay South

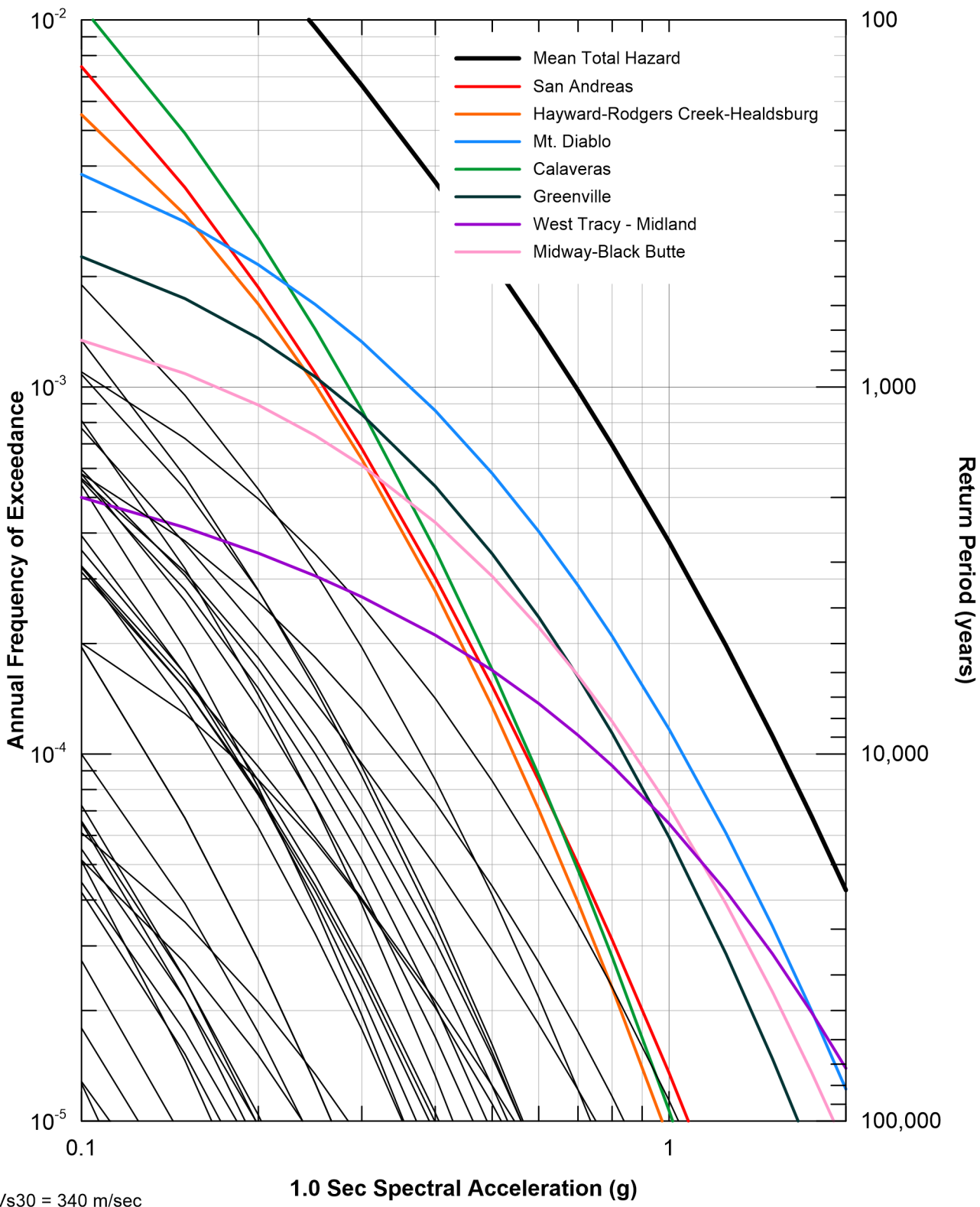


Vs30 = 260 m/sec
 Sources contributing 5% or more in
 144 to 2,475-year return period range listed.
 Other less significant sources shown in black
 not listed.



For Illustration
 Purposes Only

Figure 73
 Seismic Source Fractional Contributions
 for Mean 1.0 Sec Horizontal Spectral
 Acceleration Hazard for
 Southern Forebay South

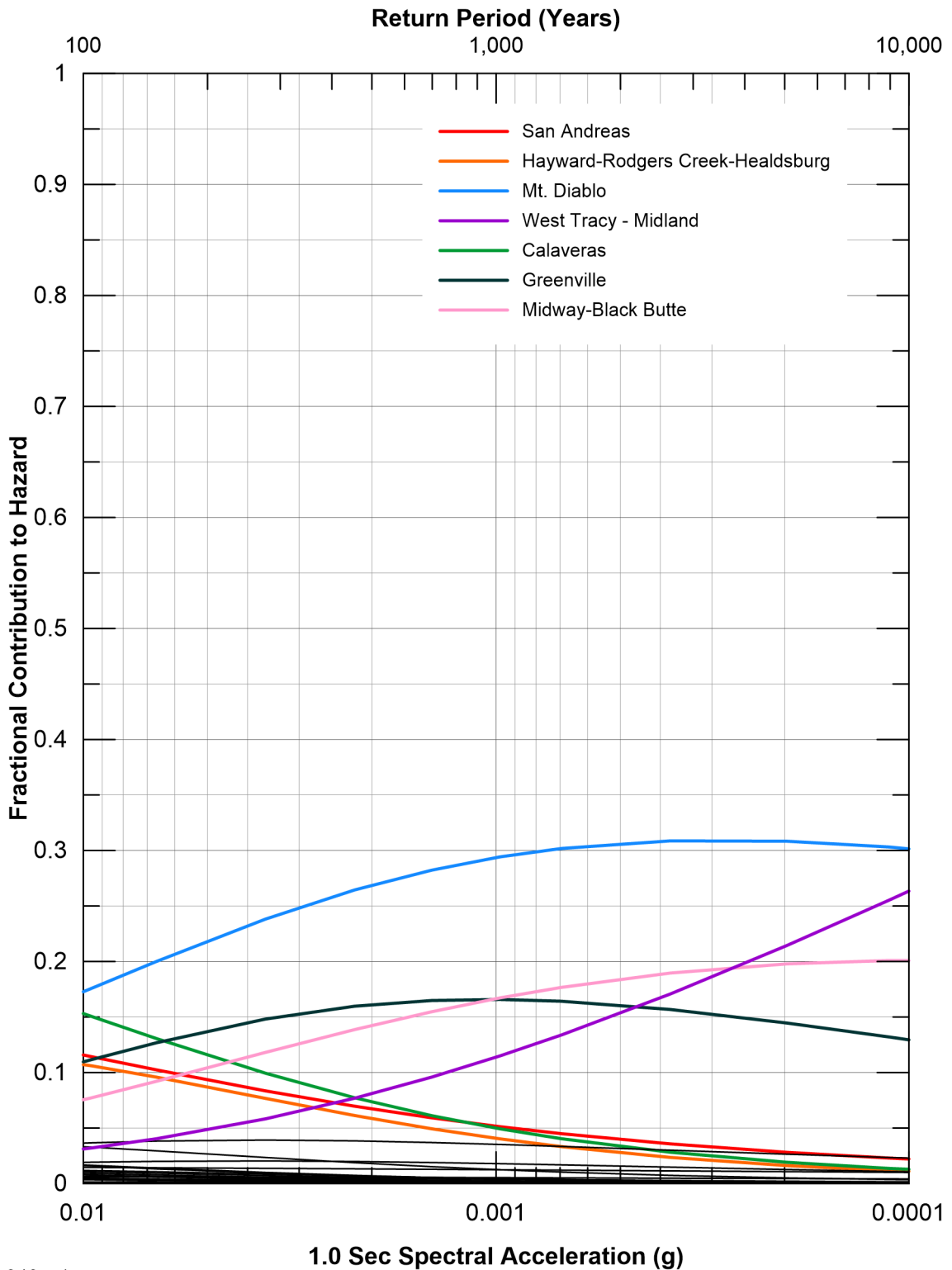


Vs30 = 340 m/sec
 Sources contributing 5% or more in
 144 to 2,475-year return period range listed.
 Other less significant sources shown in black
 not listed.



For Illustration
 Purposes Only

Figure 74
 Seismic Source Contributions for Mean
 1.0 Sec Horizontal Spectral Acceleration
 Hazard for Jones Connection

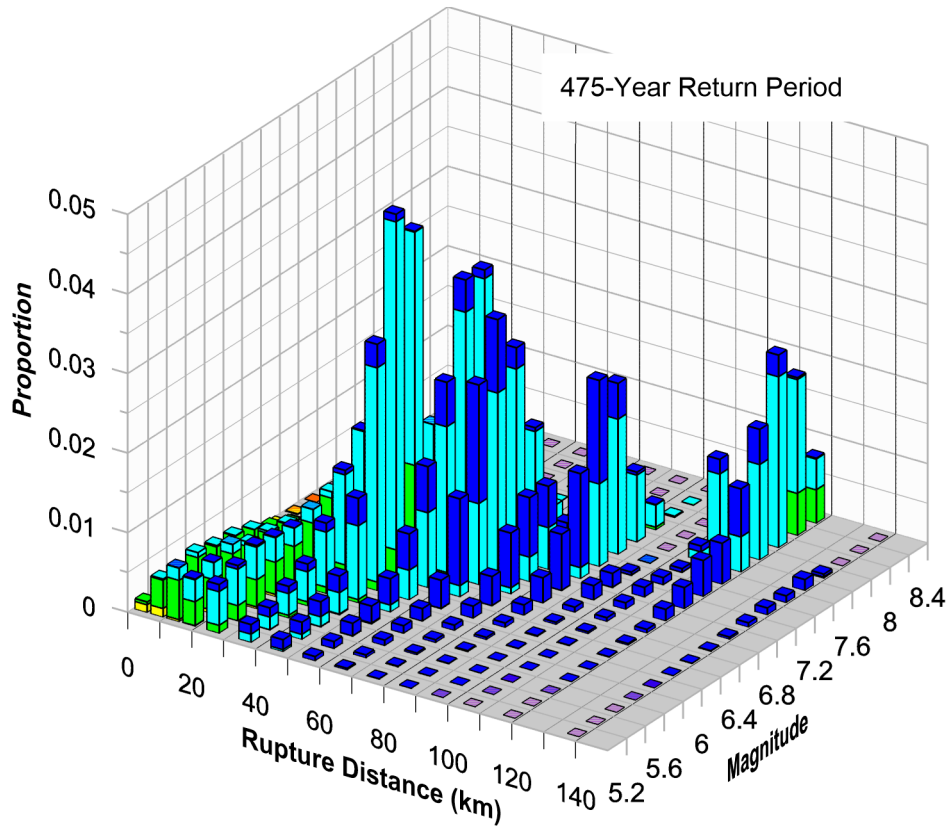


Vs30 = 340 m/sec
 Sources contributing 5% or more in
 144 to 2,475-year return period range listed.
 Other less significant sources shown in black
 not listed.

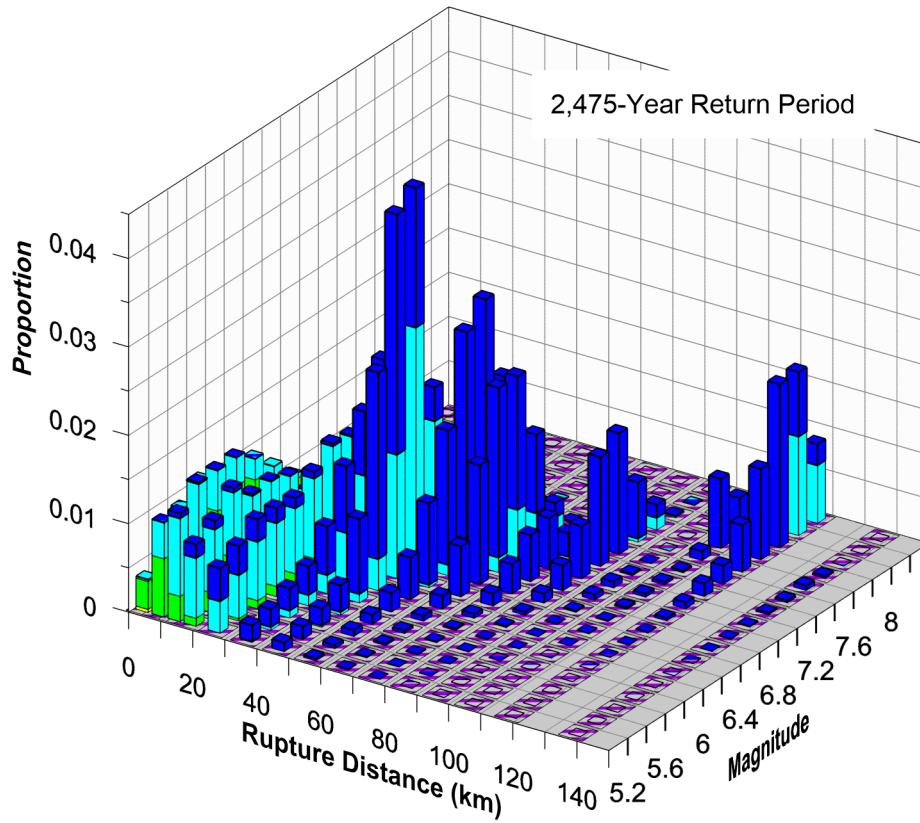


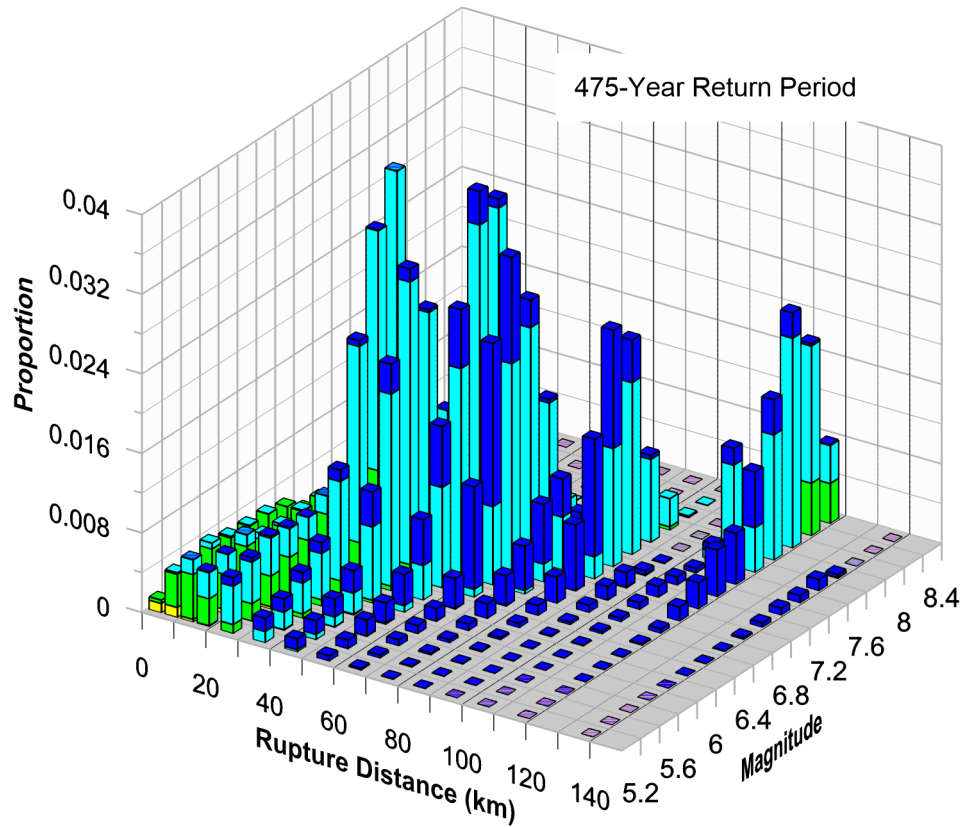
For Illustration
 Purposes Only

Figure 73
 Seismic Source Fractional Contributions
 for Mean 1.0 Sec Horizontal Spectral
 Acceleration Hazard for
 Jones Connection

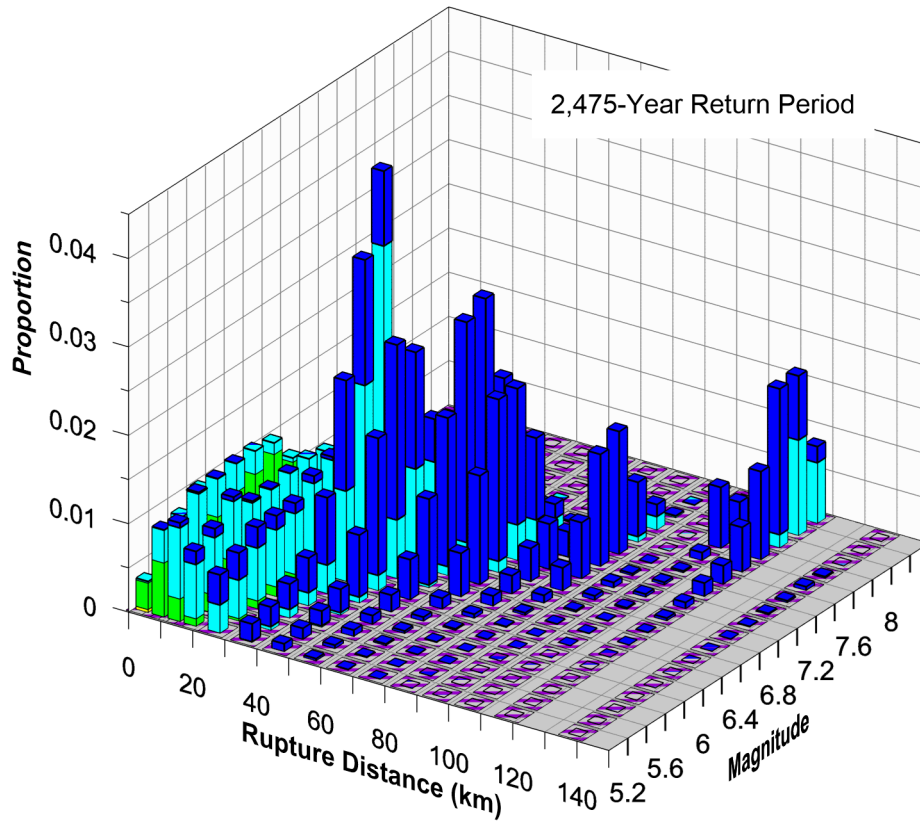


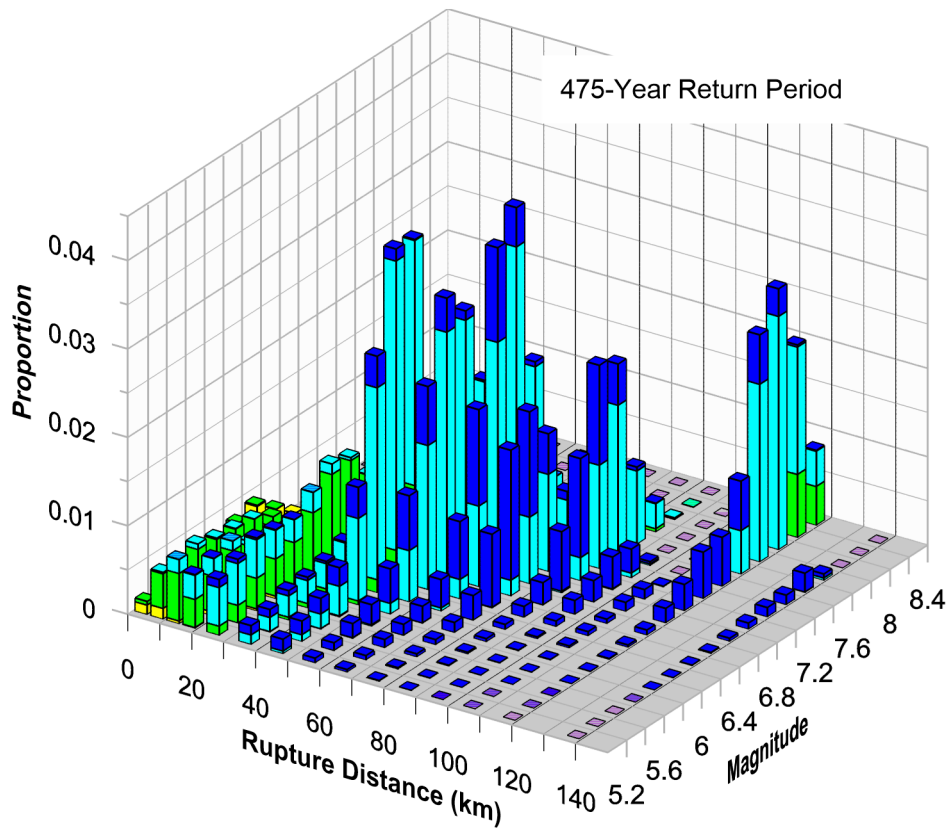
- Epsilon
- 2 to 3
 - 1 to 2
 - 0 to 1
 - 1 to 0
 - 2 to -1
 - < -2



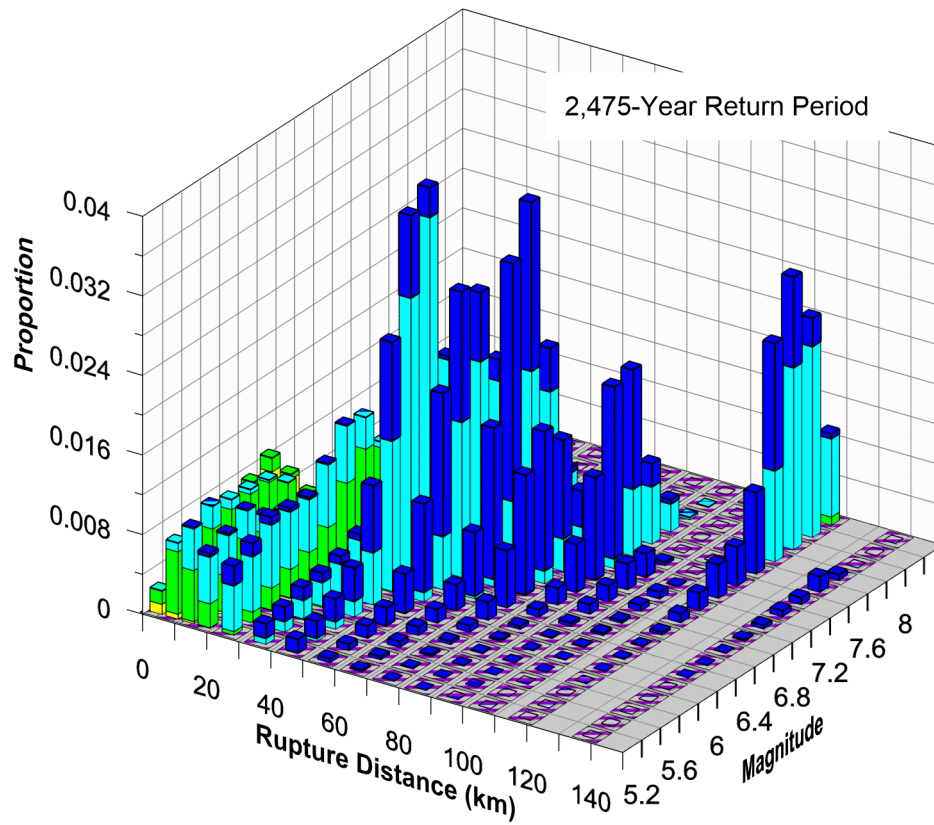


- Epsilon
- 2 to 3
 - 1 to 2
 - 0 to 1
 - -1 to 0
 - -2 to -1
 - < -2



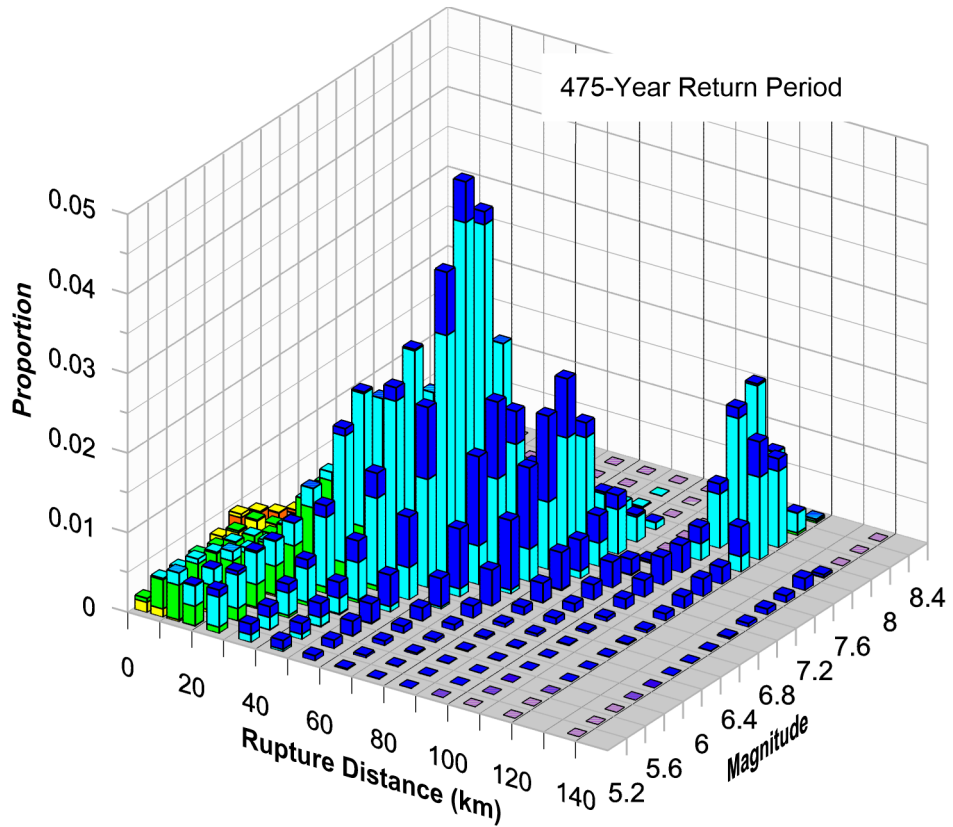


- Epsilon
- 2 to 3
 - 1 to 2
 - 0 to 1
 - 1 to 0
 - 2 to -1
 - < -2

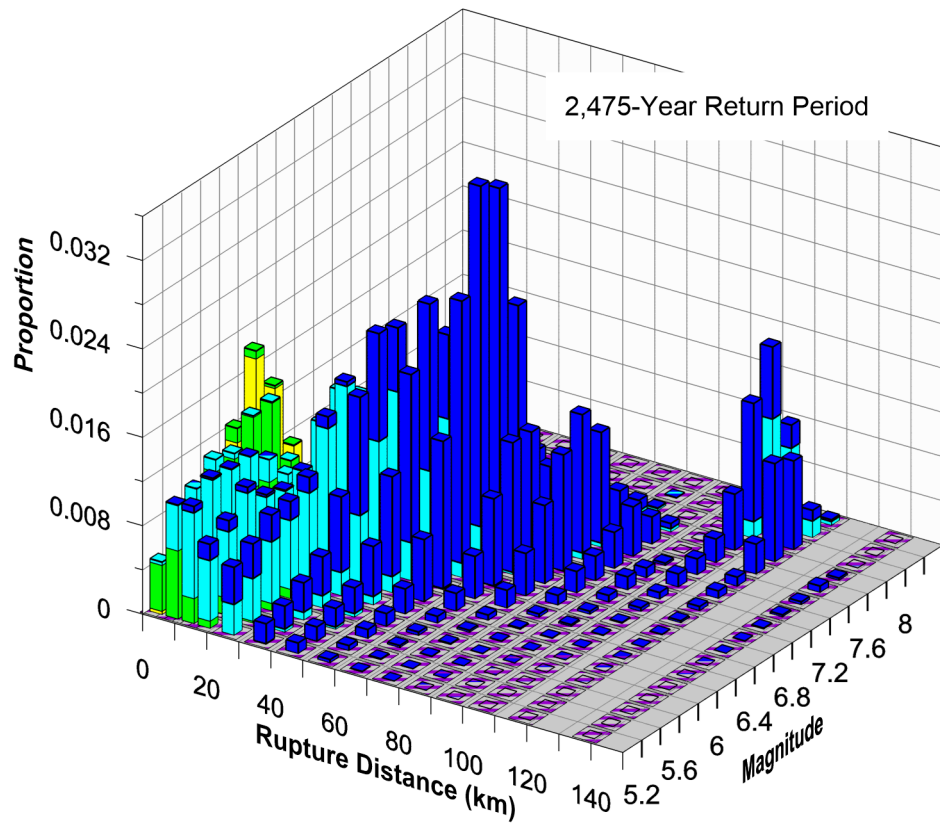


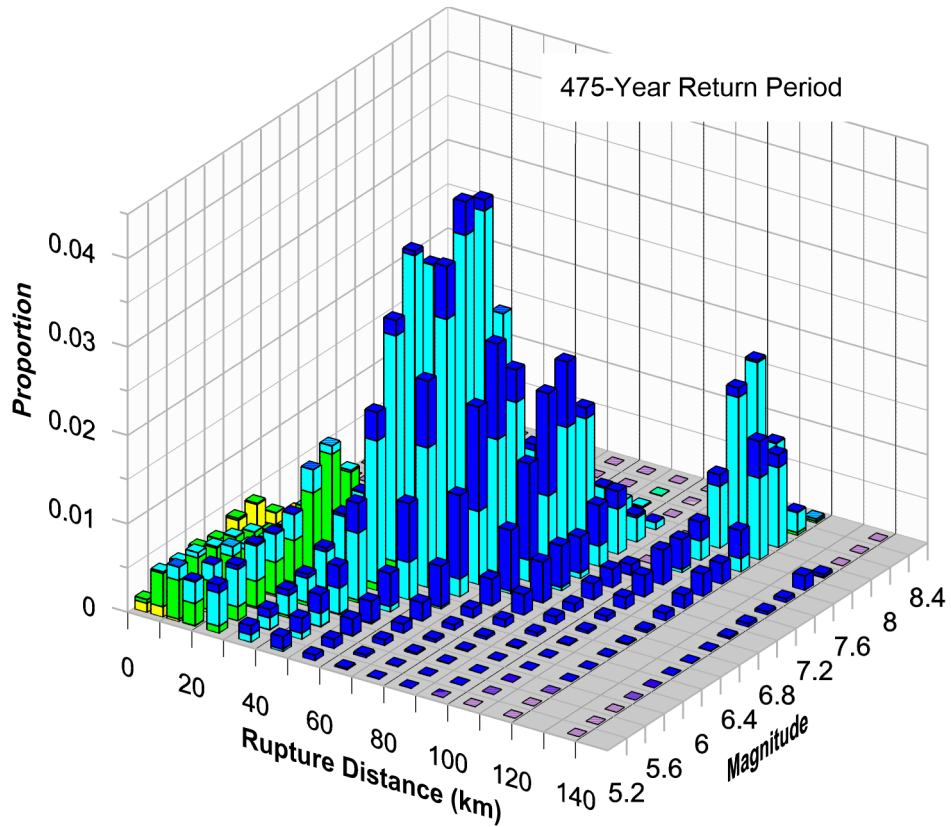
For Illustration
Purposes Only

Figure 78
Magnitude and Distance Contributions
to the Mean Peak Horizontal Hazard
at 475 and 2,475-Year Return Periods
for Twin Cities

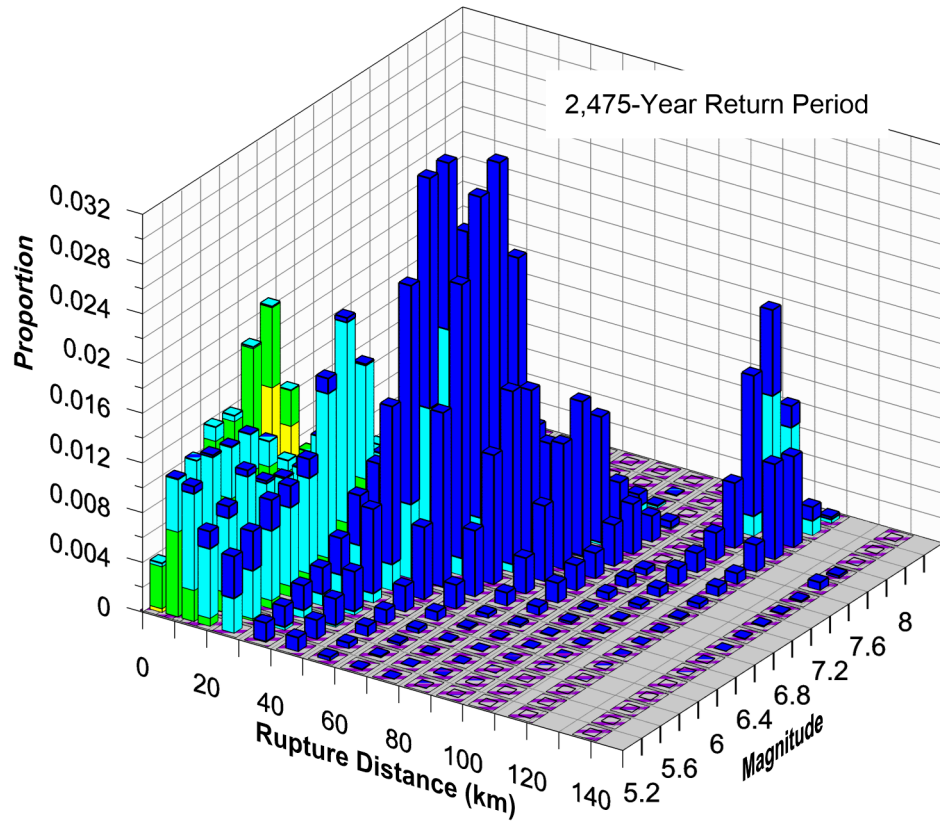


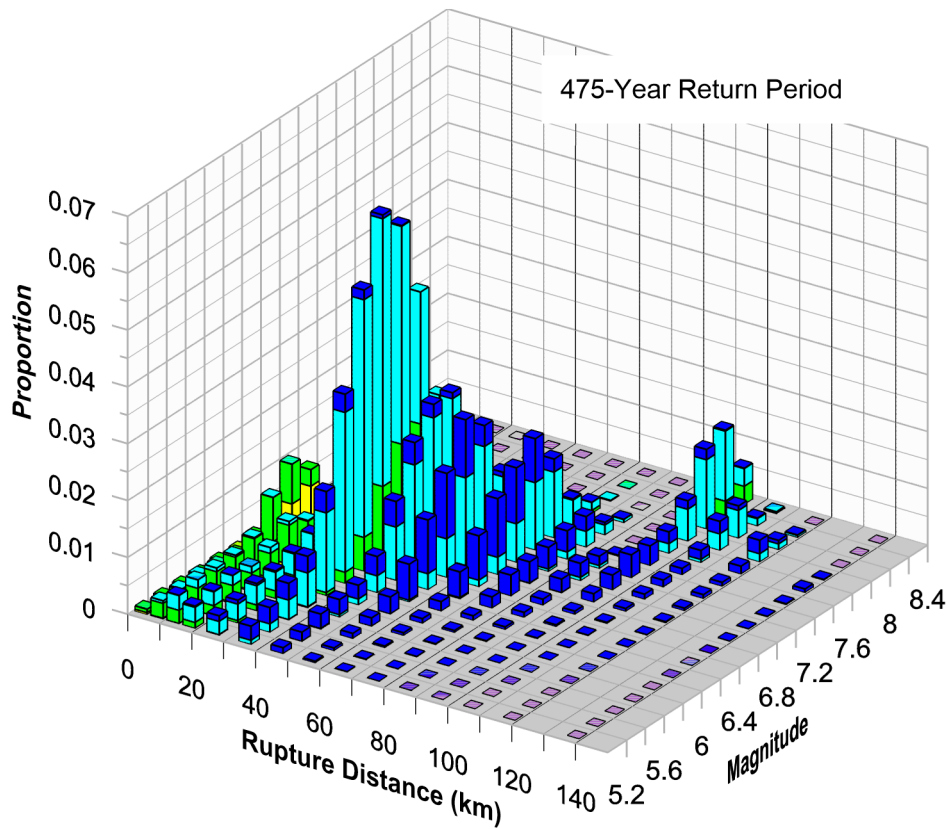
- Epsilon
- 2 to 3
 - 1 to 2
 - 0 to 1
 - 1 to 0
 - 2 to -1
 - < -2



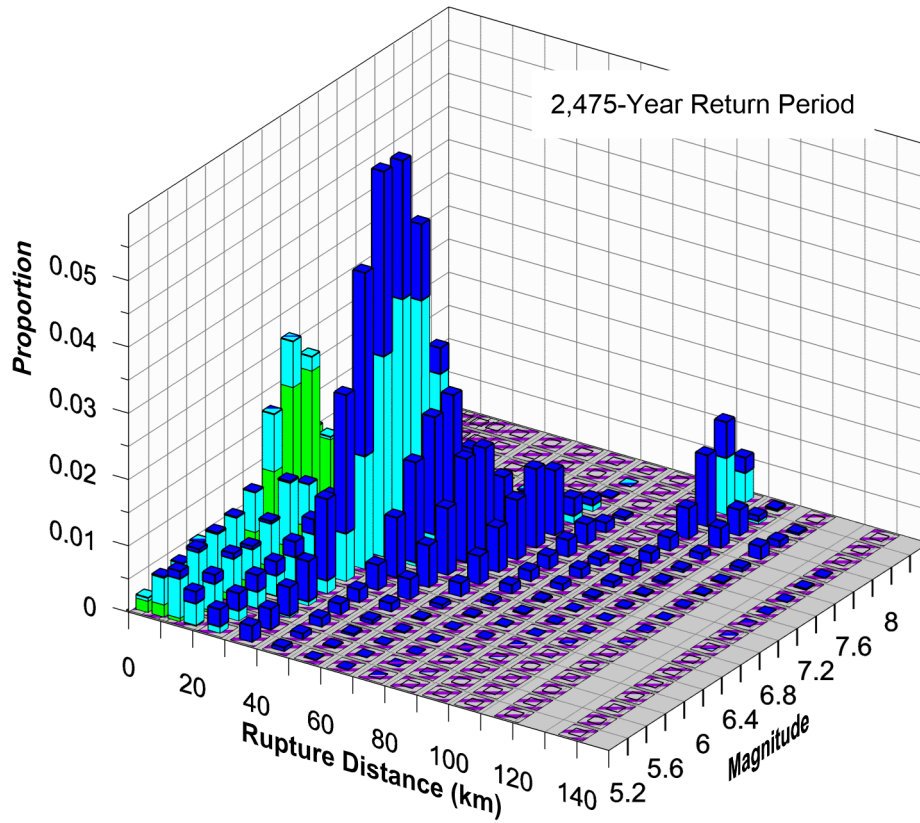


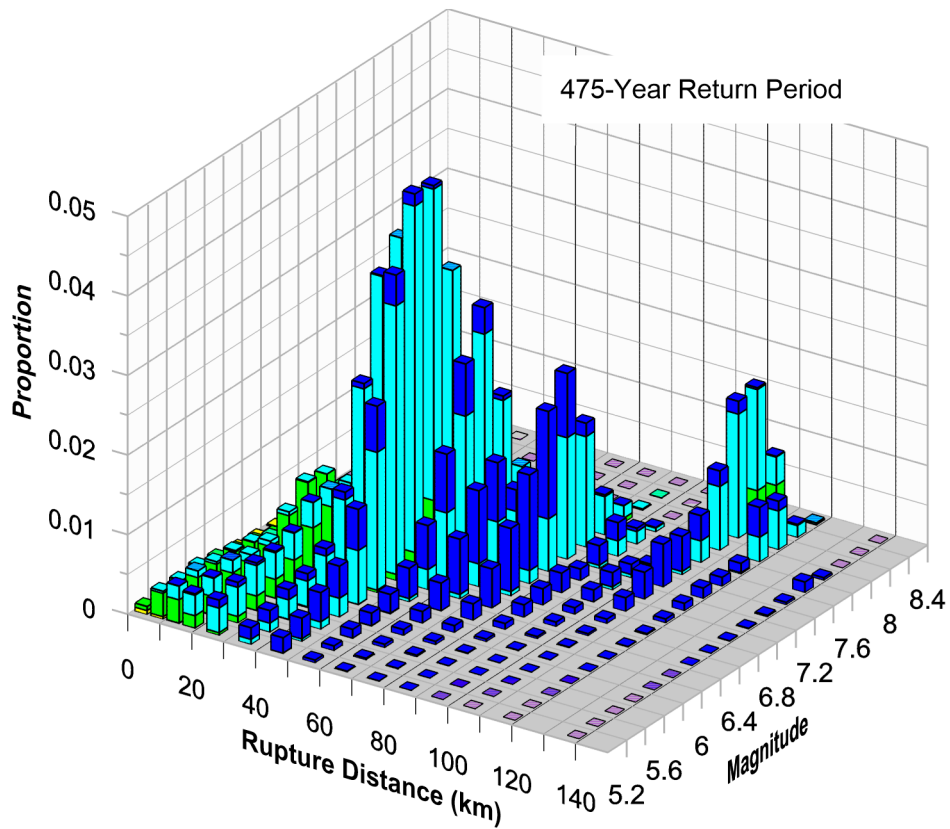
- Epsilon
- 2 to 3
 - 1 to 2
 - 0 to 1
 - 1 to 0
 - 2 to -1
 - < -2



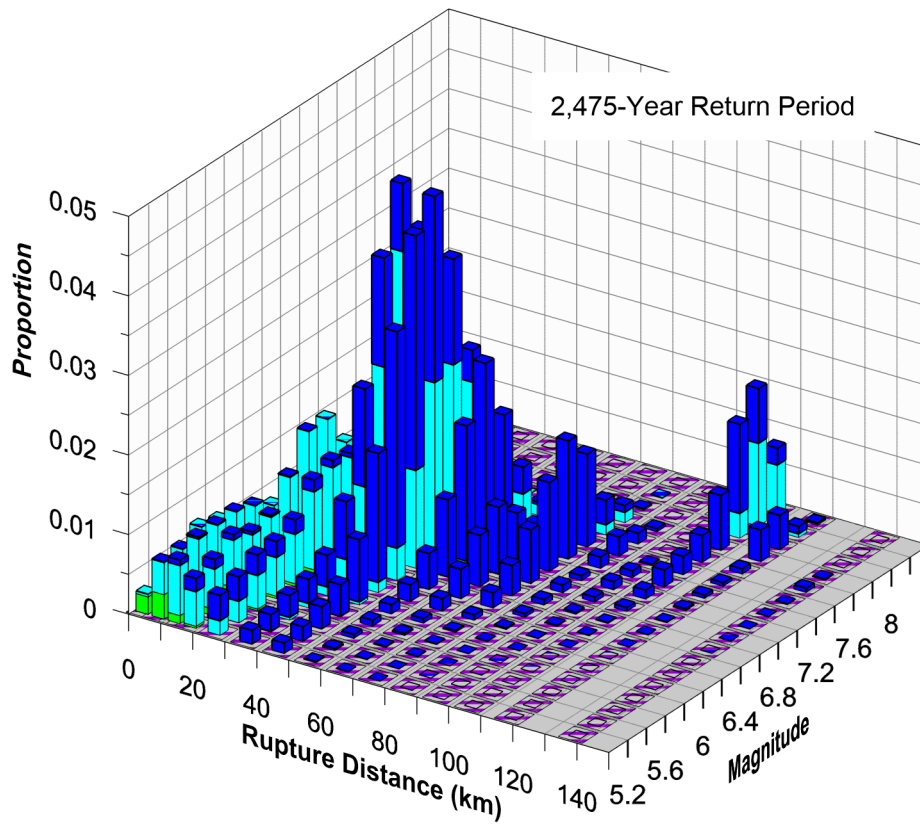


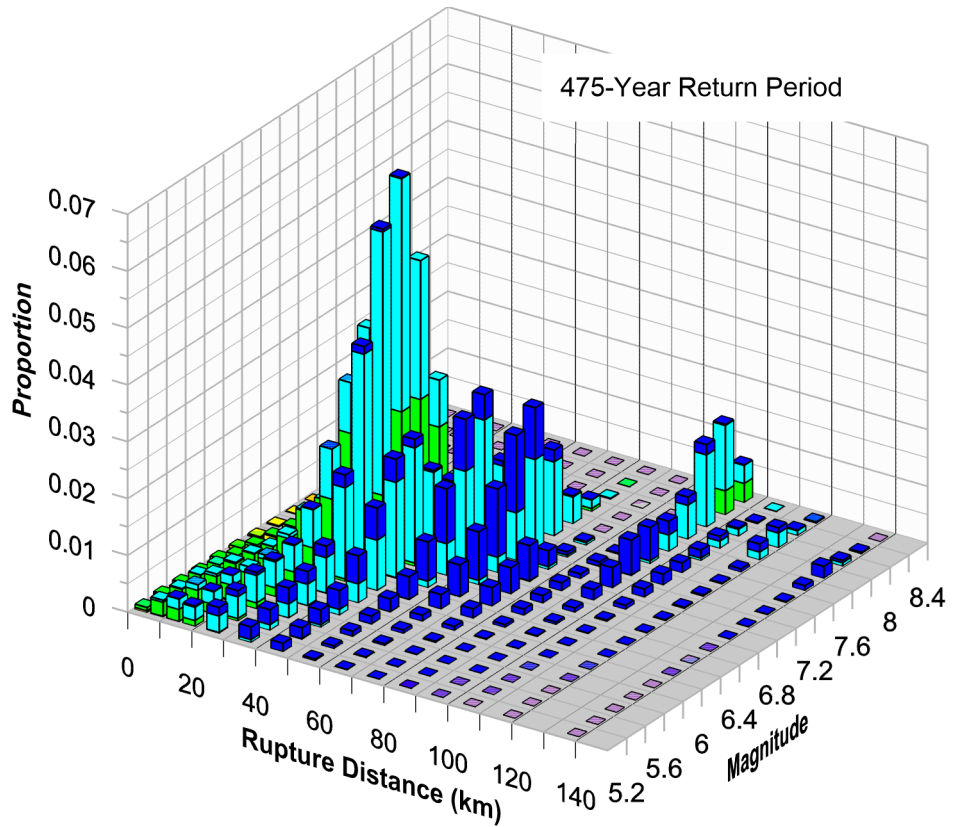
- Epsilon
- 2 to 3
 - 1 to 2
 - 0 to 1
 - -1 to 0
 - -2 to -1
 - < -2



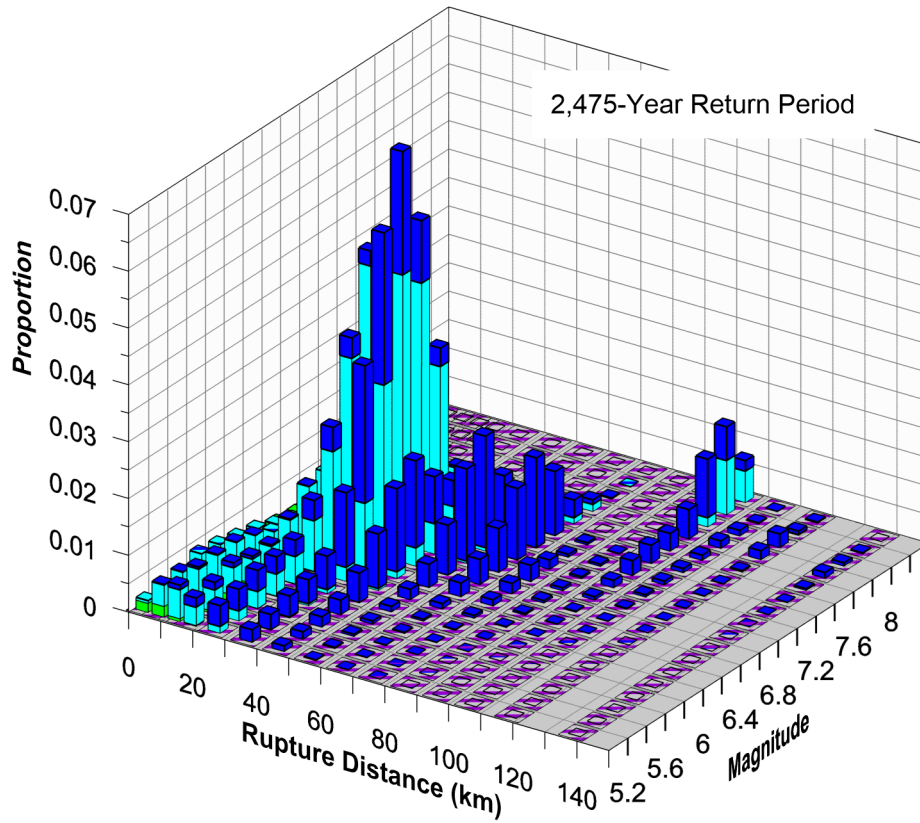


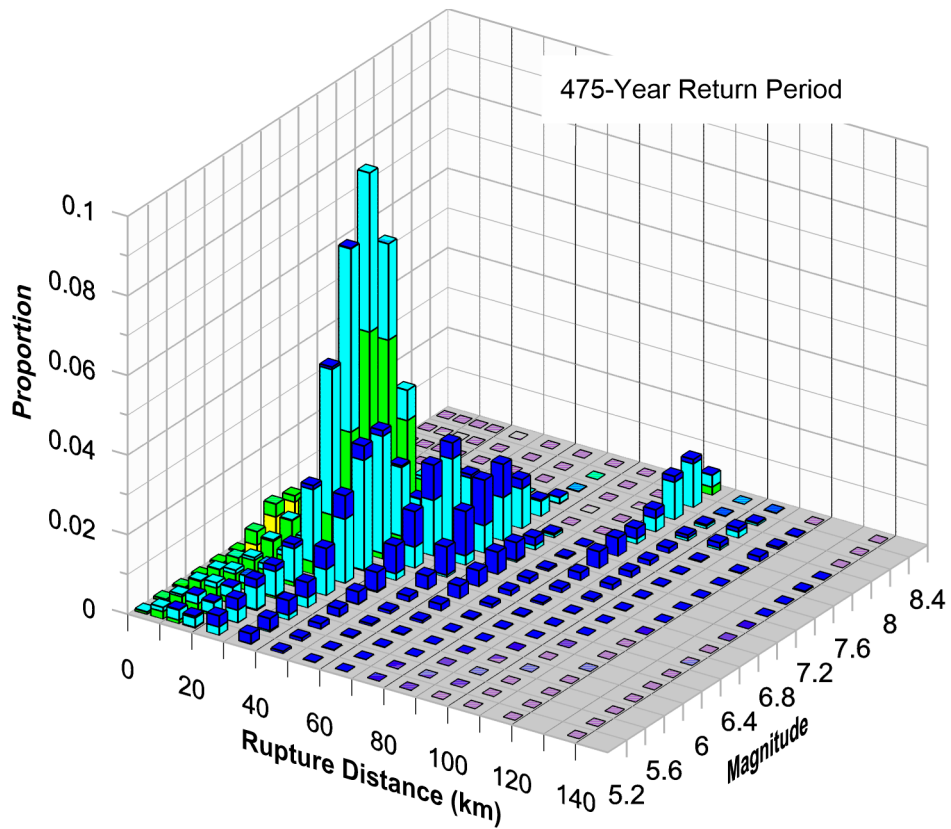
- Epsilon
- 2 to 3
 - 1 to 2
 - 0 to 1
 - 1 to 0
 - 2 to -1
 - < -2



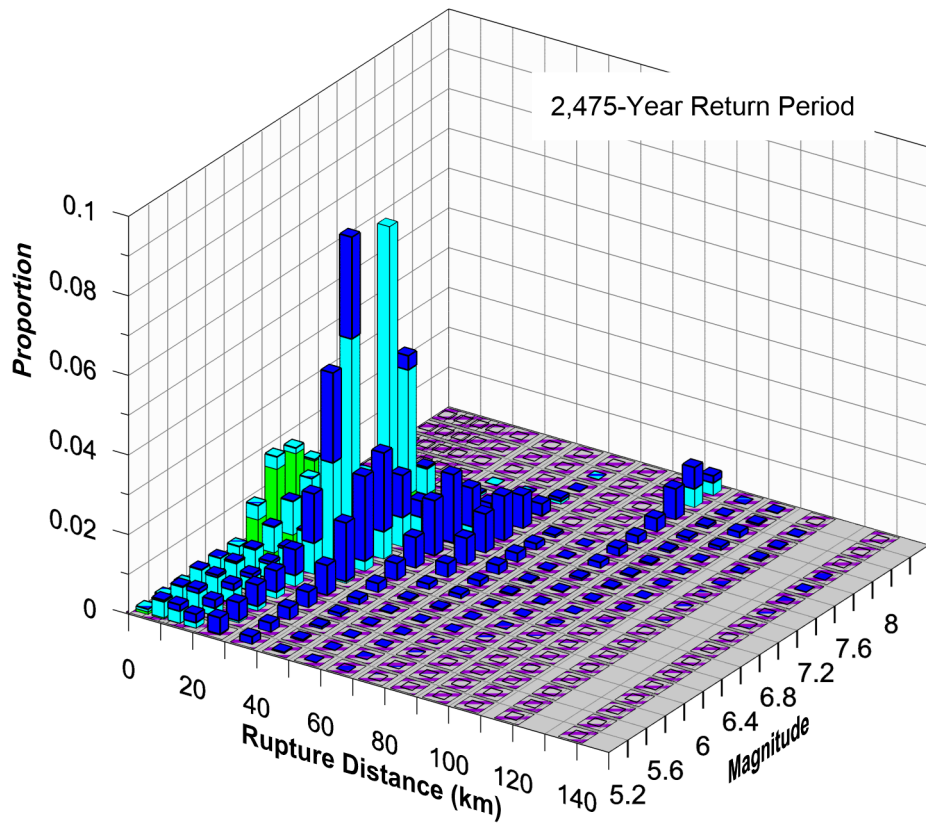


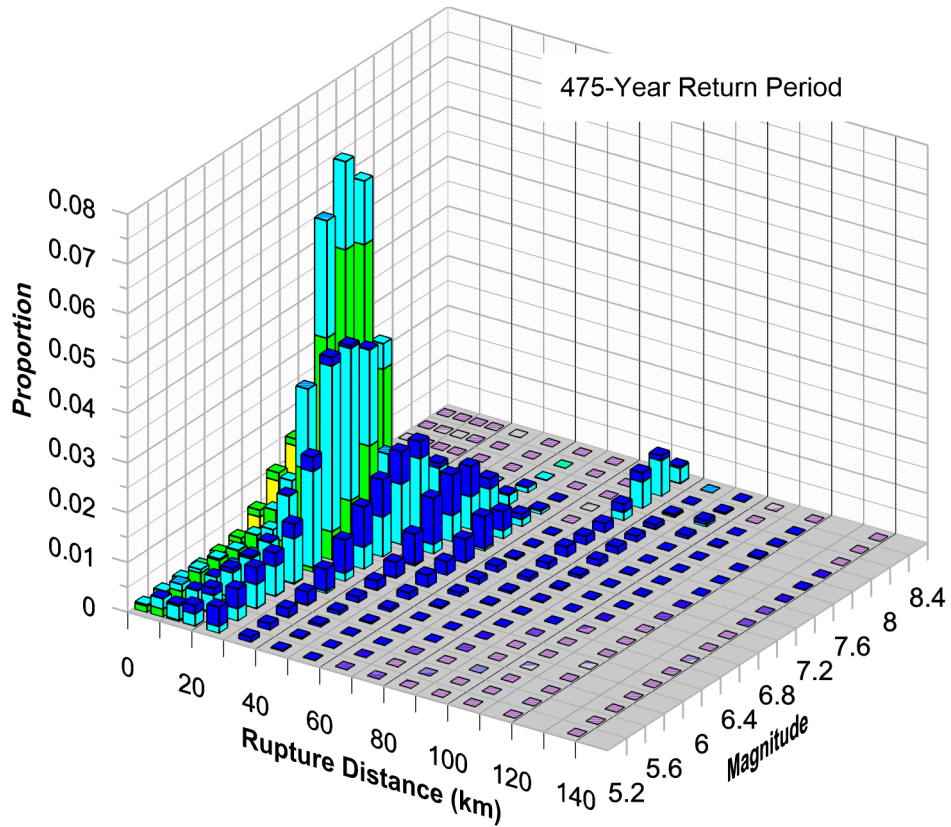
- Epsilon
- 2 to 3
 - 1 to 2
 - 0 to 1
 - -1 to 0
 - -2 to -1
 - < -2



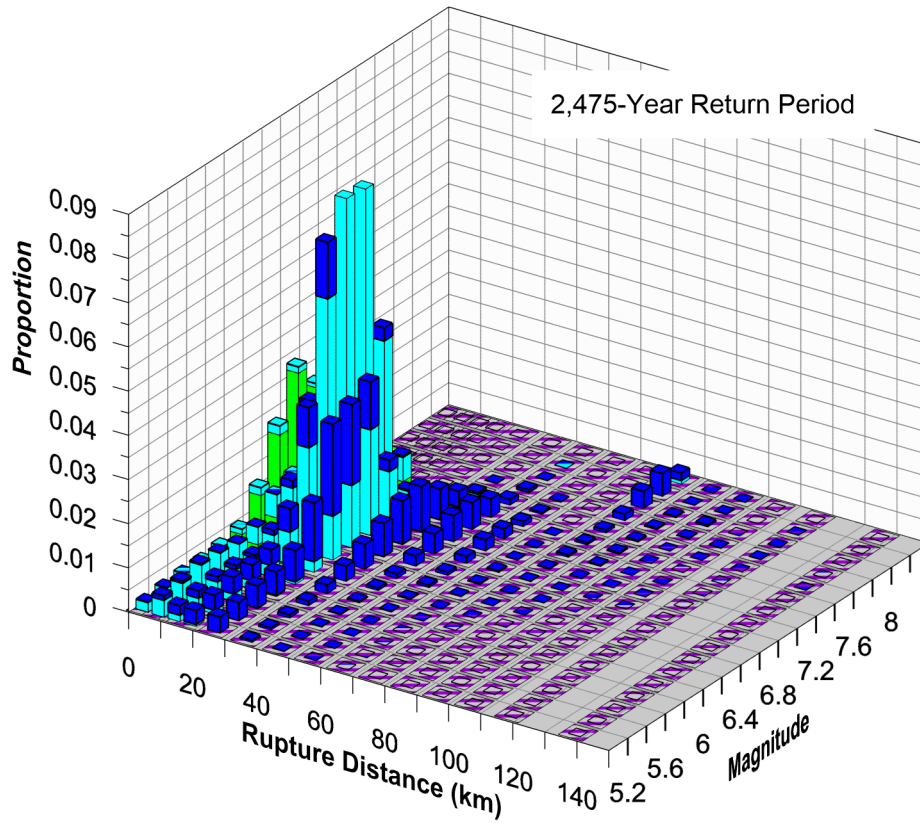


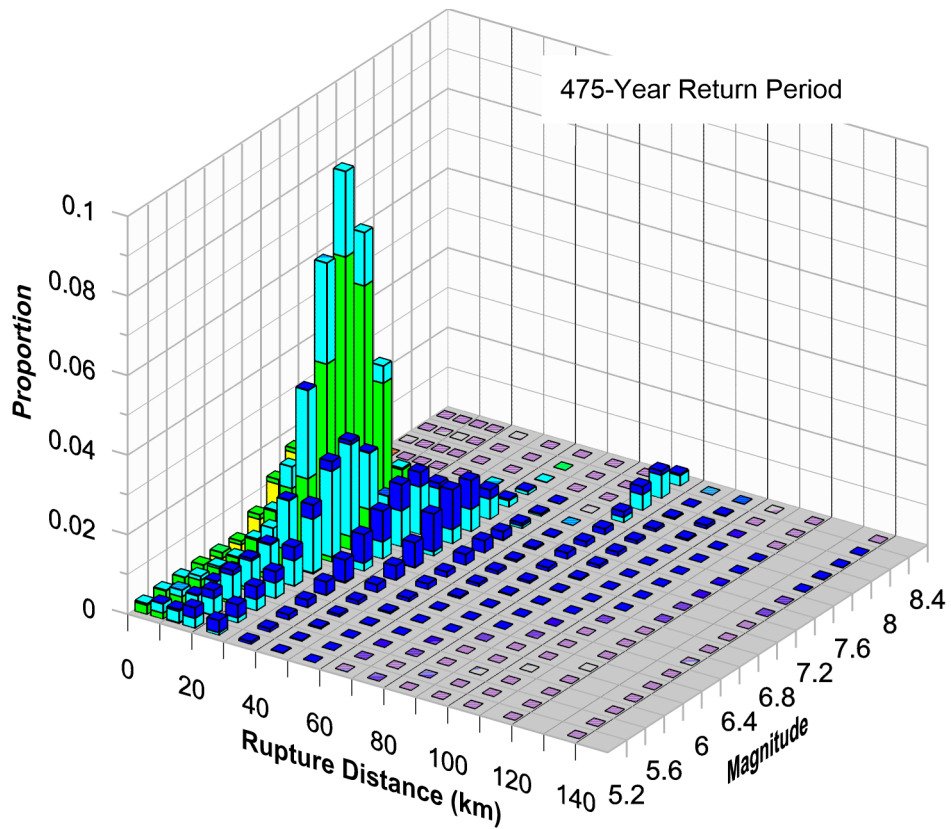
- Epsilon
- 2 to 3
 - 1 to 2
 - 0 to 1
 - 1 to 0
 - 2 to -1
 - < -2



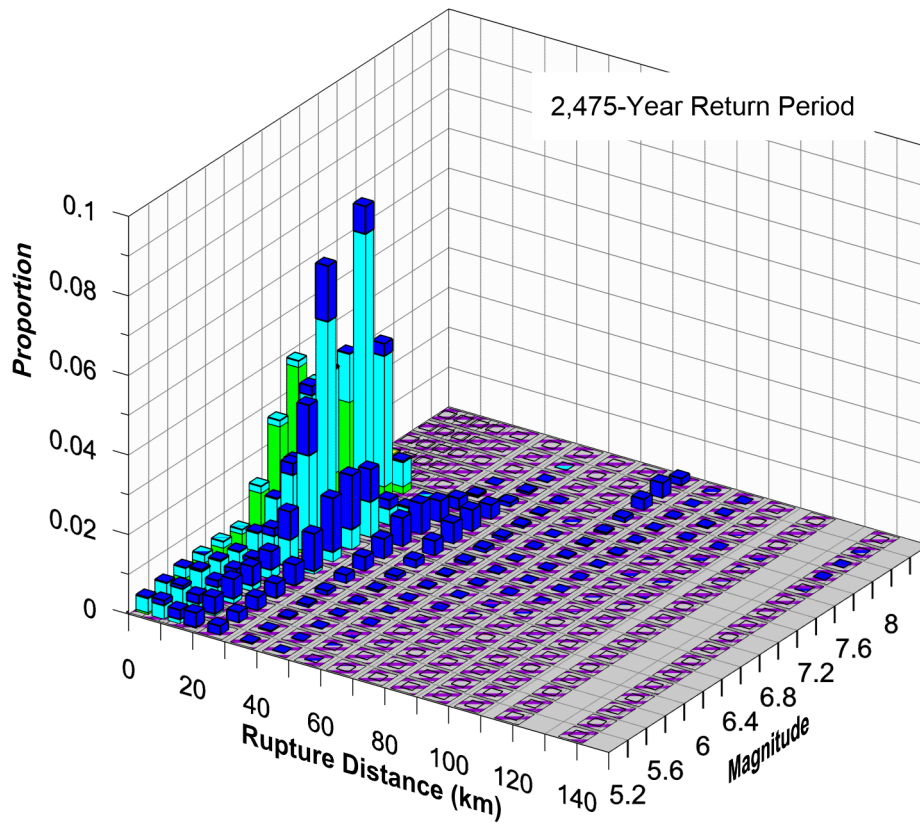


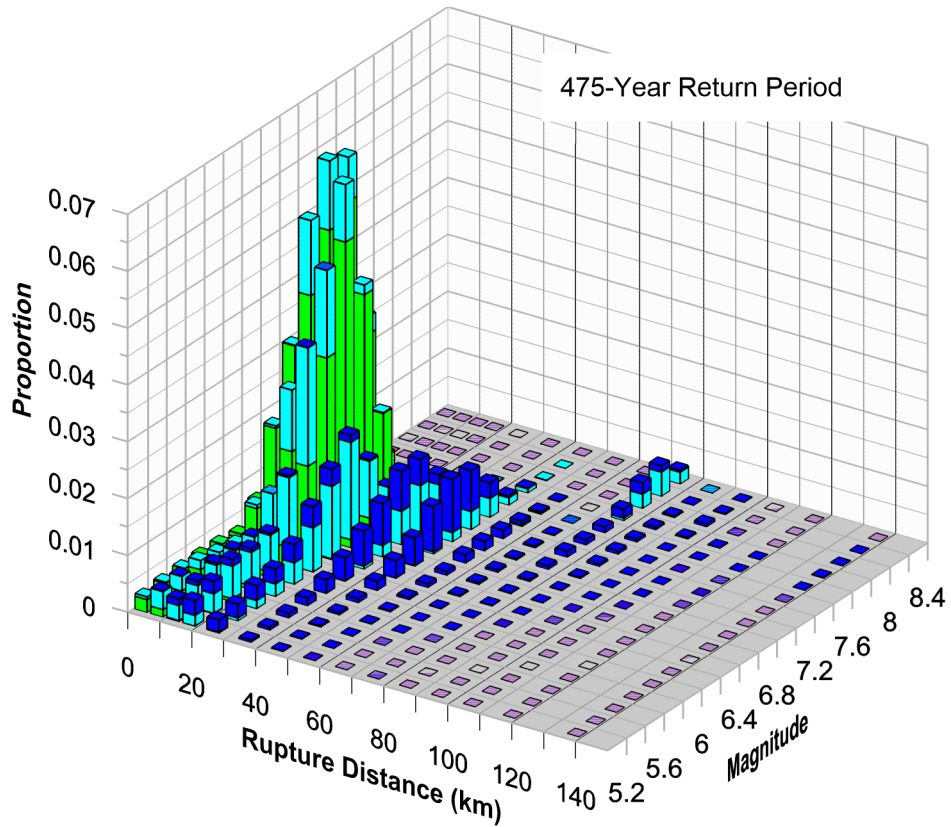
- Epsilon
- 2 to 3
 - 1 to 2
 - 0 to 1
 - 1 to 0
 - 2 to -1
 - < -2



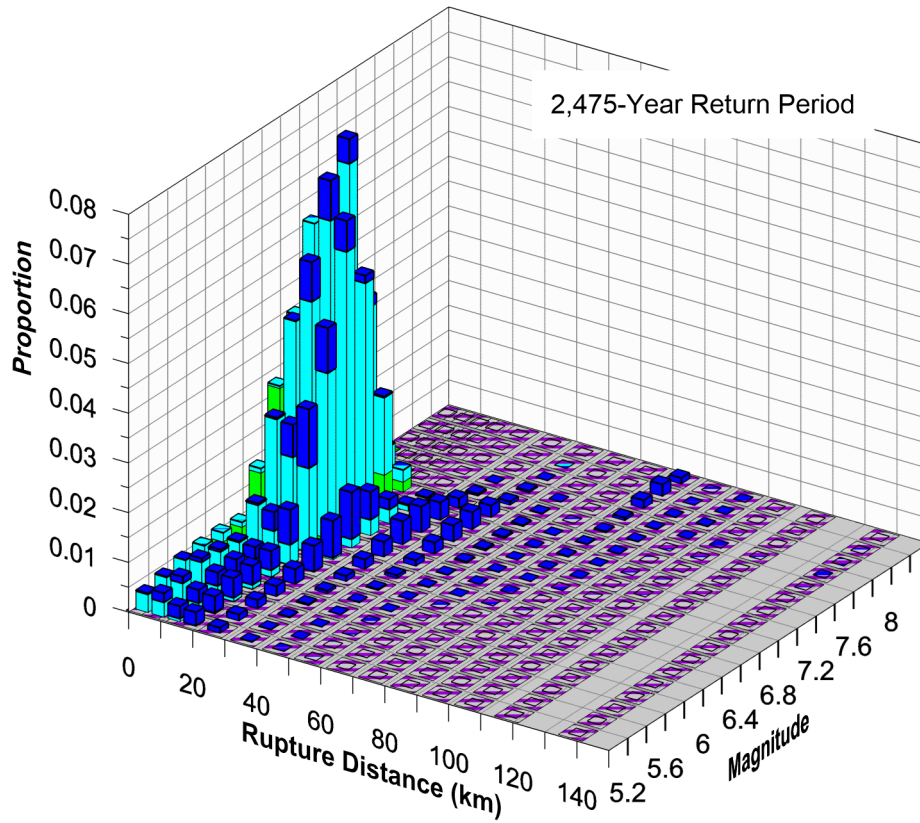


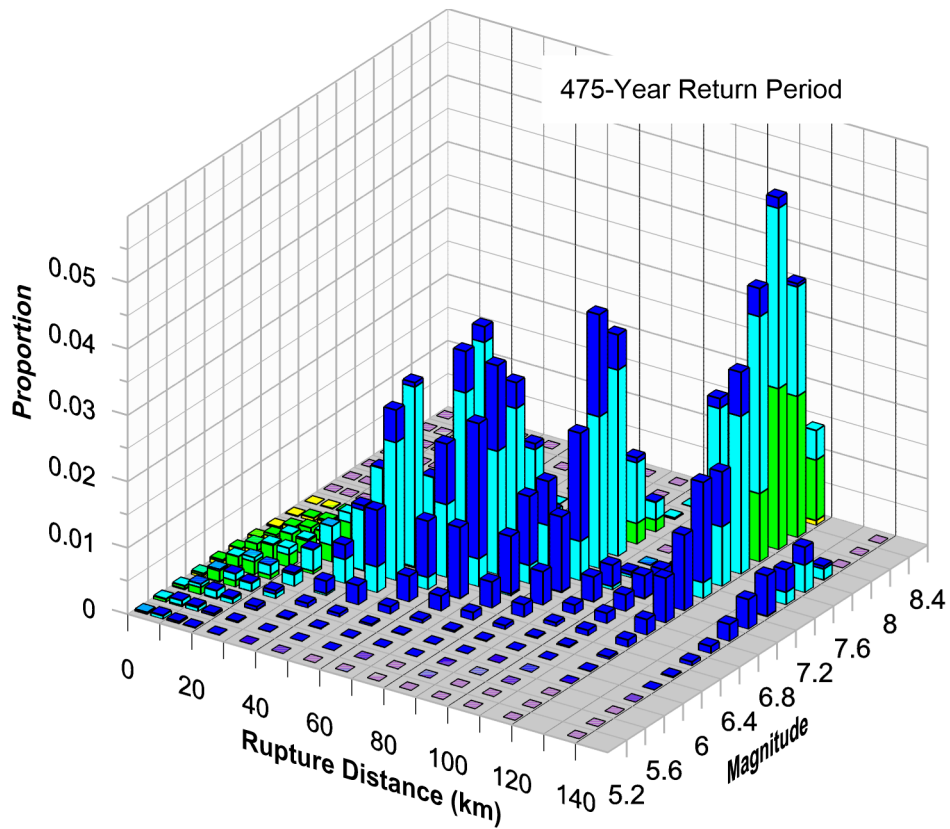
- Epsilon
- 2 to 3
 - 1 to 2
 - 0 to 1
 - 1 to 0
 - 2 to -1
 - < -2



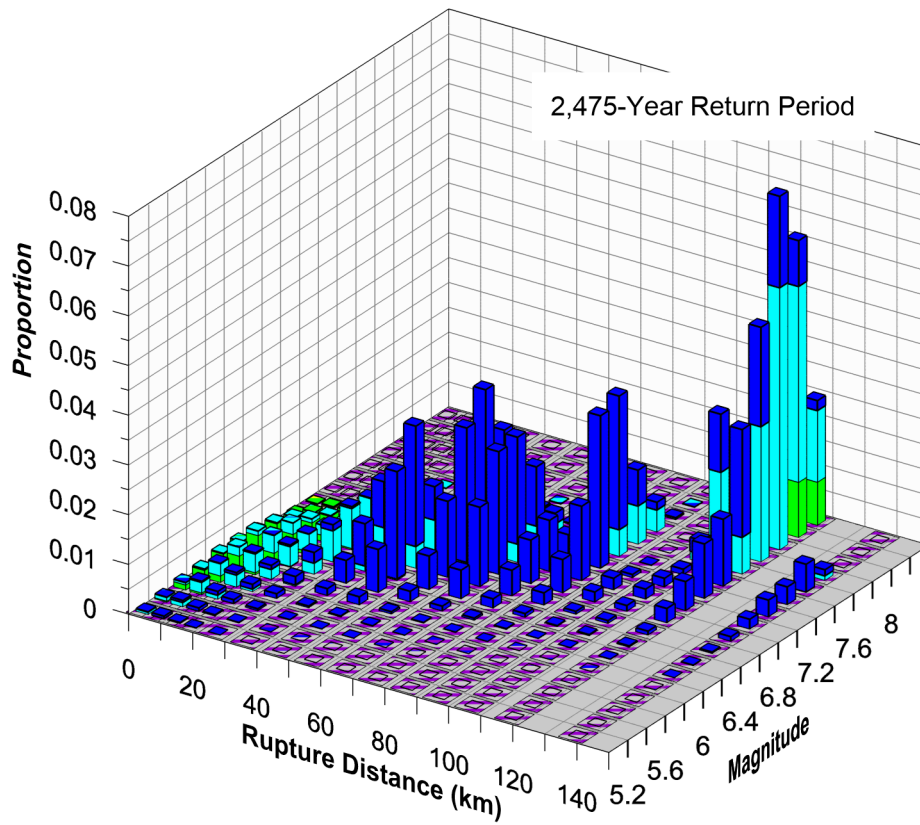


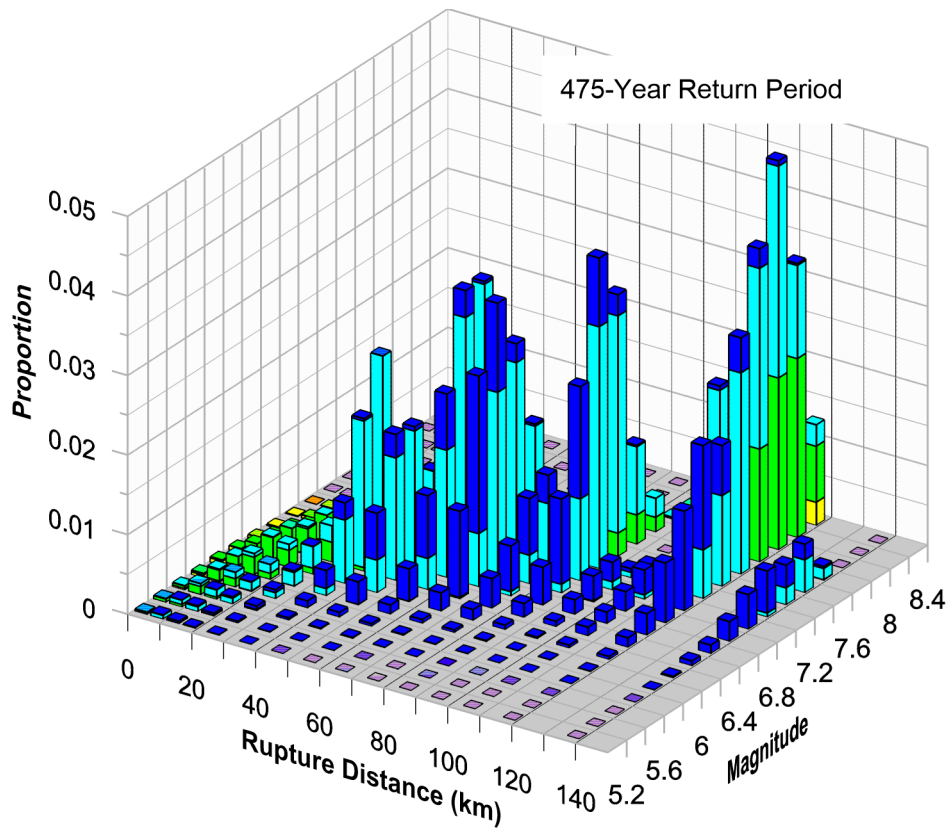
- Epsilon
- 2 to 3
 - 1 to 2
 - 0 to 1
 - 1 to 0
 - 2 to -1
 - < -2



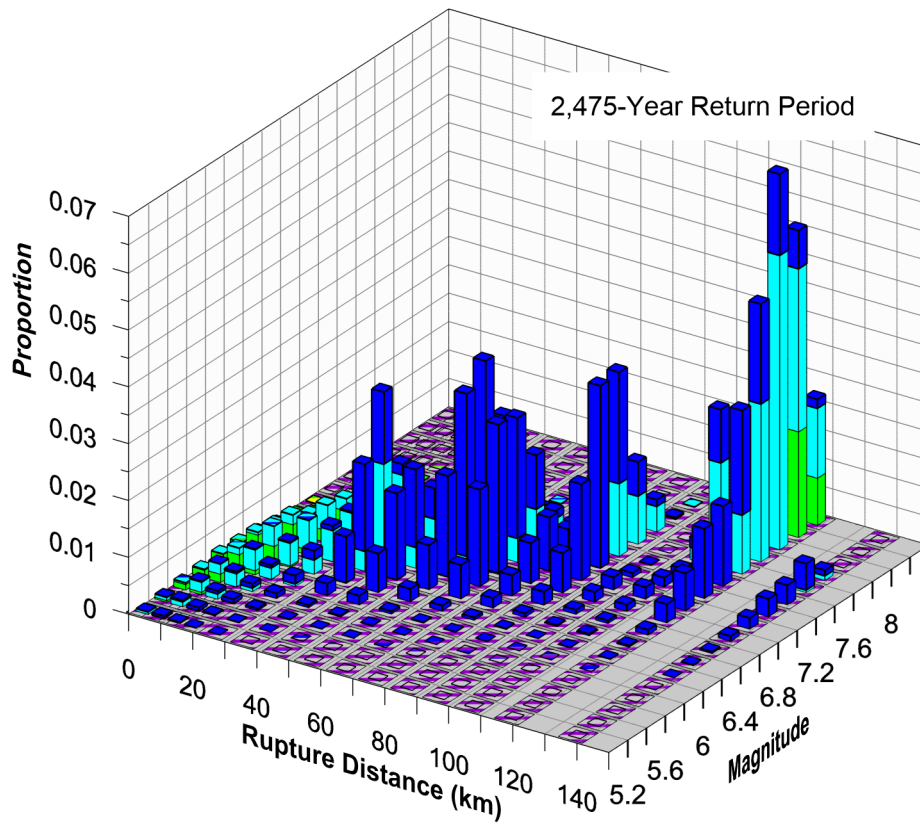


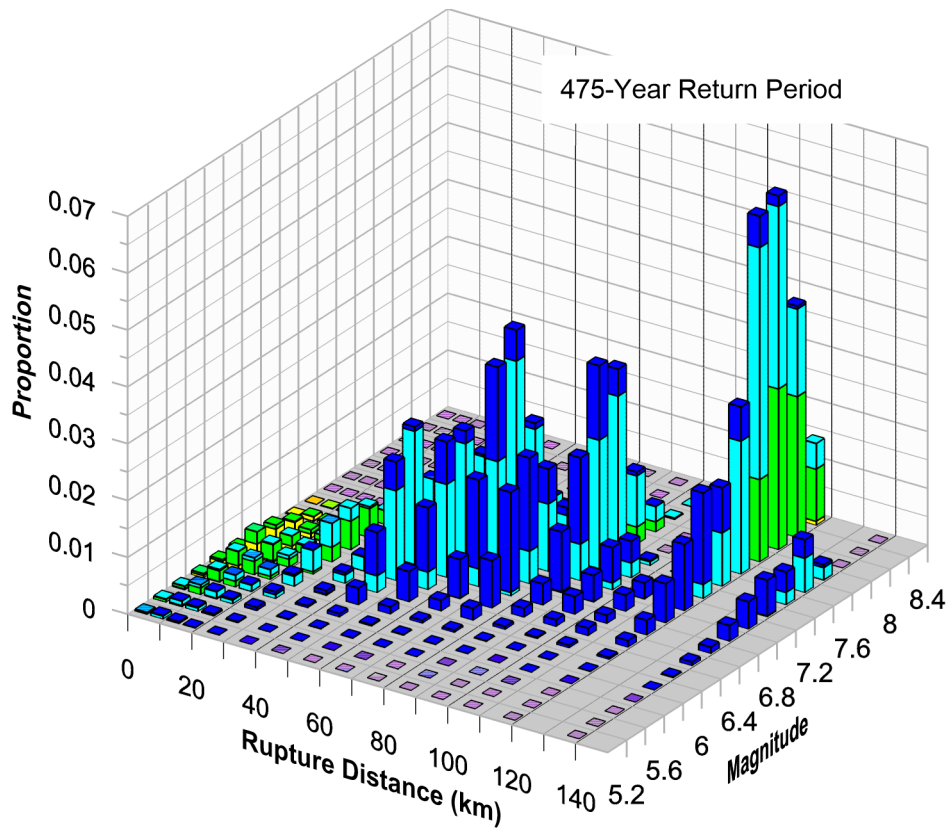
- Epsilon
- 2 to 3
 - 1 to 2
 - 0 to 1
 - 1 to 0
 - 2 to -1
 - < -2



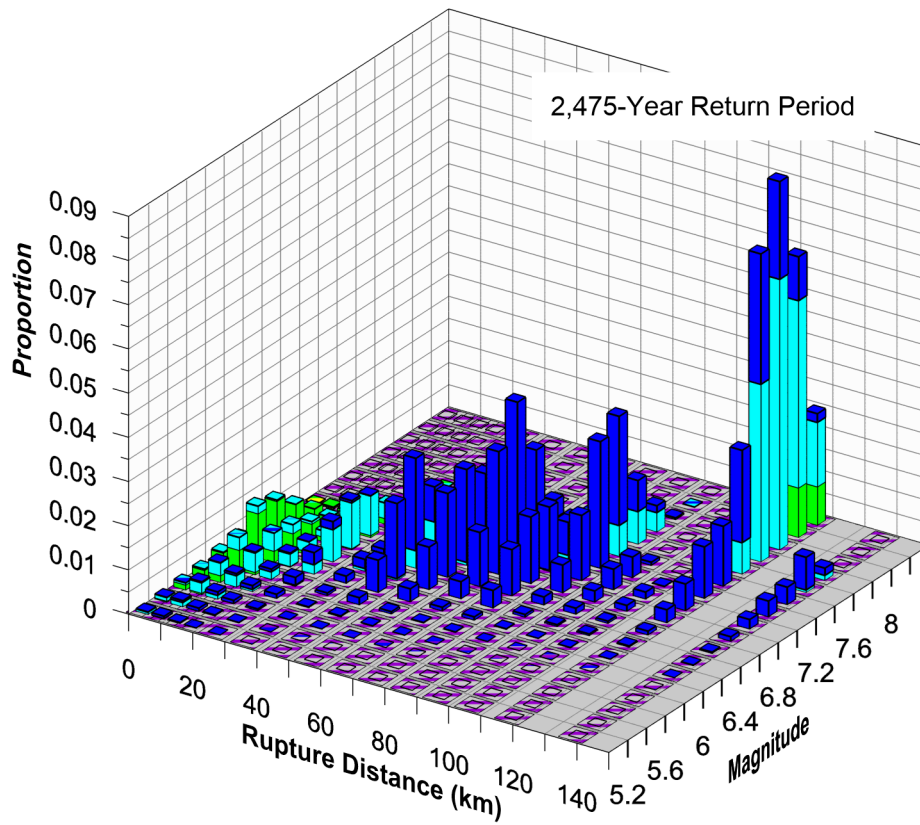


- Epsilon
- 2 to 3
 - 1 to 2
 - 0 to 1
 - -1 to 0
 - -2 to -1
 - < -2



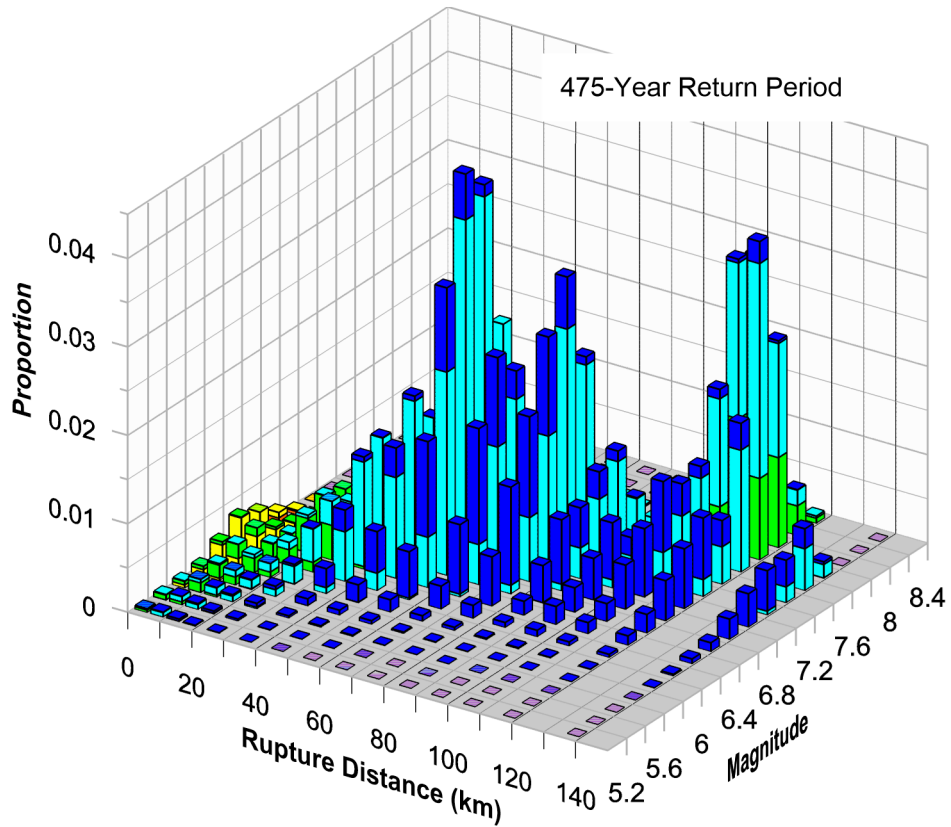


- Epsilon
- 2 to 3
 - 1 to 2
 - 0 to 1
 - 1 to 0
 - 2 to -1
 - < -2

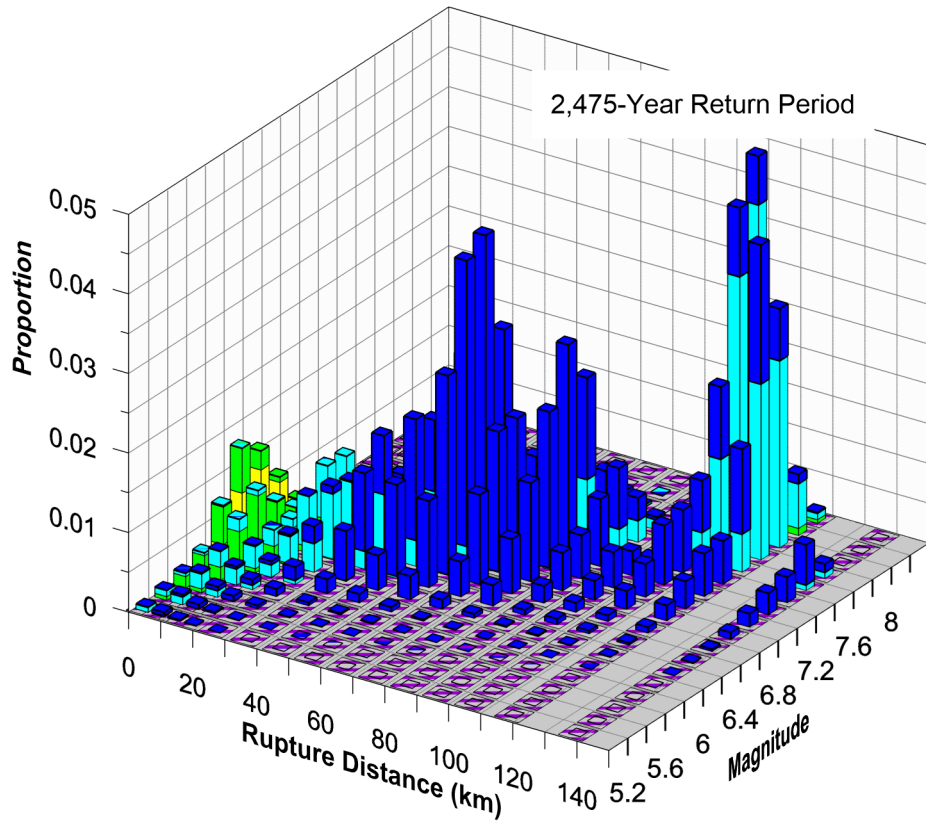


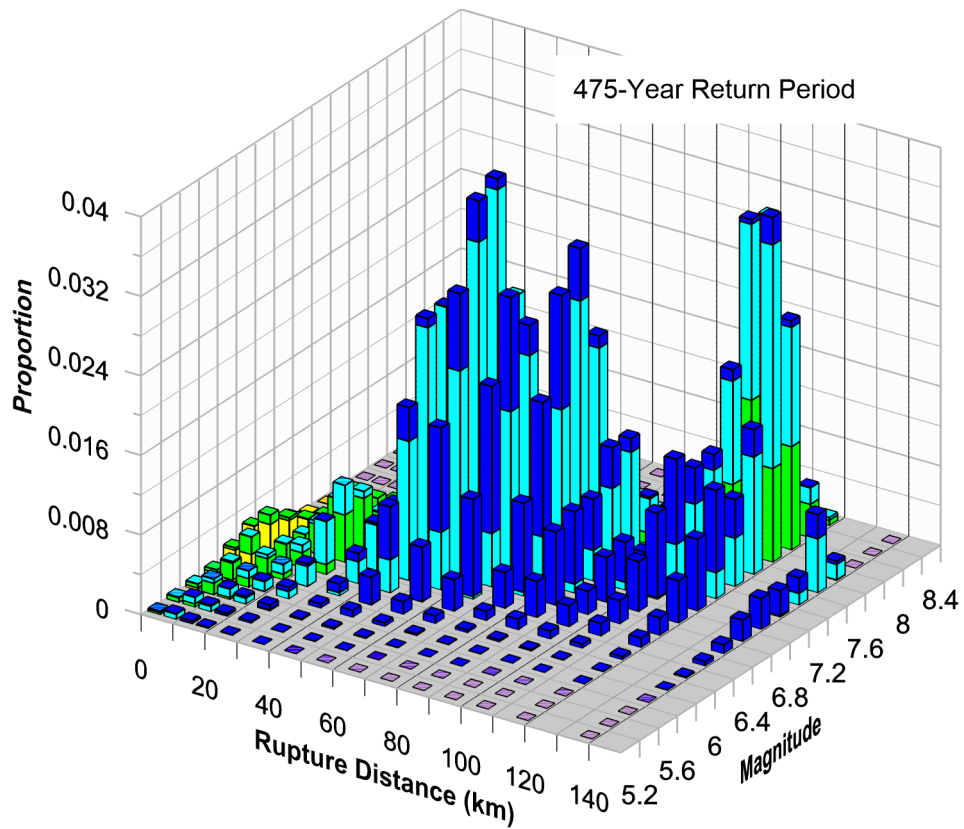
For Illustration
Purposes Only

Figure 90
Magnitude and Distance Contributions
to the Mean 1.0 Sec Spectral Hazard
at 475 and 2,475-Year Return Periods
for Twin Cities

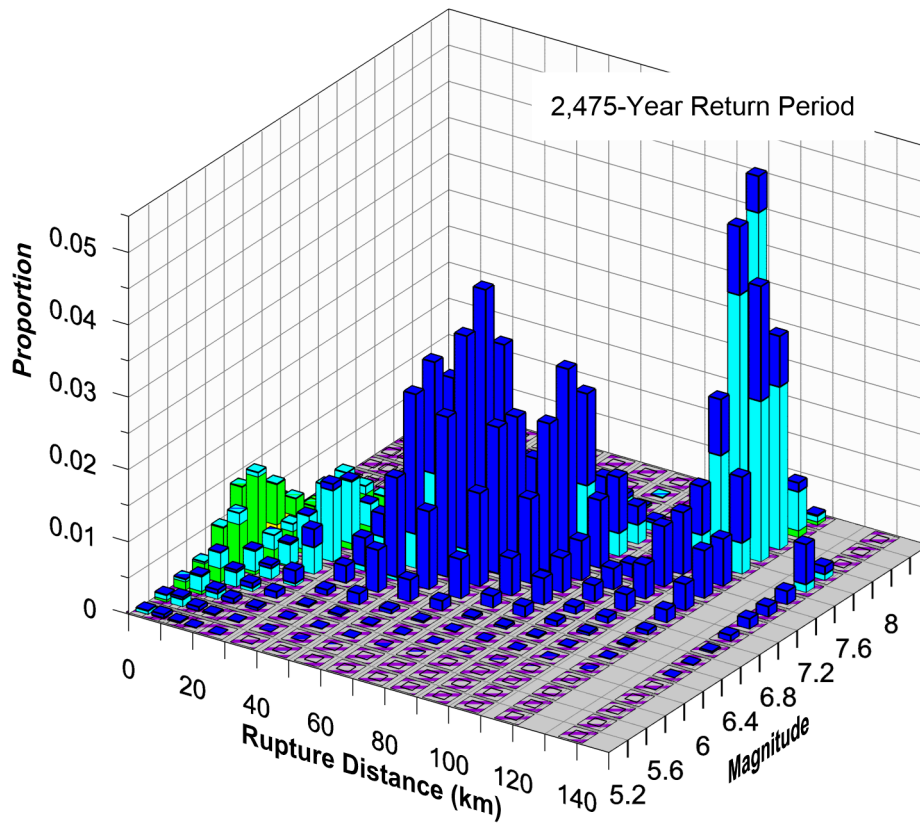


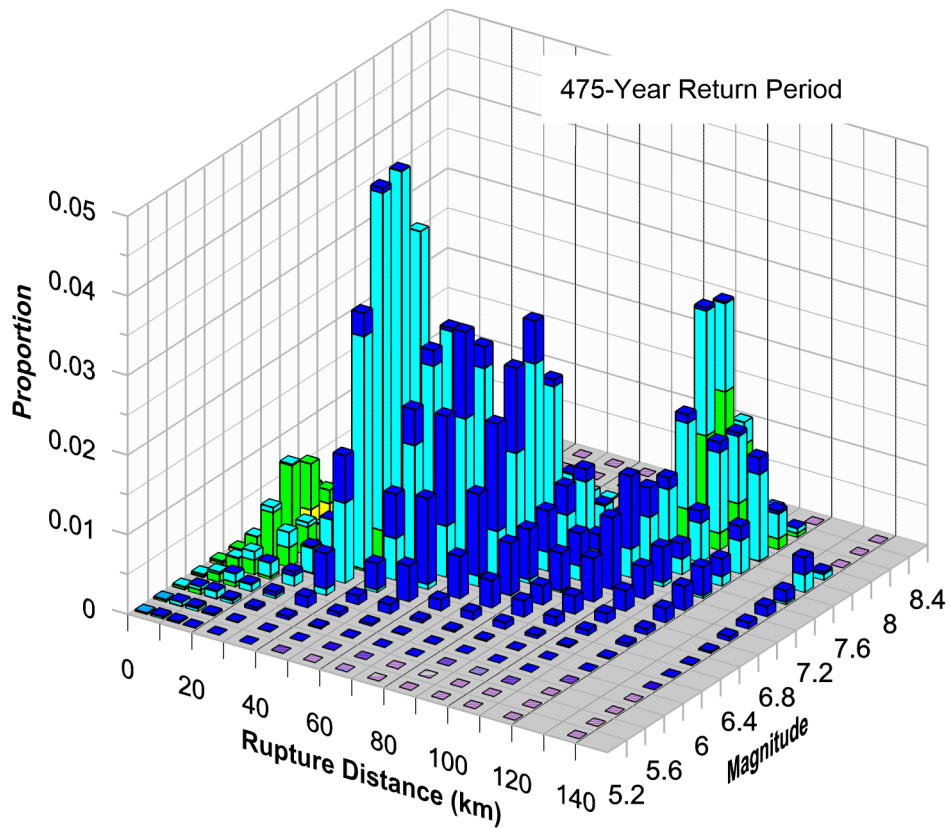
- Epsilon
- 2 to 3
 - 1 to 2
 - 0 to 1
 - 1 to 0
 - 2 to -1
 - < -2



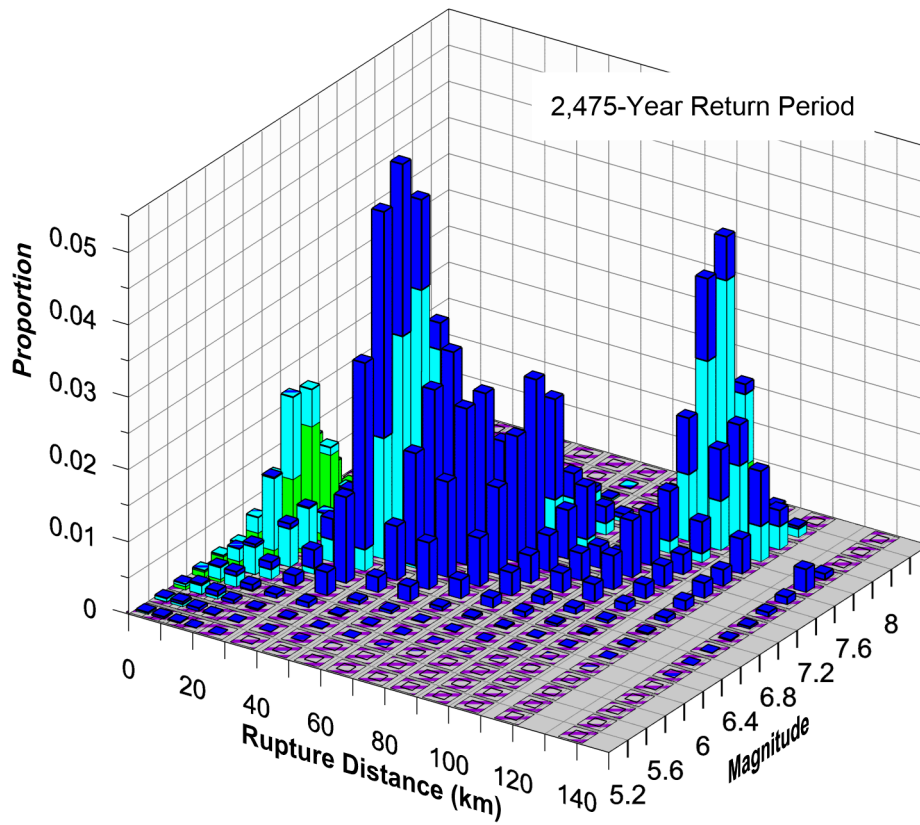


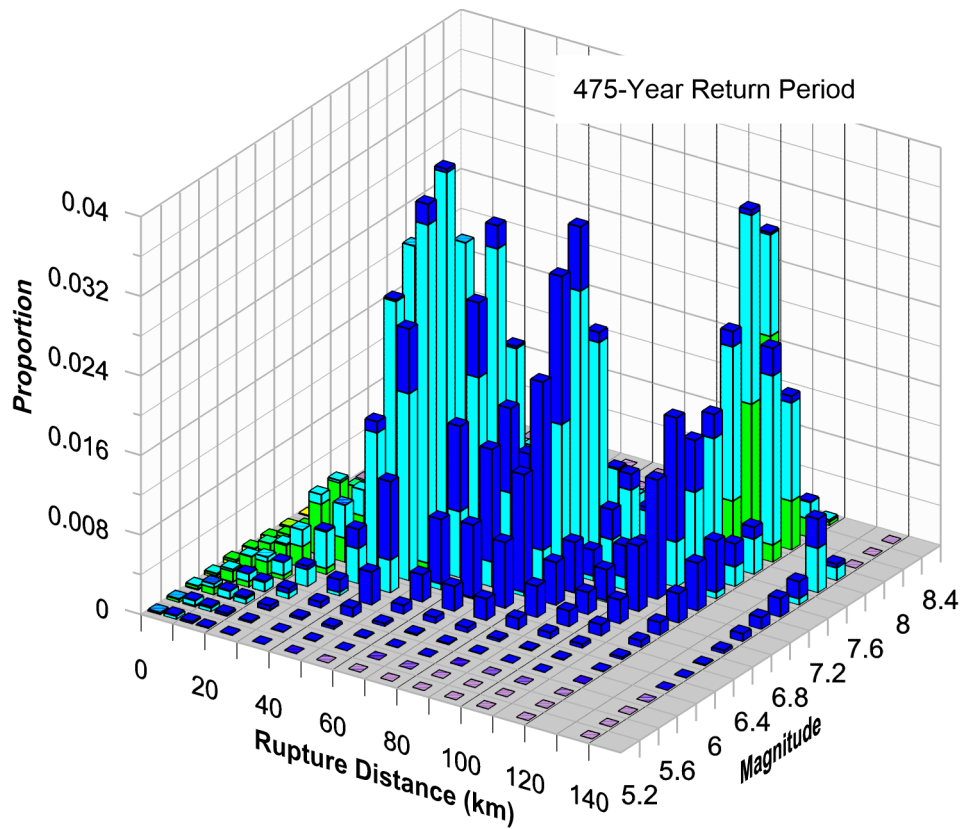
- Epsilon
- 2 to 3
 - 1 to 2
 - 0 to 1
 - 1 to 0
 - 2 to -1
 - < -2



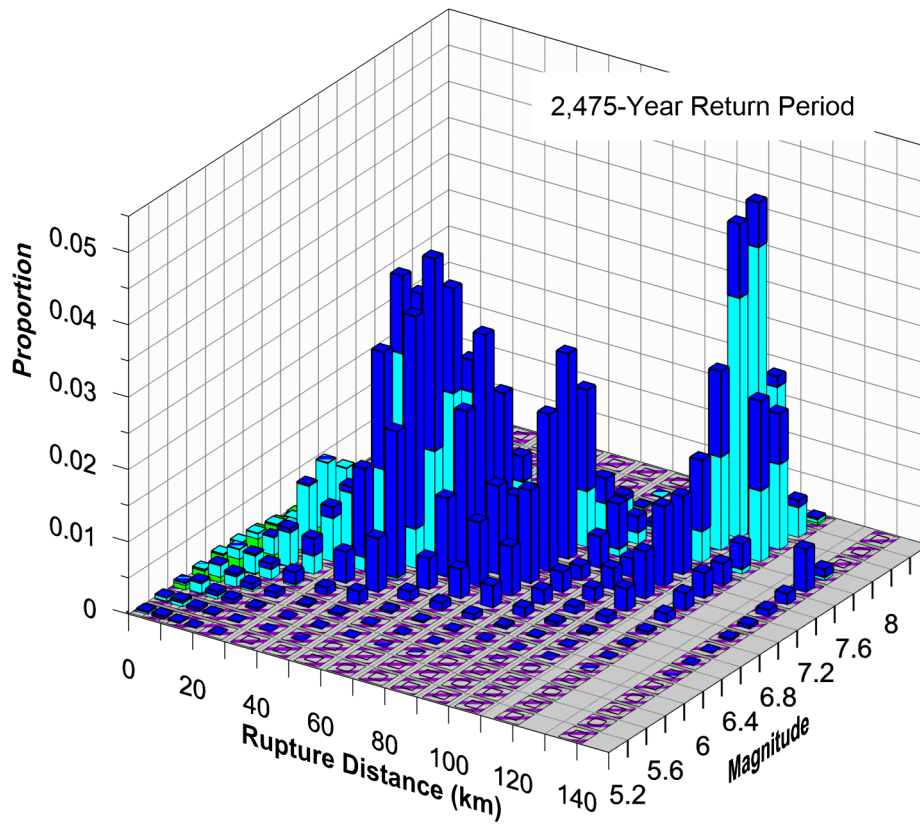


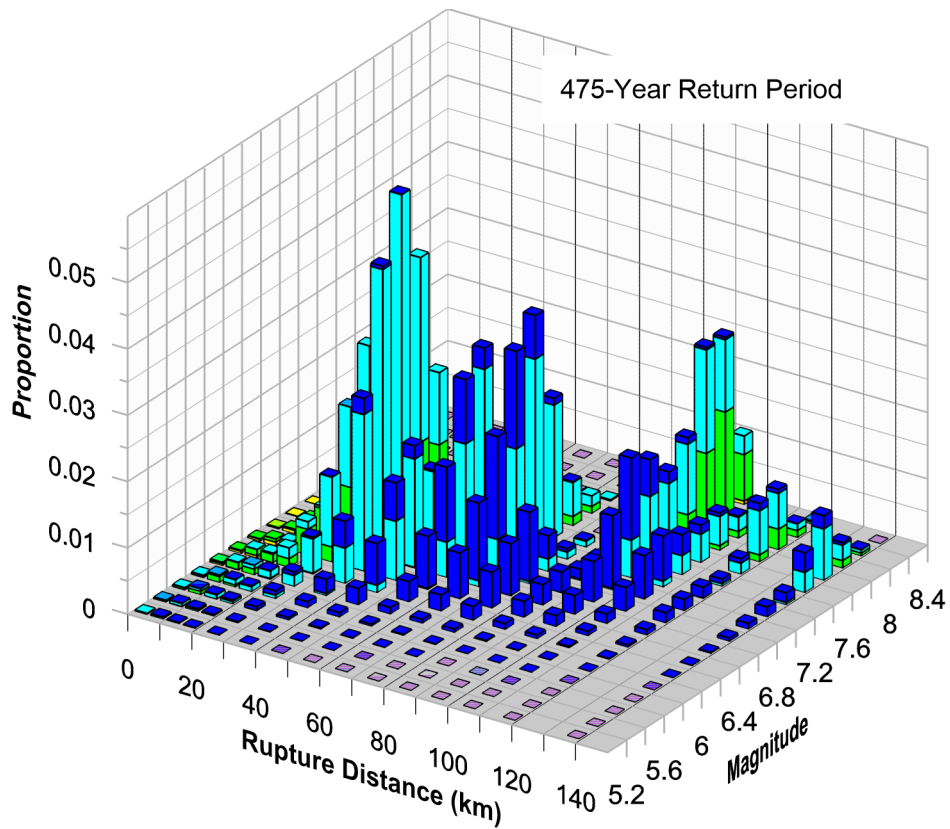
- Epsilon
- 2 to 3
 - 1 to 2
 - 0 to 1
 - 1 to 0
 - 2 to -1
 - < -2



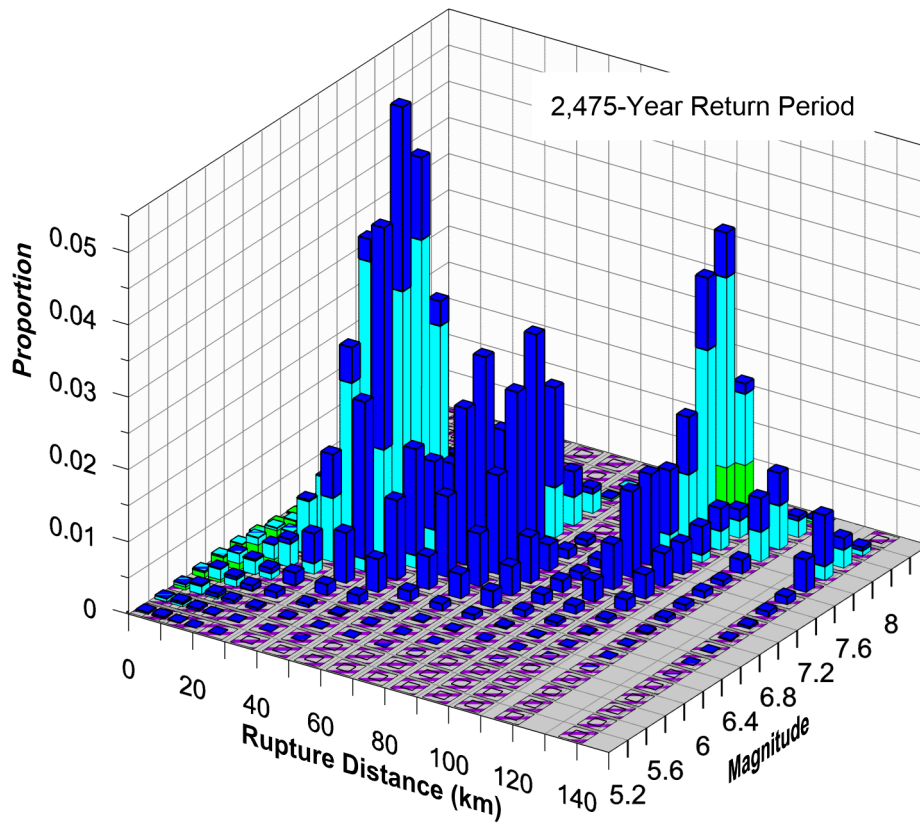


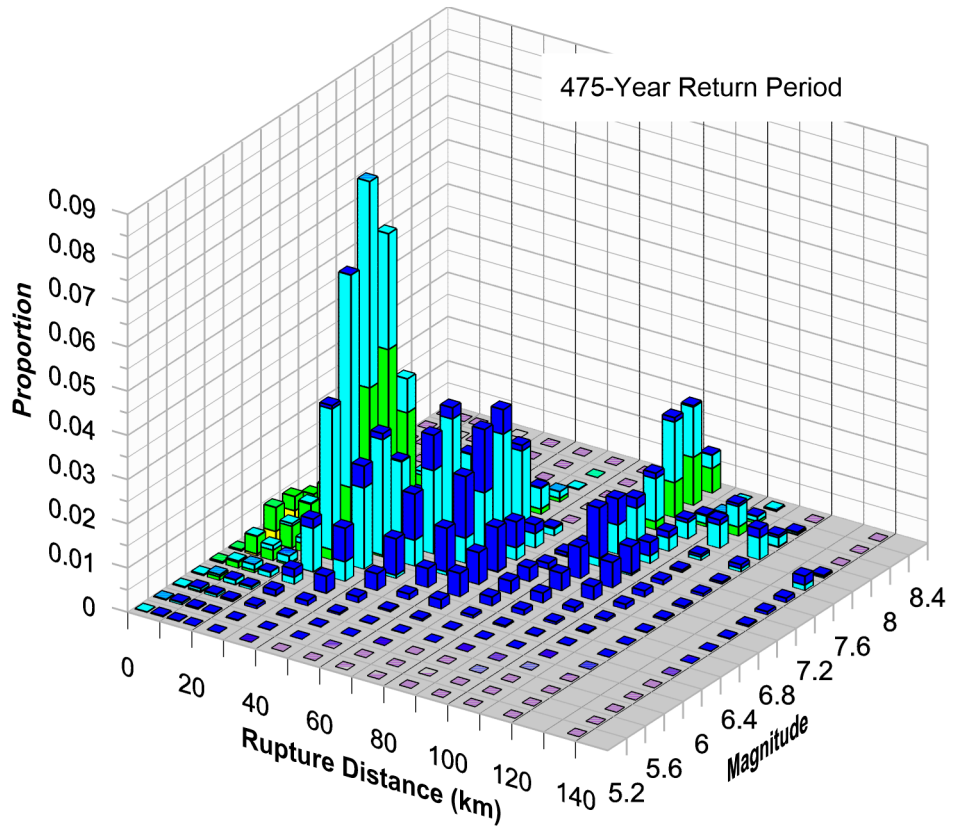
- Epsilon
- 2 to 3
 - 1 to 2
 - 0 to 1
 - 1 to 0
 - 2 to -1
 - < -2



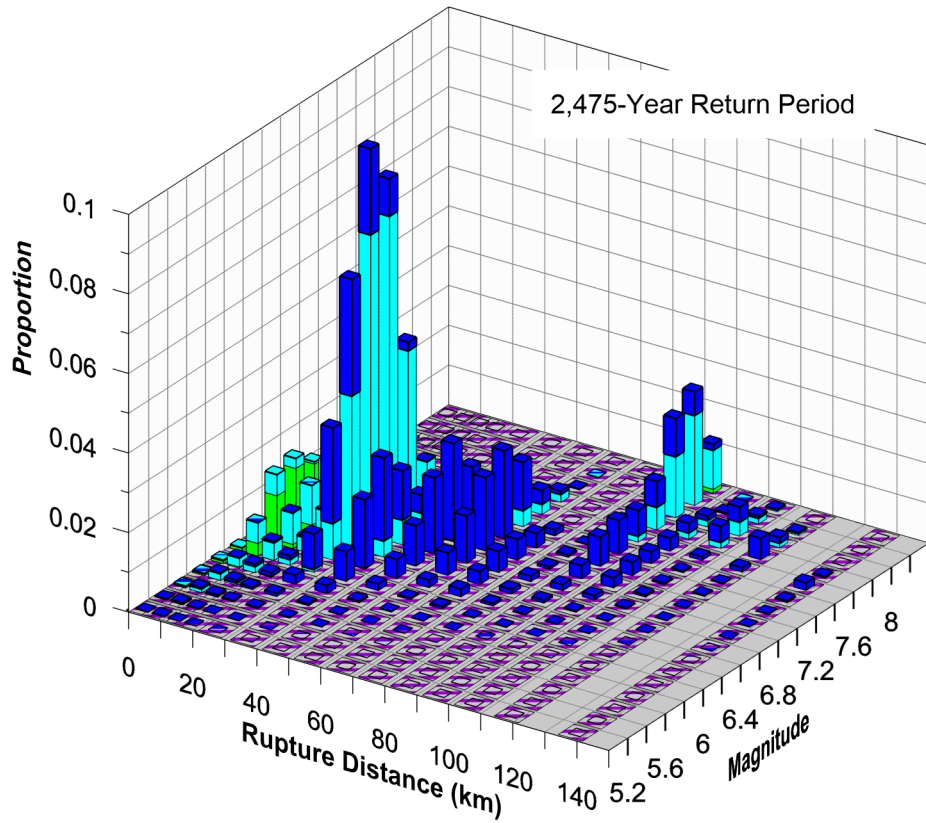


- Epsilon
- 2 to 3
 - 1 to 2
 - 0 to 1
 - -1 to 0
 - -2 to -1
 - < -2



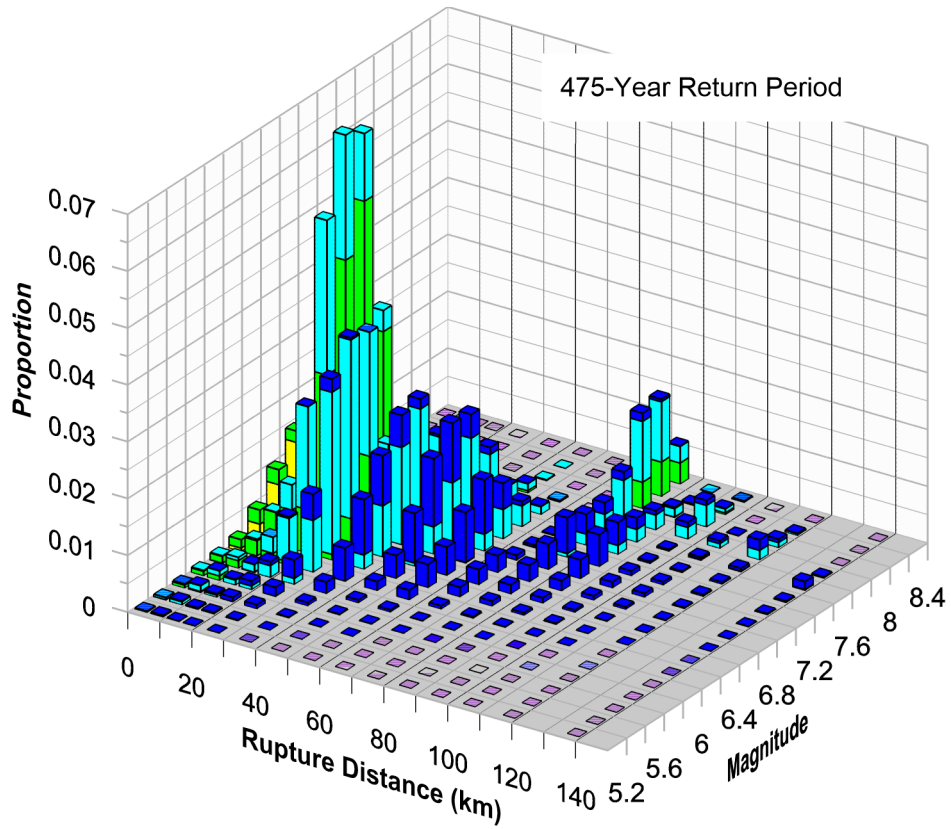


- Epsilon
- 2 to 3
 - 1 to 2
 - 0 to 1
 - -1 to 0
 - -2 to -1
 - < -2

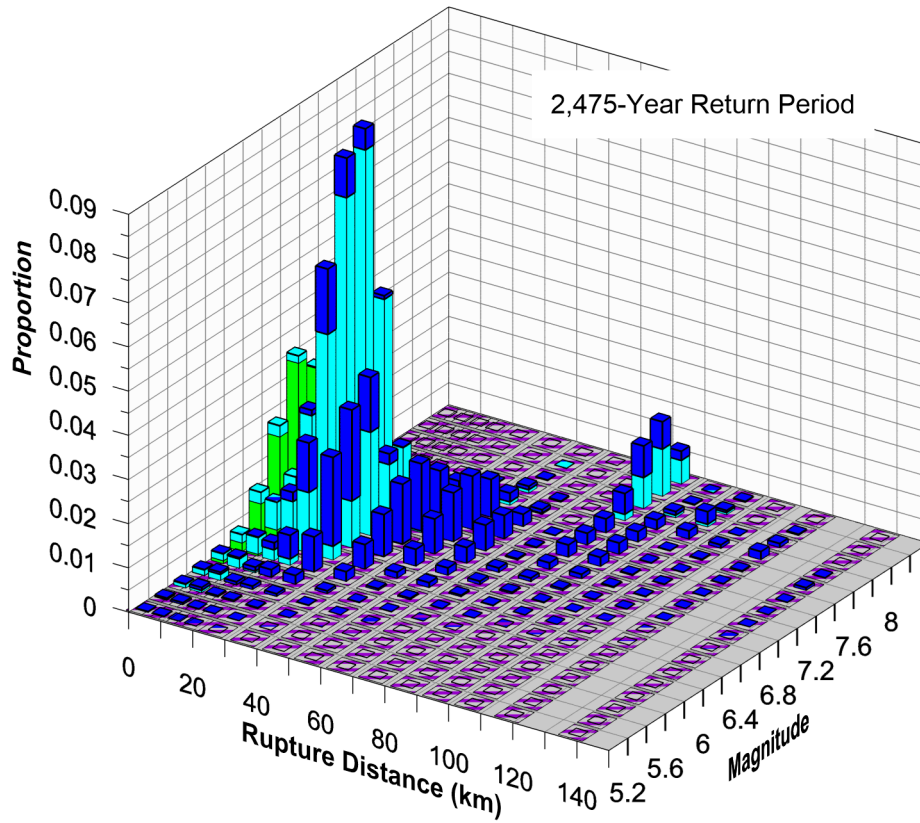


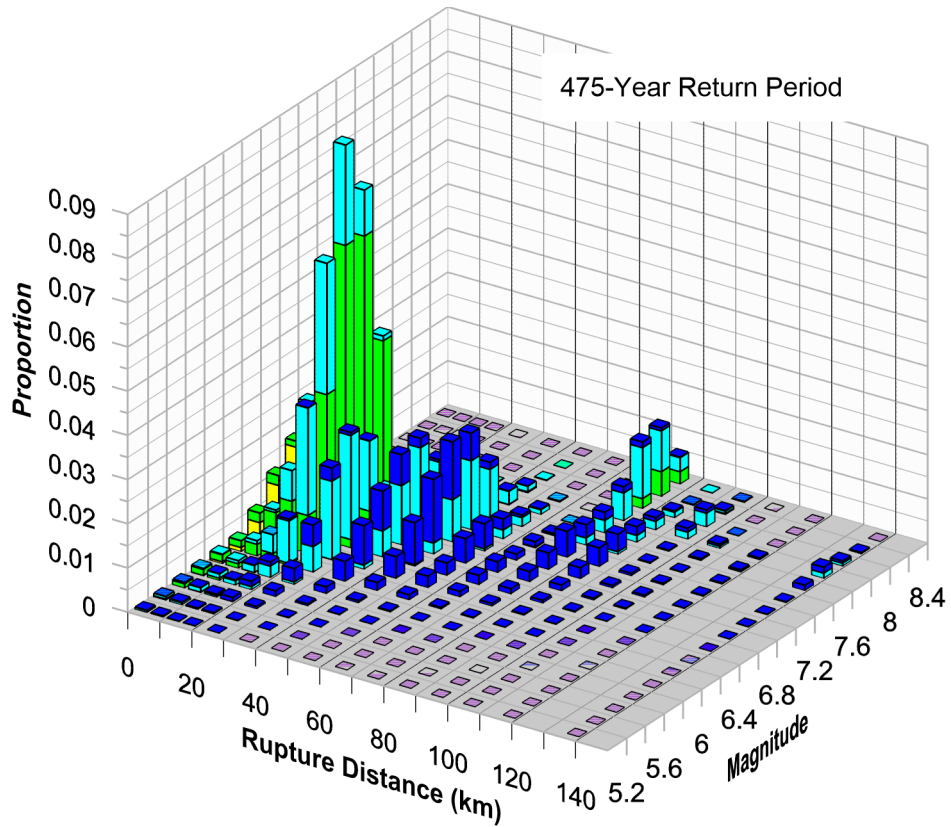
For Illustration
Purposes Only

Figure 96
Magnitude and Distance Contributions
to the Mean 1.0 Sec Spectral Hazard
at 475 and 2,475-Year Return Periods
for Bacon

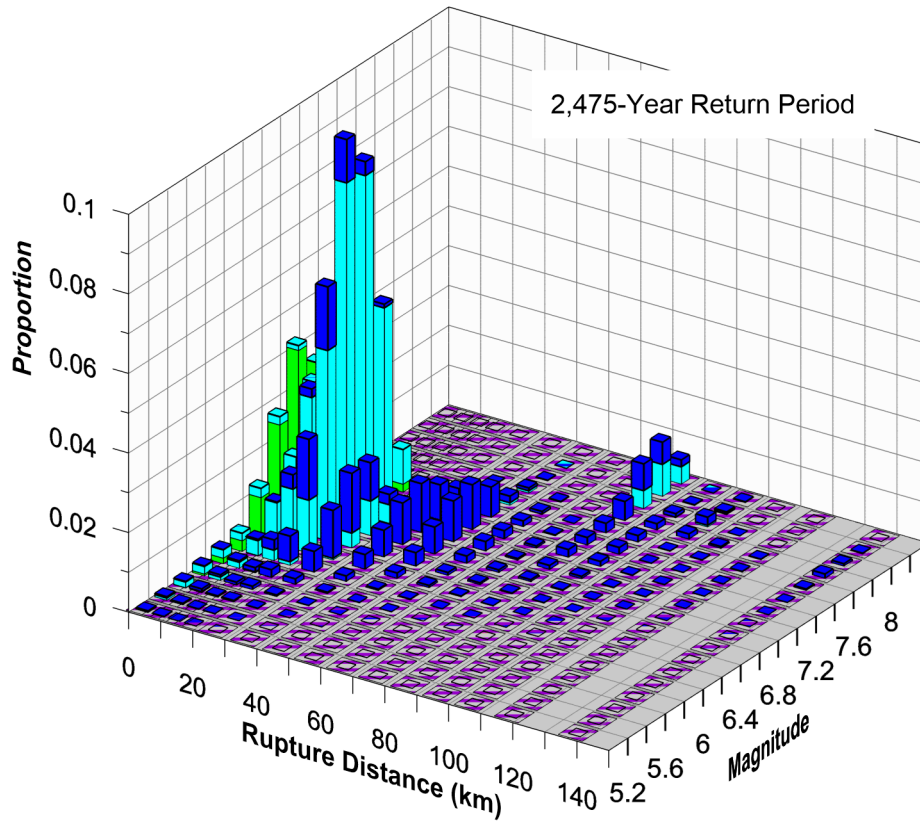


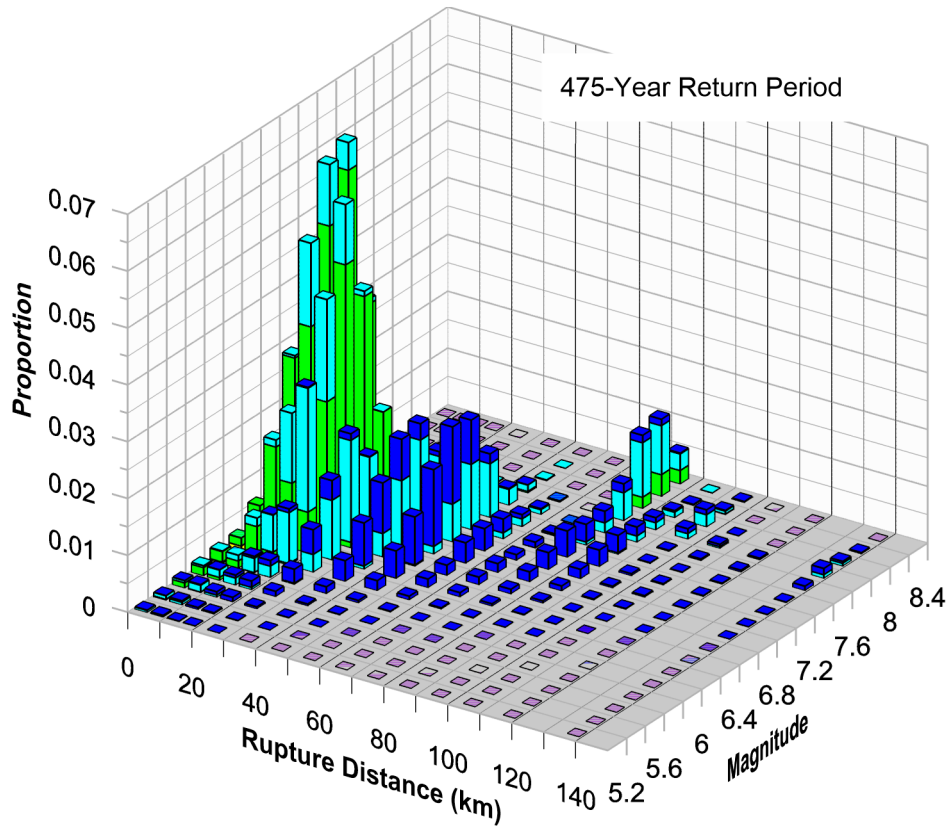
- Epsilon
- 2 to 3
 - 1 to 2
 - 0 to 1
 - 1 to 0
 - 2 to -1
 - < -2



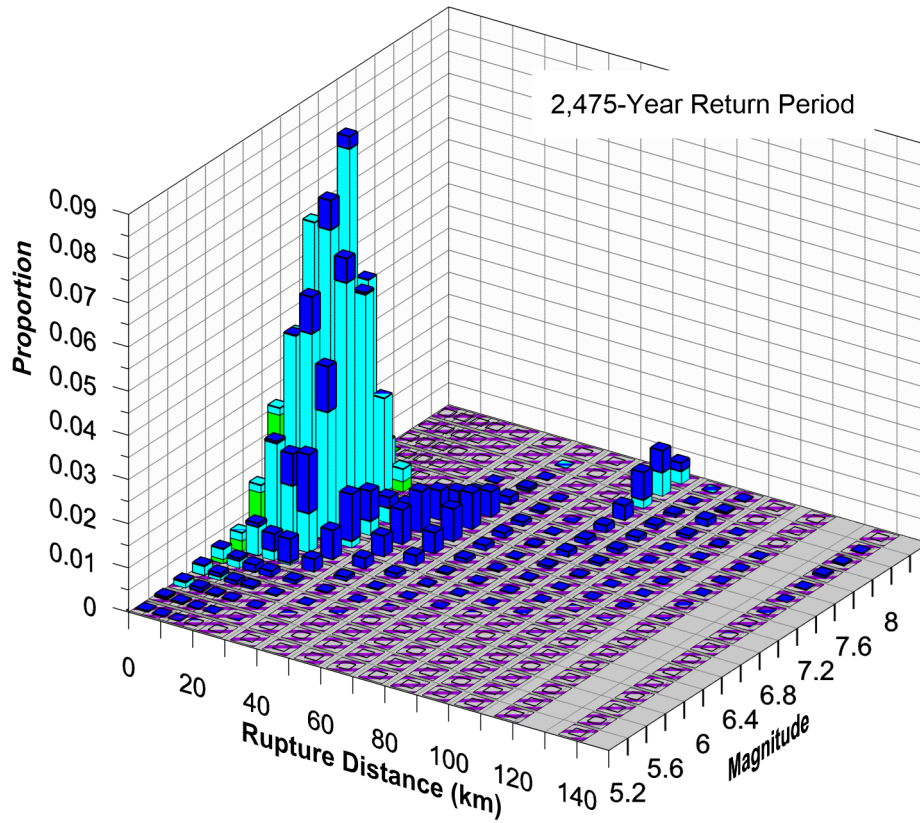


- Epsilon
- 2 to 3
 - 1 to 2
 - 0 to 1
 - 1 to 0
 - 2 to -1
 - < -2



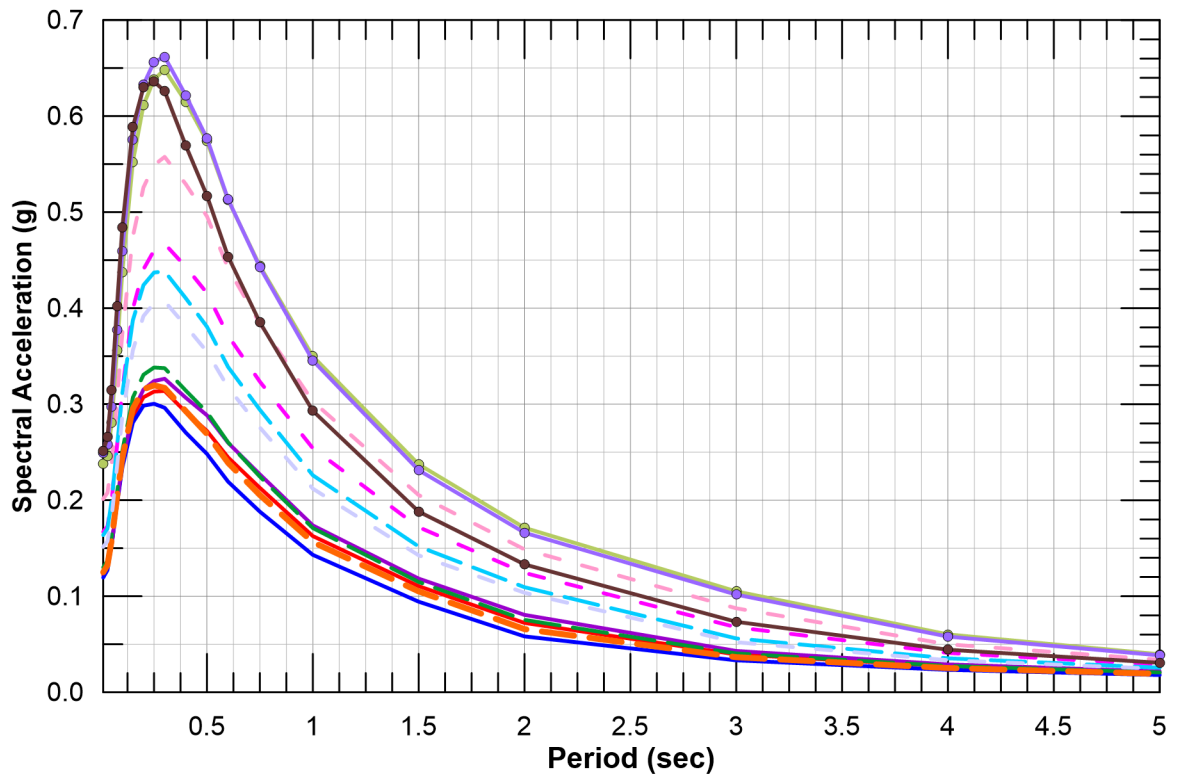
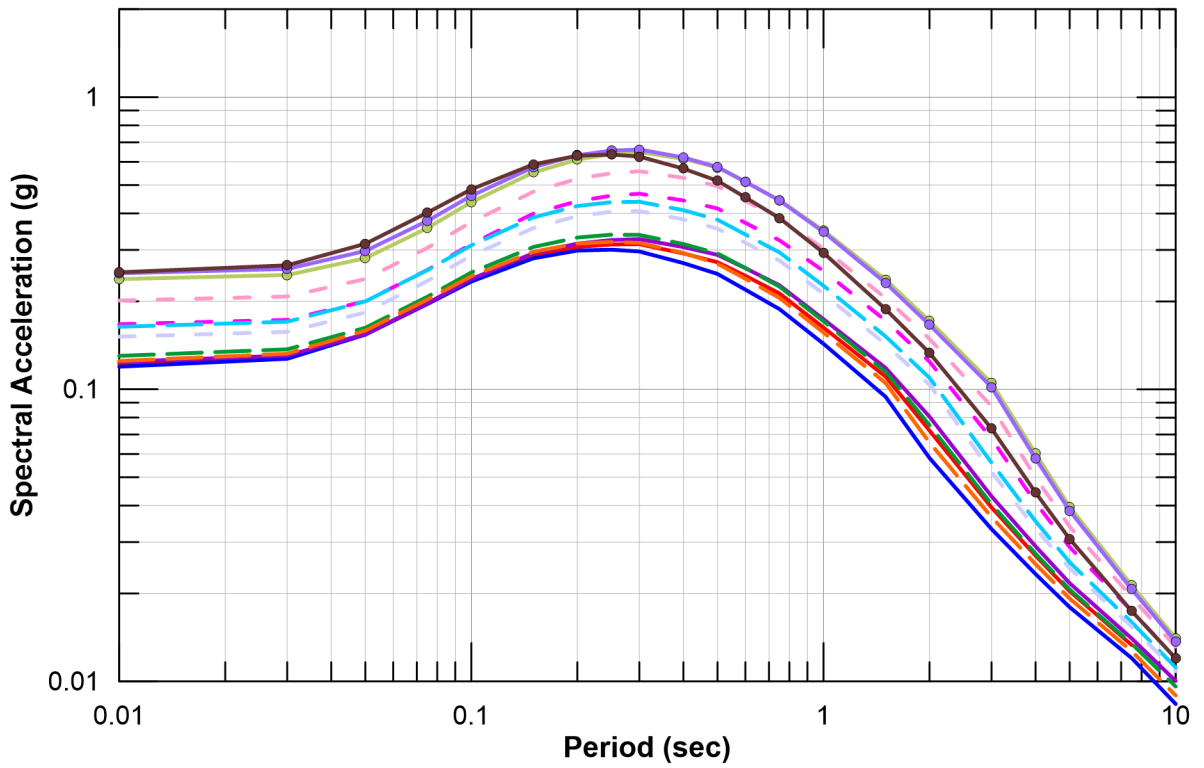


- Epsilon
- 2 to 3
 - 1 to 2
 - 0 to 1
 - 1 to 0
 - 2 to -1
 - < -2

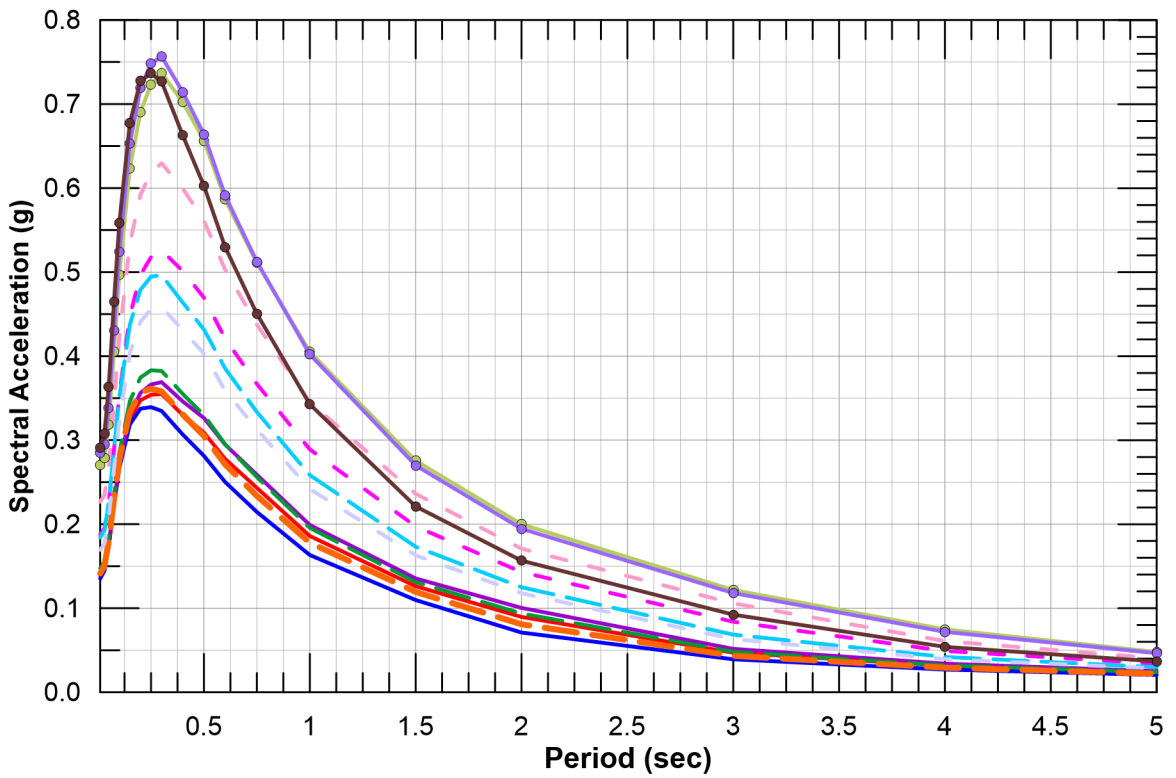
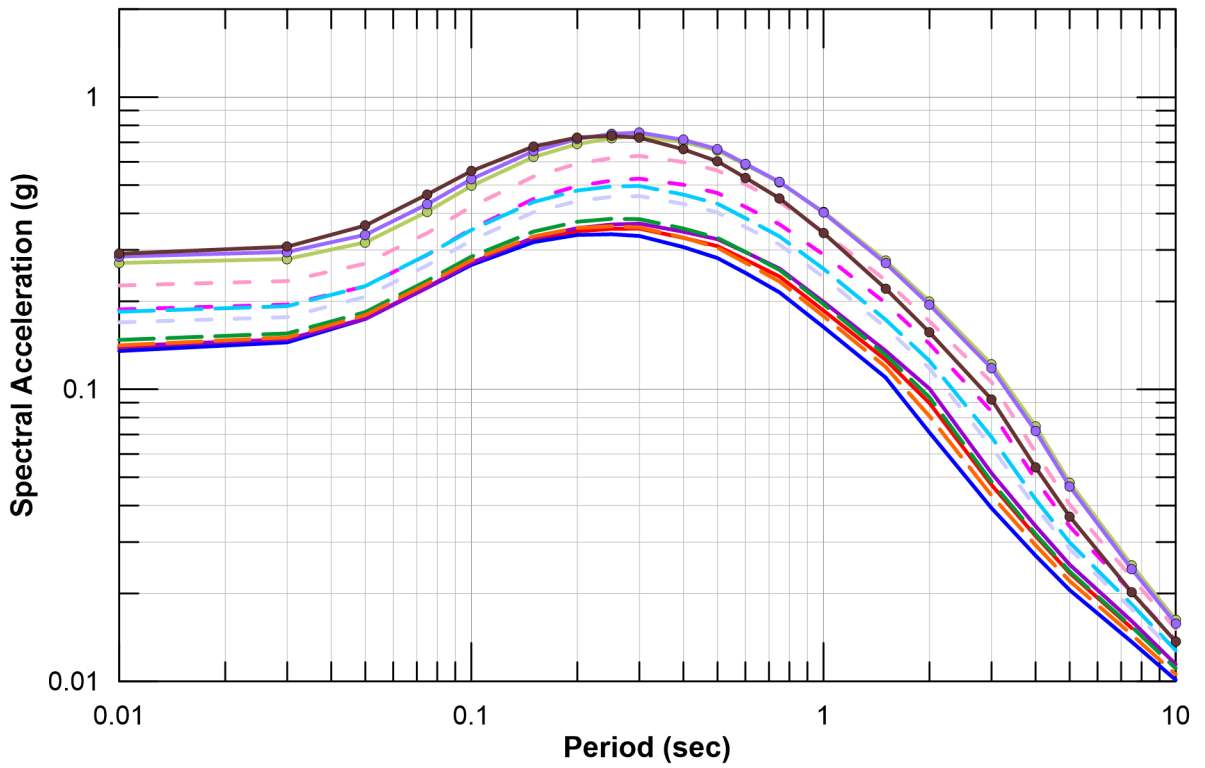


For Illustration
Purposes Only

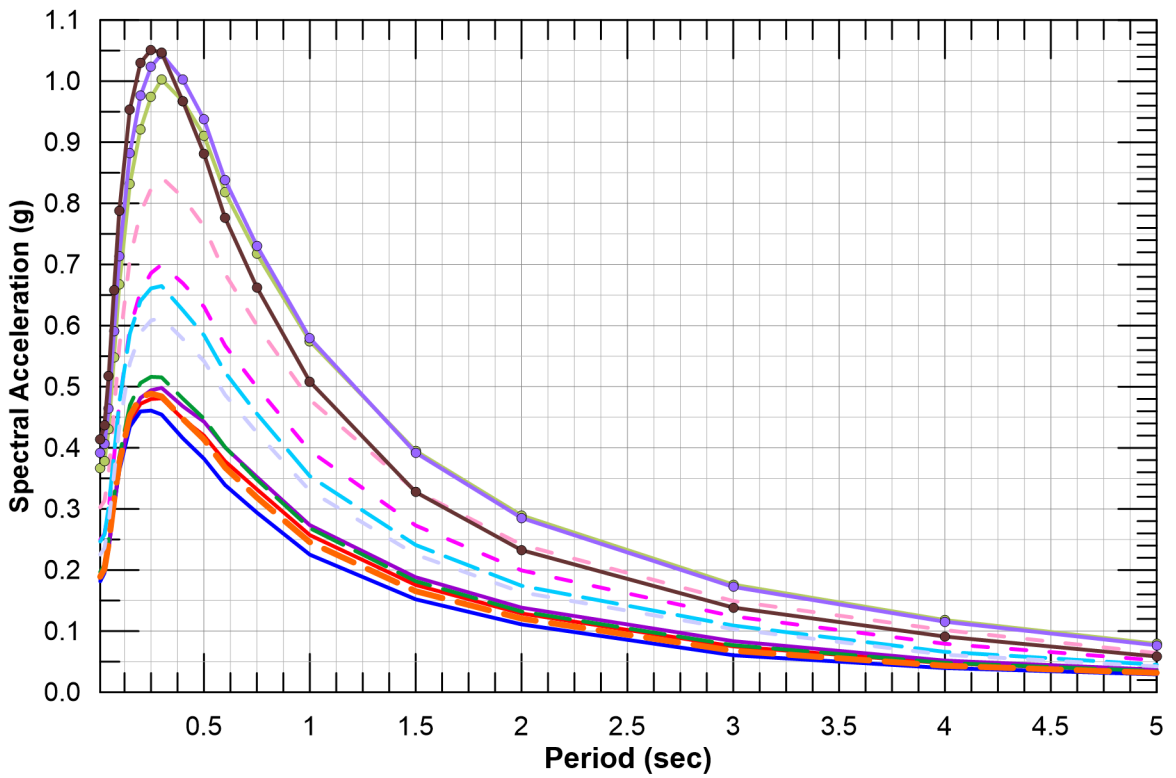
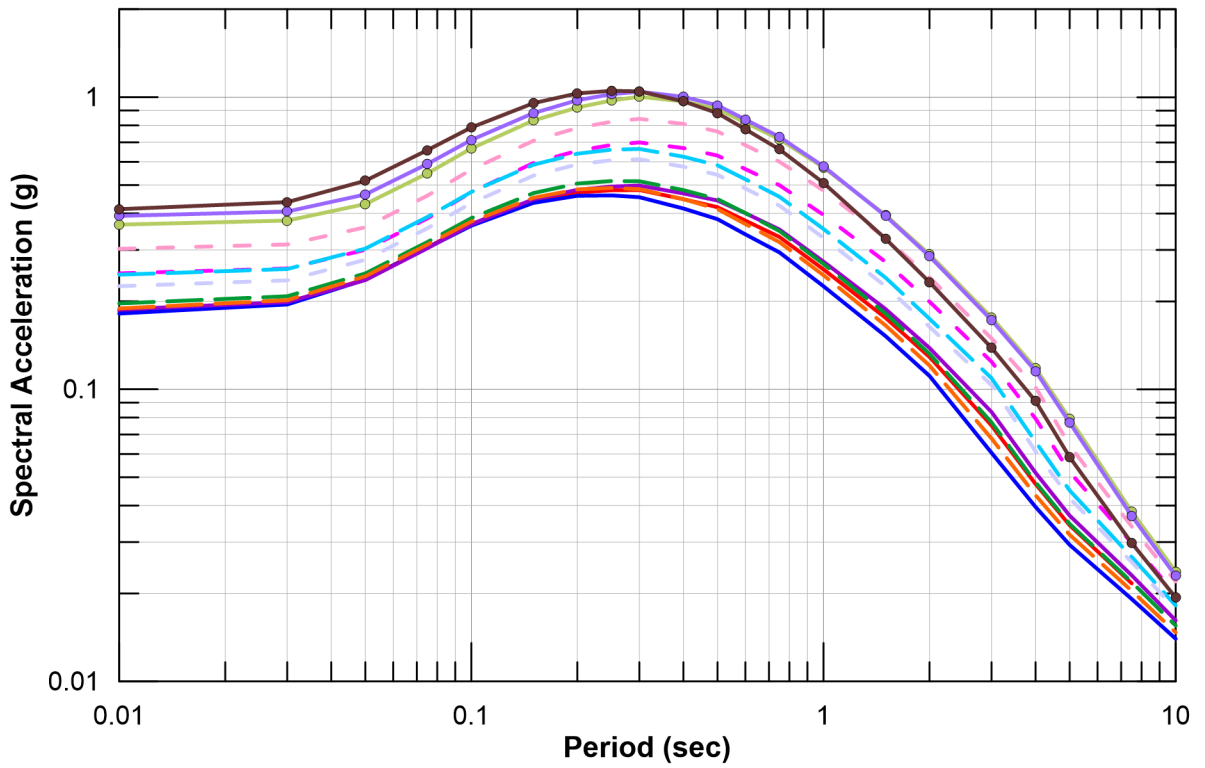
Figure 99
Magnitude and Distance Contributions
to the Mean 1.0 Sec Spectral Hazard
at 475 and 2,475-Year Return Periods
for Jones Connection



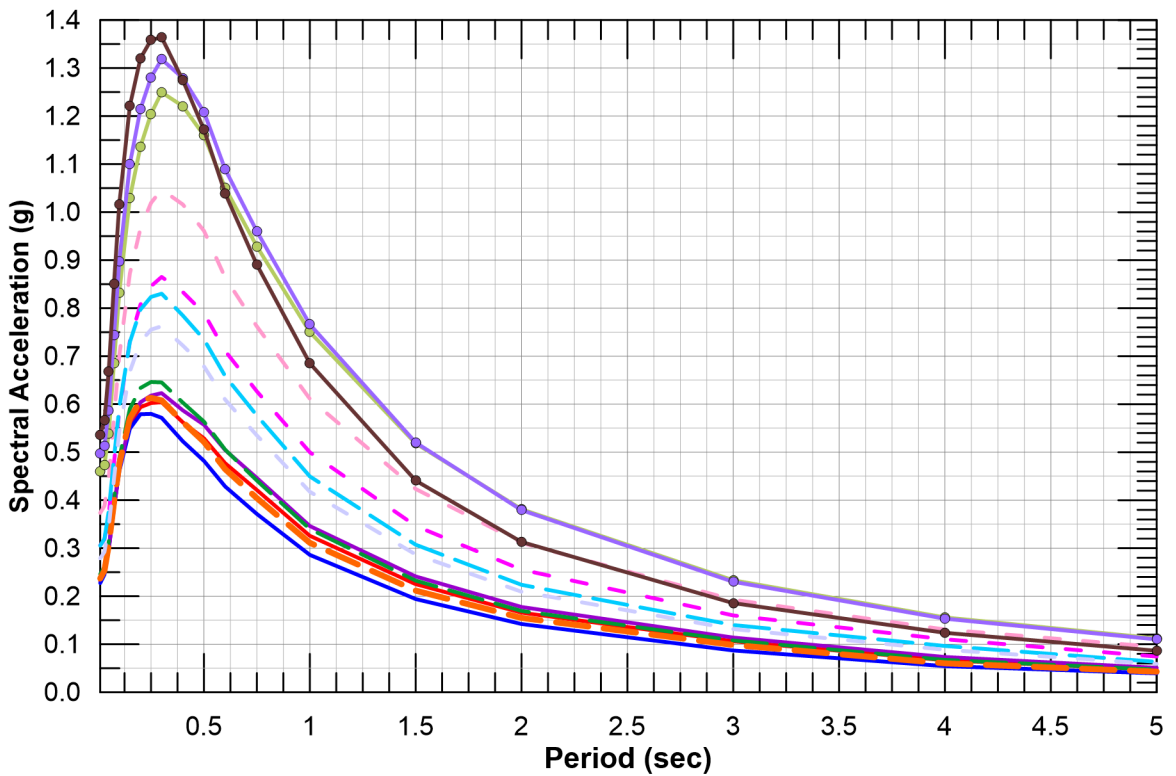
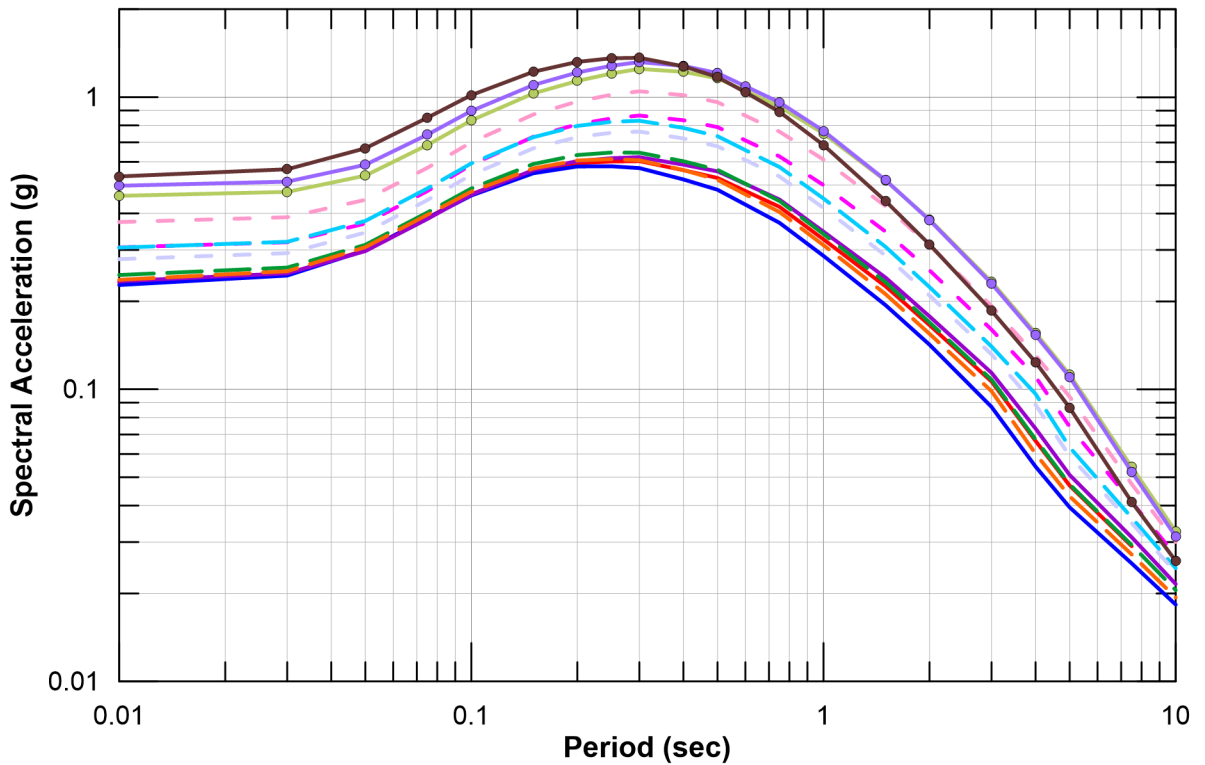
- | | | |
|---------------|-------------------|--------------------------|
| — Intake No.3 | — Canal Ranch | - - Bacon |
| — Intake No.5 | — Bouldin | — Southern Forebay North |
| — Twin Cities | - - King Island | — Southern Forebay South |
| — New Hope | - - Lower Roberts | — Jones Connection |



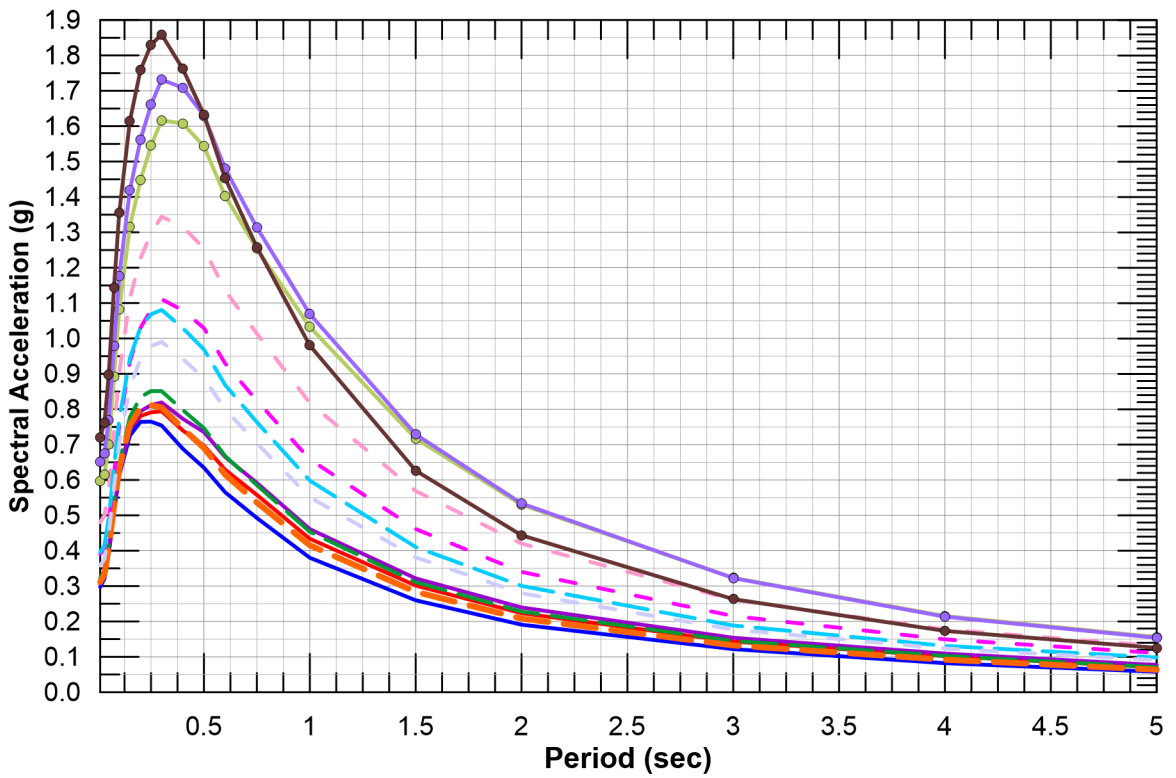
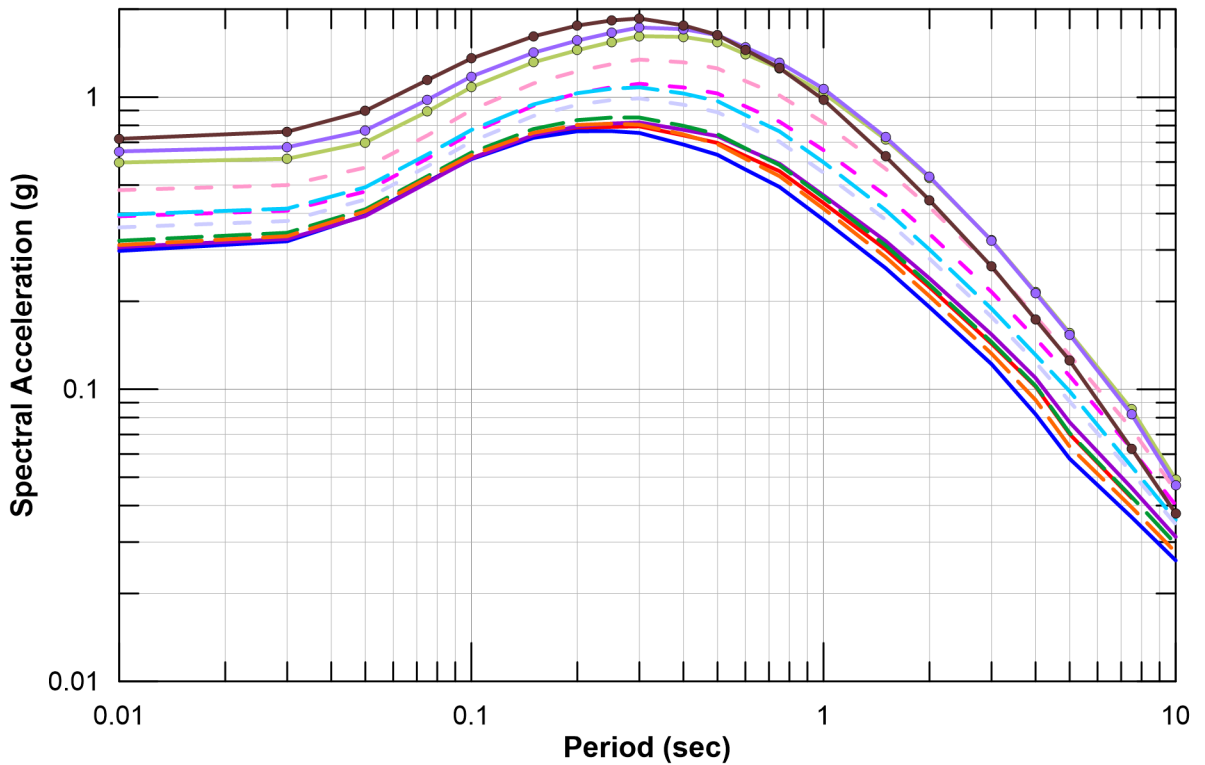
- | | | |
|---------------|-----------------|--------------------------|
| — Intake No.3 | — Canal Ranch | - - Bacon |
| — Intake No.5 | — Bouldin | — Southern Forebay North |
| — Twin Cities | — King Island | — Southern Forebay South |
| — New Hope | — Lower Roberts | — Jones Connection |



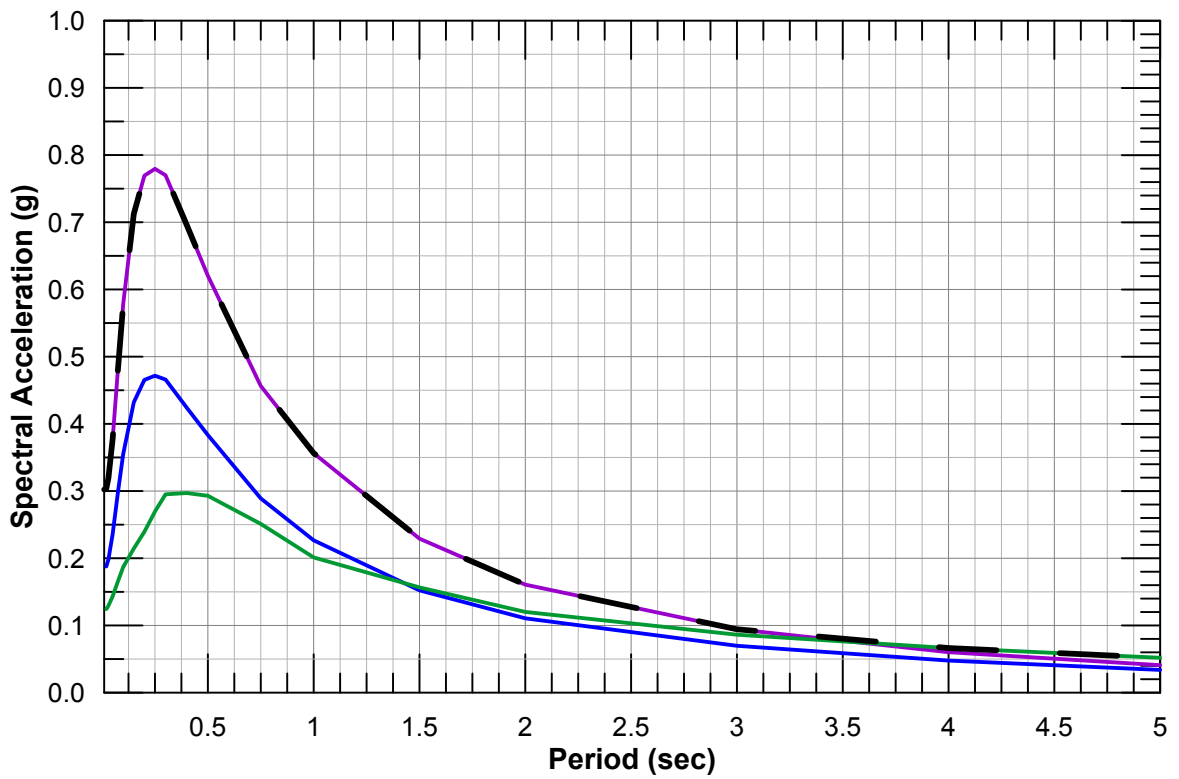
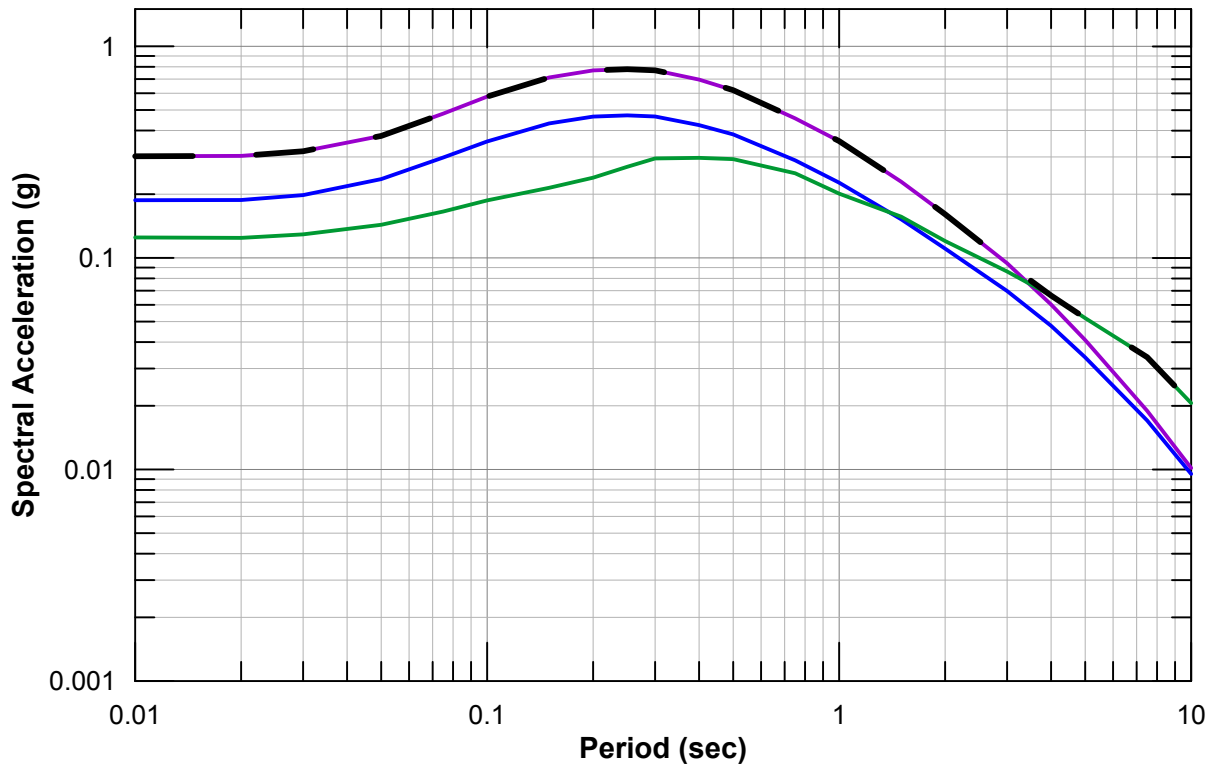
- | | | |
|---------------|-------------------|--------------------------|
| — Intake No.3 | — Canal Ranch | - - Bacon |
| — Intake No.5 | — Bouldin | — Southern Forebay North |
| — Twin Cities | - - King Island | — Southern Forebay South |
| — New Hope | - - Lower Roberts | — Jones Connection |



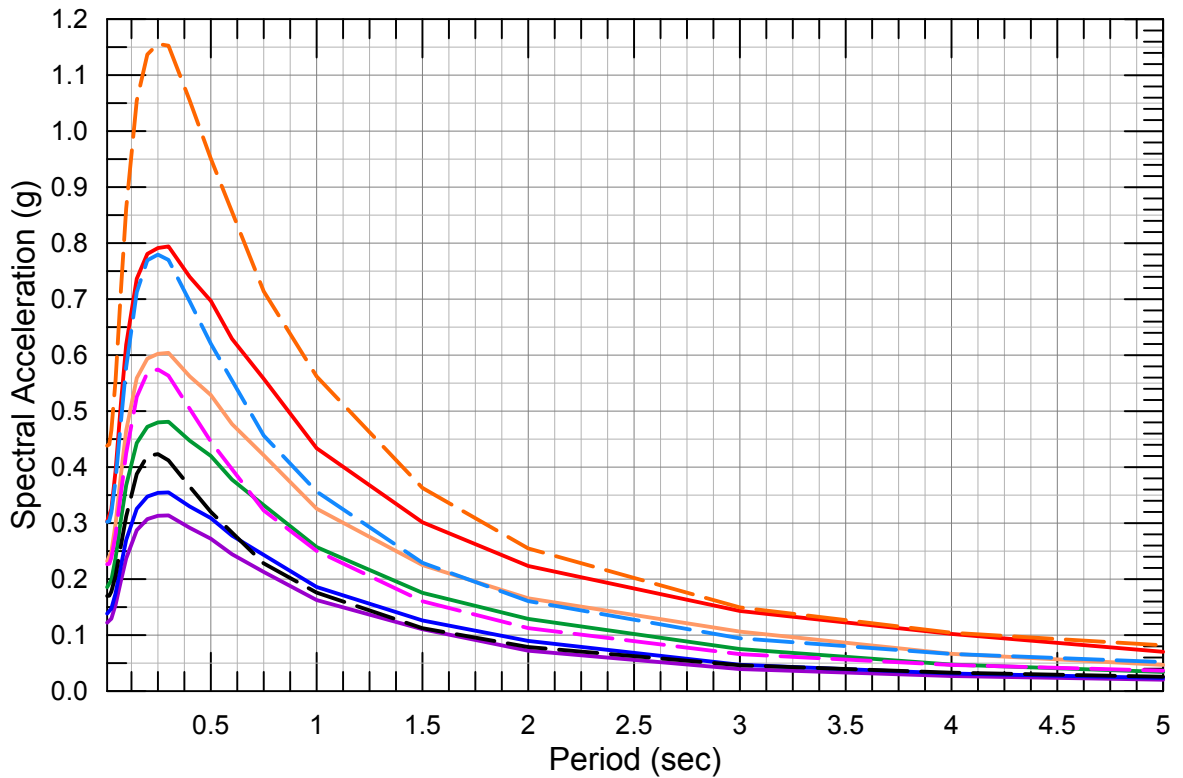
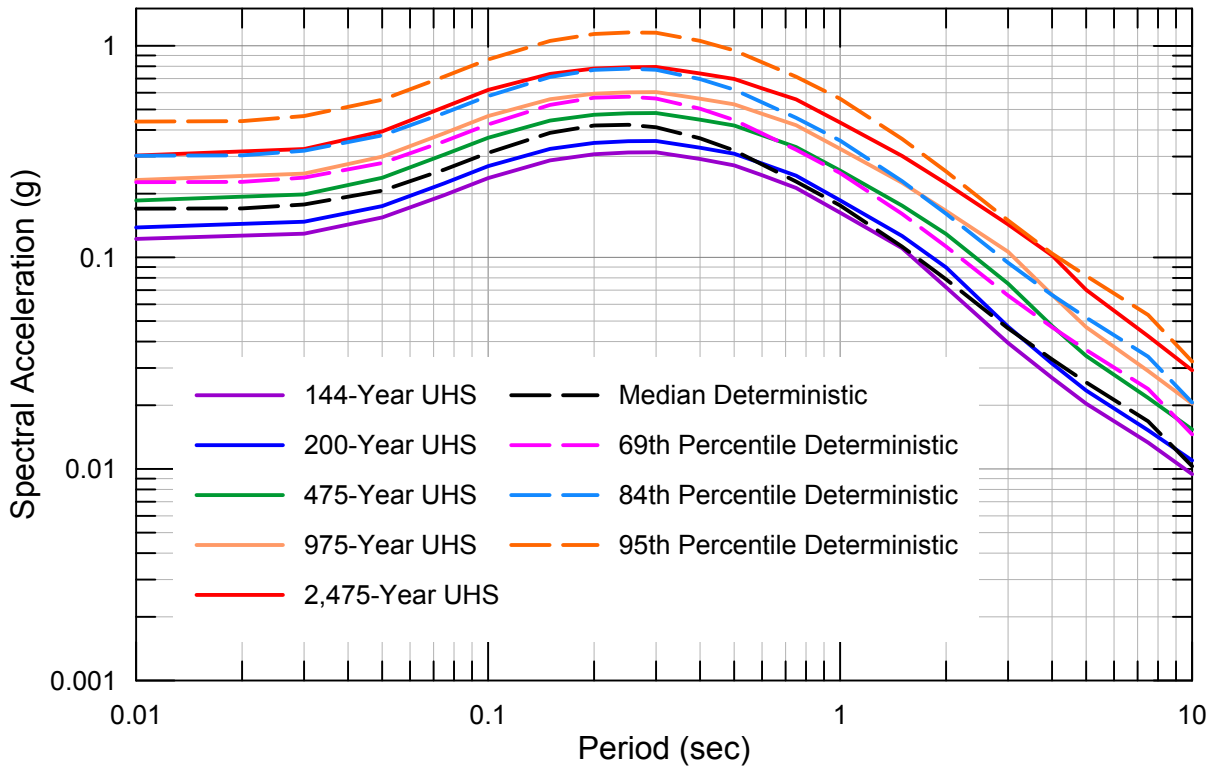
- | | | |
|---------------|-------------------|--------------------------|
| — Intake No.3 | — Canal Ranch | - - Bacon |
| — Intake No.5 | — Bouldin | — Southern Forebay North |
| — Twin Cities | - - King Island | — Southern Forebay South |
| — New Hope | - - Lower Roberts | — Jones Connection |

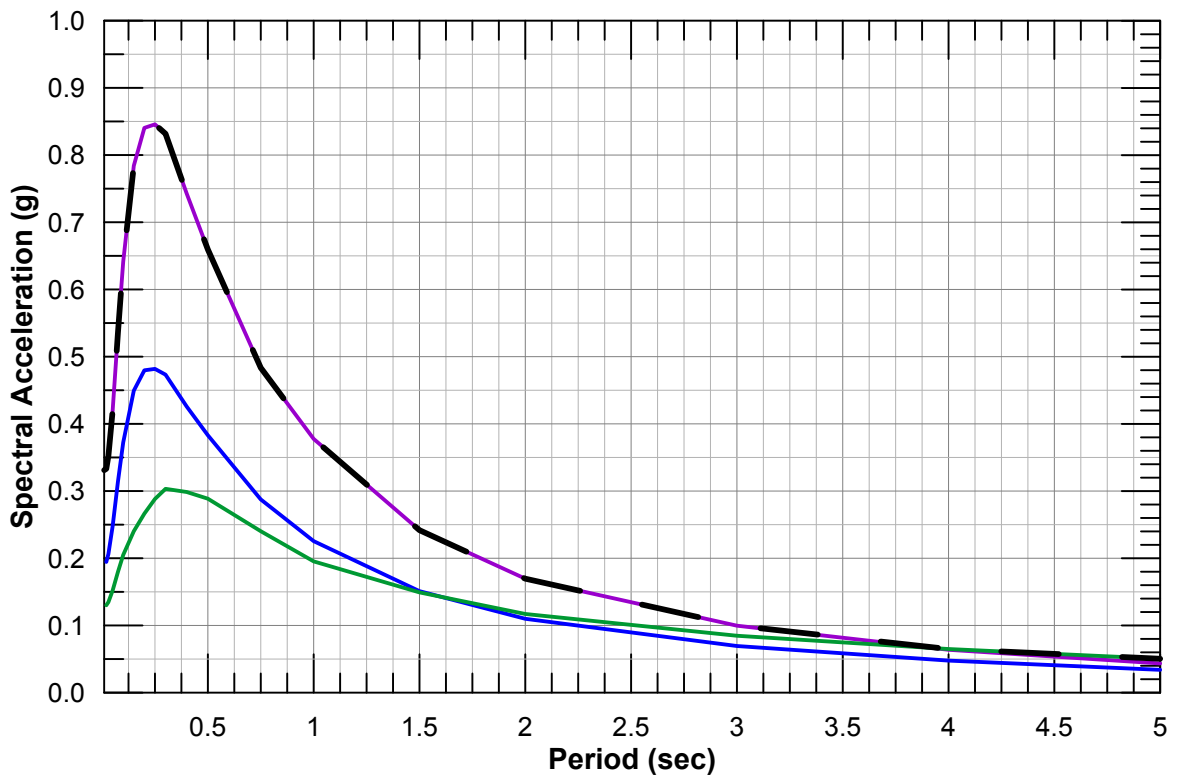
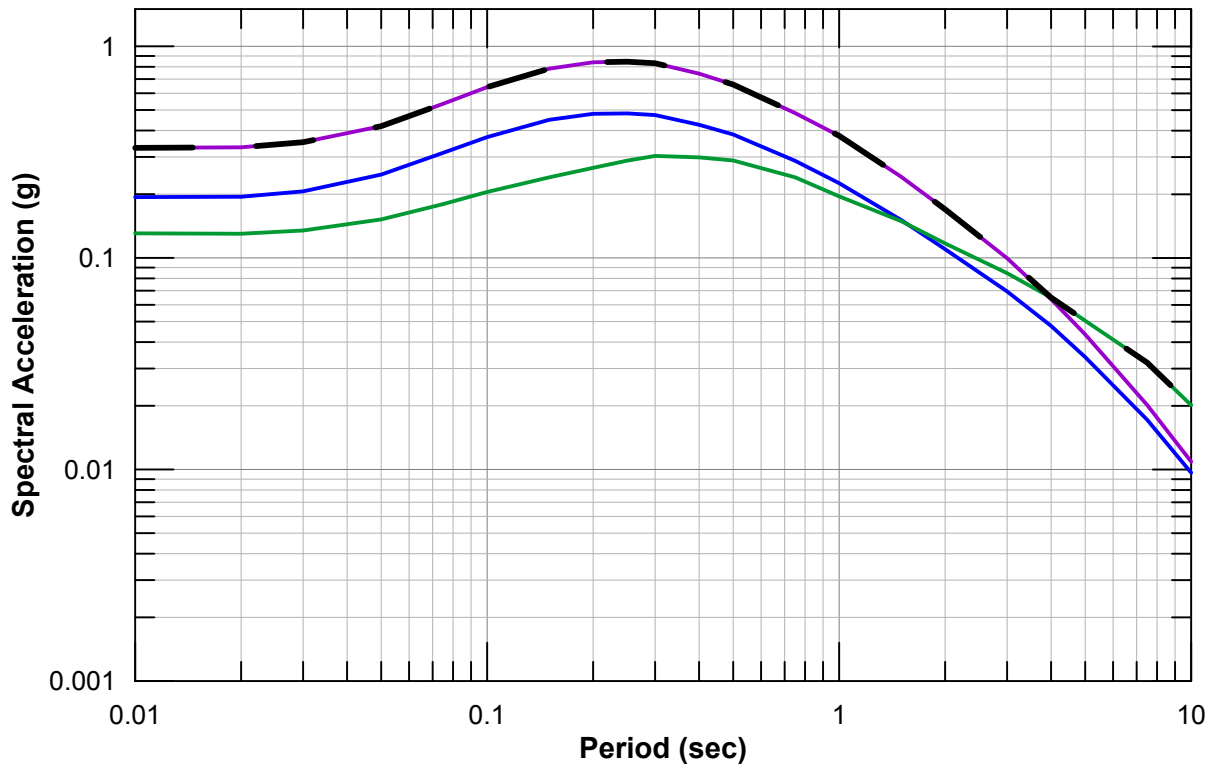


- | | | |
|---------------|-------------------|--------------------------|
| — Intake No.3 | — Canal Ranch | - - Bacon |
| — Intake No.5 | — Bouldin | — Southern Forebay North |
| — Twin Cities | - - King Island | — Southern Forebay South |
| — New Hope | - - Lower Roberts | — Jones Connection |

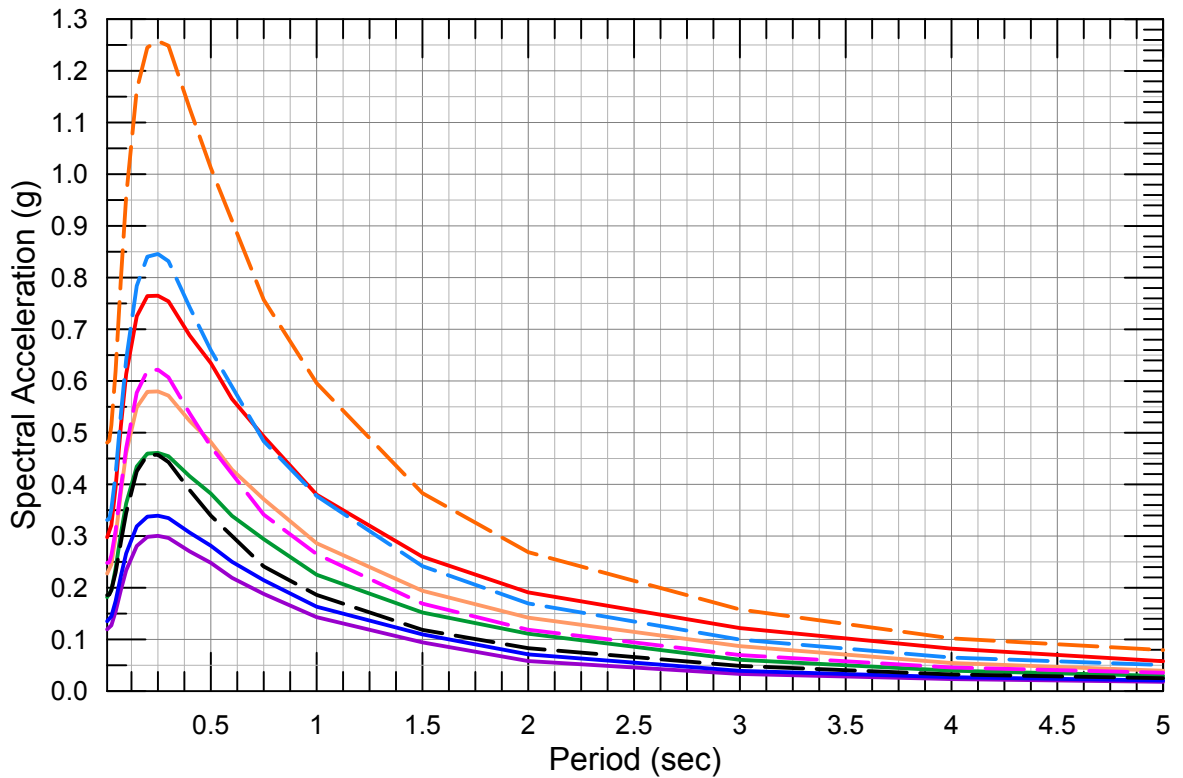
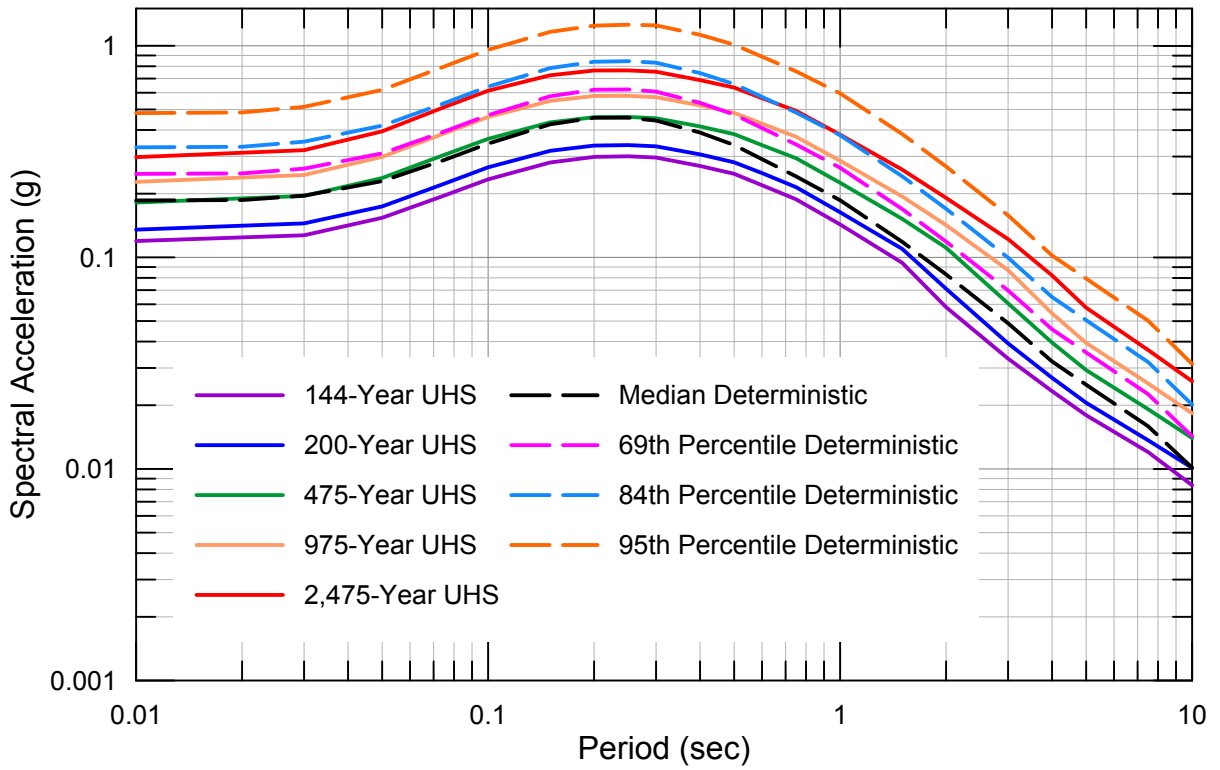


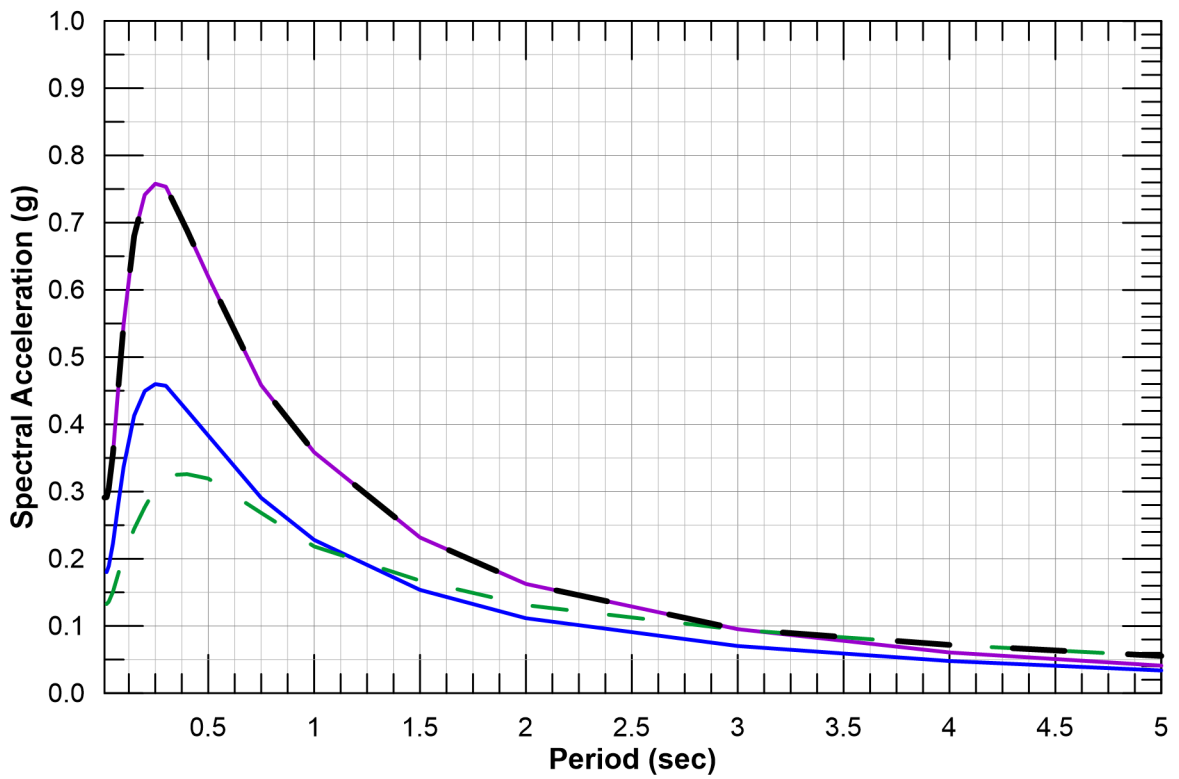
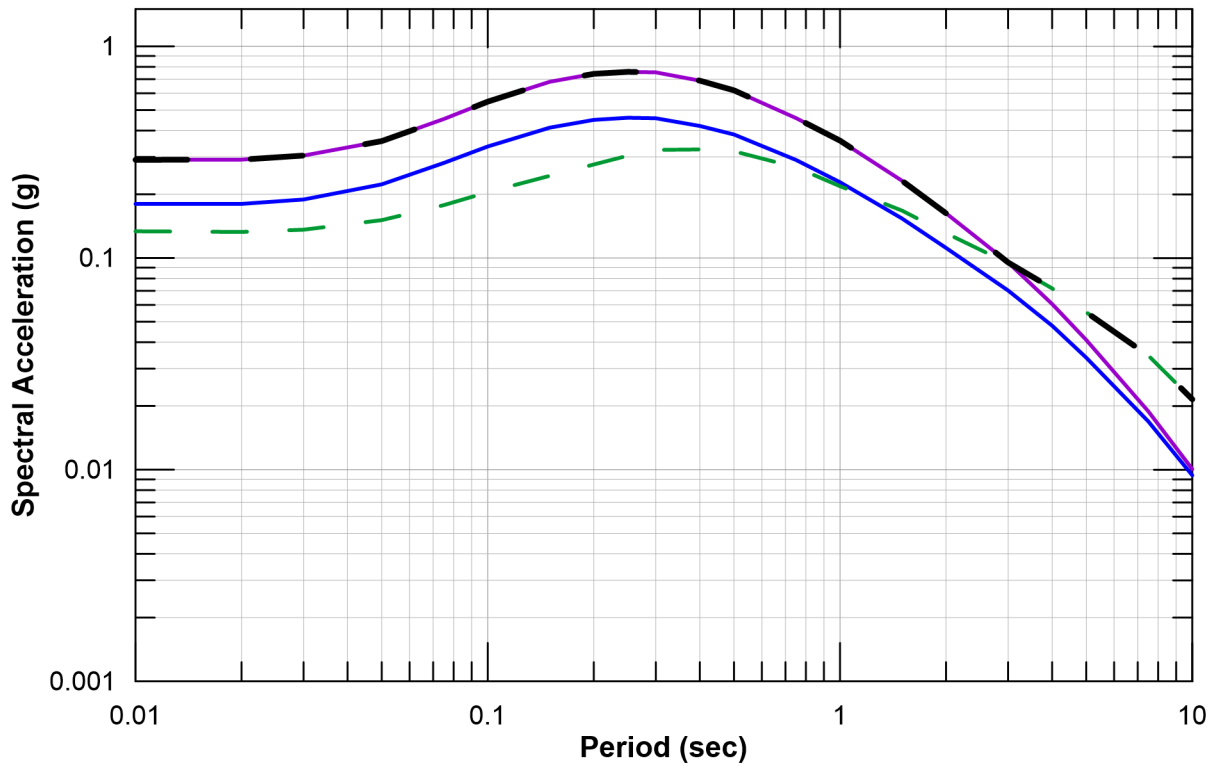
Enveloped 84th Percentile Deterministic
 Pittsburg-Kirby Hills Fault
 Midland Fault
 San Andreas Fault



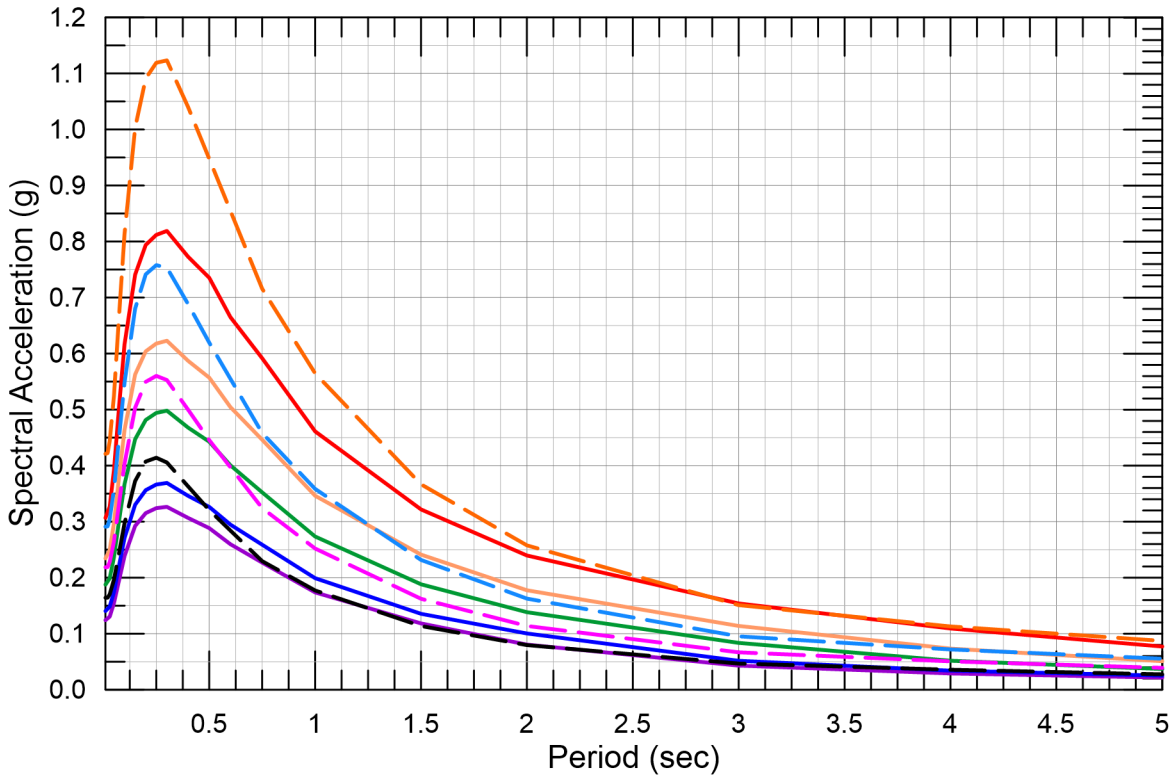
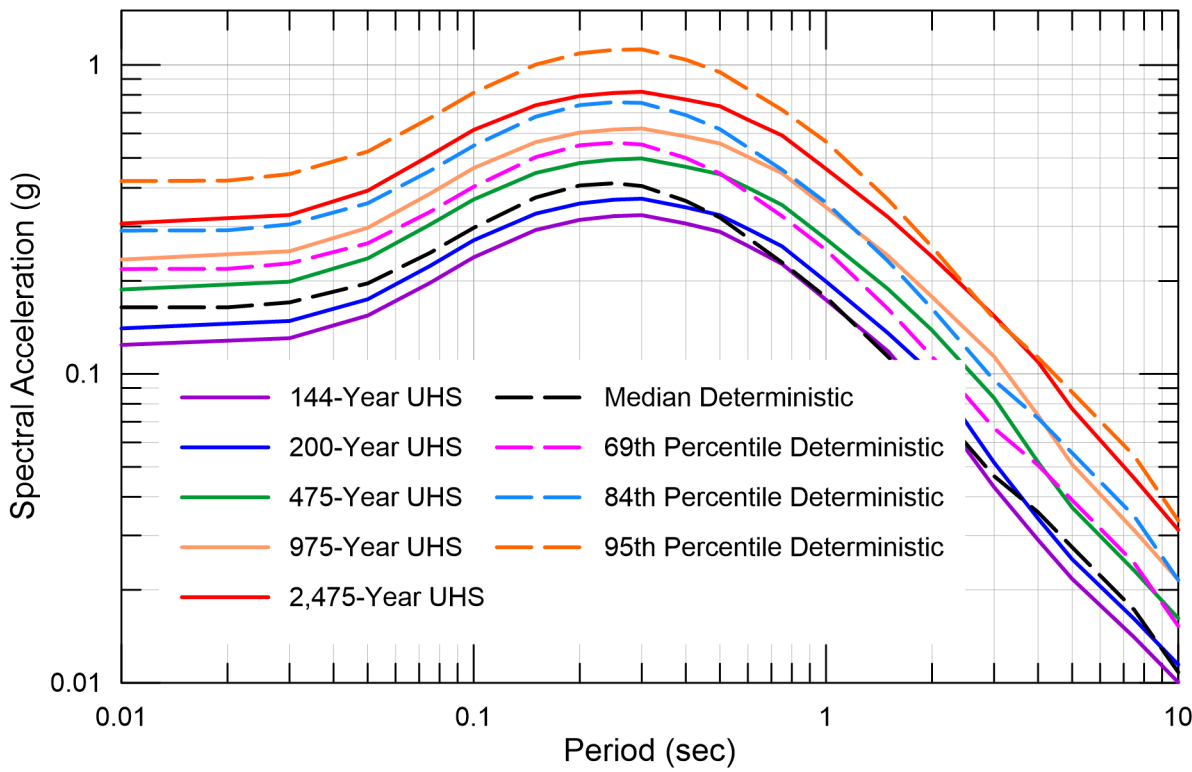


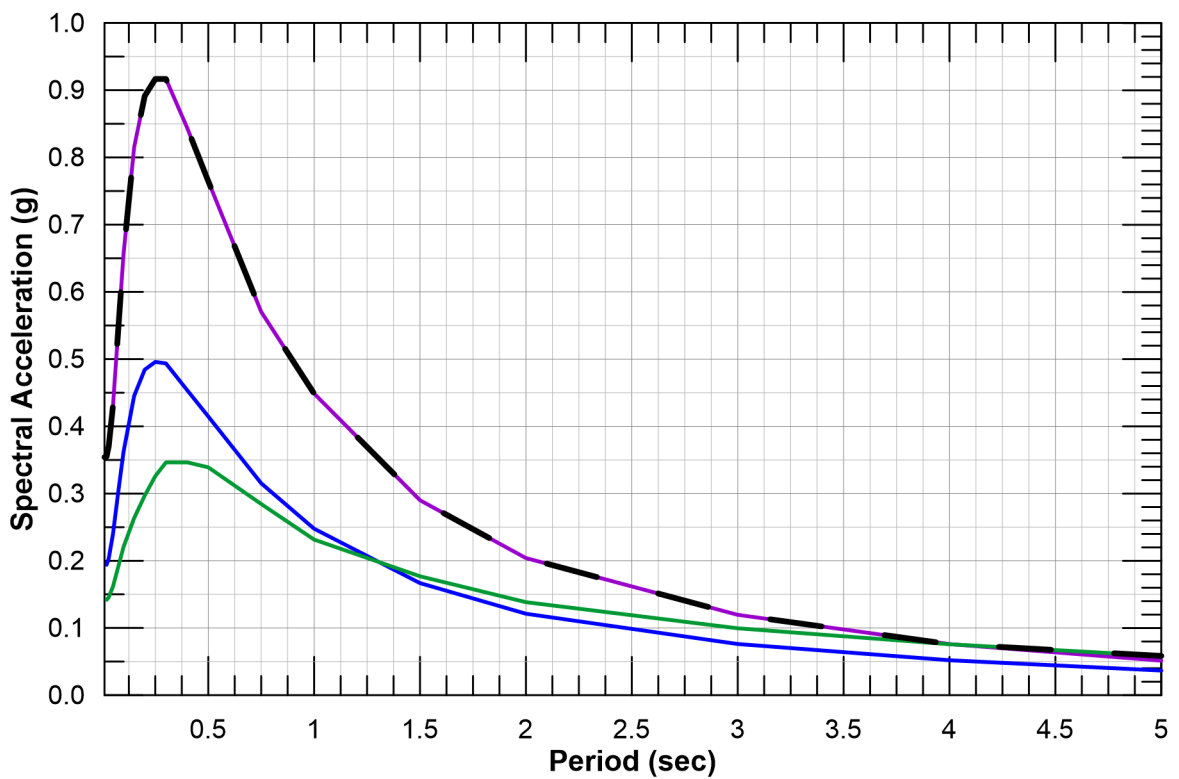
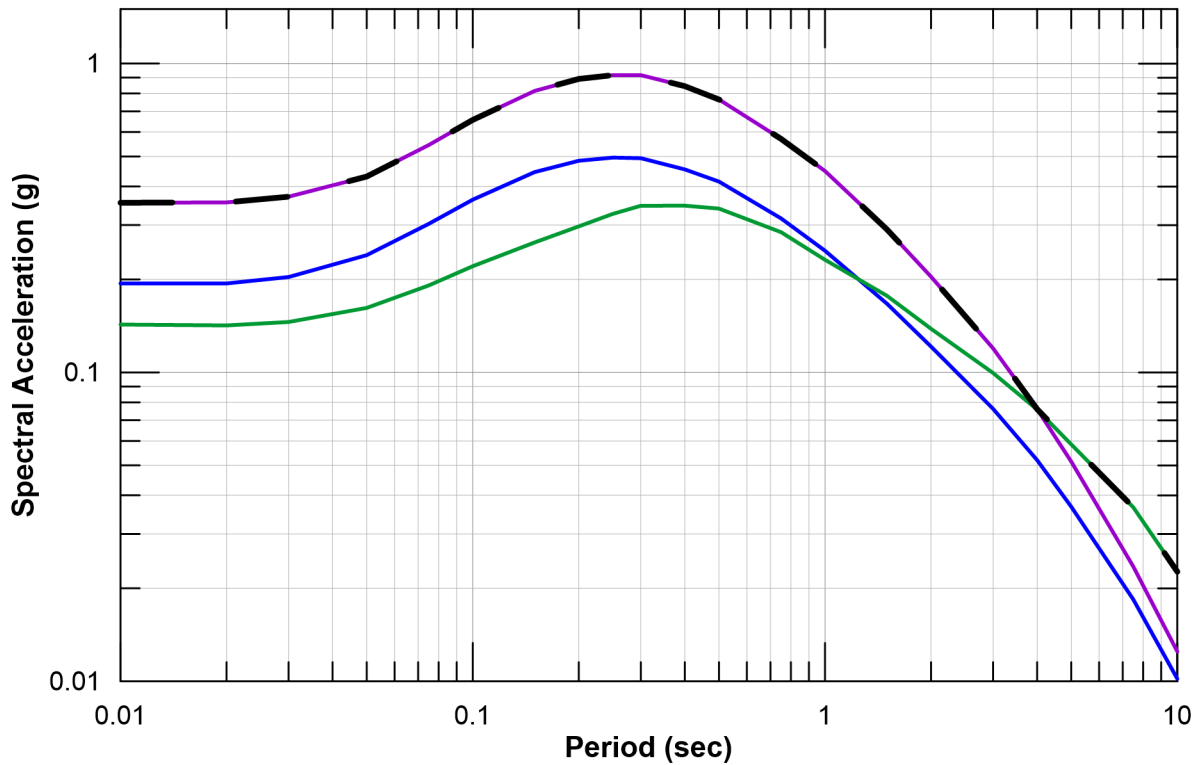
Enveloped 84th Percentile Deterministic
 Pittsburg-Kirby Hills Fault
 Midland Fault
 San Andreas Fault



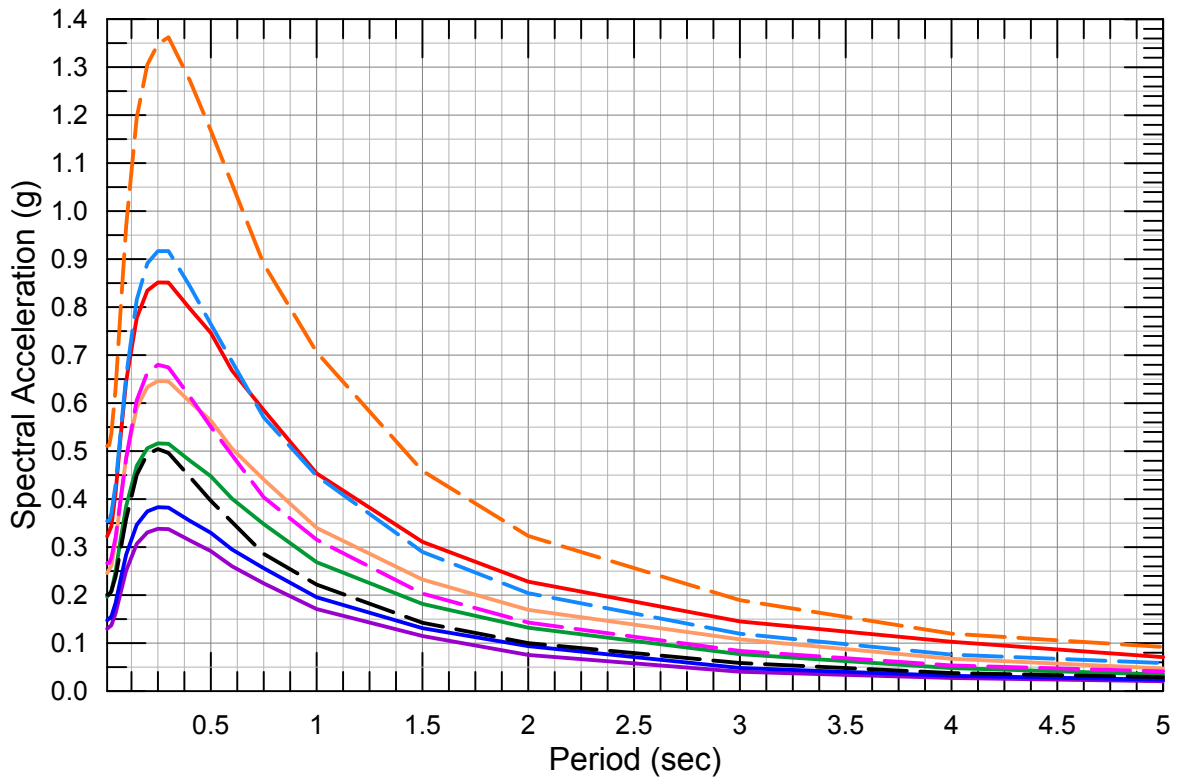
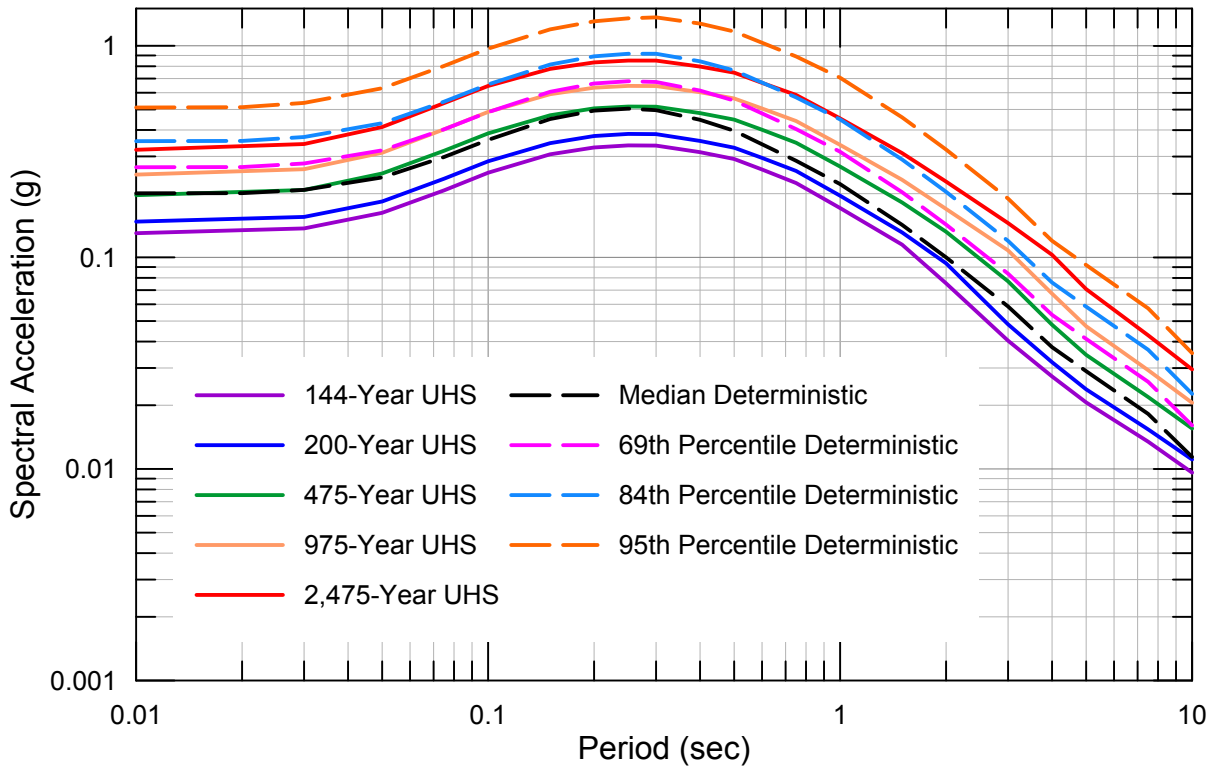


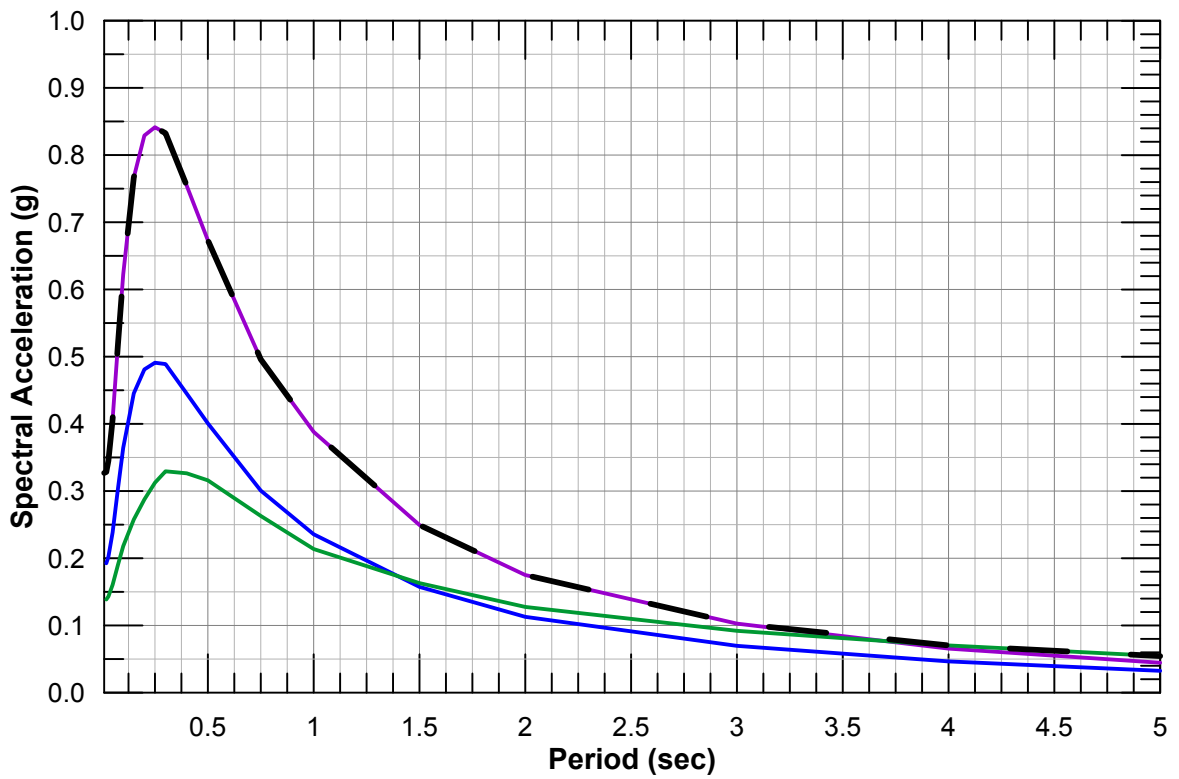
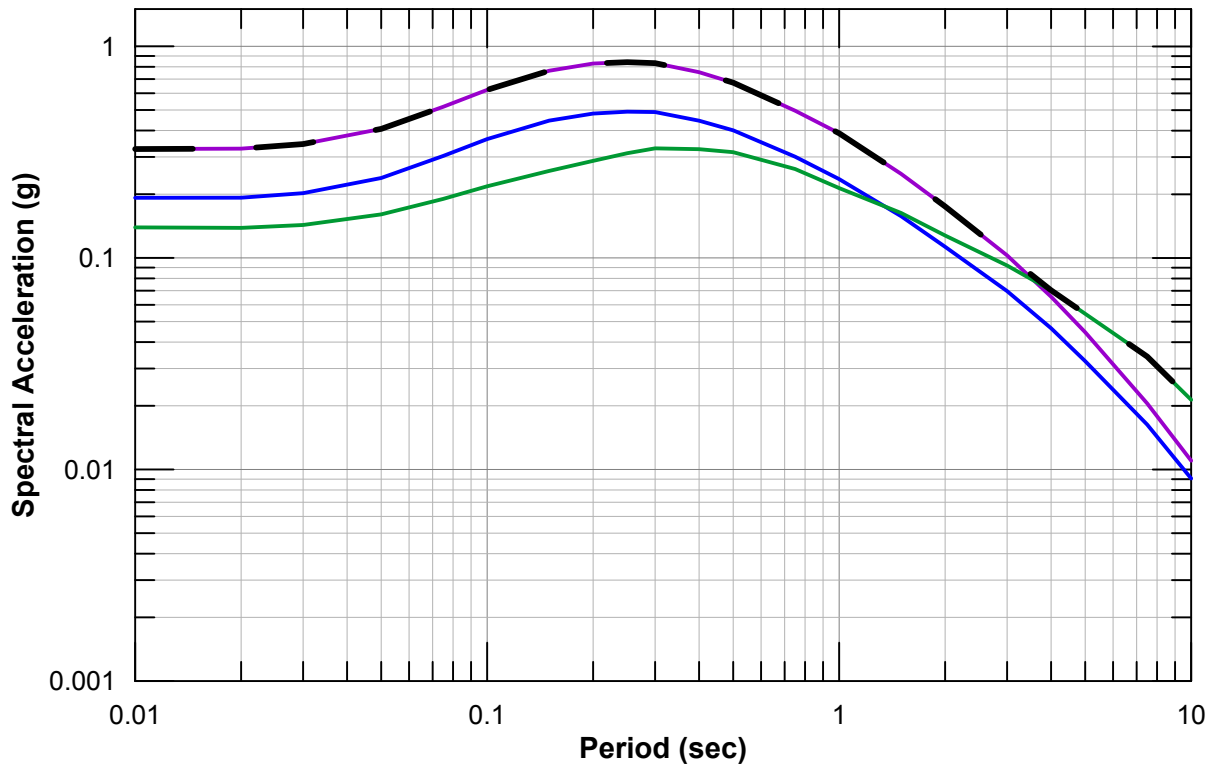
Enveloped 84th Percentile Deterministic
 Pittsburgh-Kirby Hills Fault
 Midland Fault
 San Andreas Fault



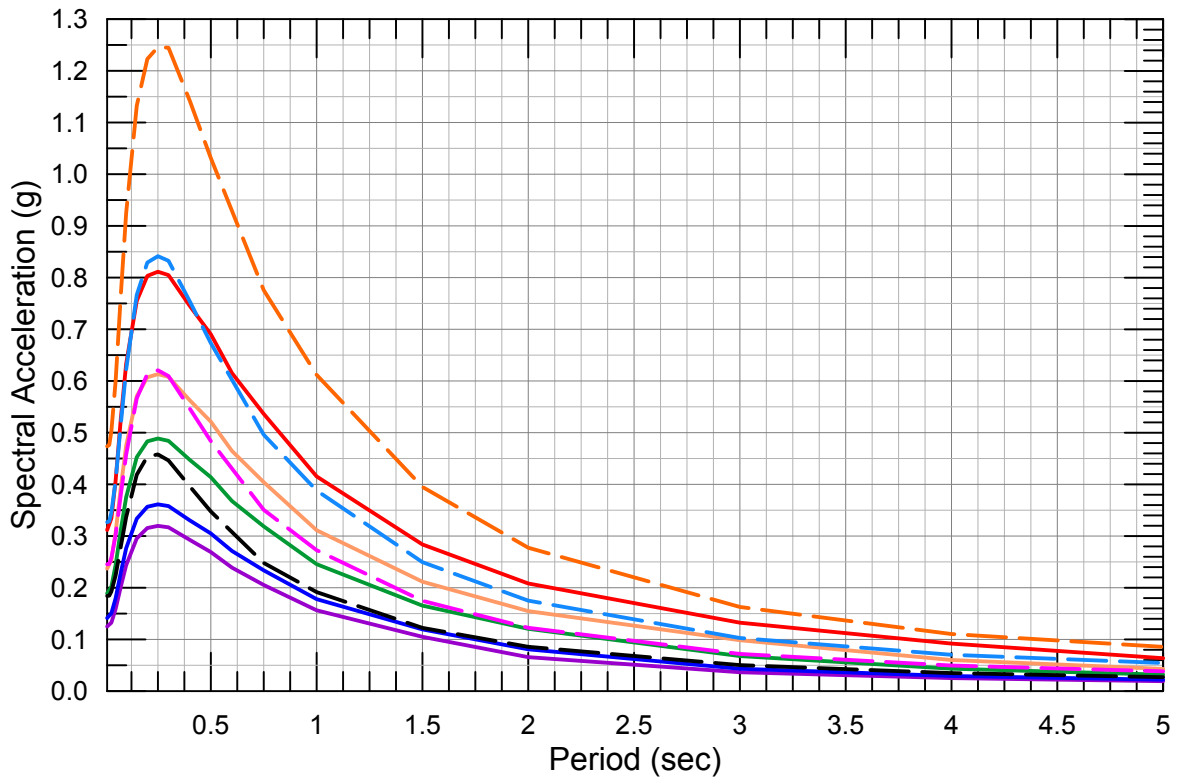
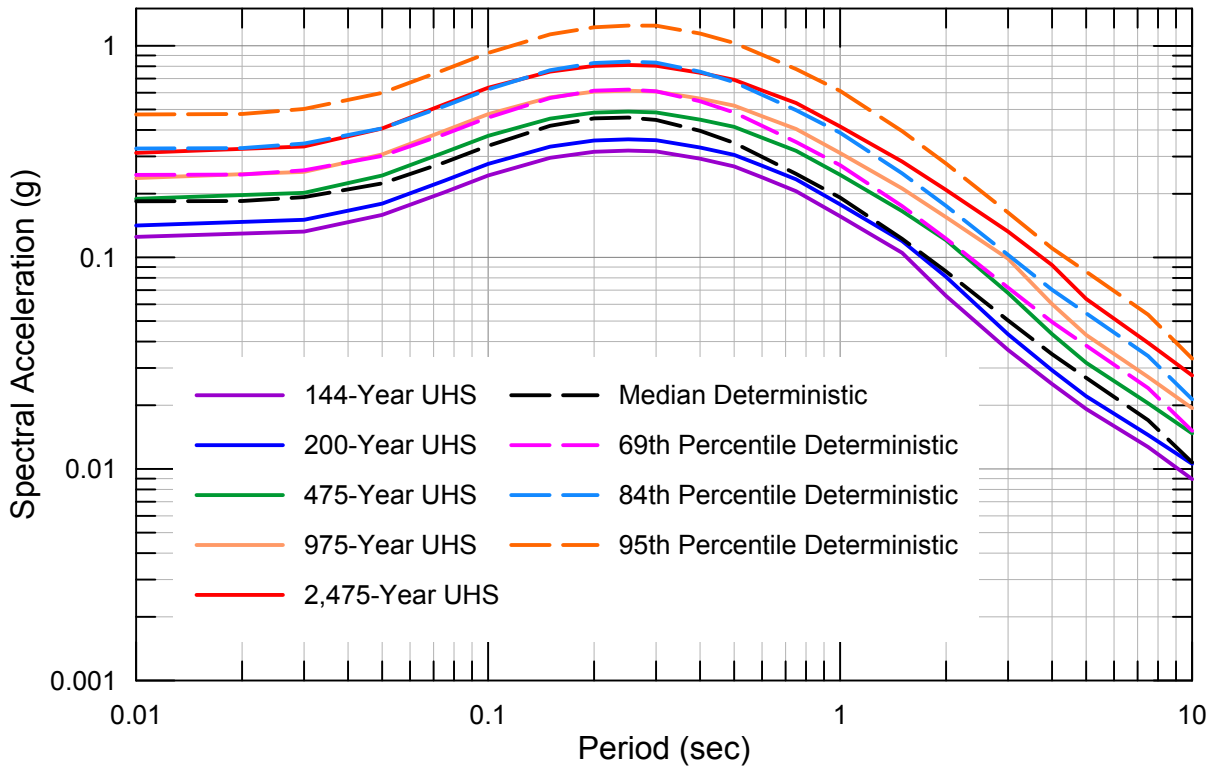


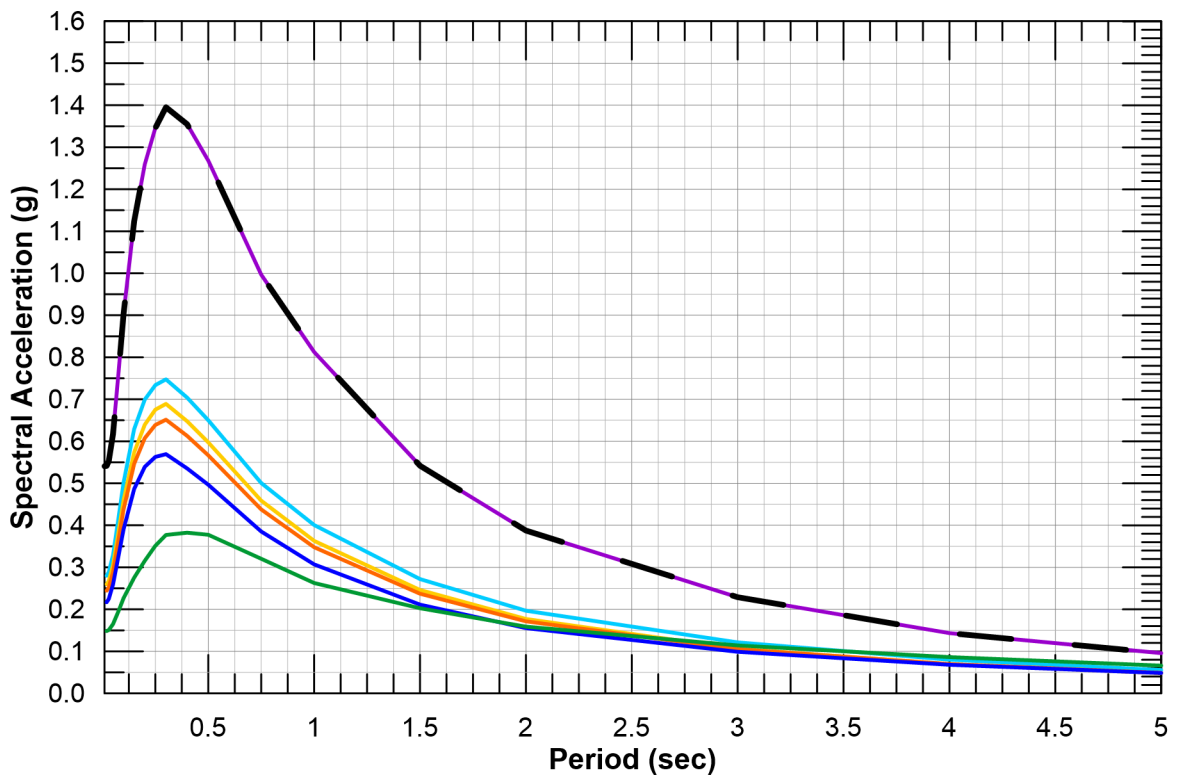
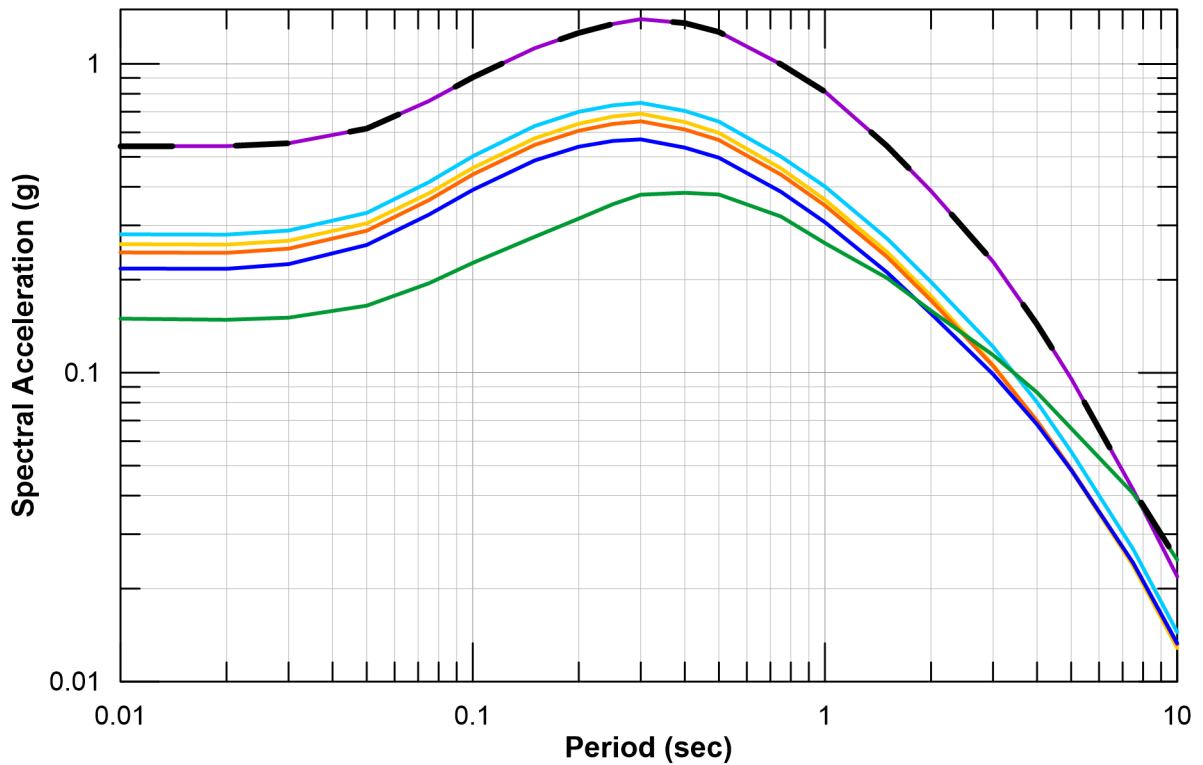
Enveloped 84th Percentile Deterministic
 Pittsburgh-Kirby Hills Fault
 Midland Fault
 San Andreas Fault



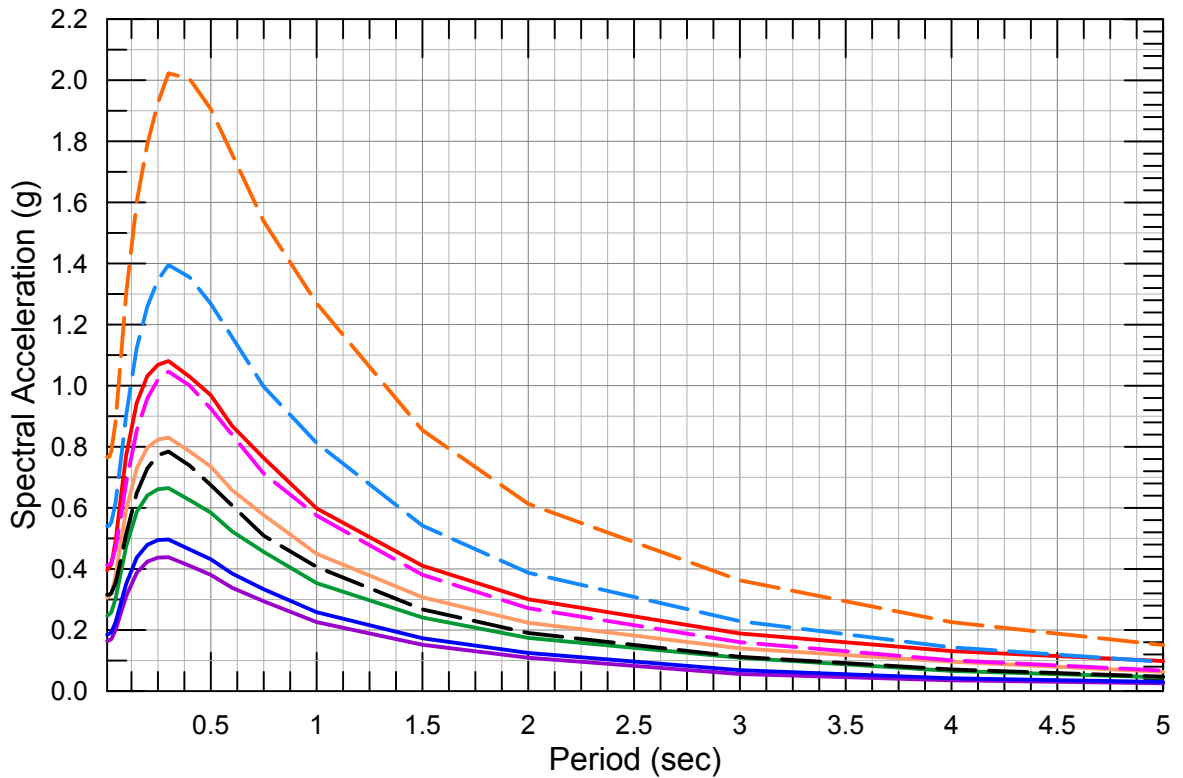
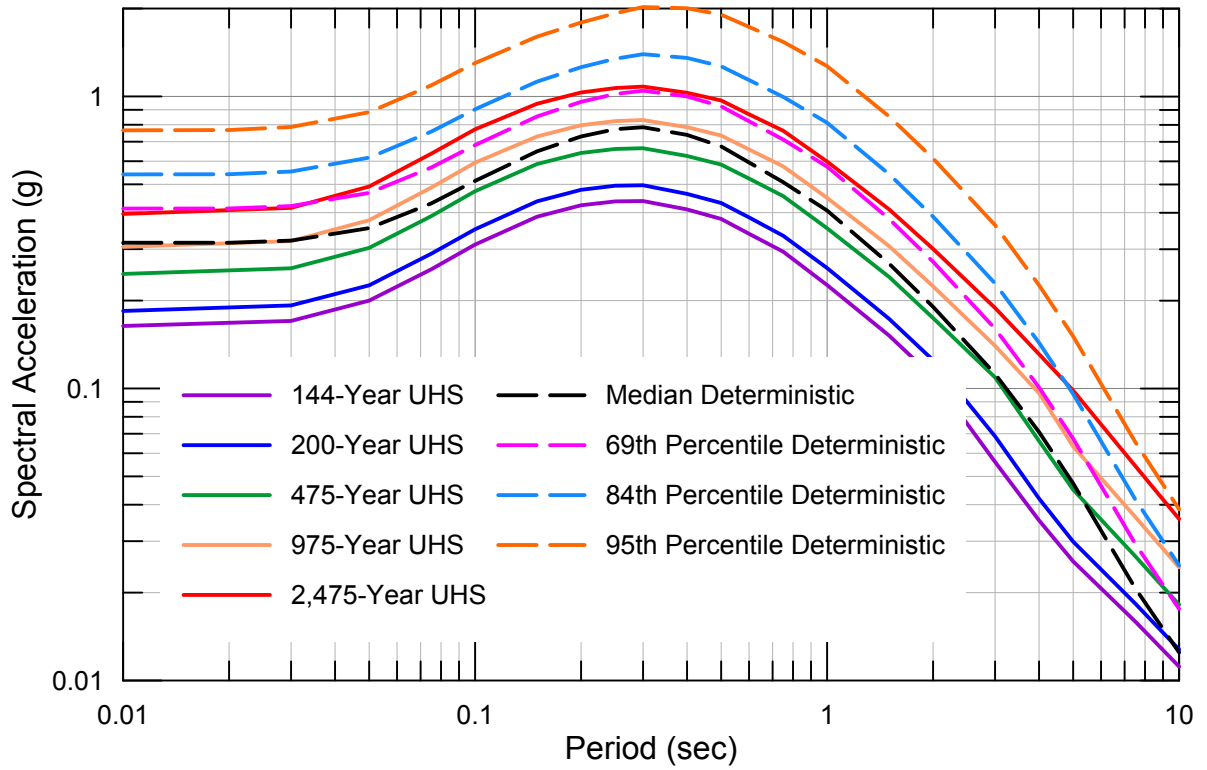


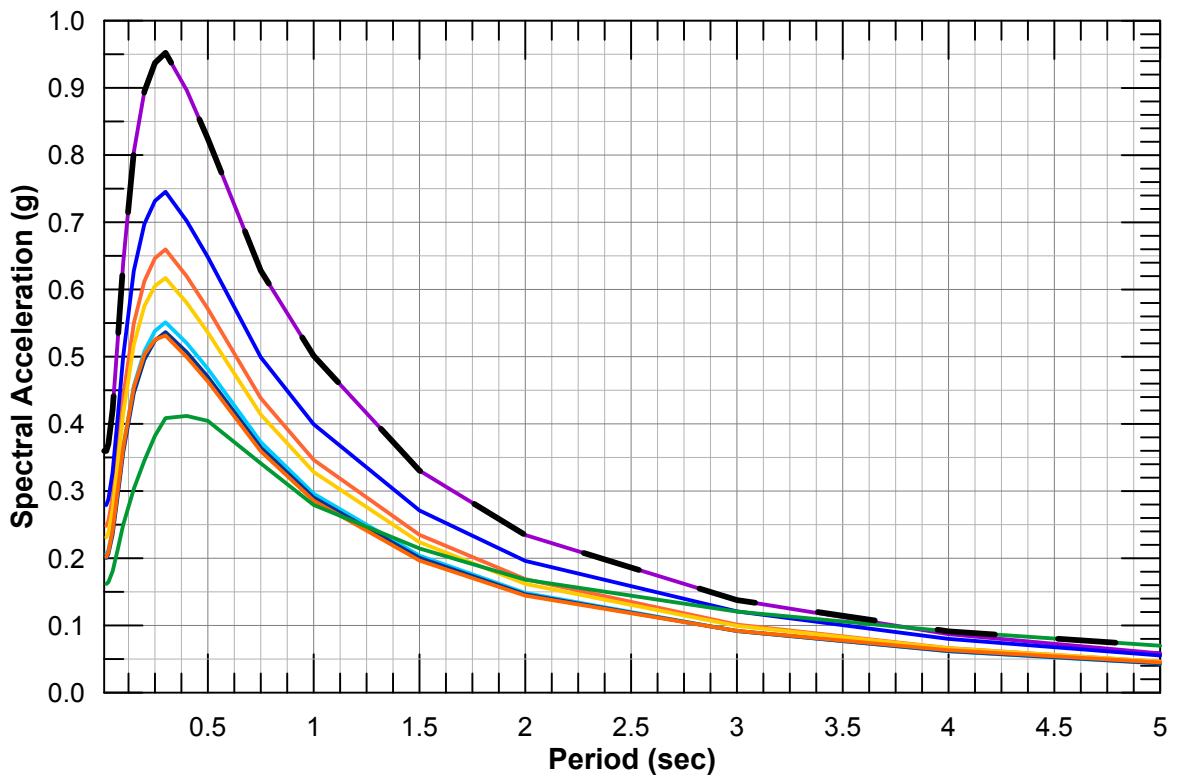
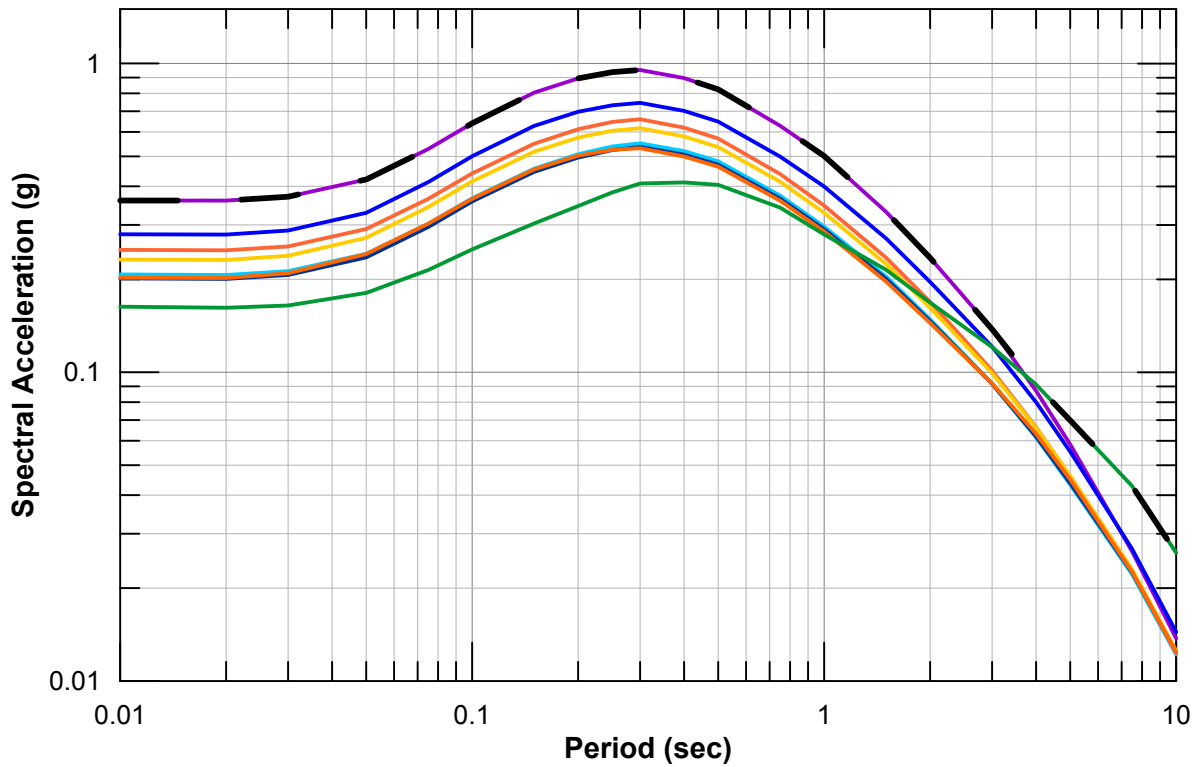
— 84th Percentile Deterministic — West Tracy Fault
 — Midland Fault — San Andreas Fault



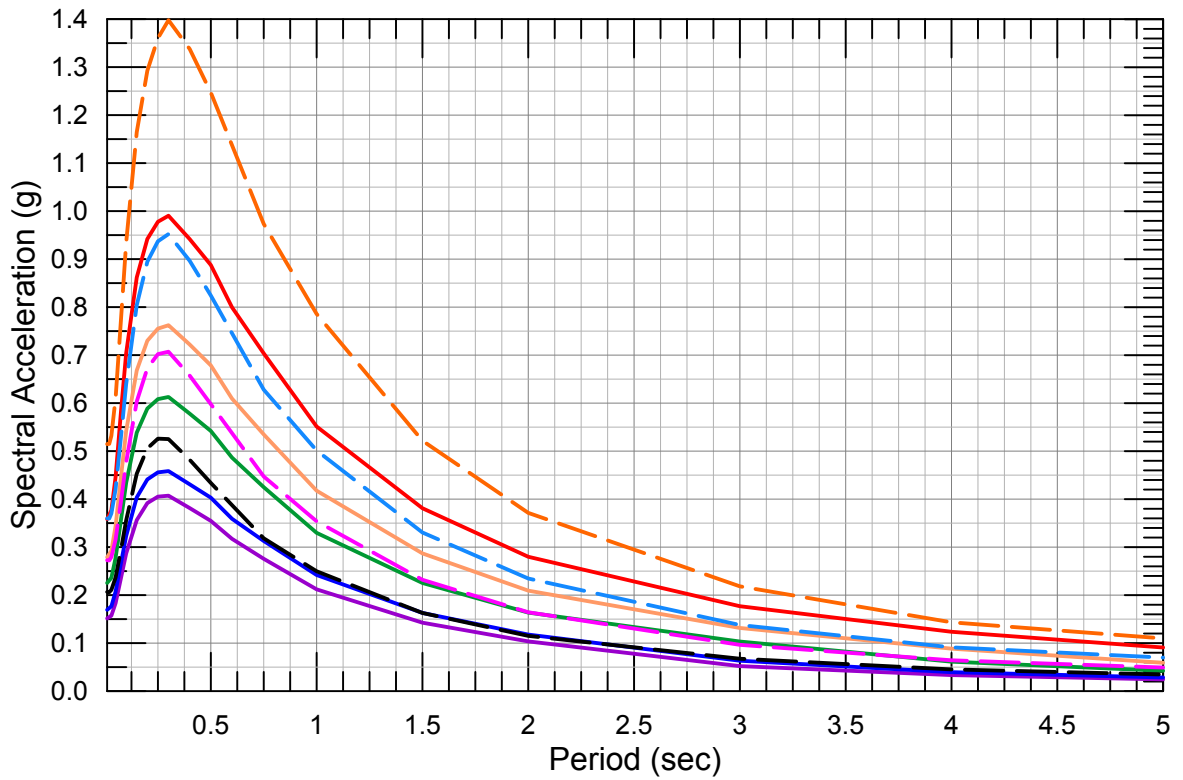
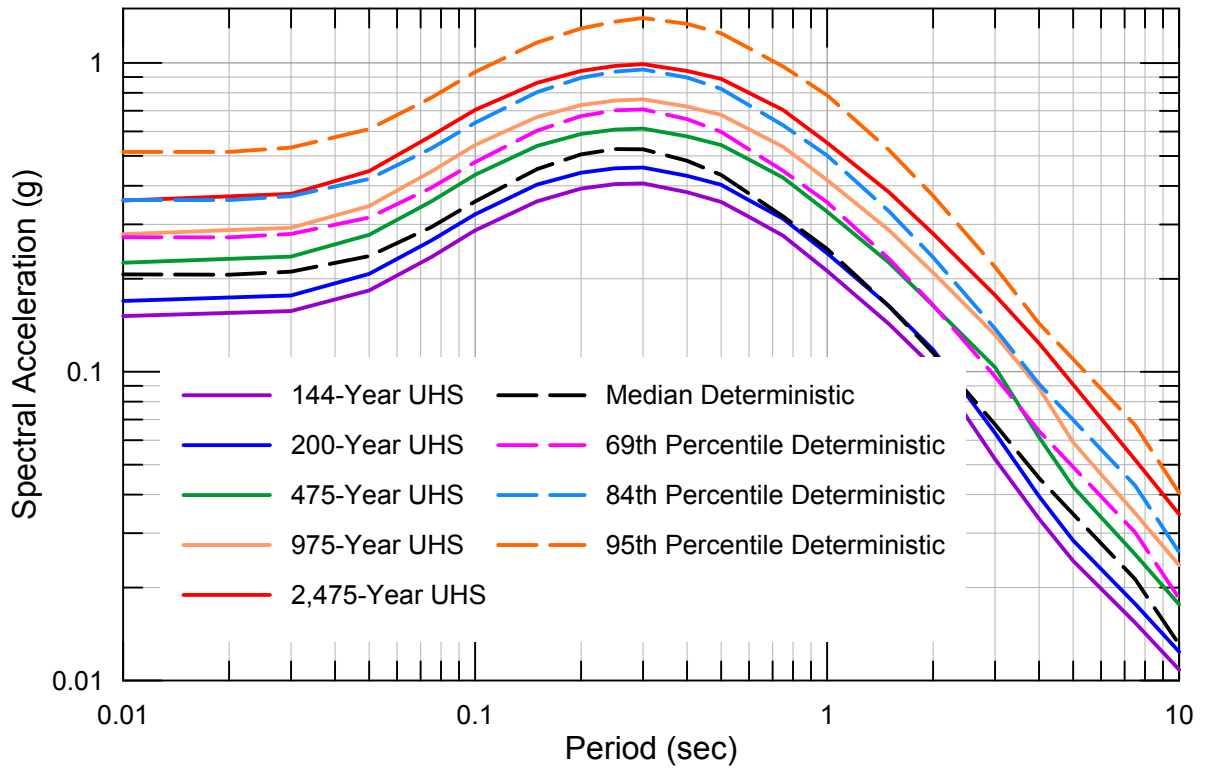


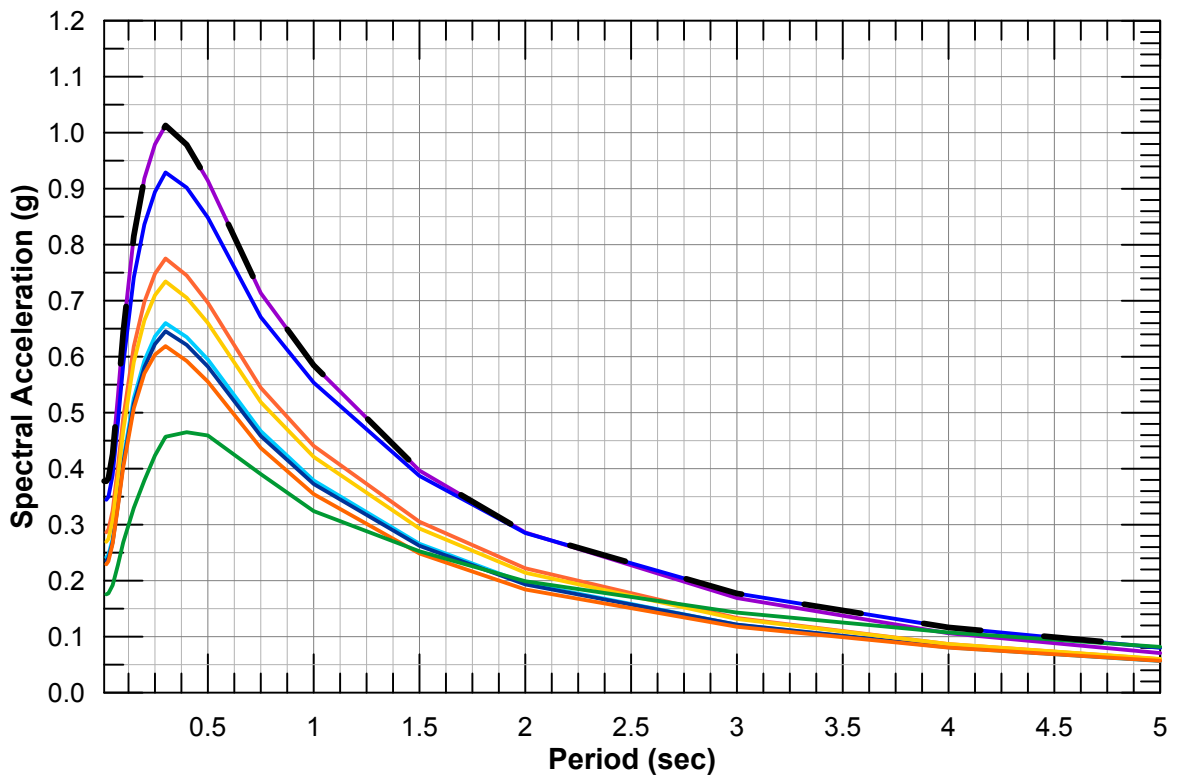
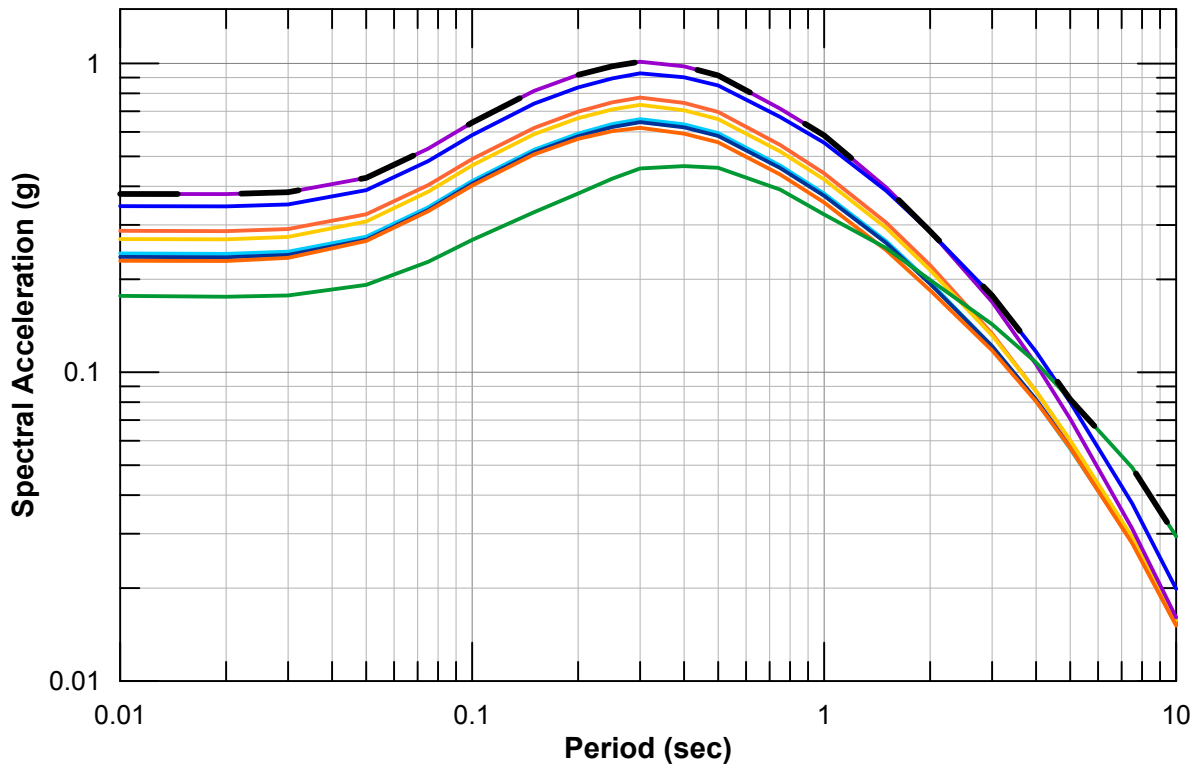
- Enveloped 84th Percentile Deterministic
- Greenville
- San Andreas Fault
- West Tracy
- Midland Fault
- Mt. Diablo, top 1km
- Mt. Diablo, top 5km



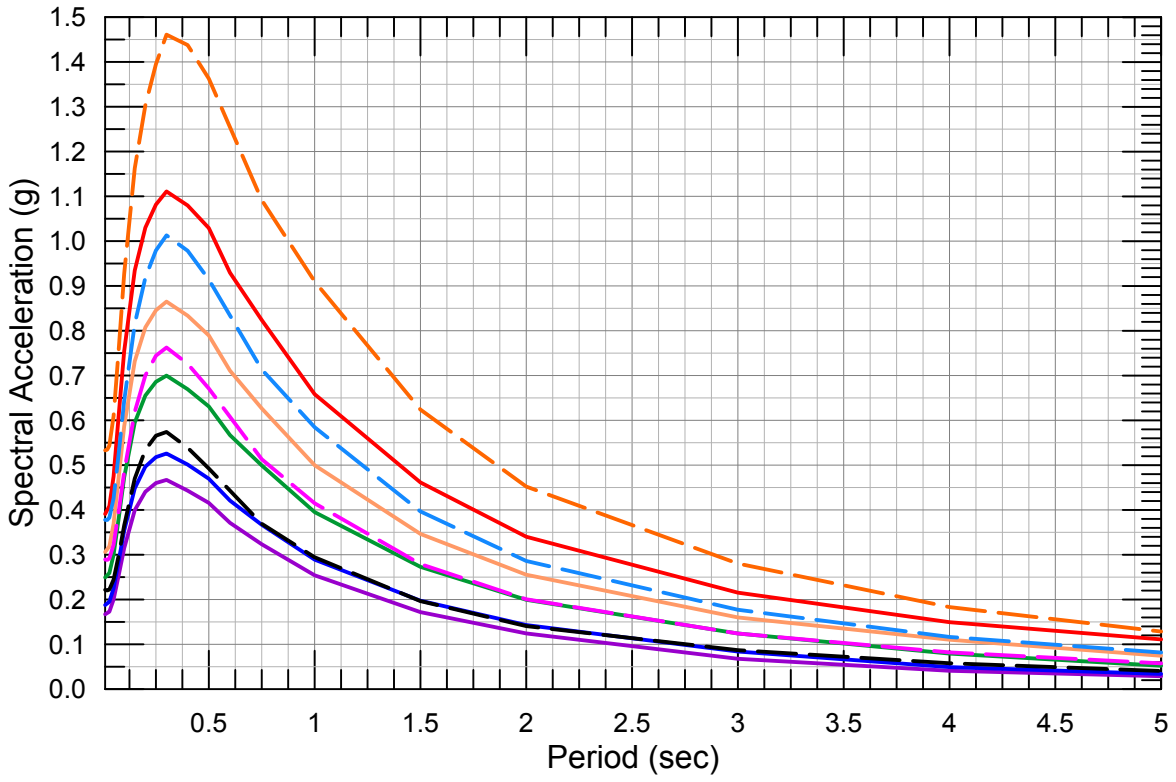
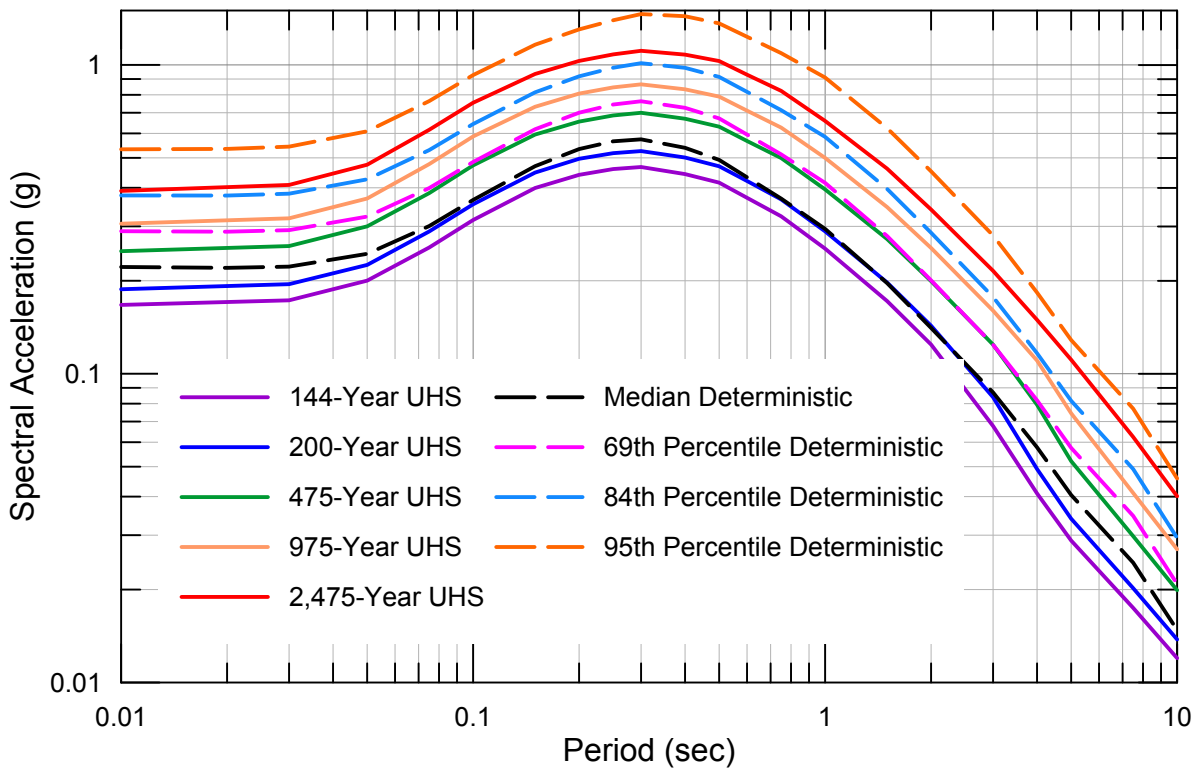


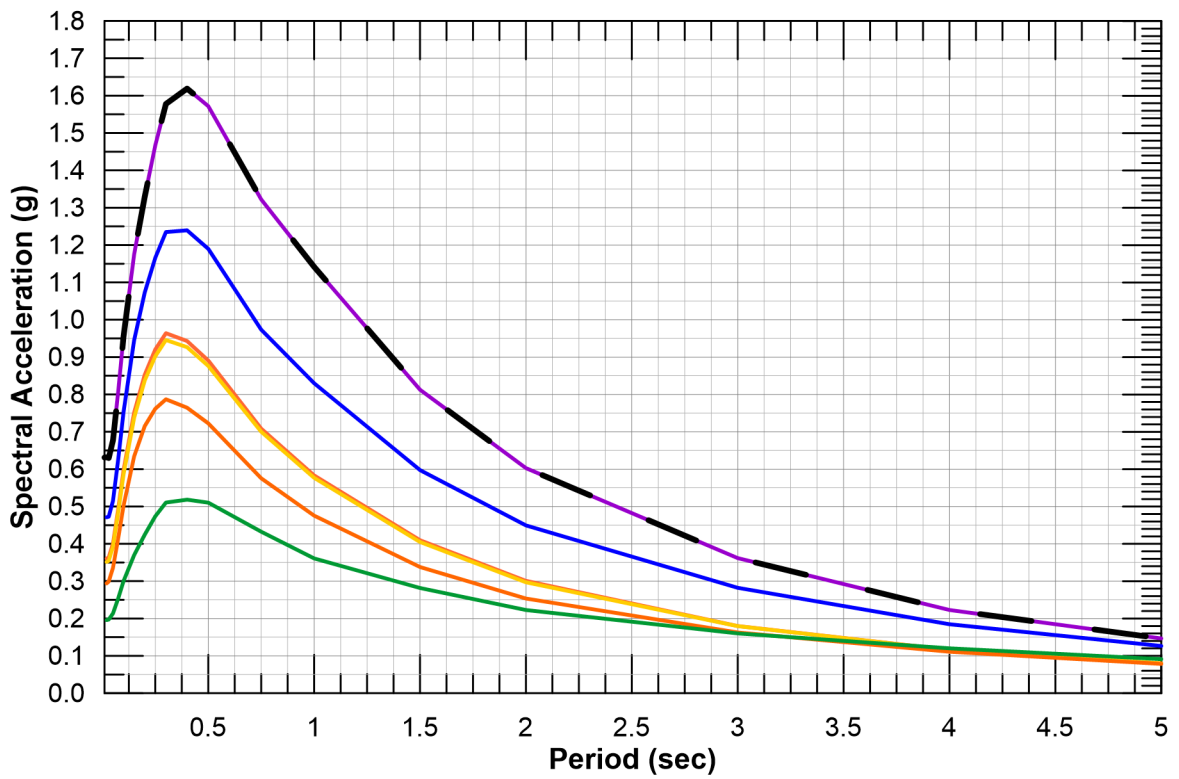
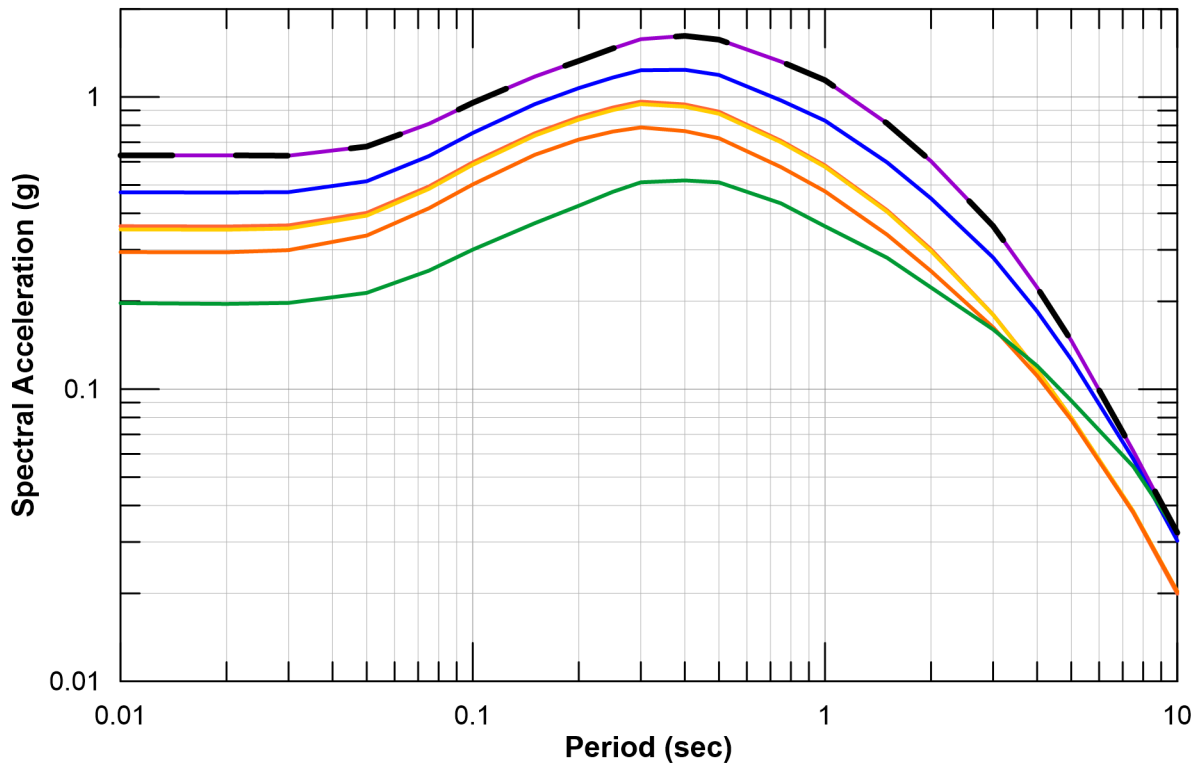
- | | |
|---|-----------------------|
| — Enveloped 84th Percentile Deterministic | — Mt. Diablo, top 1km |
| — Midland Fault | — Mt. Diablo, top 5km |
| — West Tracy Fault | — Orestimba, top 1km |
| — San Andreas Fault | — Orestimba, top 3km |
| — Greenville Fault | |



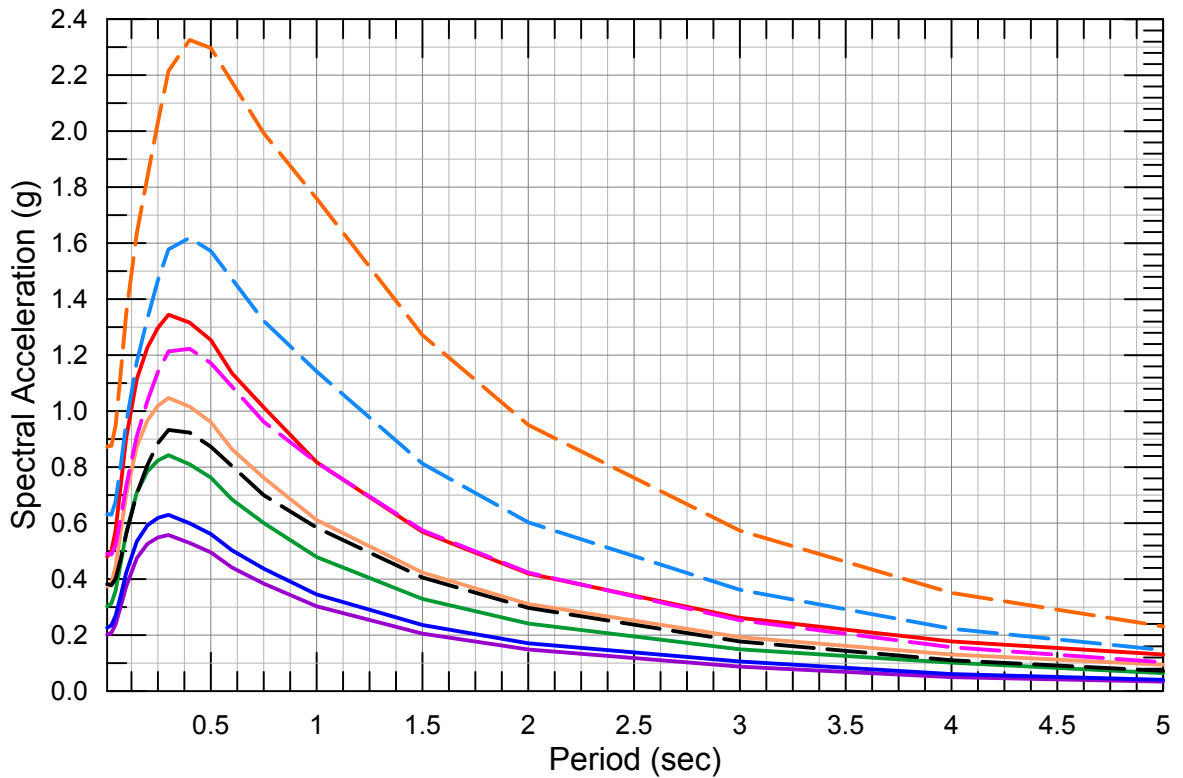
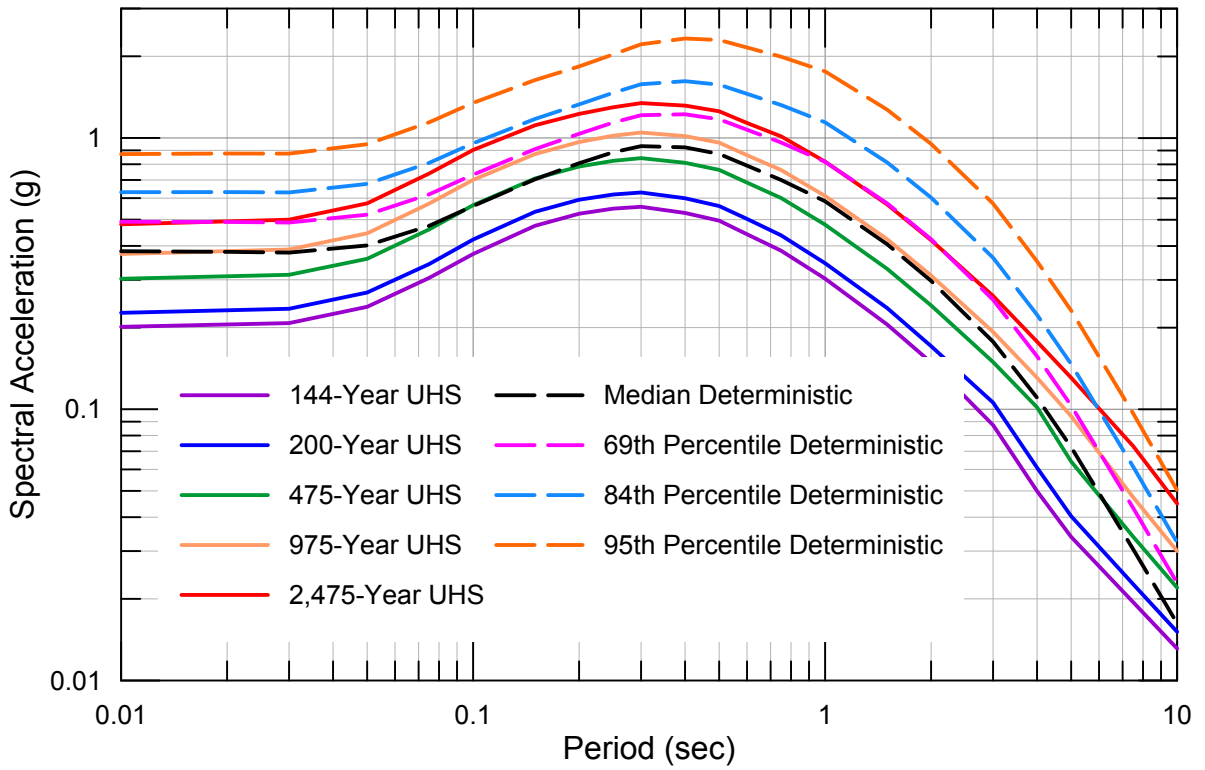


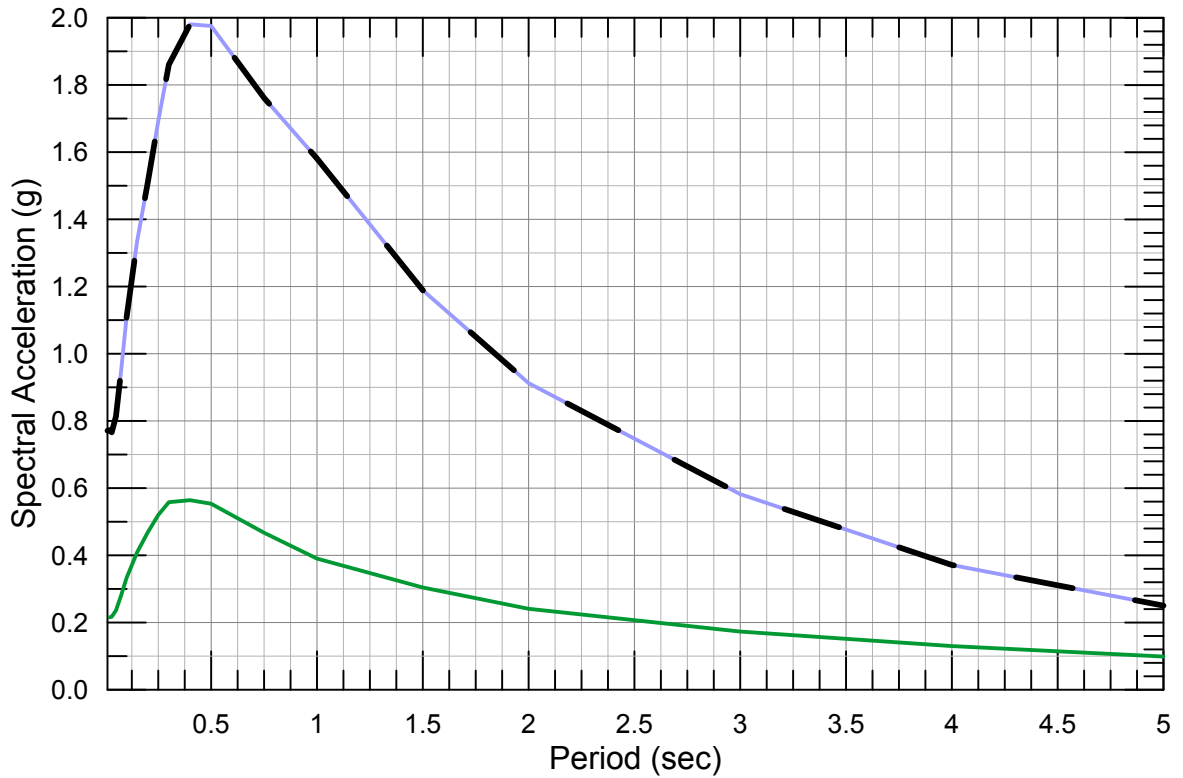
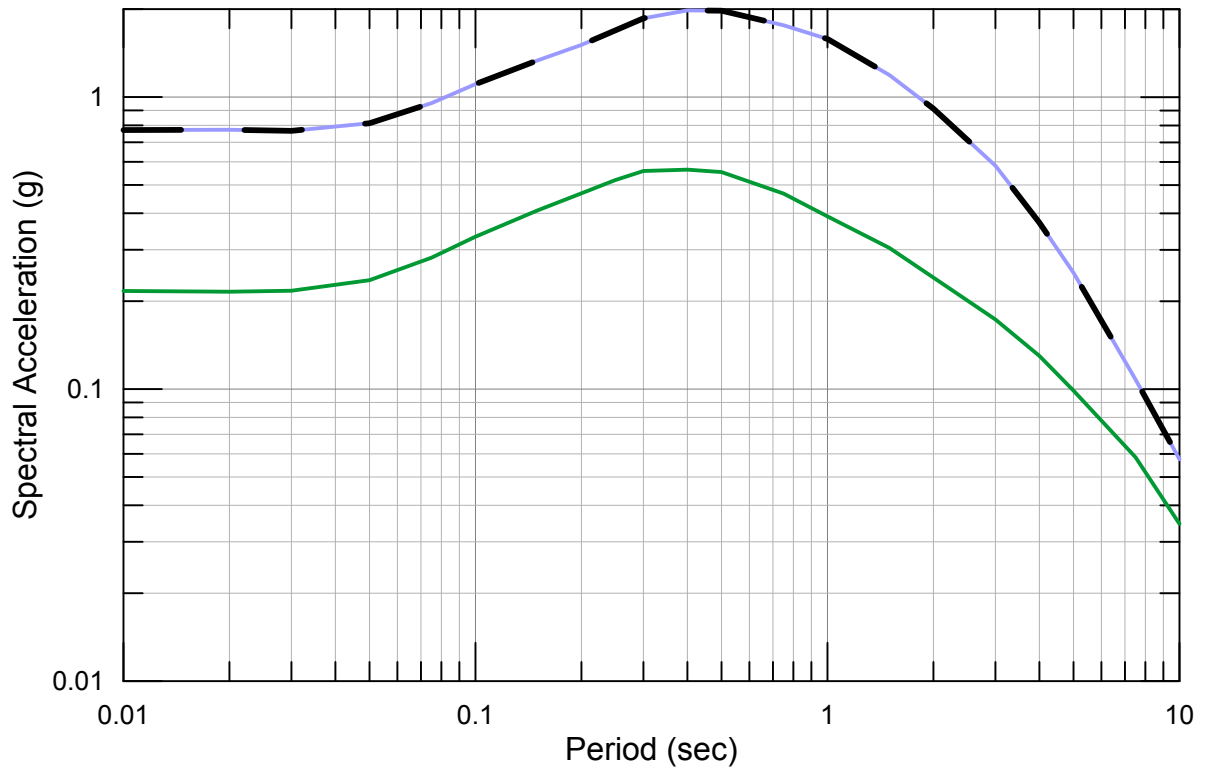
- Enveloped 84th Percentile Deterministic
- Midland Fault
- West Tracy Fault
- San Andreas Fault
- Greenville Fault
- Mt. Diablo, top 1km
- Mt. Diablo, top 5km
- Orestimba, top 1km
- Orestimba, top 3km



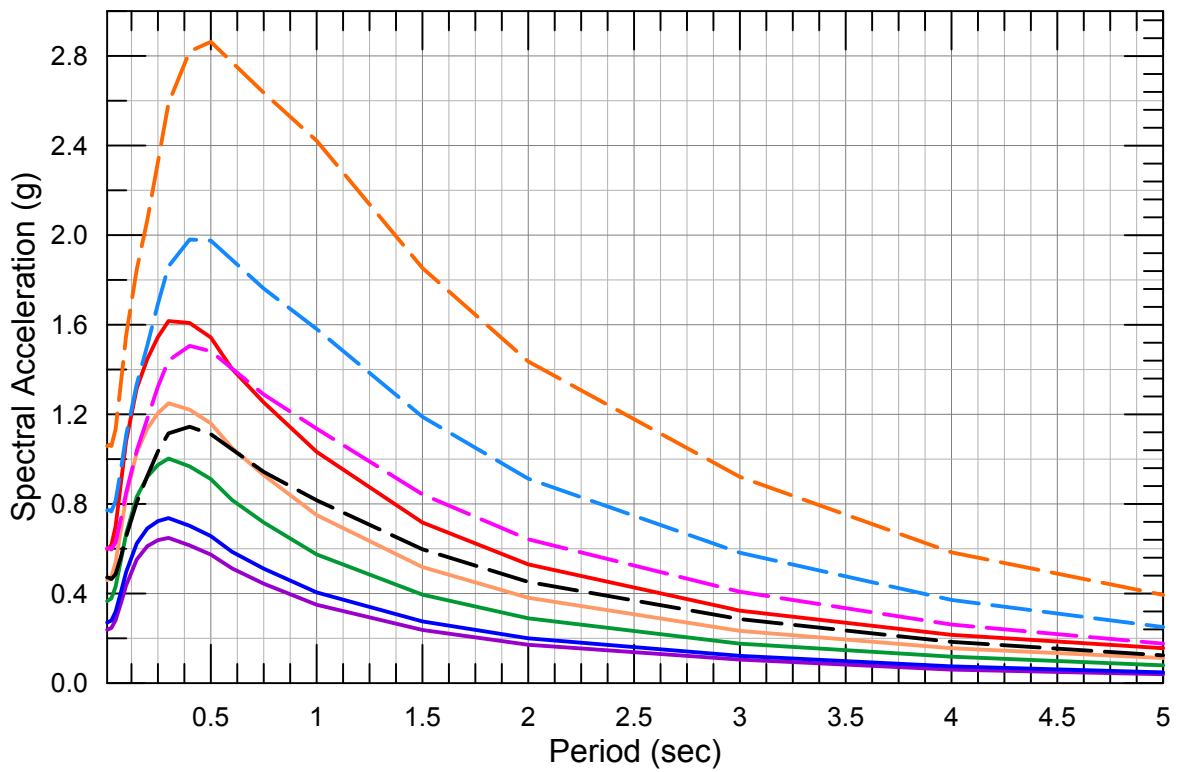
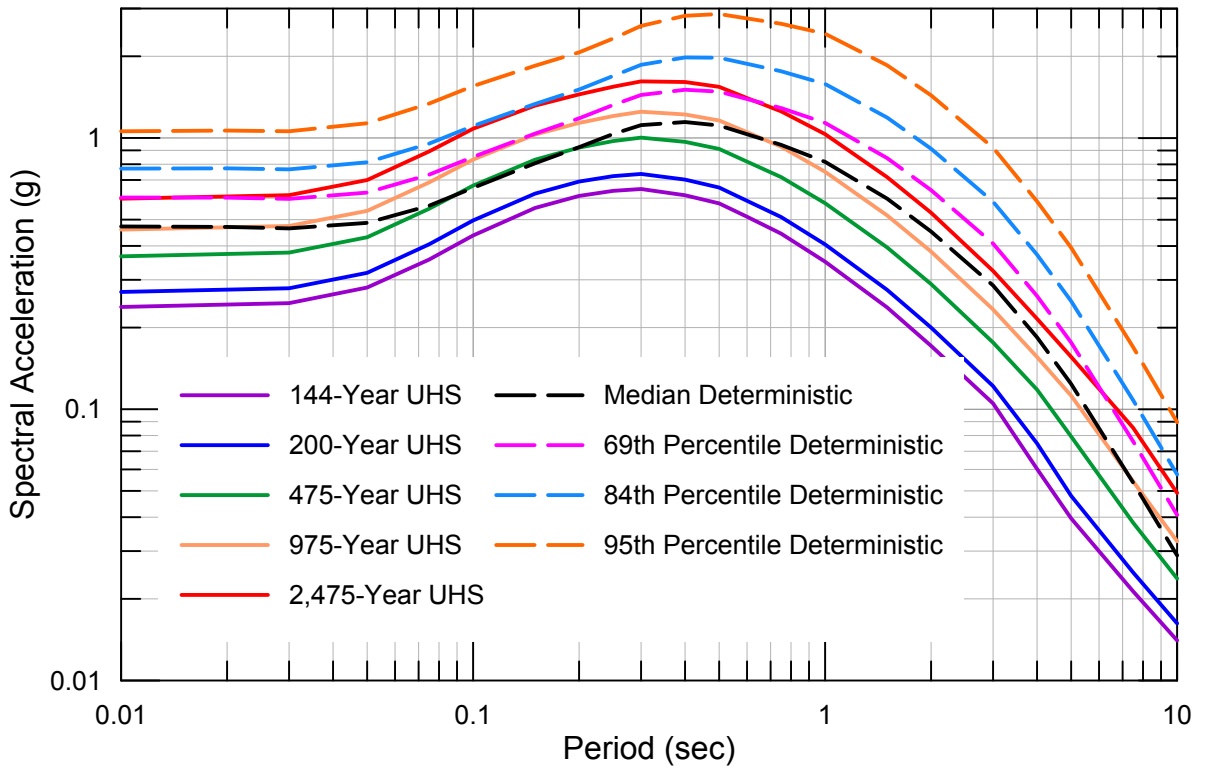


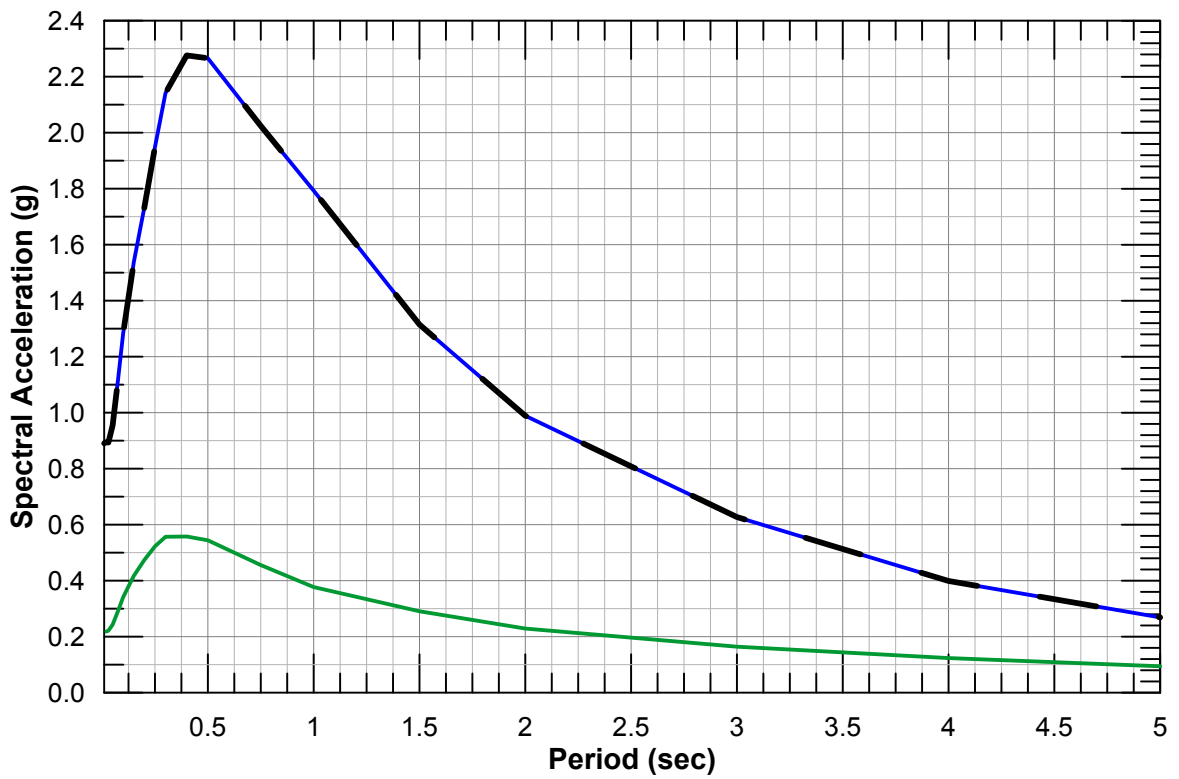
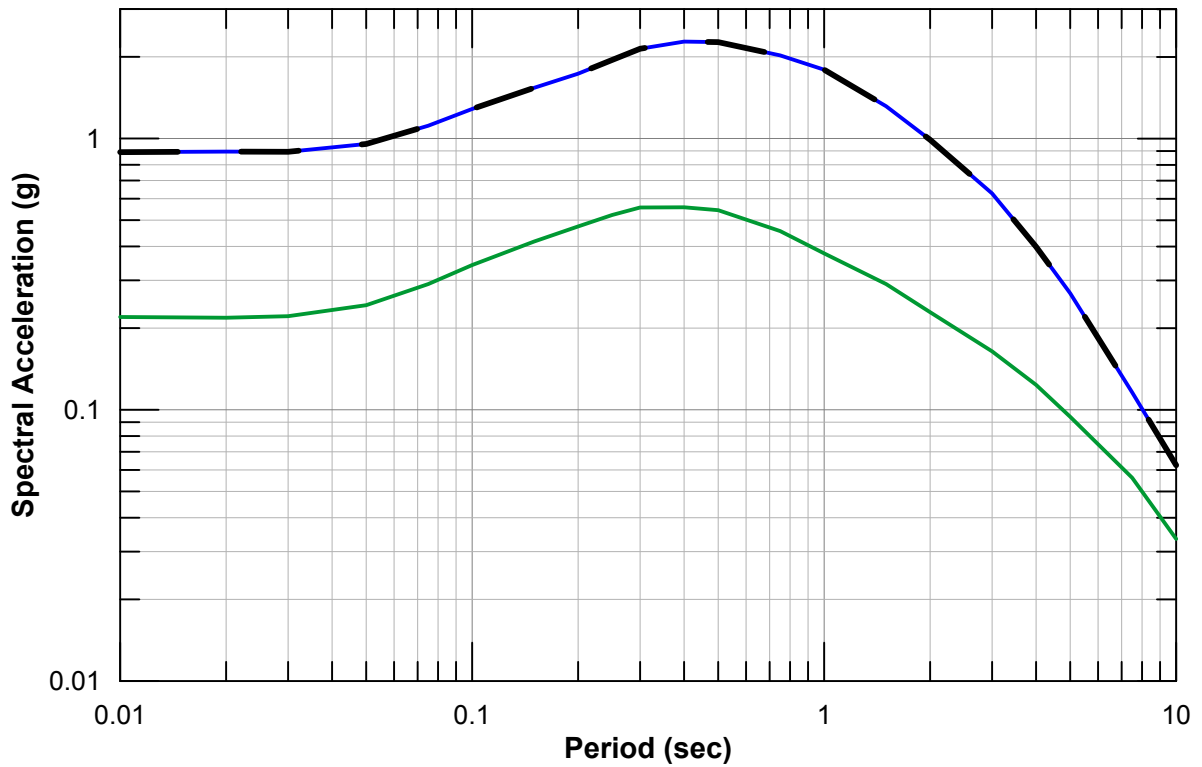
- | | | | |
|---|---|---|---------------------|
| — | Enveloped 84th Percentile Deterministic | — | Greenville Fault |
| — | Midland Fault | — | Mt. Diablo, top 1km |
| — | West Tracy Fault | — | Mt. Diablo, top 5km |
| — | San Andreas Fault | | |



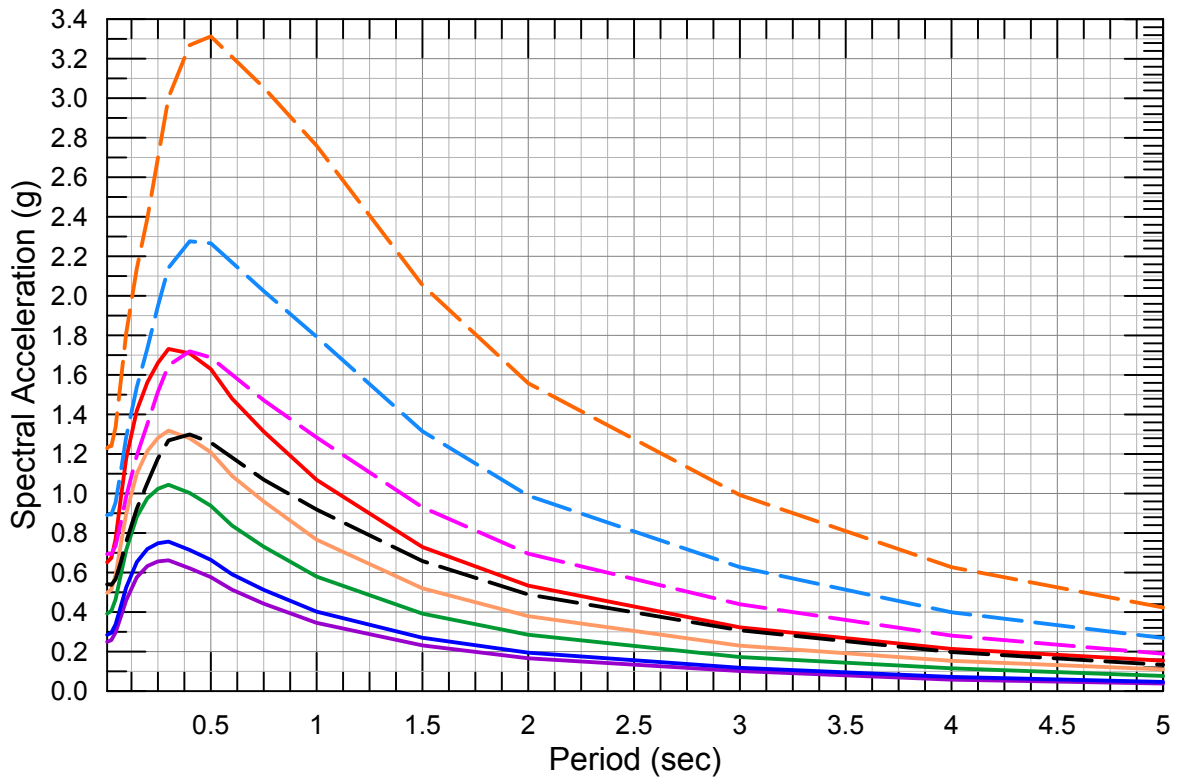
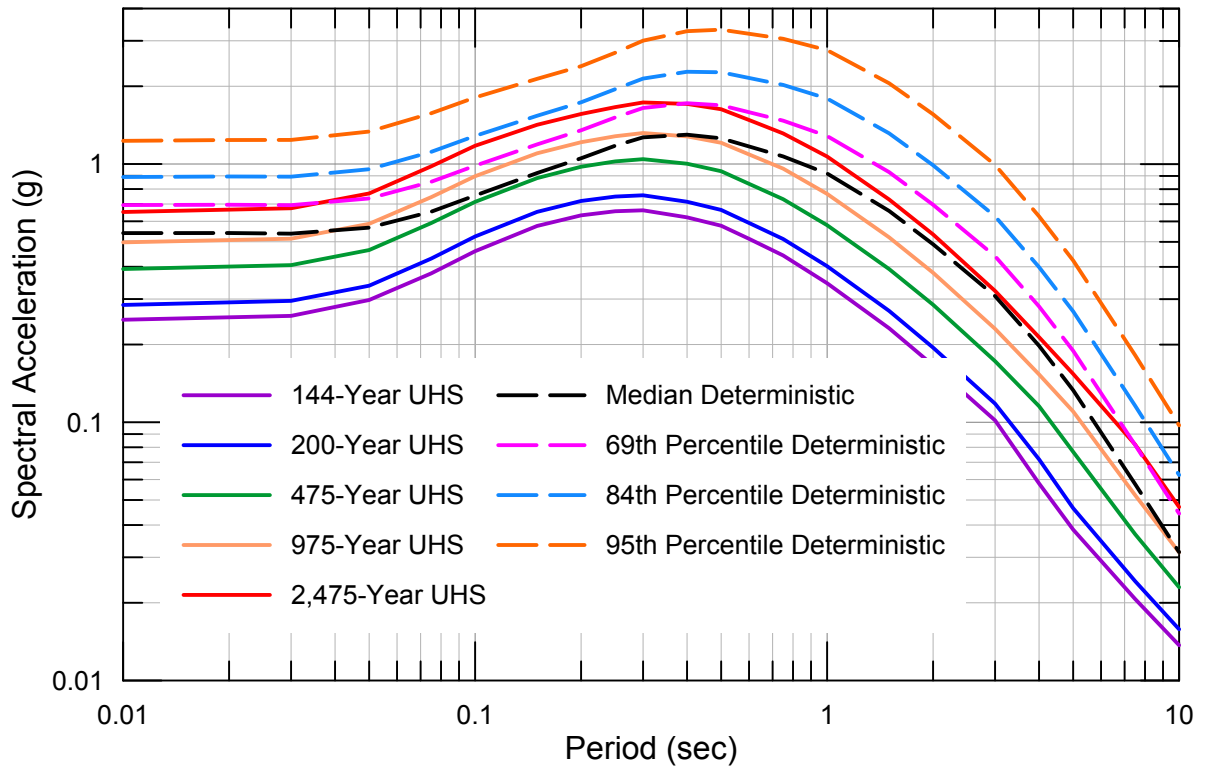


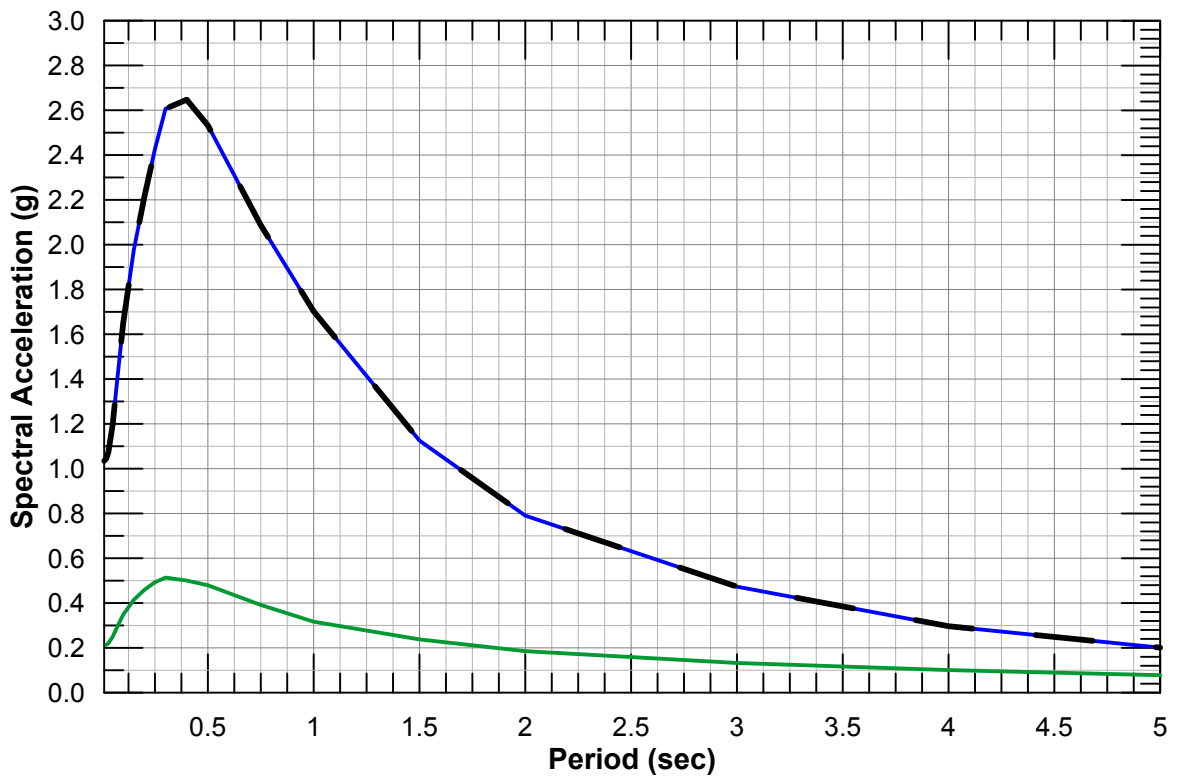
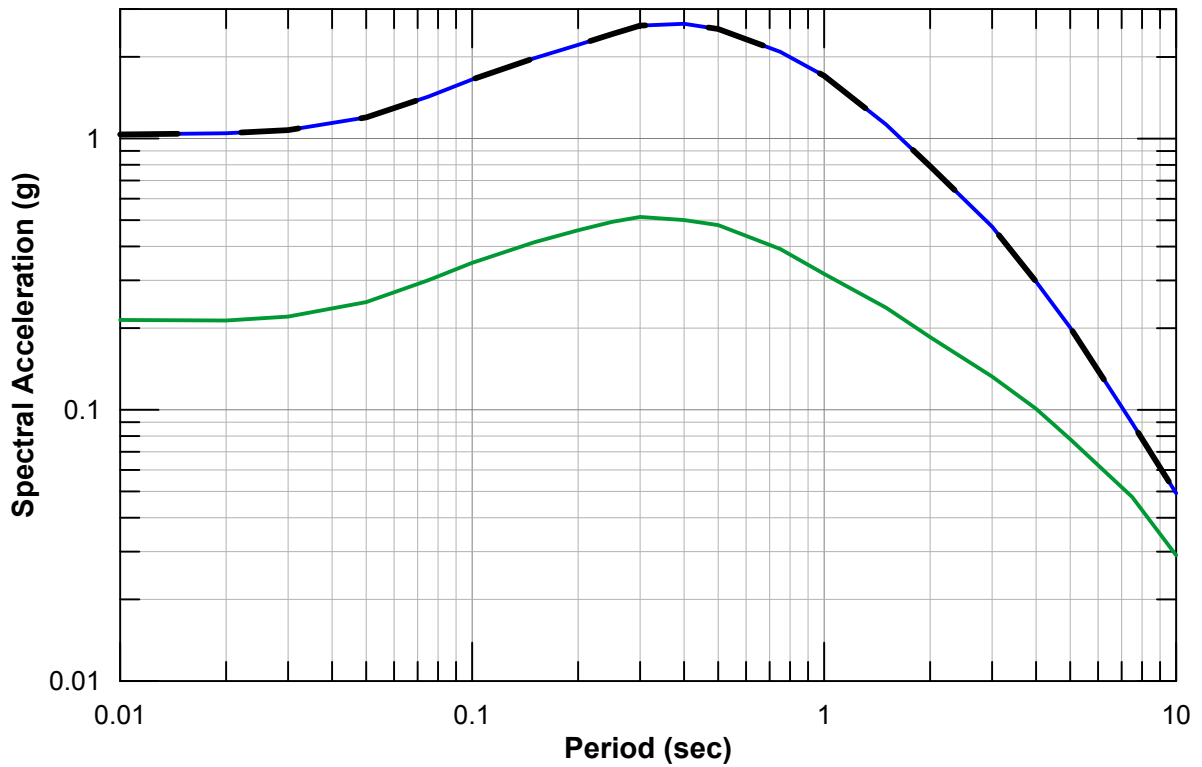
- Enveloped 84th Percentile Deterministic
- San Andreas Fault
- West Tracy



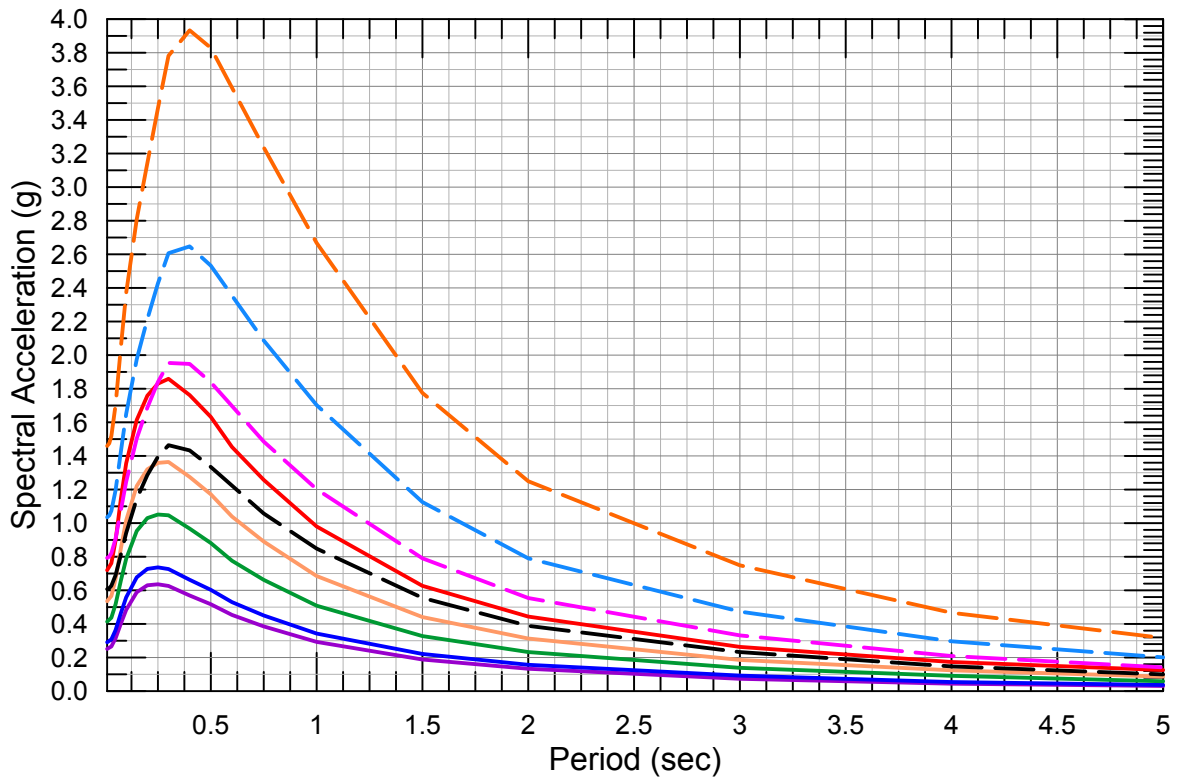
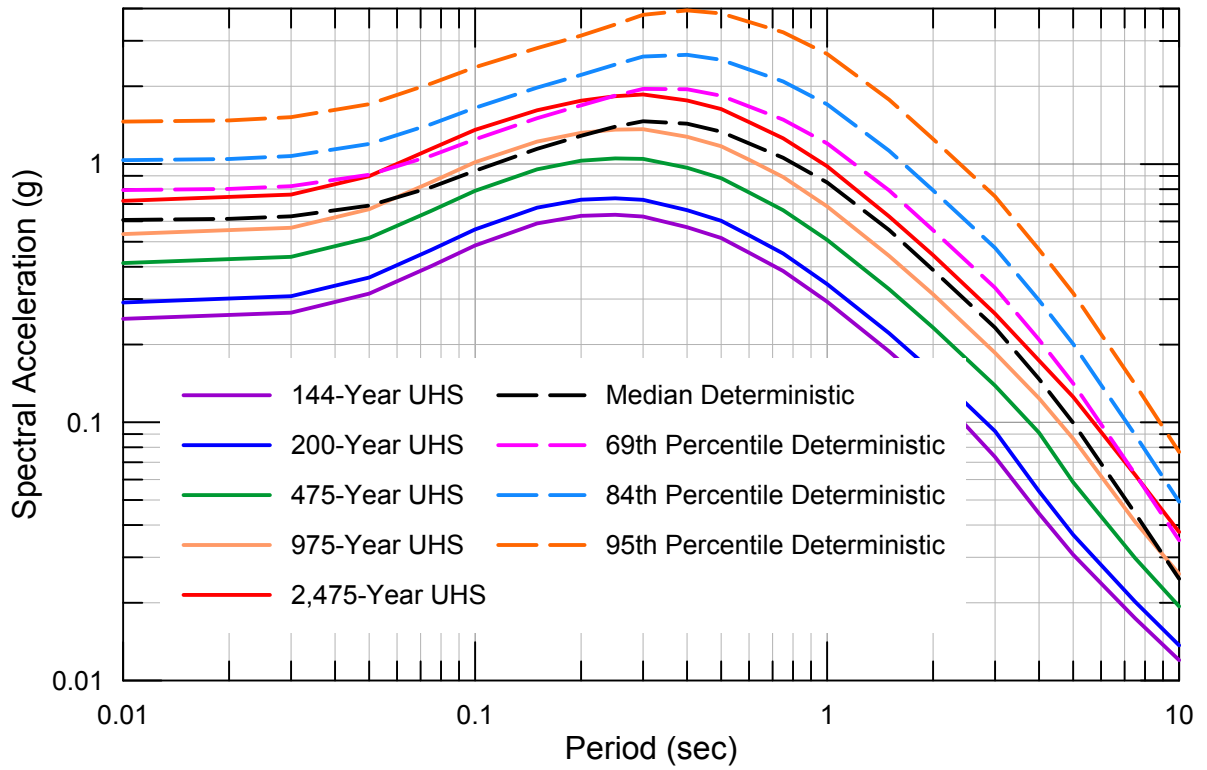


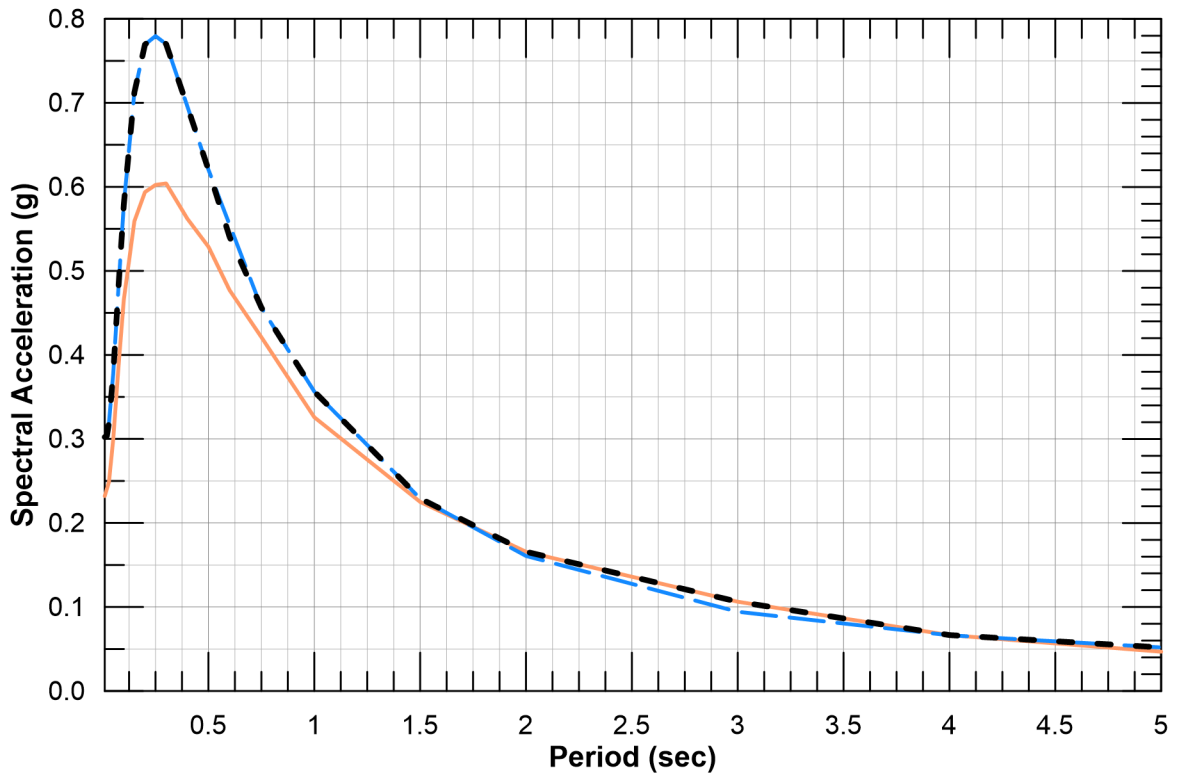
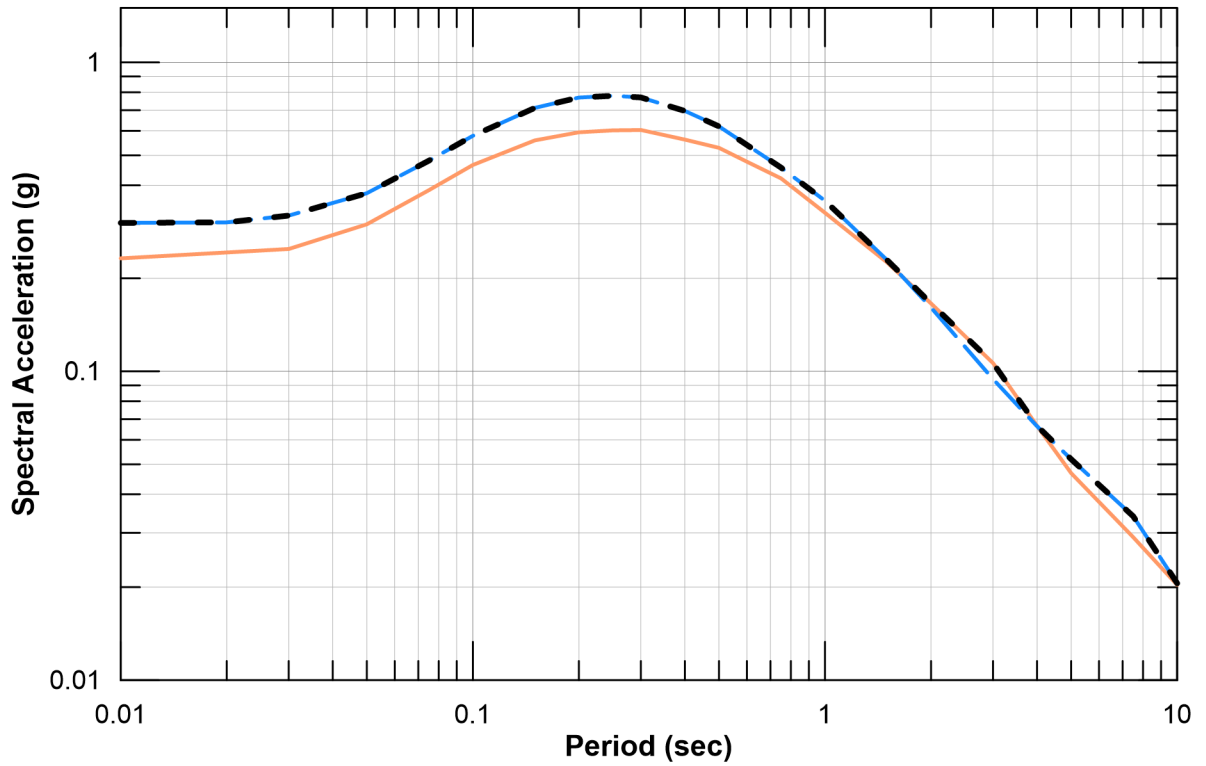
Enveloped 84th Percentile Deterministic
 San Andreas Fault
 West Tracy Fault



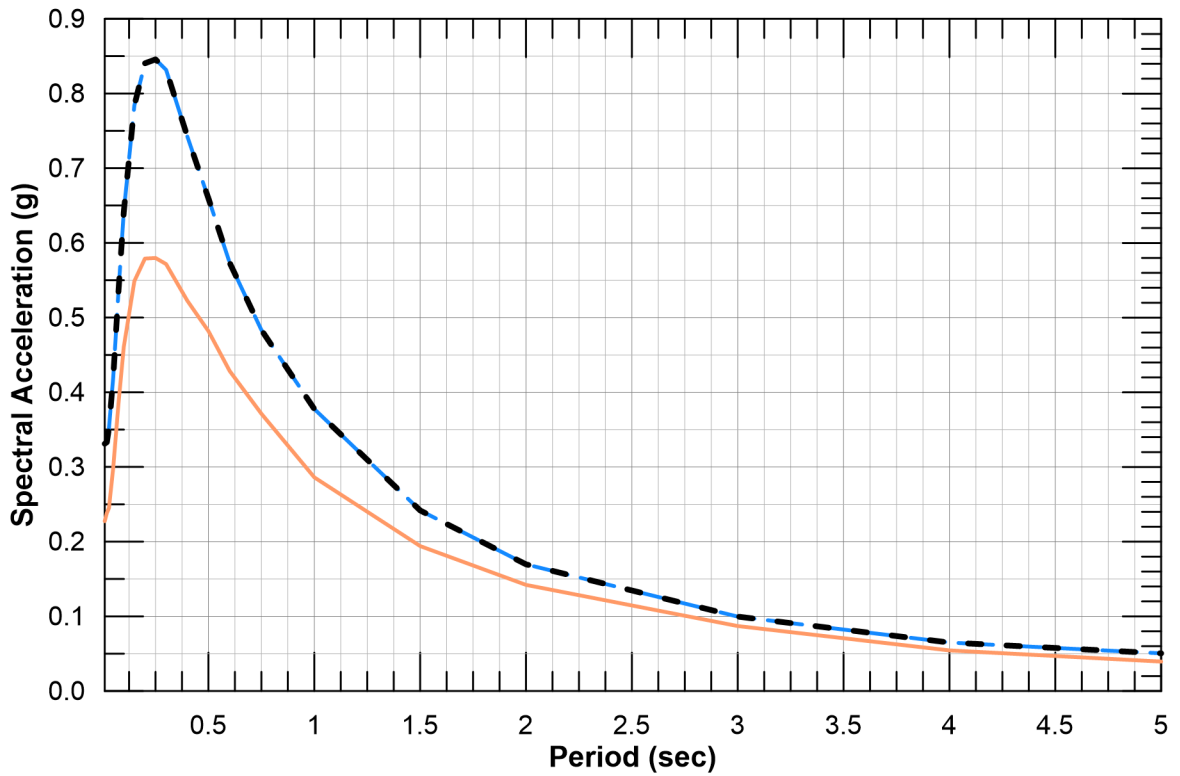
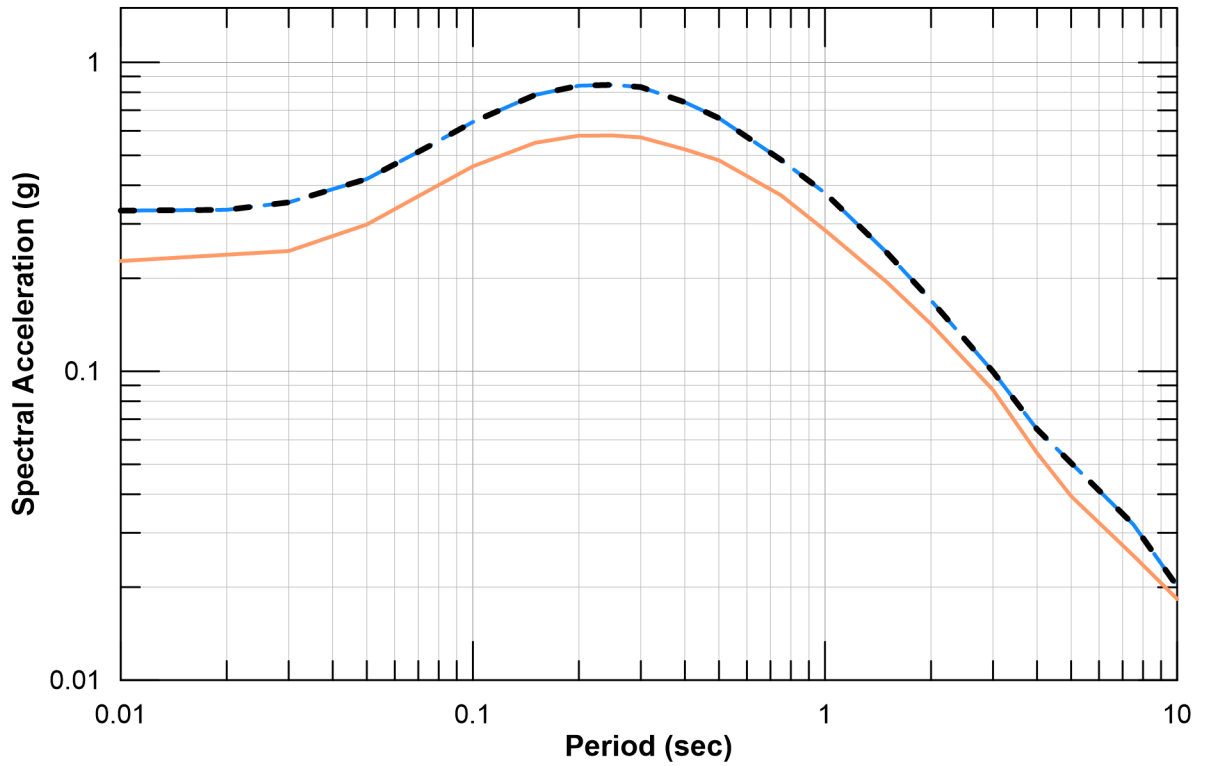


Enveloped 84th Percentile Deterministic
 San Andreas Fault
 West Tracy Fault

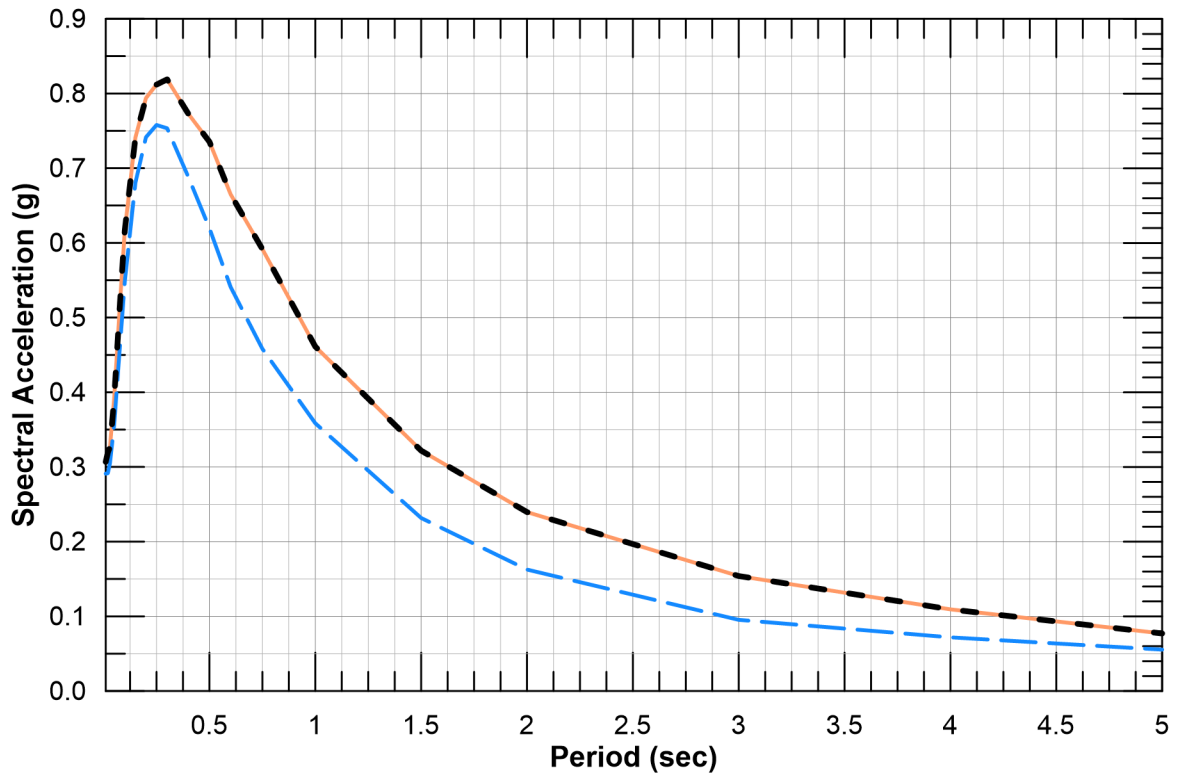
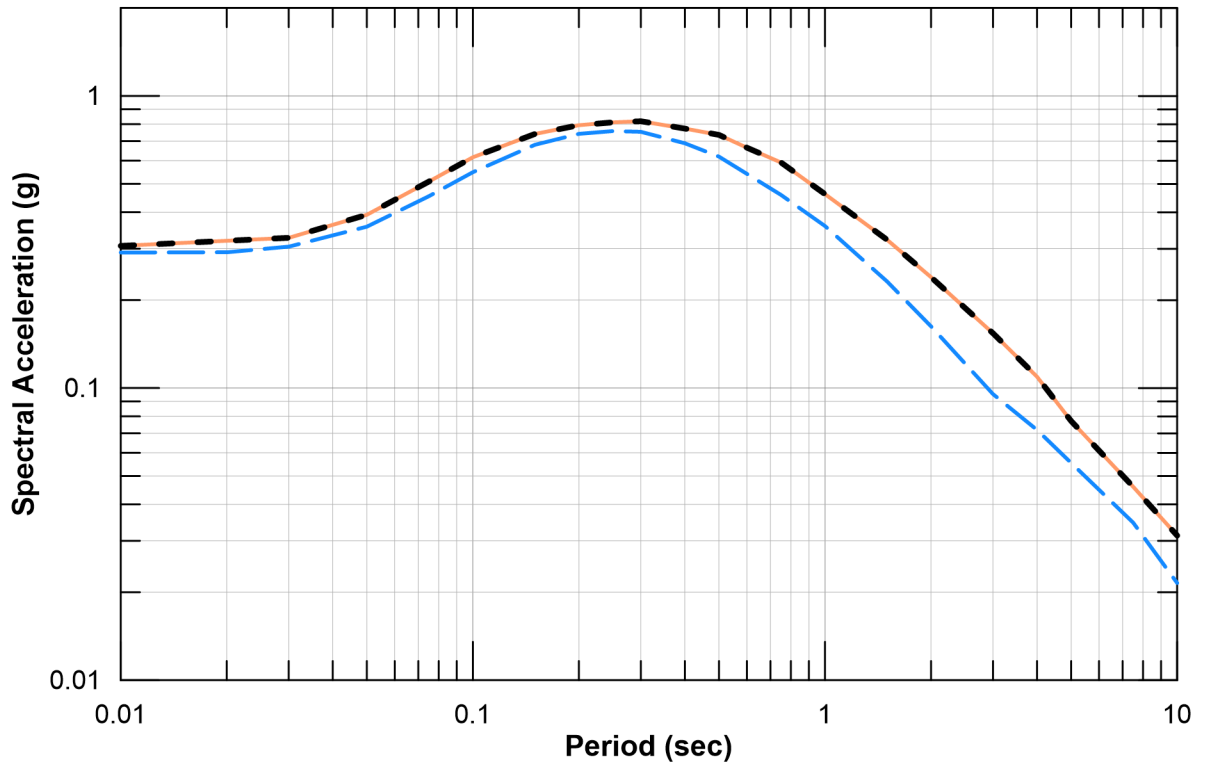




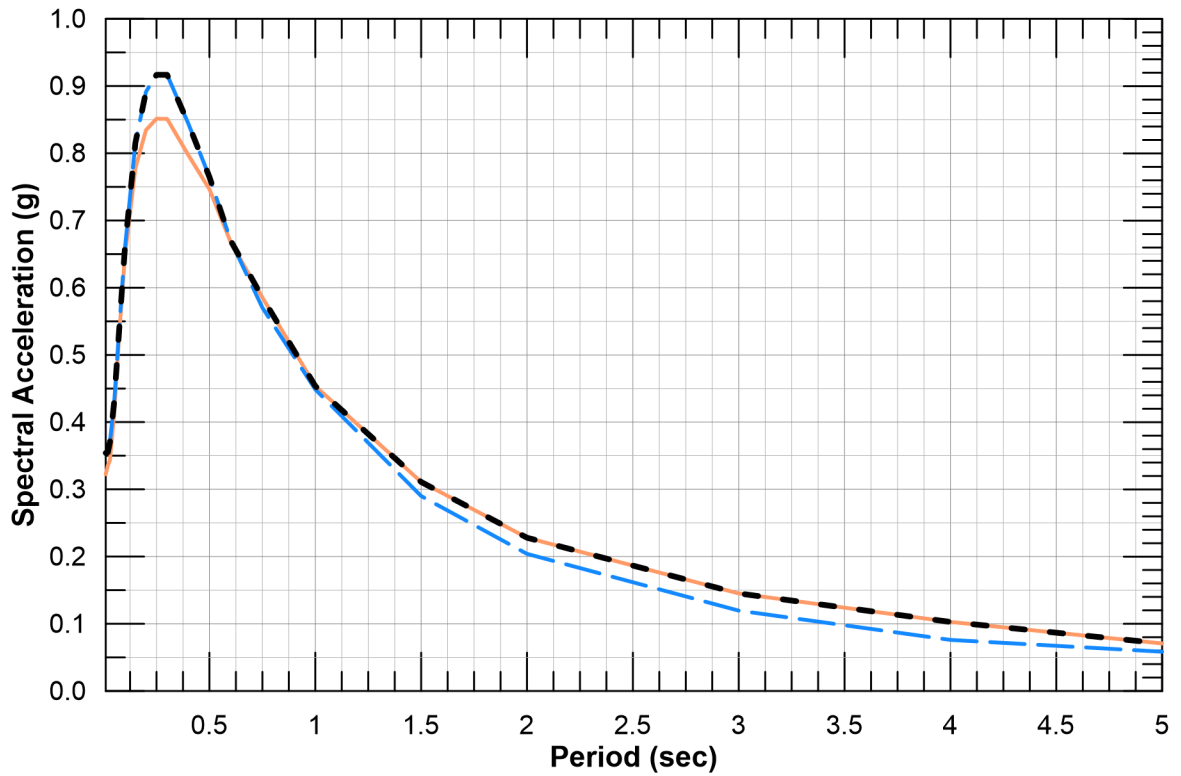
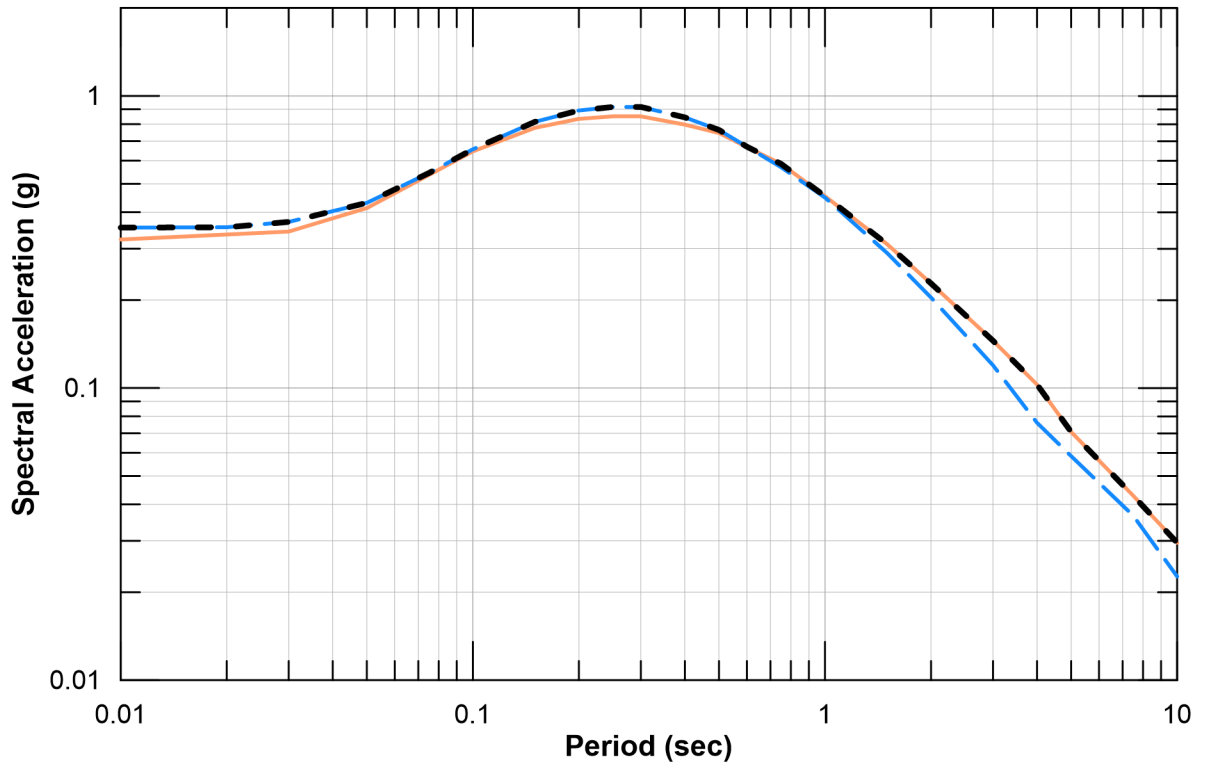
- 975-Year Uniform Hazard Spectrum
- - - 84th Percentile Deterministic Spectrum
- - - MDE Spectrum



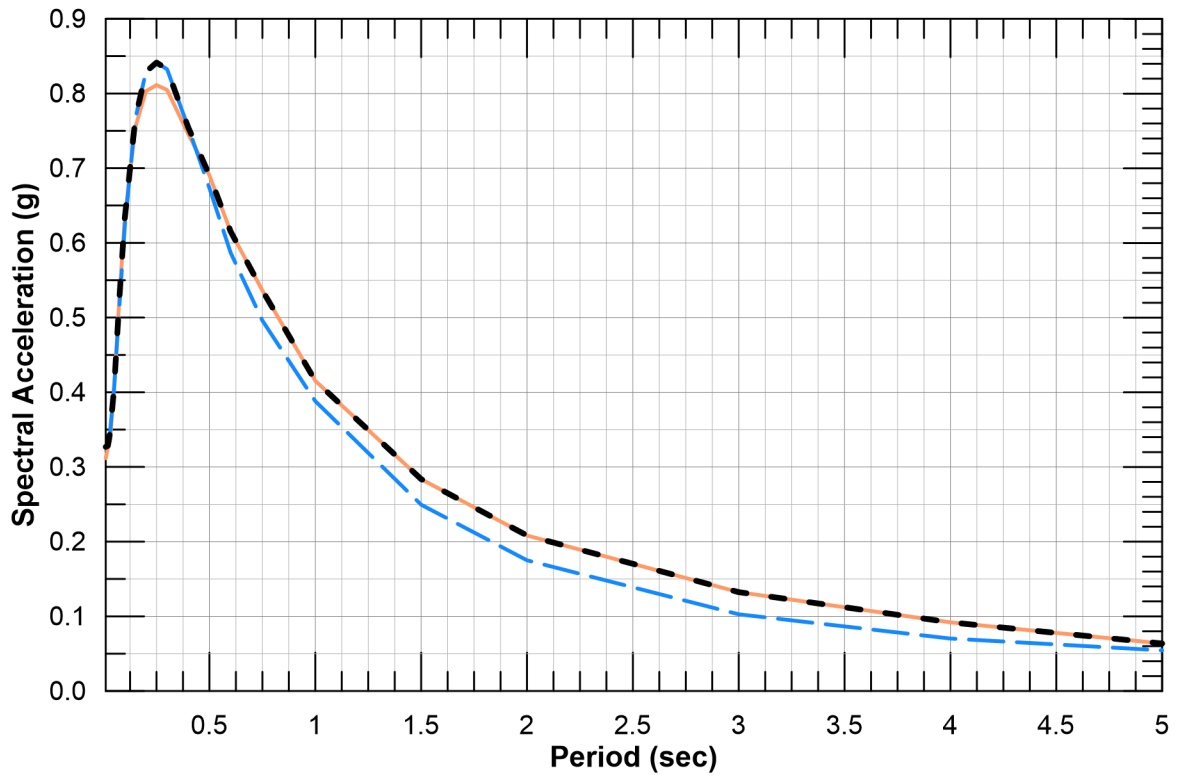
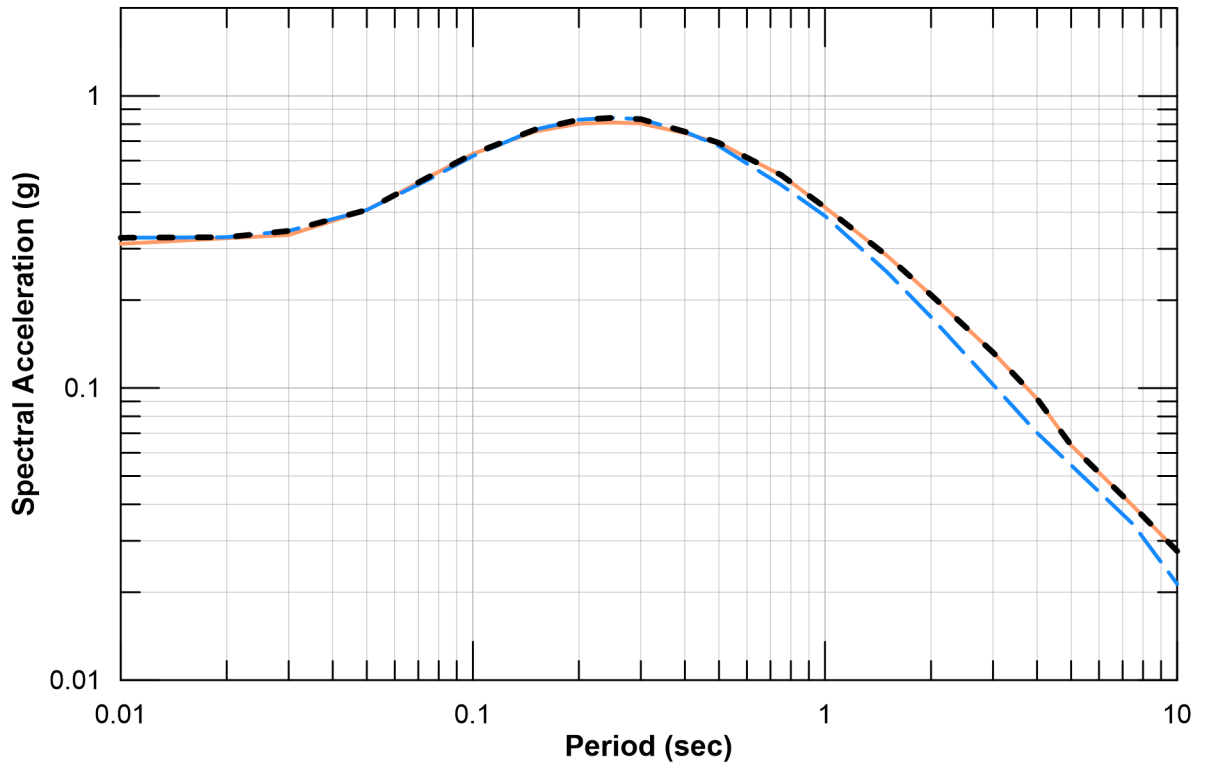
- 975-Year Uniform Hazard Spectrum
- - - 84th Percentile Deterministic Spectrum
- - - MDE Spectrum



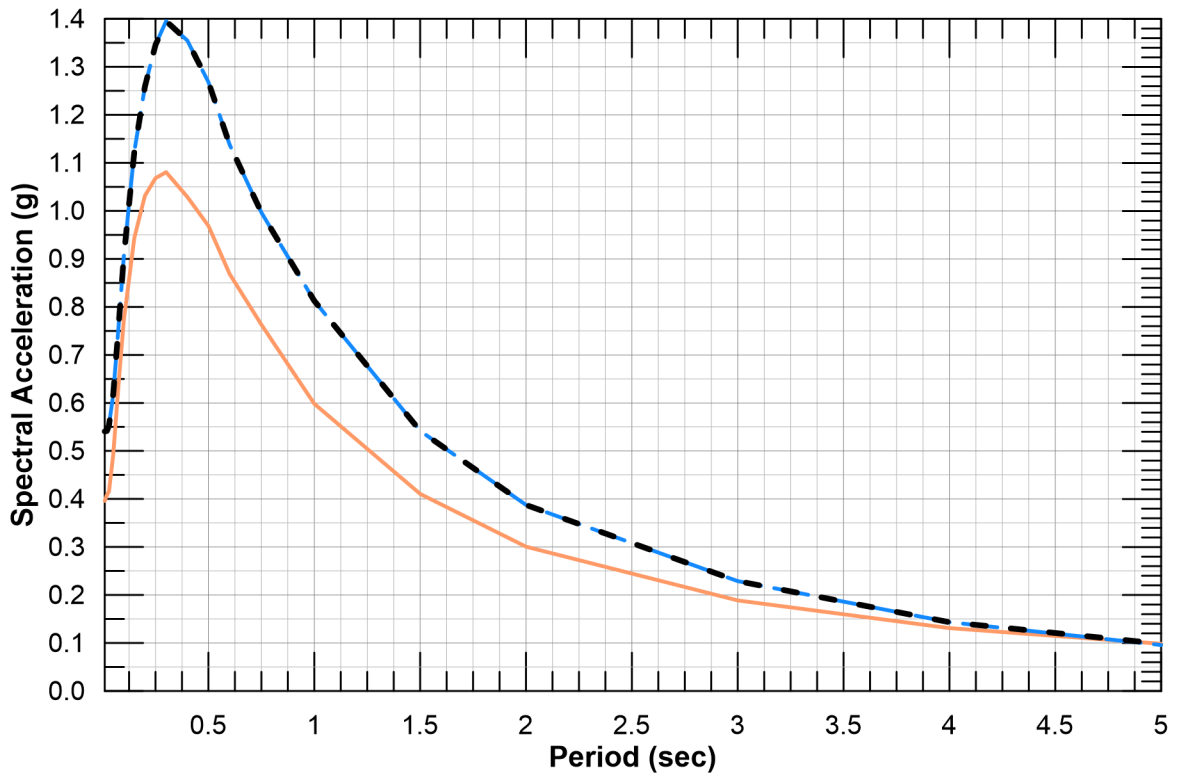
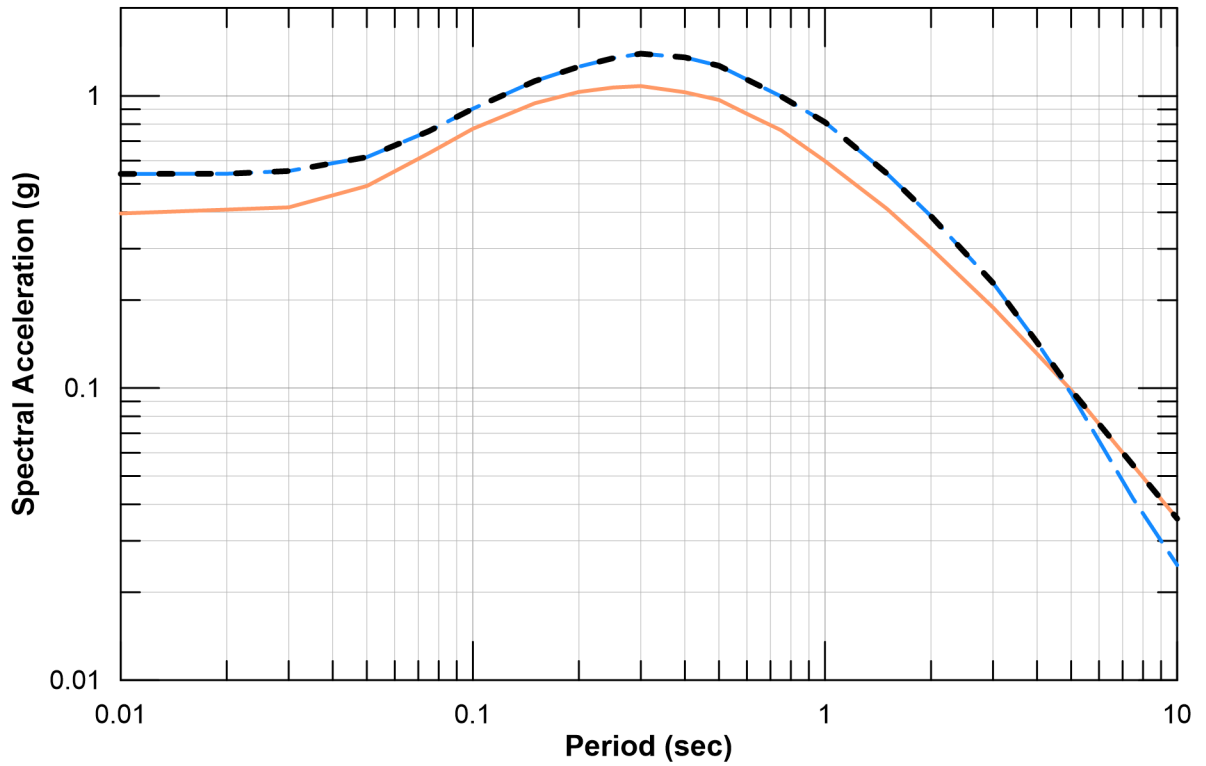
- 2,475-Year Uniform Hazard Spectrum
- - - 84th Percentile Deterministic Spectrum
- - - MDE Spectrum



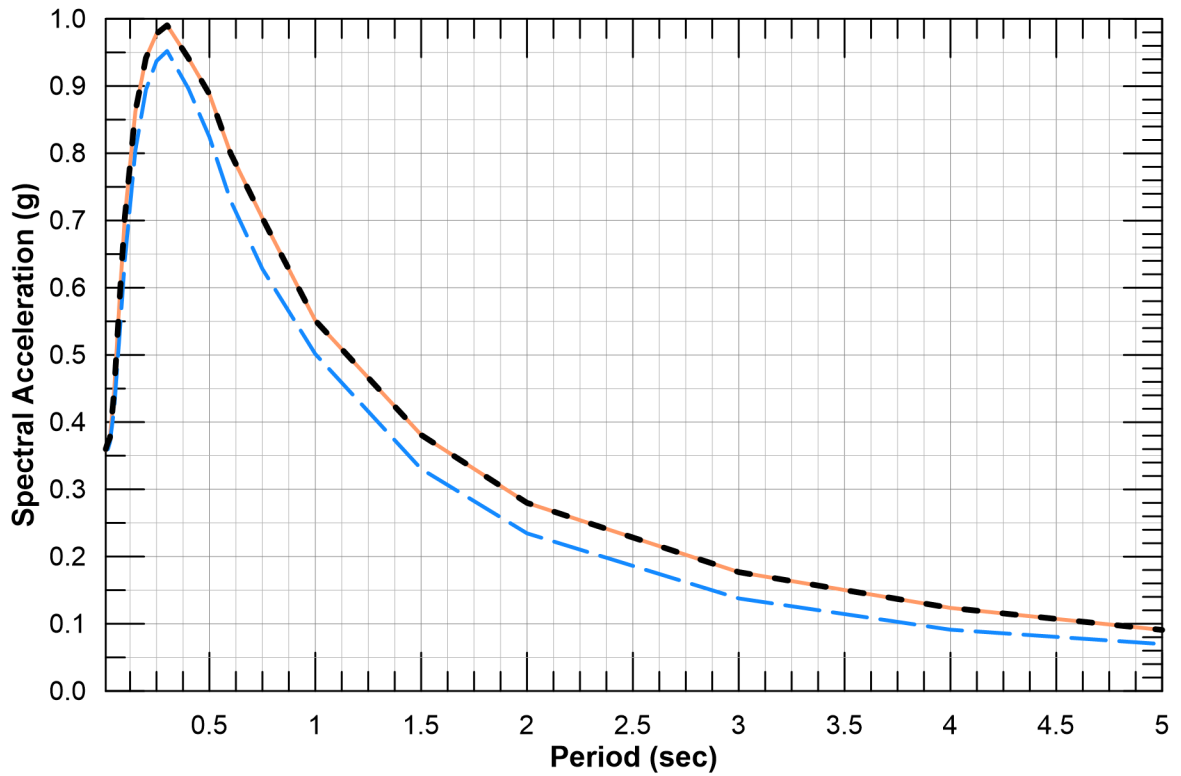
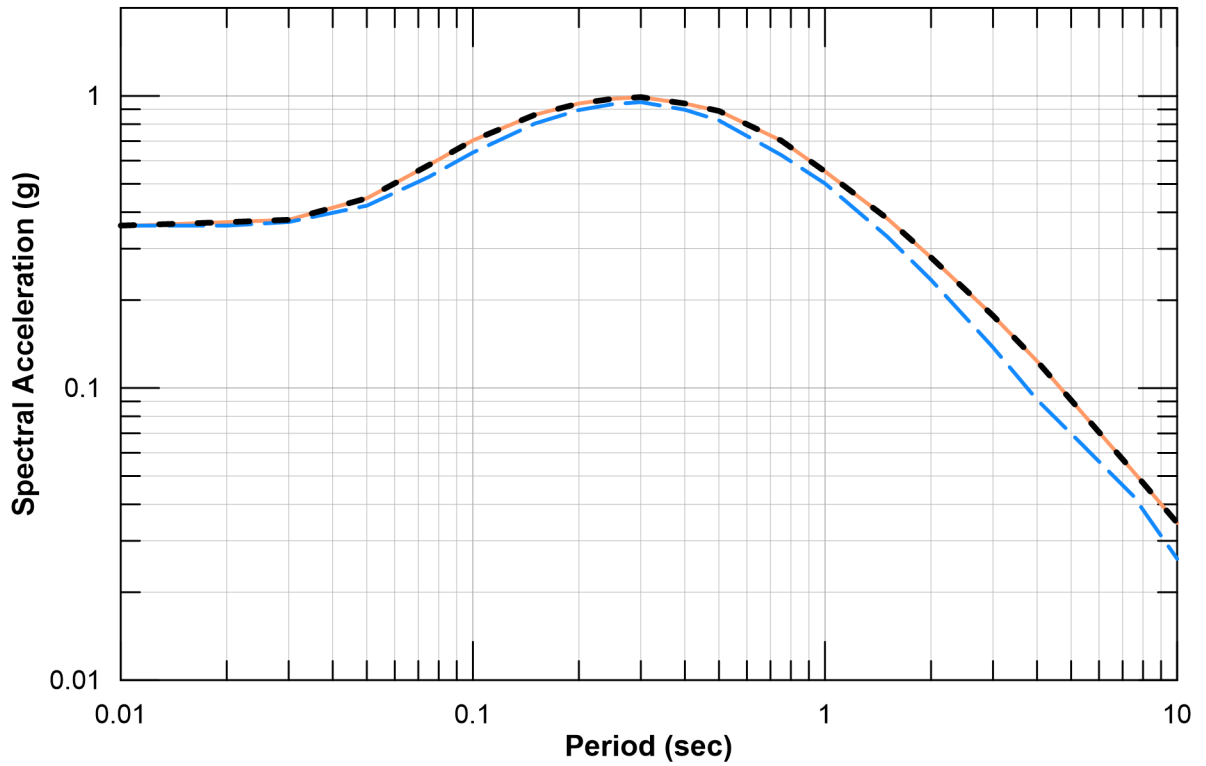
- 2,475-Year Uniform Hazard Spectrum
- - - 84th Percentile Deterministic Spectrum
- - - MDE Spectrum



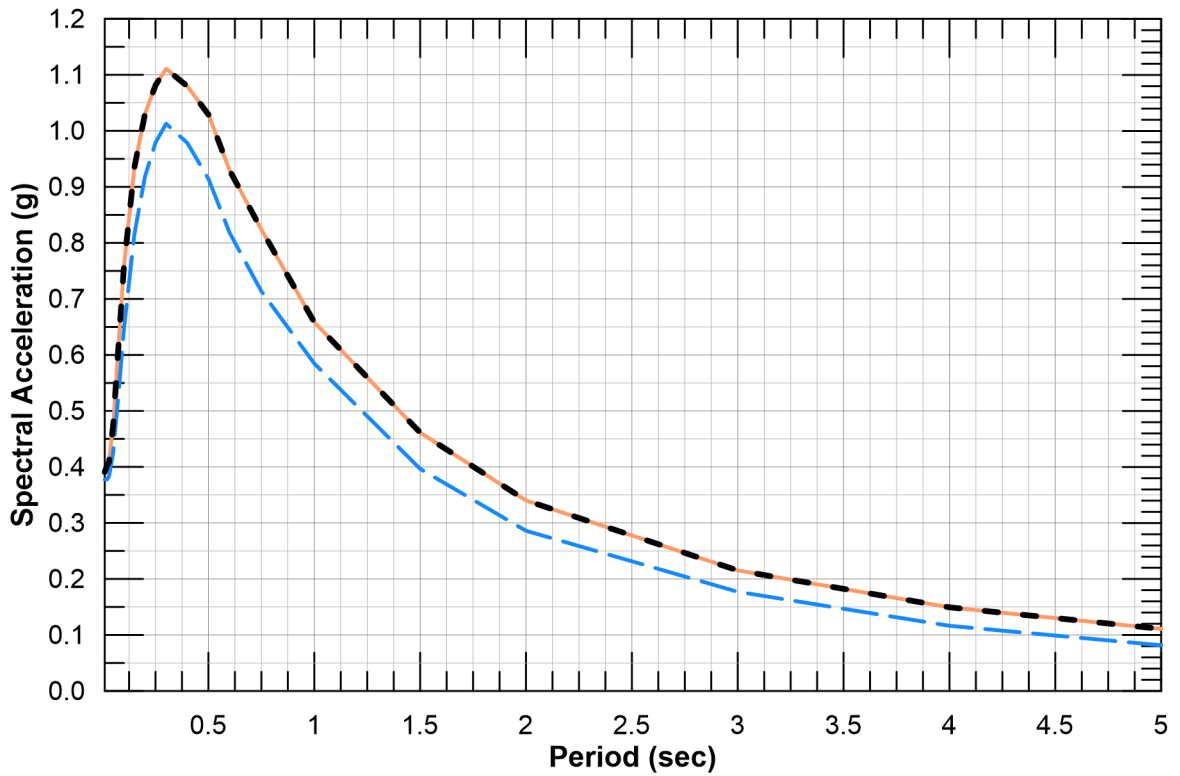
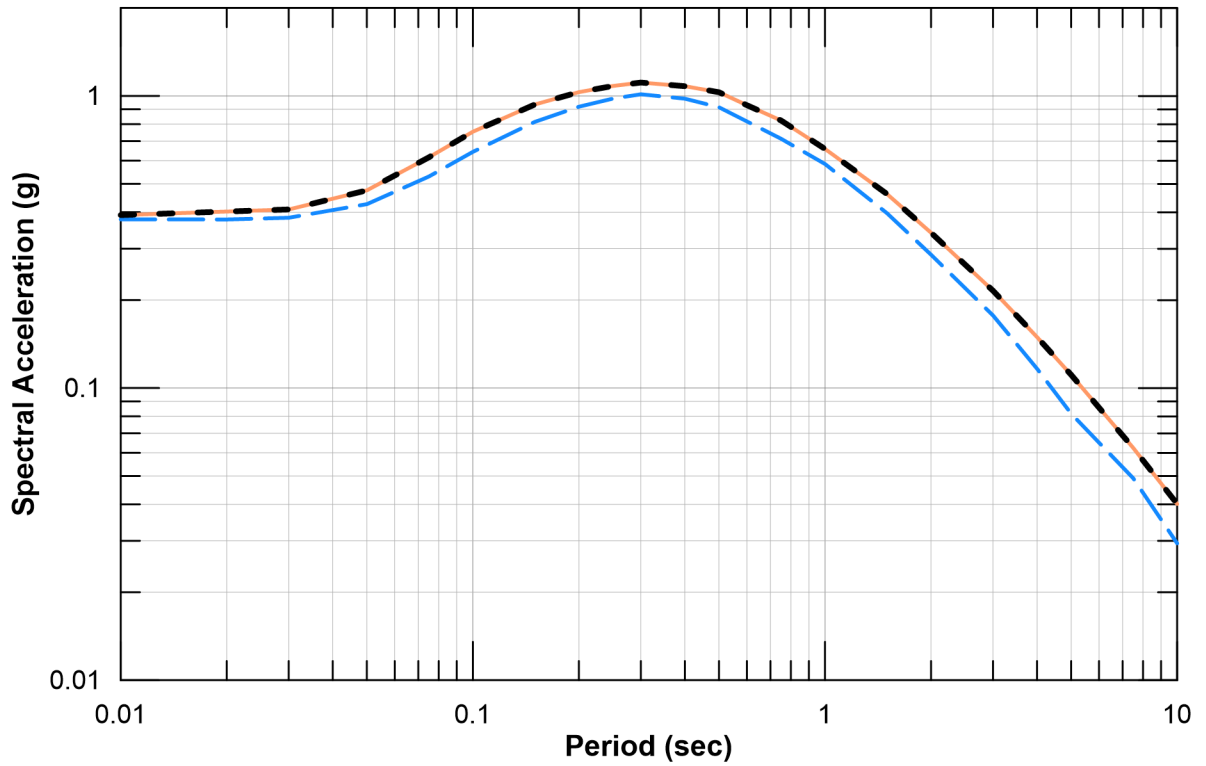
- 2,475-Year Uniform Hazard Spectrum
- - - 84th Percentile Deterministic Spectrum
- - - MDE Spectrum



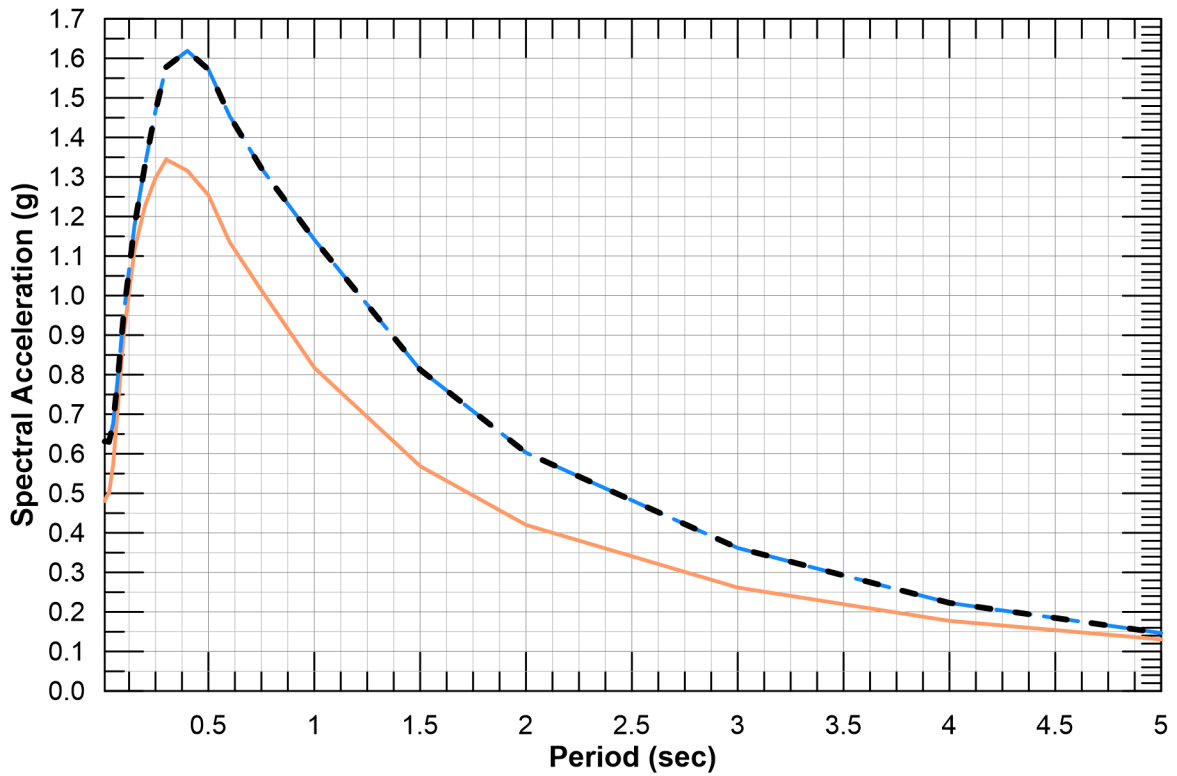
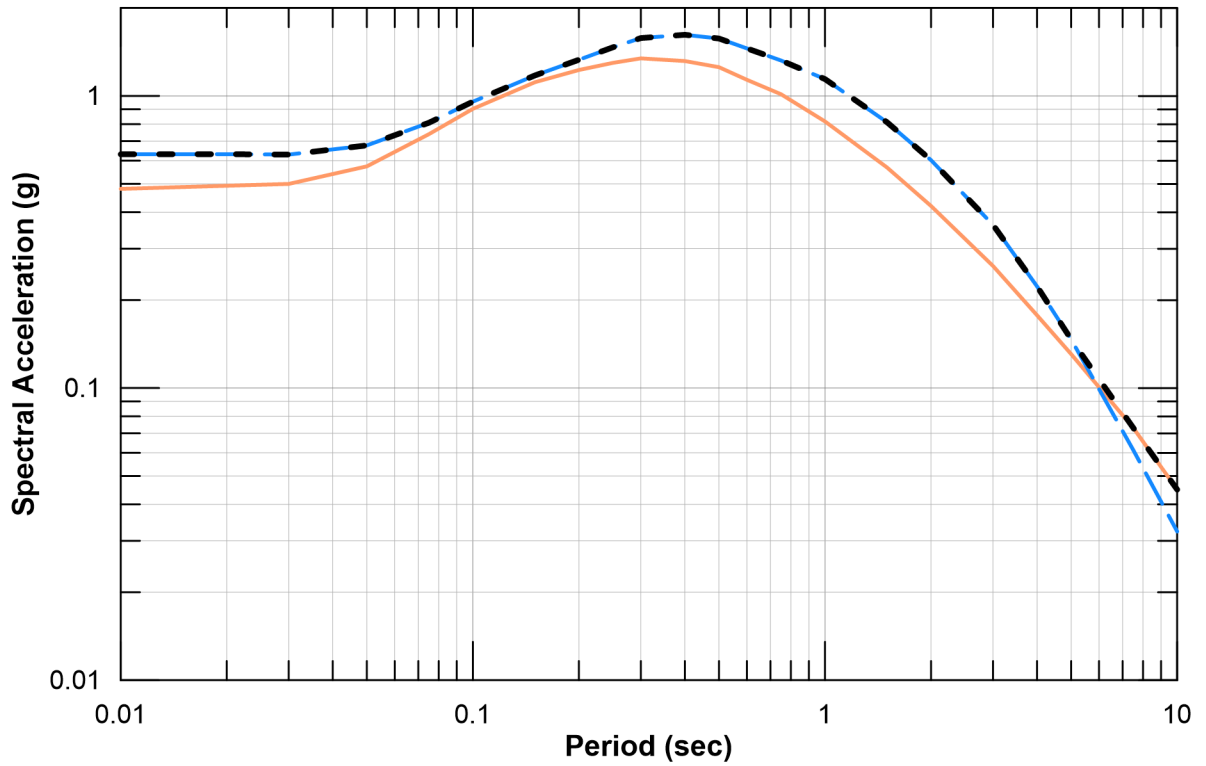
- 2,475-Year Uniform Hazard Spectrum
- - - 84th Percentile Deterministic Spectrum
- - - MDE Spectrum



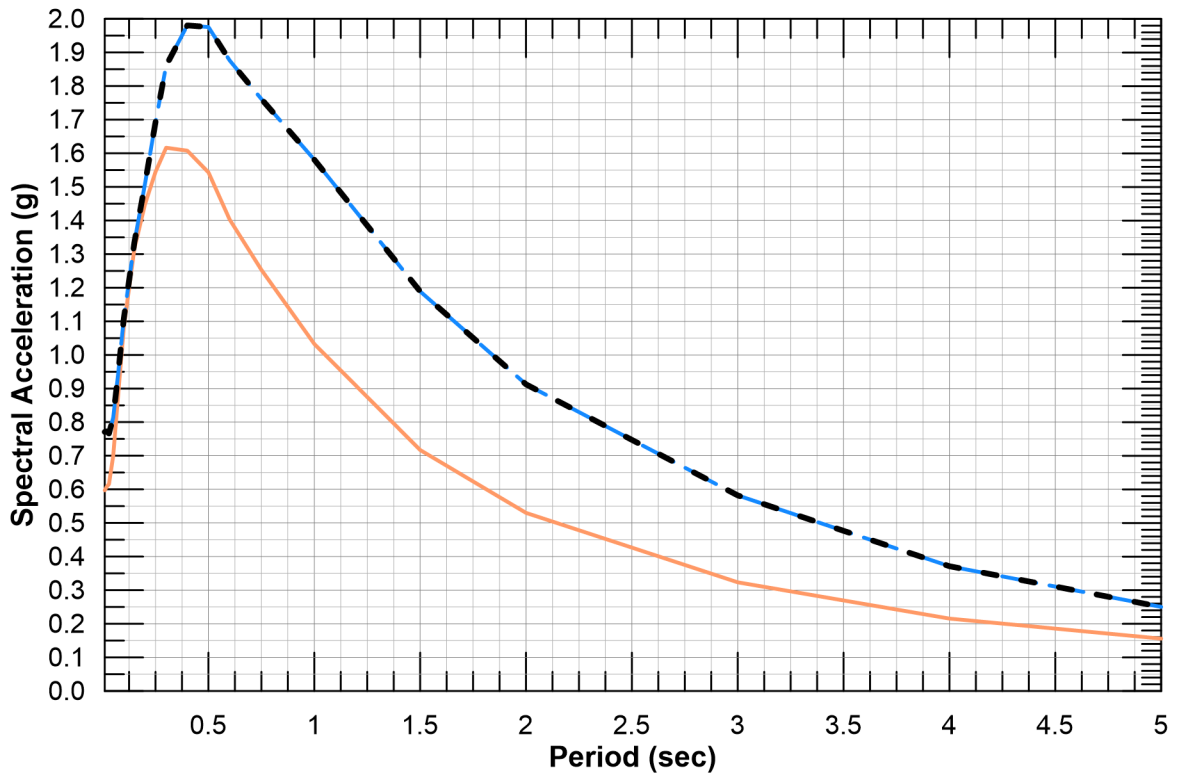
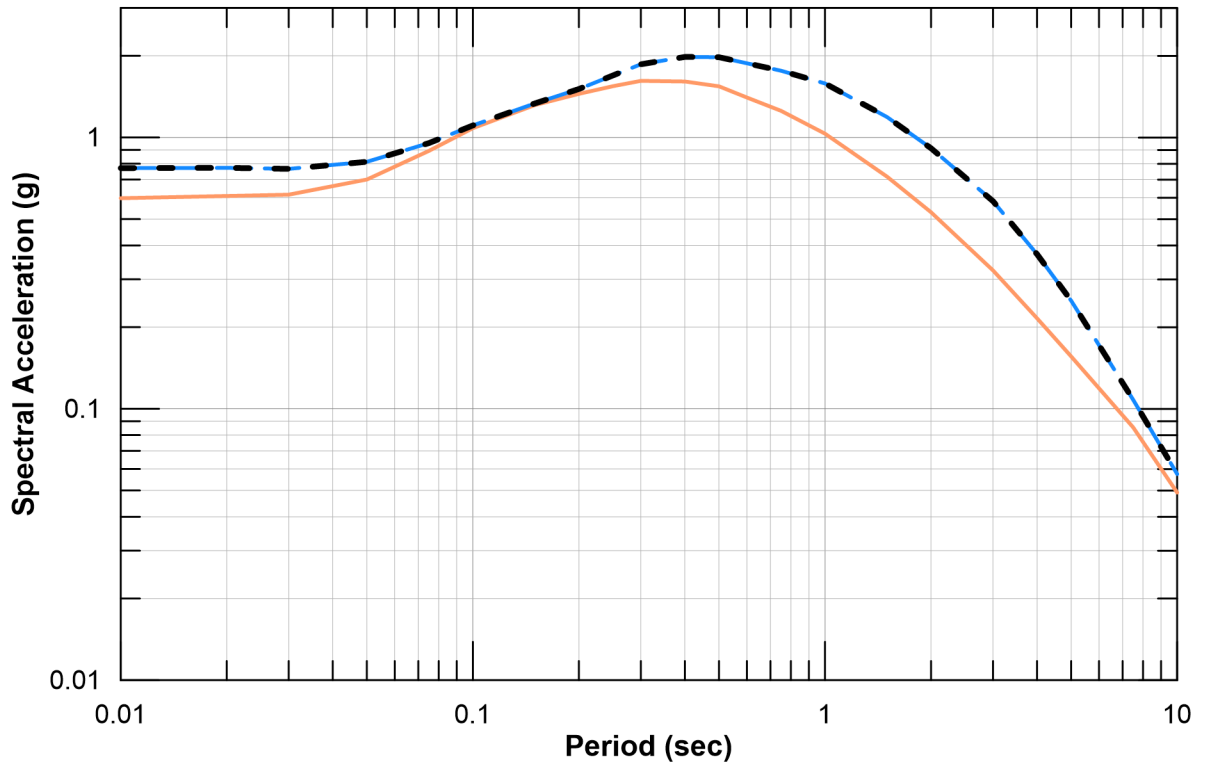
- 2,475-Year Uniform Hazard Spectrum
- - - 84th Percentile Deterministic Spectrum
- - - MDE Spectrum



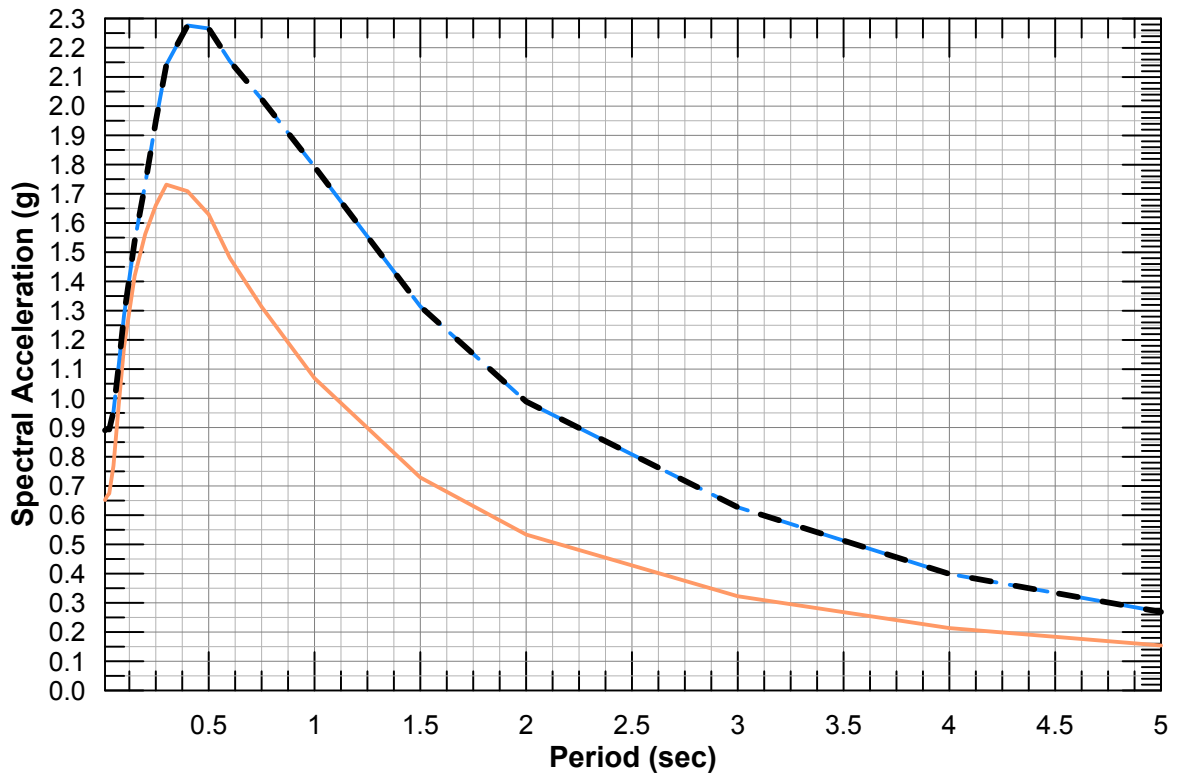
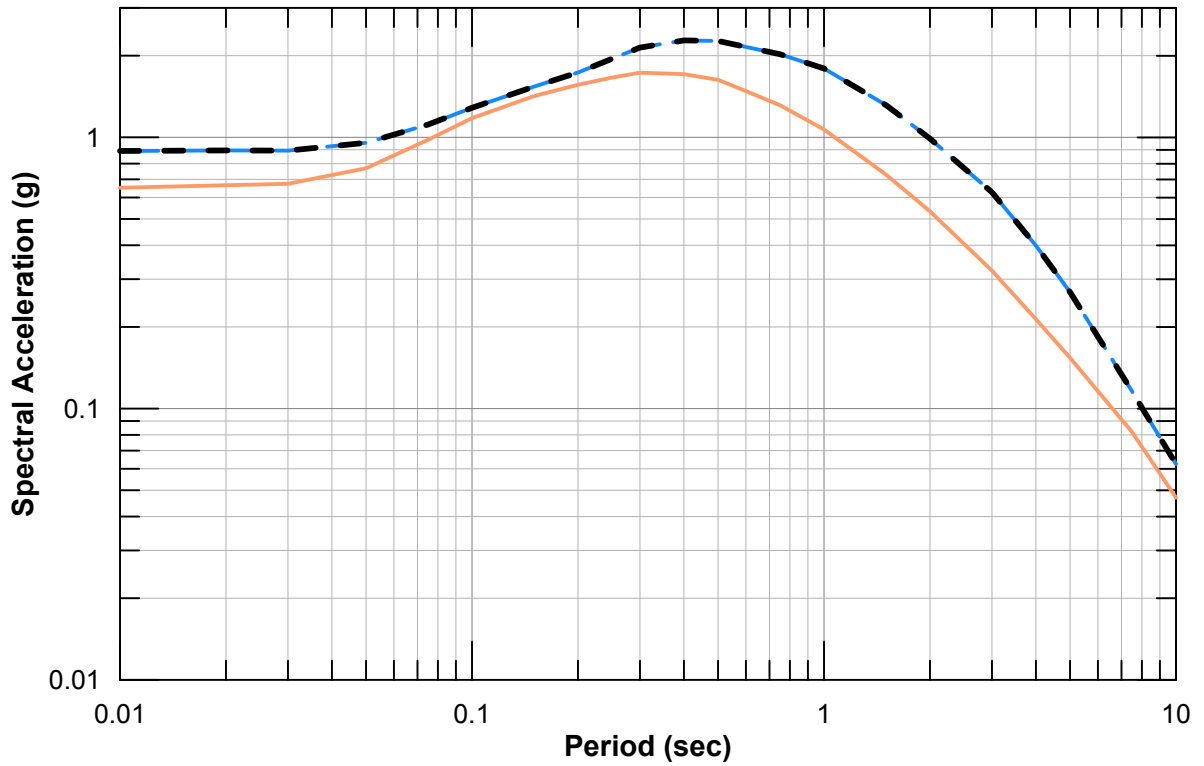
- 2,475-Year Uniform Hazard Spectrum
- - - 84th Percentile Deterministic Spectrum
- - - MDE Spectrum



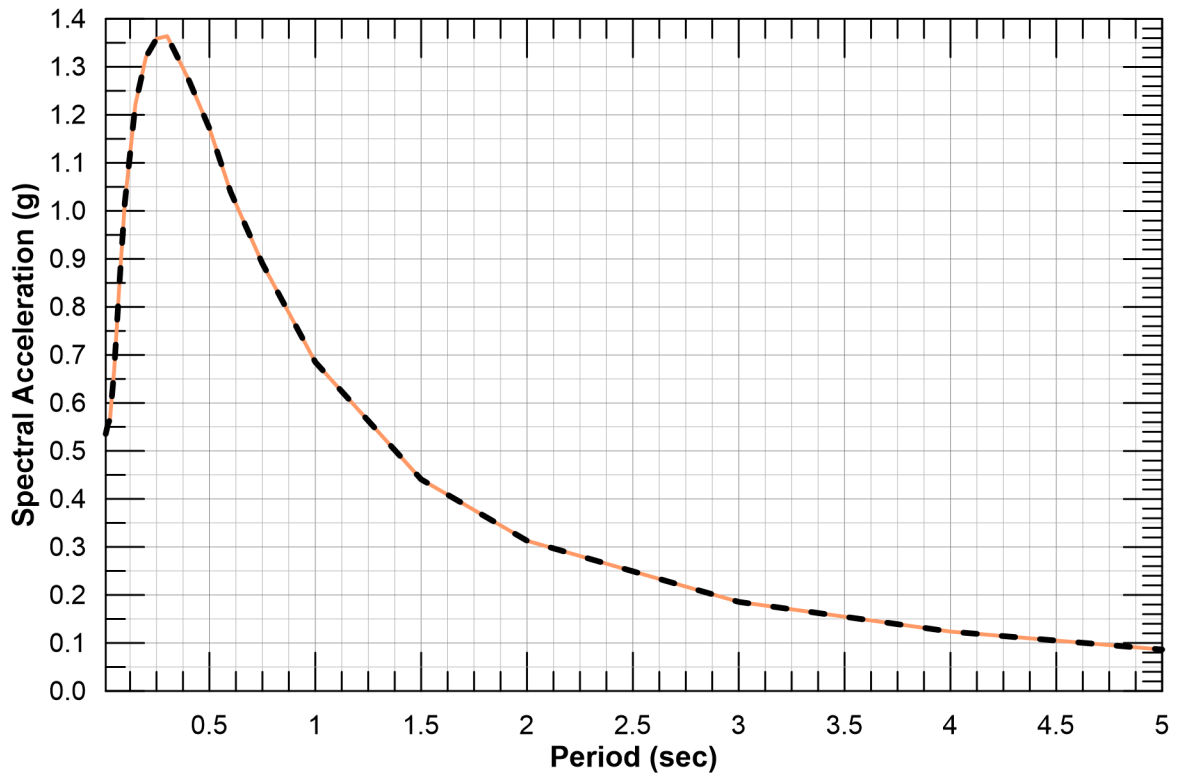
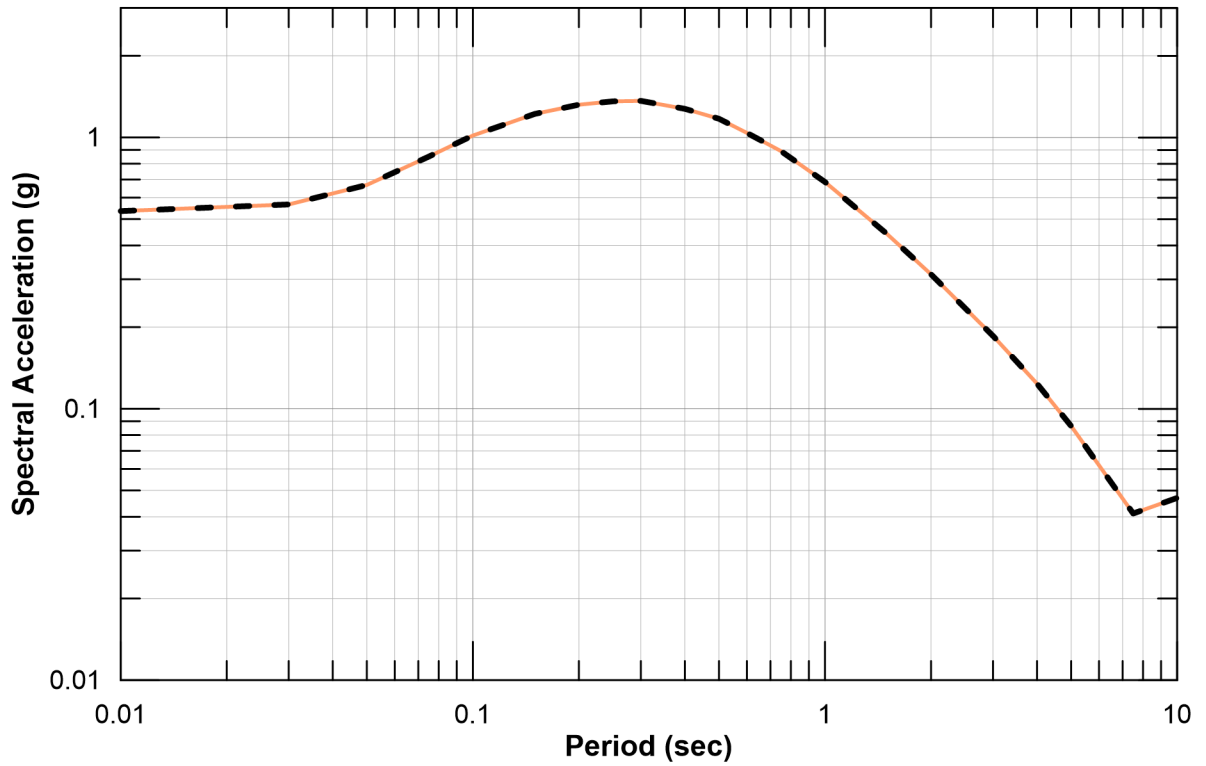
- 2,475-Year Uniform Hazard Spectrum
- - - 84th Percentile Deterministic Spectrum
- - - MDE Spectrum



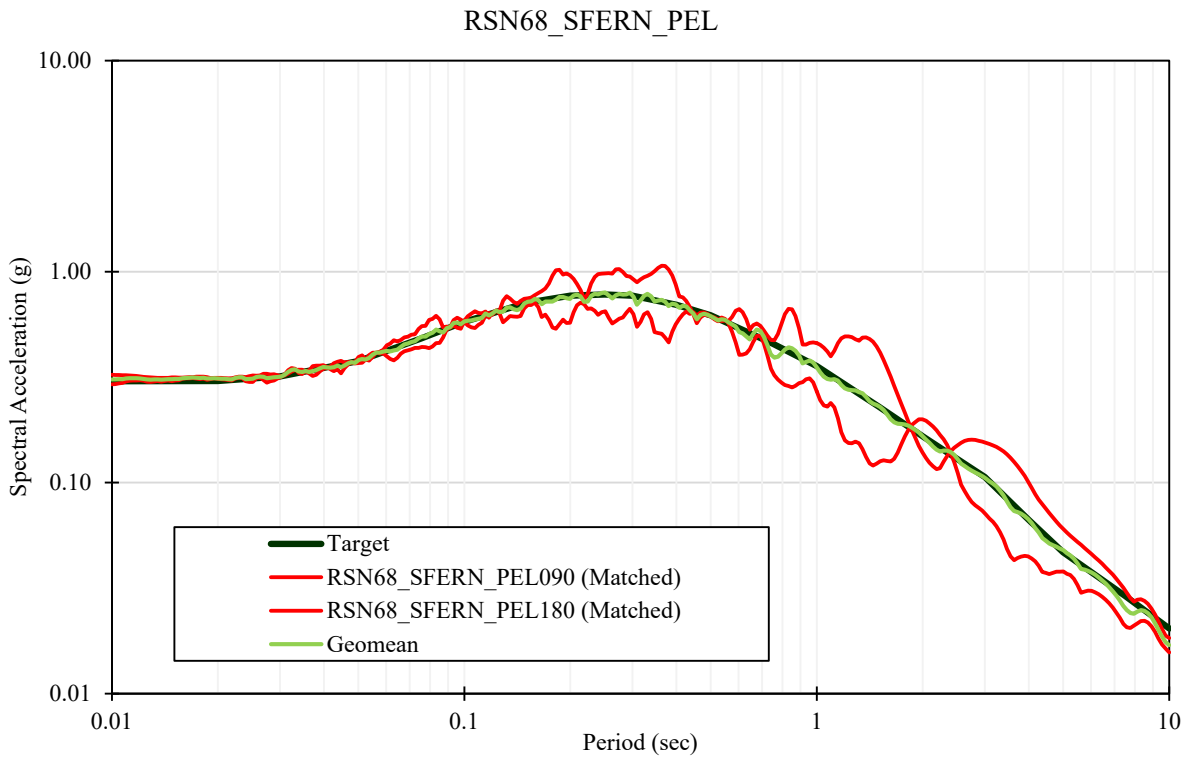
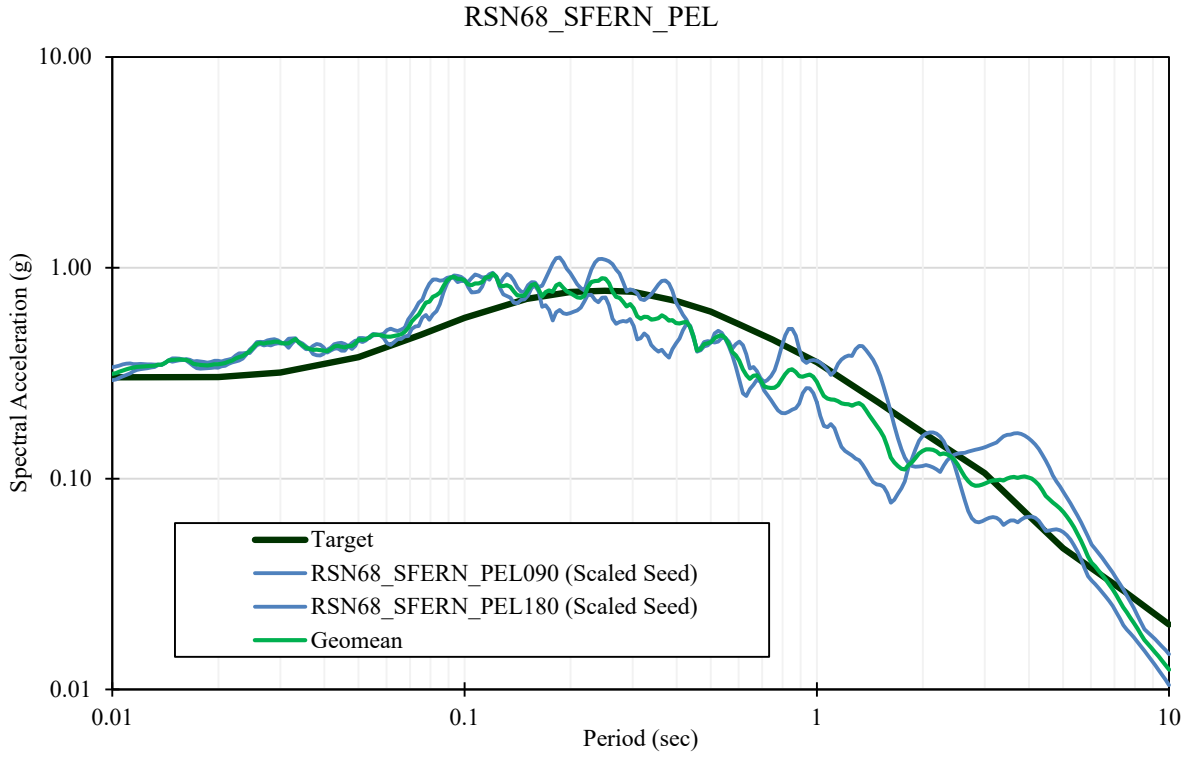
- 2,475-Year Uniform Hazard Spectrum
- - - 84th Percentile Deterministic Spectrum
- - - MDE Spectrum



- 2,475-Year Uniform Hazard Spectrum
- - - 84th Percentile Deterministic Spectrum
- - - MDE Spectrum



— 975-Year Uniform Hazard Spectrum
 - - - MDE Spectrum



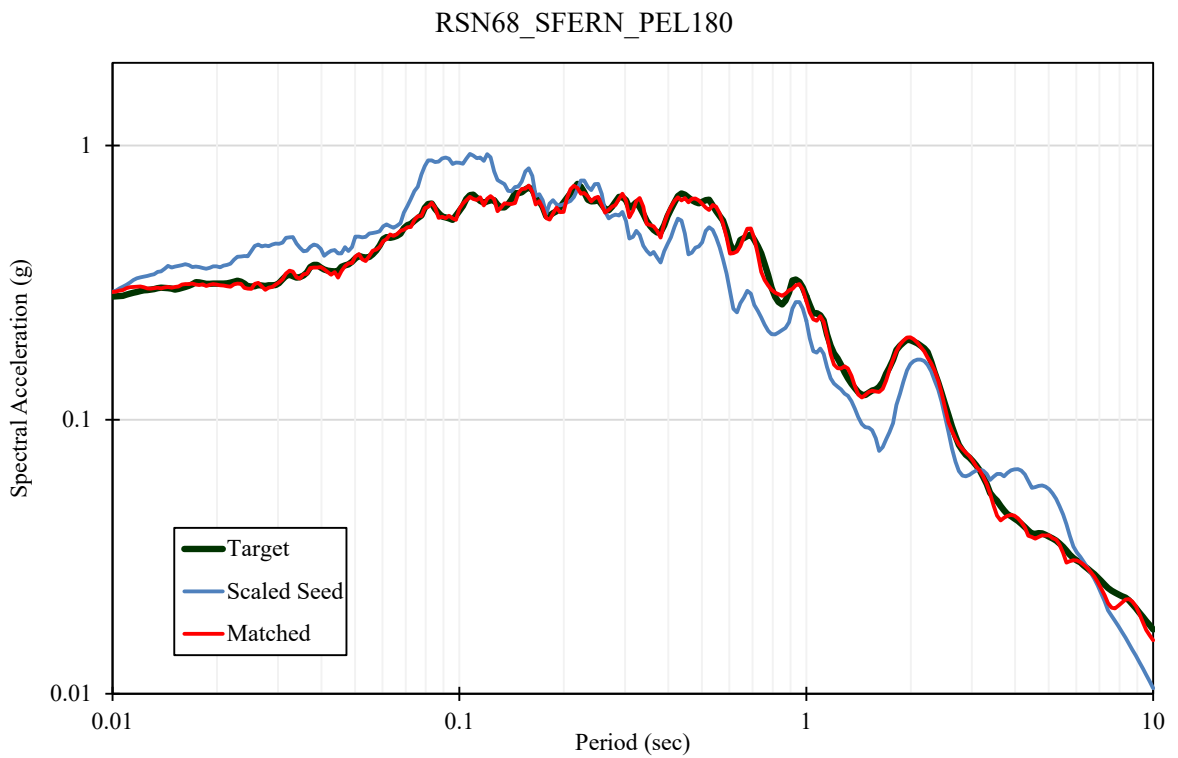
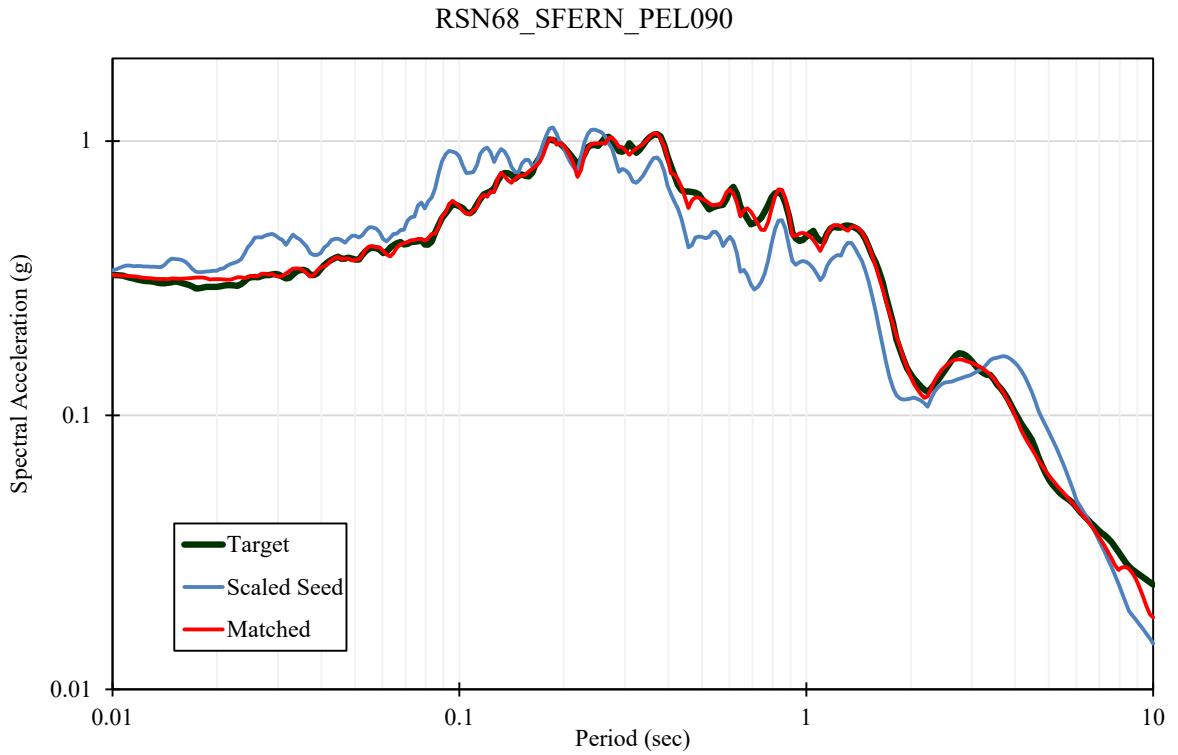
S:\1802\Figures\DCA\Figure_141.ai; Date: 05/03/2021; User: JCh.LCI



For Illustration
Purposes Only

1971 San Fernando –
LA-Hollywood Stor FF

Figure 141
Response Spectra for MDE Time
Histories for Intake No. 3, RSN 68



S:\1802\Figures\DCA\Figure_142.ai; Date: 05/03/2021; User: JCh.LCI

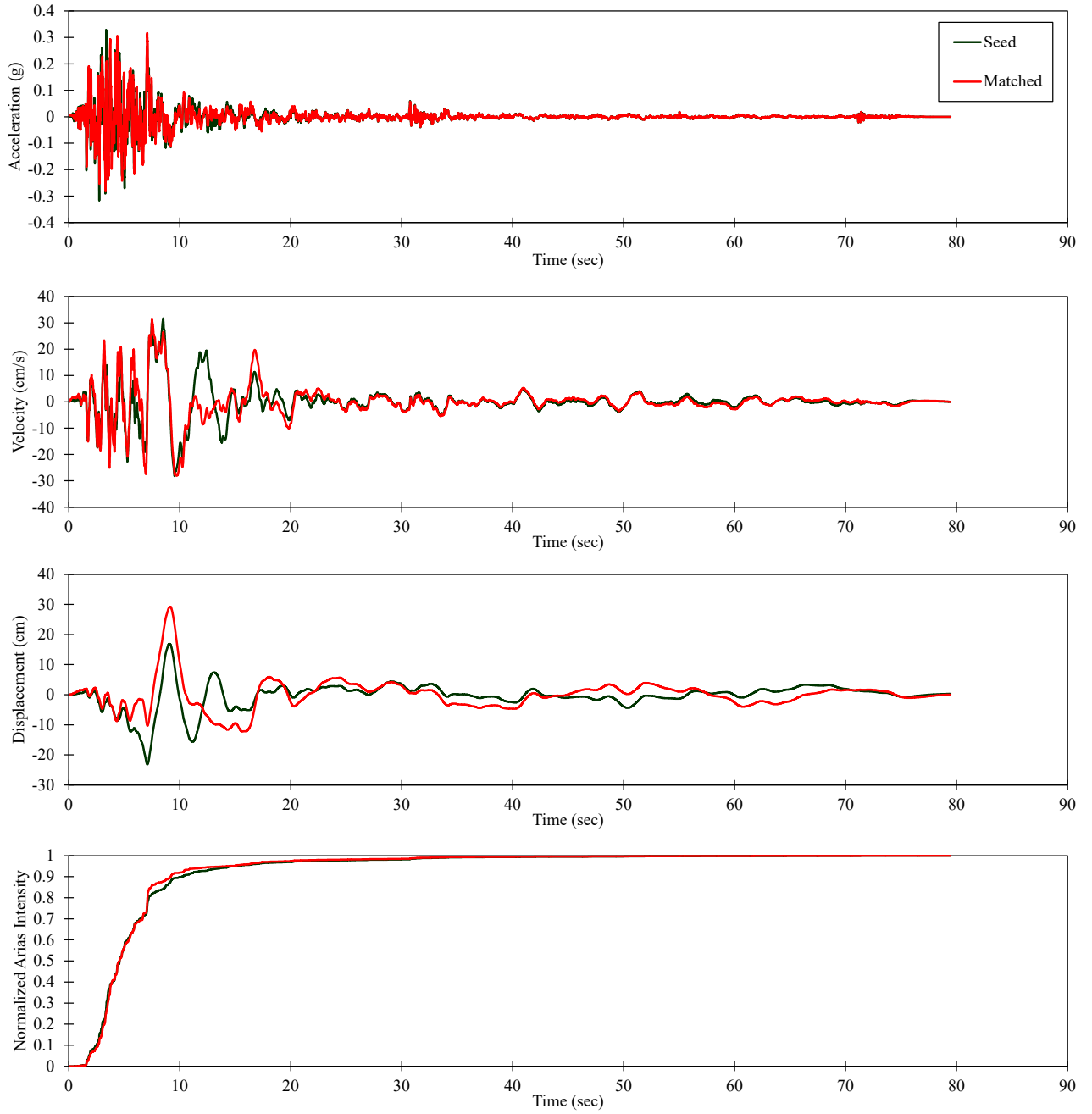


For Illustration
Purposes Only

1971 San Fernando –
LA-Hollywood Stor FF

Figure 142
Spectral Matches for MDE Time
Histories for Intake No. 3, RSN 68

RSN68_SFERN_PEL090



S:\1802\Figures\DCA\Figure_141.ai; Date: 05/03/2021; User: JCh.LCI

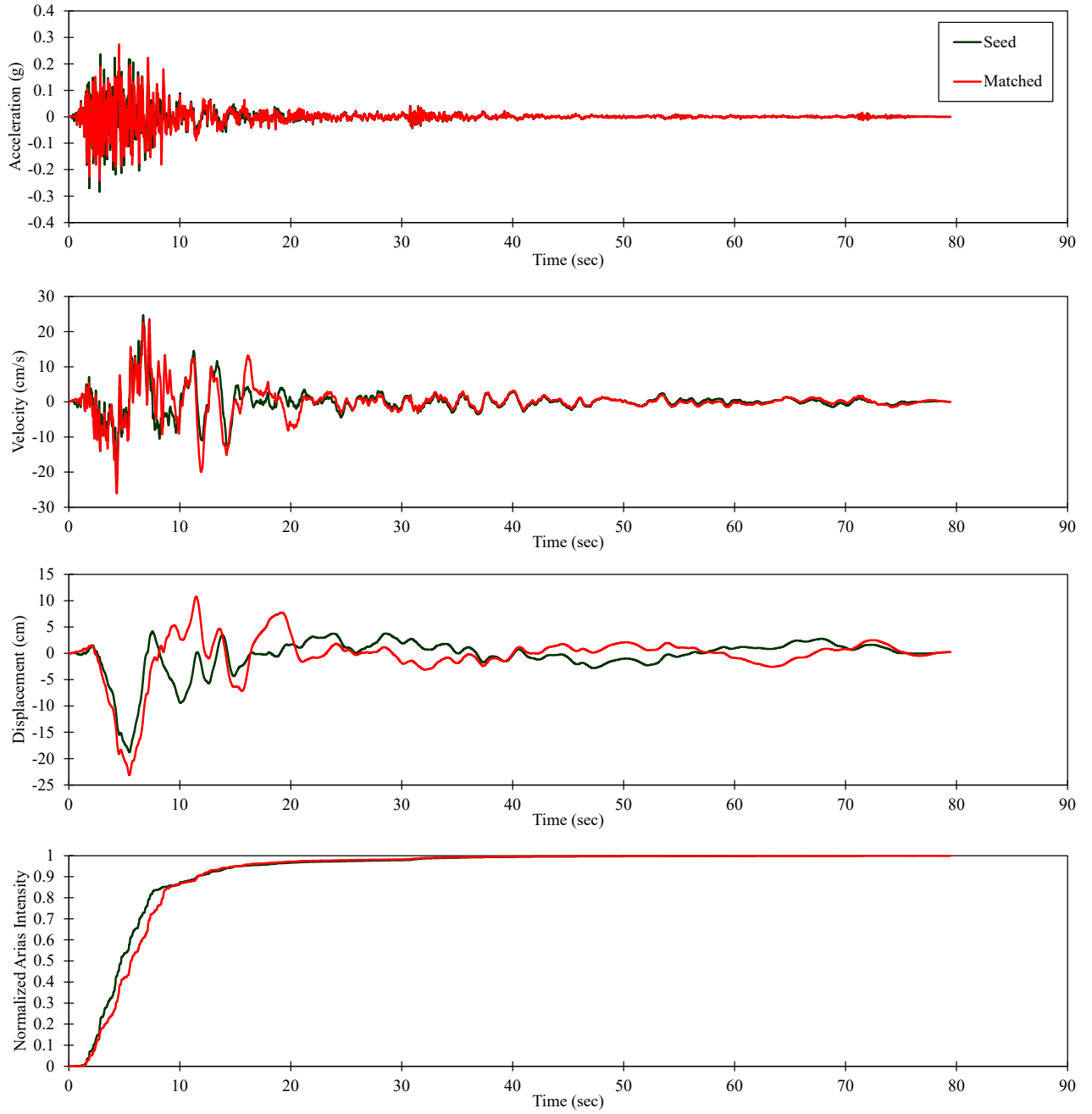


For Illustration
Purposes Only

1971 San Fernando –
LA-Hollywood Stor FF

Figure 143
Time History Spectrally-Matched to
MDE for Intake No. 3, RSN 68 (H1)

RSN68_SFERN_PEL180



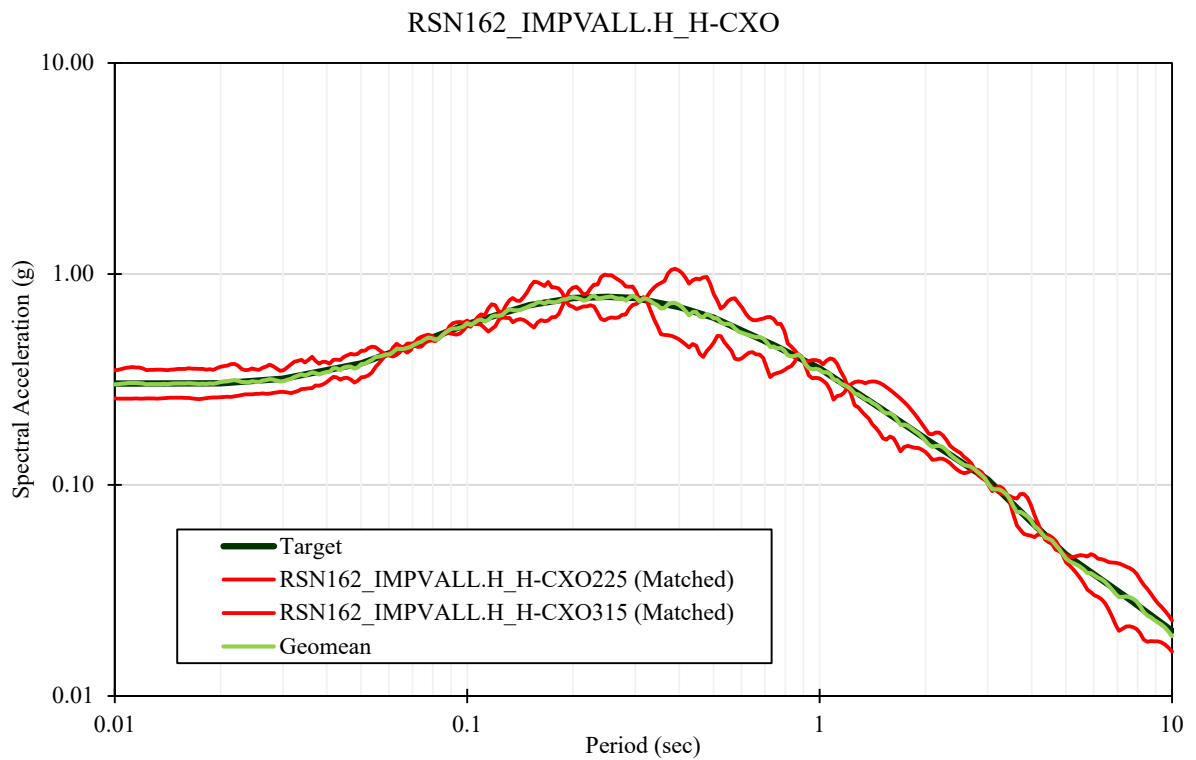
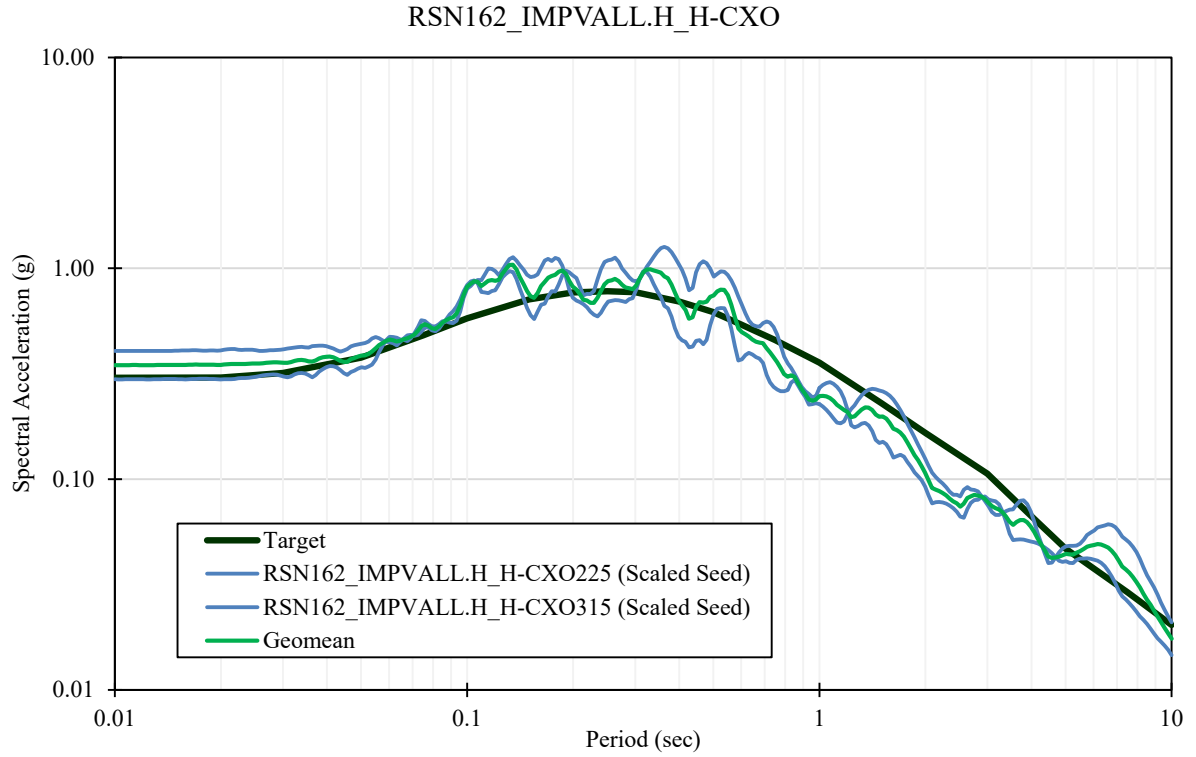
S:\1802\Figures\DCAFigure_144.ai Date: 05/03/2021, User: JCH/LCI



For Illustration
Purposes Only

1971 San Fernando –
LA-Hollywood Stor FF

Figure 144
Time History Spectrally-Matched to
MDE for Intake No. 3, RSN 68 (H2)



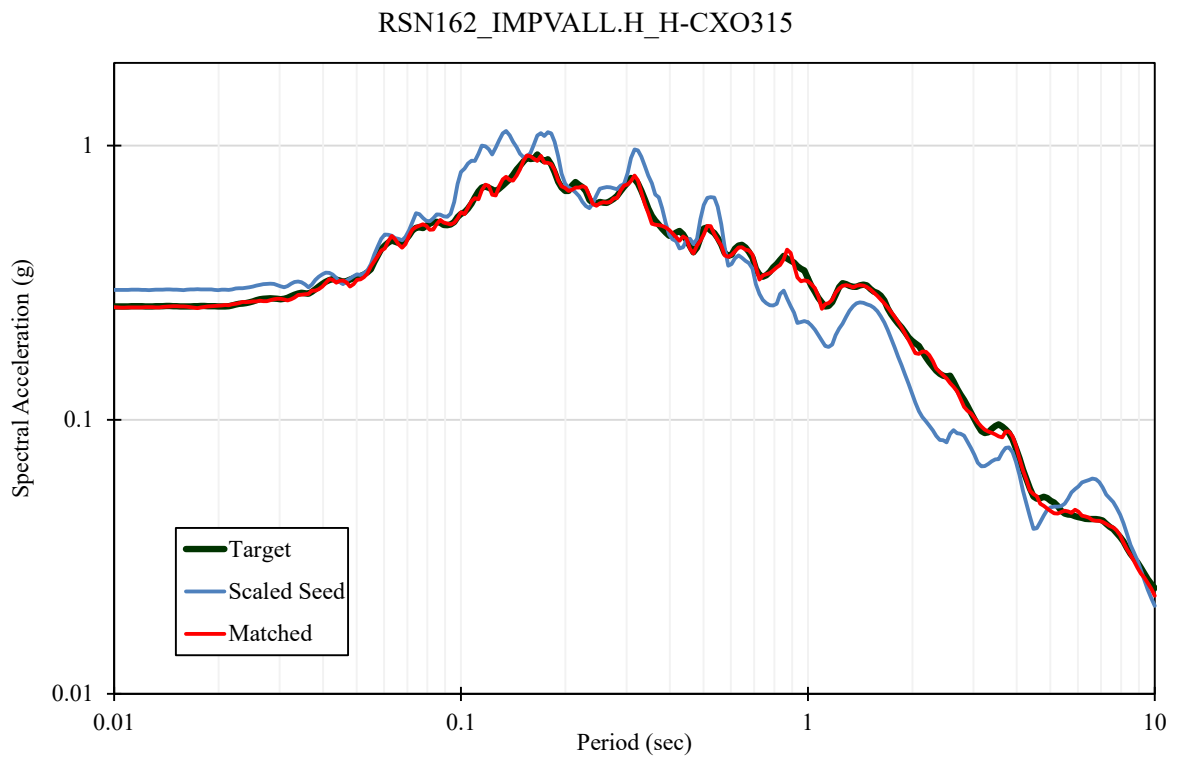
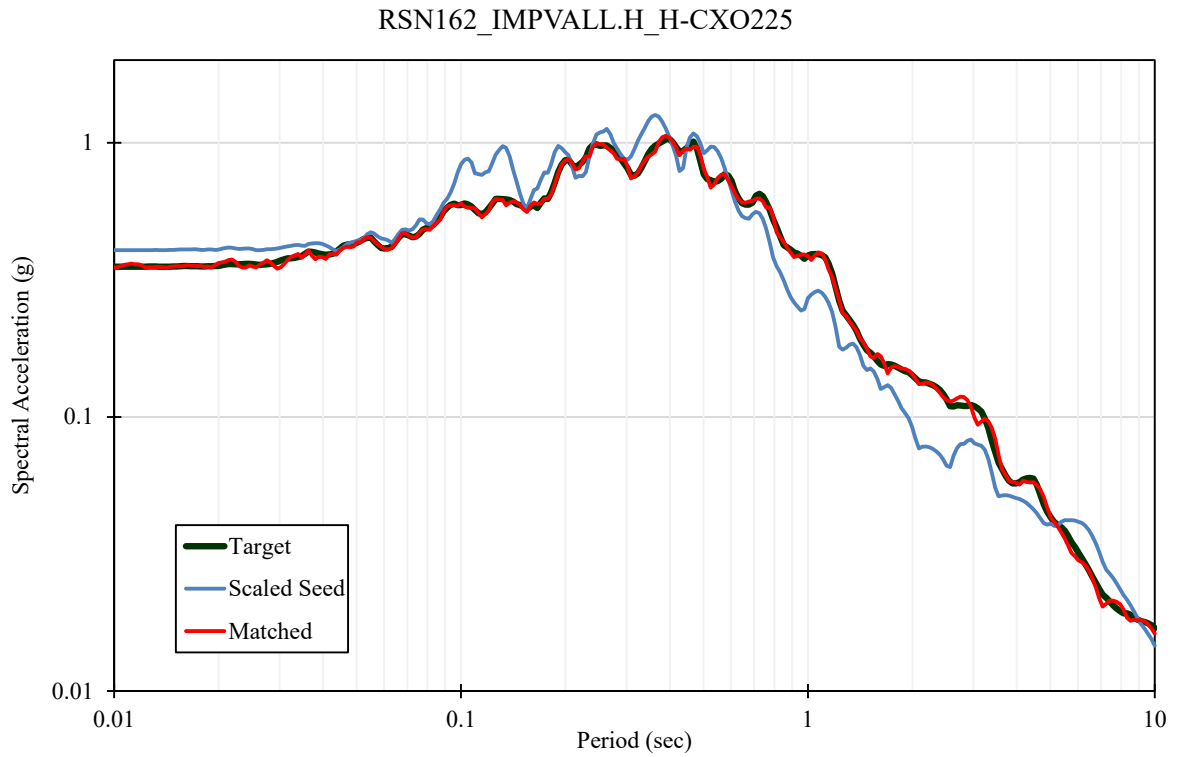
S:\1802\Figures\Figure_141.ai; Date: 05/03/2021; User: JCh.LCI



For Illustration
Purposes Only

1979 Imperial Valley-06 –
Calexico Fire Station

Figure 145
Response Spectra for MDE Time
Histories for Intake No. 3, RSN 162



S:\1802\Figures\Figure_146.ai; Date: 05/03/2021; User: JCH.LCI

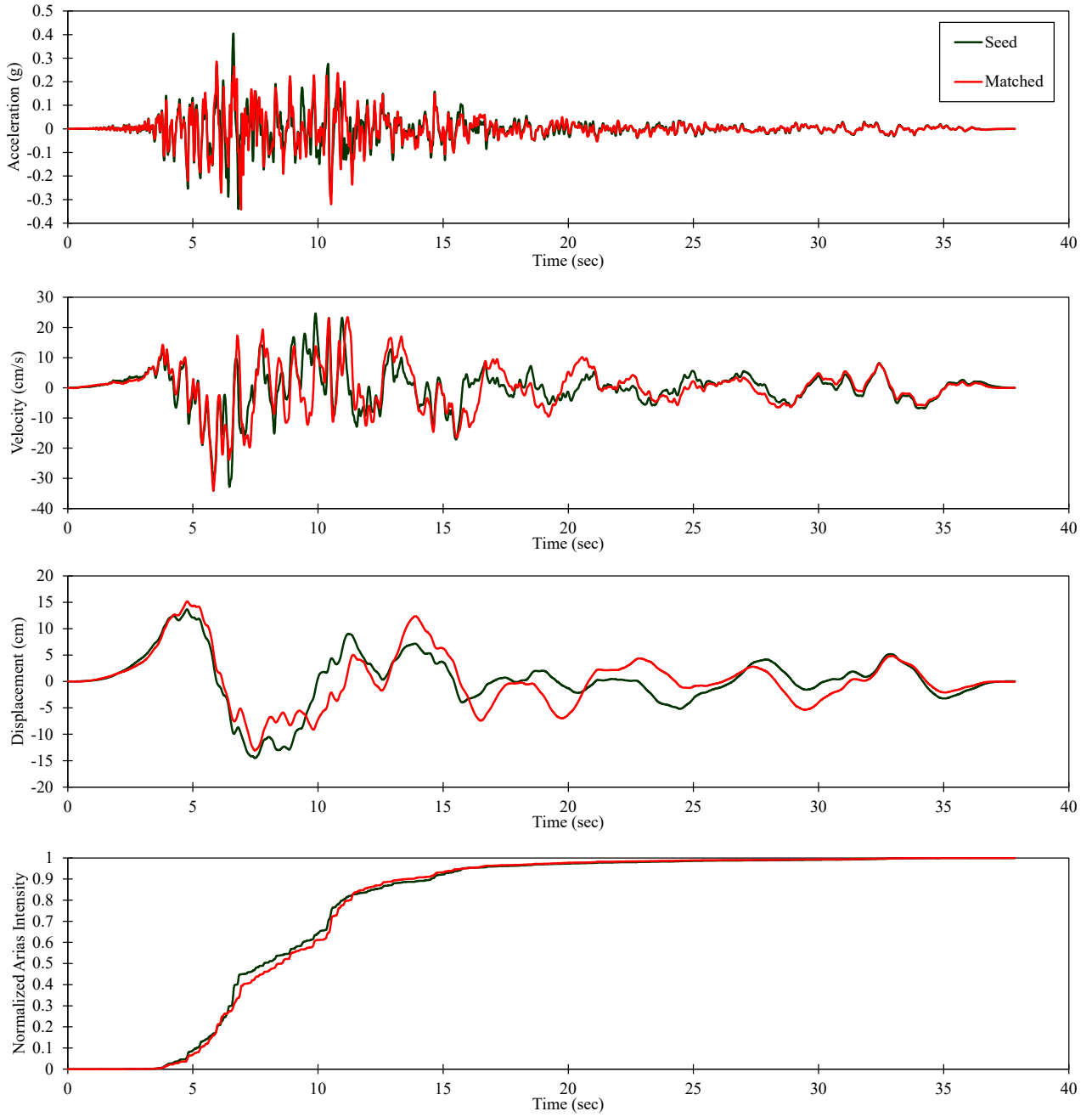


For Illustration
Purposes Only

1979 Imperial Valley-06 –
Calexico Fire Station

Figure 146
Spectral Matches for MDE Time
Histories for Intake No. 3, RSN 162

RSN162_IMPVAL.L_H_H-CXO225



S:\1802\Figures\Figure_147.ai; Date: 05/03/2021; User: JCh.LCL

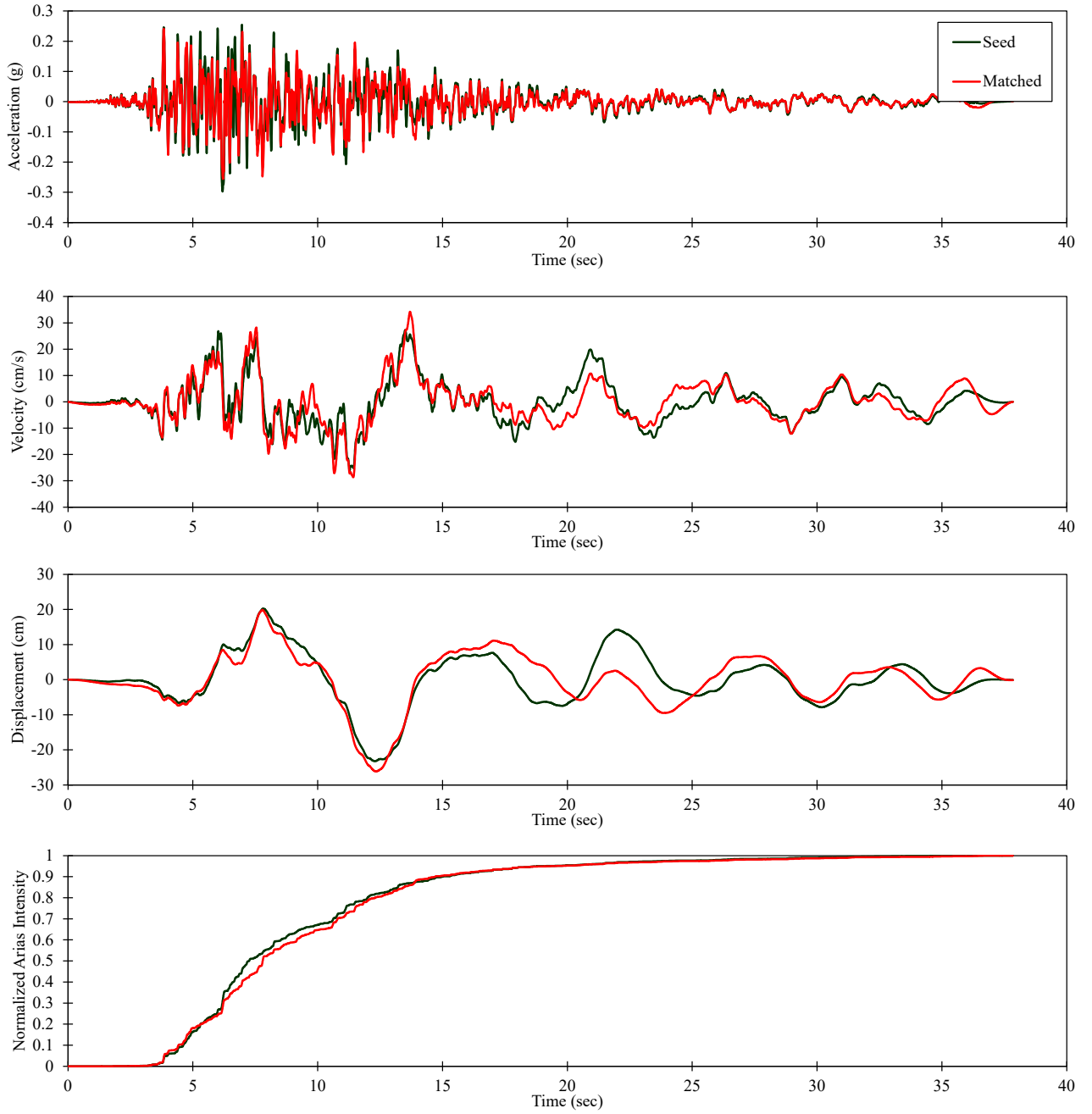


For Illustration
Purposes Only

1979 Imperial Valley-06 –
Calexico Fire Station

Figure 147
Time History Spectrally-Matched to
MDE for Intake No. 3, RSN 162 (H1)

RSN162_IMPVAL.L_H_H-CXO315



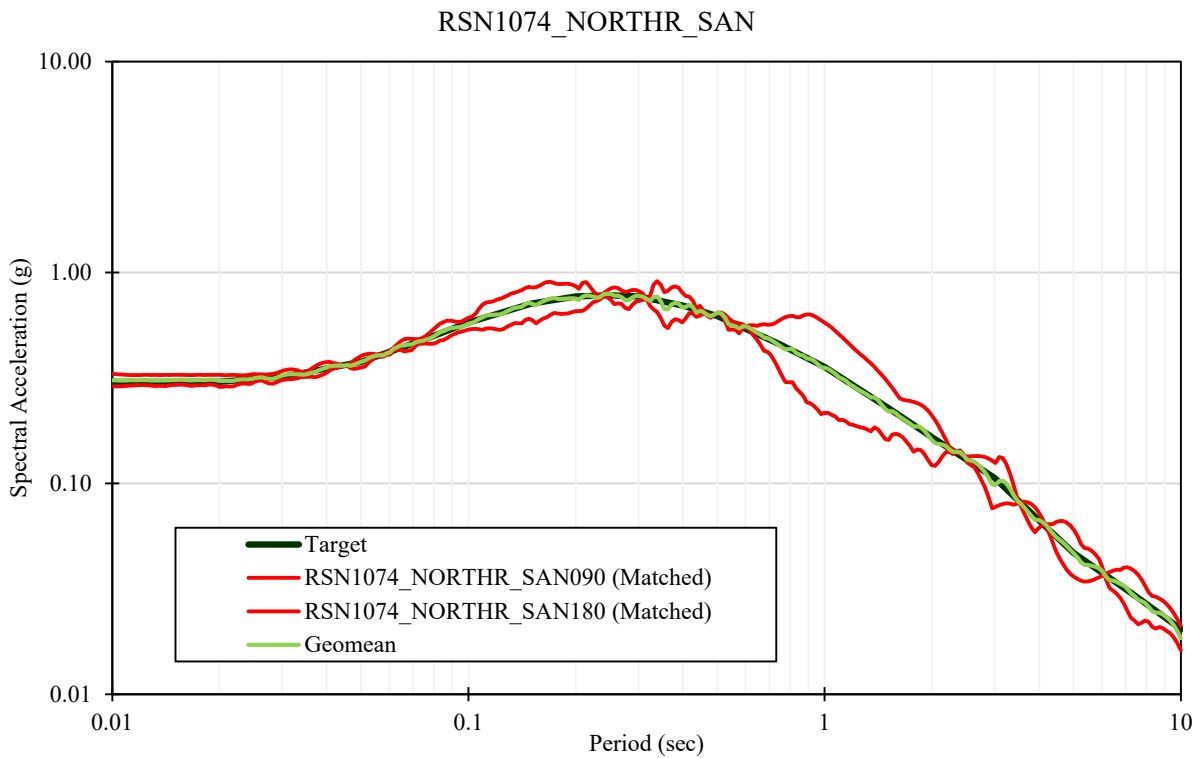
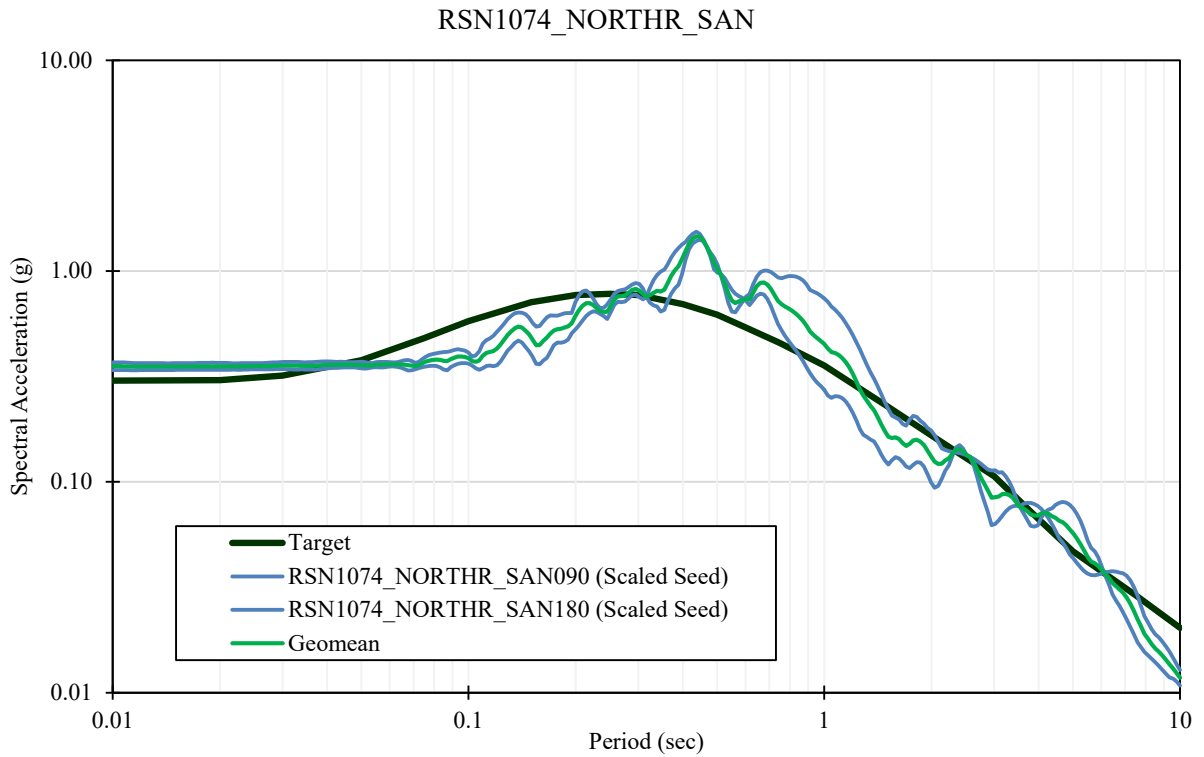
S:\1802\Figures\Figure_148.ai; Date: 05/03/2021; User: JCh.LCL



For Illustration
Purposes Only

1979 Imperial Valley-06 –
Calexico Fire Station

Figure 148
Time History Spectrally-Matched to
MDE for Intake No. 3, RSN 162 (H2)



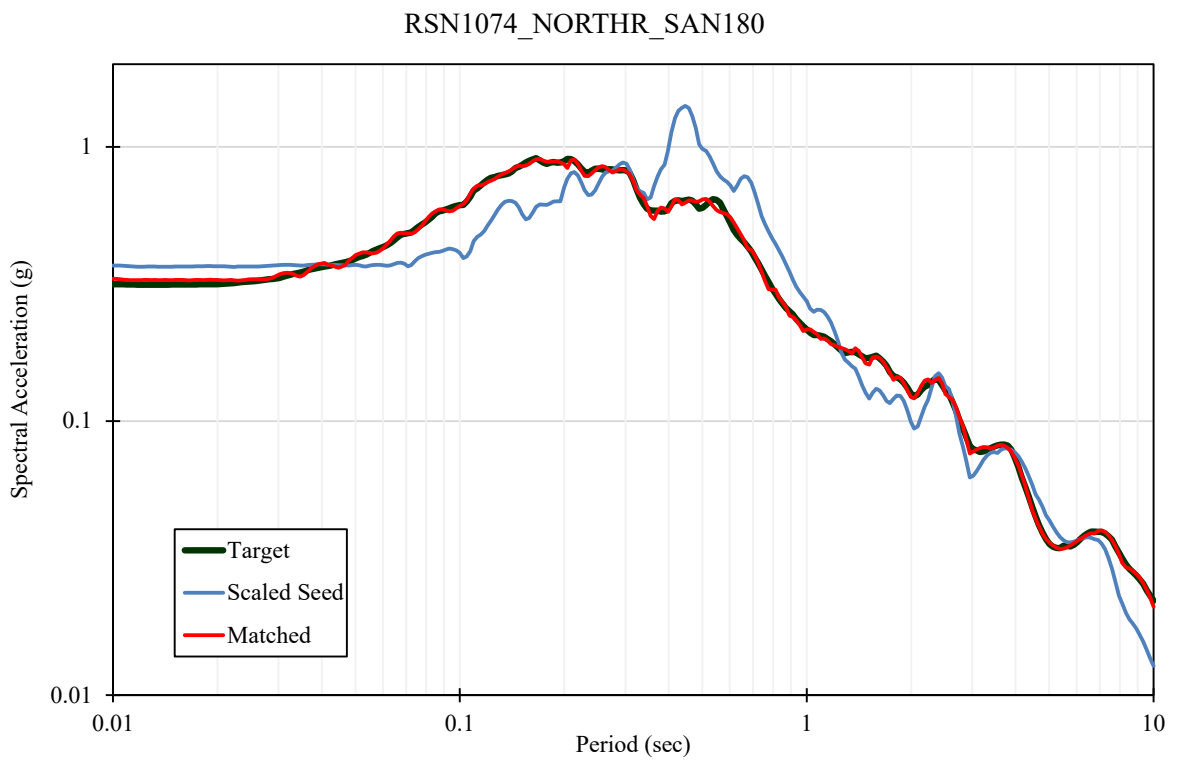
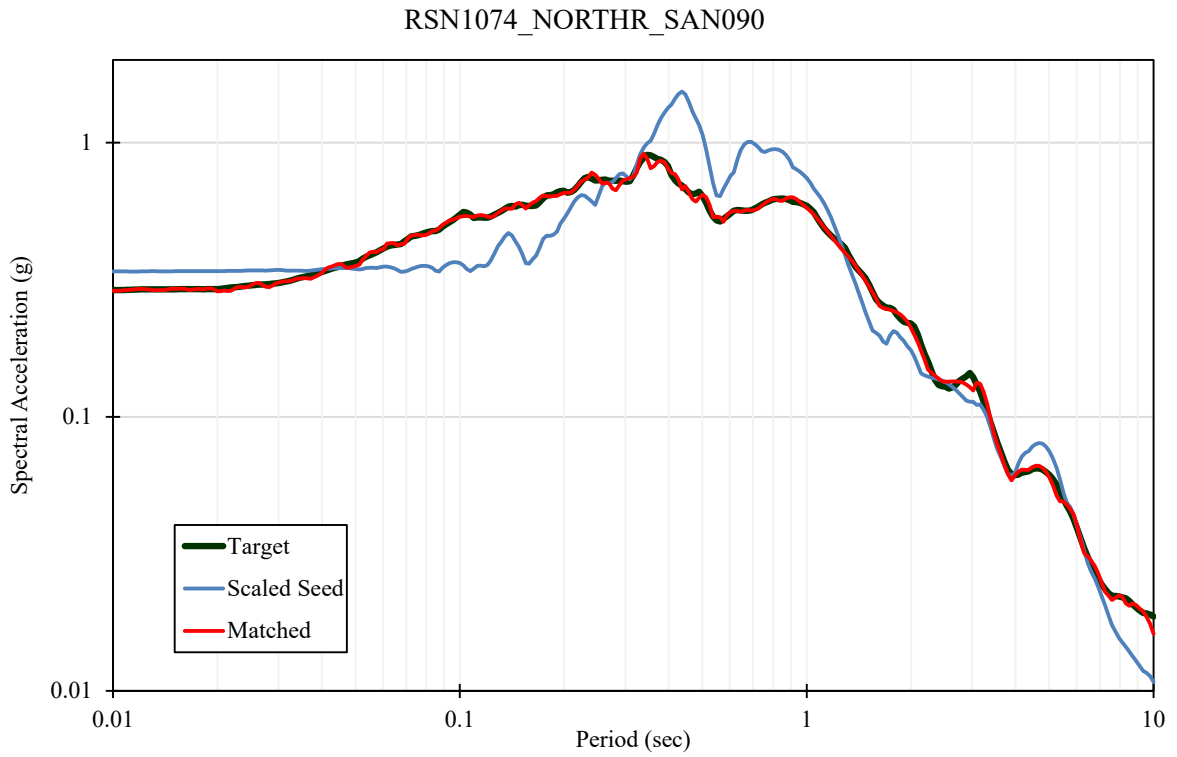
S:\1802\Figures\Figure_149.ai; Date: 05/03/2021; User: JCh.LCI



For Illustration
Purposes Only

**1995 Northridge-01 –
Sandberg-Bald Mtn**

**Figure 149
Response Spectra for MDE Time
Histories for Intake No. 3, RSN 1074**



S:\1802\Figures\Figure_150.ai; Date: 05/03/2021; User: JCh.LCL

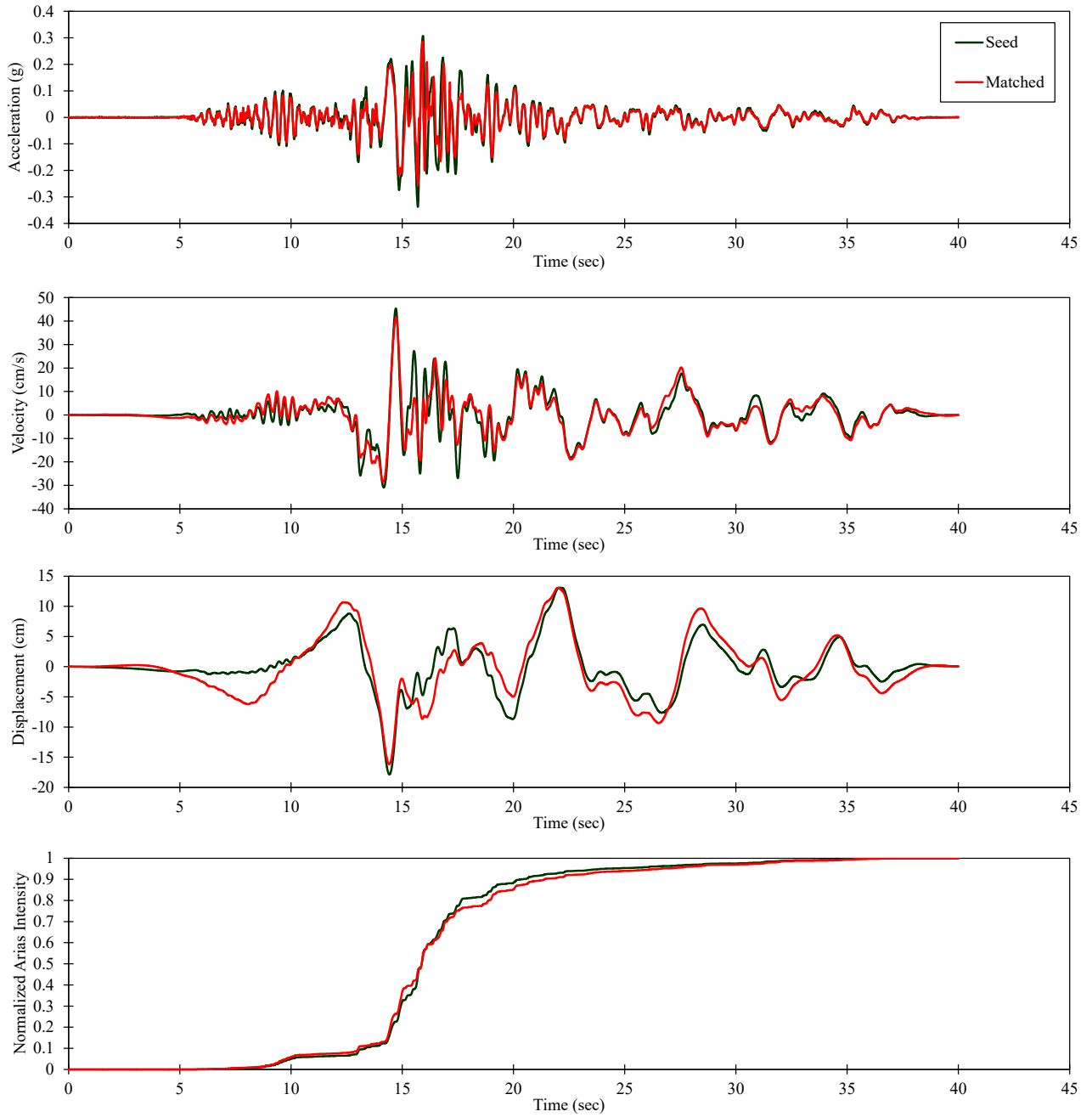


For Illustration
Purposes Only

1995 Northridge-01 –
Sandberg-Bald Mtn

Figure 150
Spectral Matches for MDE Time
Histories for Intake No. 3, RSN 1074

RSN1074_NORTHR_SAN090



S:\1802\Figures\Figure_151.ai; Date: 05/03/2021; User: JCh.LCL

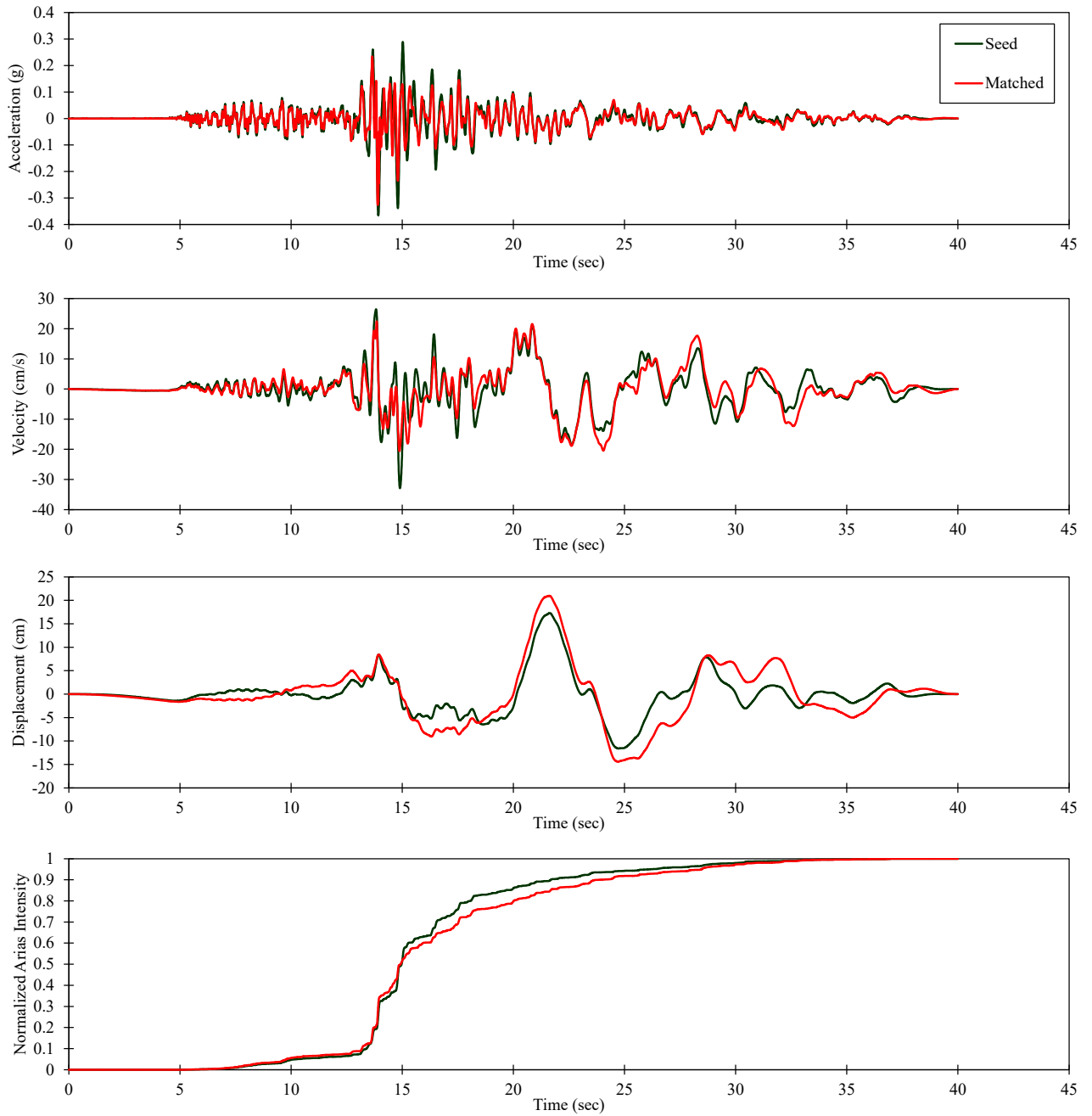


For Illustration
Purposes Only

1995 Northridge-01 –
Sandberg-Bald Mtn

Figure 151
Time History Spectrally-Matched to
MDE for Intake No. 3, RSN 1074 (H1)

RSN1074_NORTHR_SAN180



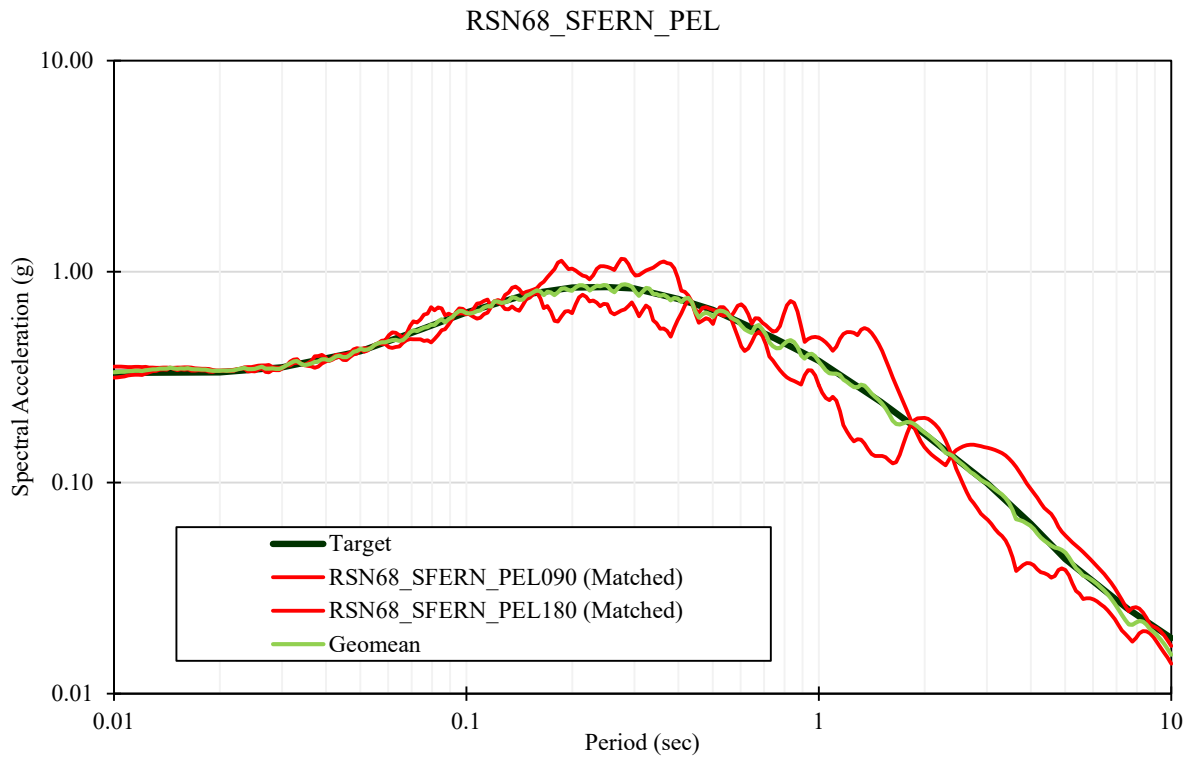
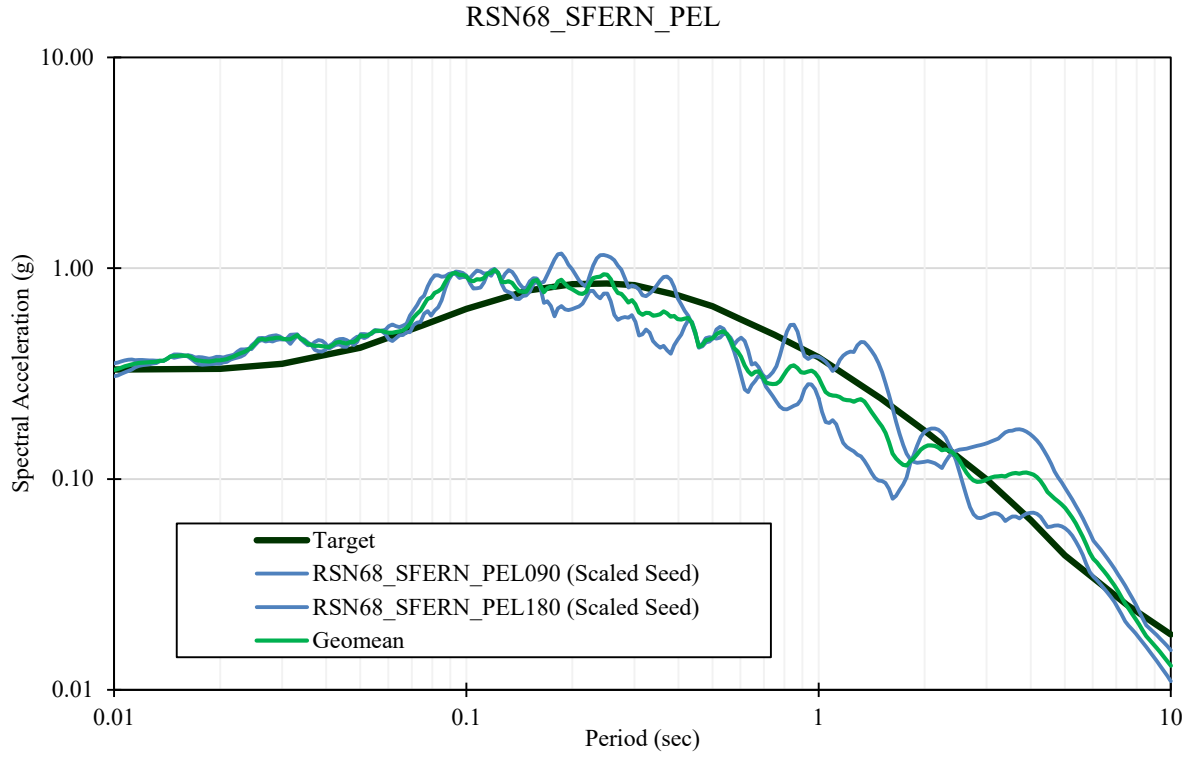
S:\1802\Figures\Figure_152.ai; Date: 05/03/2021; User: JCh.LCL



For Illustration
Purposes Only

1995 Northridge-01 –
Sandberg-Bald Mtn

Figure 152
Time History Spectrally-Matched to
MDE for Intake No. 3, RSN 1074 (H2)



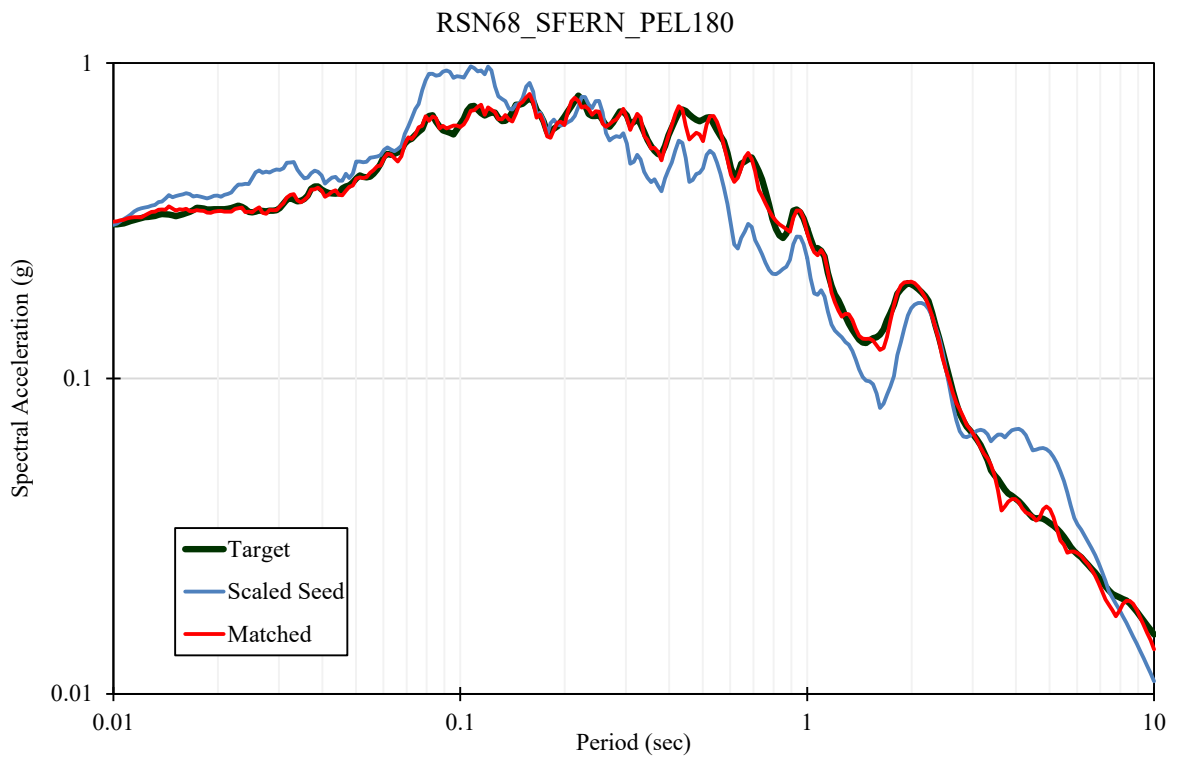
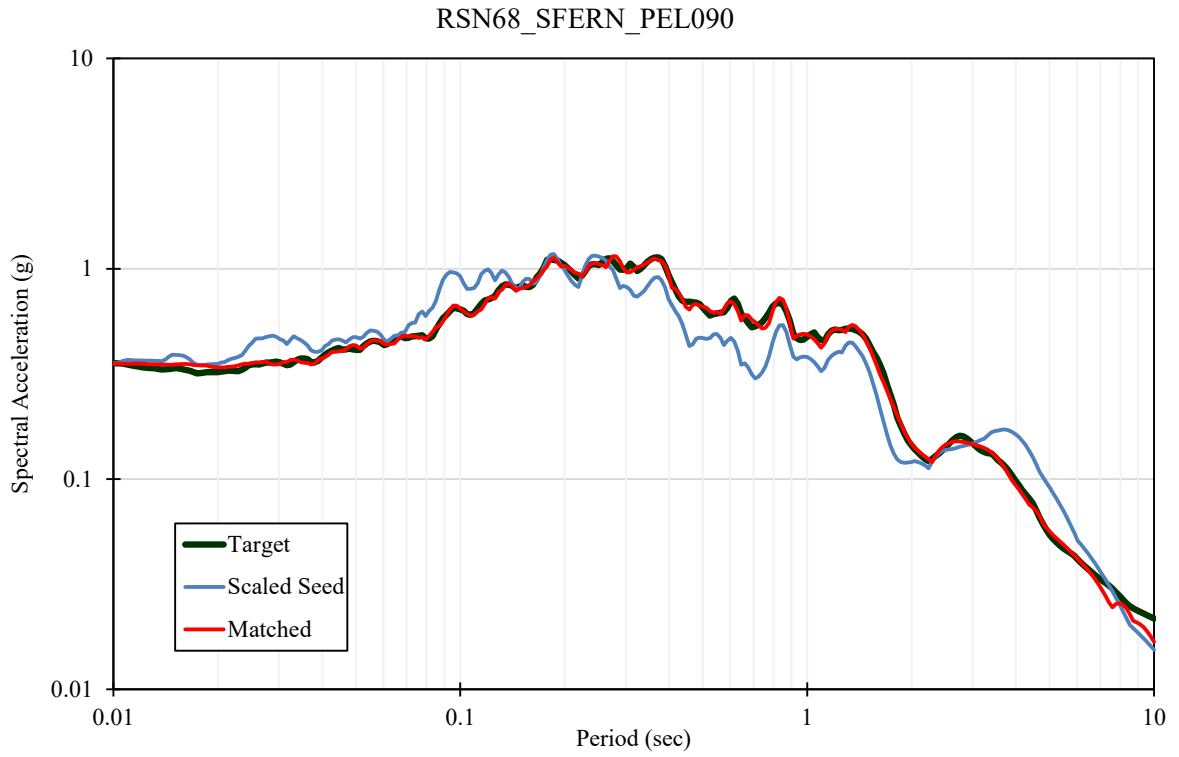
S:\1802\Figures\Figure_153.ai; Date: 05/03/2021; User: JCh.LCI



For Illustration
Purposes Only

1971 San Fernando –
LA-Hollywood Stor FF

Figure 153
Response Spectra for MDE Time
Histories for Intake No. 5, RSN 68



S:\1802\Figures\Figure_154.ai; Date: 05/03/2021; User: JCh.LCL

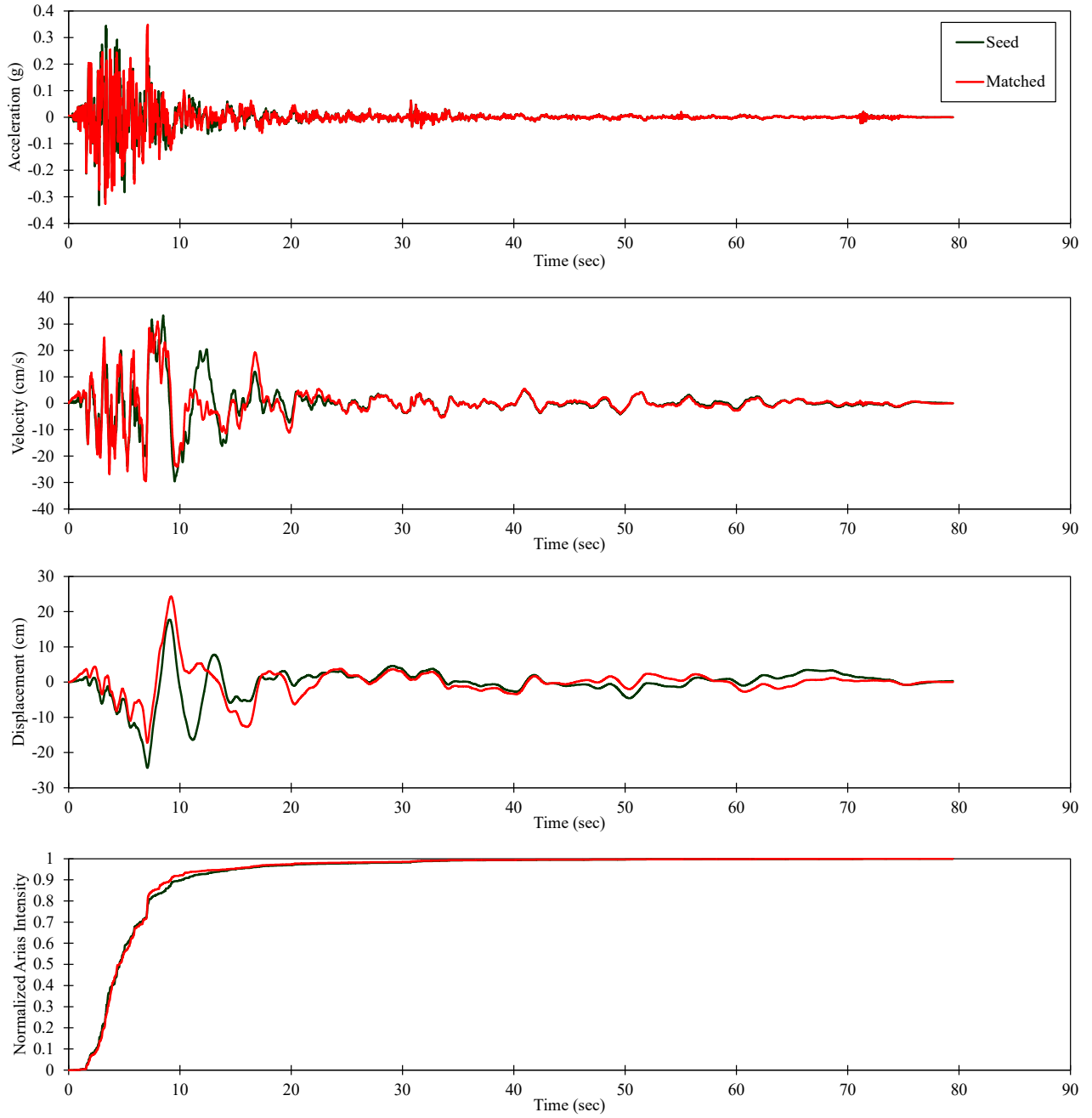


For Illustration
Purposes Only

1971 San Fernando –
LA-Hollywood Stor FF

Figure 154
Response Spectra for MDE Time
Histories for Intake No. 5, RSN 68

RSN68_SFERN_PEL090



S:\1802\Figures\Figure_155.ai; Date: 05/03/2021; User: JCh.LCL

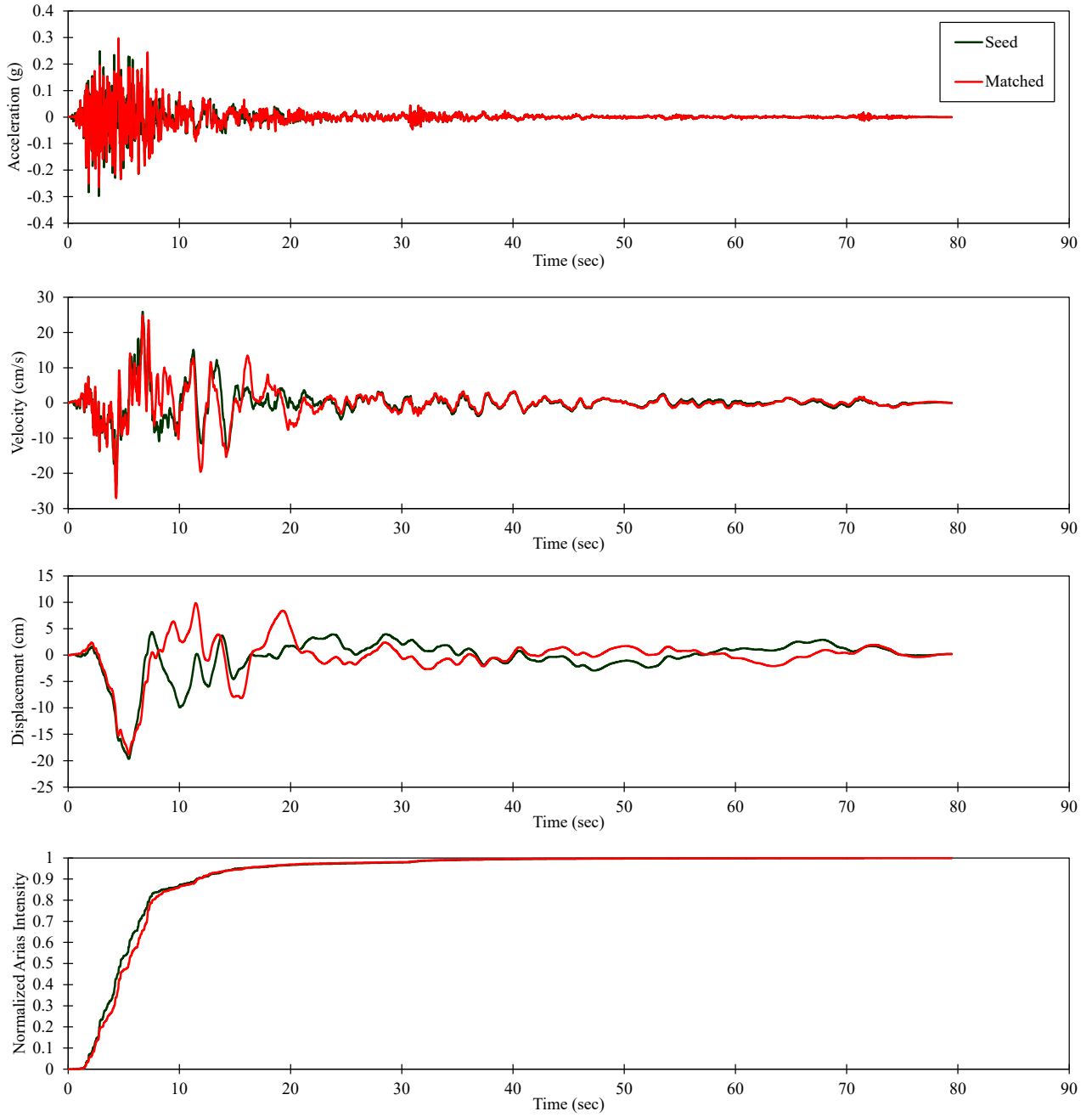


For Illustration
Purposes Only

1971 San Fernando –
LA-Hollywood Stor FF

Figure 155
Time History Spectrally-Matched to
MDE for Intake No. 5, RSN 68 (H1)

RSN68_SFERN_PEL180



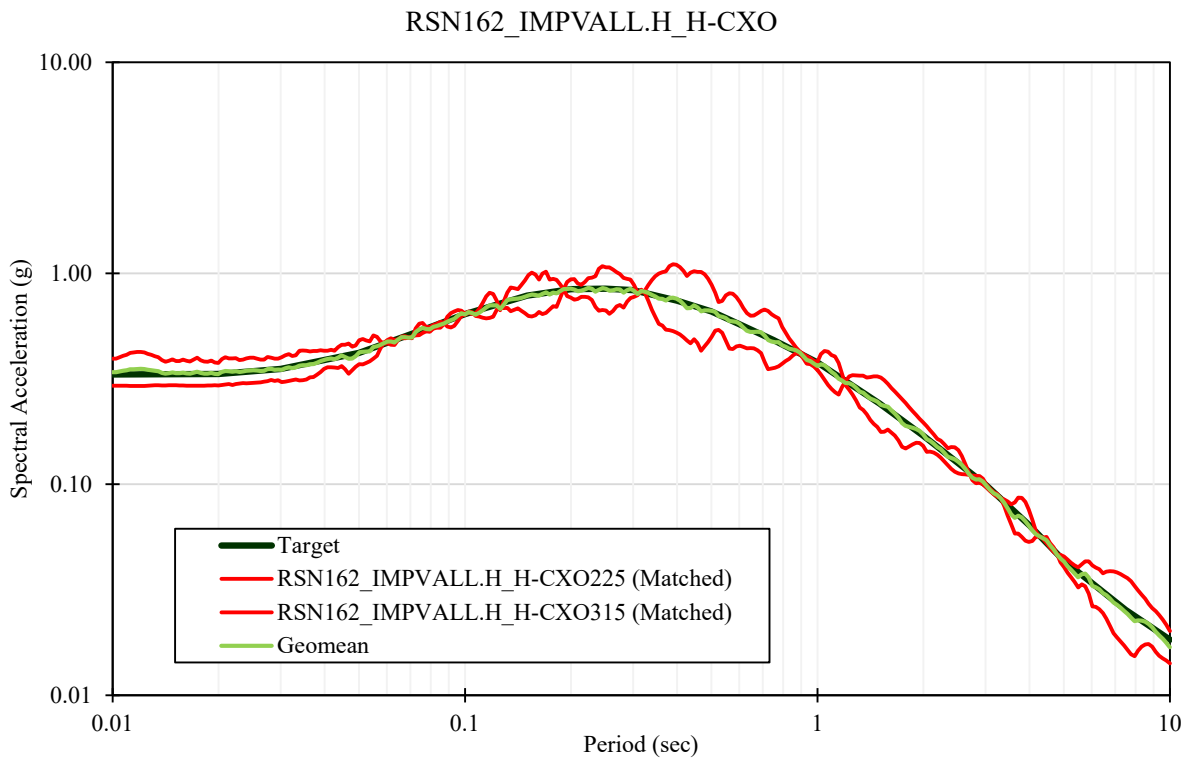
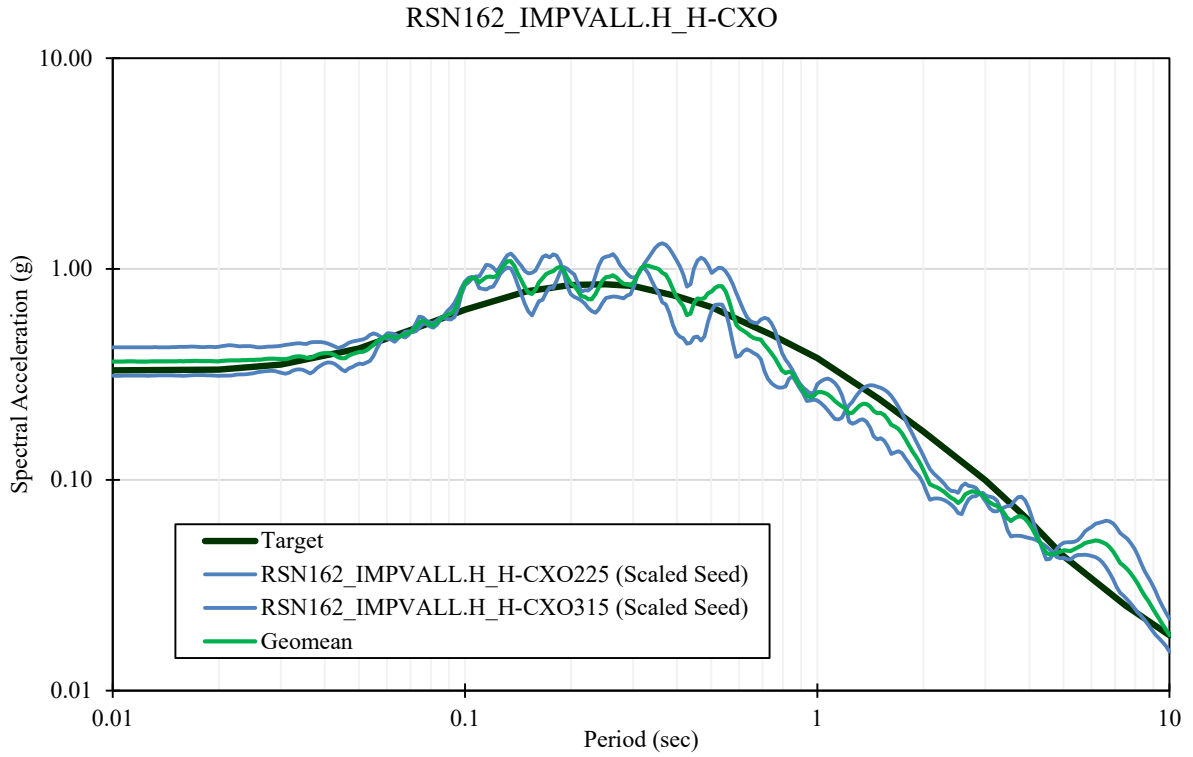
S:\1802\Figures\Figure_156.ai; Date: 05/03/2021; User: JCh.LCL



For Illustration
Purposes Only

1971 San Fernando –
LA-Hollywood Stor FF

Figure 156
Time History Spectrally-Matched to
MDE for Intake No. 5, RSN 68 (H2)



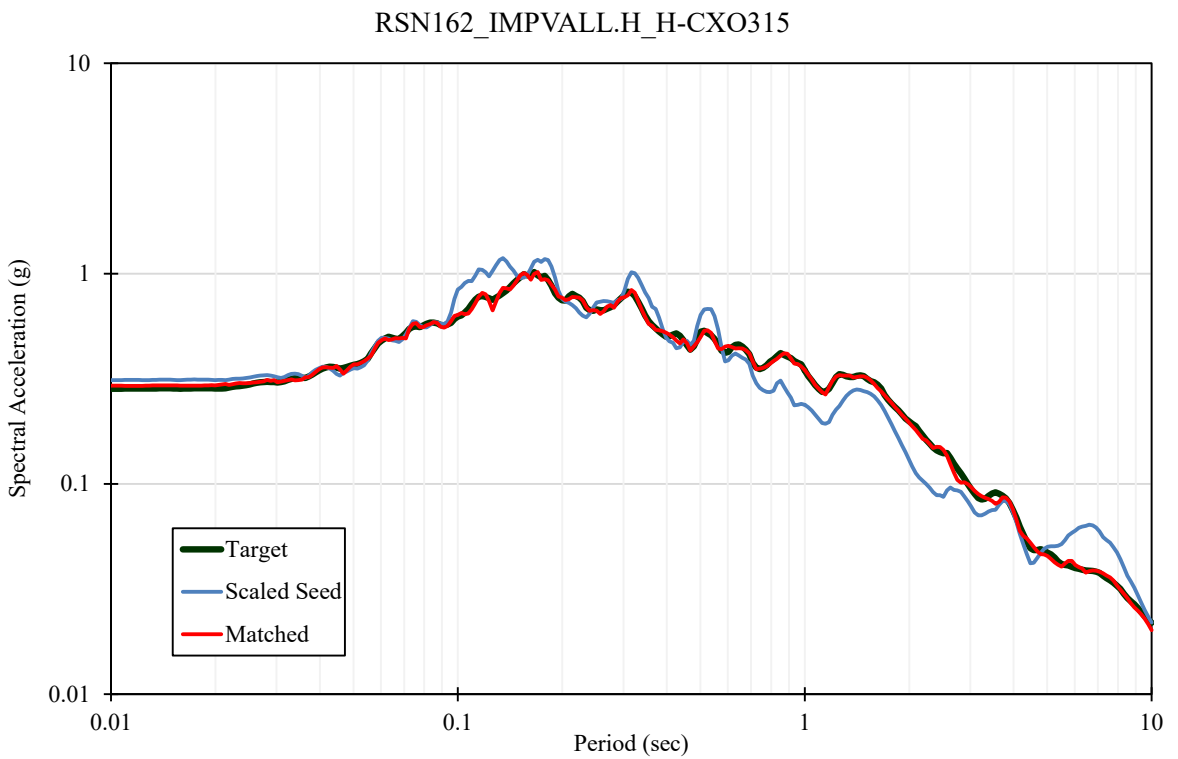
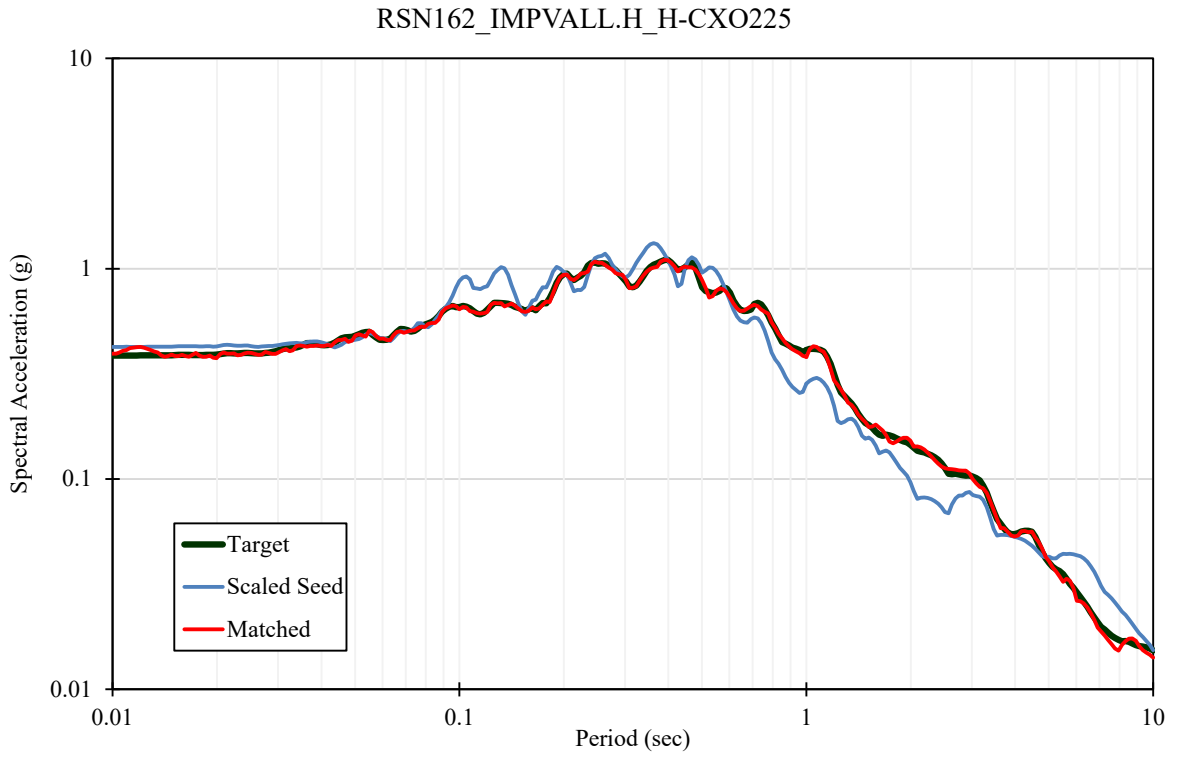
S:\1802\Figure_157.ai; Date: 05/03/2021; User: JCh.LCI



For Illustration
Purposes Only

1979 Imperial Valley-06 –
Calexico Fire Station

Figure 157
Response Spectra for MDE Time
Histories for Intake No. 5, RSN 162



S:\1802\Figures\Figure_158.ai; Date: 05/03/2021; User: JCh.LCL

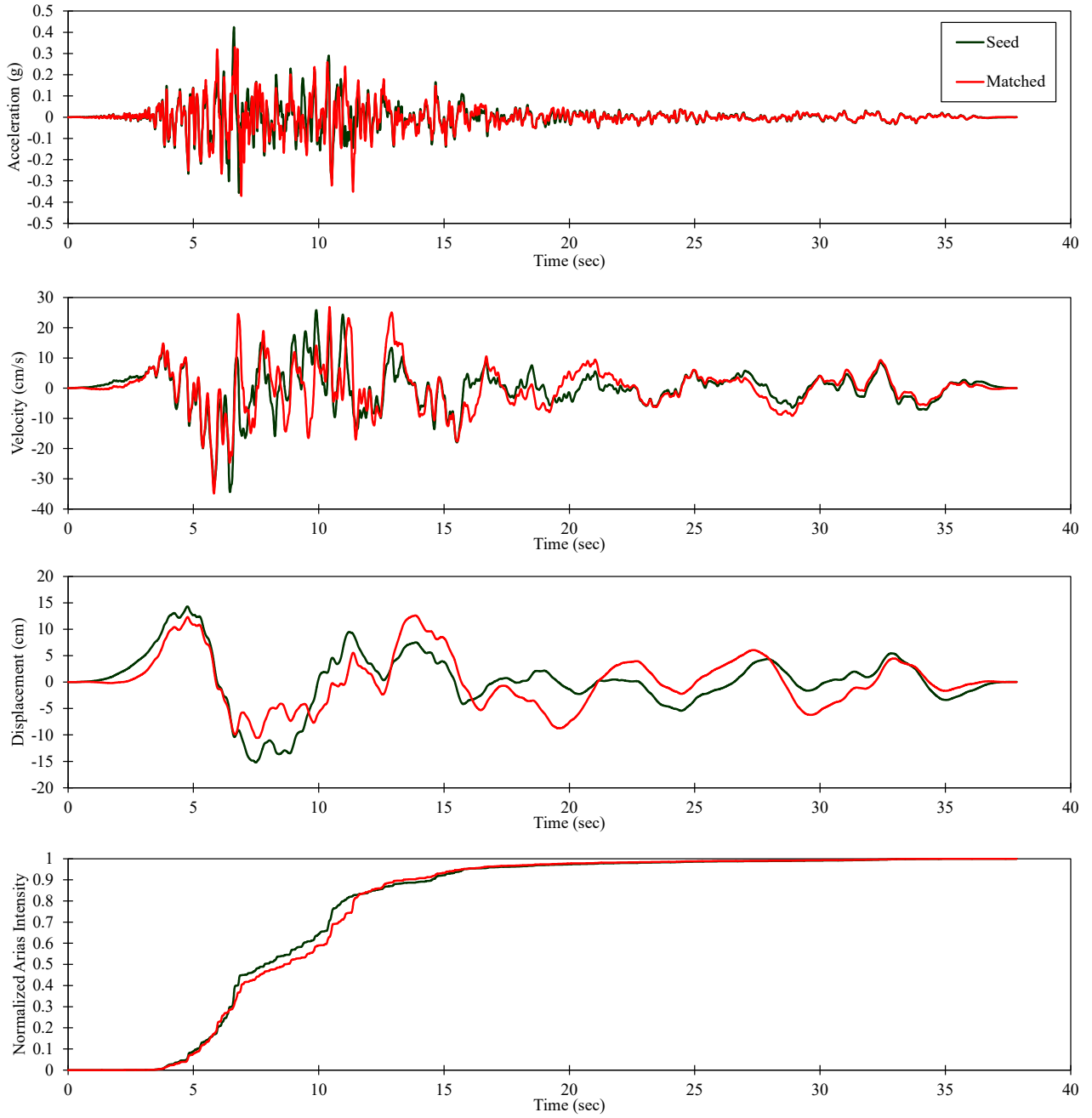


For Illustration
Purposes Only

1979 Imperial Valley-06 –
Calexico Fire Station

Figure 158
Spectral Matches for MDE Time
Histories for Intake No. 5, RSN 162

RSN162_IMPVAL.L_H_CXO225



S:\1802\Figures\Figure_159.ai; Date: 05/03/2021; User: JCh.LCL

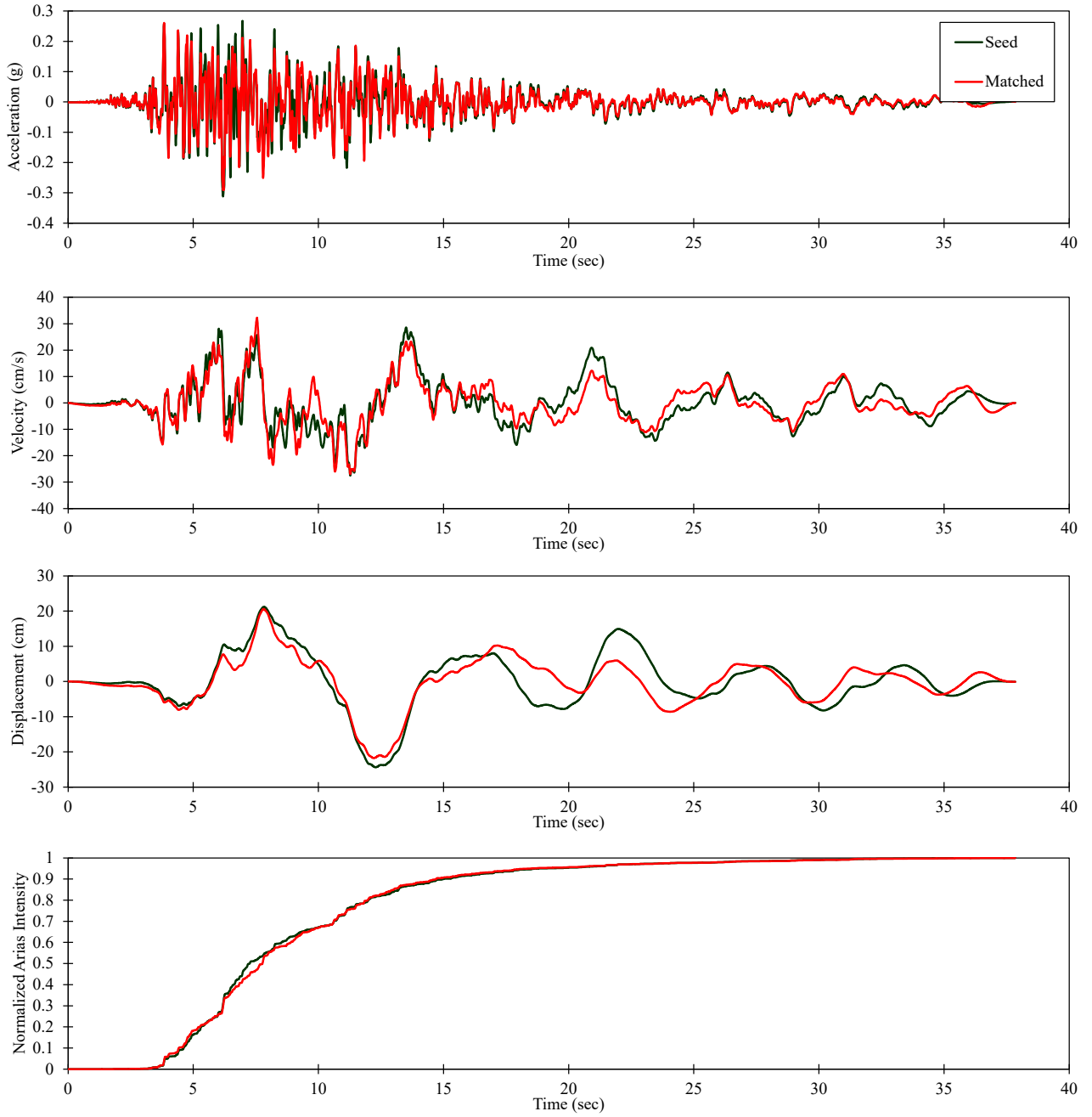


For Illustration
Purposes Only

1979 Imperial Valley-06 –
Calexico Fire Station

Figure 159
Time History Spectrally-Matched to
MDE for Intake No. 5, RSN 162 (H1)

RSN162_IMPVAL.L_H_H-CXO315



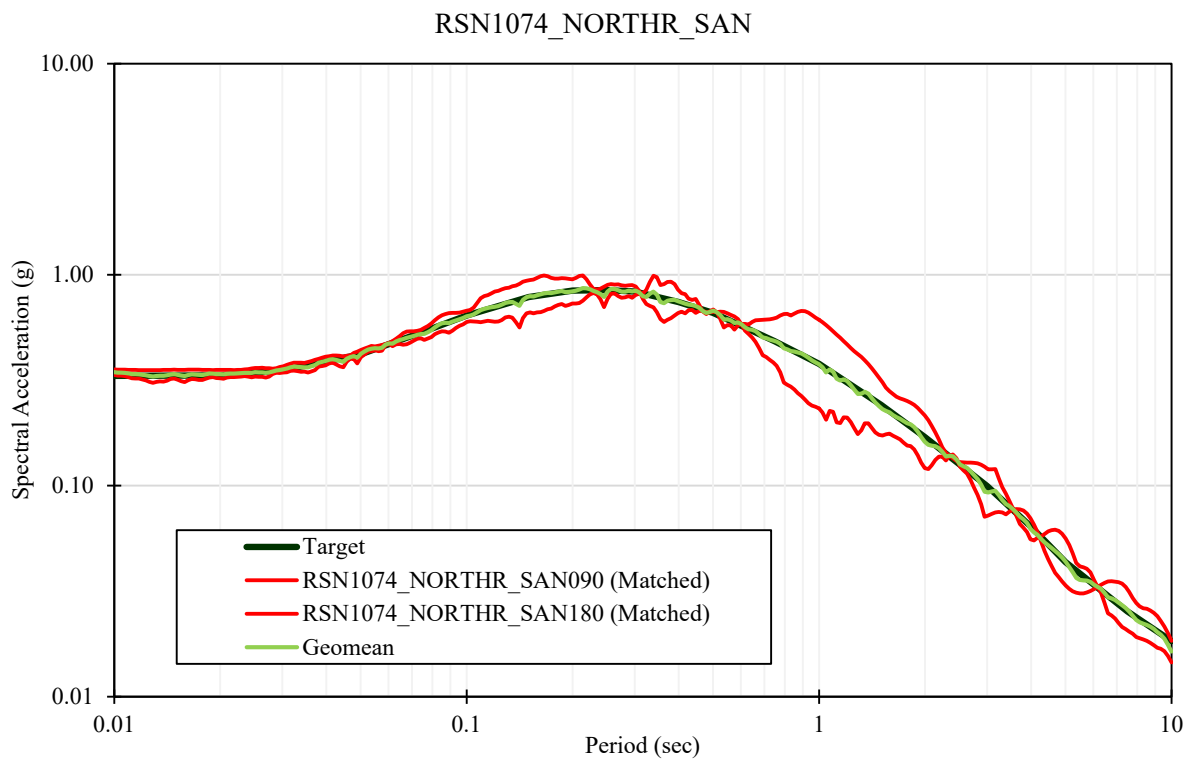
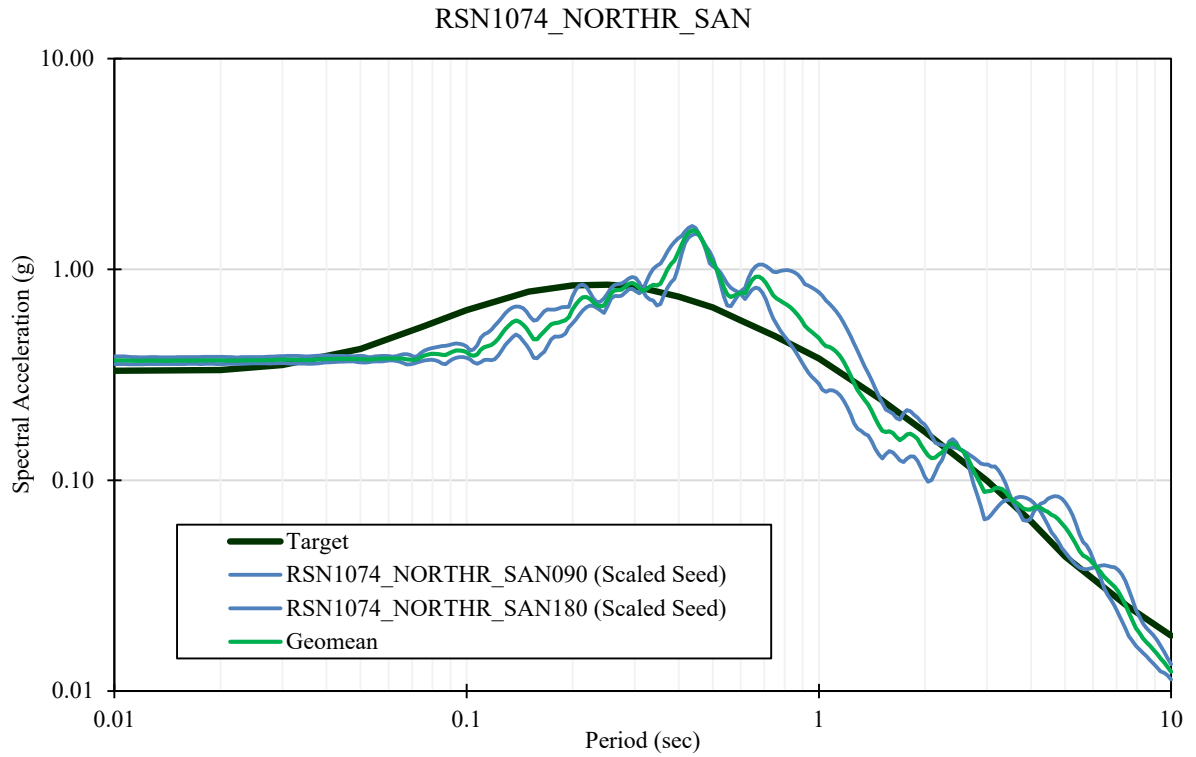
S:\1802\Figures\Figure_160.ai; Date: 05/03/2021; User: JCH.LCI



For Illustration
Purposes Only

1979 Imperial Valley-06 –
Calexico Fire Station

Figure 160
Time History Spectrally-Matched to
MDE for Intake No. 5, RSN 162 (H2)



S:\1802\Figures\Figure_161.ai; Date: 05/03/2021; User: JCh.LCI

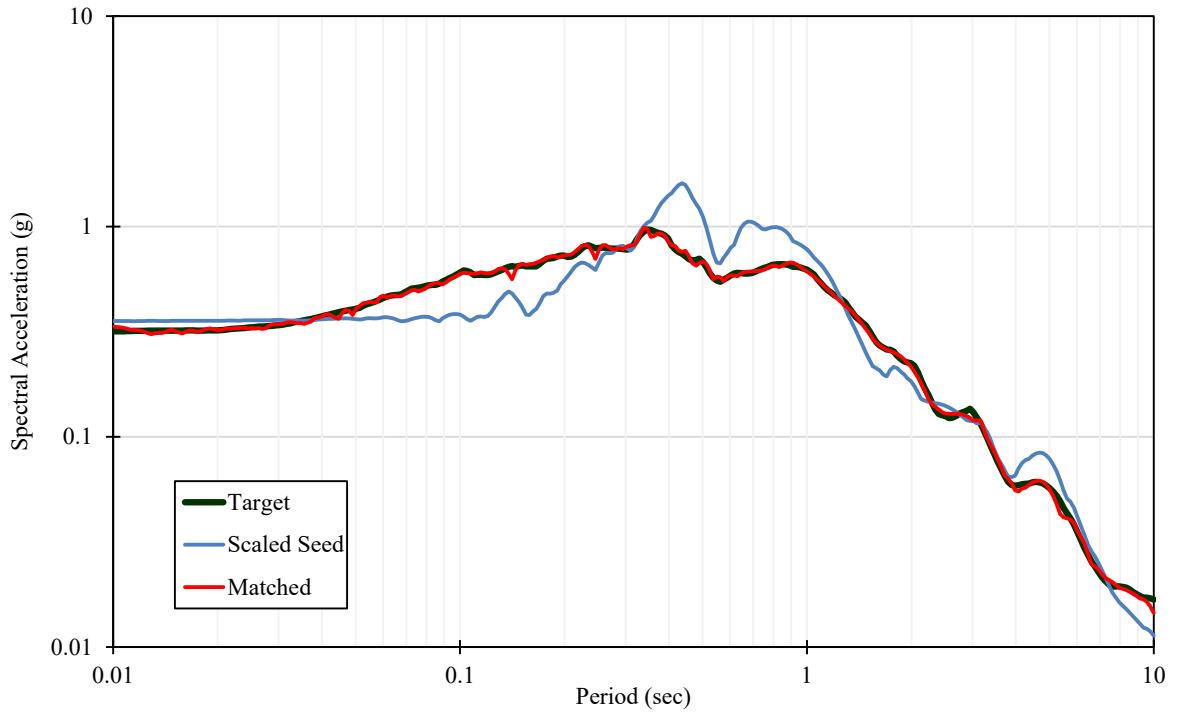


For Illustration
Purposes Only

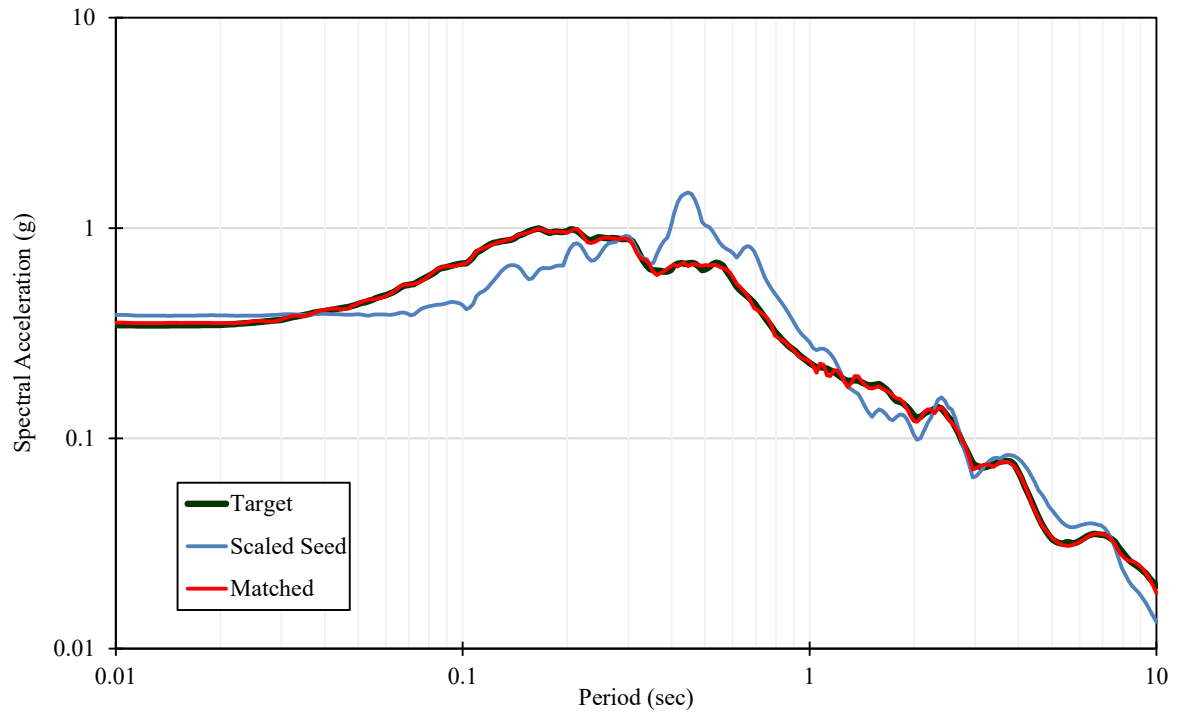
1995 Northridge-01 –
Sandberg-Bald Mtn

Figure 161
Response Spectra for MDE Time
Histories for Intake No. 5, RSN 1074

RSN1074_NORTHR_SAN090



RSN1074_NORTHR_SAN180



S:\1802\Figures\Figure_162.ai; Date: 05/03/2021; User: JCh.LCL

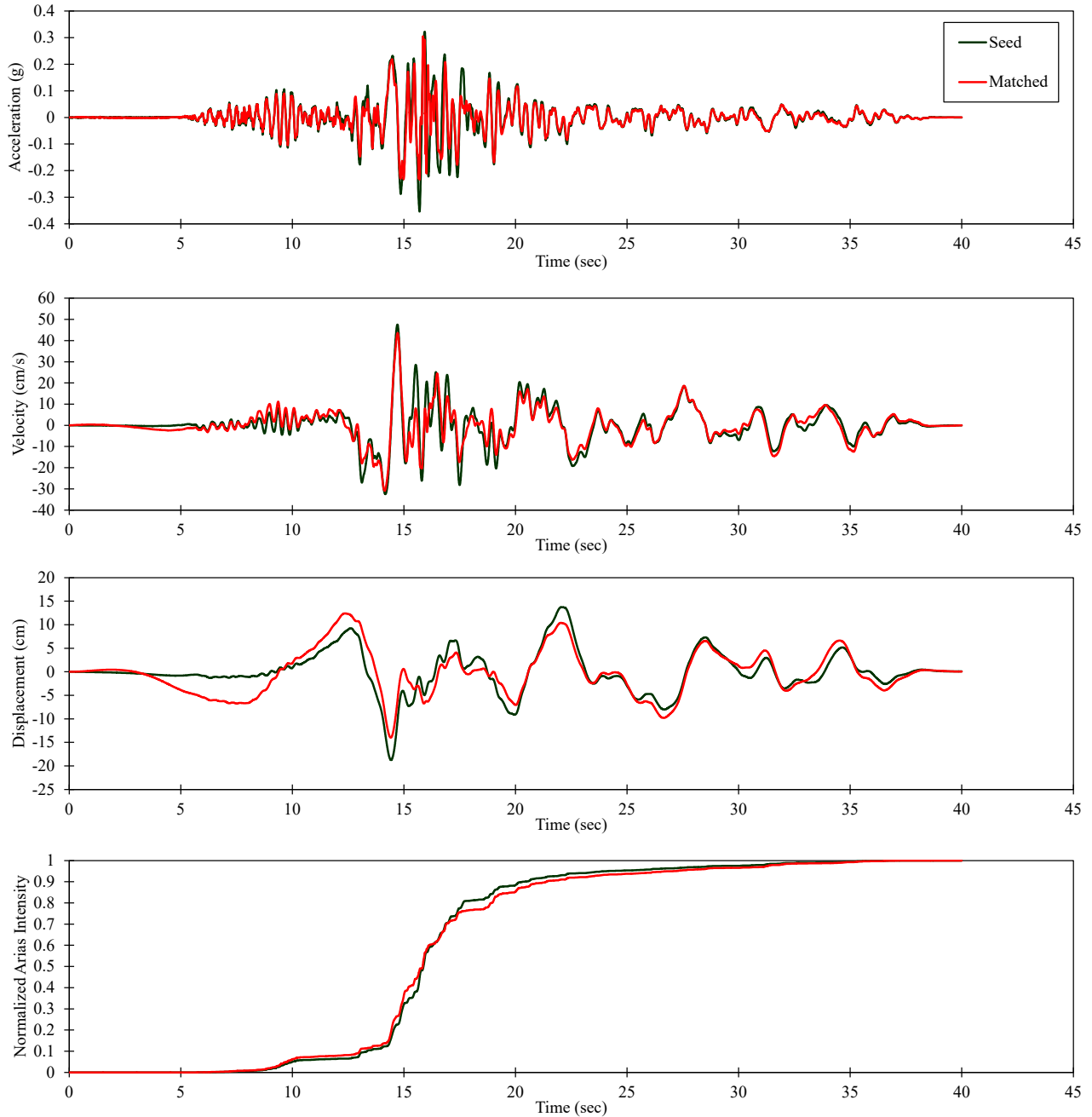


For Illustration
Purposes Only

1995 Northridge-01 –
Sandberg-Bald Mtn

Figure 162
Spectral Matches for MDE Time
Histories for Intake No. 5, RSN 1074

RSN1074_NORTHR_SAN090



S:\1802\Figures\Figure_163.ai; Date: 05/03/2021; User: JCh.LCL

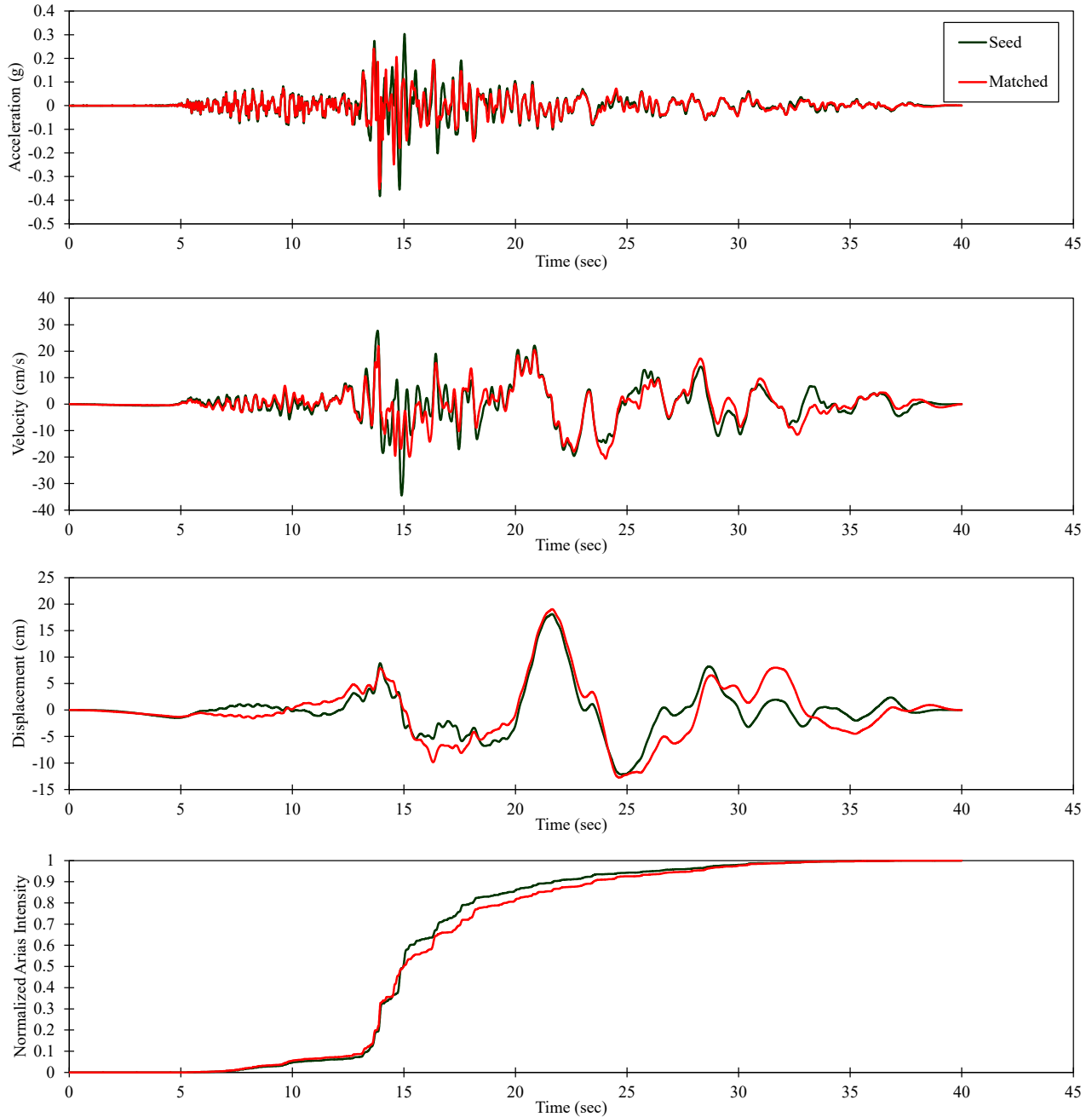


For Illustration
Purposes Only

1995 Northridge-01 –
Sandberg-Bald Mtn

Figure 163
Time History Spectrally-Matched to
MDE for Intake No. 5, RSN 1074 (H1)

RSN1074_NORTHR_SAN180



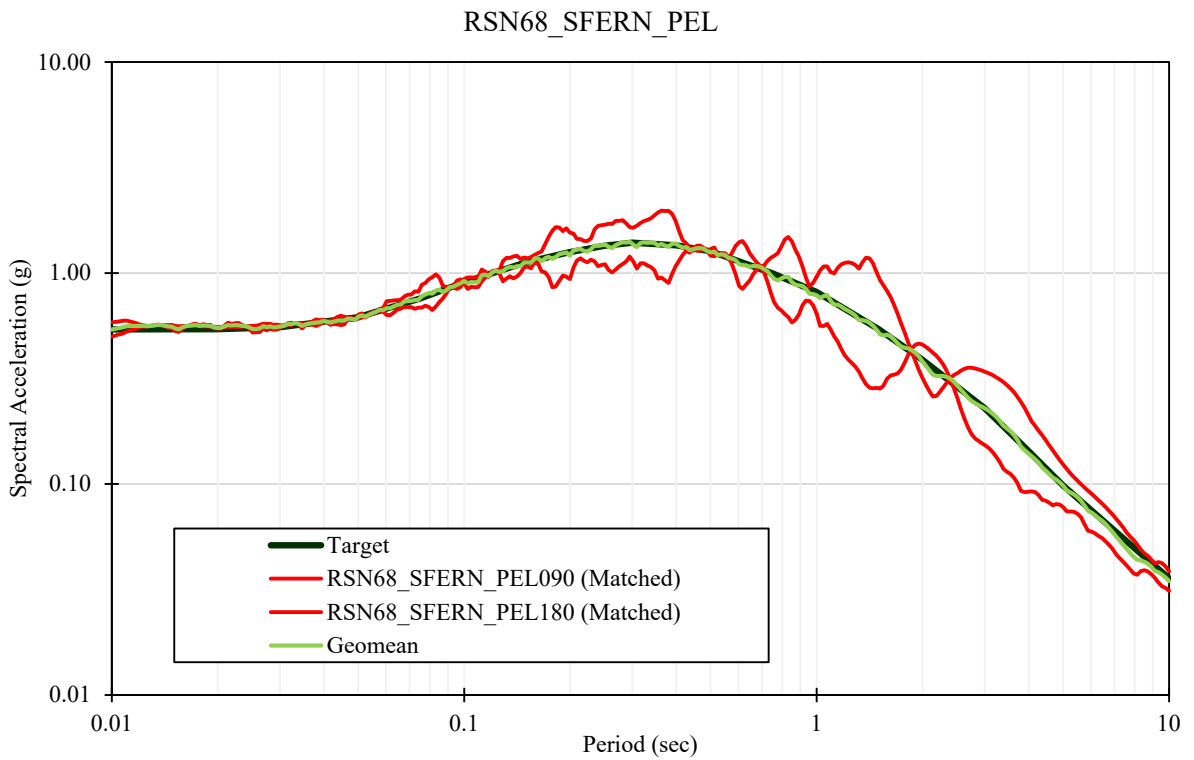
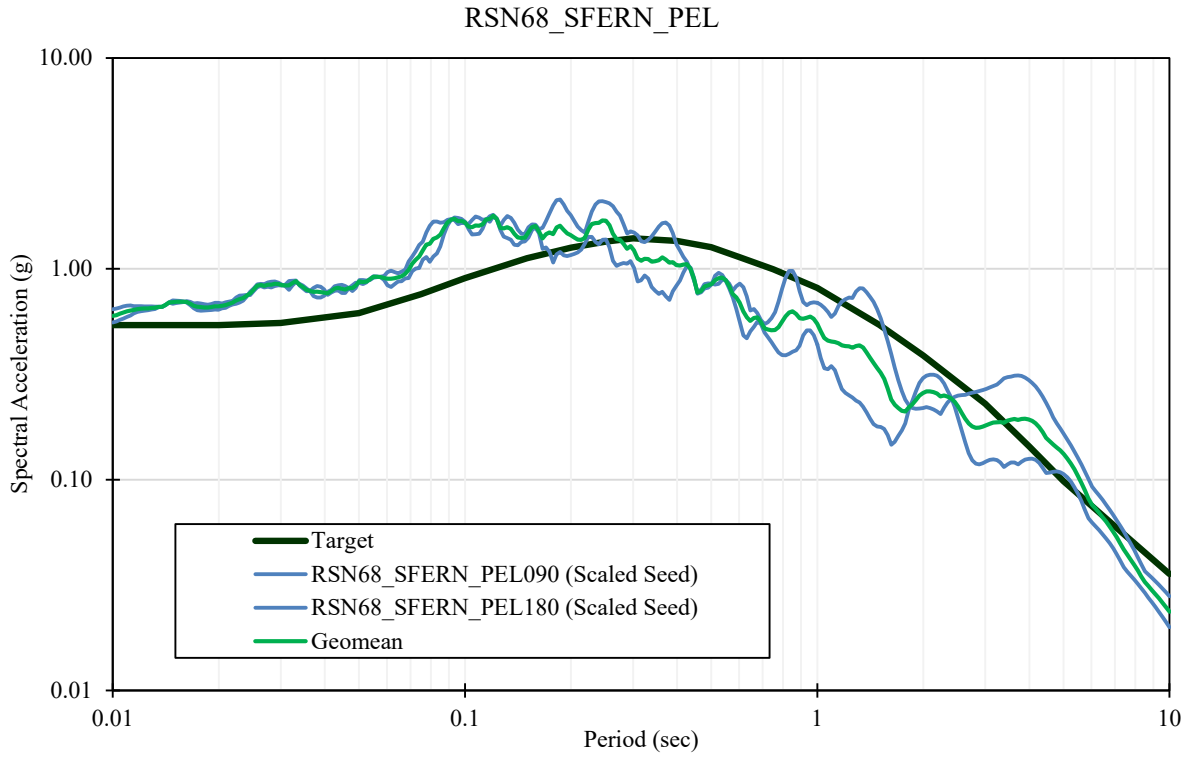
S:\1802\Figures\Figure_164.ai; Date: 05/03/2021; User: JCh.LCL



For Illustration
Purposes Only

1995 Northridge-01 –
Sandberg-Bald Mtn

Figure 164
Time History Spectrally-Matched to
MDE for Intake No. 5, RSN 1074 (H2)



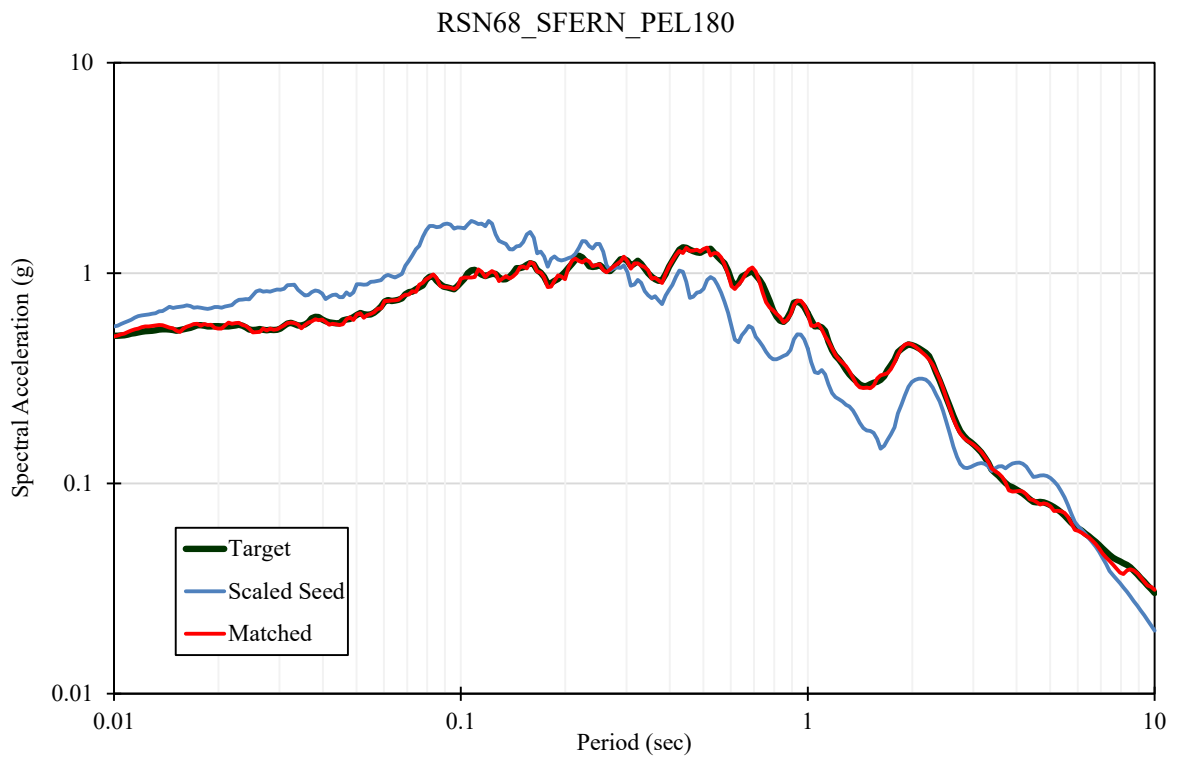
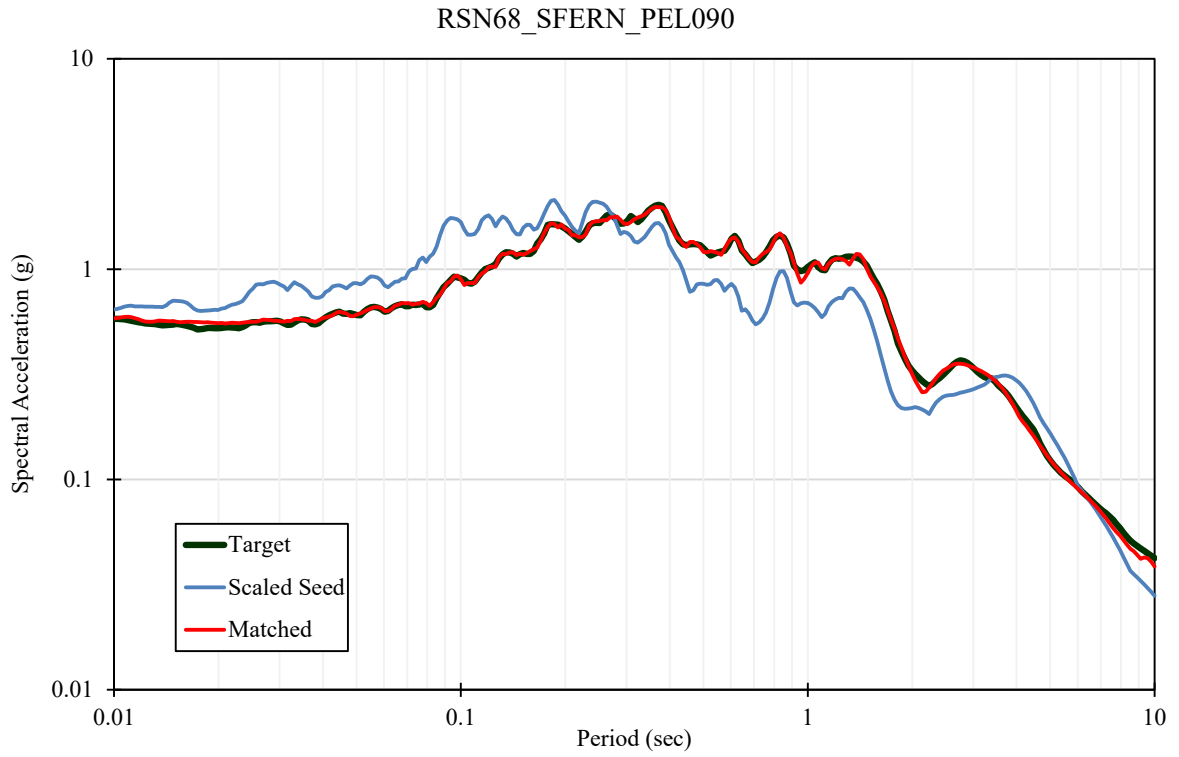
S:\1802\Figures\Figure_165.ai; Date: 05/03/2021; User: JCh.LCI



For Illustration
Purposes Only

1971 San Fernando –
LA-Hollywood Stor FF

Figure 165
Response Spectra for MDE Time
Histories for Bouldin, RSN 68



S:\1802\Figures\Figure_166.ai; Date: 05/03/2021; User: JCh.LCL

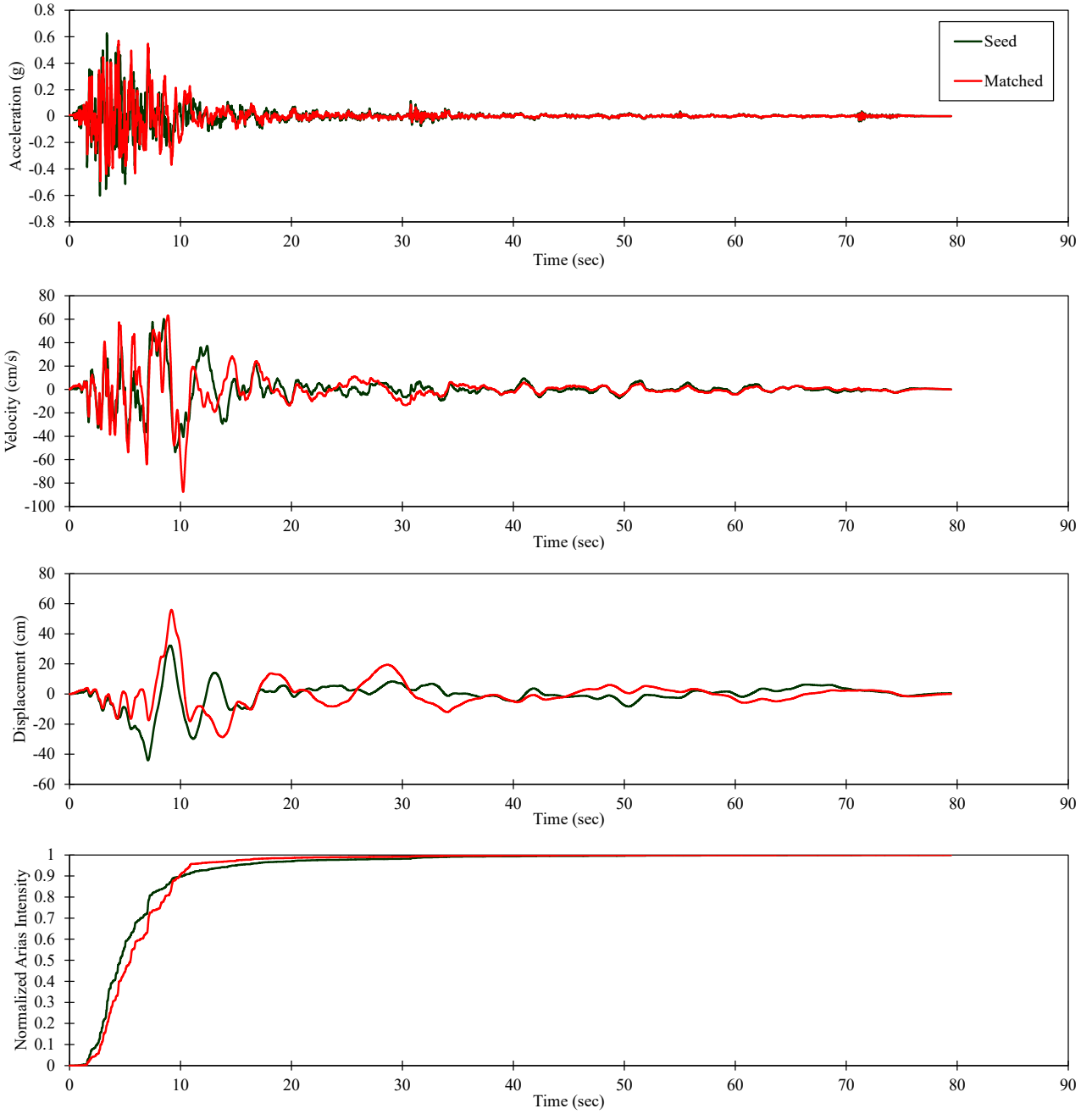


For Illustration
Purposes Only

1971 San Fernando –
LA-Hollywood Stor FF

Figure 166
Spectral Matches for MDE Time
Histories for Bouldin, RSN 68

RSN68_SFERN_PEL090



S:\1802\Figures\Figure_167.ai; Date: 05/03/2021; User: JCh.LCL

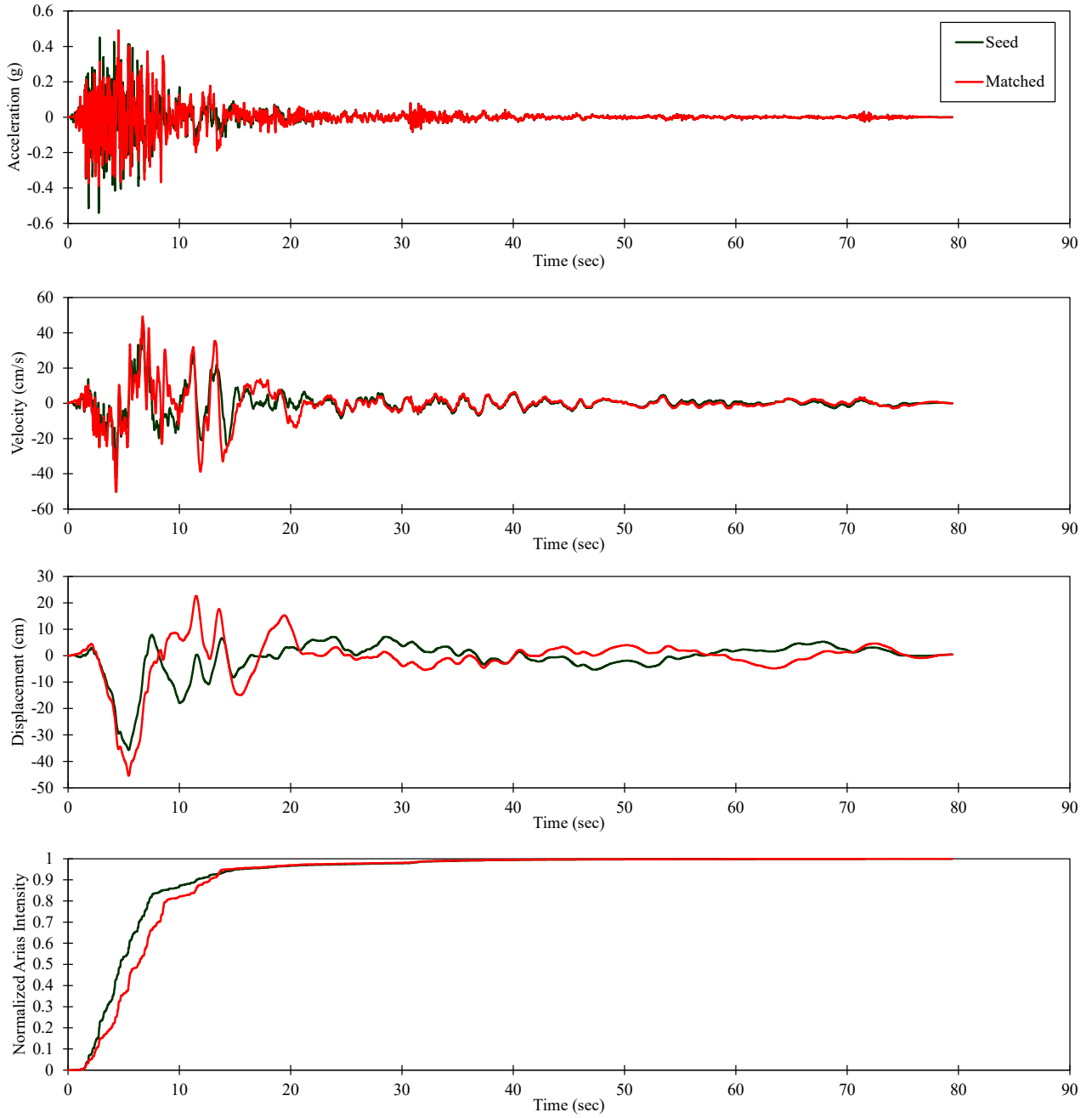


For Illustration
Purposes Only

1971 San Fernando –
LA-Hollywood Stor FF

Figure 167
Time History Spectrally-Matched to
MDE for Bouldin, RSN 68 (H1)

RSN68_SFERN_PEL180



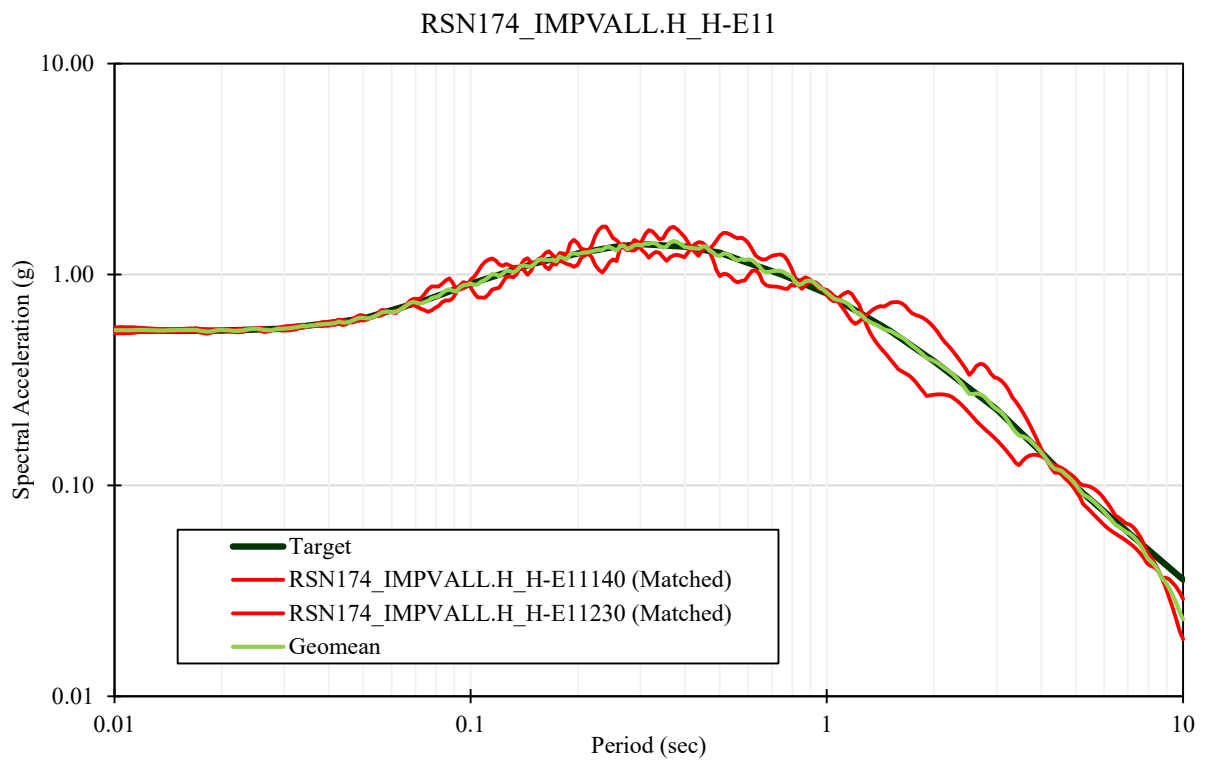
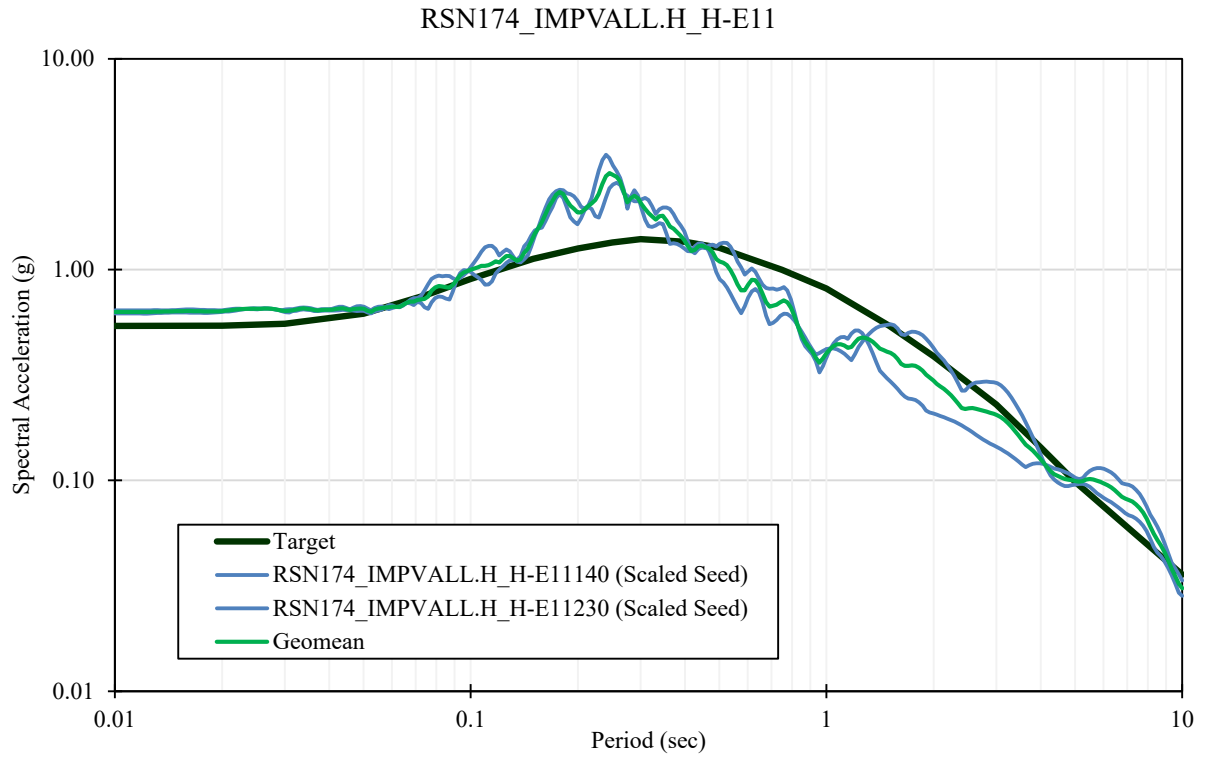
S:\1802\Figures\Figure_168.ai; Date: 05/03/2021; User: JCh.LCL



For Illustration
Purposes Only

1971 San Fernando –
LA-Hollywood Stor FF

Figure 168
Time History Spectrally-Matched to
MDE for Bouldin, RSN 68 (H2)



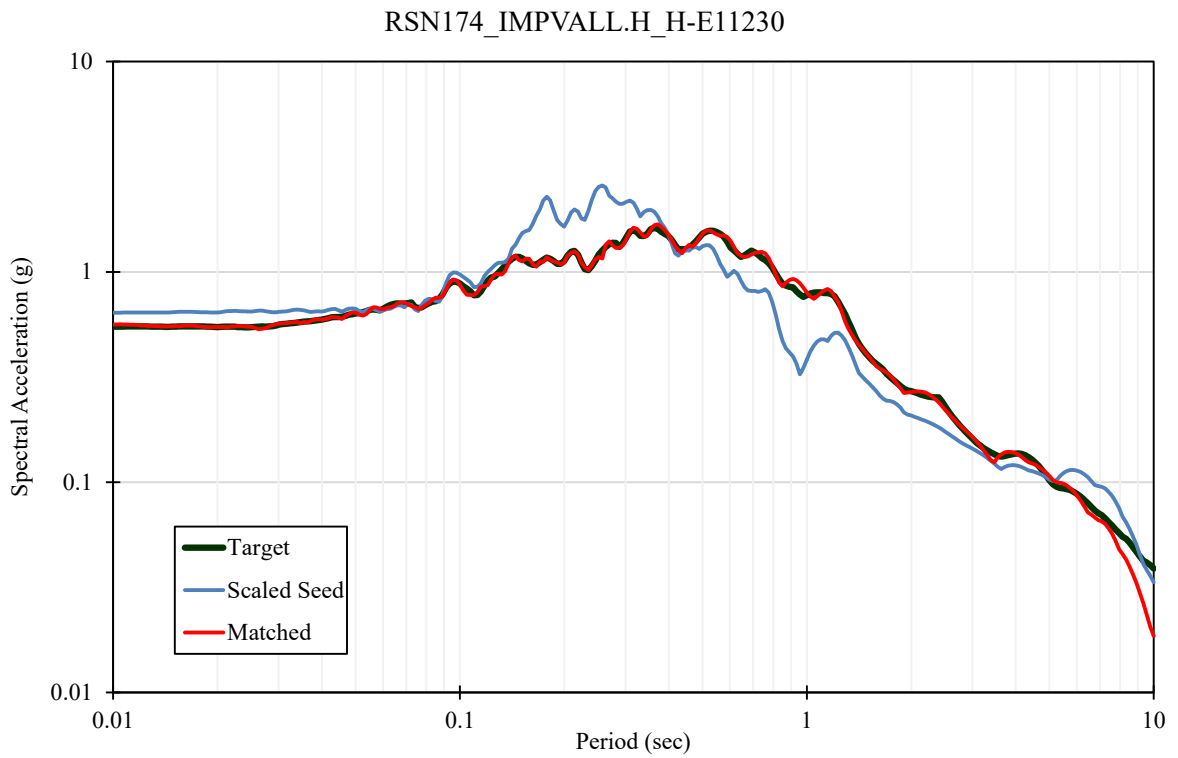
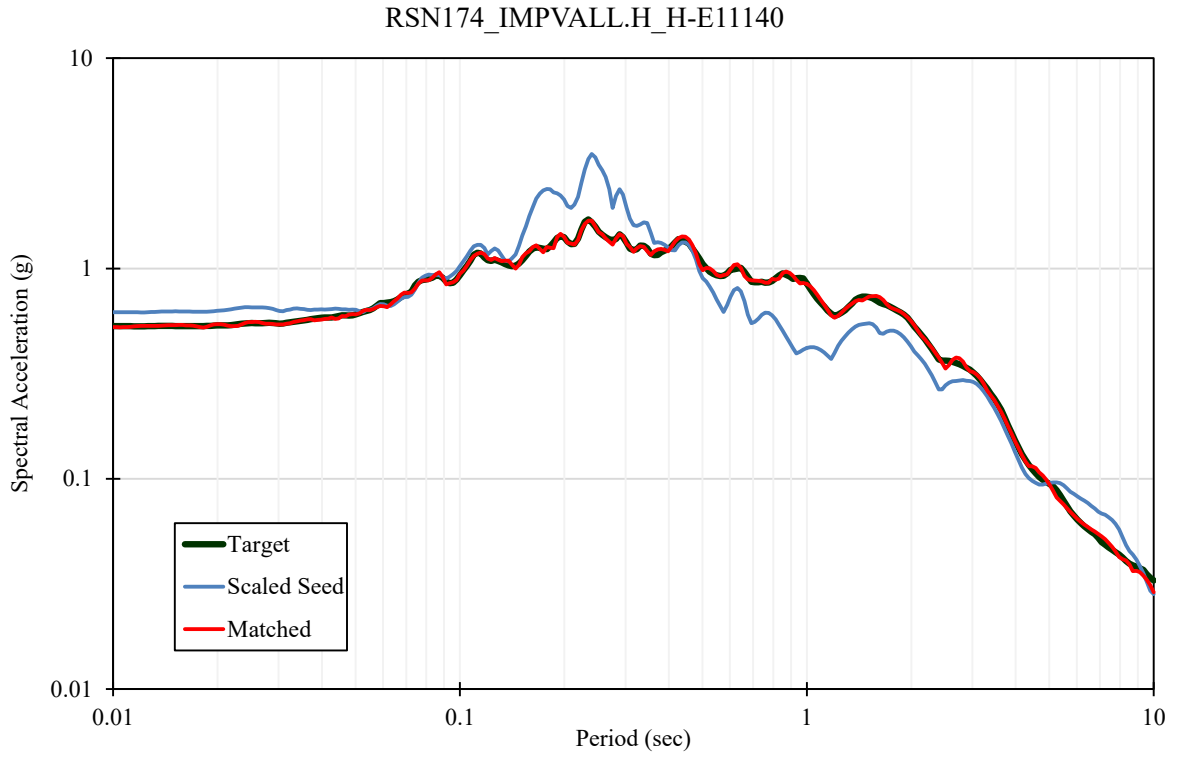
S:\1802\Figures\Figure_169.ai; Date: 05/03/2021; User: JCh.LCI



For Illustration
Purposes Only

1979 Imperial Valley-06 –
EI Centro Array No.11

Figure 169
Response Spectra for MDE Time
Histories for Bouldin, RSN 174



S:\1802\Figures\Figure_170.ai; Date: 05/04/2021; User: JCh.LCL

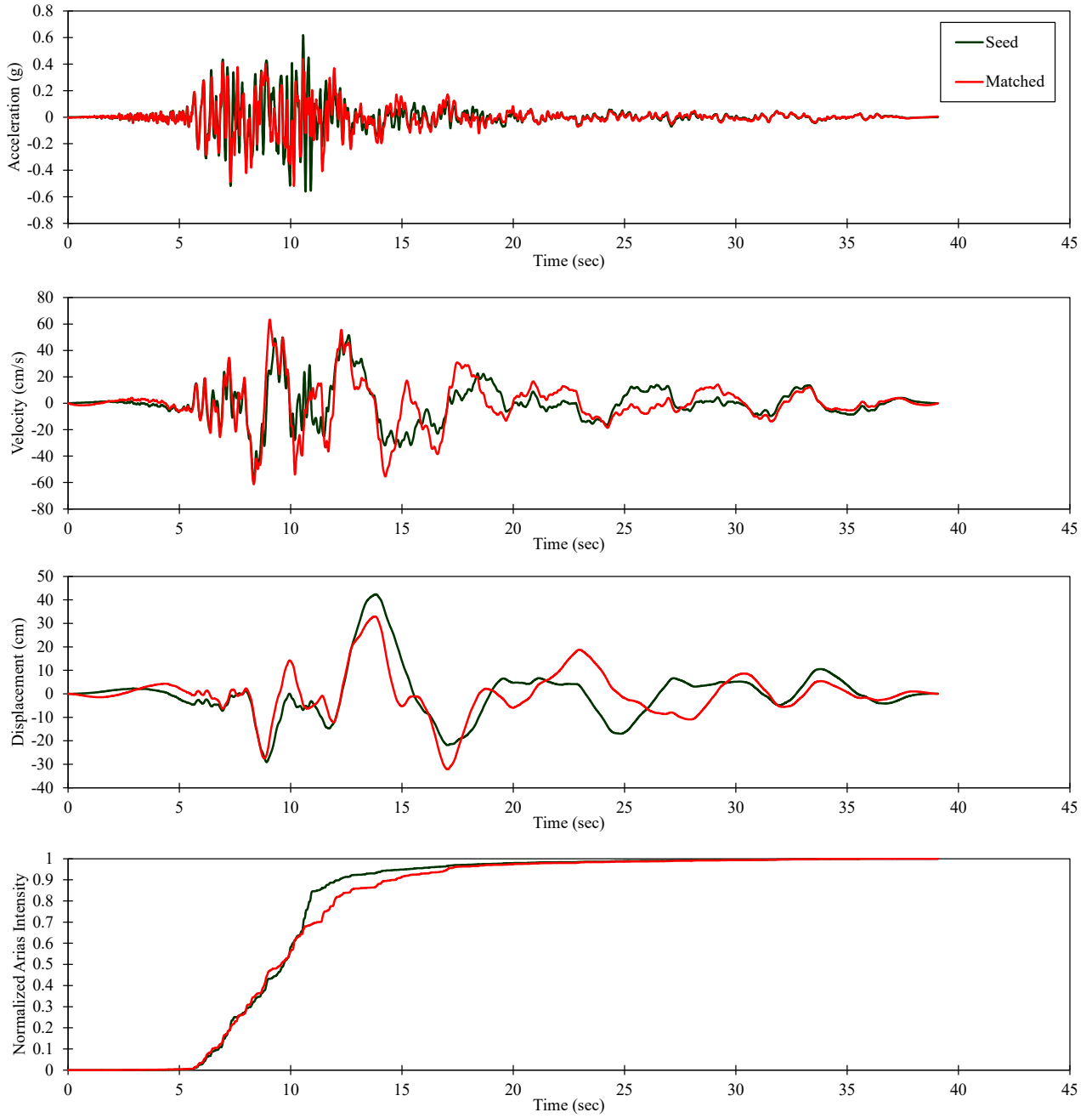


For Illustration
Purposes Only

1979 Imperial Valley-06 –
El Centro Array No.11

Figure 170
Spectral Matches for MDE Time
Histories for Bouldin, RSN 174

RSN174_IMPVALL.H_H-E11140



S:\1802\Figures\Figure_170.ai; Date: 05/04/2021; User: JCh.LCL

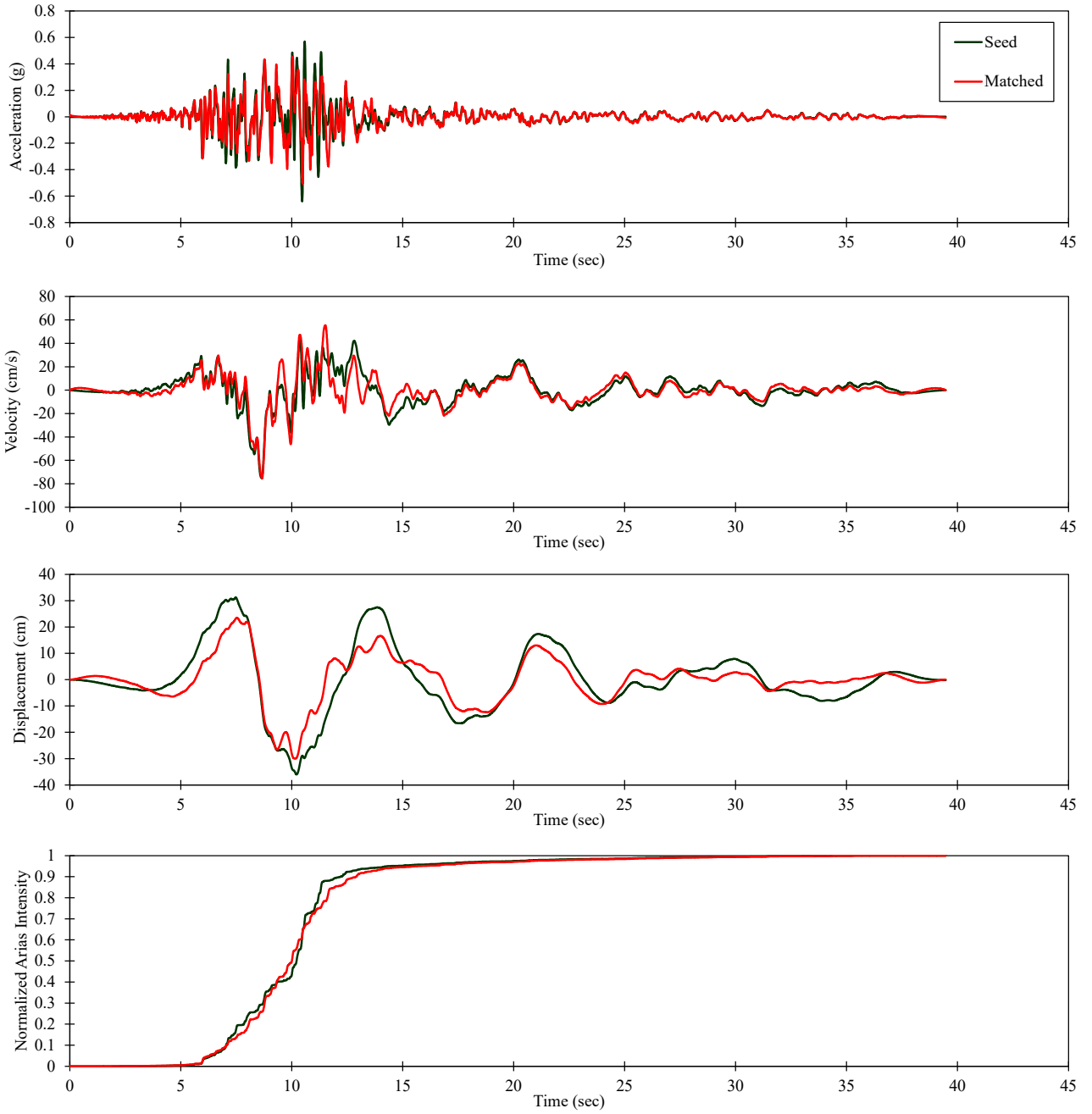


For Illustration
Purposes Only

1979 Imperial Valley-06 –
EI Centro Array No.11

Figure 171
Time History Spectrally-Matched to
MDE for Bouldin, RSN 174 (H1)

RSN174_IMPVAL.L.H_H-E11230



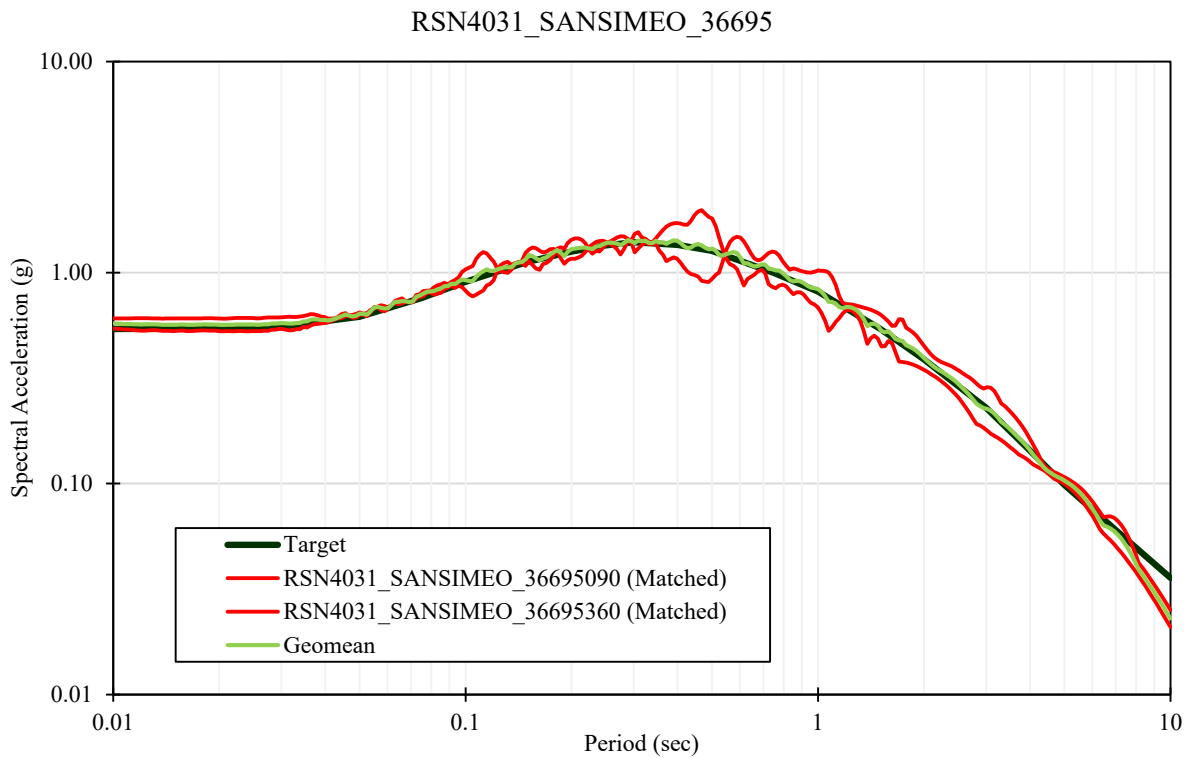
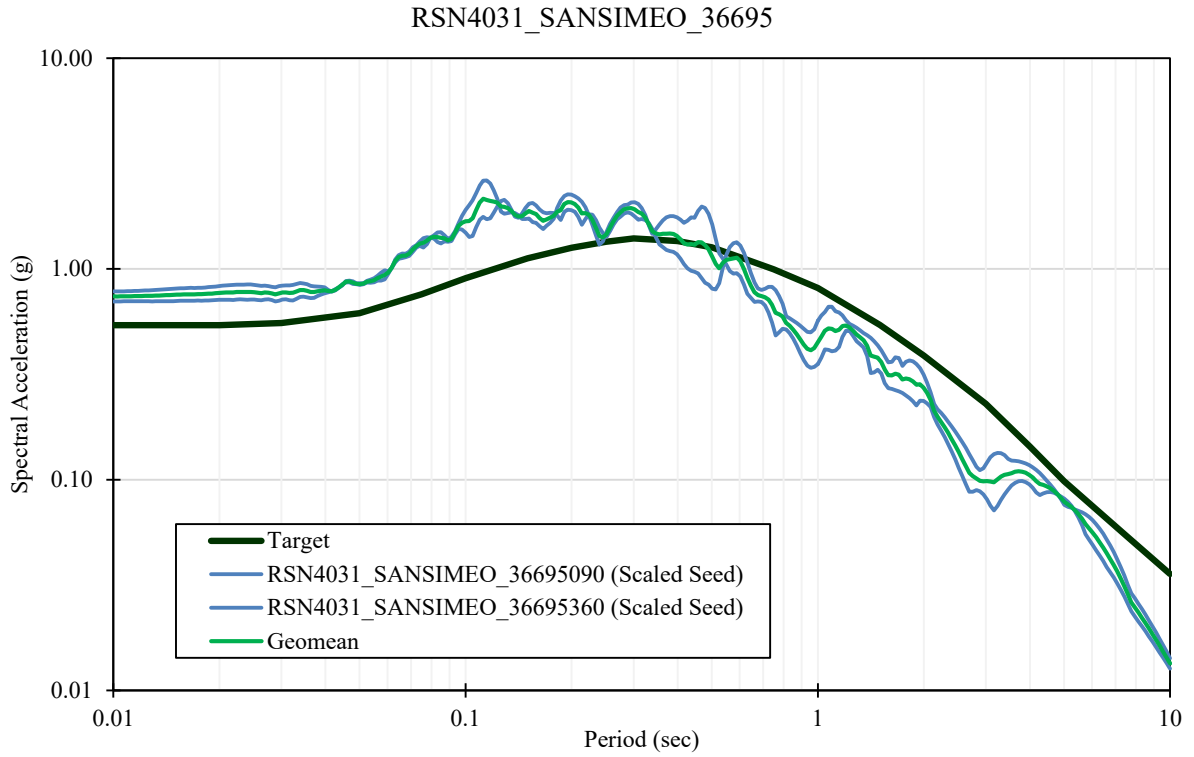
S:\1802\Figures\Figure_172.ai; Date: 05/04/2021 User: JCH.LCI



For Illustration
Purposes Only

1979 Imperial Valley-06 –
EI Centro Array No.11

Figure 172
Time History Spectrally-Matched to
MDE for Bouldin, RSN 174 (H2)



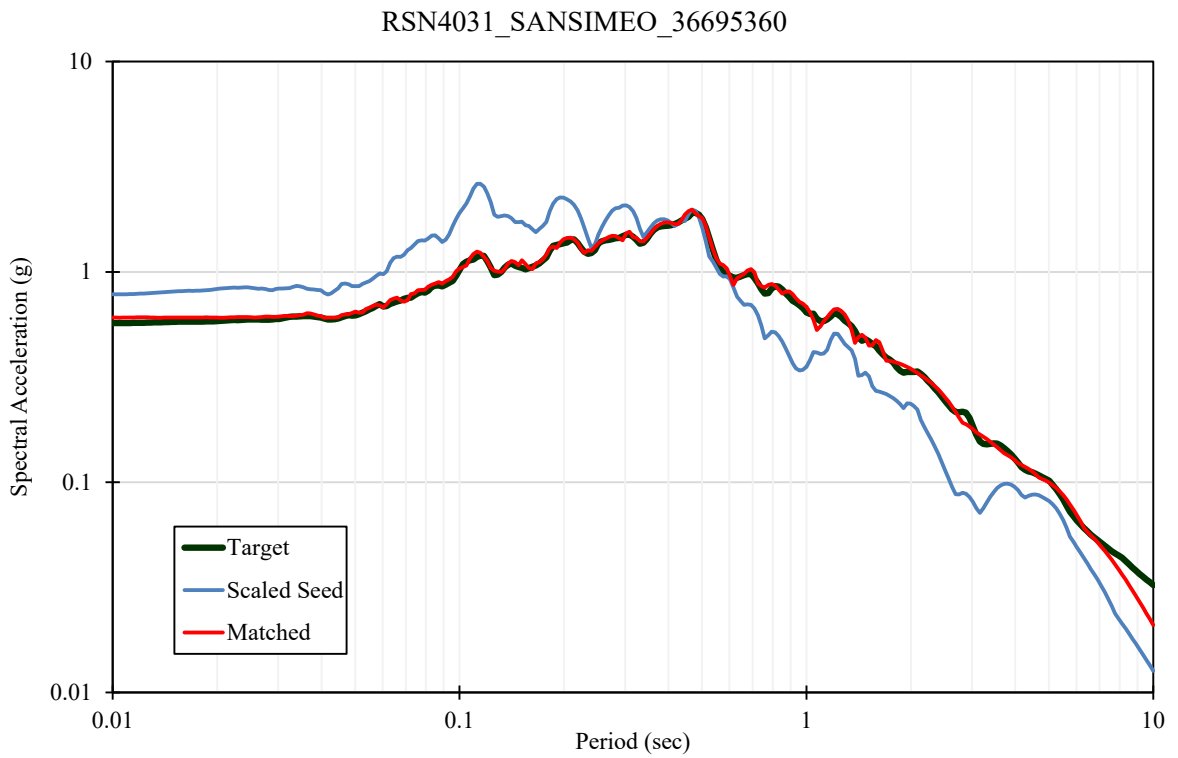
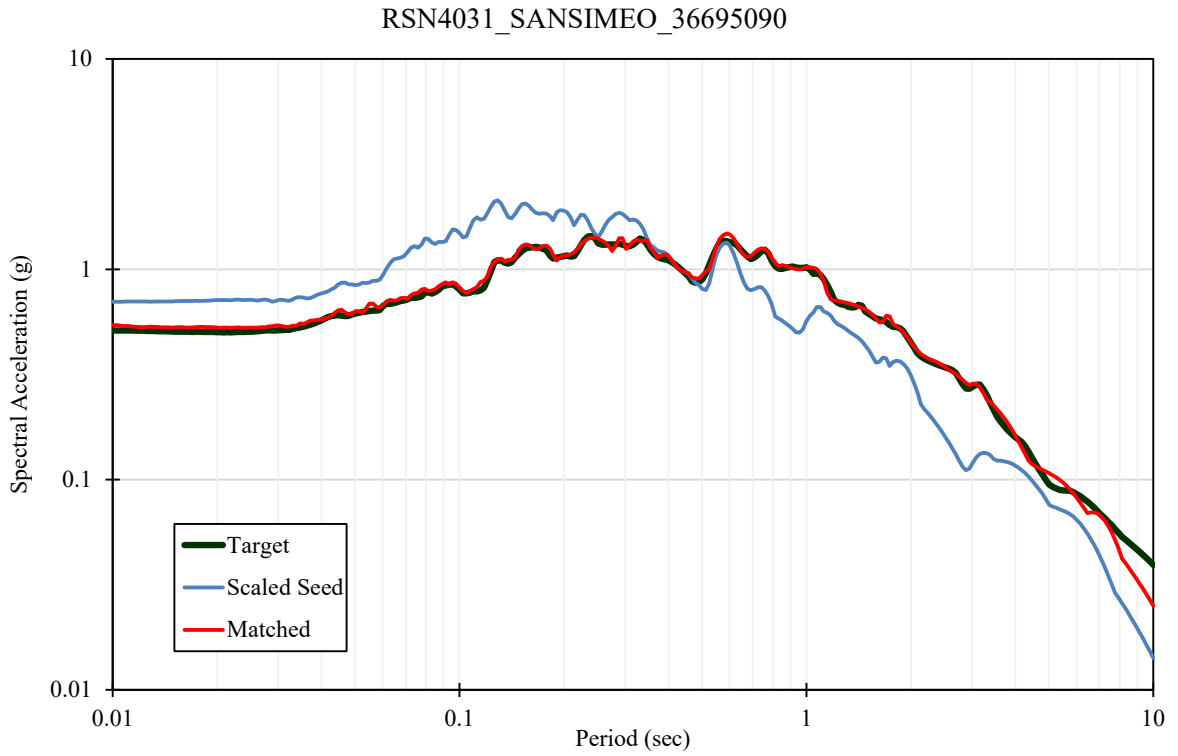
S:\1802\Figures\Figure_173.ai; Date: 05/04/2021; User: JCh.LCI



For Illustration
Purposes Only

2003 San Simeon –
Templeton -1 story

Figure 173
Response Spectra for MDE Time
Histories for Bouldin, RSN 4031



S:\1802\Figures\Figure_174.ai; Date: 05/04/2021; User: JCh.LCL

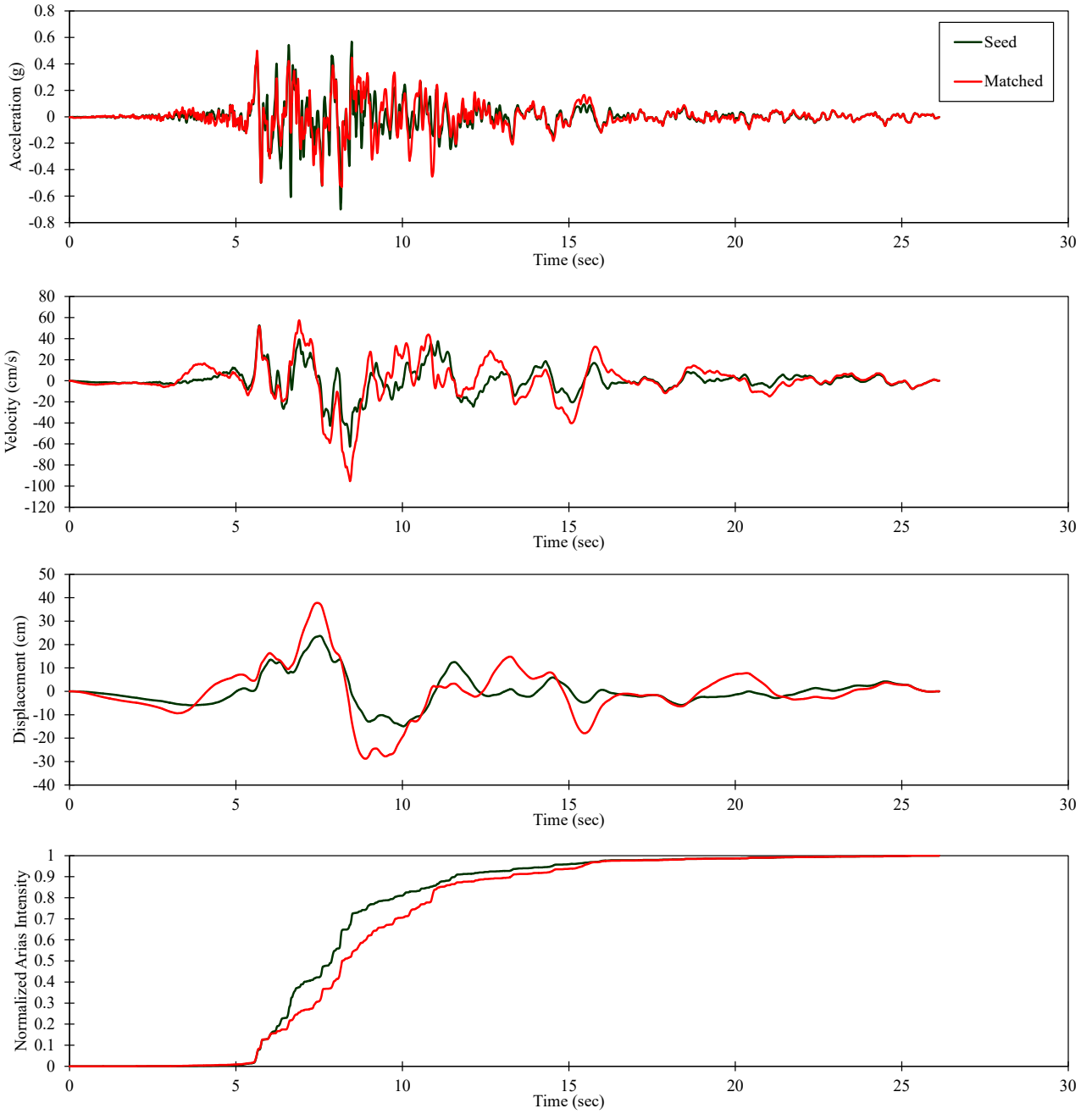


For Illustration
Purposes Only

**2003 San Simeon –
Templeton -1 story**

**Figure 174
Spectral Matches for MDE Time
Histories for Bouldin, RSN 4031**

RSN4031_SANSIMEO_36695090



S:\1802\Figures\Figure_175.ai; Date: 05/04/2021; User: JCh.LCL

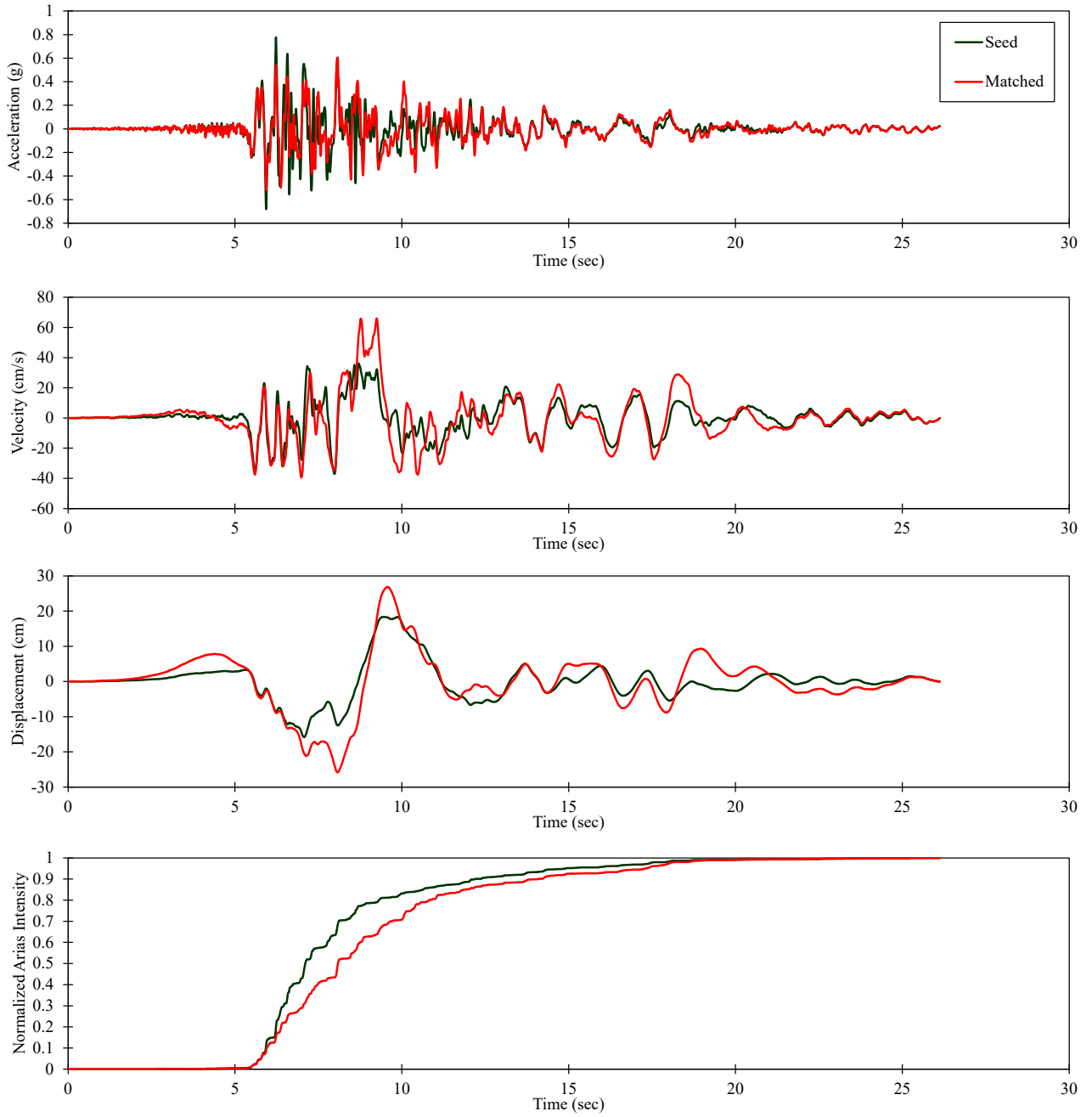


For Illustration
Purposes Only

2003 San Simeon –
Templeton -1 story

Figure 175
Time History Spectrally-Matched to
MDE for Bouldin, RSN 4031 (H1)

RSN4031_SANSIMEO_36695360



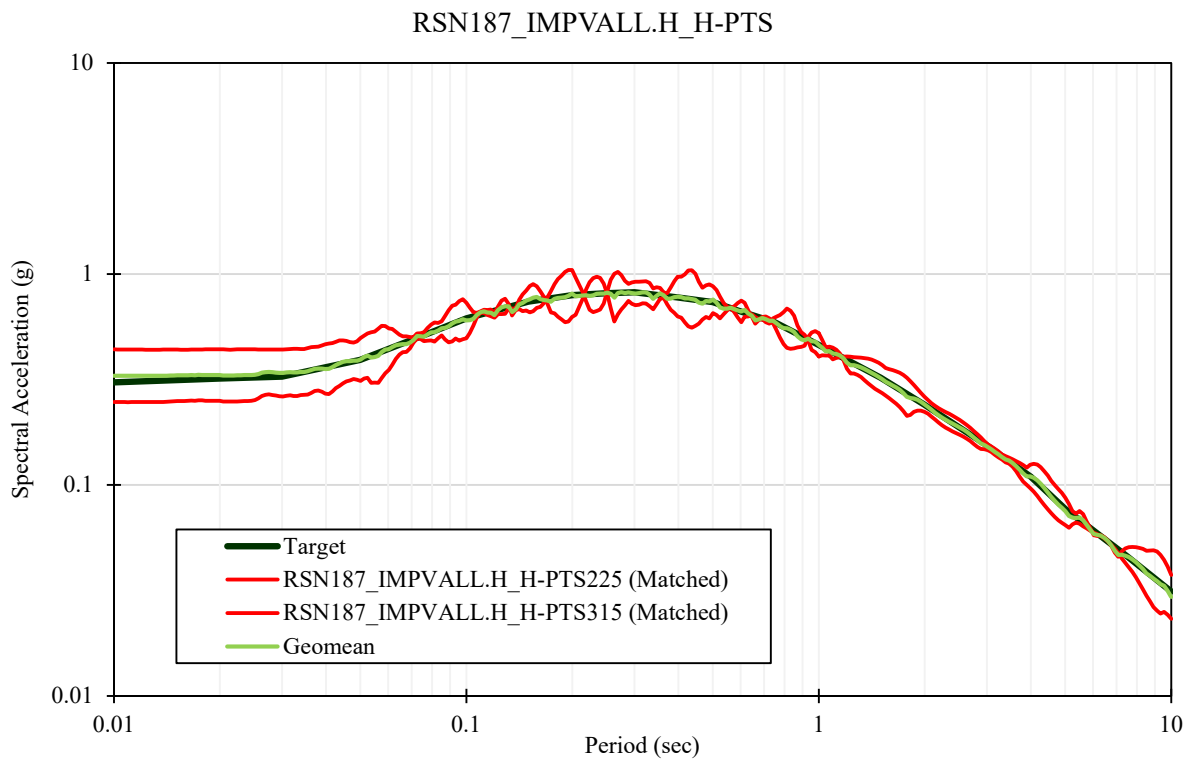
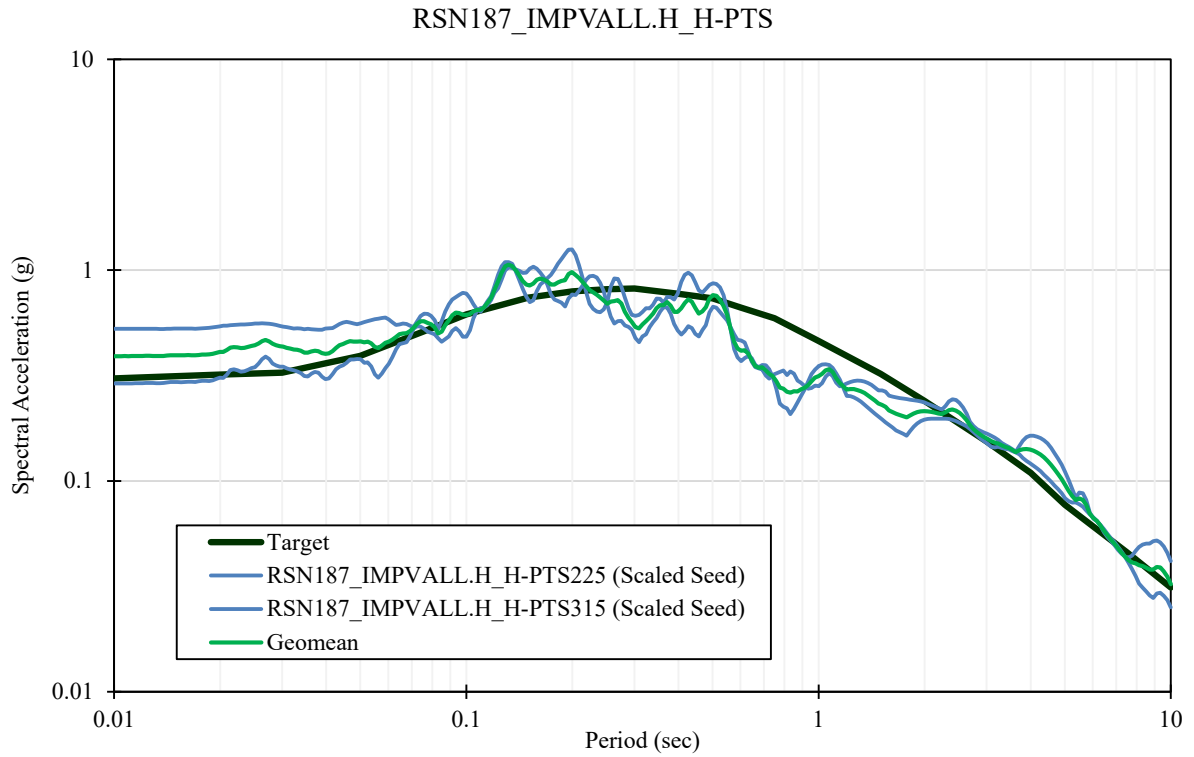
S:\1802\Figures\Figure_176.ai; Date: 05/04/2021; User: JCh.LCL



For Illustration
Purposes Only

2003 San Simeon –
Templeton -1 story

Figure 176
Time History Spectrally-Matched to
MDE for Bouldin, RSN 4031 (H2)



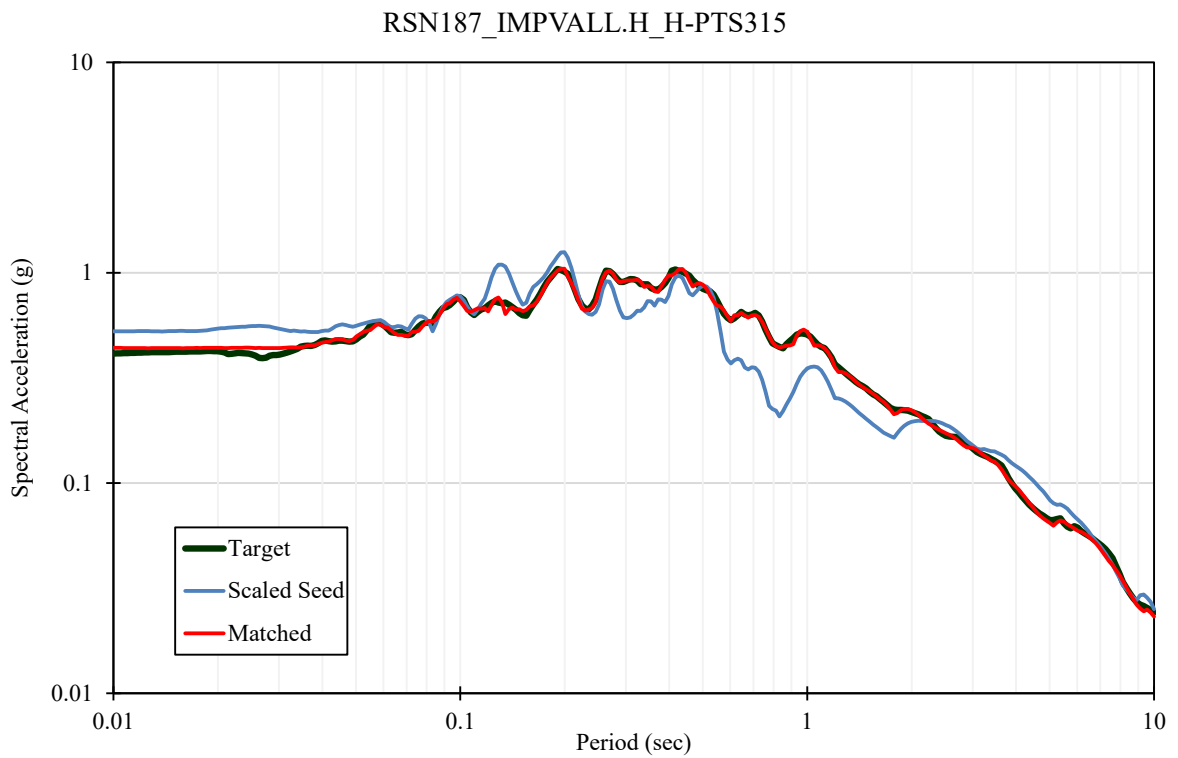
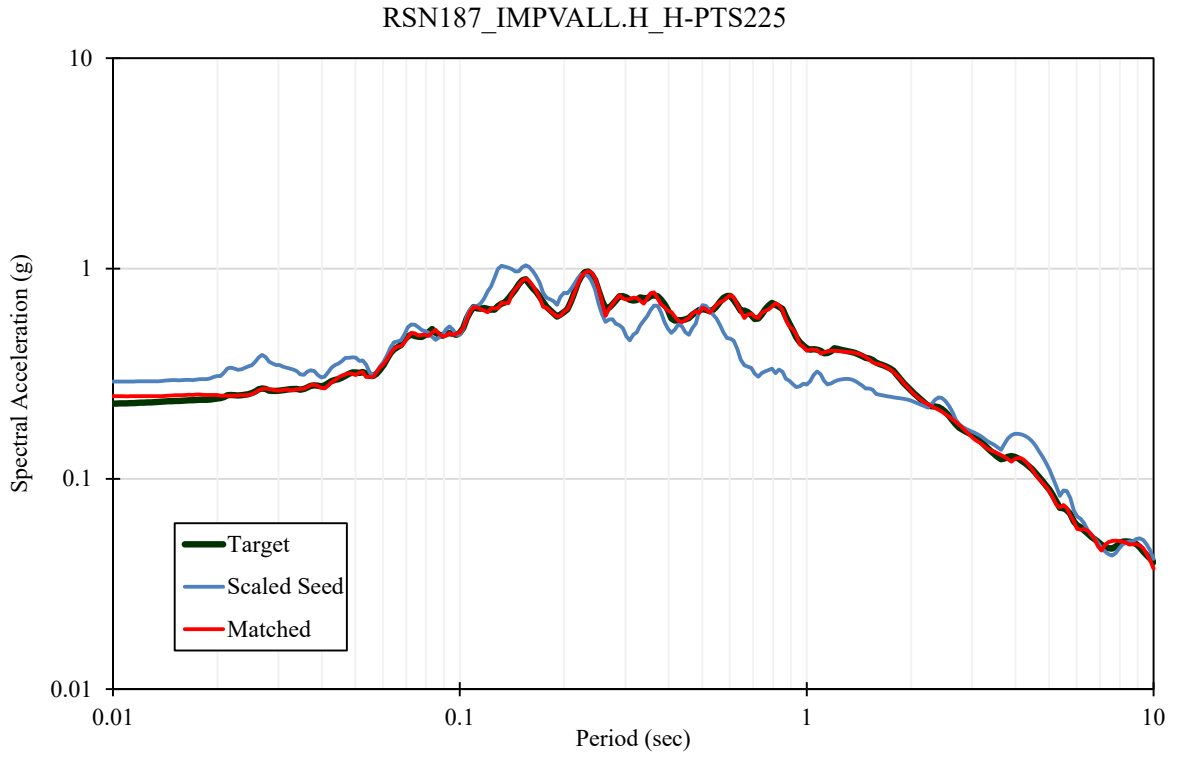
S:\1802\Figures\Figure_177.ai; Date: 05/04/2021; User: JCh.LCI



For Illustration
Purposes Only

1979 Imperial Valley-06 –
Parachute Test Site

Figure 177
Response Spectra for MDE Time
Histories for Twin Cities, RSN 187



S:\1802\Figures\Figure_178.ai; Date: 05/04/2021; User: JCh.LCL

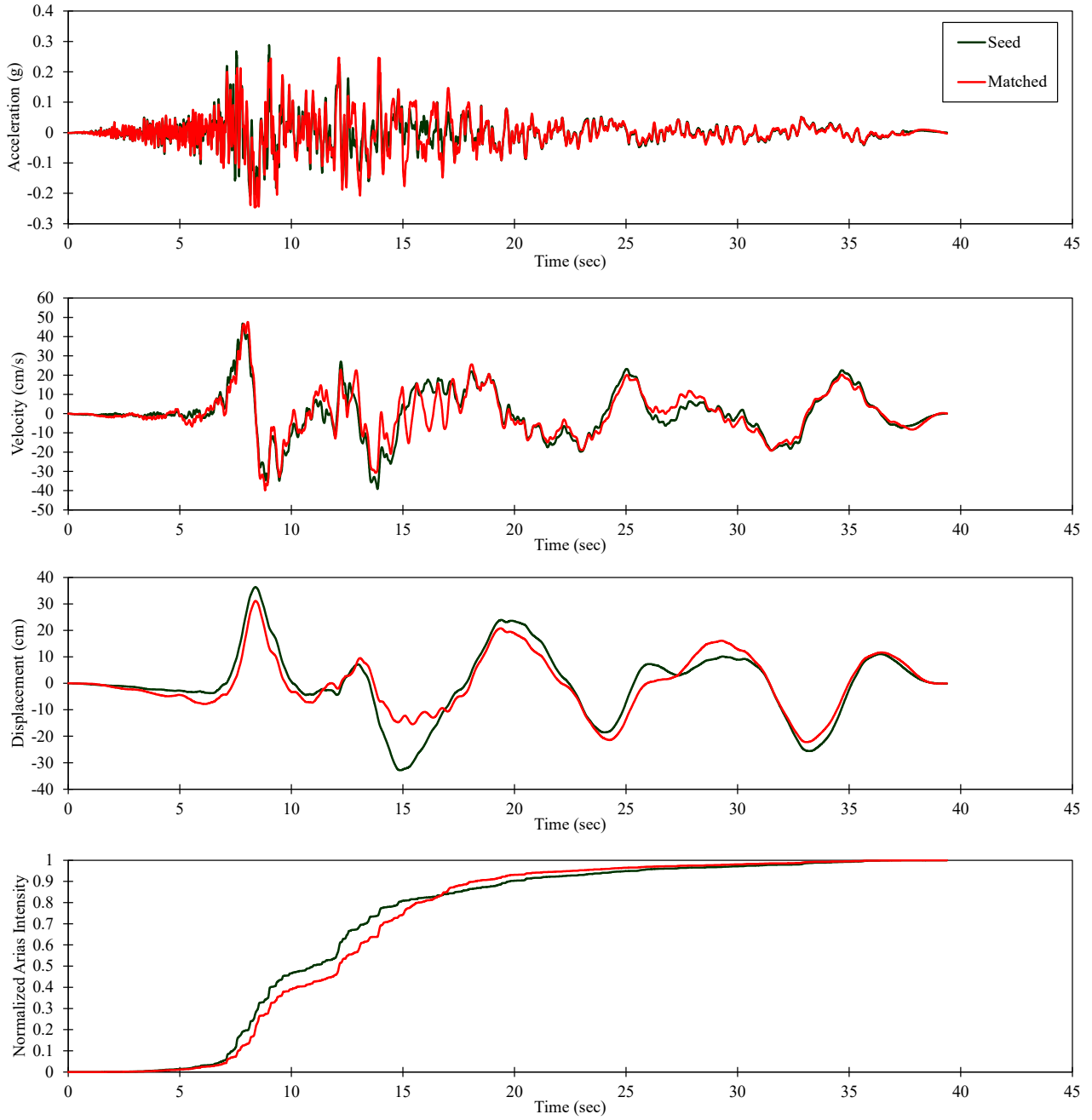


For Illustration
Purposes Only

1980 Imperial Valley-06 –
Parachute Test Site

Figure 178
Spectral Matches for MDE Time
Histories for Twin Cities, RSN 187

RSN187_IMPVAL.L_H_H-PTS225



S:\1802\Figures\Figure_179.ai; Date: 05/04/2021; User: JCh.LCL

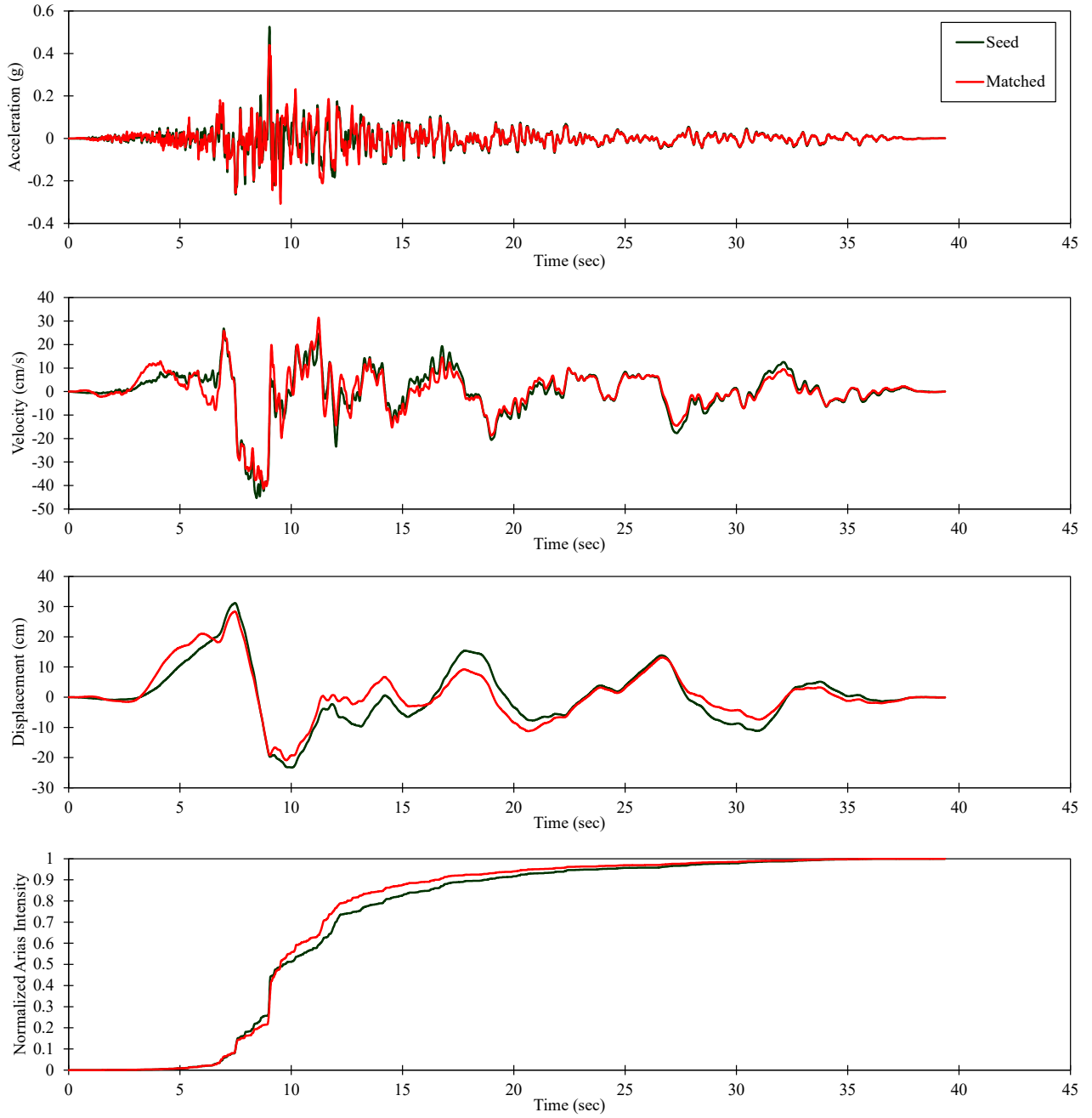


For Illustration
Purposes Only

1981 Imperial Valley-06 –
Parachute Test Site

Figure 179
Time History Spectrally-Matched to
MDE for Twin Cities, RSN 187 (H1)

RSN187_IMPVAL.L_H_H-PTS315



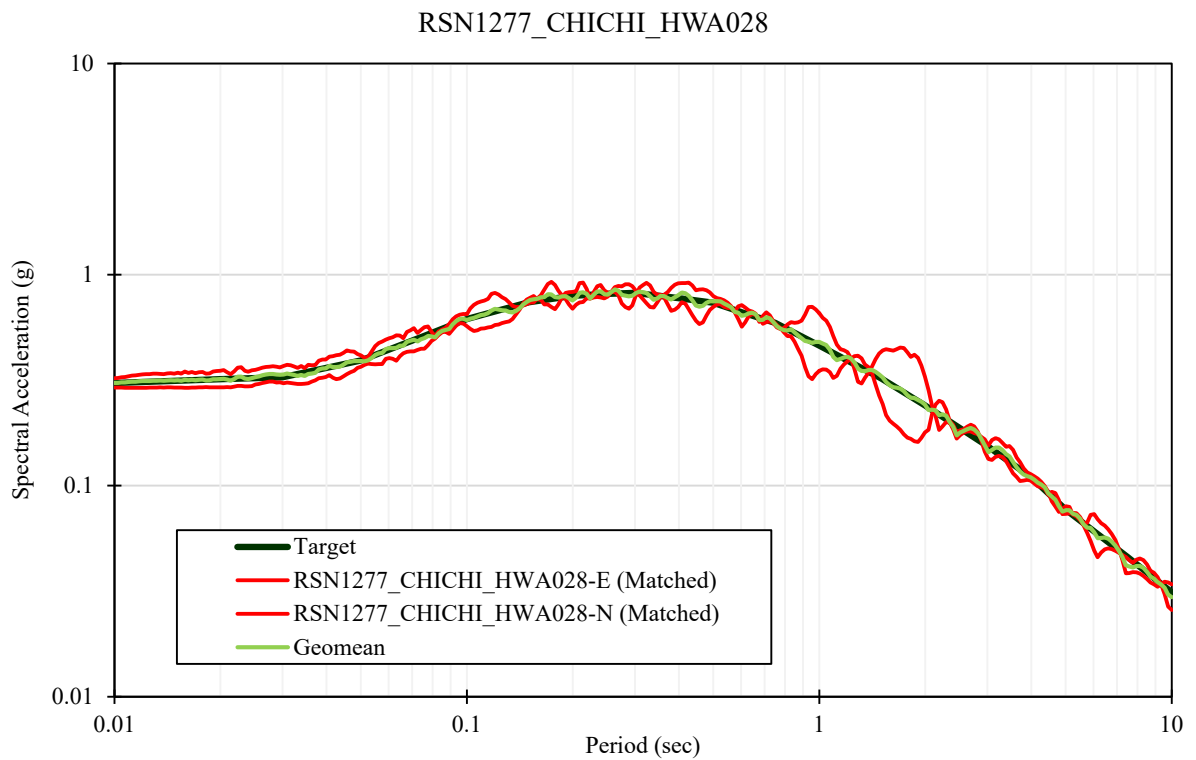
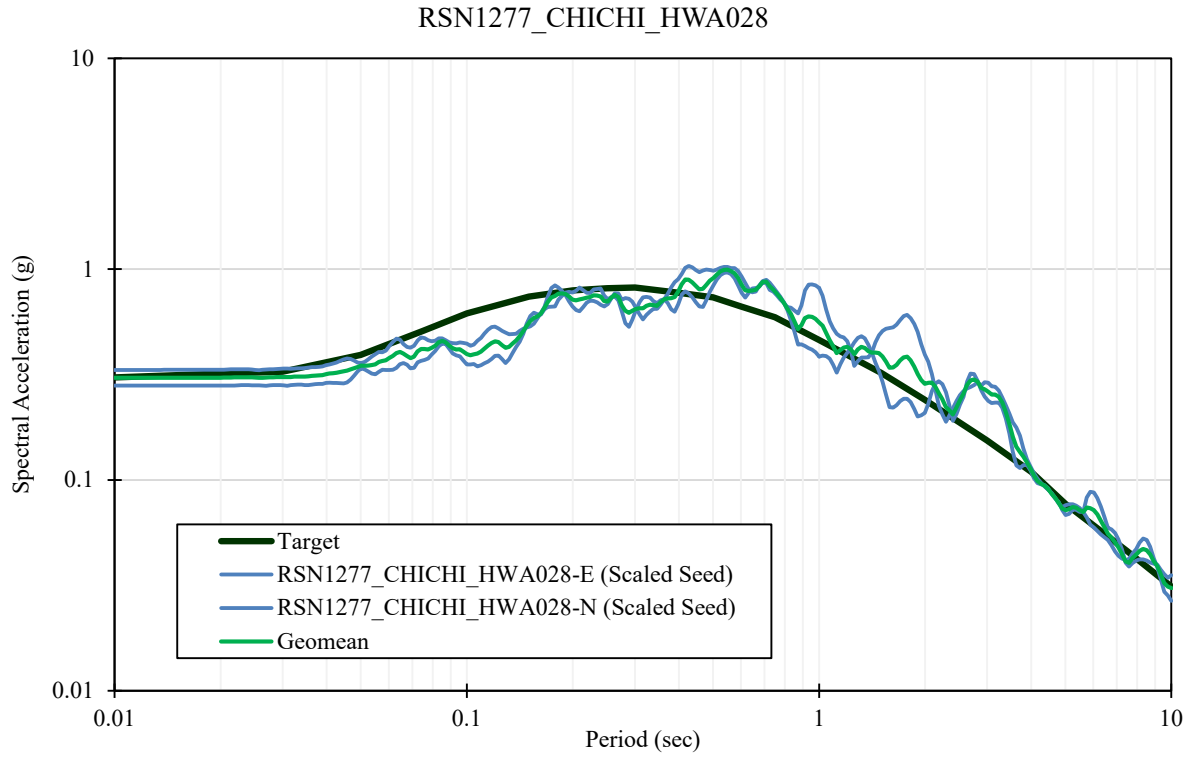
S:\1802\Figures\Figure_180.ai; Date: 05/04/2021; User: JCh.LCL



For Illustration
Purposes Only

1982 Imperial Valley-06 –
Parachute Test Site

Figure 180
Time History Spectrally-Matched to
MDE for Twin Cities, RSN 187 (H2)



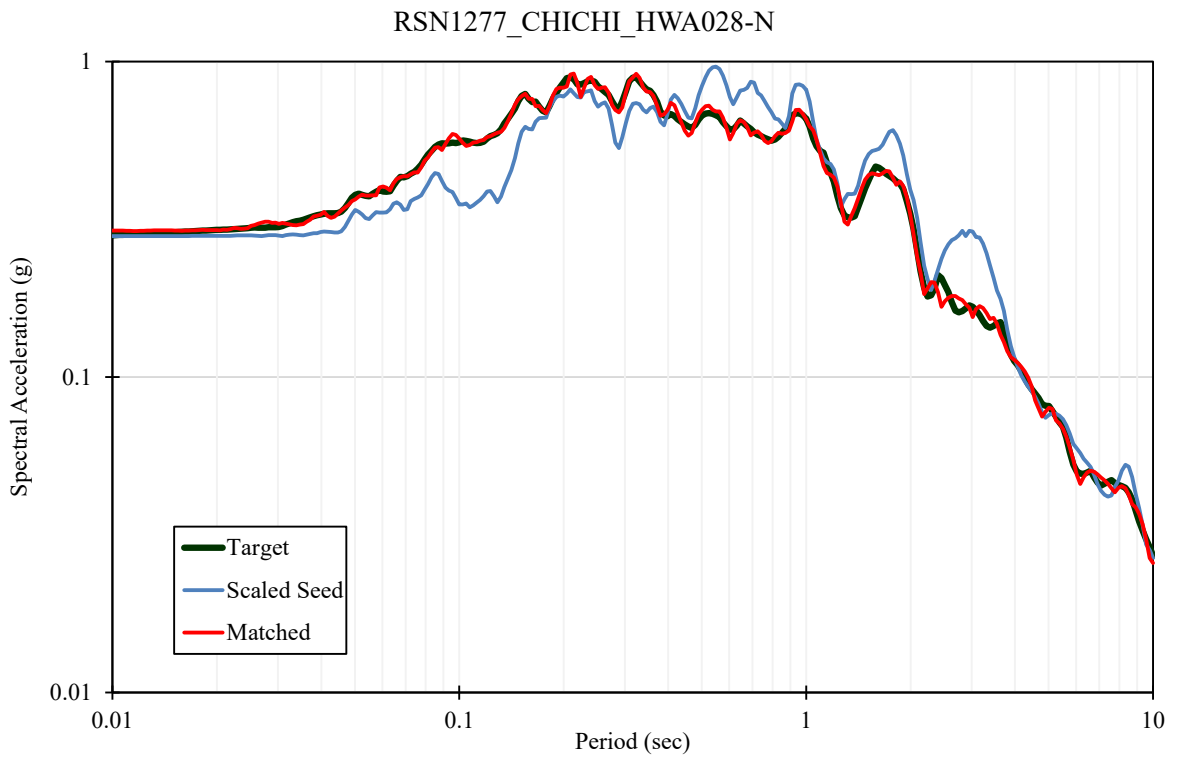
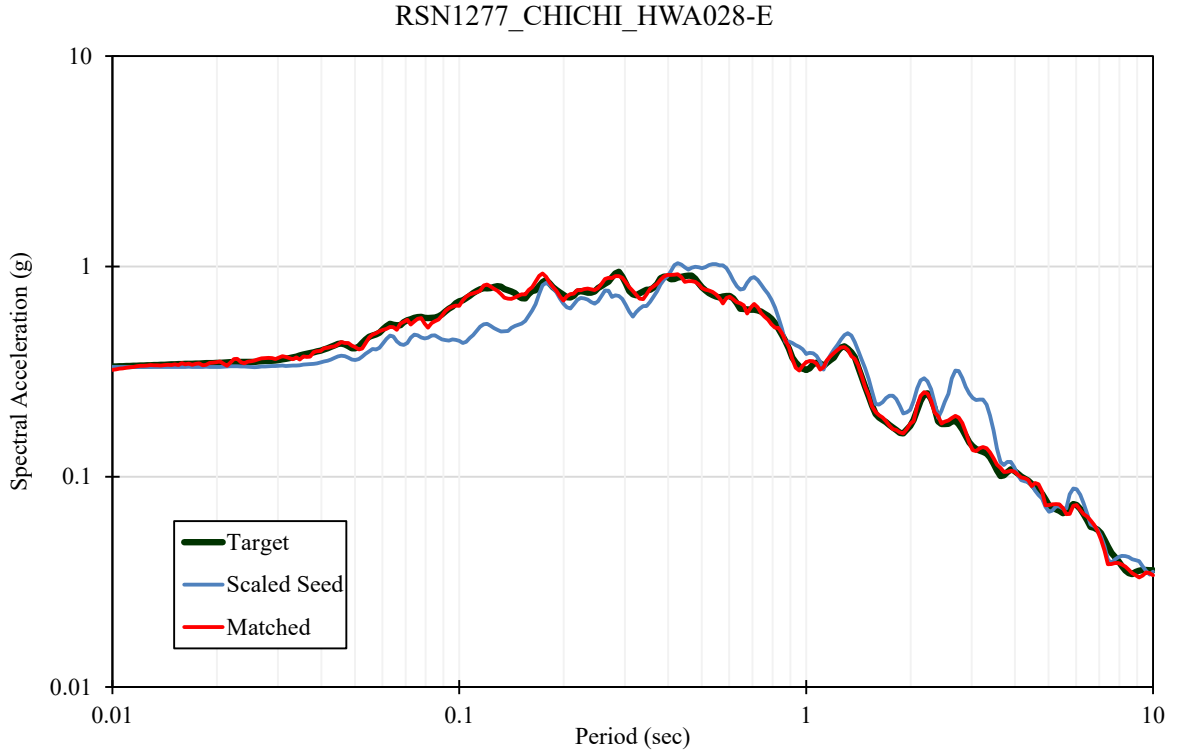
S:\1802\Figures\Figure_181.ai; Date: 05/04/2021 10: User: JCh.LCI.



For Illustration
Purposes Only

1999 Chi-Chi, Taiwan –
HWA028

Figure 181
Response Spectra for MDE Time
Histories for Twin Cities, RSN 1277



S:\1802\Figures\Figure_182.ai; Date: 05/04/2021; User: JCh.LCL

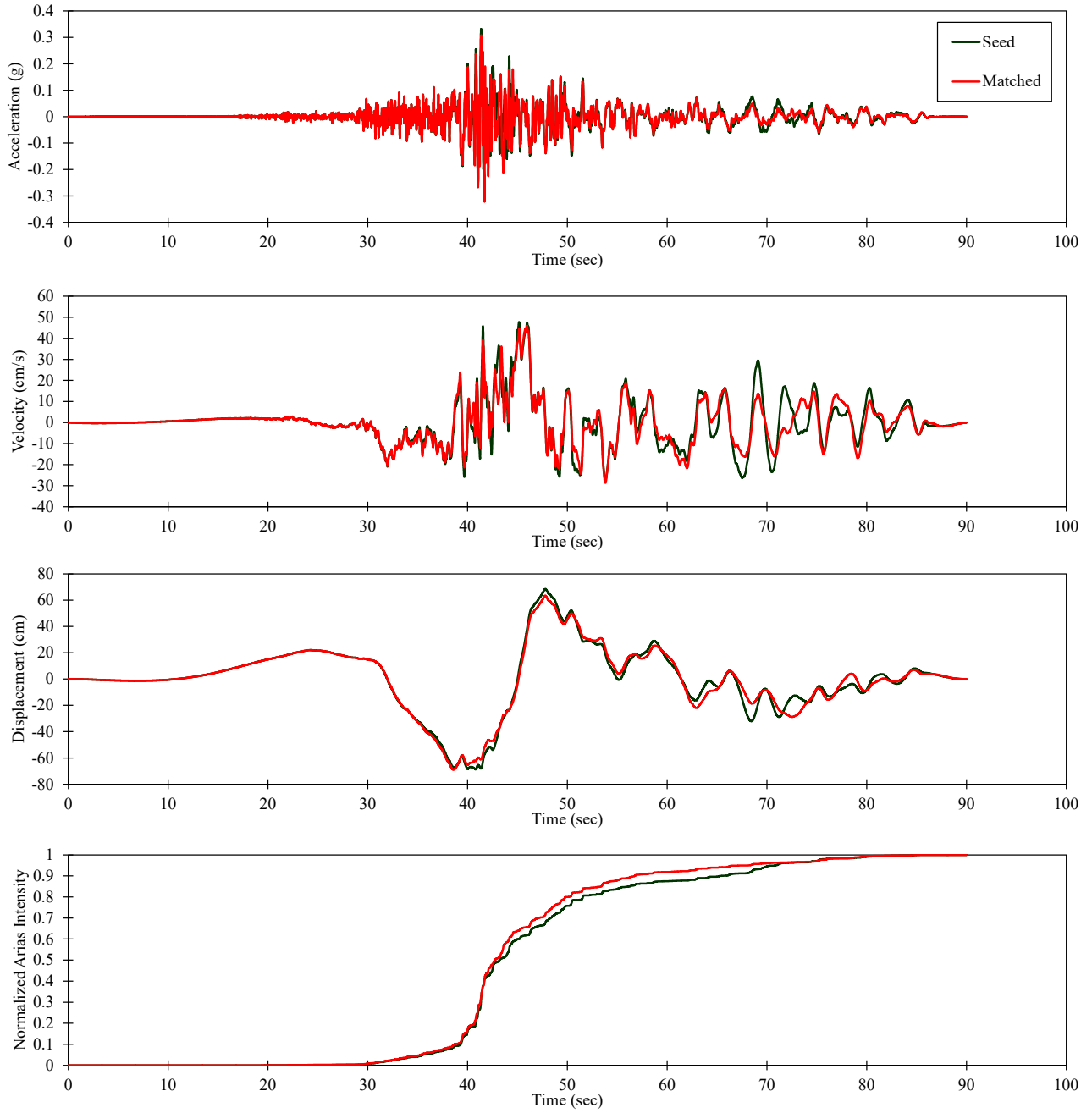


For Illustration
Purposes Only

1999 Chi-Chi, Taiwan –
HWA028

Figure 182
Spectral Matches for MDE Time
Histories for Twin Cities, RSN 1277

RSN1277_CHICHI_HWA028-E



S:\1802\Figures\Figure_183.ai; Date: 05/04/2021; User: JCh.LCL

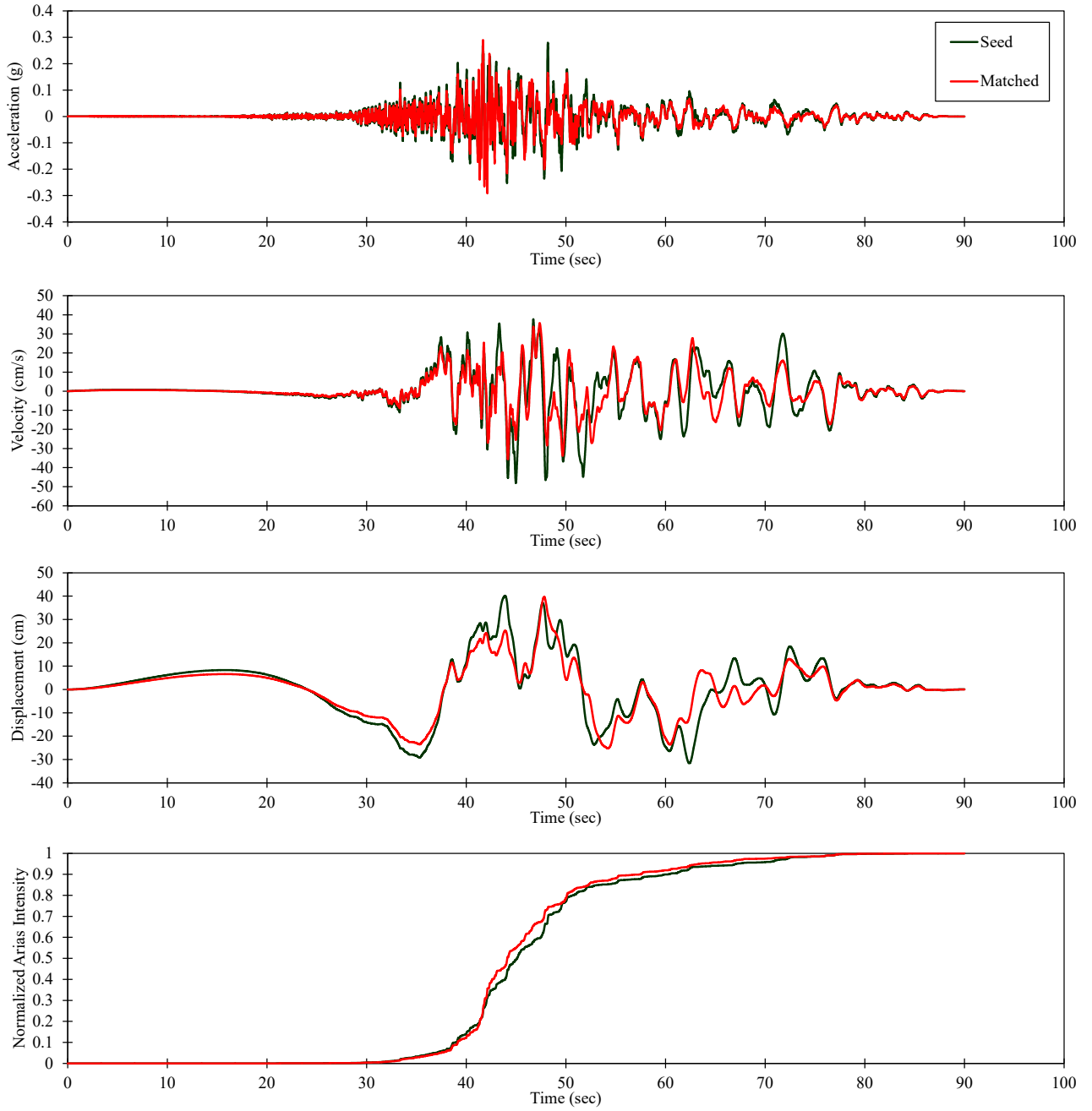


For Illustration
Purposes Only

1999 Chi-Chi, Taiwan –
HWA028

Figure 183
Time History Spectrally-Matched to
MDE for Twin Cities, RSN 1277 (H1)

RSN1277_CHICHI_HWA028-N



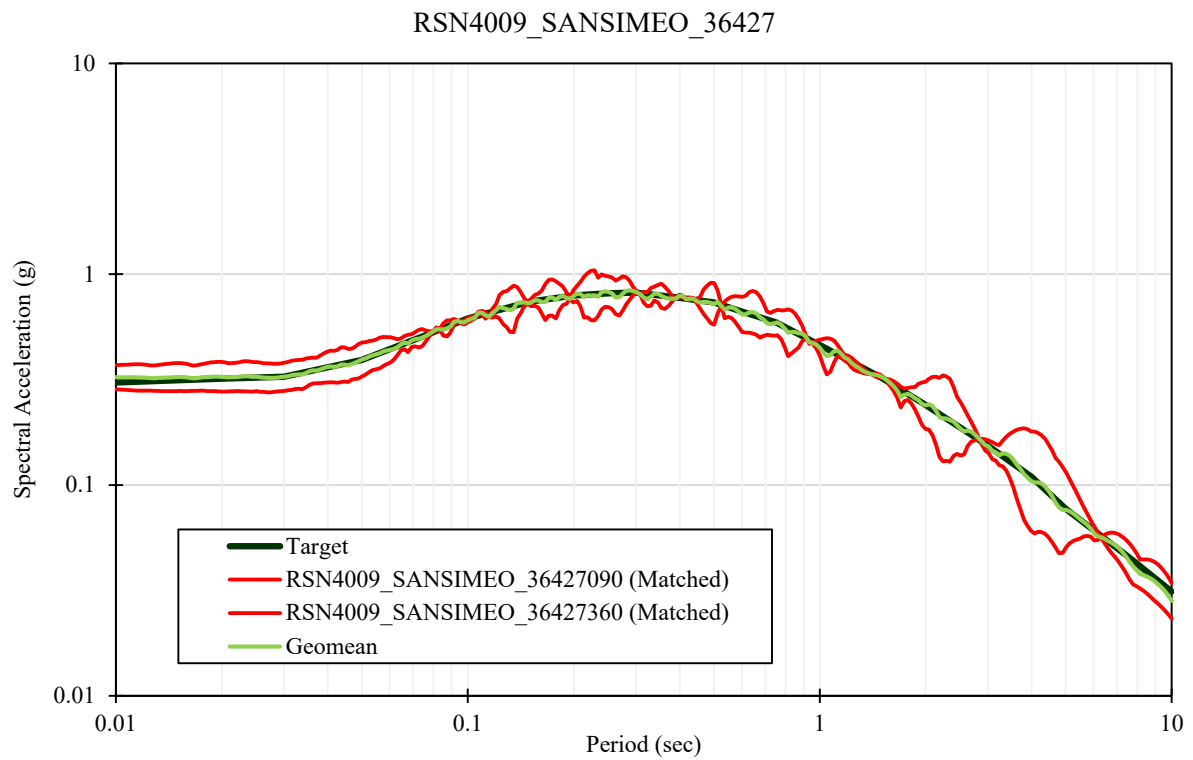
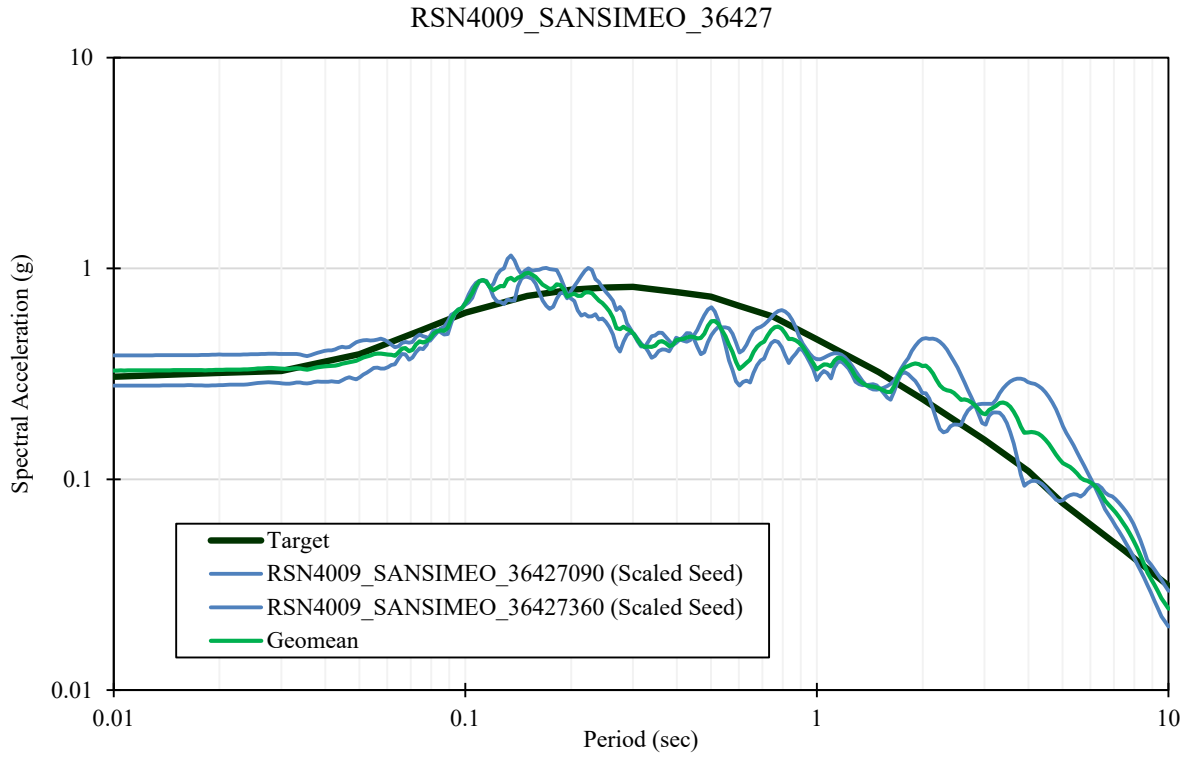
S:\1802\Figures\Figure_184.ai; Date: 05/04/2021; User: JCh.LCL



For Illustration
Purposes Only

1999 Chi-Chi, Taiwan –
HWA028

Figure 184
Time History Spectrally-Matched to
MDE for Twin Cities, RSN 1277 (H2)



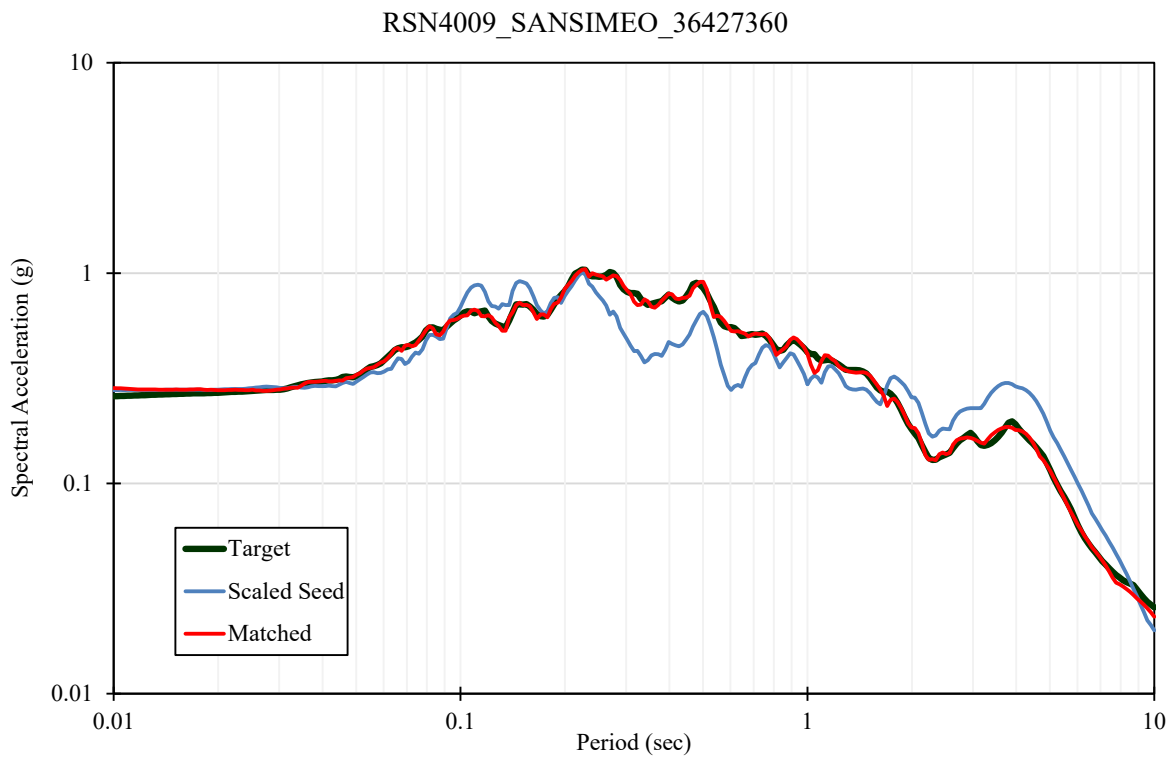
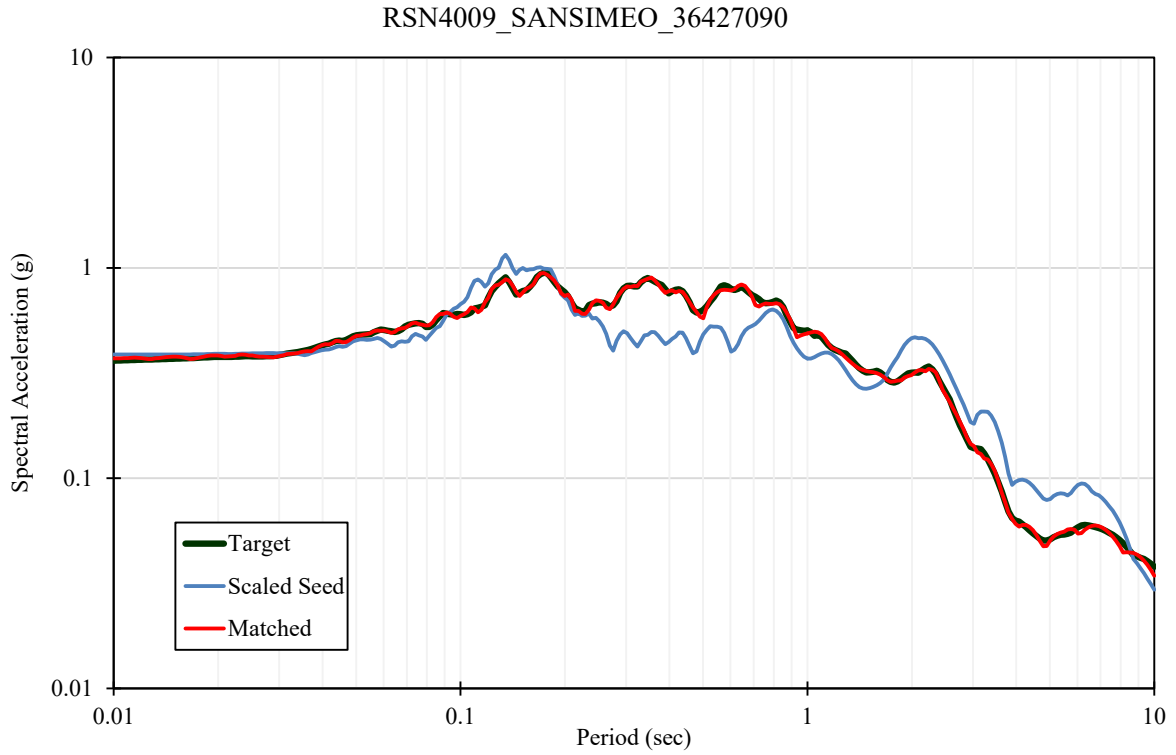
S:\1802\Figures\Figure_185.ai; Date: 05/04/2021; User: JCh.LCI



For Illustration
Purposes Only

**2003 San Simeon – Point
Buchon-Los Osos**

**Figure 185
Response Spectra for MDE Time
Histories for Twin Cities, RSN 4009**



S:\1802\Figures\Figure_186.ai; Date: 05/04/2021; User: JCh.LCL

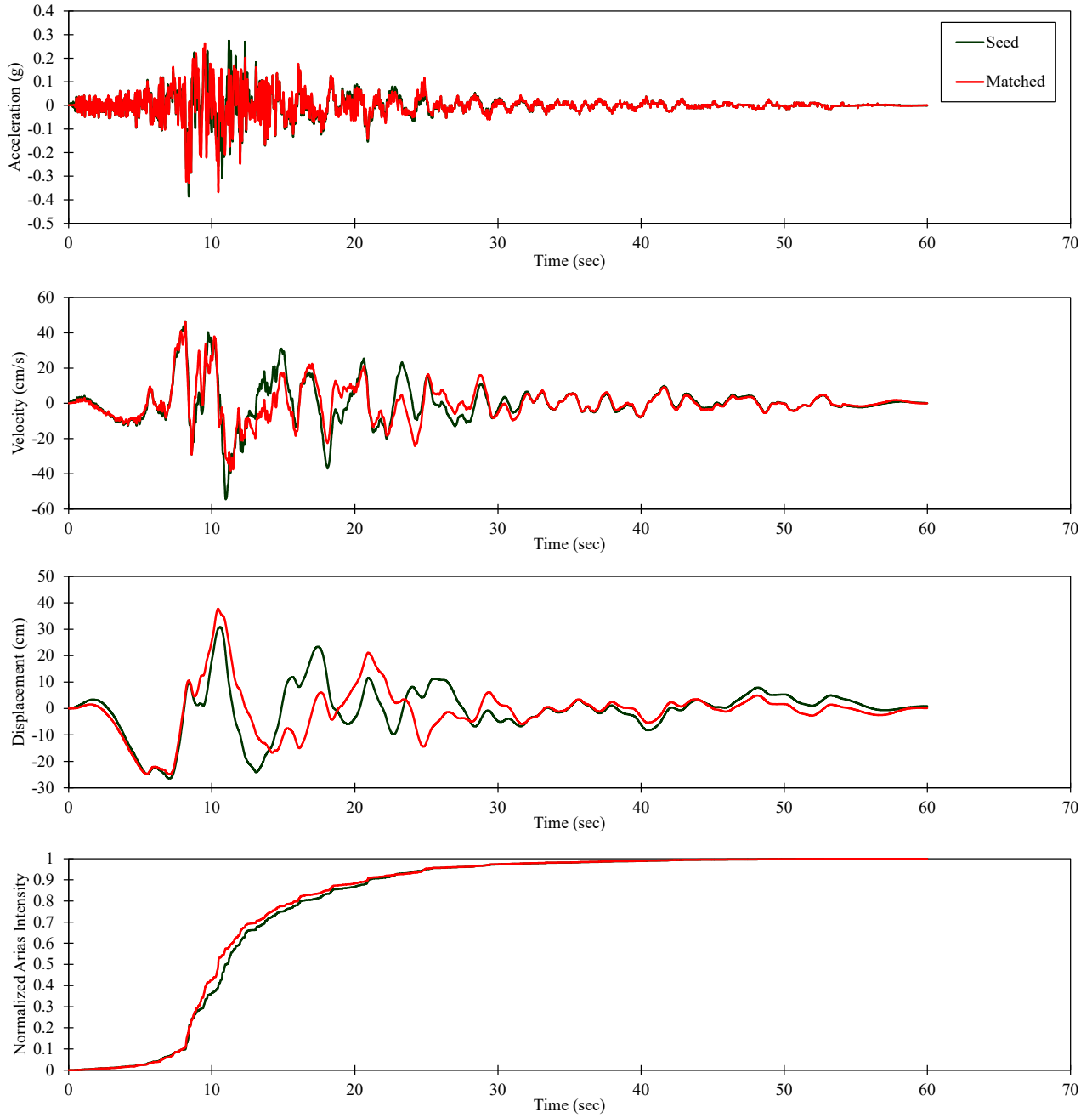


For Illustration
Purposes Only

**2004 San Simeon – Point
Buchon-Los Osos**

**Figure 186
Spectral Matches for MDE Time
Histories for Twin Cities, RSN 4009**

RSN4009_SANSIMEO_36427090



S:\1802\Figures\Figure_187.ai; Date: 05/04/2021; User: JCh.LCL



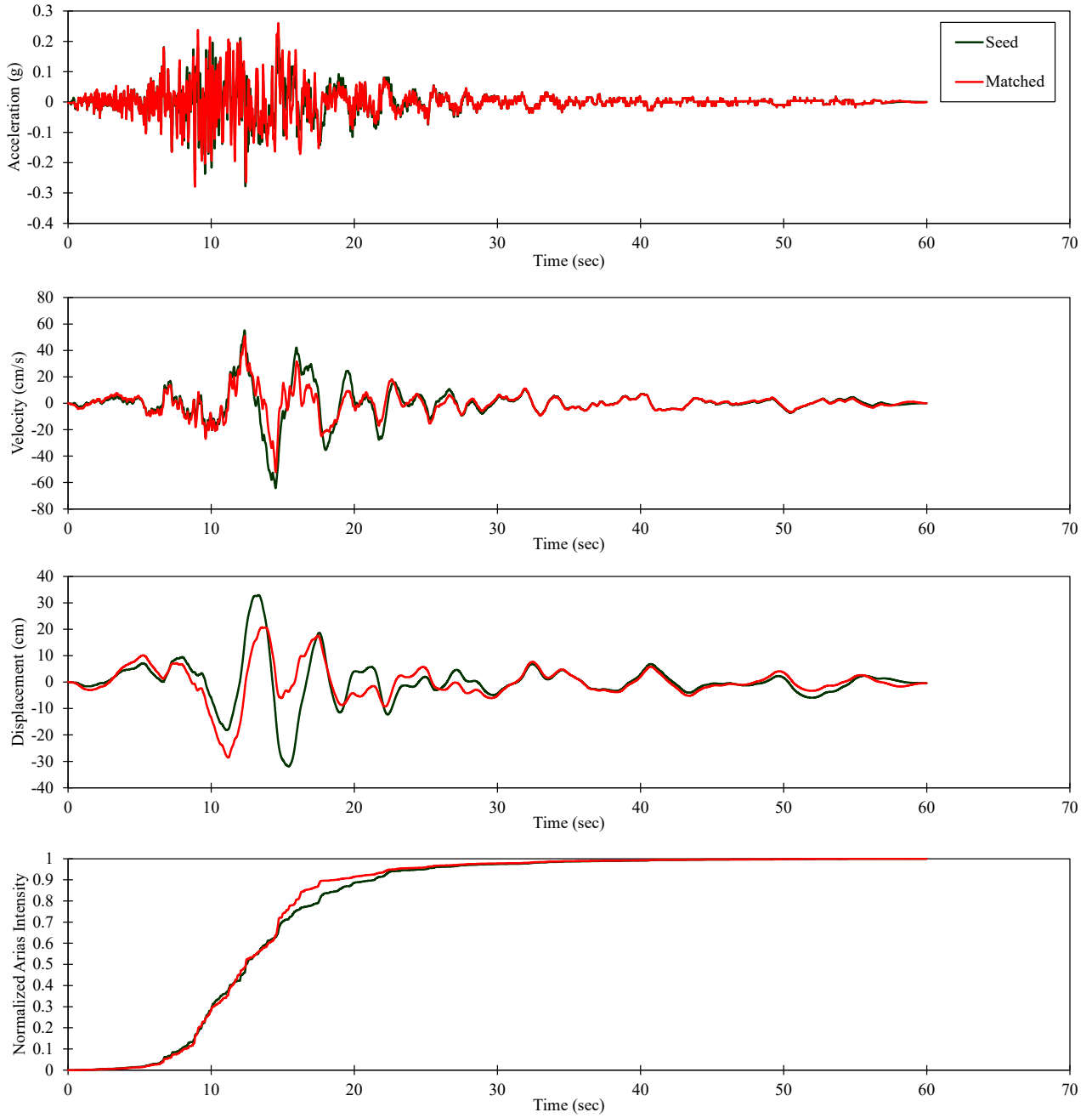
For Illustration
Purposes Only

2005 San Simeon – Point
Buchon-Los Osos

Figure 187
Time History Spectrally-Matched to
MDE for Twin Cities, RSN 4009 (H1)

Data Source: DCA, DWR

RSN4009_SANSIMEO_36427360



S:\1802\Figures\Figure_188.ai; Date: 05/04/2021; User: JCh.LCL

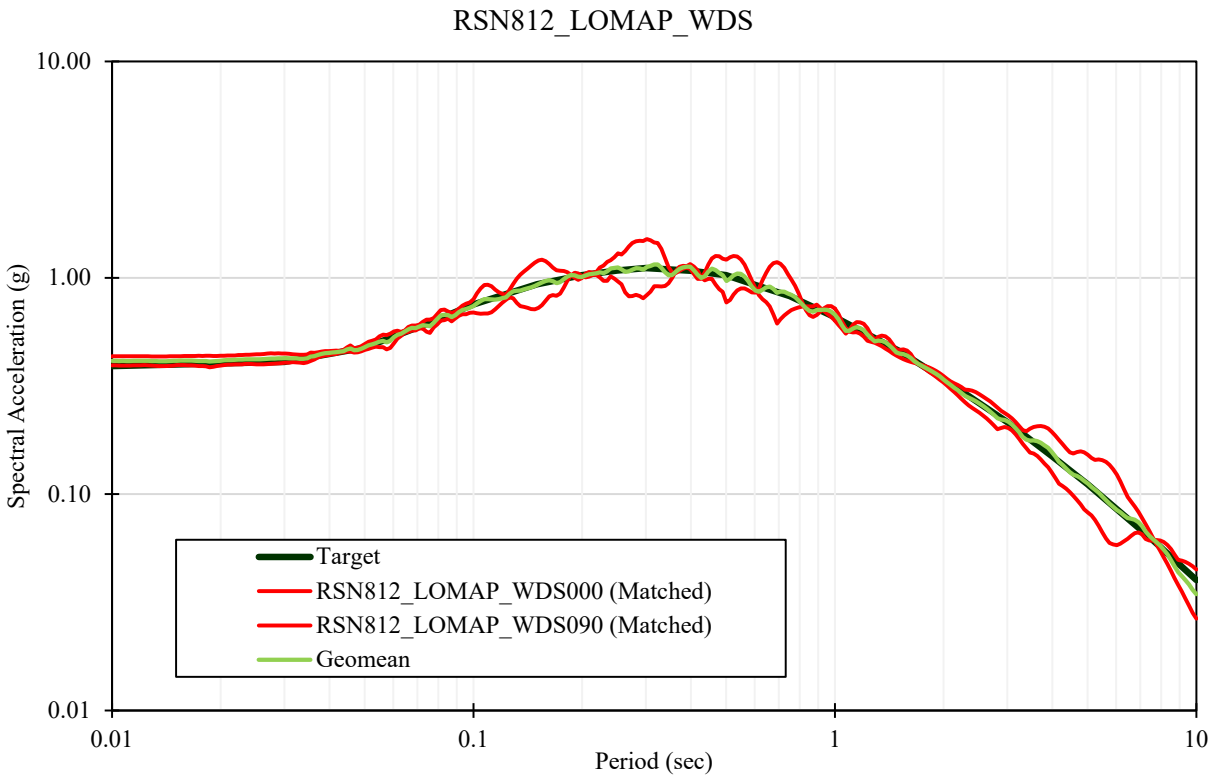
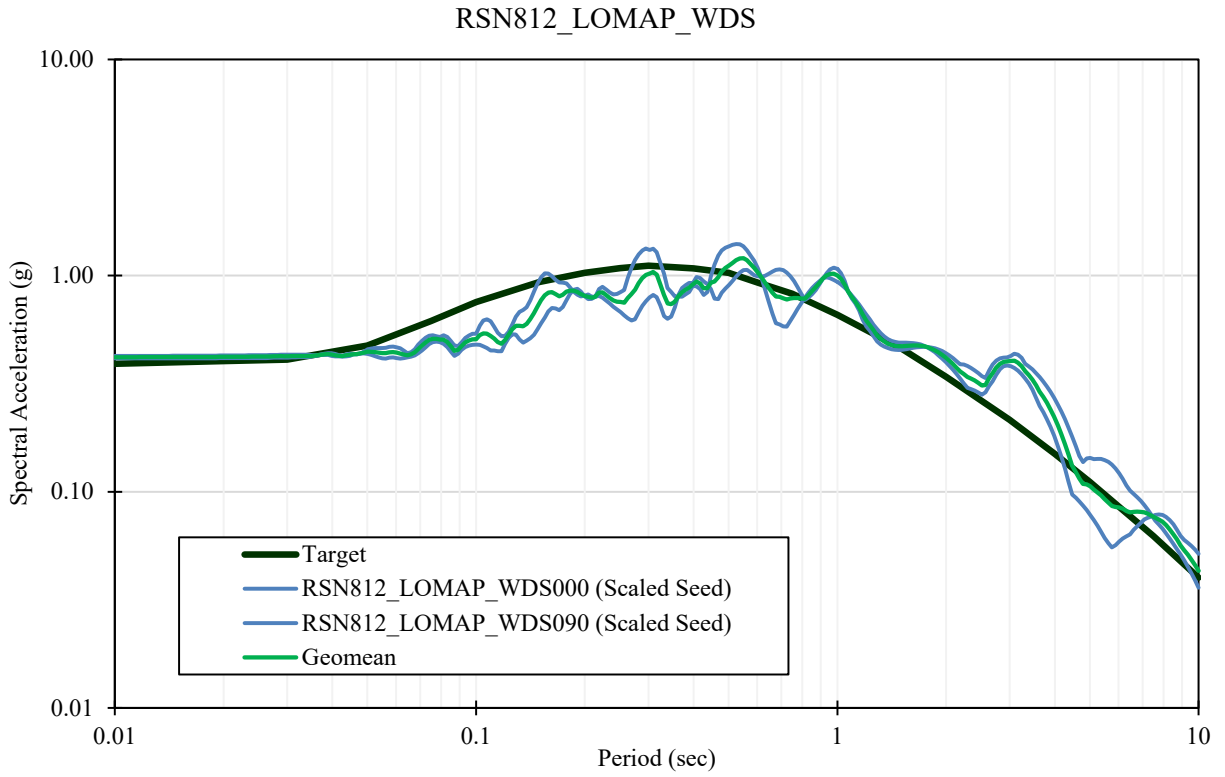


For Illustration
Purposes Only

2006 San Simeon – Point
Buchon-Los Osos

Figure 188
Time History Spectrally-Matched to
MDE for Twin Cities, RSN 4031 (H2)

Data Source: DCA, DWR



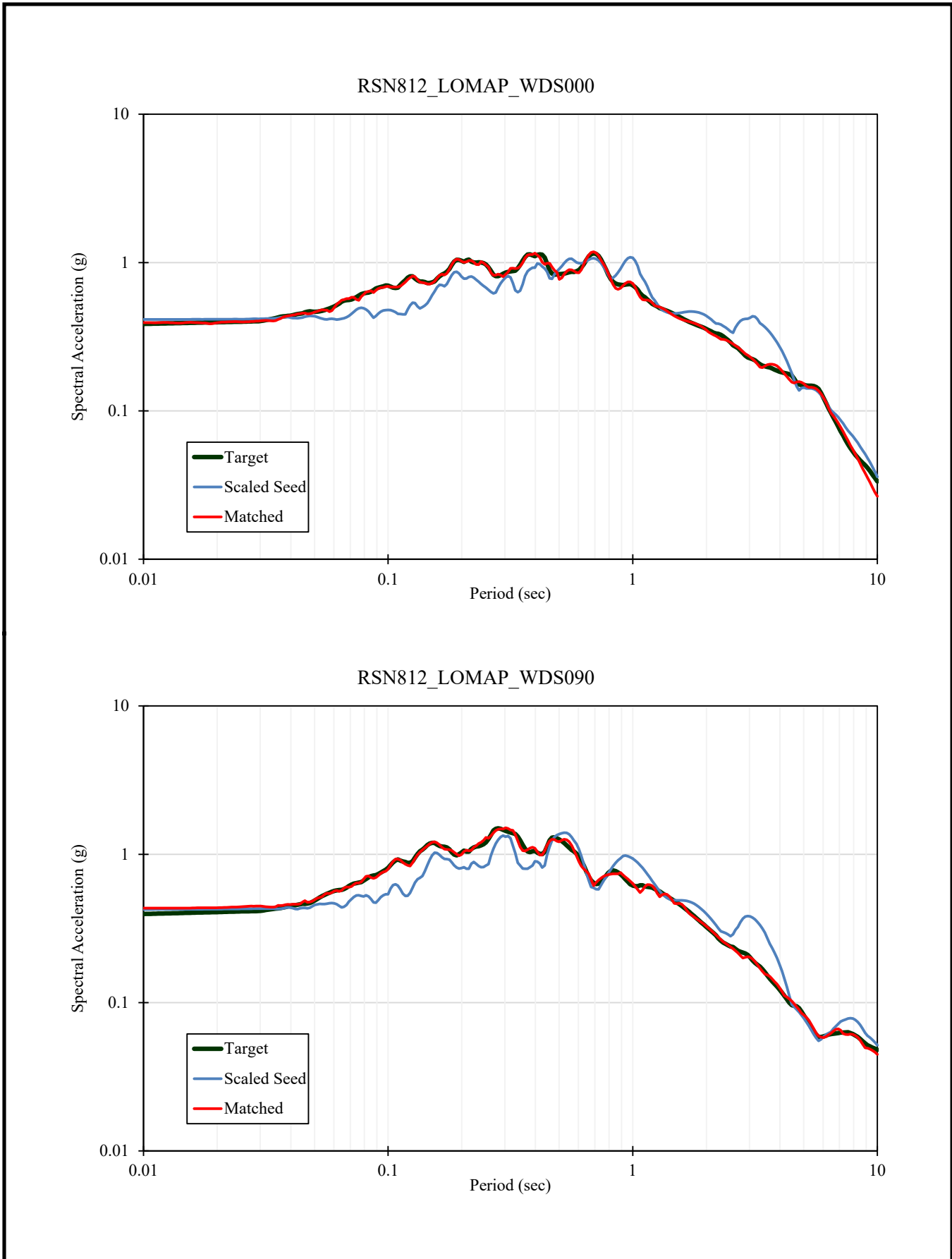
S:\1802\Figures\DCA\Figure_189.ai; Date: 05/04/2021; User: JCh.LCI



For Illustration
Purposes Only

1989 Loma Prieta – Woodside

Figure 189
Response Spectra for MDE Time
Histories for Lower Roberts,
RSN 812



S:\1802\Figures\DCA\Figure_190.ai; Date: 05/04/2021; User: JCh.LCI

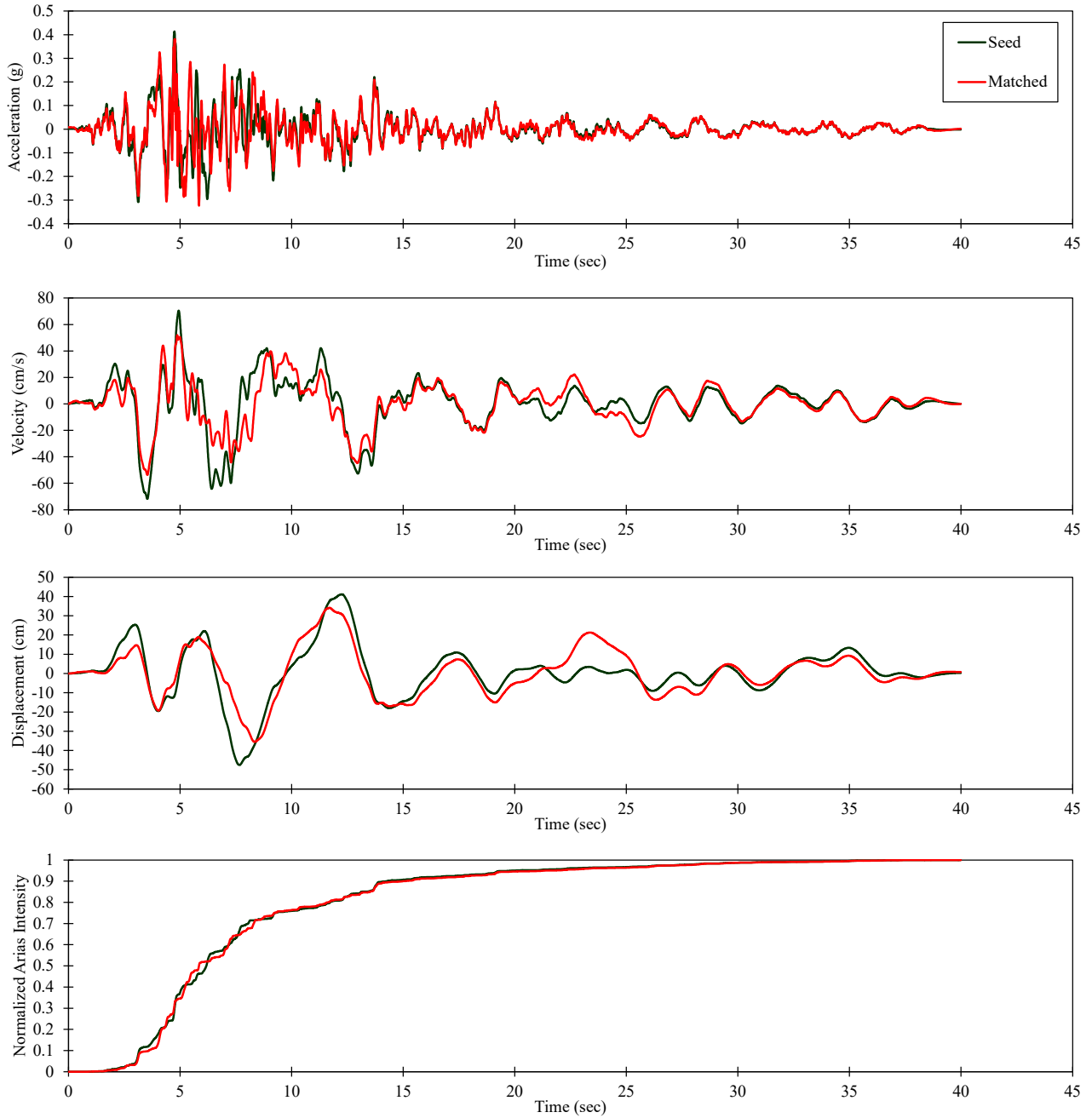


For Illustration
Purposes Only

1989 Loma Prieta – Woodside

Figure 190
Spectral Matches for MDE Time
Histories for Lower Roberts,
RSN 812

RSN812_LOMAP_WDS000



S:\1802\Figures\DCA\Figure_191.ai; Date: 05/04/2021; User: JCh.LCI

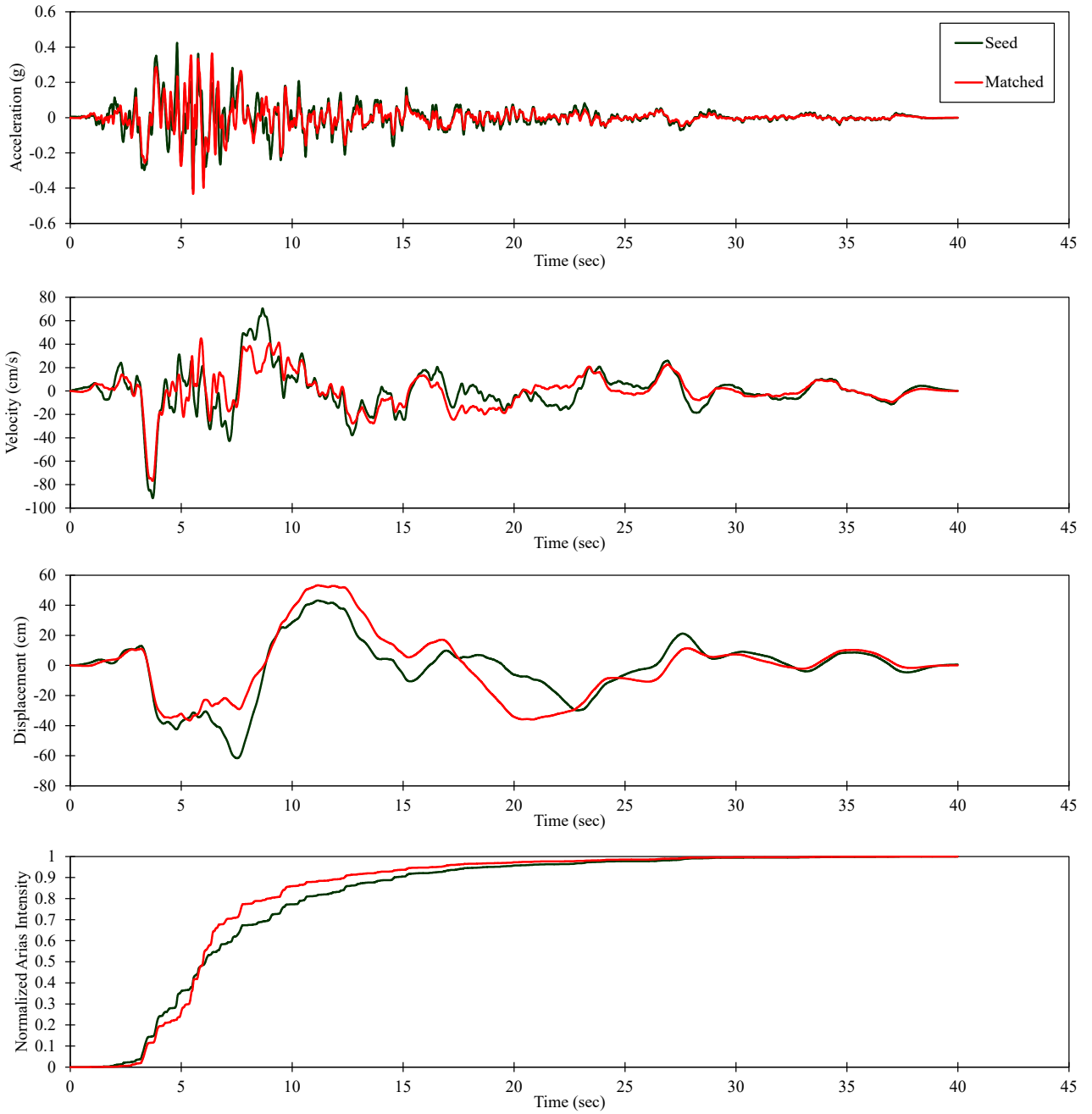


For Illustration
Purposes Only

1989 Loma Prieta – Woodside

Figure 191
Time History Spectrally-Matched
to MDE for Lower Roberts,
RSN 812 (H1)

RSN812_LOMAP_WDS090



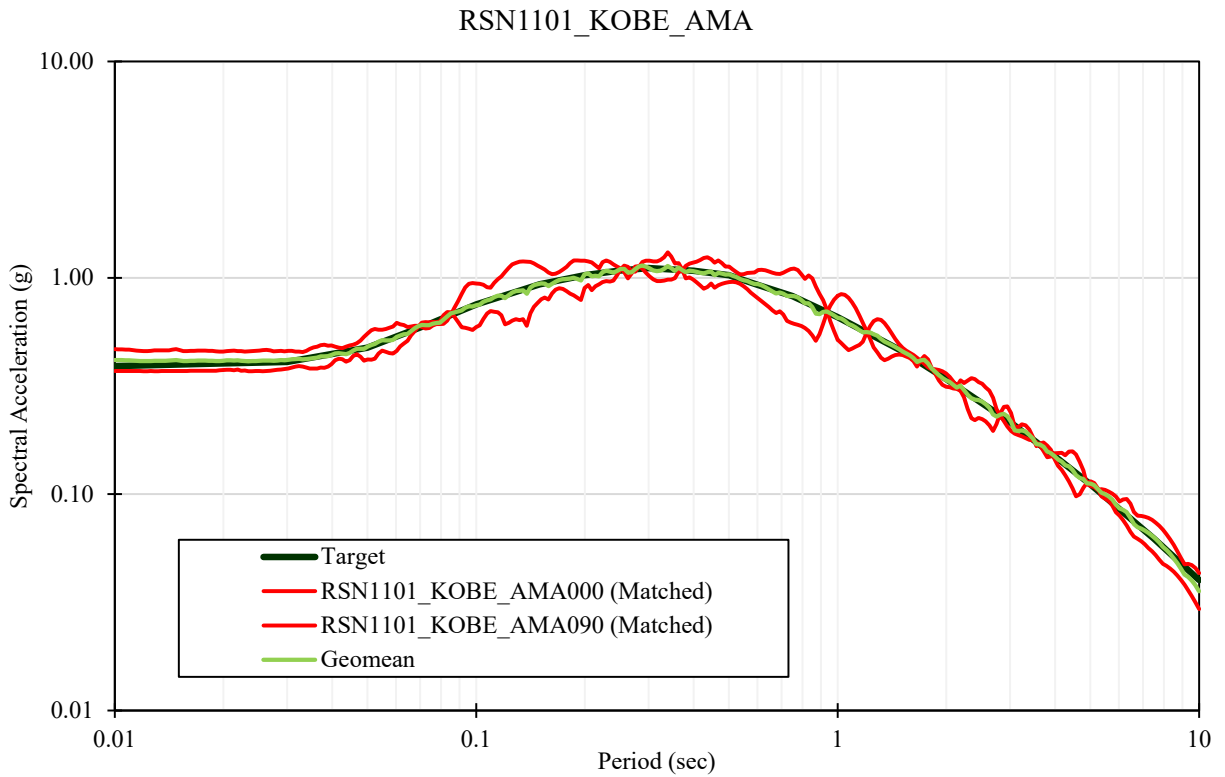
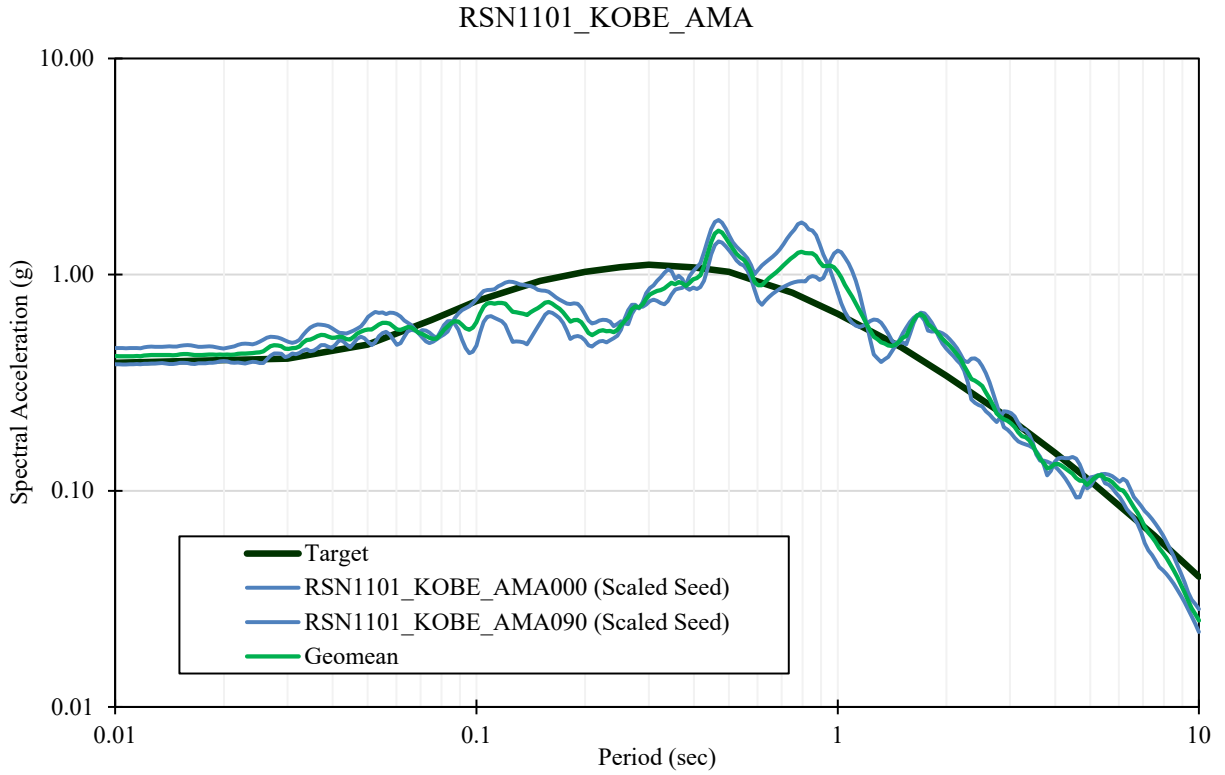
S:\1802\Figures\DCA\Figure_192.ai; Date: 05/04/2021; User: JCh.LCI



For Illustration
Purposes Only

1989 Loma Prieta – Woodside

Figure 192
Time History Spectrally-Matched
to MDE for Lower Roberts, RSN
812 (H2)



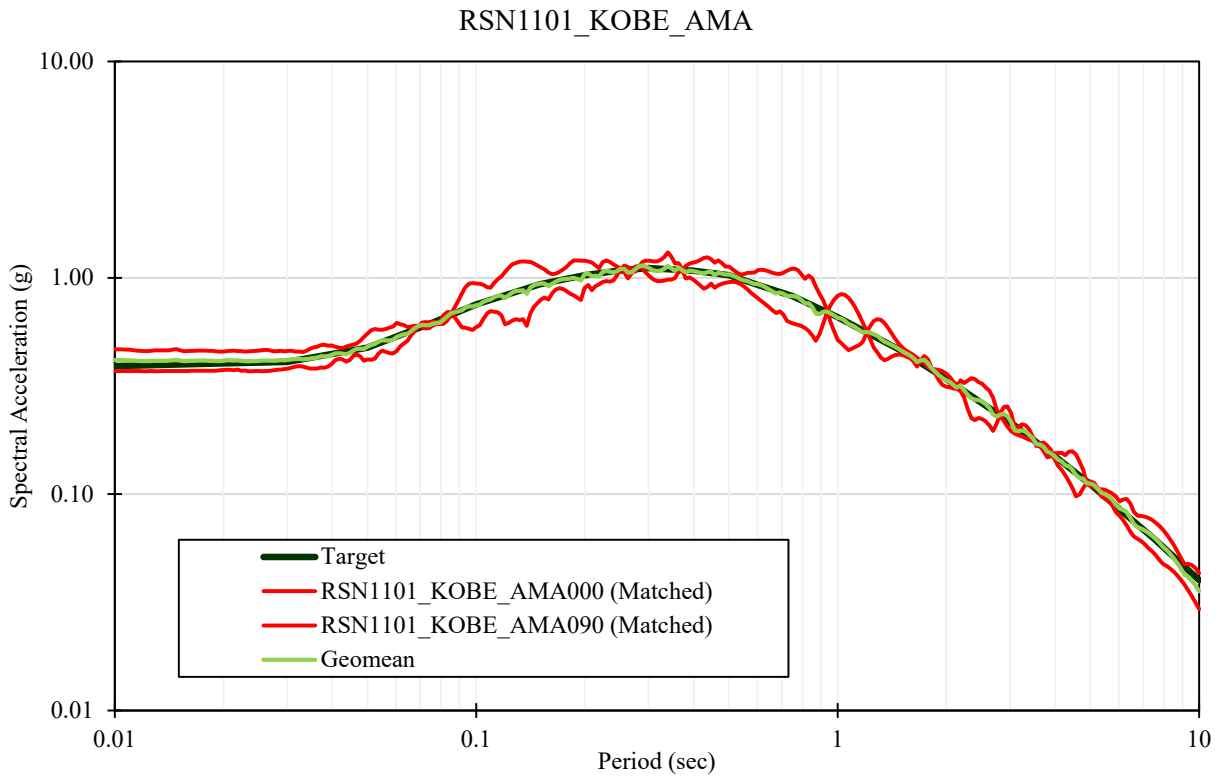
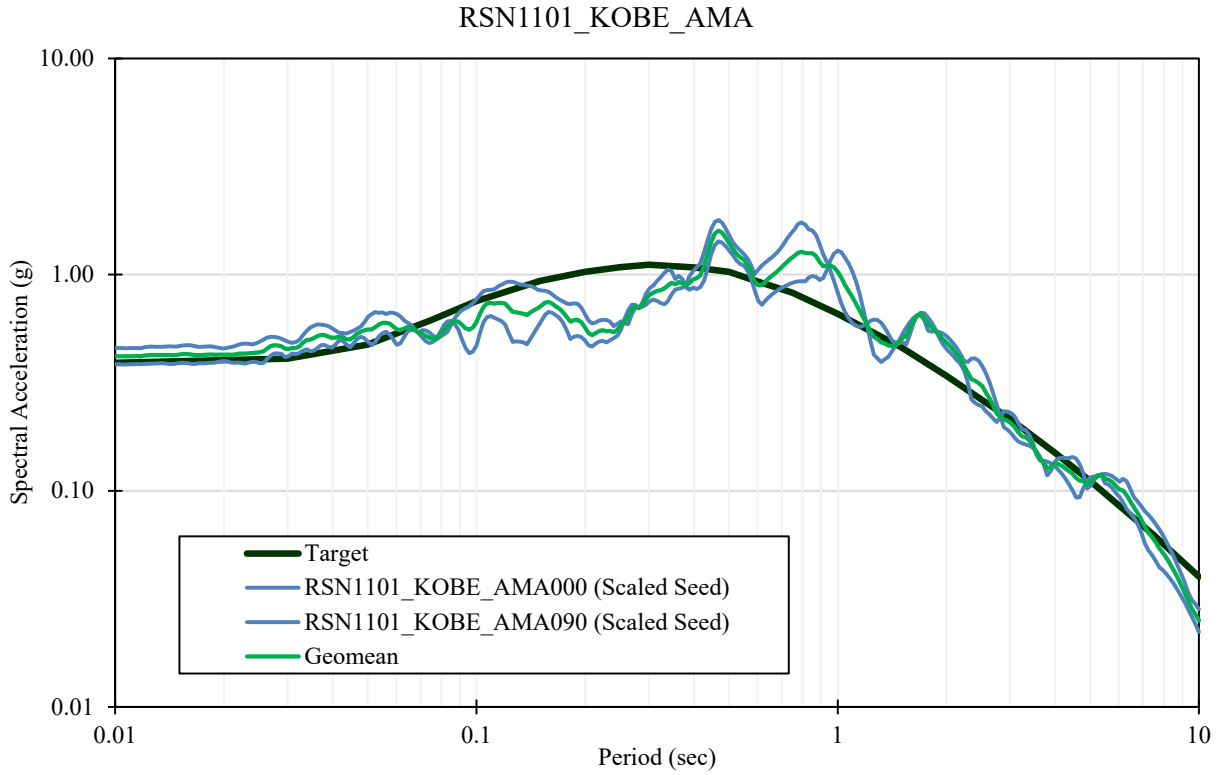
S:\1802\Figures\DCA\Figure_193.ai Date: 05/04/2021 User: JChLCL



For Illustration
Purposes Only

1995 Kobe, Japan – Amagasaki

Figure 193
Response Spectra for MDE Time
Histories for Lower Roberts,
RSN 1101



S:\1802\Figures\DCA\Figure_194.ai; Date: 05/04/2021; User: JCh.LCI

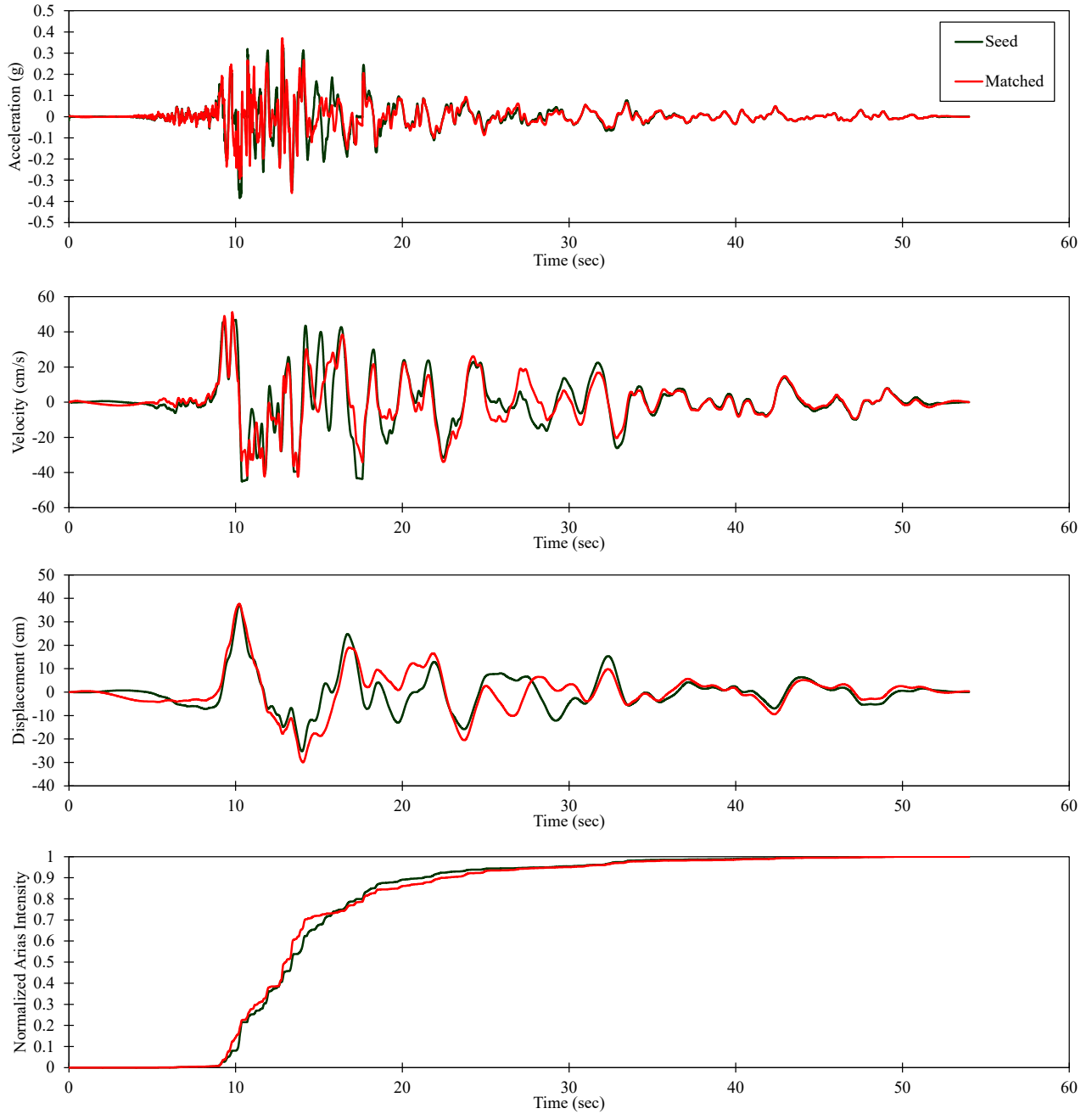


For Illustration
Purposes Only

1996 Kobe, Japan – Amagasaki

Figure 194
Spectral Matches for MDE Time
Histories for Lower Roberts,
RSN 1101

RSN1101_KOBE_AMA000



S:\1802\Figures\DCA\Figure_195.ai; Date: 05/04/2021; User: JCh.LC1

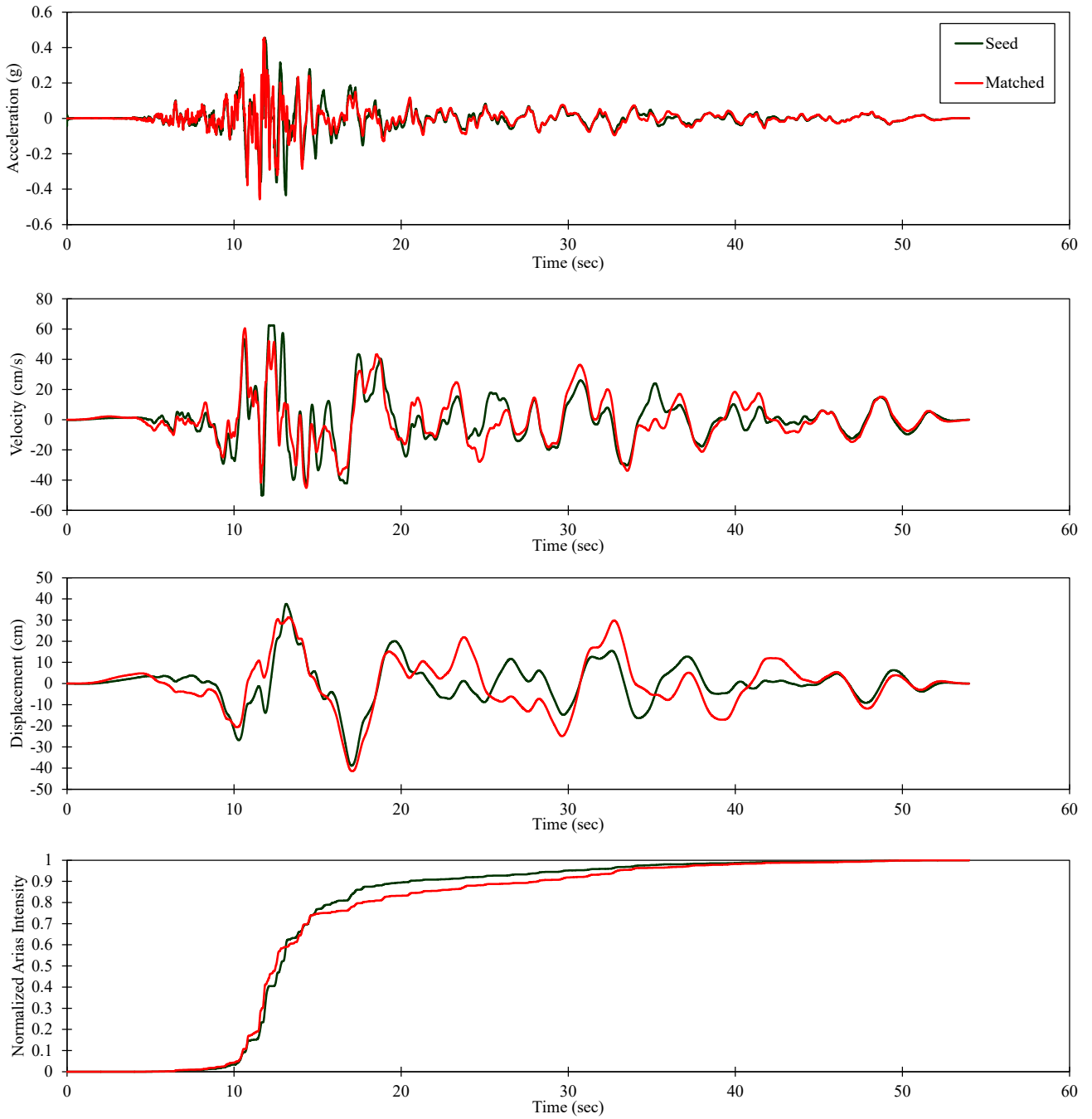


For Illustration
Purposes Only

1997 Kobe, Japan – Amagasaki

Figure 195
Time History Spectrally-Matched
to MDE for Lower Roberts, RSN
1101 (H1)

RSN1101_KOBE_AMA090



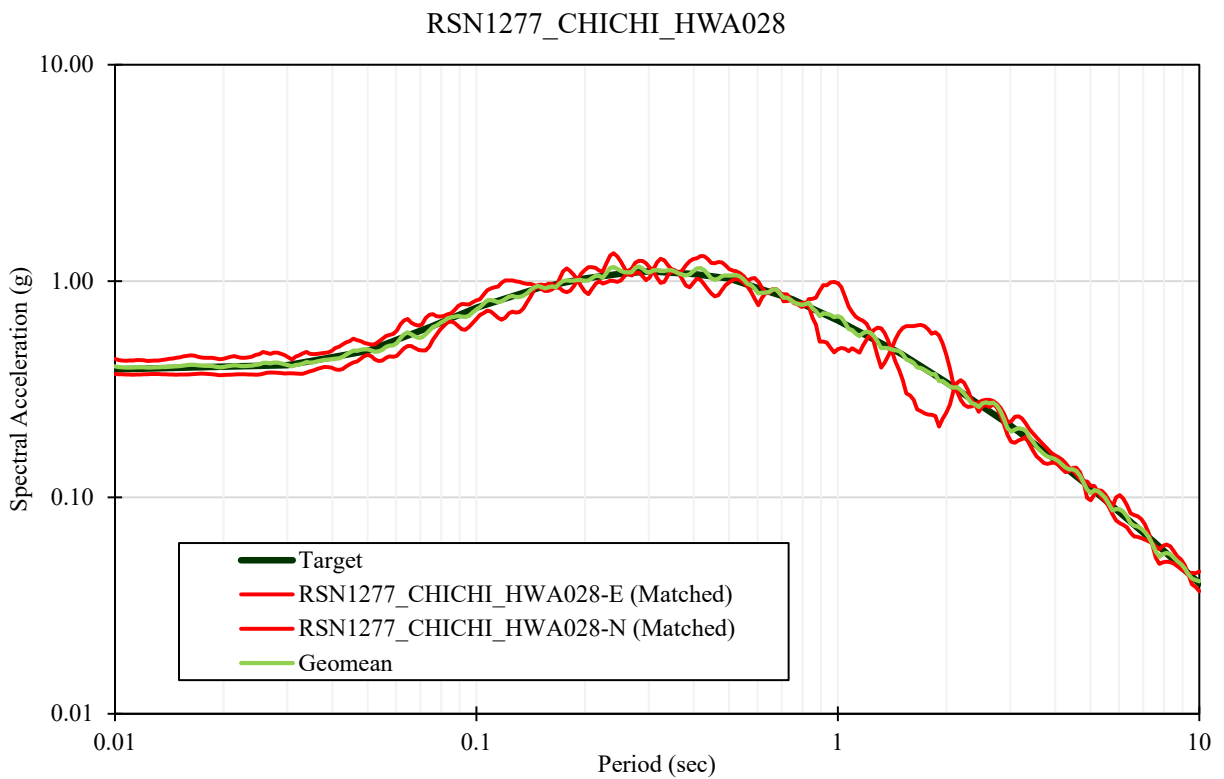
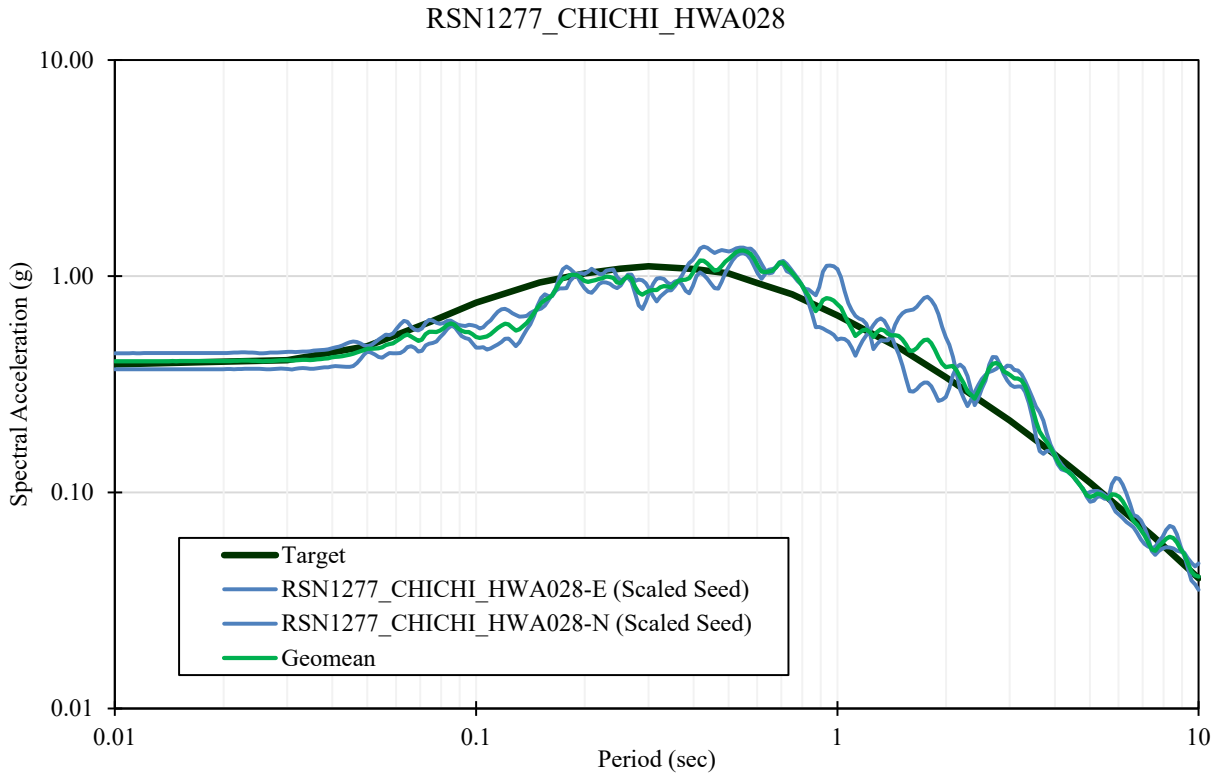
S:\1802\Figures\DCA\Figure_196.ai; Date: 05/04/2021; User: JCh.LCl



For Illustration
Purposes Only

1998 Kobe, Japan – Amagasaki

Figure 196
Time History Spectrally-Matched
to MDE for Lower Roberts, RSN
1101 (H2)



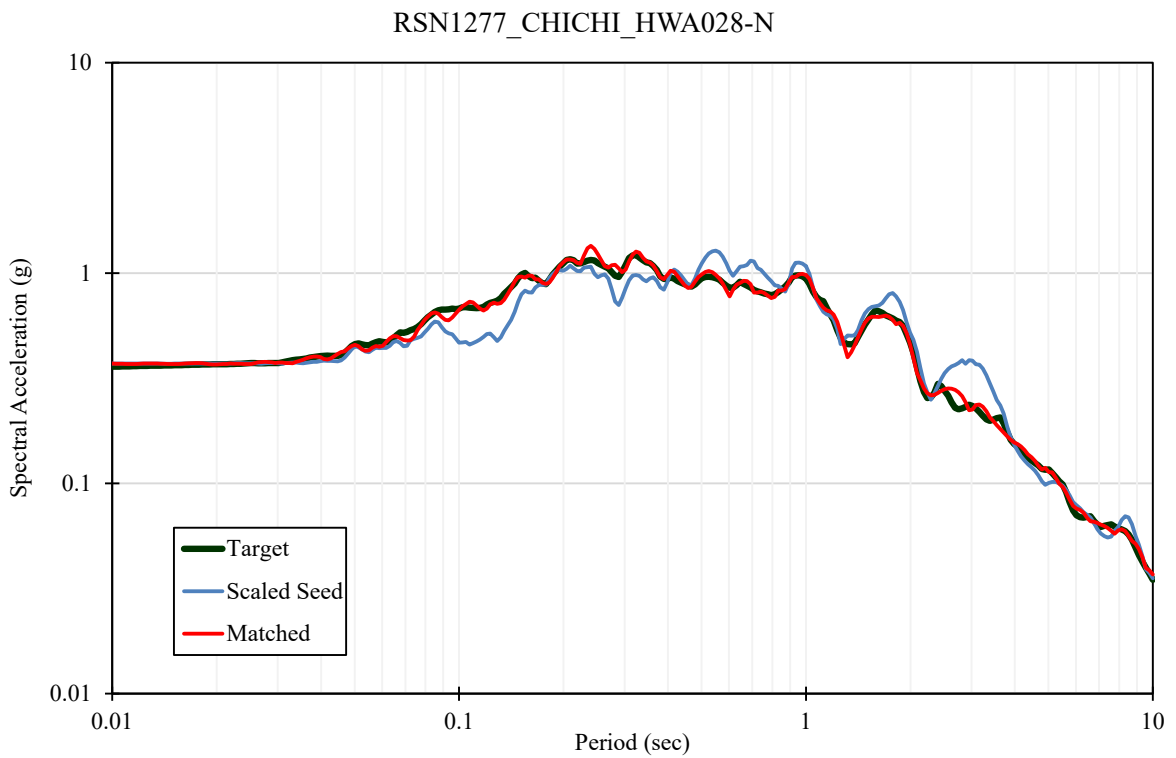
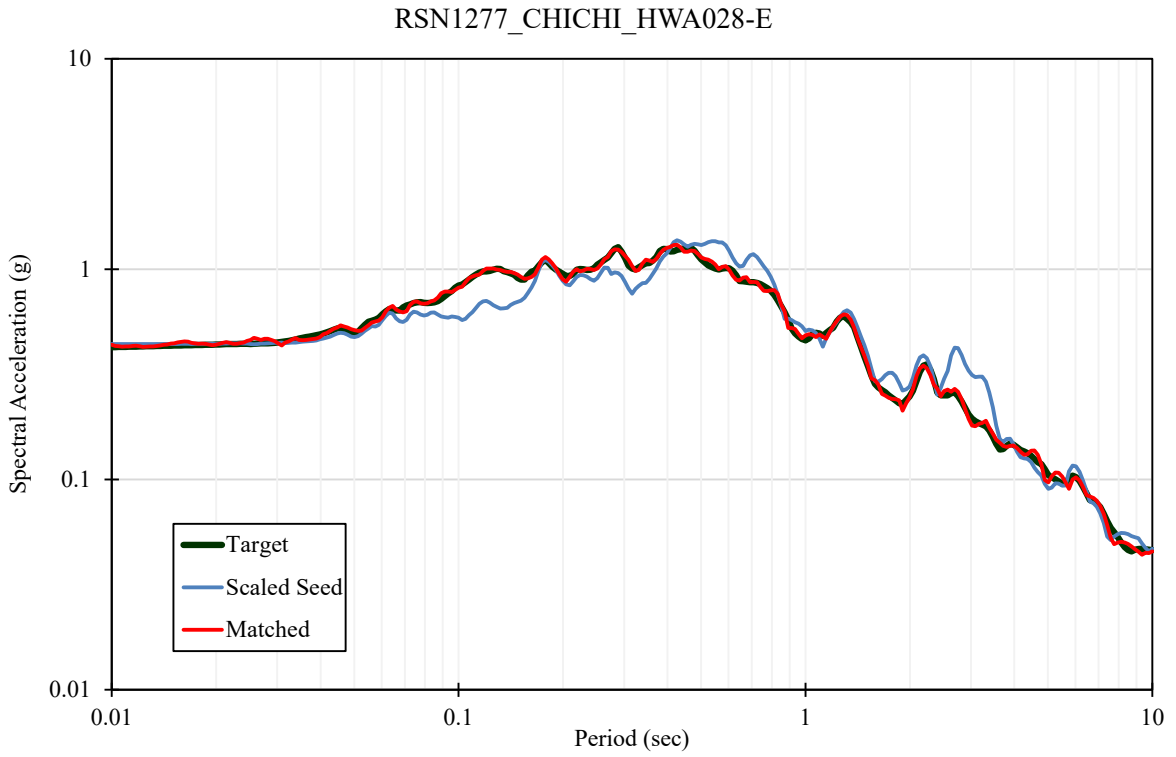
S:\1802\Figures\DCA\Figure_197.ai; Date: 05/04/2021; User: JCh.LCJ



For Illustration
Purposes Only

1999 Chi-Chi, Taiwan – HWA028

Figure 197
Response Spectra for MDE Time
Histories for Lower Roberts,
RSN 1277



S:\1802\Figures\DCA\Figure_198.ai; Date: 05/04/2021; User: JCh.LCJ

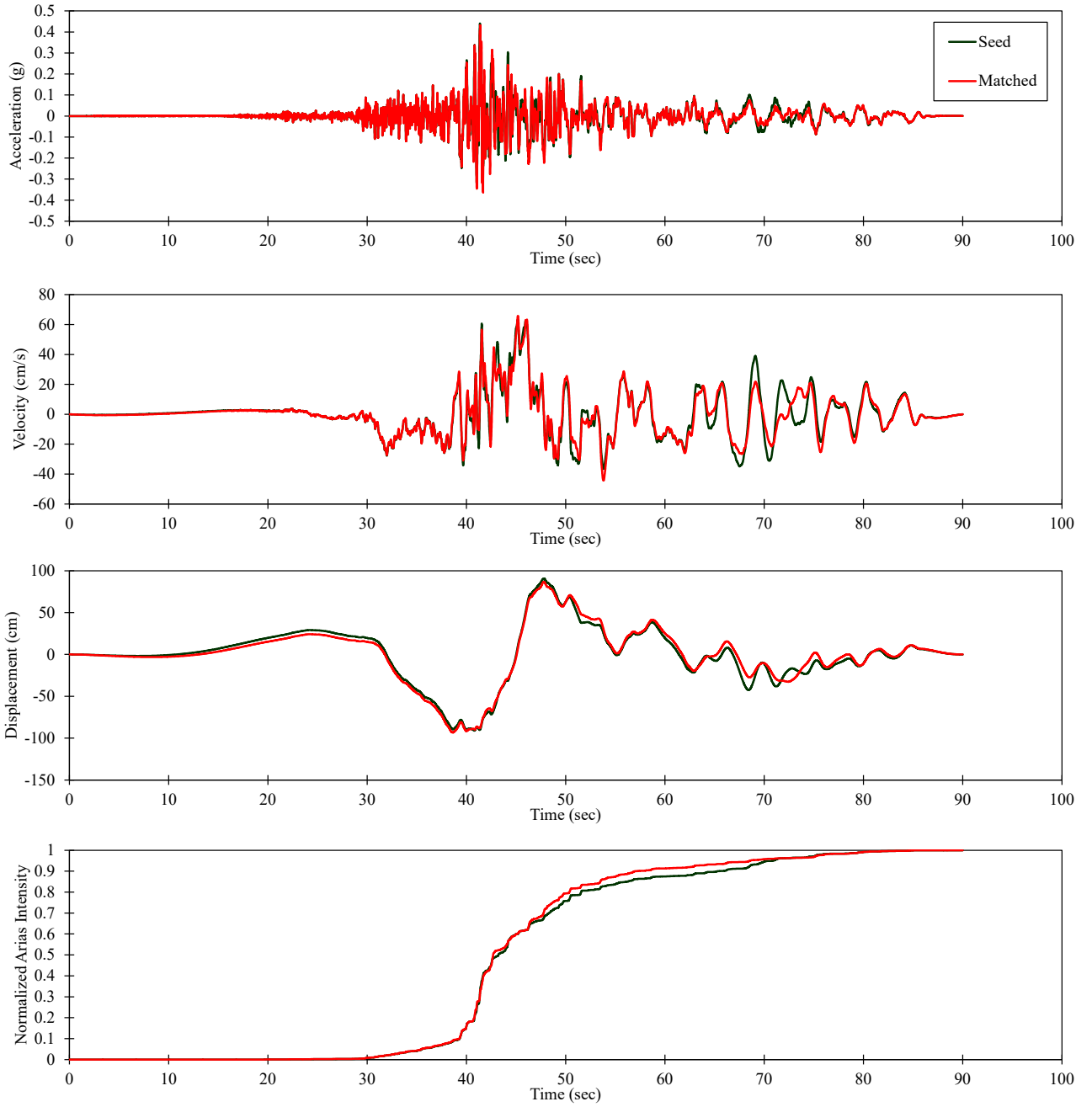


For Illustration
Purposes Only

2000 Chi-Chi, Taiwan – HWA028

Figure 198
Spectral Matches for MDE Time
Histories for Lower Roberts,
RSN 1277

RSN1277_CHICHI_HWA028-E



S:\1802\Figures\DCA\Figure_199.ai; Date: 05/04/2021; JCH.LCI

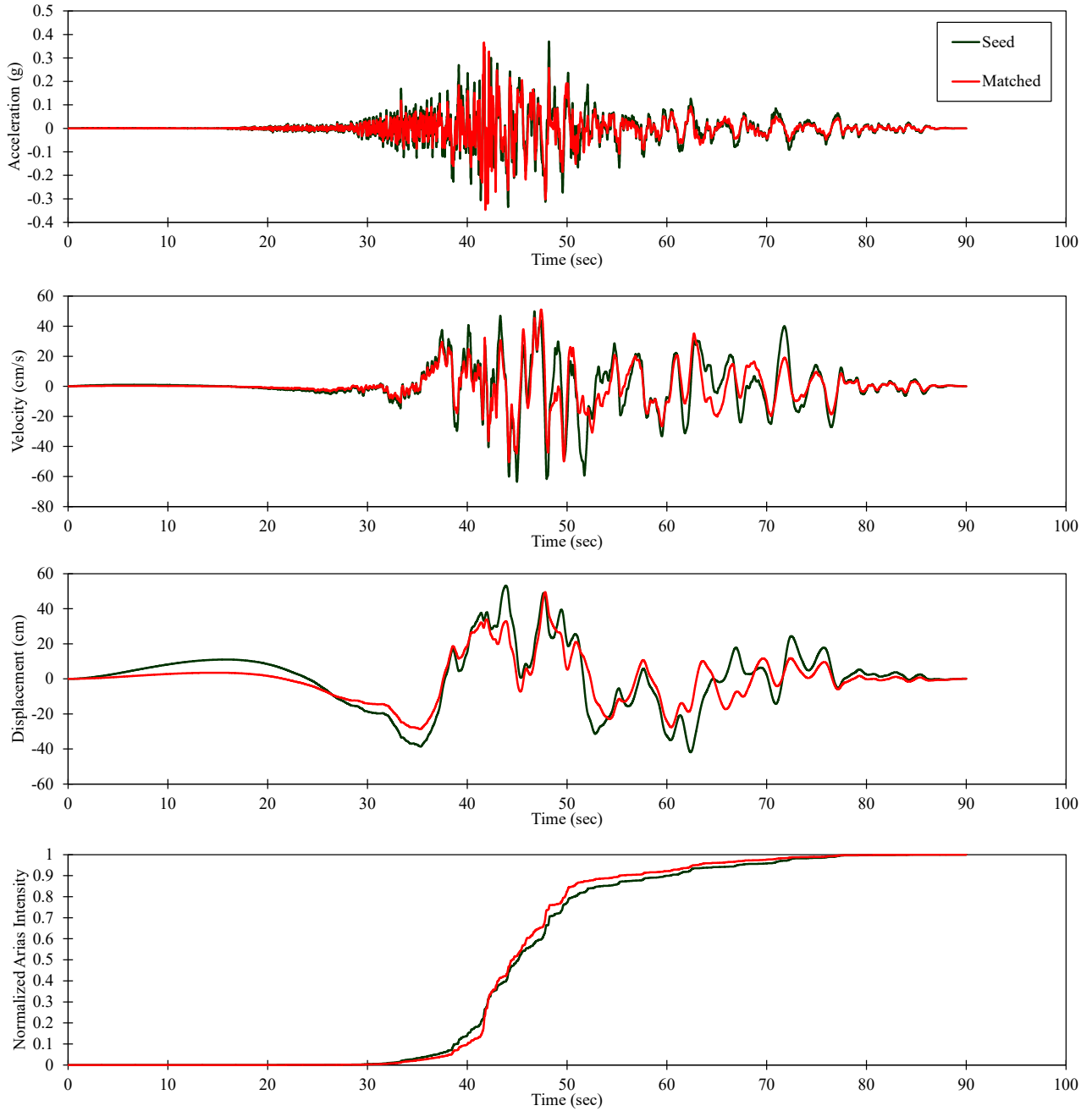


For Illustration
Purposes Only

2001 Chi-Chi, Taiwan – HWA028

Figure 199
Time History Spectrally-Matched
to MDE for Lower Roberts,
RSN 1277 (H1)

RSN1277_CHICHI_HWA028-N



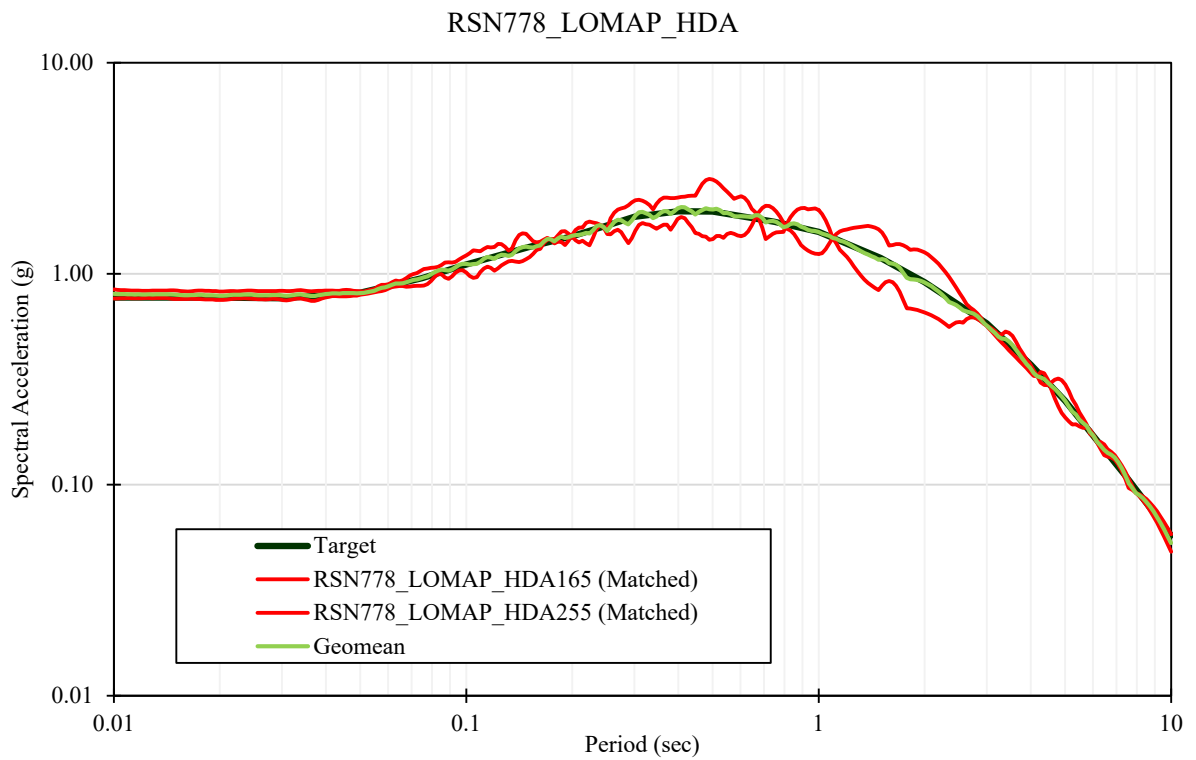
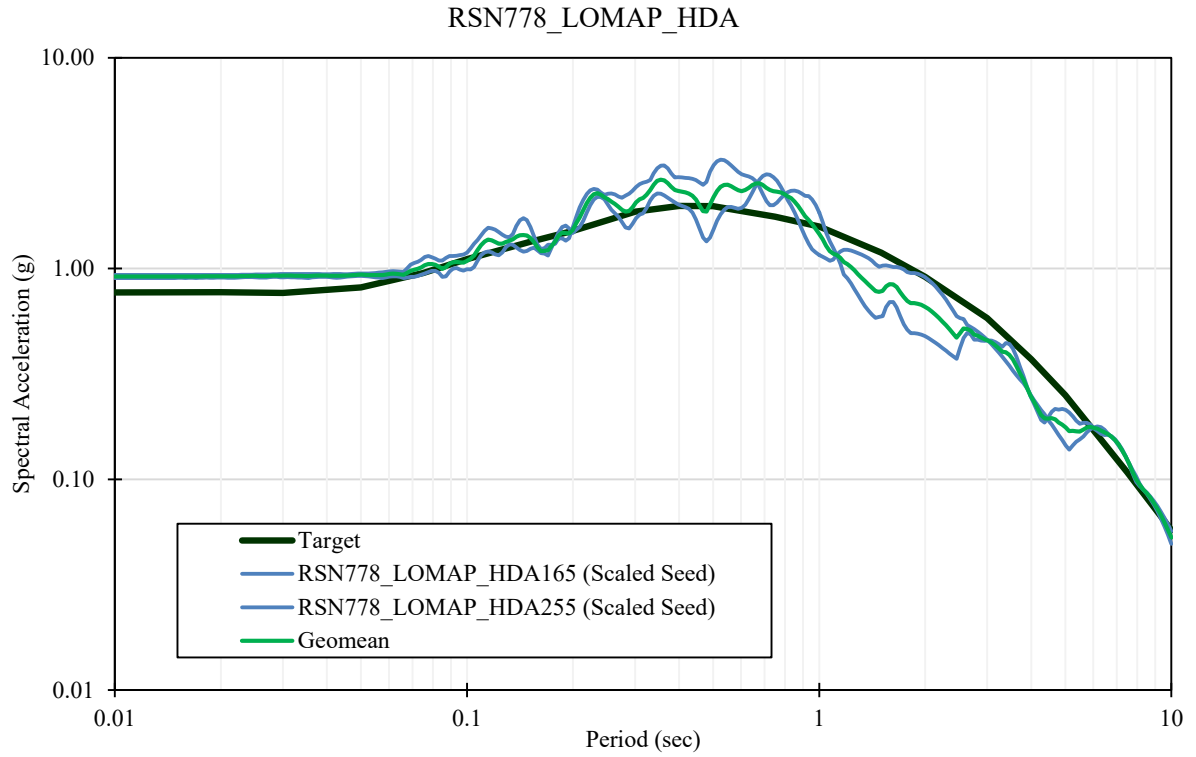
S:\1802\Figures\DCA\Figure_200.ai; Date: 05/04/2021; User: JCh.LC1



For Illustration
Purposes Only

2002 Chi-Chi, Taiwan – HWA028

Figure 200
Time History Spectrally-Matched
to MDE for Lower Roberts,
RSN 1277(H2)



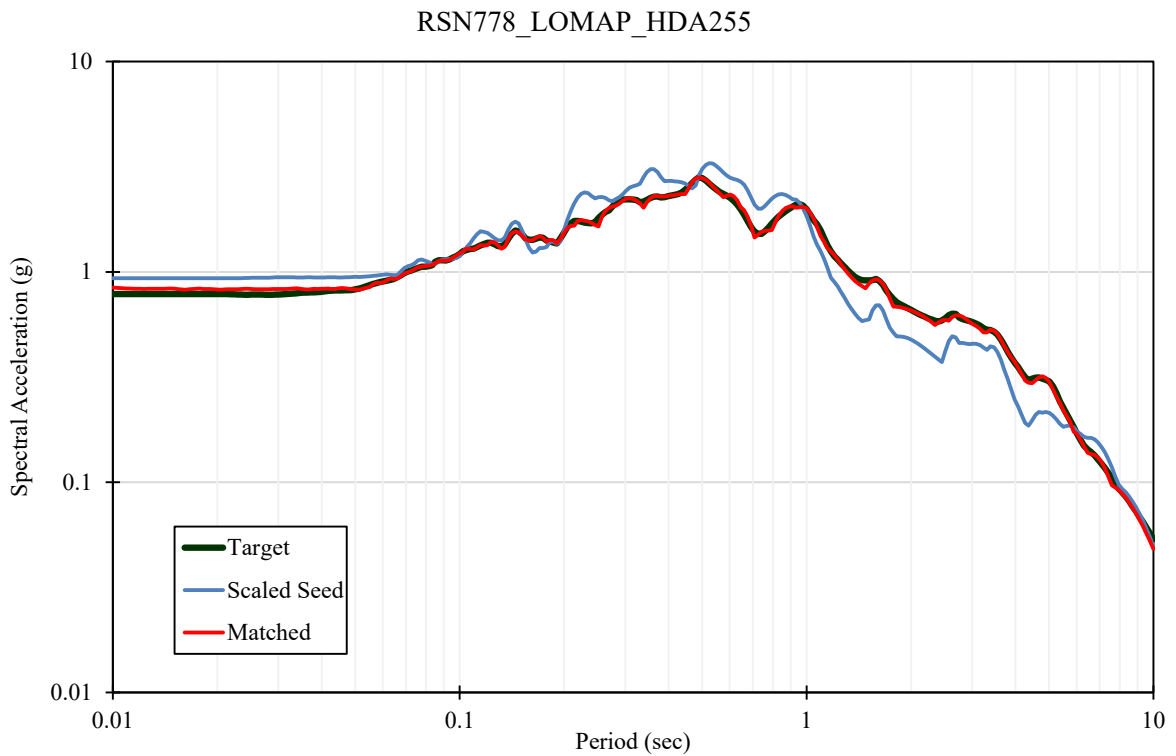
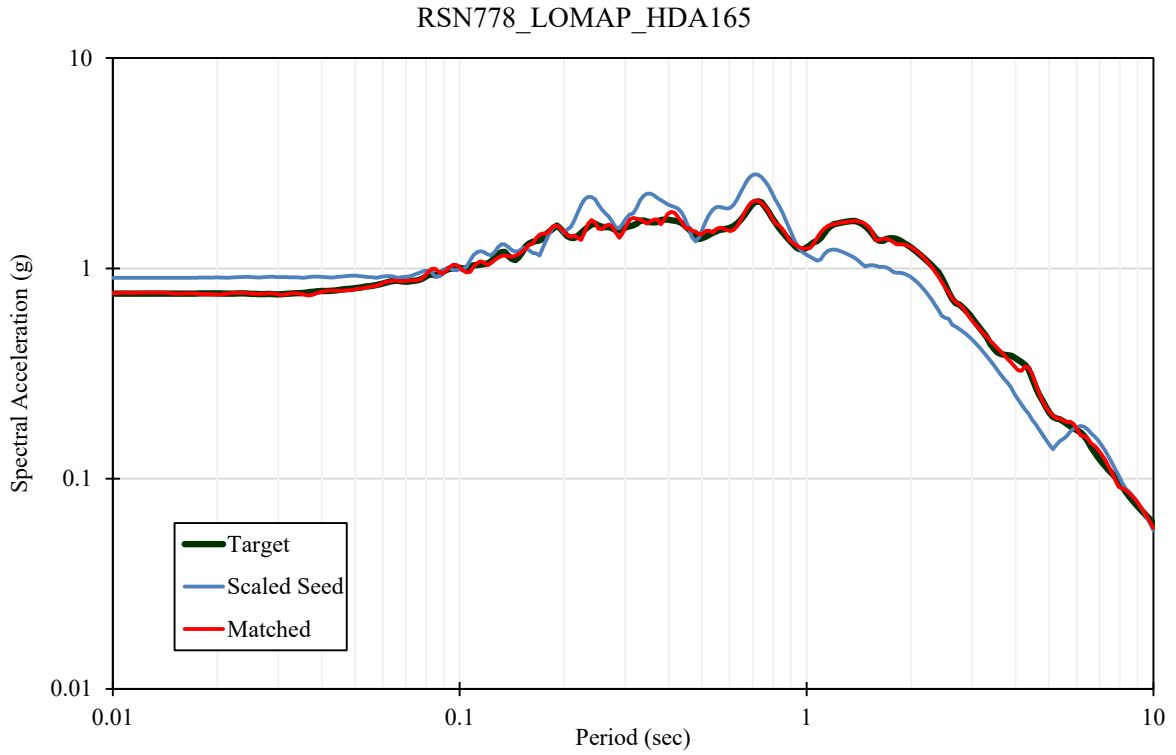
S:\1802\Figures\Figure_201.ai; Date: 05/04/2021; User: JCh.LCI



For Illustration
Purposes Only

1989 Loma Prieta – Hollister
Differential Array

Figure 201
Response Spectra for MDE Time
Histories for Southern Forebay
North, RSN 778



S:\1802\Figures\Figure_201.ai; Date: 05/04/2021; User: JCh.LCI

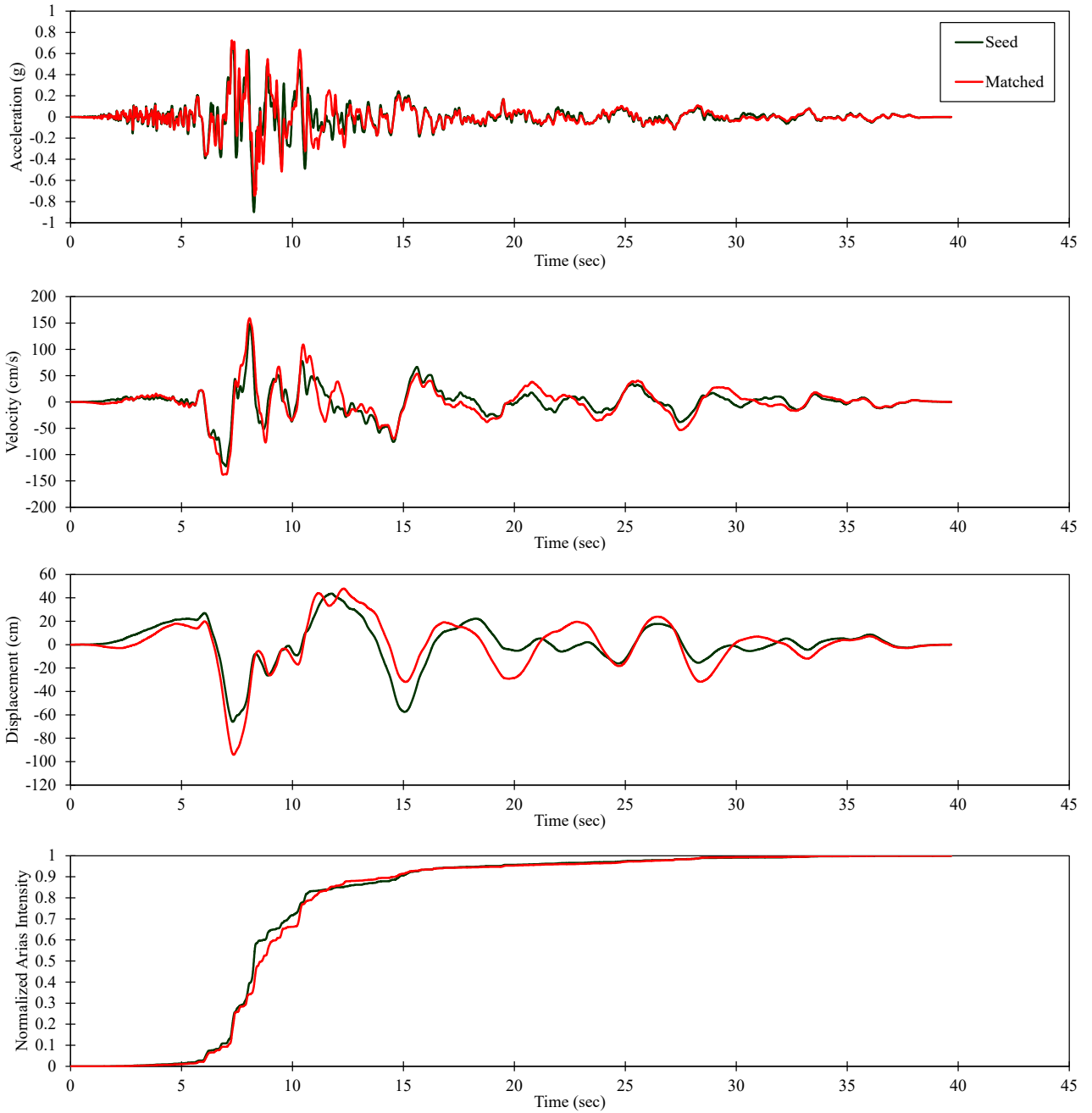


For Illustration
Purposes Only

1989 Loma Prieta – Hollister
Differential Array

Figure 202
Spectral Matches for MDE Time
Histories for Southern Forebay
North, RSN 778

RSN778_LOMAP_HDA165



S:\1802\Figures\Figure_203.ai; Date: 05/04/2021; User: JCh.LCL

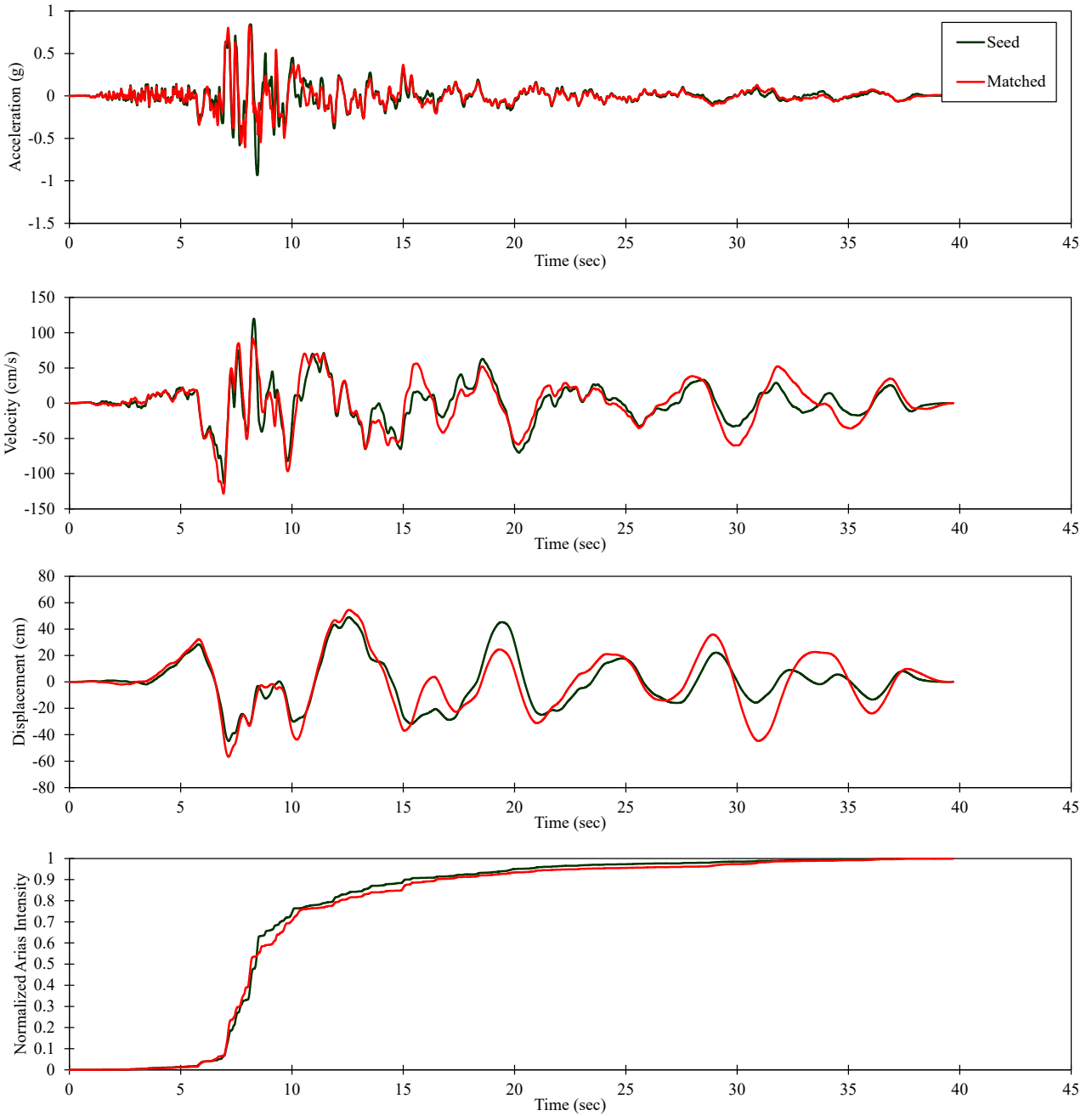


For Illustration
Purposes Only

1989 Loma Prieta – Hollister
Differential Array

Figure 203
Time History Spectrally-Matched to
MDE for Southern Forebay North,
RSN 778 (H1)

RSN778_LOMAP_HDA255



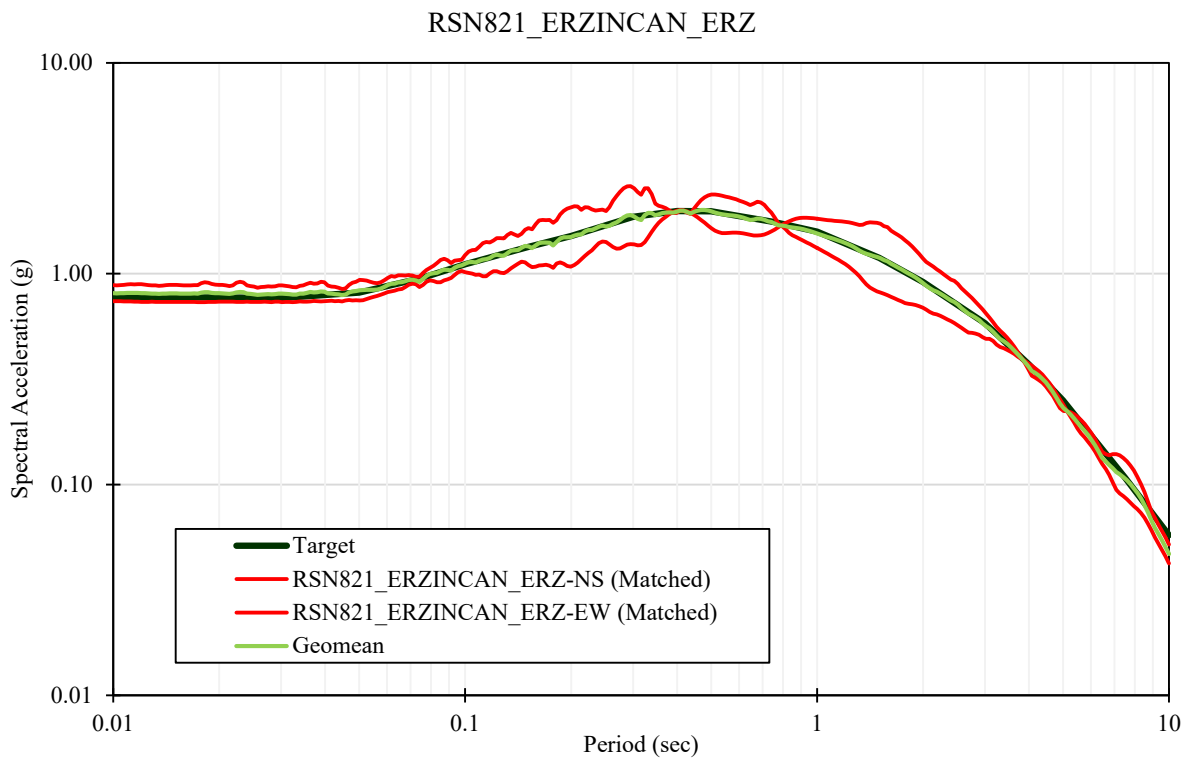
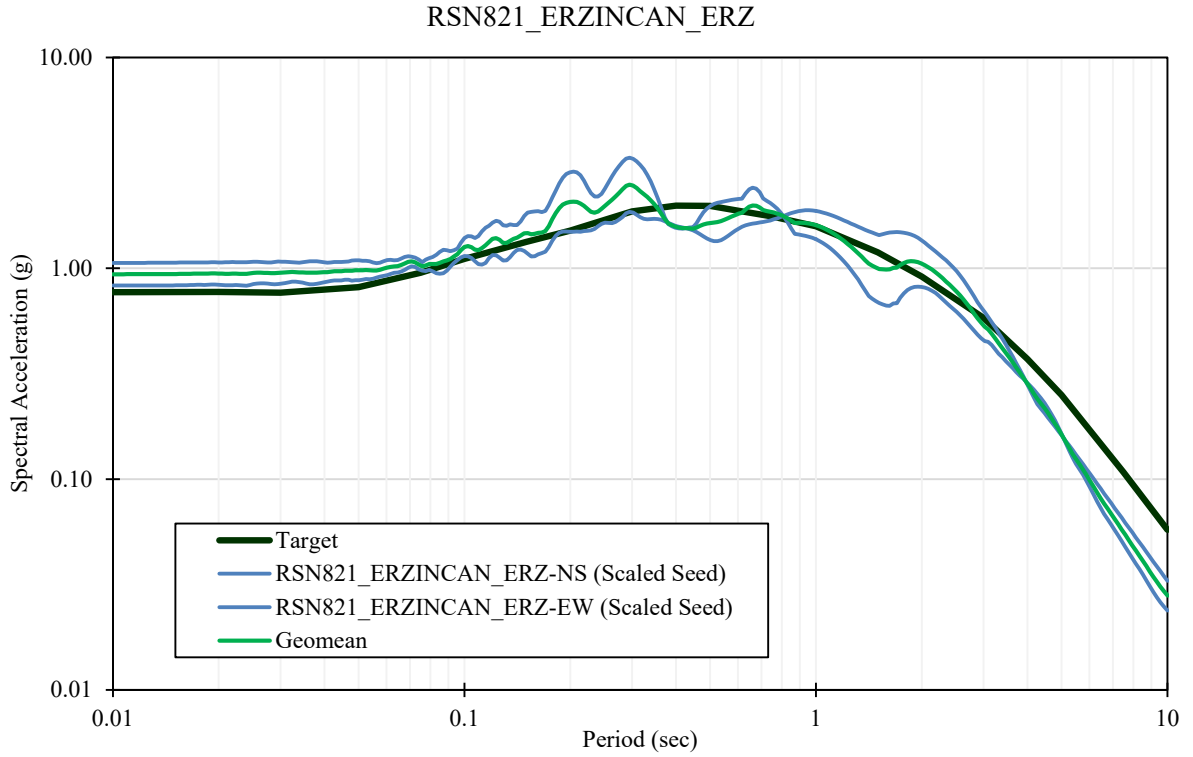
S:\1802\Figures\Figure_204.ai; Date: 05/04/2021; User: JCh.LCL



For Illustration
Purposes Only

1989 Loma Prieta – Hollister
Differential Array

Figure 204
Time History Spectrally-Matched to
MDE for Southern Forebay North,
RSN 778 (H2)



S:\1802\Figures\Figure_205.ai; Date: 05/04/2021; User: JCh.LCI

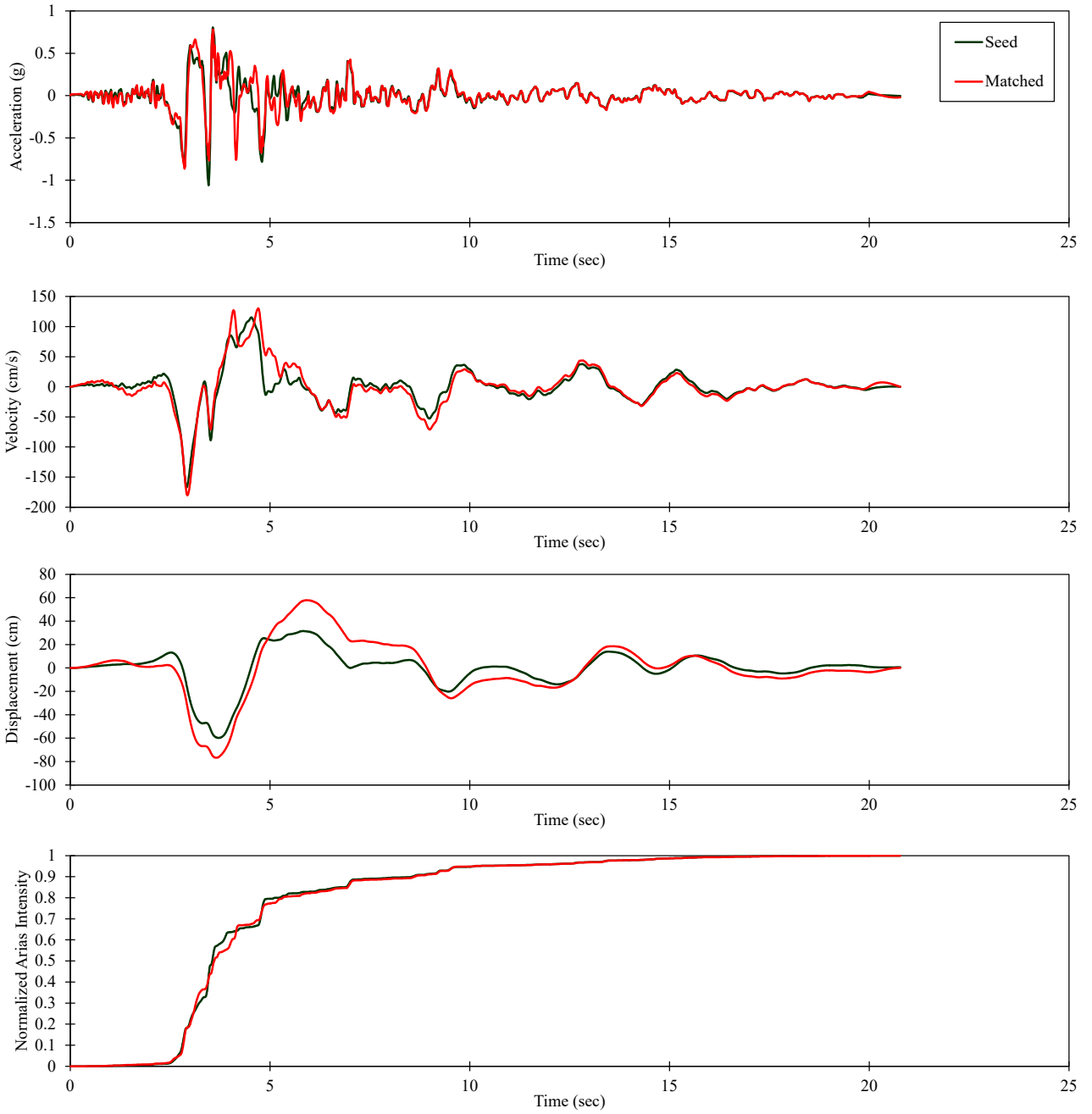


For Illustration
Purposes Only

1992 Erzican, Turkey – Erzican

Figure 205
Response Spectra for MDE Time
Histories for Southern Forebay
North, RSN 821

RSN821_ERZINCAN_ERZ-EW



S:\1802\Figures\Figure_207.ai; Date: 05/04/2021; User: JCh.LCL

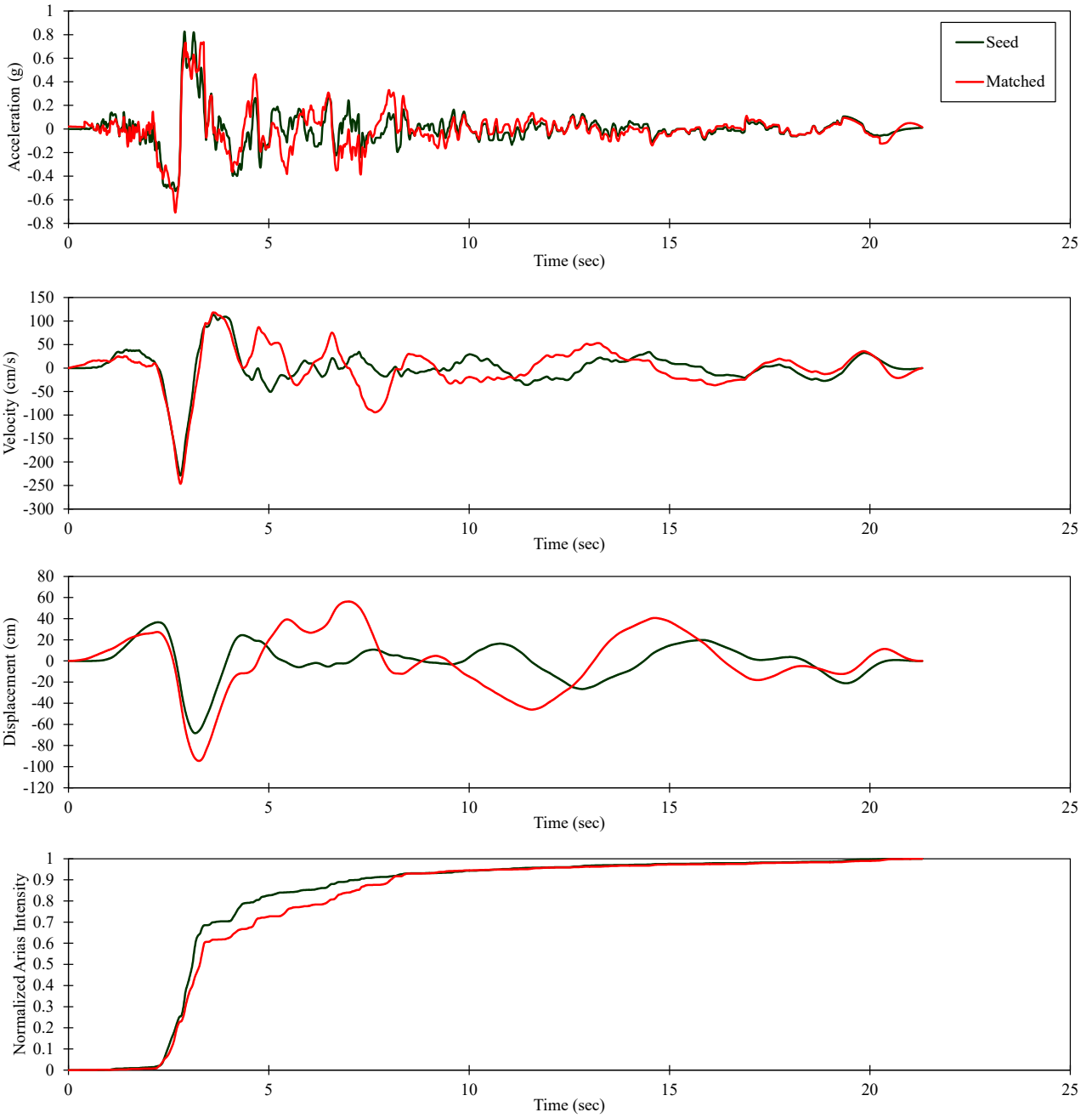


For Illustration
Purposes Only

1992 Erzican, Turkey – Erzican

Figure 207
Time History Spectrally-Matched to
MDE for Southern Forebay North,
RSN 821 (H1)

RSN821_ERZINCAN_ERZ-NS



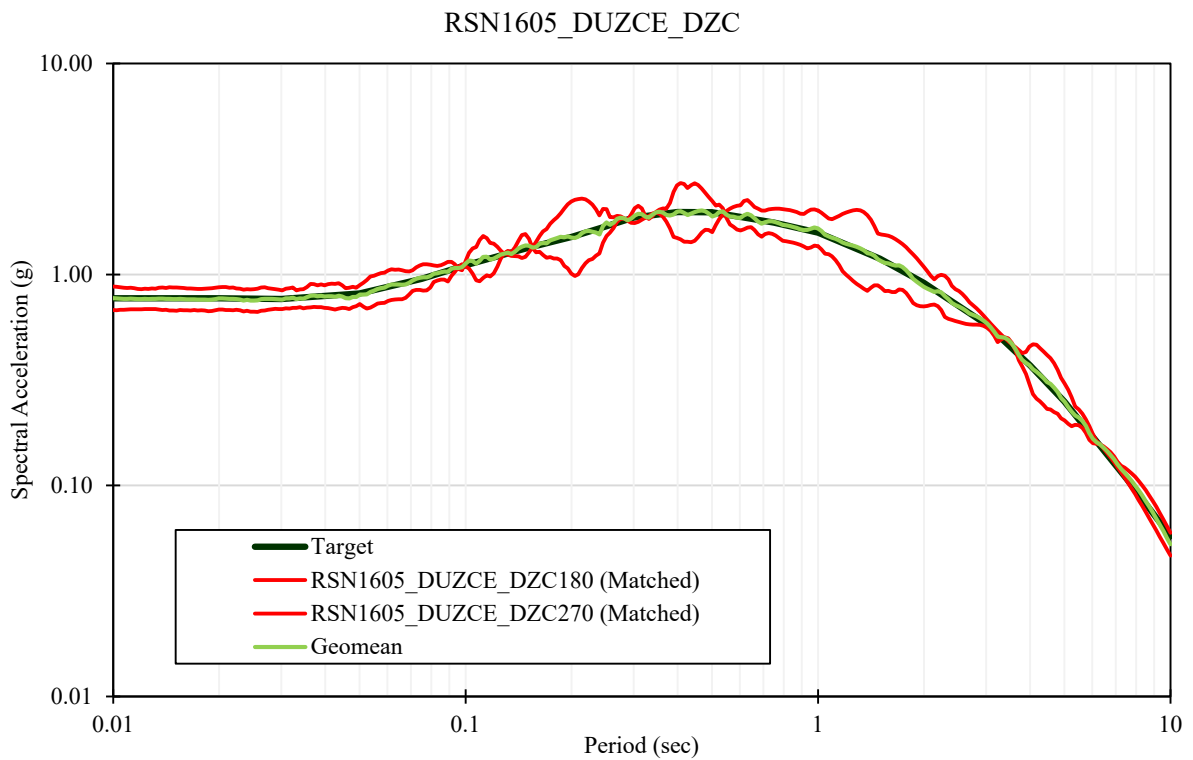
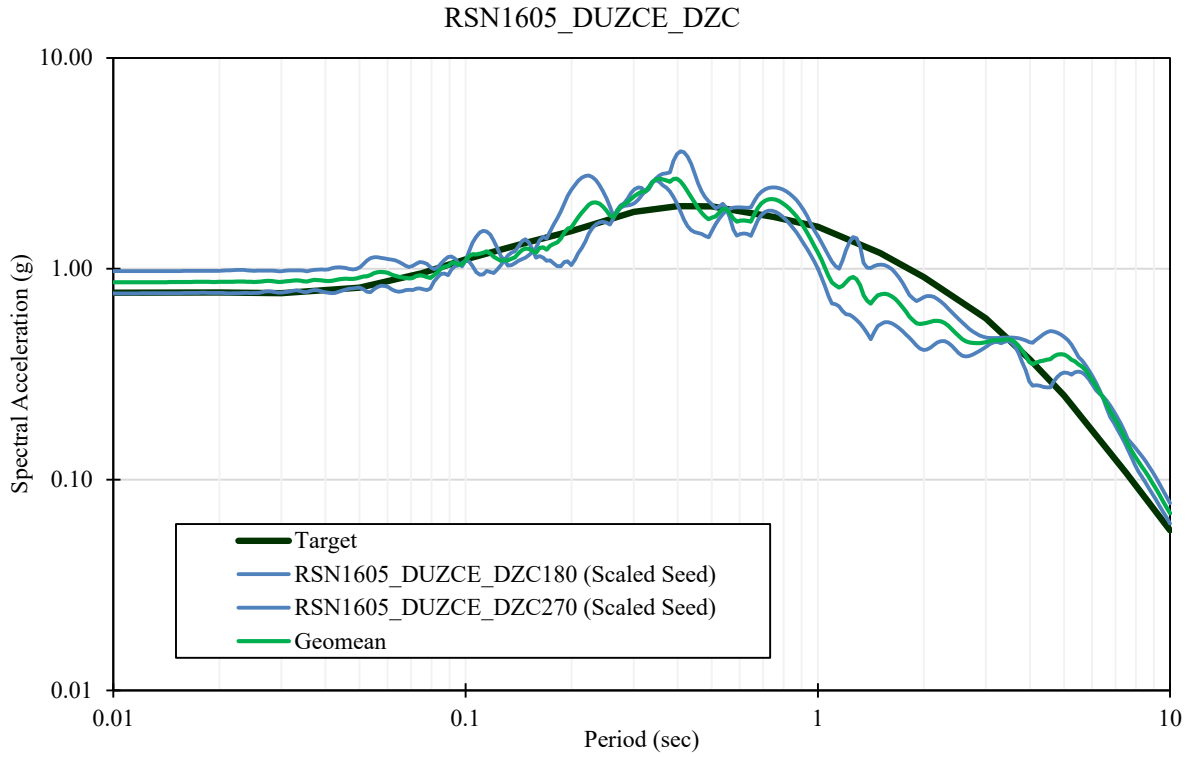
S:\1802\Figures\Figure_208.ai; Date: 05/04/2021; User: JCh.LCL



For Illustration
Purposes Only

1992 Erzican, Turkey – Erzican

Figure 208
Time History Spectrally-Matched to
MDE for Southern Forebay North,
RSN 821 (H2)



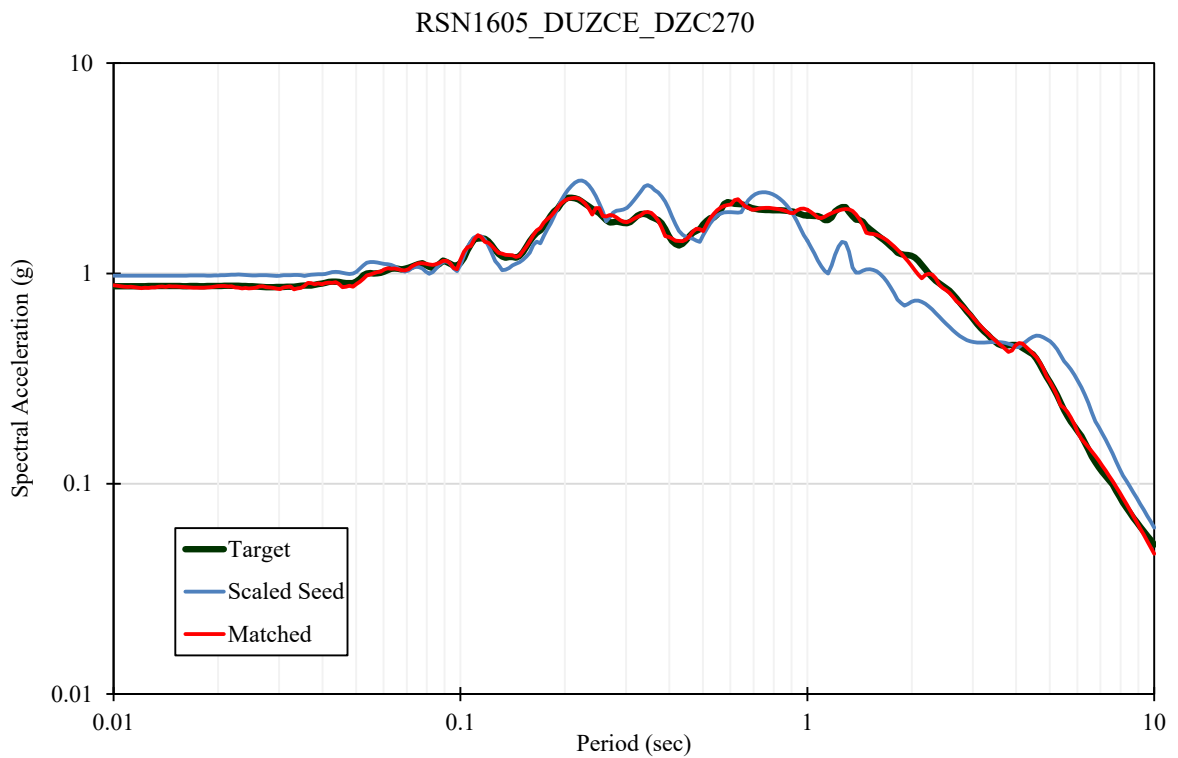
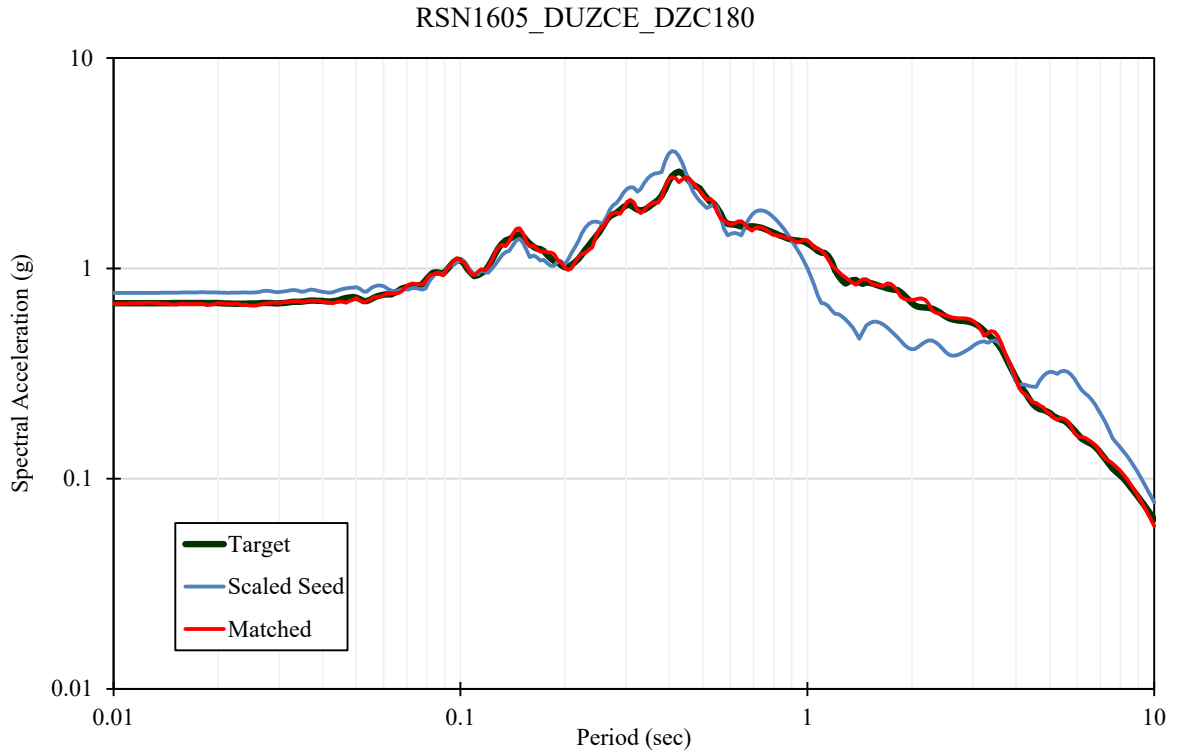
S:\1802\Figures\Figure_209.ai; Date: 05/04/2021; User: JCh.LCI



For Illustration
Purposes Only

1999 Duzce, Turkey – Duzce

Figure 209
Response Spectra for MDE Time
Histories for Southern Forebay
North, RSN 1605



S:\1802\Figures\Figure_210.ai; Date: 05/04/2021; User: JCH.LCI

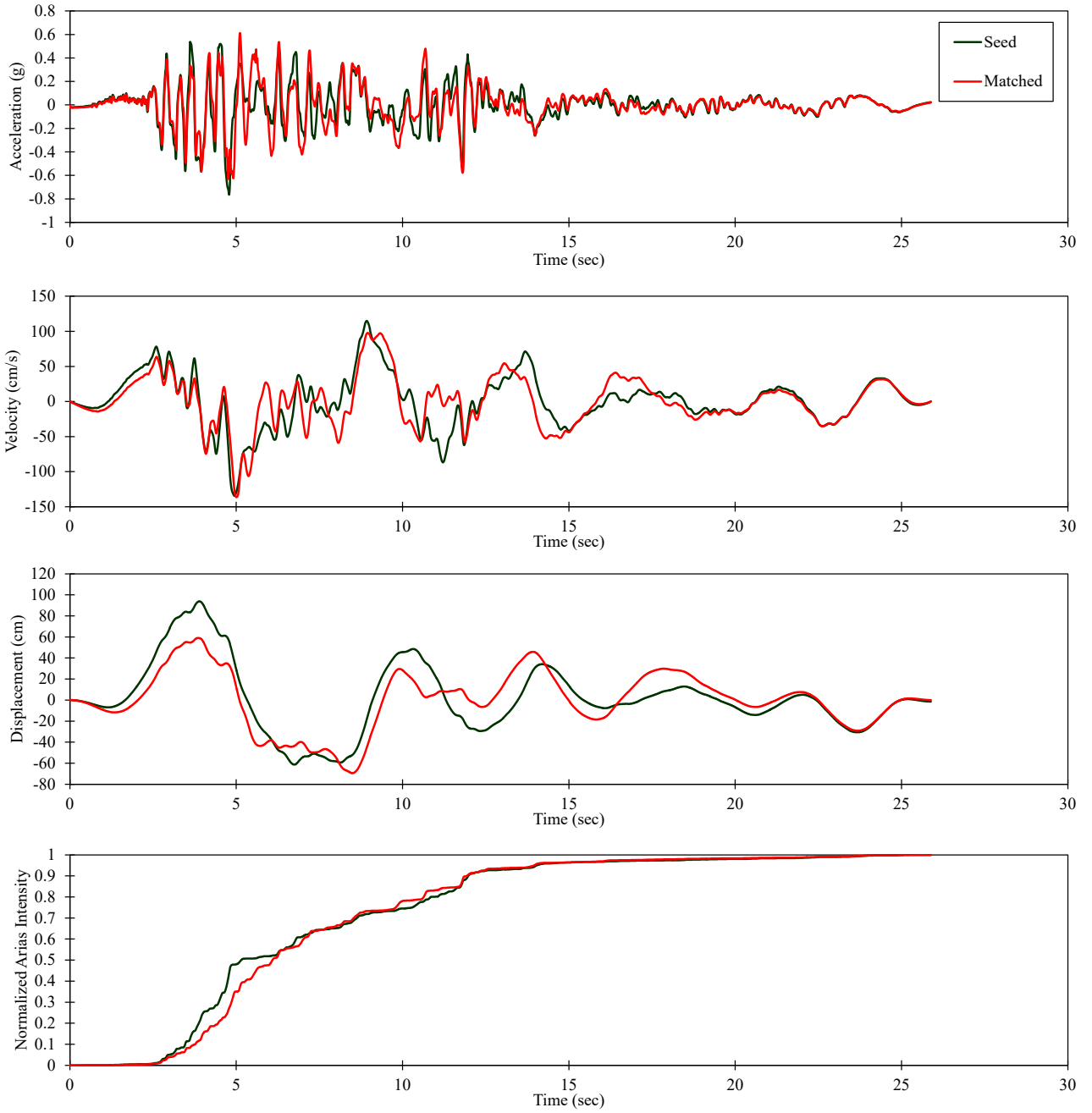


For Illustration
Purposes Only

2000 Duzce, Turkey – Duzce

Figure 210
Spectral Matches for MDE Time
Histories for Southern Forebay
North, RSN 1605

RSN1605_DUZCE_DZC180



S:\1802\Figures\Figure_211.ai; Date: 05/04/2021; User: JCh.LCL

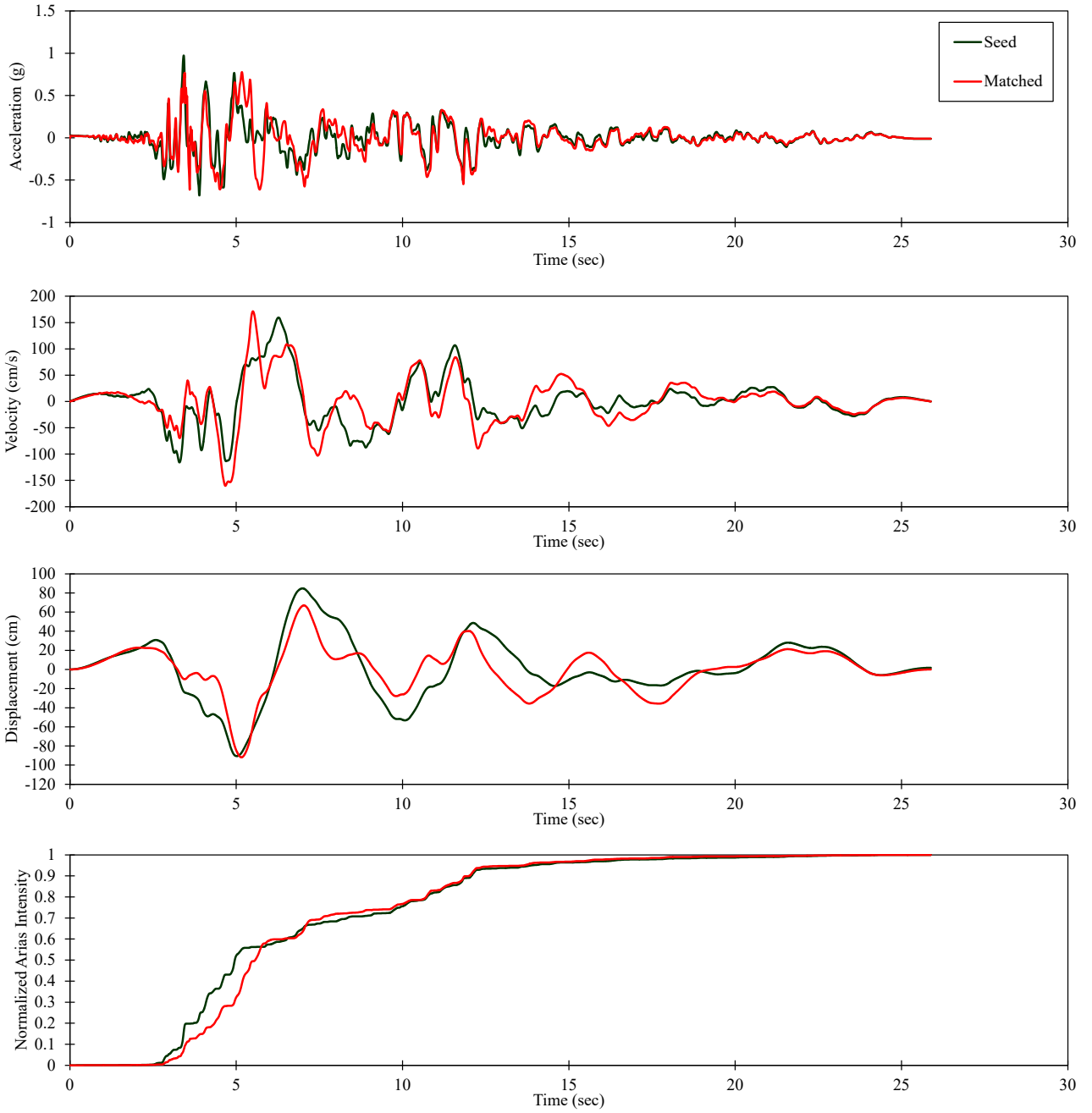


For Illustration
Purposes Only

2001 Duzce, Turkey – Duzce

Figure 211
Time History Spectrally-Matched to
MDE for Southern Forebay North,
RSN 1605 (H1)

RSN1605_DUZCE_DZC270



S:\1802\Figures\Figure_212.ai; Date: 05/04/2021; User: JCh.LCL



For Illustration
Purposes Only

2002 Duzce, Turkey – Duzce

Figure 212
Time History Spectrally-Matched to
MDE for Southern Forebay North,
RSN 4031 (H2)



MEMORANDUM OF TRANSMITTAL

Date: 1 September 2021
 To: Andrew Finney and Dario Rosidi
 From: Patricia Thomas, Sarah Smith, and Ivan Wong

SUBJECT: Data Transmittal – Delta Conveyance Probabilistic and Deterministic Ground Motions for Bethany Alternative Sites

Lettis Consultants International, Inc. (LCI) is pleased to provide these probabilistic and deterministic peak horizontal ground accelerations (PGAs) for the three sites along the Bethany Alternative of the Delta Conveyance Project (Figure 1). These values supplement the values provided in reports by Wong *et al.* (2021) for 12 sites along the two original alignments. All sites are shown on Figure 1. Consistent with those previous analyses, the ground motions computed herein are for a generic stiff soil site condition with a time-averaged shear-wave velocity in the top 30 m (V_{s30}) of 1,100 ft/sec (335 m/sec).

The seismic source model used in the May 2019 analyses for WaterFix (LCI, 2019) has since been updated. Specifically the characterizations of the West Tracy, Midland, and Greenville faults were revised based on new information (Figure 1). The updates to the seismic source model are described in Wong *et al.* (2021). Table 1 provides mean and 85th percentile PGAs at 500, 1,000, and 2,475-year return periods.

Table 1. Probabilistic PGAs for California Delta Conveyance¹

LOCATION ¹	LATITUDE	LONGITUDE	500-YEAR PGA		1,000-YEAR PGA		2,475-YEAR PGA	
			MEAN (g)	85TH % (g)	MEAN (g)	85TH % (g)	MEAN (g)	85TH % (g)
Bethany Reservoir Shaft	37.779498°	-121.605939°	0.46	0.53	0.59	0.67	0.78	0.89
Pumping Plant	37.801215°	-121.575039°	0.41	0.47	0.53	0.60	0.70	0.79
Union Island Shaft	37.866588°	-121.523912°	0.33	0.37	0.41	0.46	0.54	0.61

¹ Stiff Soil, Site Class D was assumed for each location.

Notes:

% = percentile

PGA = peak horizontal acceleration



The results of the PSHA show that the highest probabilistic hazard is at the Bethany Reservoir shaft followed by the Pumping Plant. The lowest hazard is at the Union Island shaft. The probabilistic PGA hazard at the three sites is controlled by the active faults to the west including the Greenville and Mt. Diablo faults (Figure 1). Unlike the DSHA, the West Tracy fault is not a major contributor to the probabilistic hazard because of its low slip rate.

A DSHA was also performed for the three sites. All three sites are within 6 km of the West Tracy fault, and so, deterministic PGAs are computed for the **M** 6.9 scenario on the West Tracy fault. Deterministic scenarios on other faults in the region result in lower PGAs.

Table 2. Deterministic PGA Values¹

LOCATION	DETERMINISTIC MEDIAN PGA (g)	DETERMINISTIC 84 TH PERCENTILE PGA (g)	DETERMINISTIC 69 TH PERCENTILE PGA (g)	DETERMINISTIC 95 TH PERCENTILE PGA (g)
Bethany Reservoir Shaft	0.54	0.93	0.71	1.31
Pumping Plant	0.60	1.02	0.78	1.44
Union Island Shaft	0.42	0.72	0.55	1.03

¹Controlling deterministic scenario for all three sites is **M** 6.9 earthquake on the West Tracy fault.

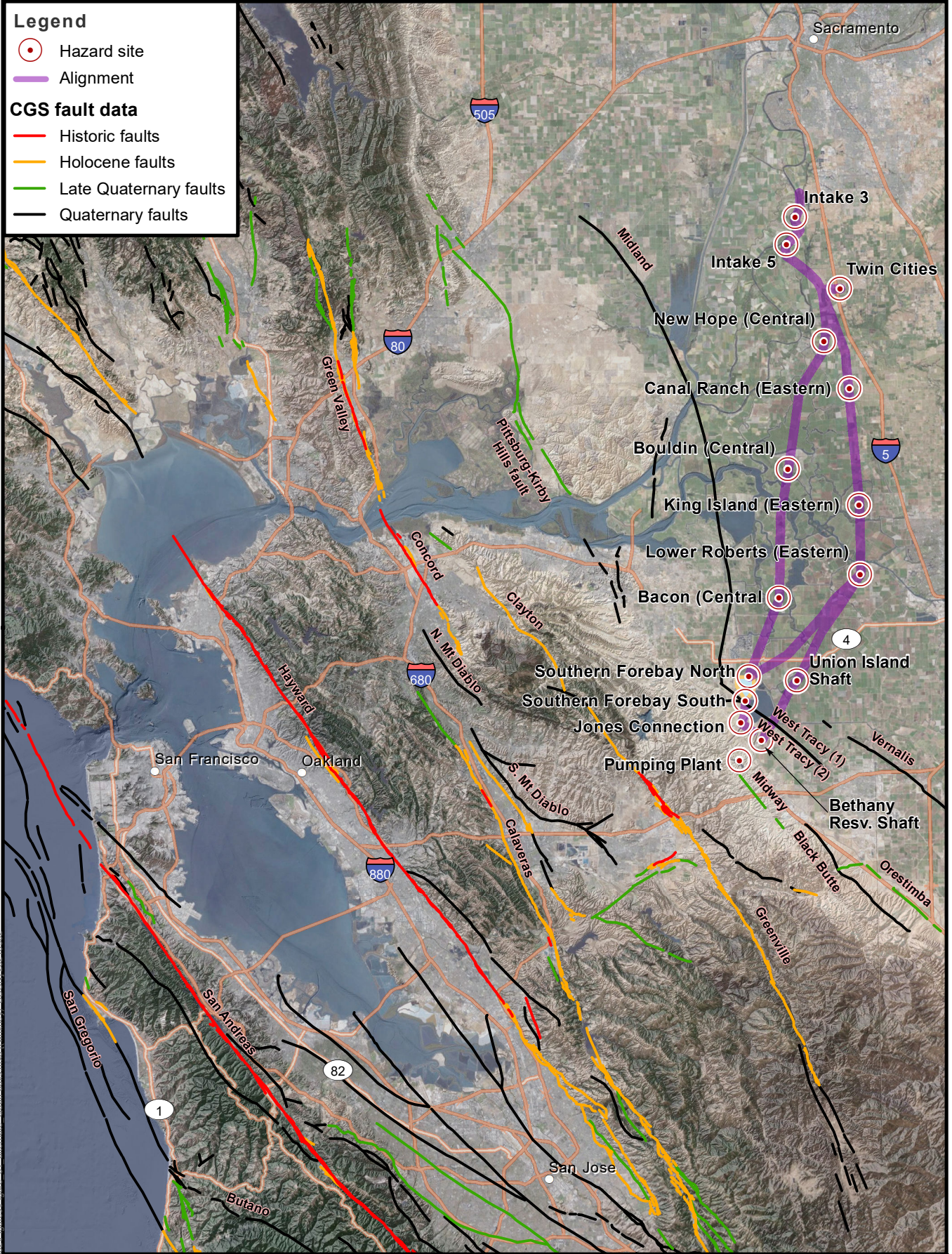
The Bethany Reservoir Shaft and Pumping Plant sites are located on the hanging wall of the West Tracy fault resulting in larger ground motions than at the Union Island Shaft site. The Pumping Plant hazard is highest because it is closest to the West Tracy fault (Figure 1).

The probabilistic and deterministic ground motions represent free-field motions for a reference site condition of stiff soil ($V_{s30} = 1,100$ ft/sec). These preliminary ground motions should be revised at a later date using site response analysis to model the effects of the softer, near surface materials.

REFERENCES

Lettis Consultants International, 2019, Date transmittal – WaterFix probabilistic and deterministic ground motions for CER Section 4, letter of transmittal to Andrew Finney dated 1 May 2019.

Wong, I., Thomas, P., Zandieh, A., Lewandowski, N., Smith, S., and Unruh, J., 2021, Seismic hazard analyses and development of conceptual seismic design ground motions for the Delta Conveyance, unpublished final report (Rev 2 dated 1 Sep 2021) prepared by Lettis Consultants International for the Delta Conveyance Design and Construction Office.



Legend

- Hazard site
- Alignment

CGS fault data

- Historic faults
- Holocene faults
- Late Quaternary faults
- Quaternary faults

DCA
DELTA CONVEYANCE DESIGN
& CONSTRUCTION AUTHORITY

**For Illustration
Purposes Only**

N

0 5 10 15 Miles

Figure 1
Quaternary Faults in the
San Francisco Bay Region

S:\181021E\Figures\18102_002\Figures\Figure_01_alternate_CrossFaults.mxd (Montreux) BD:SNL 2/12/2012 10:00:02

Data Source: DCA, CGS (2005)



MEMORANDUM OF TRANSMITTAL

Date: 1 September 2021

To: Andrew Finney and Dario Rosidi

From: Patricia Thomas and Ivan Wong

SUBJECT: Data Transmittal – Delta Conveyance Probabilistic and Deterministic Ground Motions for Union Island Shaft

As requested, the following are probabilistic and deterministic peak horizontal ground acceleration (PGA) values and spectral acceleration (SA) values for spectral periods from 0.01 to 10.0 sec, as well as Operating Basis Earthquake (OBE) and Maximum Design Earthquake (MDE) design response spectra for the Union Island Shaft site along the Bethany Alternative alignment of the Delta Conveyance Project (Figure 1). These values supplement the values provided in reports by Wong *et al.* (2021) for 12 sites along the two original alignments and Thomas *et al.* (2021) for three sites along the Bethany Alternative. All sites are shown on Figure 1. Consistent with those previous analyses, the ground motions computed herein are for a generic stiff soil site condition with a time-averaged shear-wave velocity in the top 30 m (V_{s30}) of 1,100 ft/sec (335 m/sec).

The seismic source model used in the 2019 analyses for WaterFix (LCI, 2019) was subsequently updated. Specifically the characterizations of the West Tracy, Midland, and Greenville faults were revised based on new information (Figure 1). The updates to the seismic source model are described in the Wong *et al.* (2021). The results for the three Bethany Alternative presented in Thomas *et al.* (2021) are based on the updated source model, as are the expanded results presented herein for Union Island Shaft site. These results for the Union Island Shaft site supersede those in Thomas *et al.* (2021).

Probabilistic Ground Motion Results

The probabilistic seismic hazard analysis (PSHA) methodology, including documentation of the seismic source model and ground motion models, used to develop the Union Island Shaft ground motions are provided in Wong *et al.* (2021). The results of the PSHA for the Union Island Shaft are presented in terms of ground motion as a function of annual exceedance frequency (AEF). AEF is the reciprocal of the average return period. Figure 2 shows the mean, median (50th percentile), 5th, 15th, 85th, and 95th percentile PGA hazard curves. The range of uncertainty between the the 5th and 95th percentile (fractiles) is a factor of 1.6 at a return period of 2,475 years. These fractiles indicate the range of epistemic uncertainty about the mean hazard. The 1.0 sec horizontal SA hazard curves are shown on Figure 3, which also have a factor of 1.6 at a return

period of 2,475 years. Table 1 provides mean and 5th to 95th percentile PGA and 1.0 sec values at return periods of 144, 200, 475, 975, and 2,475 years.

Table 1. Summary of PGA and 1.0 Sec Horizontal Spectral Accelerations¹

	PGA (g)	1.0 SEC SA (g)
144-Year Return Period		
Mean	0.20	0.25
5th-95th Percentiles	0.16 - 0.25	0.19 - 0.31
200-Year Return Period		
Mean	0.23	0.29
5th-95th Percentiles	0.18 - 0.29	0.22 - 0.36
475-Year Return Period		
Mean	0.32	0.41
5th-95th Percentiles	0.25 - 0.4	0.32 - 0.51
975-Year Return Period		
Mean	0.41	0.54
5th-95th Percentiles	0.32 - 0.5	0.41 - 0.66
2,475-Year Return Period		
Mean	0.54	0.74
5th-95th Percentiles	0.42 - 0.66	0.56 - 0.92

¹ Stiff Soil, Site Class D was assumed for Union Island Shaft site.

Notes: % = percentile

PGA = peak horizontal acceleration

The contributions of the various seismic sources to the mean PGA hazard are shown on Figures 4 and 5 as hazard curves and fractional contribution plots, respectively. Seismic sources that contribute at least 5 percent to the hazard over the period range of 144 to 2,475 years are identified on these figures. Figures 4 and 5 show that the PGA hazard is controlled by the Mt. Diablo fault for return periods between 100 and 10,000 years. Although the site is located 25 km from the Mt. Diablo fault, it has a preferred slip rate of 2.0 mm/year, while the closer faults such as Greenville and West Tracy have significantly lower slip rates. The 1.0 sec SA hazard results are similar with some increased relative contribution from the Greenville and Midway-Black Butte faults (Figures 6 and 7).

The hazard can also be deaggregated in terms of the joint magnitude-distance-epsilon probability conditional on the ground motion parameter (PGA or SA exceeding a specific values). Epsilon is the difference between the logarithm of the ground motion amplitude and the mean logarithm of ground motion (for that M and D) measured in units of standard deviation (σ). Thus, positive epsilons indicated larger-than-average ground motions. By deaggregating the PGA and 1.0 sec SA hazard by magnitude, distance, and epsilon bins, we can illustrate the contribution by events at various return periods. Figure 8 shows the deaggregation of the PGA hazard for the return periods of 475 and 2,475 years. The contributions to the PGA hazard are coming from a wide

range of M and D reflecting the contribution from several seismic sources (Figures 4 and 5). The majority of the PGA hazard at both the 475 and 2,475 year return periods is coming from events with magnitudes **M** 6.4 to 7.4 at distances less than 60 km. Deaggregation of the 1.0 sec SA hazard shows contribution from events of the same magnitude and distance ranges, but with additional contribution from events of magnitude **M** 7.2 to 8.4 between 80 and 90 km on the San Andreas fault (Figure 9).

Based on the magnitude and distance deaggregated results, the controlling earthquakes as defined by the mean magnitude (\bar{M}) and modal magnitude (M^*), and mean distance (\bar{D}) and modal distance (D^*) can be calculated. Table 2 lists the \bar{M} , M^* , \bar{D} , and D^* for the five return periods (144, 200, 475, 975, and 2,475 years) and for PGA and 1.0 sec horizontal SA.

Table 2. Magnitude and Distance Deaggregation

PERIOD (SEC)	PGA	1.0 Sec SA
144-Year Return Period		
Modal M	6.7	6.7
Modal R_{RUP} (km)	25	25
Mean M	6.6	6.8
Mean R_{RUP} (km)	35.6	48.0
200-Year Return Period		
Modal M	6.7	6.7
Modal R_{RUP} (km)	25	25
Mean M	6.6	6.8
Mean R_{RUP} (km)	33.1	45.4
475-Year Return Period		
Modal M	6.7	6.7
Modal R_{RUP} (km)	25	25
Mean M	6.6	6.8
Mean R_{RUP} (km)	27.9	39.2
975-Year Return Period		
Modal M	6.7	6.7
Modal R_{RUP} (km)	25	25
Mean M	6.6	6.8
Mean R_{RUP} (km)	24.6	41.9
2,475-Year Return Period		
Modal M	6.7	6.7
Modal R_{RUP} (km)	25	25
Mean M	6.6	6.8
Mean R_{RUP} (km)	21.4	30.2

Figure 10 shows a suite of mean uniform hazard spectra (UHS) at the return periods of 144, 200, 475, 975, and 2475 years. A UHS depicts the ground motions at all spectral periods with the same

annual exceedance frequency or return period. The mean UHS shown on Figure 10 are tabulated in Table 3.

Table 3. Mean Uniform Hazard Spectra

PERIOD (SEC)	144-YEAR RETURN PERIOD, SA (g)	200-YEAR RETURN PERIOD, SA (g)	475-YEAR RETURN PERIOD, SA (g)	975-YEAR RETURN PERIOD, SA (g)	2,475-YEAR RETURN PERIOD, SA (g)
0.01	0.20	0.23	0.32	0.41	0.54
0.03	0.22	0.25	0.34	0.43	0.57
0.05	0.26	0.29	0.41	0.51	0.68
0.075	0.33	0.38	0.52	0.66	0.88
0.10	0.40	0.45	0.63	0.80	1.05
0.15	0.49	0.55	0.76	0.96	1.27
0.20	0.52	0.59	0.82	1.04	1.37
0.25	0.53	0.60	0.83	1.06	1.41
0.30	0.52	0.60	0.83	1.06	1.41
0.40	0.48	0.55	0.76	0.99	1.33
0.50	0.43	0.50	0.70	0.91	1.23
0.60	0.38	0.44	0.62	0.81	1.10
0.75	0.33	0.38	0.53	0.69	0.95
1.0	0.25	0.29	0.41	0.54	0.74
1.5	0.16	0.19	0.27	0.35	0.48
2.0	0.12	0.13	0.19	0.25	0.35
3.0	0.061	0.076	0.12	0.15	0.21
4.0	0.038	0.045	0.073	0.11	0.14
5.0	0.027	0.032	0.049	0.070	0.11
7.5	0.016	0.019	0.027	0.037	0.055
10.0	0.011	0.013	0.018	0.024	0.035

Deterministic Ground Motion Results

A deterministic seismic hazard analysis (DSHA) was also performed for the Union Island Shaft site. The site is on the footwall and within 6 km of the West Tracy fault, and so, deterministic ground motions are computed for the characteristic **M** 6.9 scenario on the West Tracy fault (Figure 11). Deterministic ground motions were also computed for the larger, but more distant, **M** 8.0 scenario for the San Andreas fault (Figure 11). Deterministic scenarios for the San Andreas fault scenario and on other faults in the region result in lower ground motions. Inputs for the DSHA are provided in Table 4 and the resulting deterministic ground motions are provided in Table 5. Median, 69th, 84th, and 95th PGA values were computed to illustrate the range of uncertainty in the computed ground motions due to the aleatory sigma of the ground motion models. Figure 12 compares the enveloped (West Tracy scenario) deterministic ground motions to the suite of UHS for return periods of 144 to 2,475-year return periods. The median deterministic ground motions are similar to the 975-year UHS, while the 84th and 95th percentile deterministic ground motions exceed the 2,475-year UHS (Figure 12).

Table 4. DSHA Inputs

INPUT PARAMETER	INPUT PARAMETER DEFINITION	WEST TRACY	SAN ANDREAS
<i>M</i>	Moment magnitude	6.9	8.0
<i>R_{RUP}</i>	Closest distance to coseismic rupture (km)	5.9	81.9
<i>R_{JB}</i>	Closest distance to surface projection of coseismic rupture (km)	5.9	81.9
<i>R_X</i>	Horizontal distance from top of rupture measured perpendicular to fault strike (km)	-5.9	81.9
<i>R_{y0}</i>	The horizontal distance off the end of the rupture measured parallel to strike (km)	0	0
<i>U</i>	Unspecified-mechanism factor: 1 for unspecified; 0 otherwise	0	0
<i>F_{RV}</i>	Reverse-faulting factor: 0 for strike slip, normal, normal-oblique; 1 for reverse, reverse-oblique and thrust	1	0
<i>F_N</i>	Normal-faulting factor: 0 for strike slip, reverse, reverse-oblique, thrust and normal-oblique; 1 for normal	0	0
<i>F_{HW}</i>	Hanging-wall factor: 1 for site on down-dip side of top of rupture; 0 otherwise	0	0
<i>Z_{TOR}</i>	Depth to top of coseismic rupture (km)	0	0
<i>Dip</i>	Average dip of rupture plane (degrees)	70	90
<i>V_{S30}</i>	The average shear-wave velocity (m/s) over a subsurface depth of 30 m	335	335
<i>F_{Measured}</i>	0 = inferred, 1 = measured	1	1
<i>Z_{HYP}</i>	Hypocentral depth from the earthquake	Default	Default
<i>Z_{1.0}</i>	Depth to Vs=1 km/sec	0.7	0.7
<i>Z_{2.5}</i>	Depth to Vs=2.5 km/sec	4.0	4.0
<i>W</i>	Fault rupture width (km)	20.3	13
<i>Region</i>	Specific Regions considered in the models	California	California



Table 5. DSHA Results

PERIOD (SEC)	WEST TRACY				SAN ANDREAS				ENVELOPE			
	MEDIAN (g)	69 TH PERC. (g)	84 TH PERC.(g)	95 TH PERC. (g)	MEDIAN (g)	69 TH PERC. (g)	84 TH PERC.(g)	95 TH PERC. (g)	MEDIAN (g)	69 TH PERC. (g)	84 TH PERC.(g)	95 TH PERC. (g)
0.01	0.42	0.55	0.72	1.03	0.11	0.15	0.19	0.28	0.42	0.55	0.72	1.03
0.02	0.42	0.56	0.73	1.04	0.11	0.15	0.19	0.28	0.42	0.56	0.73	1.04
0.03	0.43	0.57	0.75	1.07	0.11	0.15	0.20	0.29	0.43	0.57	0.75	1.07
0.05	0.48	0.64	0.84	1.21	0.12	0.17	0.22	0.33	0.48	0.64	0.84	1.21
0.075	0.58	0.77	1.02	1.48	0.14	0.20	0.27	0.40	0.58	0.77	1.02	1.48
0.10	0.68	0.91	1.20	1.74	0.17	0.23	0.31	0.47	0.68	0.91	1.20	1.74
0.15	0.85	1.12	1.48	2.11	0.20	0.27	0.37	0.56	0.85	1.12	1.48	2.11
0.20	0.94	1.25	1.65	2.35	0.22	0.31	0.41	0.61	0.94	1.25	1.65	2.35
0.25	1.01	1.33	1.77	2.55	0.24	0.33	0.45	0.67	1.01	1.33	1.77	2.55
0.30	1.03	1.38	1.85	2.70	0.25	0.34	0.47	0.70	1.03	1.38	1.85	2.70
0.40	0.98	1.34	1.82	2.71	0.24	0.33	0.46	0.70	0.98	1.34	1.82	2.71
0.50	0.90	1.24	1.72	2.60	0.23	0.32	0.44	0.68	0.90	1.24	1.72	2.60
0.75	0.69	0.98	1.37	2.13	0.18	0.26	0.36	0.57	0.69	0.98	1.37	2.13
1.0	0.56	0.80	1.13	1.77	0.15	0.21	0.29	0.46	0.56	0.80	1.13	1.77
1.5	0.37	0.53	0.76	1.20	0.11	0.16	0.22	0.35	0.37	0.53	0.76	1.20
2.0	0.27	0.38	0.55	0.86	0.085	0.12	0.17	0.27	0.27	0.38	0.55	0.86
3.0	0.17	0.24	0.34	0.54	0.061	0.087	0.12	0.20	0.17	0.24	0.34	0.54
4.0	0.11	0.16	0.22	0.35	0.047	0.066	0.094	0.15	0.11	0.16	0.22	0.35
5.0	0.076	0.11	0.15	0.24	0.036	0.051	0.073	0.11	0.076	0.11	0.15	0.24
7.5	0.035	0.049	0.070	0.11	0.022	0.032	0.045	0.070	0.035	0.049	0.070	0.11
10.0	0.019	0.027	0.038	0.059	0.014	0.019	0.027	0.043	0.019	0.027	0.038	0.059

Design Ground Motions

MDE and OBE design response spectra were developed for the Union Island Shaft site. In accordance with the Delta Conveyance seismic design criteria (DCA, 2021), MDE for shafts is defined as the envelope of the 2,475-year UHS and 84th percentile deterministic response spectra. Figure 13 compares these spectra and shows that for this site, the MDE is controlled by the 84th percentile deterministic spectra for all spectral periods. The OBE is defined as the 475-year UHS (Figure 10). Table 6 provides the MDE and OBE for the Union Island Shaft site.

Table 6. MDE and OBE Design Ground Motions

PERIOD (SEC)	MDE, SA (g)	OBE, SA (g)
0.01	0.72	0.32
0.02	0.73	0.33
0.03	0.75	0.34
0.05	0.84	0.41
0.075	1.02	0.52
0.10	1.20	0.63
0.15	1.48	0.76
0.20	1.65	0.82
0.25	1.77	0.83
0.30	1.85	0.83
0.40	1.82	0.76
0.50	1.72	0.70
0.60	1.55	0.62
0.75	1.37	0.53
1.0	1.13	0.41
1.5	0.76	0.27
2.0	0.55	0.19
3.0	0.339	0.118
4.0	0.222	0.073
5.0	0.153	0.049
7.5	0.070	0.027
10.0	0.038	0.018

The probabilistic and deterministic ground motions represent free-field motions for a reference site condition of stiff soil ($V_{s30} = 1,100$ ft/sec). These ground motions should be revised at a later date using site response analysis to model the effects of the softer, near-surface materials.

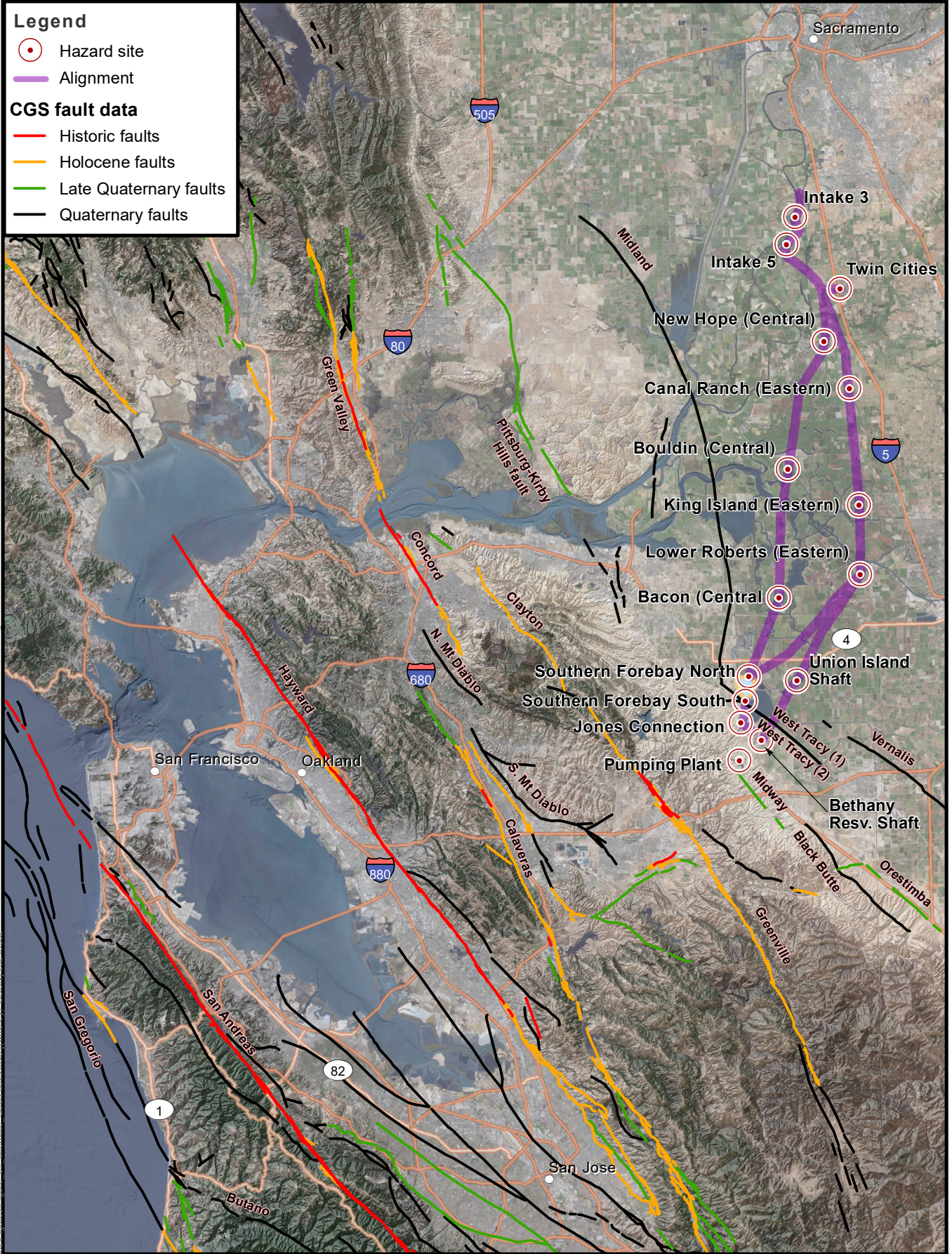
REFERENCES

DCA (Delta Conveyance Design and Construction Authority), 2021, Conceptual-Level Seismic Design Criteria, prepared for DWR/Delta Conveyance Office, 26 p.

Lettis Consultants International, 2019, Data transmittal – WaterFix probabilistic and deterministic ground motions for CER Section 4, letter of transmittal to Andrew Finney dated 1 May 2019.

Thomas, P., Smith, S., and Wong, I., 2021, Data transmittal – Delta Conveyance probabilistic and deterministic ground motions for Bethany Alternative sites, memorandum of transmittal to Andrew Finney and Dario Rosidi prepared by Lettis Consultants International dated 1 September 2021.

Wong, I., Thomas, P., Zandieh, A., Lewandowski, N., Smith, S., and Unruh, J., 2021, Seismic hazard analyses and development of conceptual seismic design ground motions for the Delta Conveyance, unpublished final report (Rev 2 dated 1 Sep 2021) prepared by Lettis Consultants International for the Delta Conveyance Design and Construction Office.



Legend

- Hazard site
- Alignment

CGS fault data

- Historic faults
- Holocene faults
- Late Quaternary faults
- Quaternary faults

DCA
DELTA CONVEYANCE DESIGN
& CONSTRUCTION AUTHORITY

**For Illustration
Purposes Only**

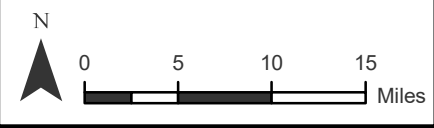
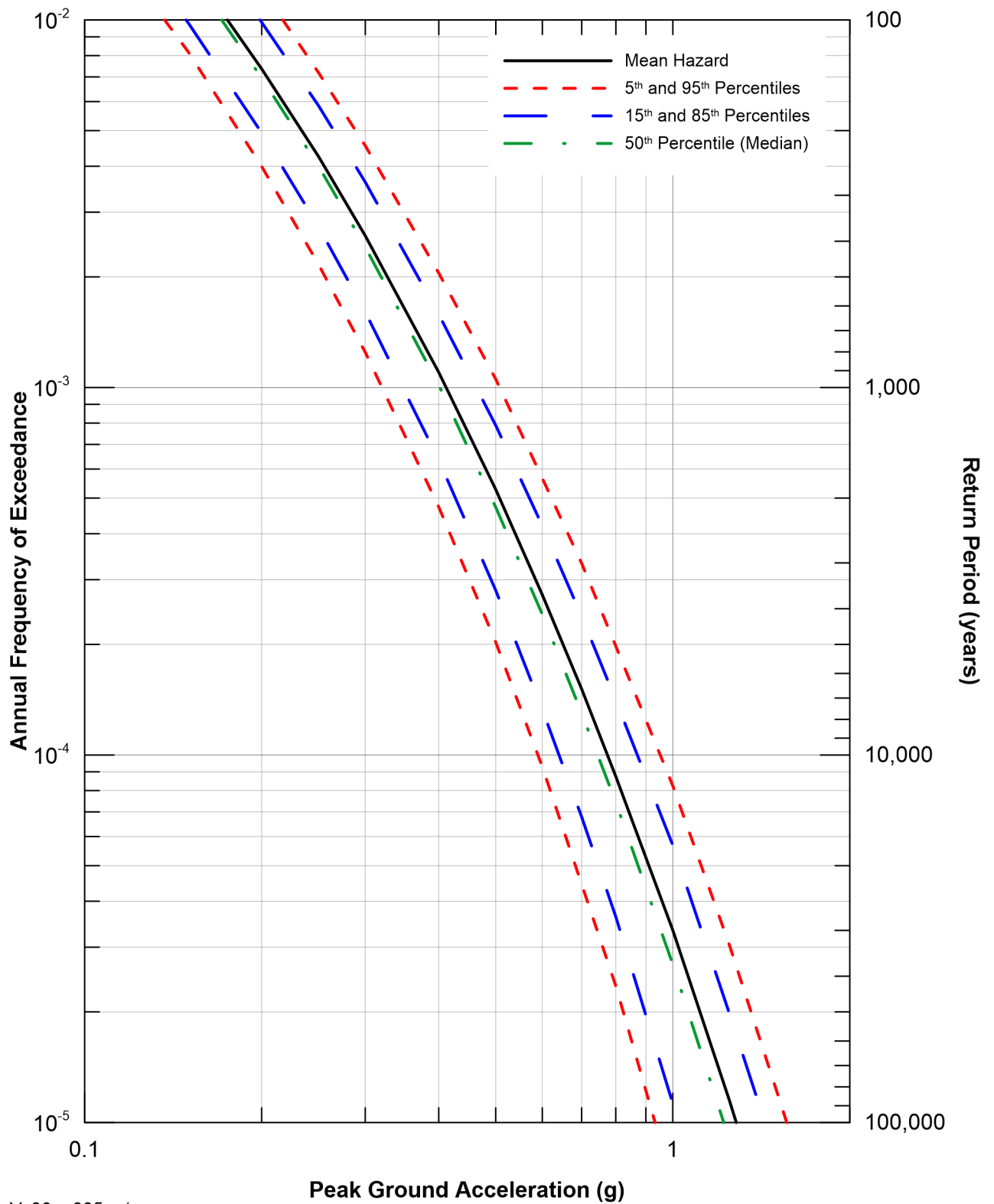
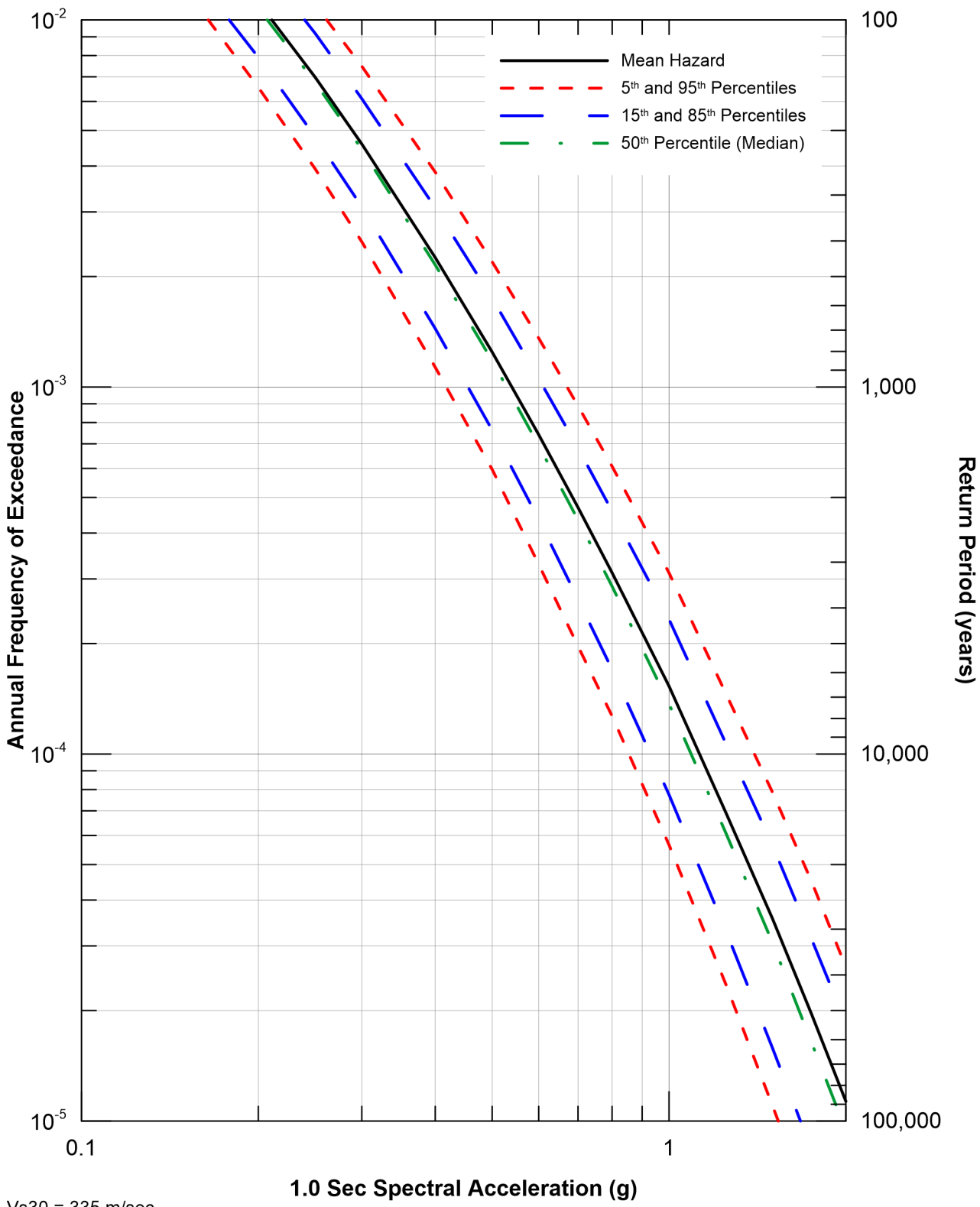


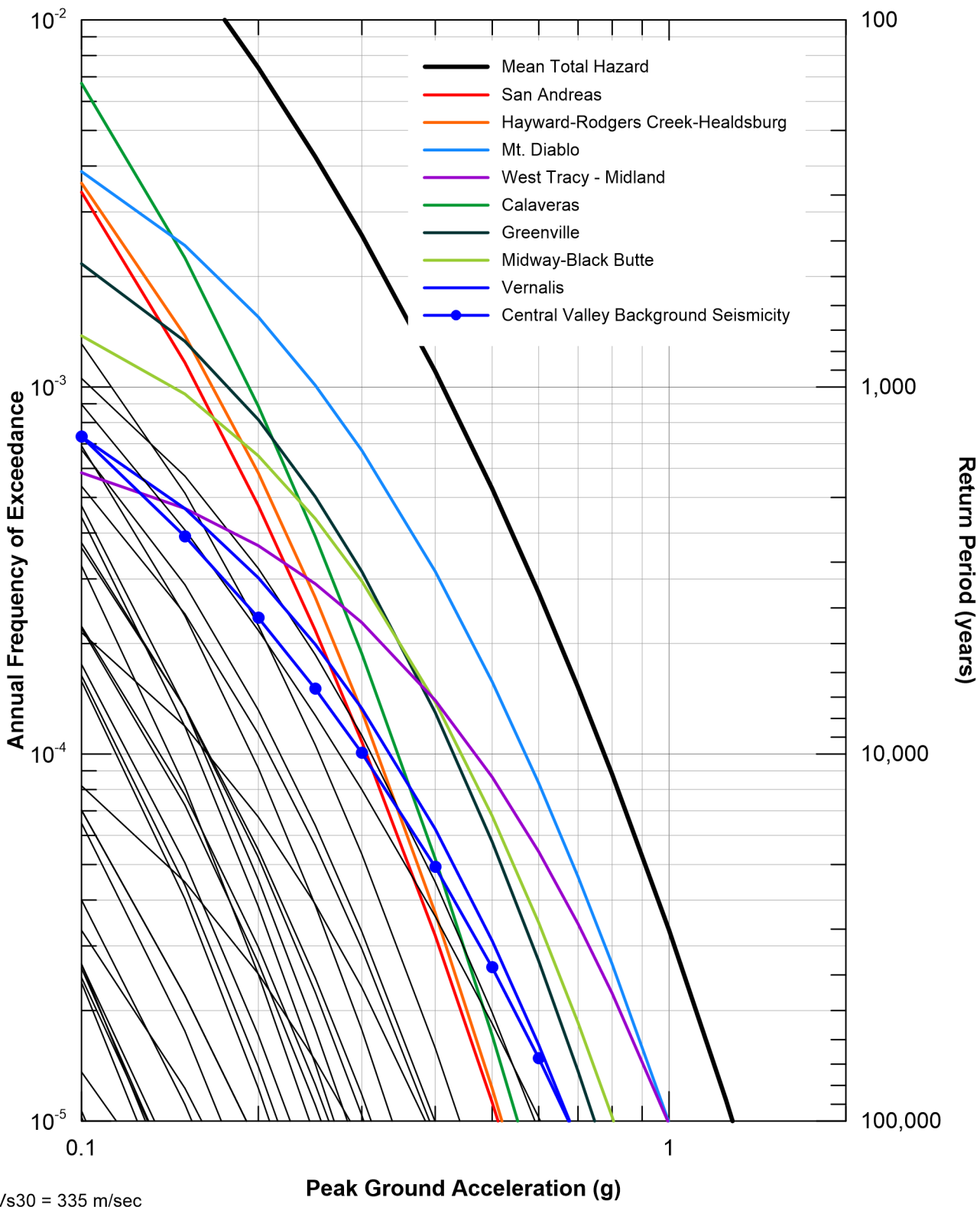
Figure 1
Quaternary Faults in the
San Francisco Bay Region

S:\18102\Figures\18102_002\Figures\Figure_01_alternate_CrossFaults.mxd (Montreux) BD:SNL 2/12/10 09:02

Data Source: DCA, CGS (2005)





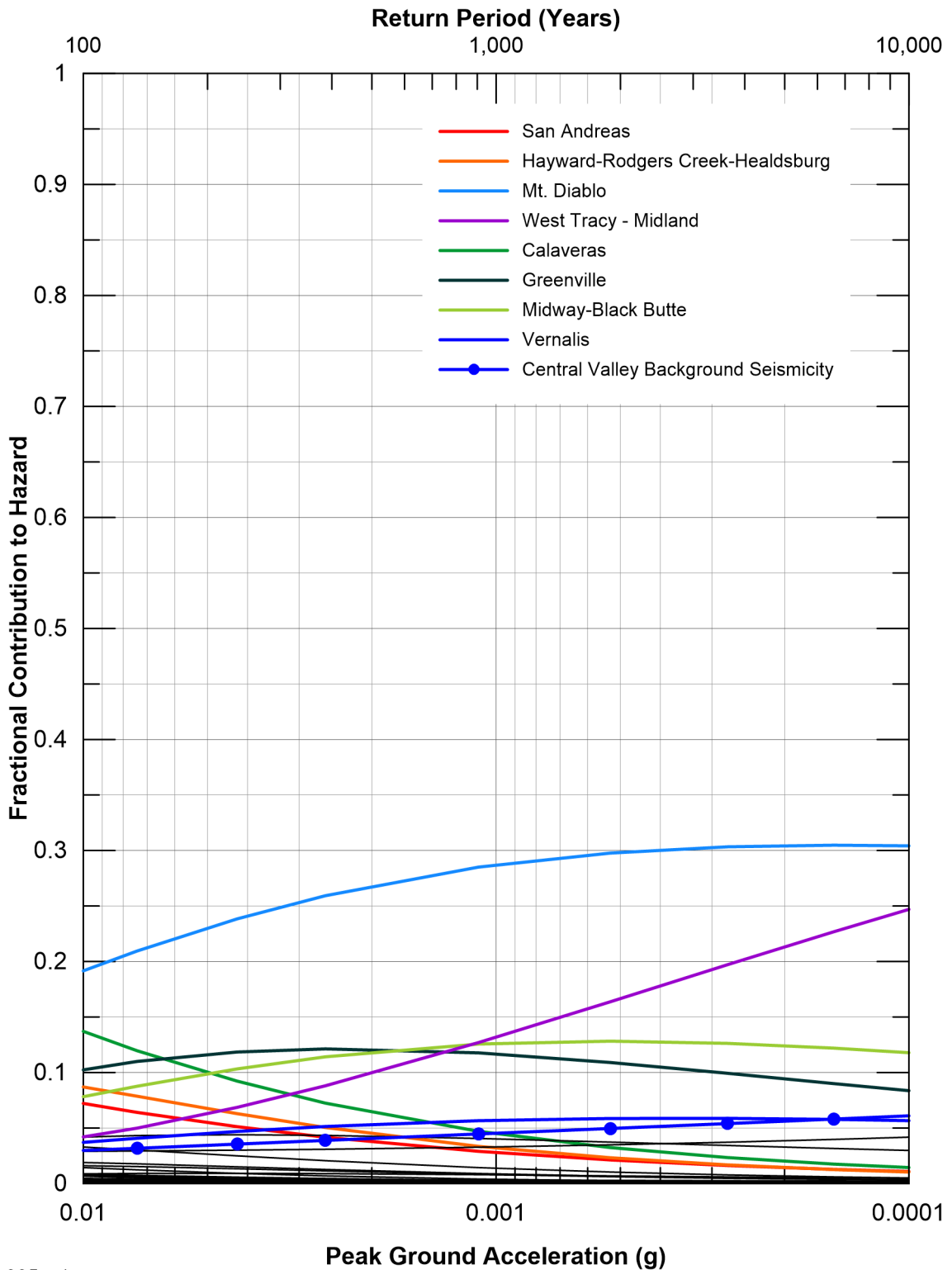


Vs30 = 335 m/sec
 Sources contributing 5% or more in
 144 to 2,475-year return period range listed.
 Other less significant sources shown in black
 not listed.



For Illustration
Purposes Only

Figure 4
 Seismic Source Contributions
 for Mean Peak Horizontal Acceleration
 Hazard for Union Island Shaft

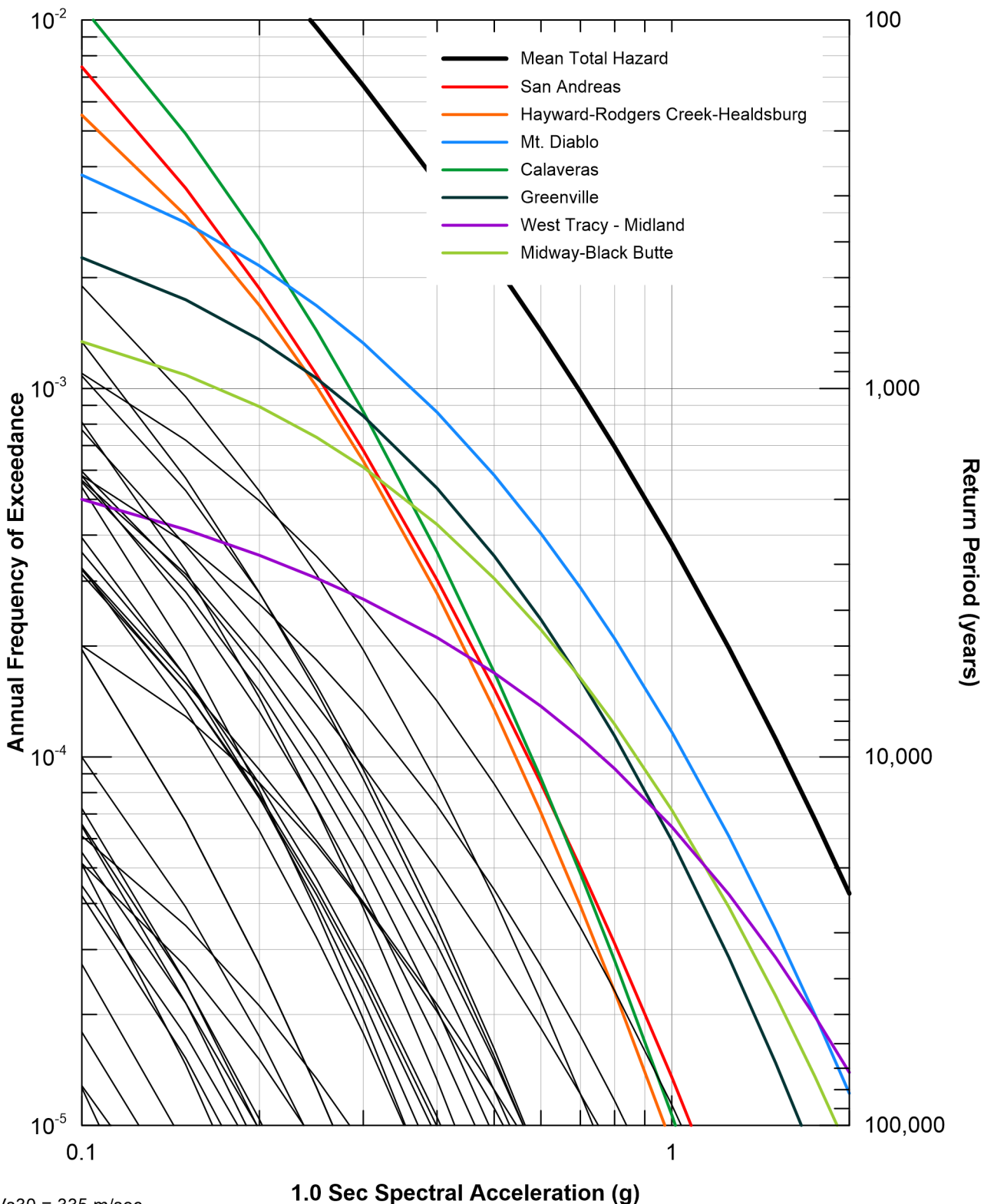


Vs30 = 335 m/sec
 Sources contributing 5% or more in
 144 to 2,475-year return period range listed.
 Other less significant sources shown in black
 not listed.



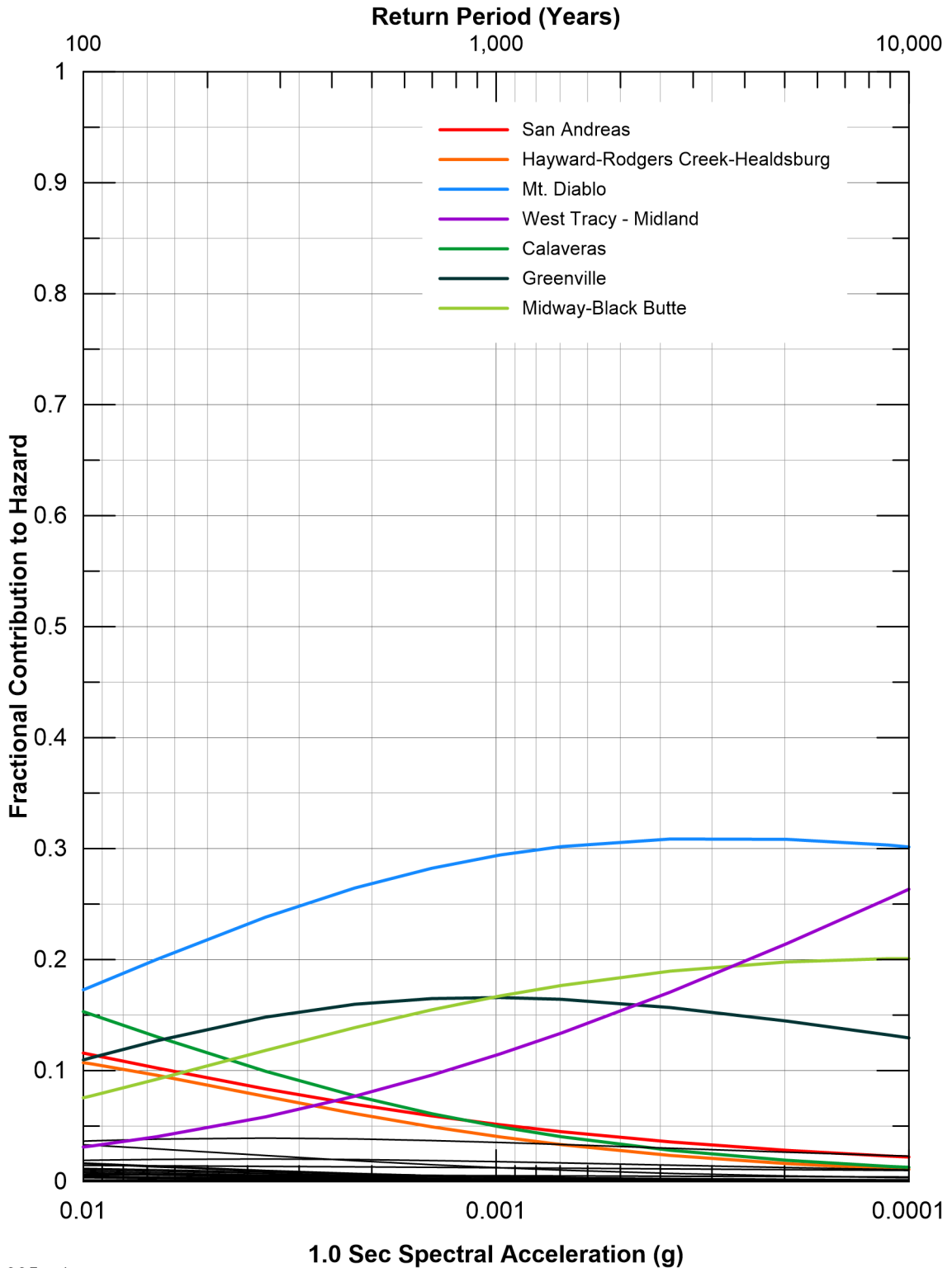
For Illustration
 Purposes Only

Figure 5
 Seismic Source Fractional Contributions
 for Mean Peak Horizontal Acceleration
 Hazard for Union Island Shaft



$V_{s30} = 335 \text{ m/sec}$
 Sources contributing 5% or more in
 144 to 2,475-year return period range listed.
 Other less significant sources shown in black
 not listed.

Figure 6
 Seismic Source Contributions
 for Mean 1.0 Sec Horizontal Spectral
 Acceleration Hazard for
 Union Island Shaft

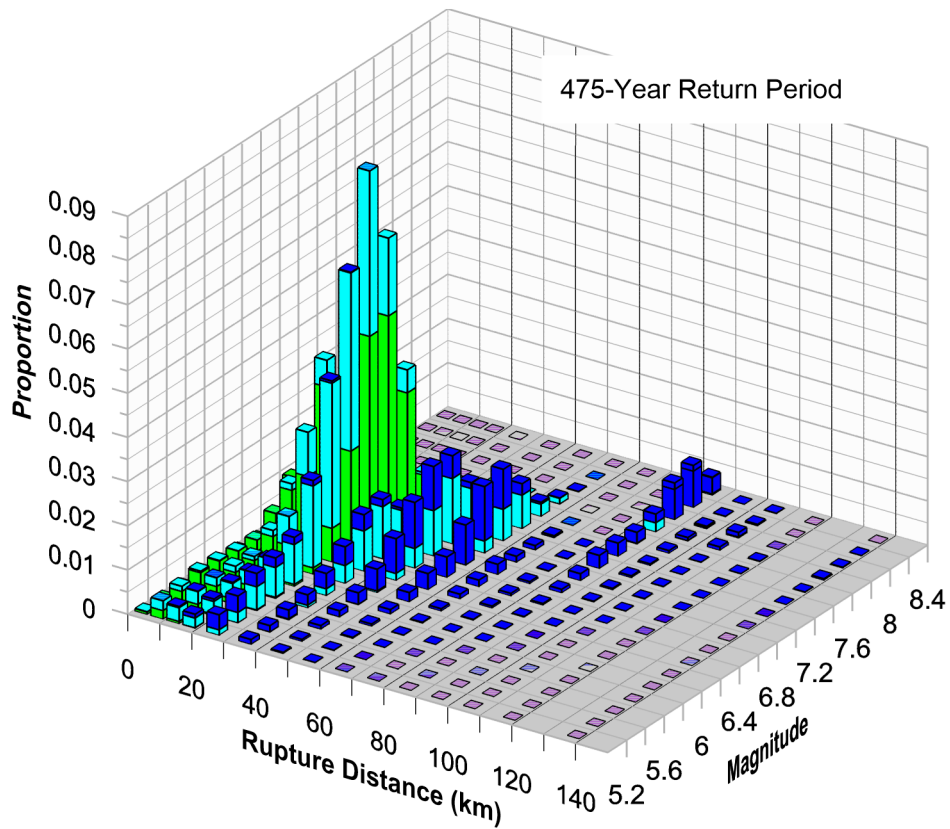


Vs30 = 335 m/sec
 Sources contributing 5% or more in
 144 to 2,475-year return period range listed.
 Other less significant sources shown in black
 not listed.

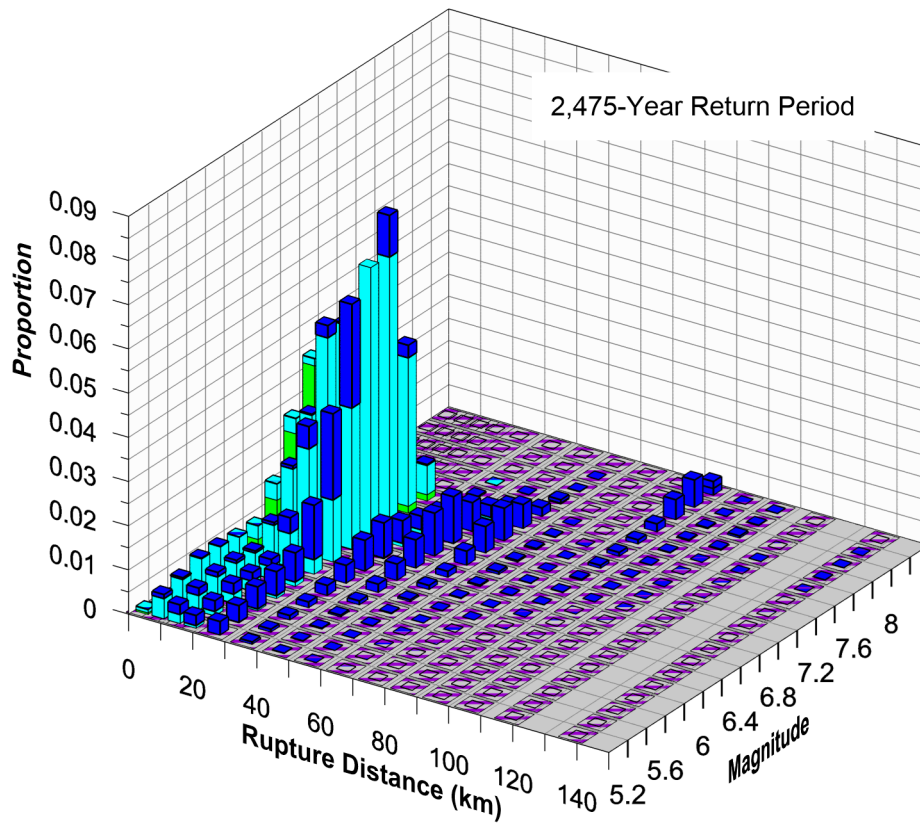


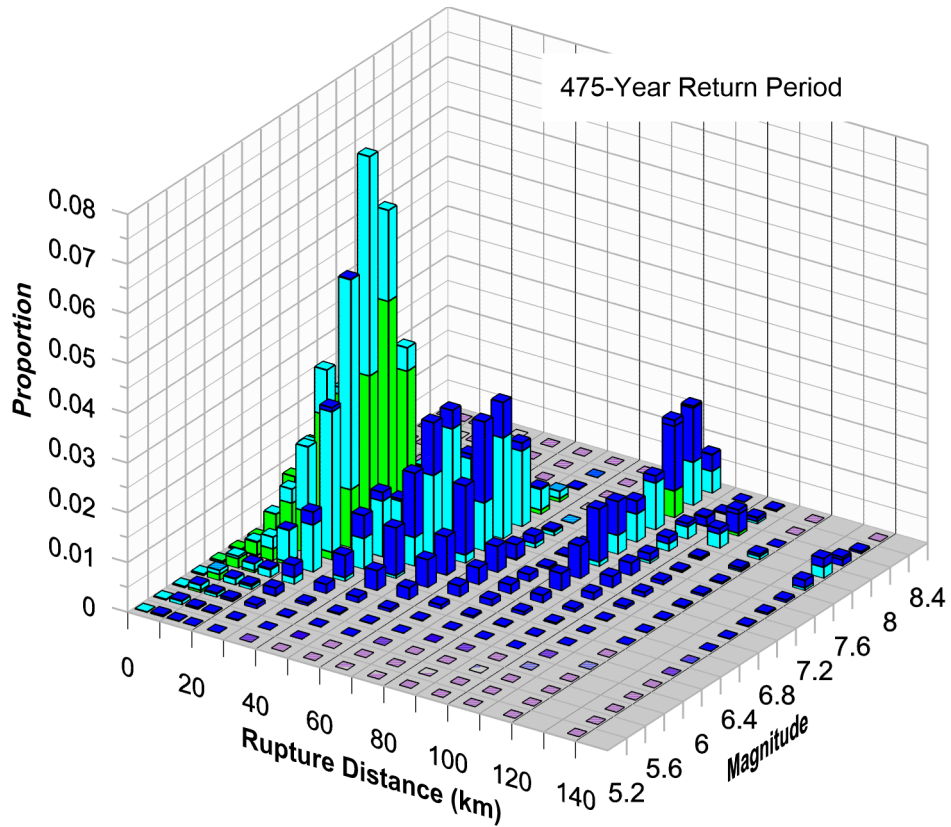
For Illustration
 Purposes Only

Figure 7
 Seismic Source Fractional Contributions
 for Mean 1.0 Sec Horizontal Spectral
 Acceleration Hazard for
 Union Island Shaft

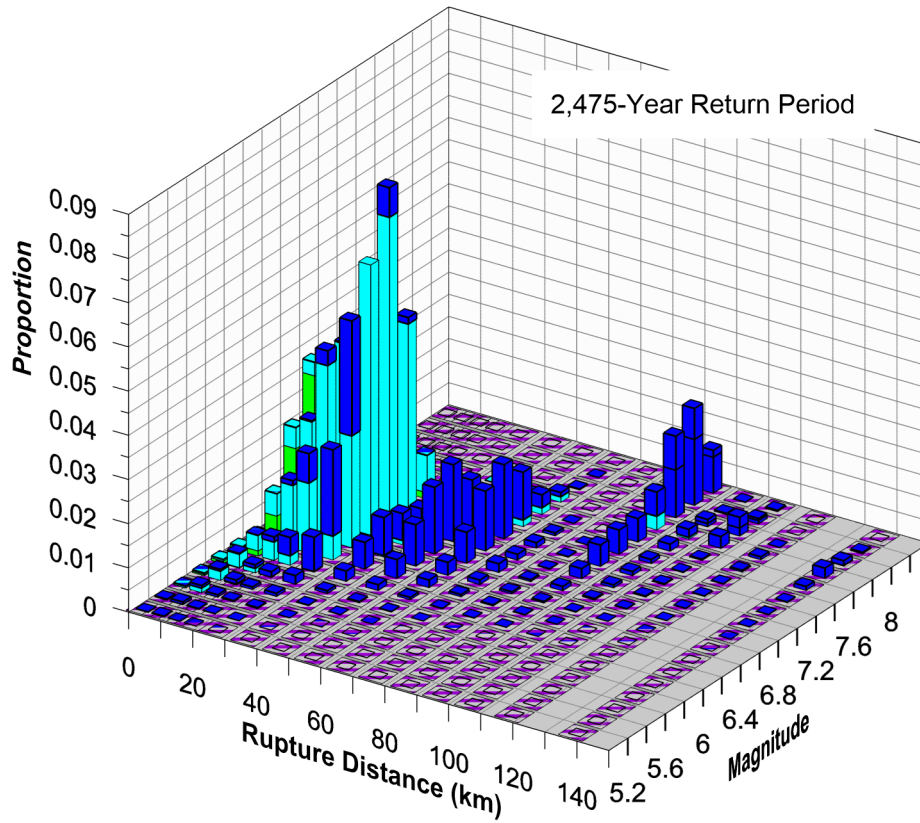


- Epsilon
- 2 to 3
 - 1 to 2
 - 0 to 1
 - 1 to 0
 - 2 to -1
 - < -2



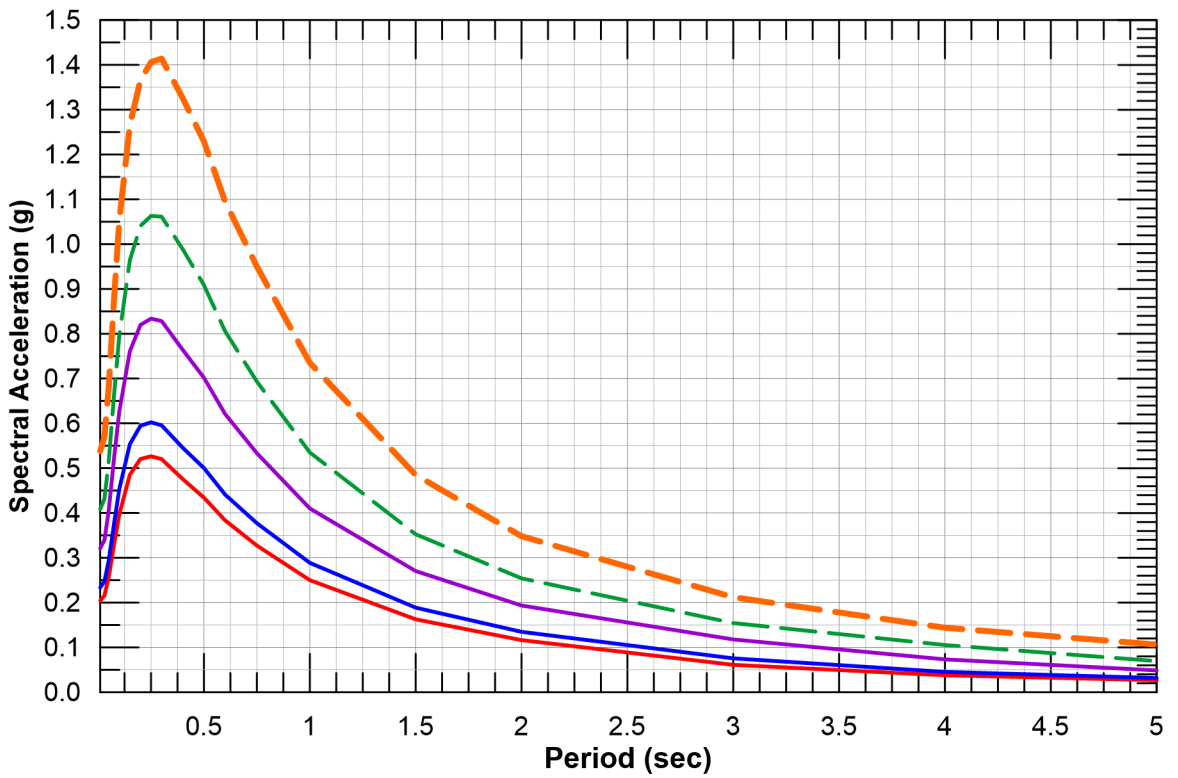
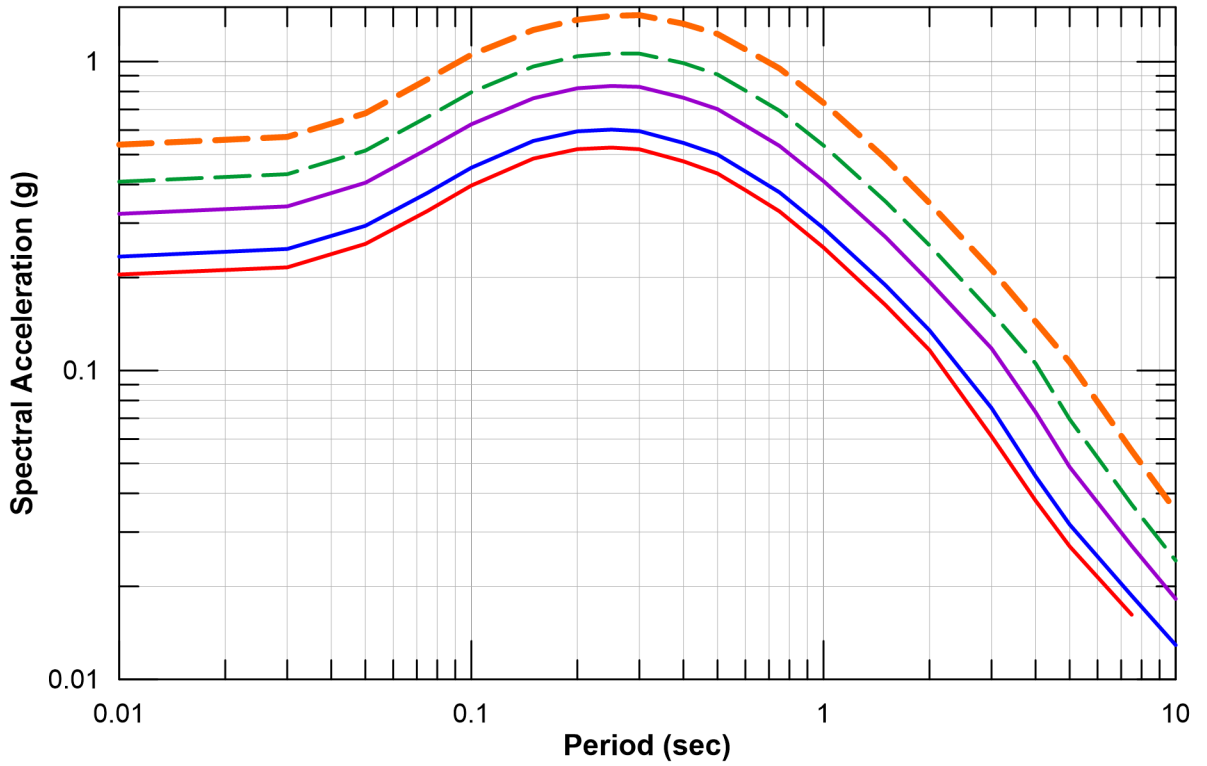


- Epsilon
- 2 to 3
 - 1 to 2
 - 0 to 1
 - -1 to 0
 - -2 to -1
 - < -2



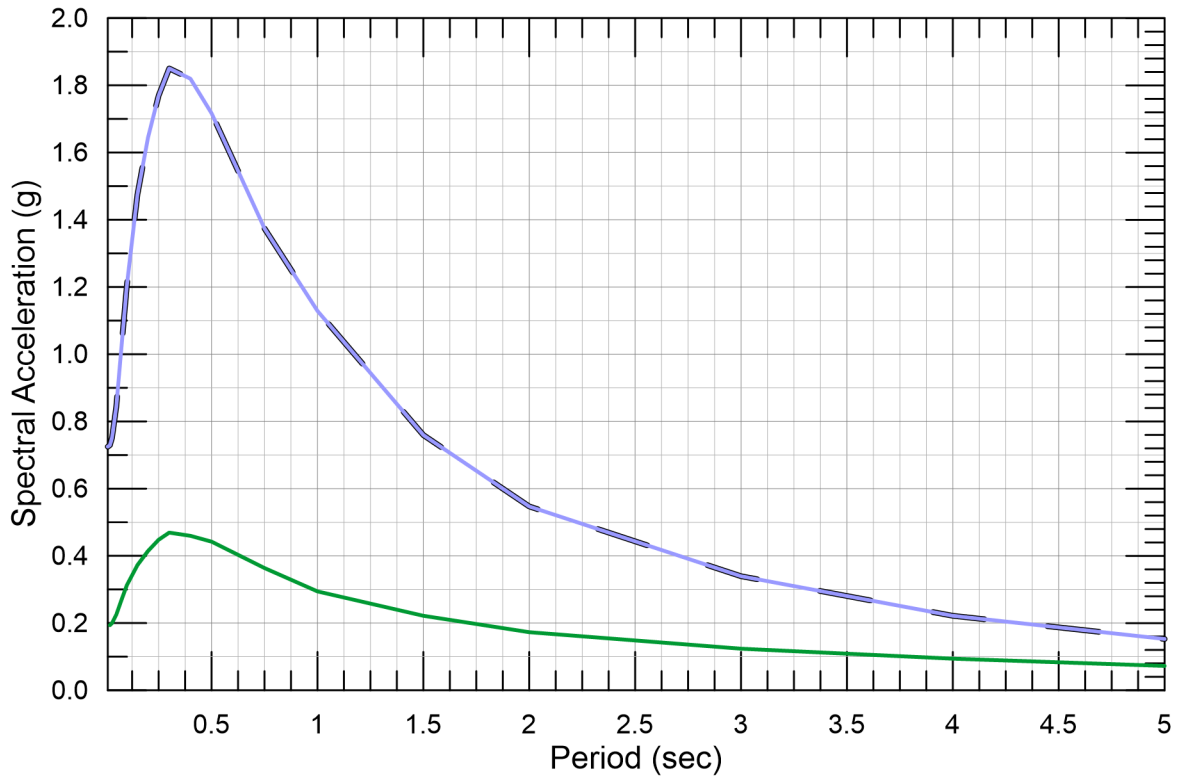
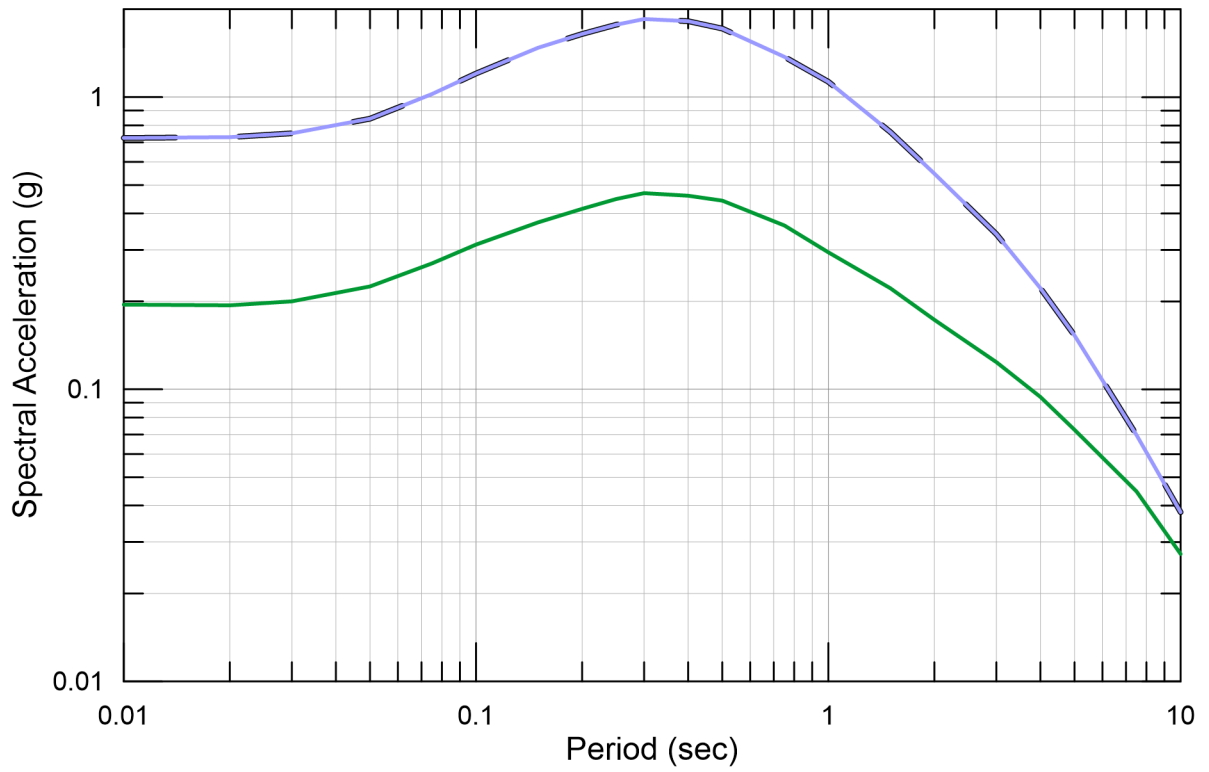
For Illustration
Purposes Only

Figure 9
Magnitude and Distance Contributions
to the Mean 1.0 Sec Spectral Hazard
at 475 and 2,475-Year Return Periods
for Union Island Shaft

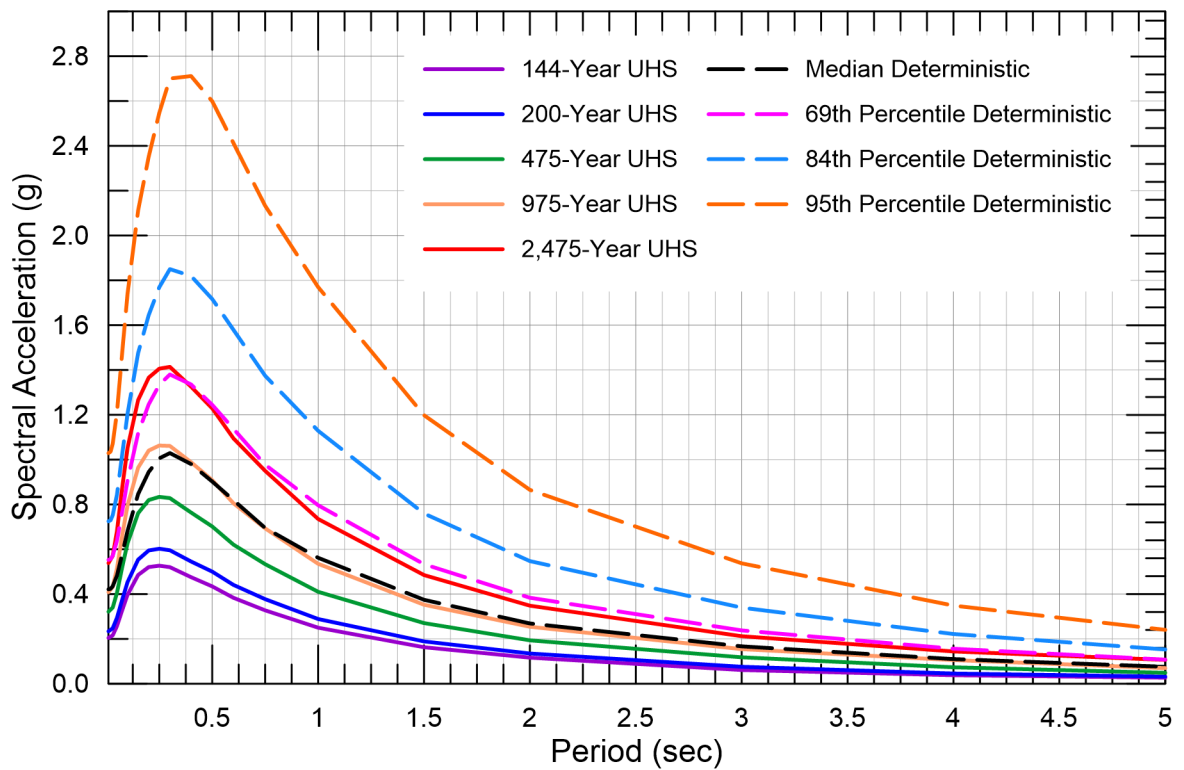
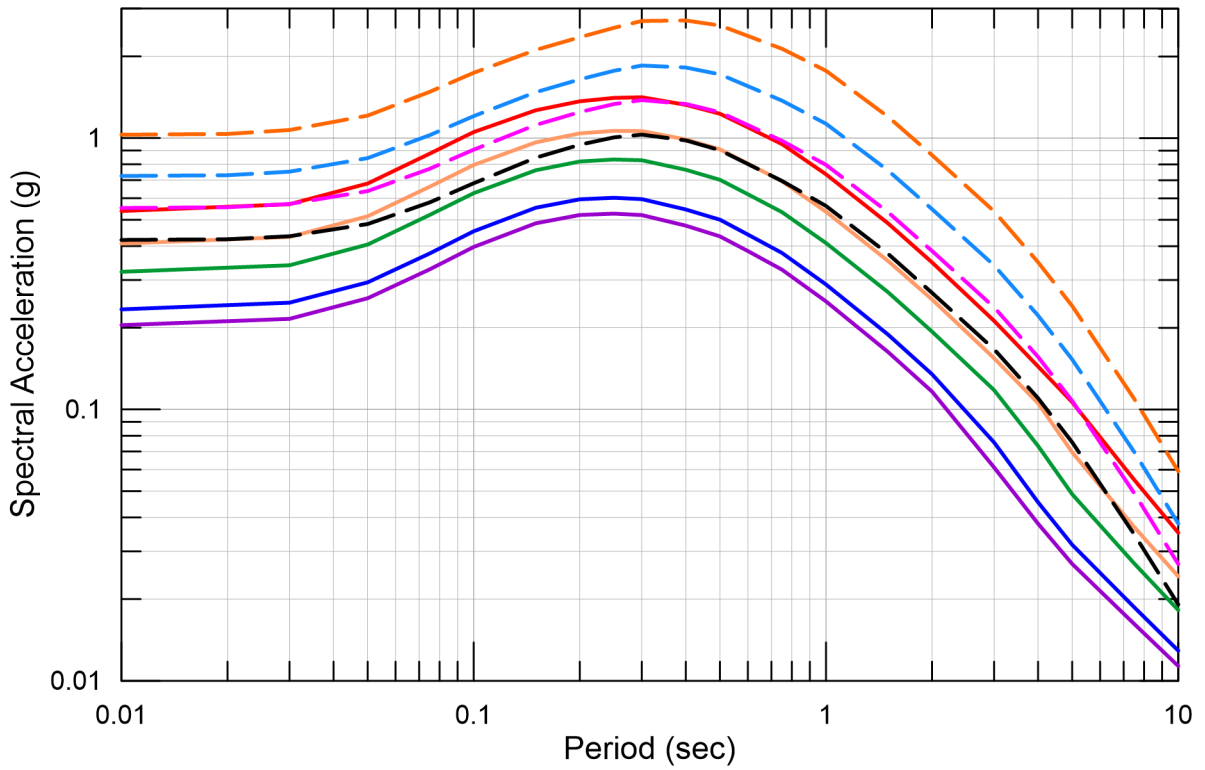


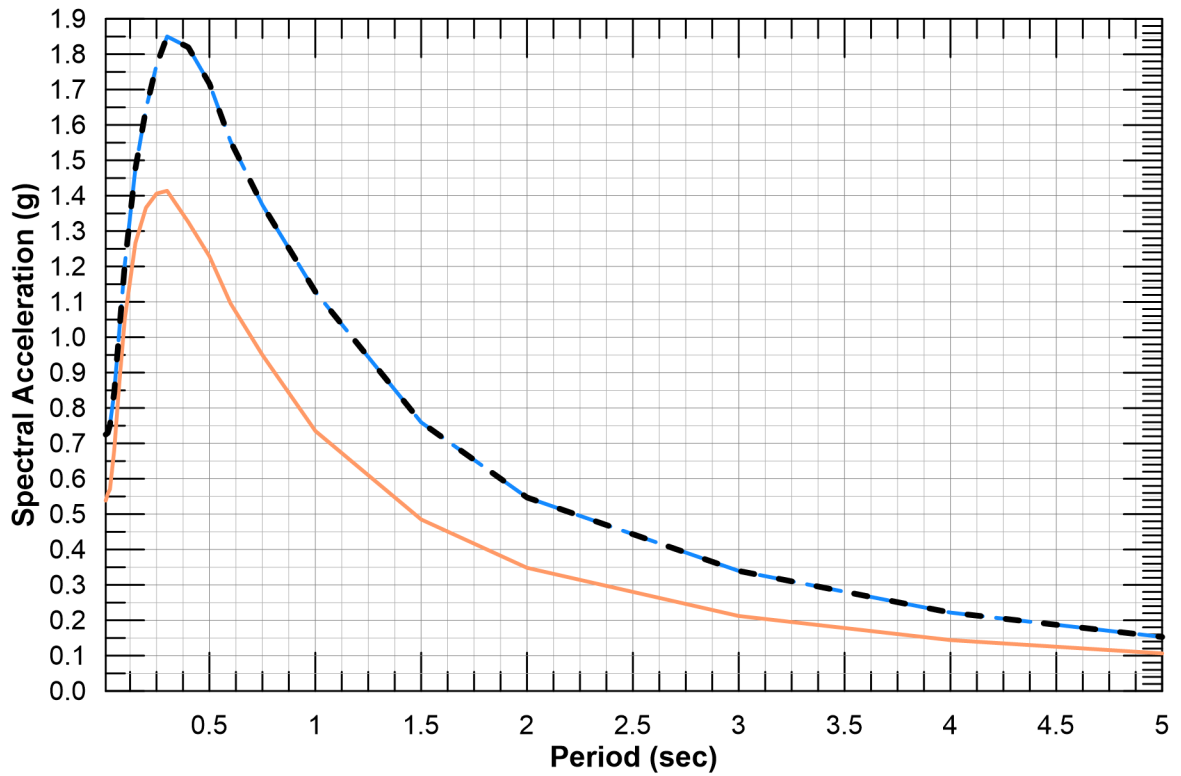
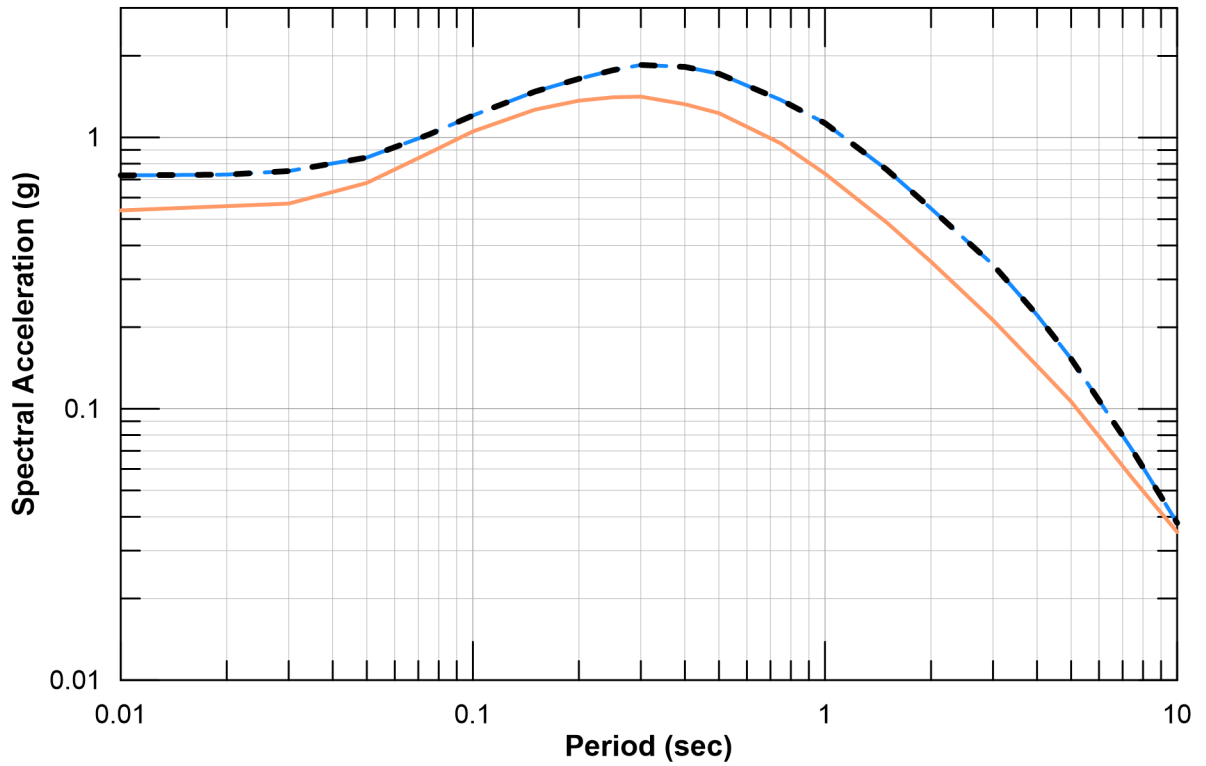
Return Period (years)

— 144 — 200 — 475 — 975 — 2475



- Enveloped 84th Percentile Deterministic
- San Andreas Fault
- West Tracy





- 2,475-Year Uniform Hazard Spectrum
- - - 84th Percentile Deterministic Spectrum
- - - MDE Spectrum

Attachment 2
Development of Design and Maximum Considered
Earthquake (MCE_R) for Bethany Reservoir
Pumping Plant

ATTACHMENT 2
DEVELOPMENT OF DESIGN AND MAXIMUM CONSIDERED EARTHQUAKE (MCE_R)
FOR BETHANY RESERVOIR PUMPING PLANT

Bethany Reservoir Pumping Plant

Seismic Parameters

Seismic Parameters (2019 CBC/ASCE 7-16)	Values
Project site geographic coordinates	37.801°N, 121.575°W
Site Class	D
S _s – Mapped MCE _R spectral acceleration at short periods (g)	1.293
S ₁ – Mapped MCE _R spectral acceleration at 1.0-second period (g)	0.453
F _a – Site coefficient at short periods	1.0
F _v – Site coefficient at 1.0-second period	1.85 ¹
S _{MS} – Site-adjusted MCE _R spectral acceleration at short periods (g)	1.293
S _{M1} – Site-adjusted MCE _R spectral acceleration at 1.0-second period (g)	0.838
S _{DS} – Site-adjusted design spectral acceleration at short periods (g)	0.862
S _{D1} – Site-adjusted design spectral acceleration at 1.0-second period (g)	0.559
T ₀ = 0.2 (S _{D1} /S _{DS}) (sec)	0.130
T _s = S _{D1} /S _{DS} (sec)	0.648
T _L – Long-period transition period (sec)	8

Notes:

°N = degrees North; °W = degrees West; g = acceleration caused by gravity

¹: Assume Exception #2 of Section 11.4.8 (ASCE 7-16) applies, so no site-specific ground motion hazard analysis is required.

Site-adjusted Design and MCE_R Response Spectra

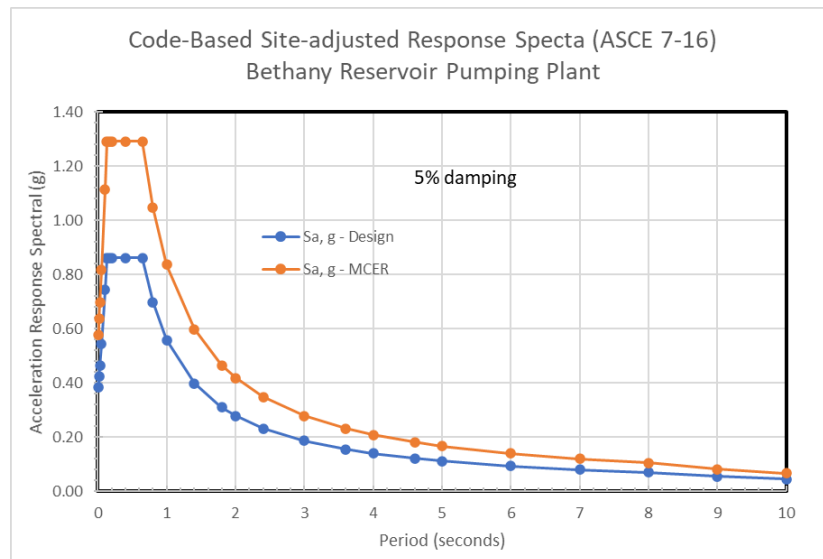


Figure A4-1. Site-adjusted Design and MCE_R Response Spectra for Bethany Reservoir Pumping Plant

Attachment 3
DEEPSOIL Model Calibrations

Soil Profile Definition

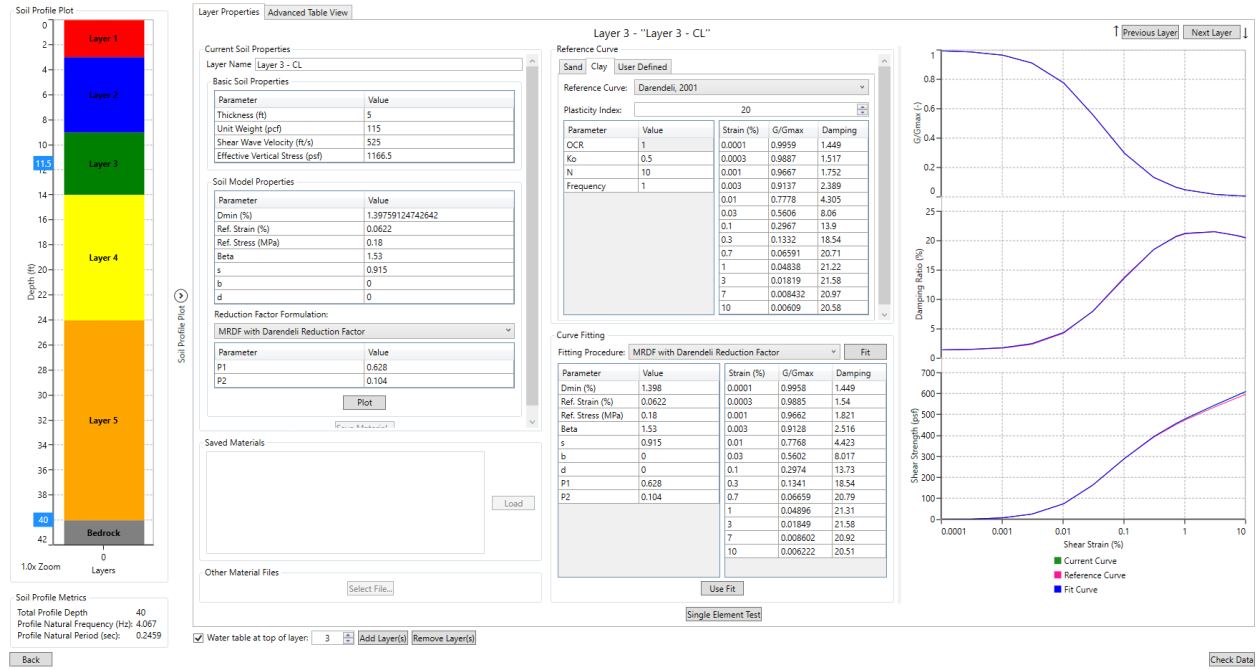


Figure A3-1. Representative Fine-Grained Layer Properties at the Bethany Reservoir Pumping Plant Facility Site

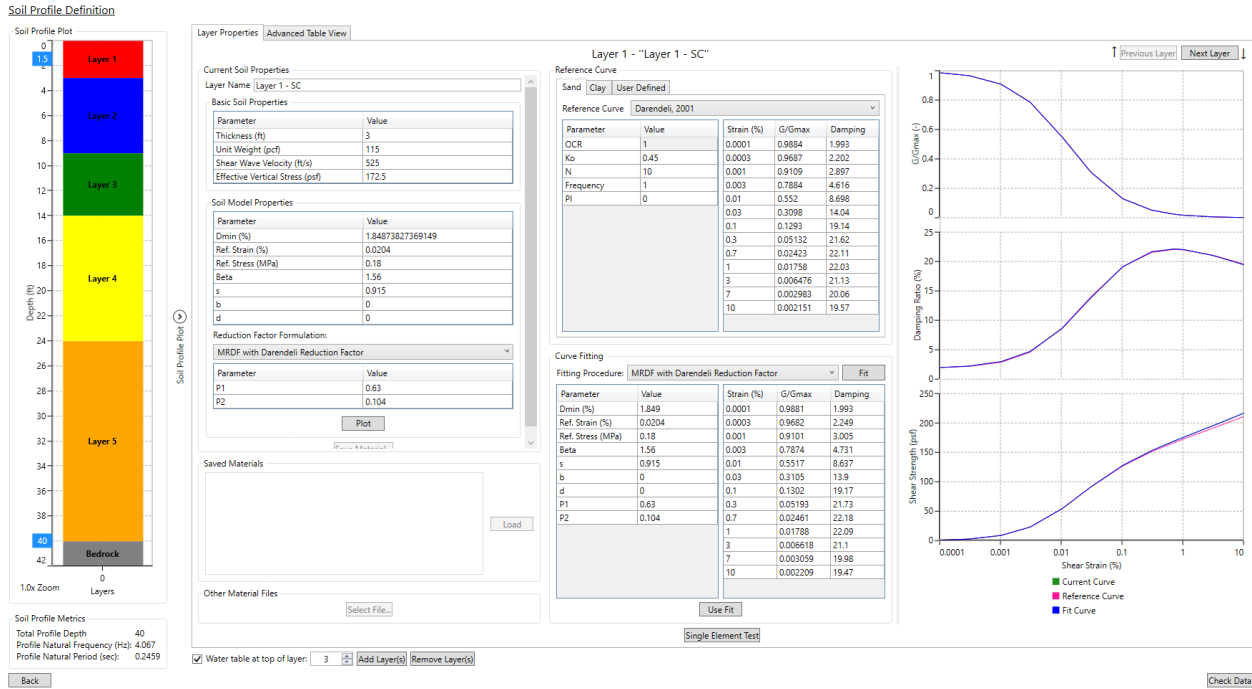


Figure A3-2. Representative Coarse-Grained Layer Properties at the Bethany Reservoir Pumping Plant Facility Site

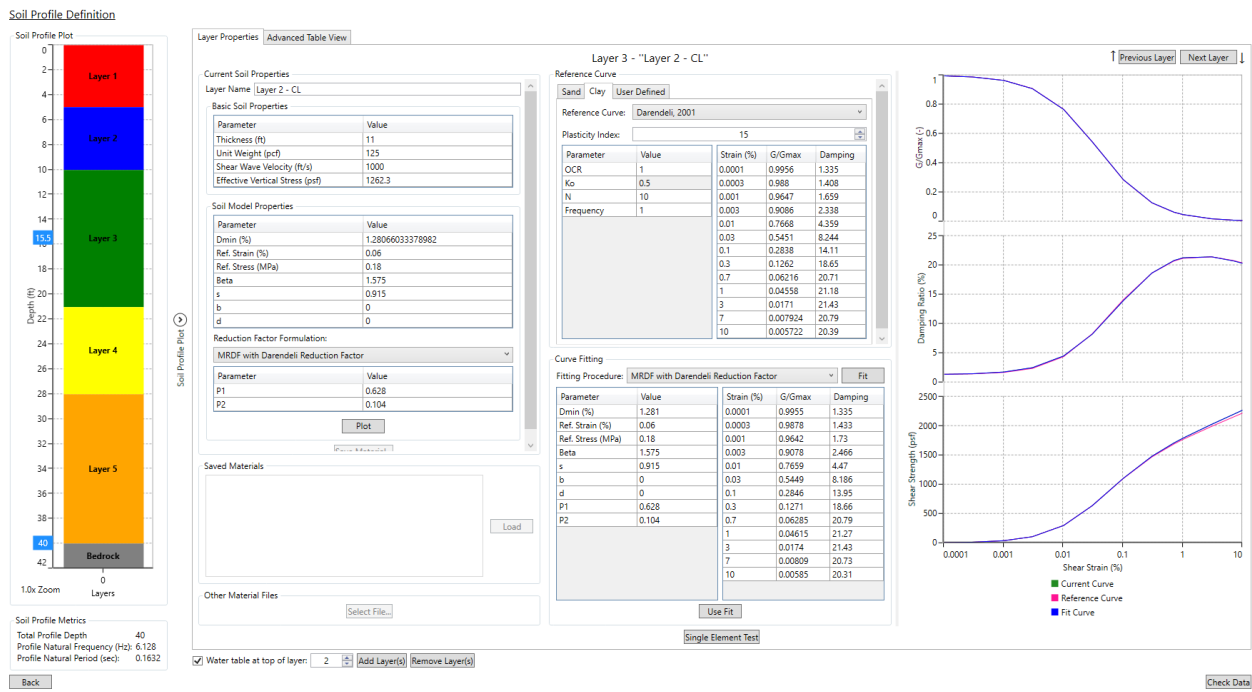


Figure A3-3. Representative Fine-Grained Layer Properties at the Canal Ranch Tract Facility Site

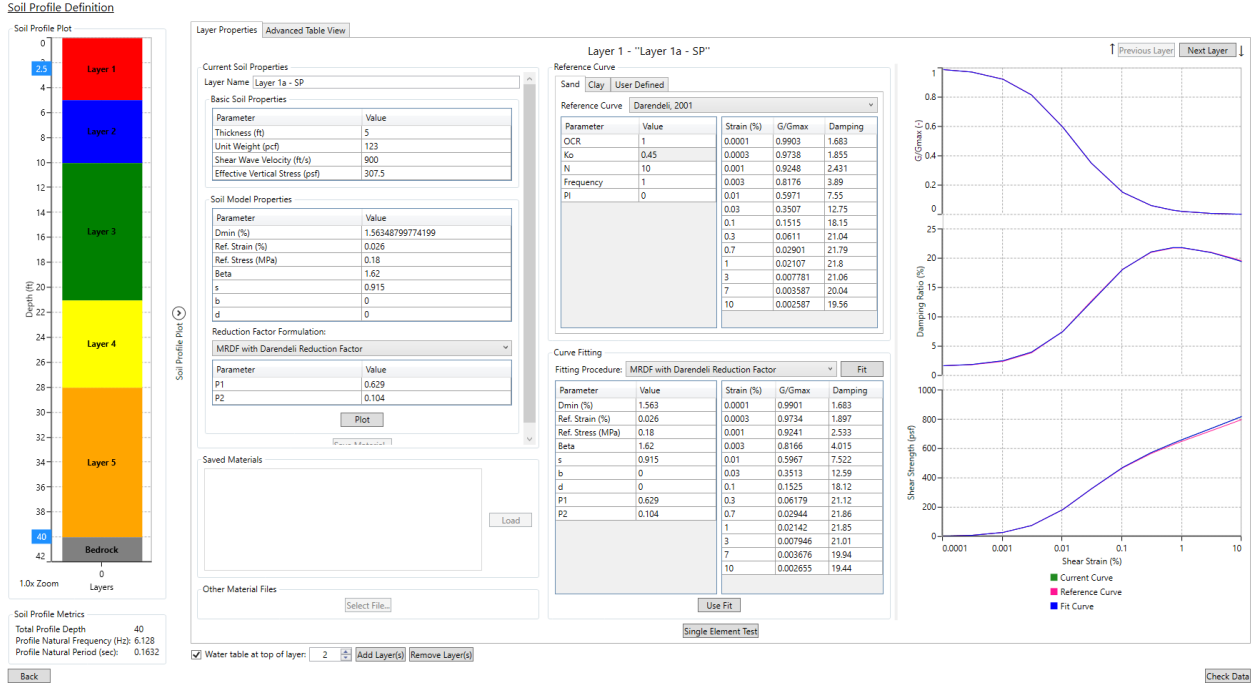


Figure A3-4. Representative Coarse-Grained Layer Properties at the Canal Ranch Tract Facility Site

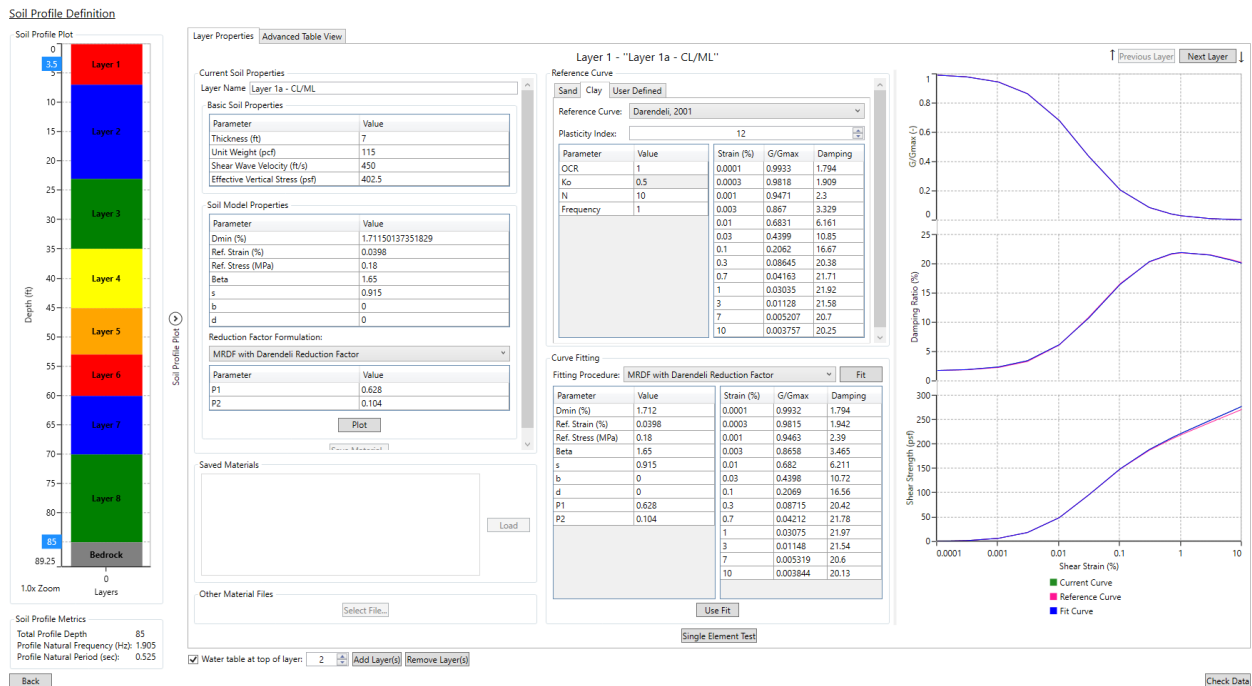


Figure A3-5. Representative Fine-Grained Layer Properties at the Intake 3 Facility Site

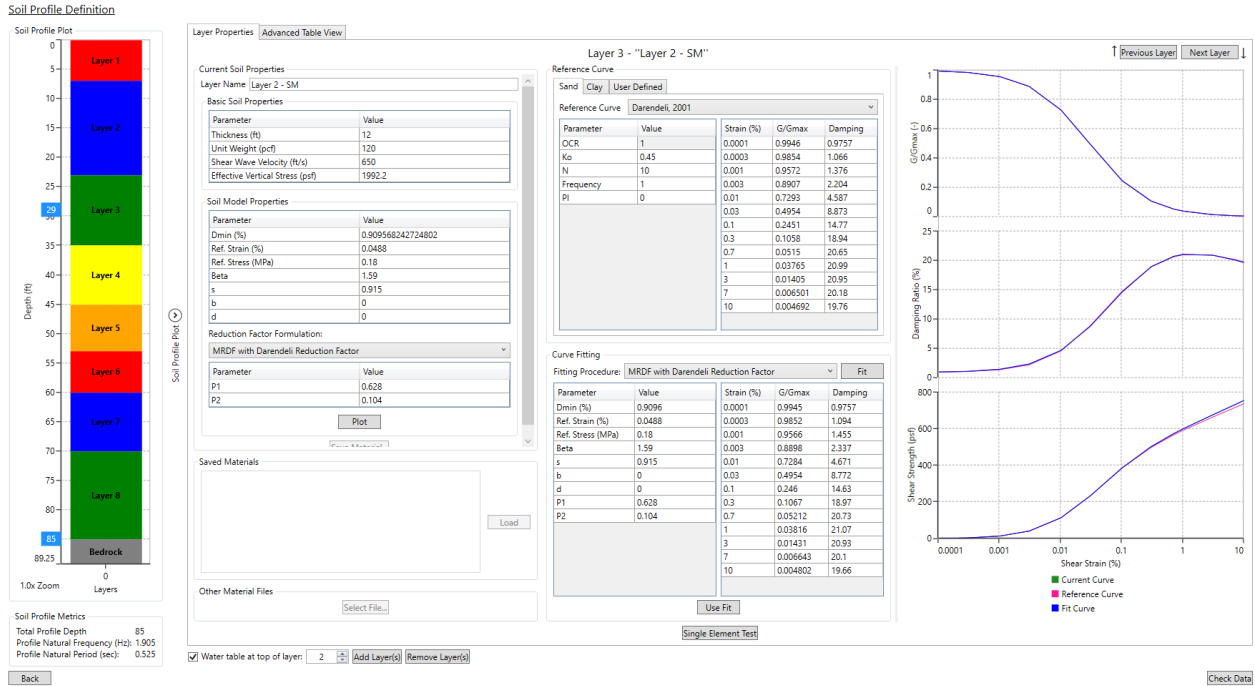


Figure A3-6. Representative Coarse-Grained Layer Properties at the Intake 3 Facility Site

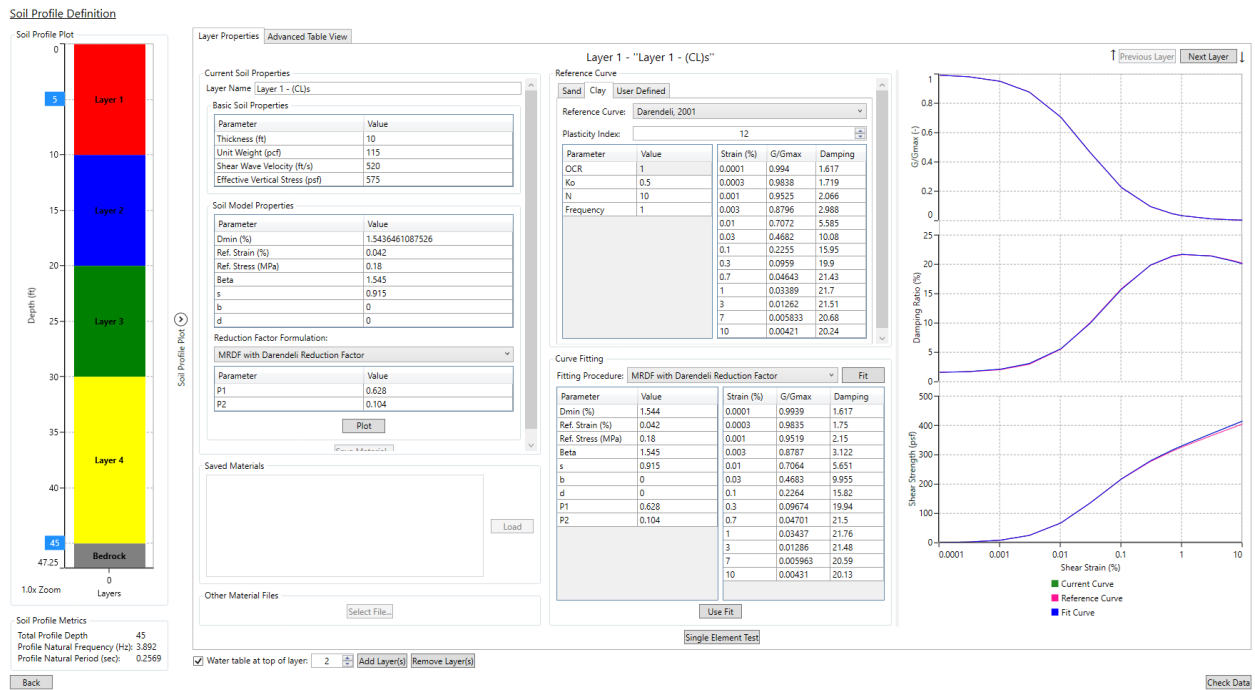


Figure A3-7. Representative Fine-Grained Layer Properties at the Intake 5 Facility Site

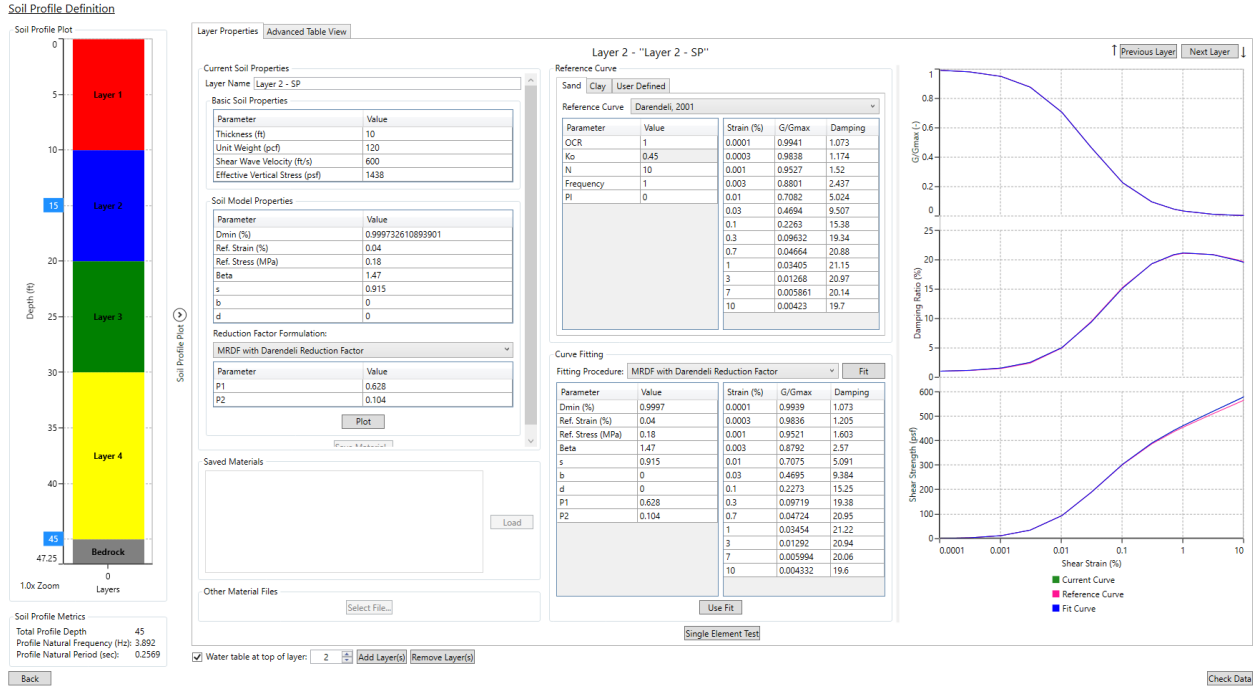


Figure A3-8. Representative Coarse-Grained Layer Properties at the Intake 5 Facility Site

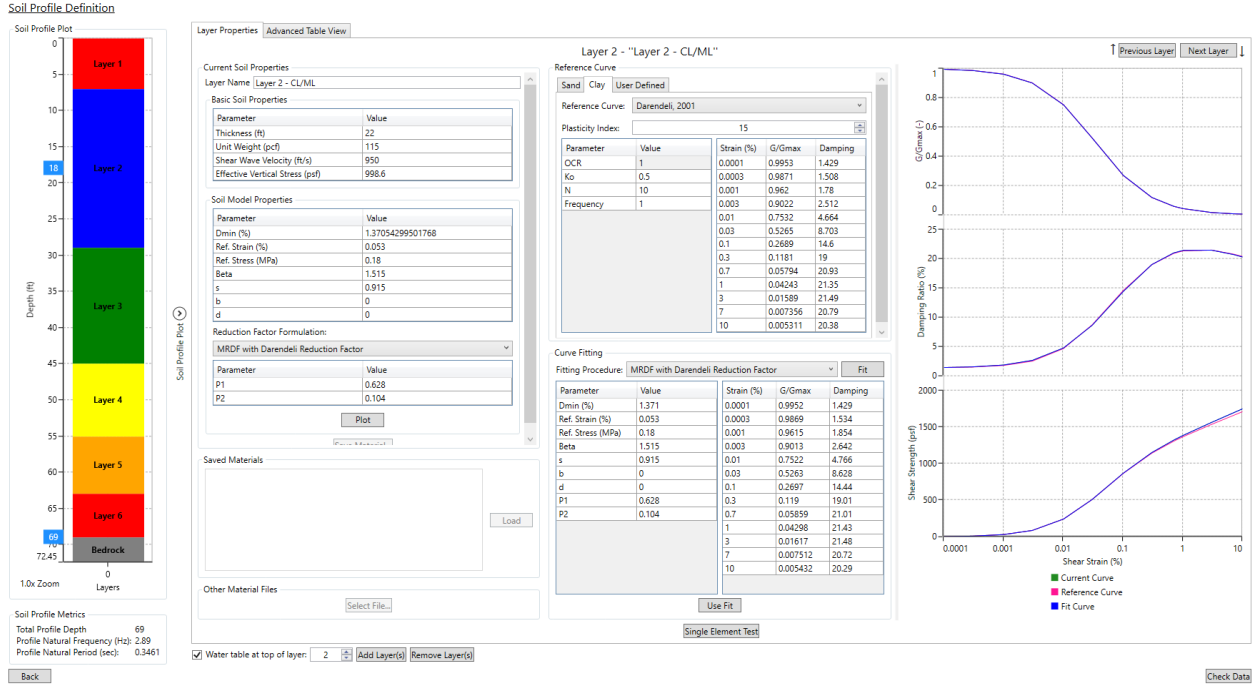


Figure A3-9. Representative Fine-Grained Layer Properties at the King Island Facility Site

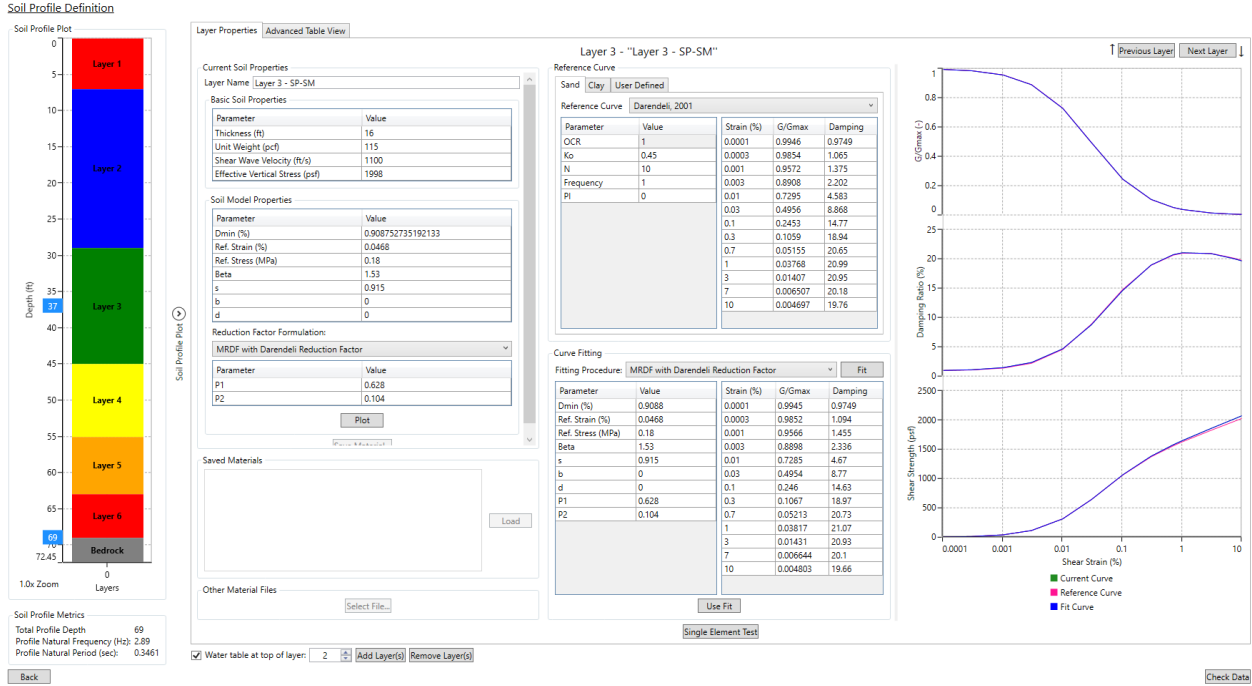


Figure A3-10. Representative Coarse-Grained Layer Properties at the King Island Facility Site

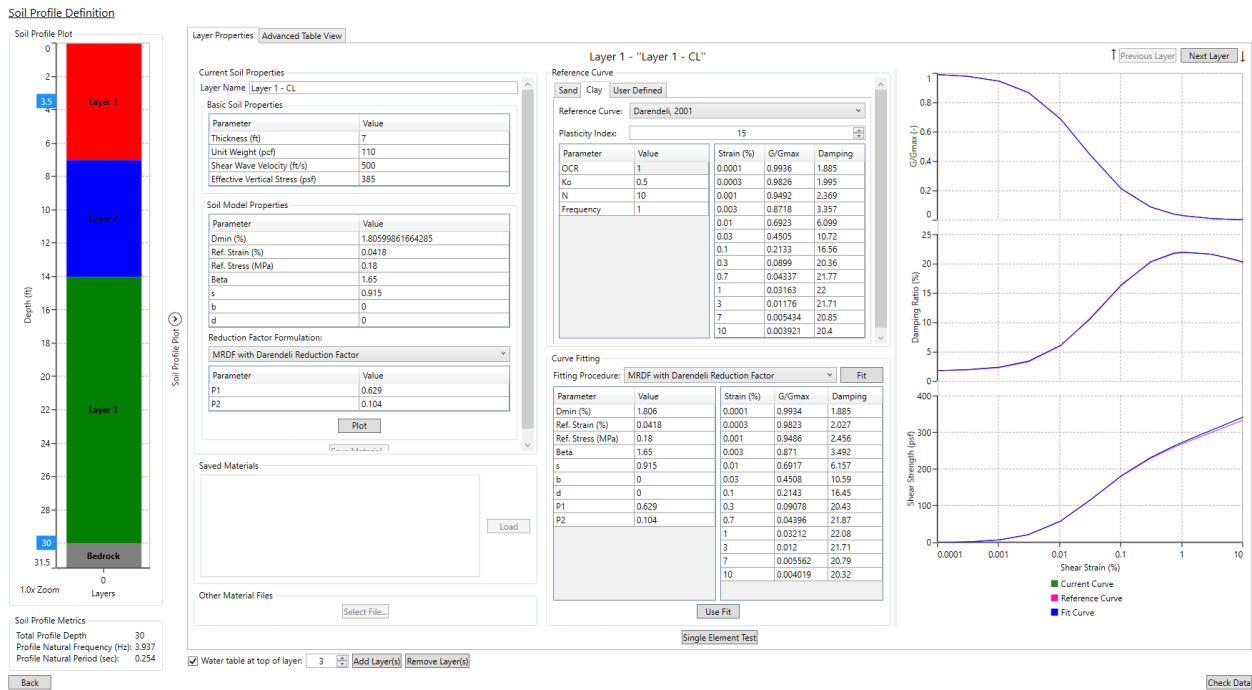


Figure A3-11. Representative Fine-Grained Layer Properties at the Lower Roberts Island Facility Site

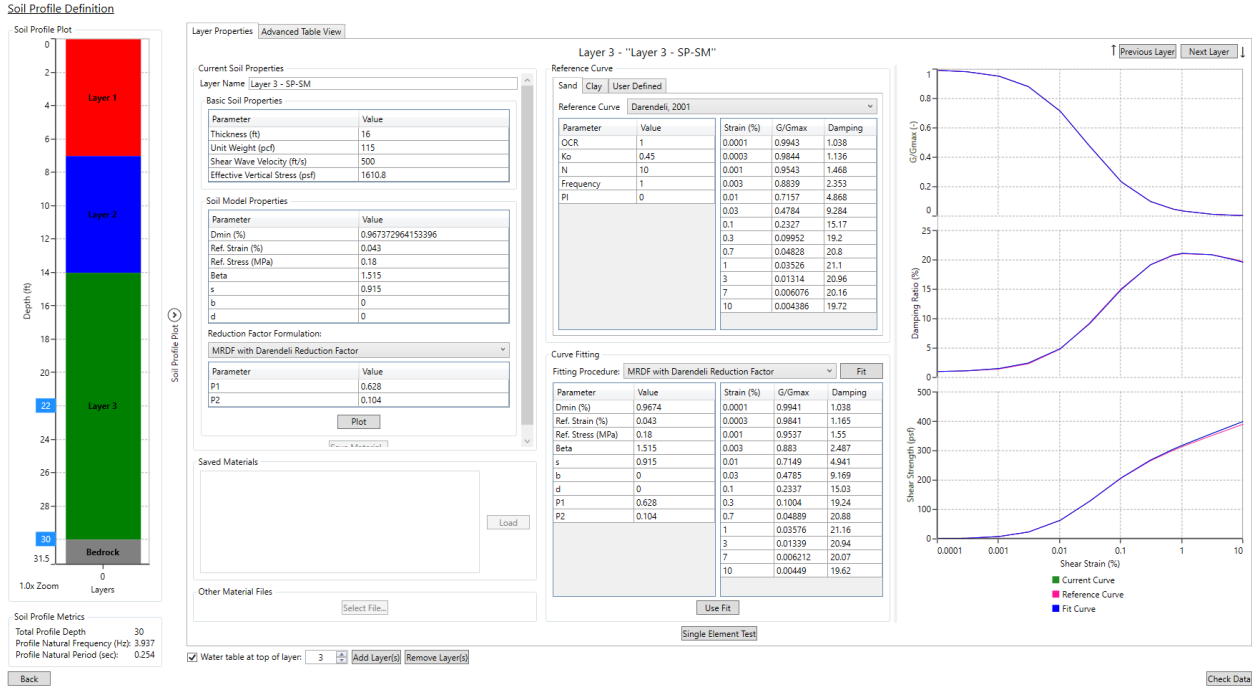


Figure A3-12. Representative Coarse-Grained Layer Properties at the Lower Roberts Island Facility Site

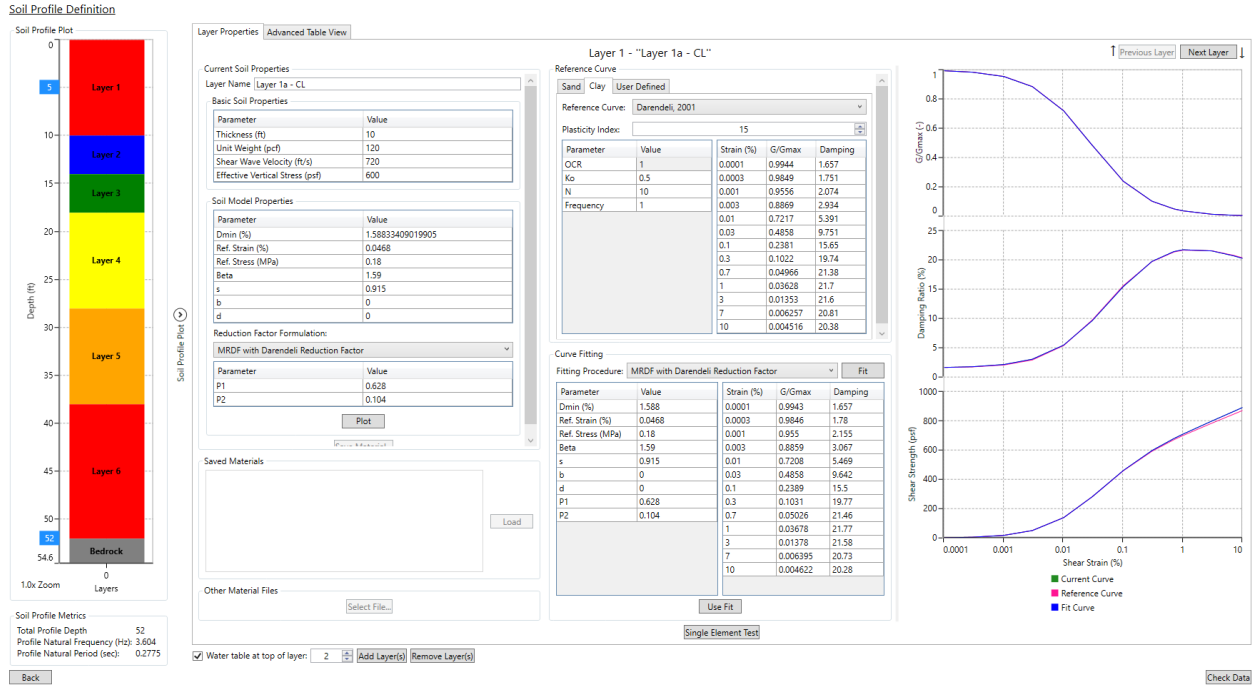


Figure A3-13. Representative Fine-Grained Layer Properties at the New Hope Tract Facility Site

Soil Profile Definition

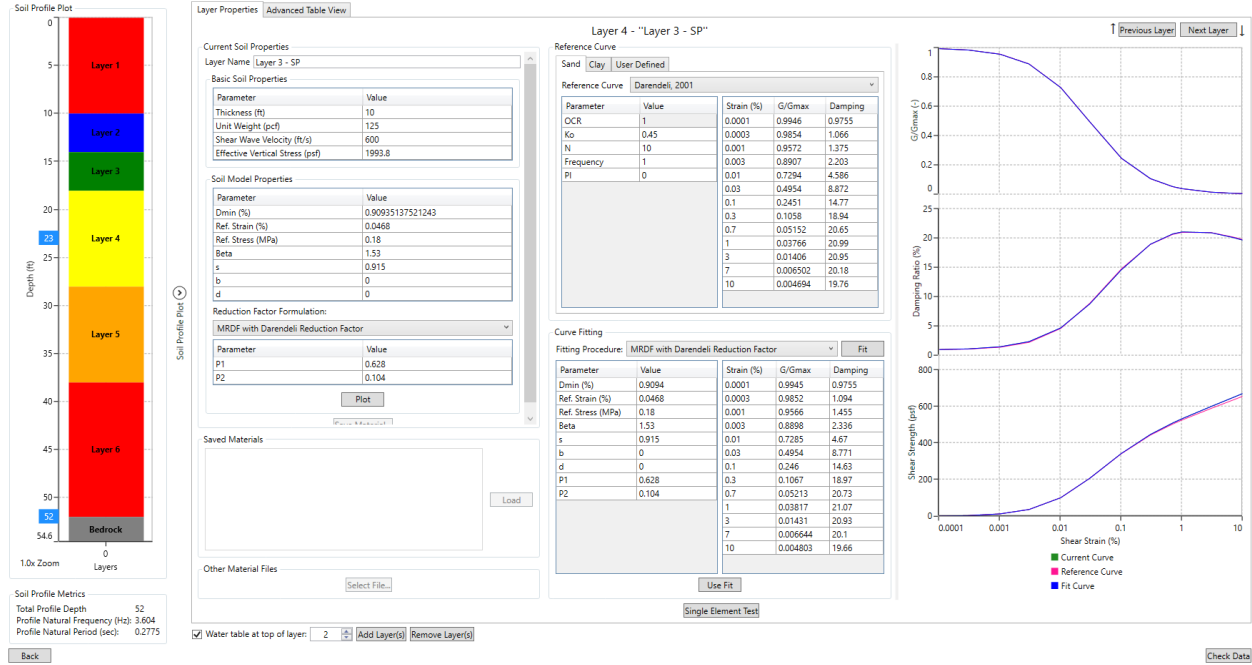


Figure A3-14. Representative Coarse-Grained Layer Properties at the New Hope Tract Facility Site

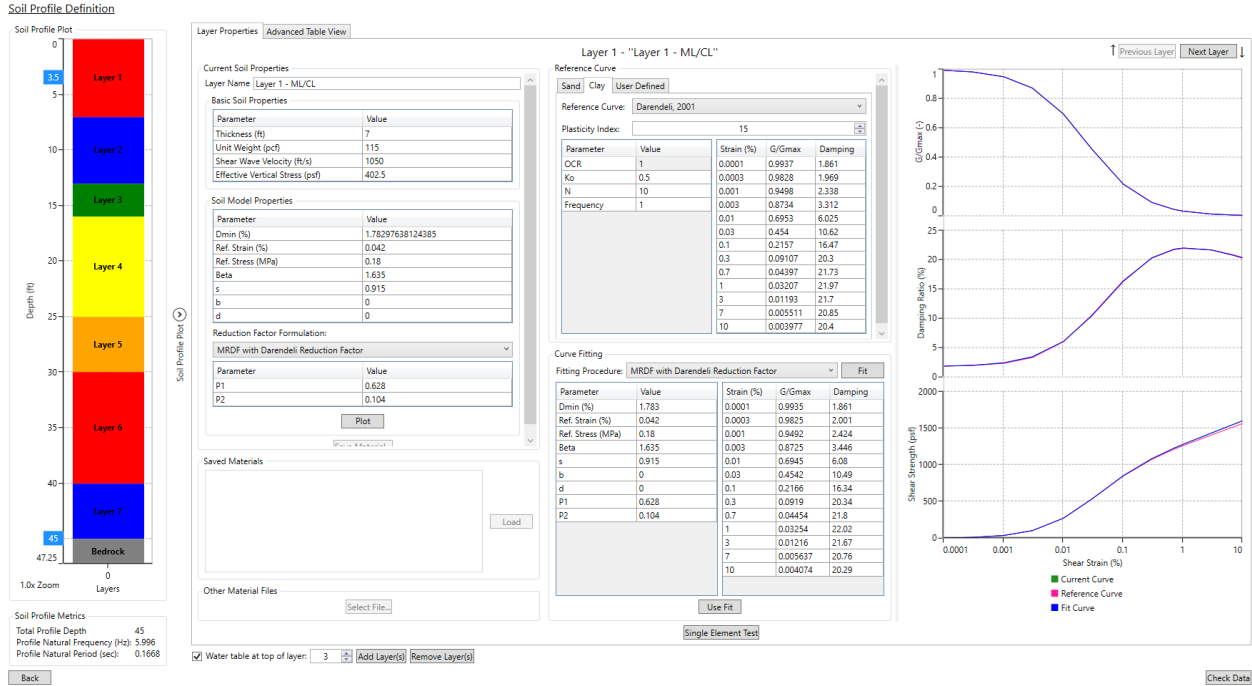


Figure A3-15. Representative Fine-Grained Layer Properties at the Twin Cities Road Facility Site

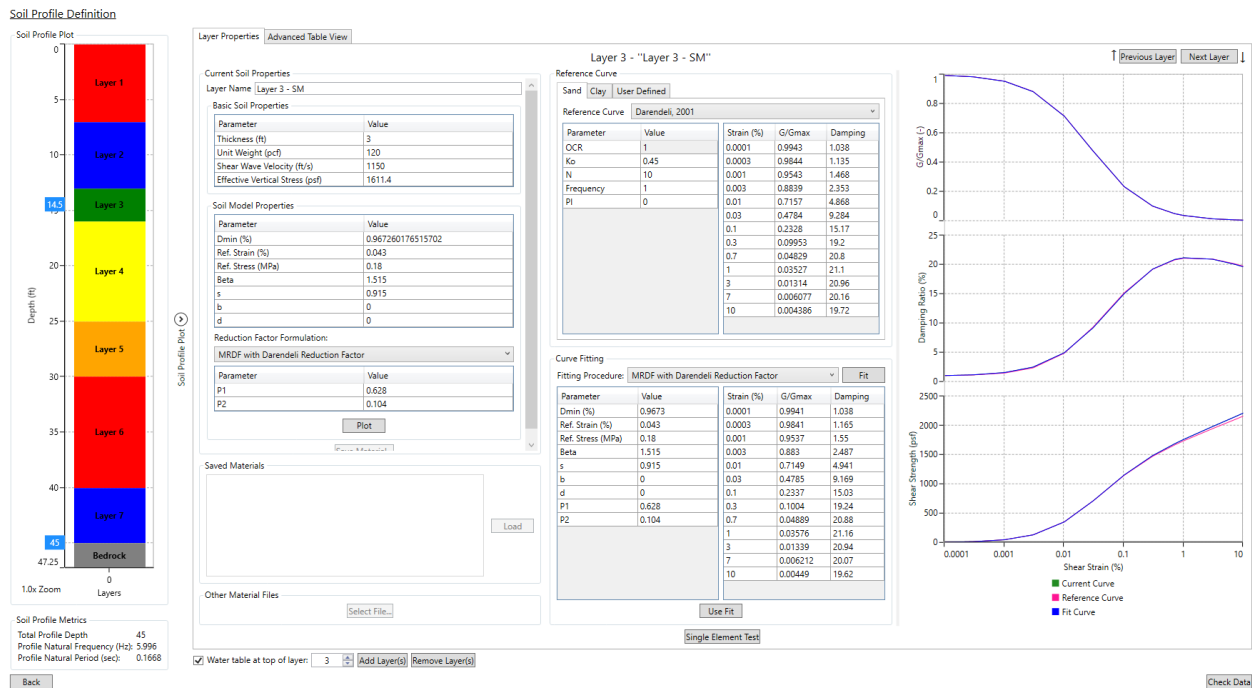


Figure A3-16. Representative Coarse-Grained Layer Properties at the Twin Cities Road Facility Site

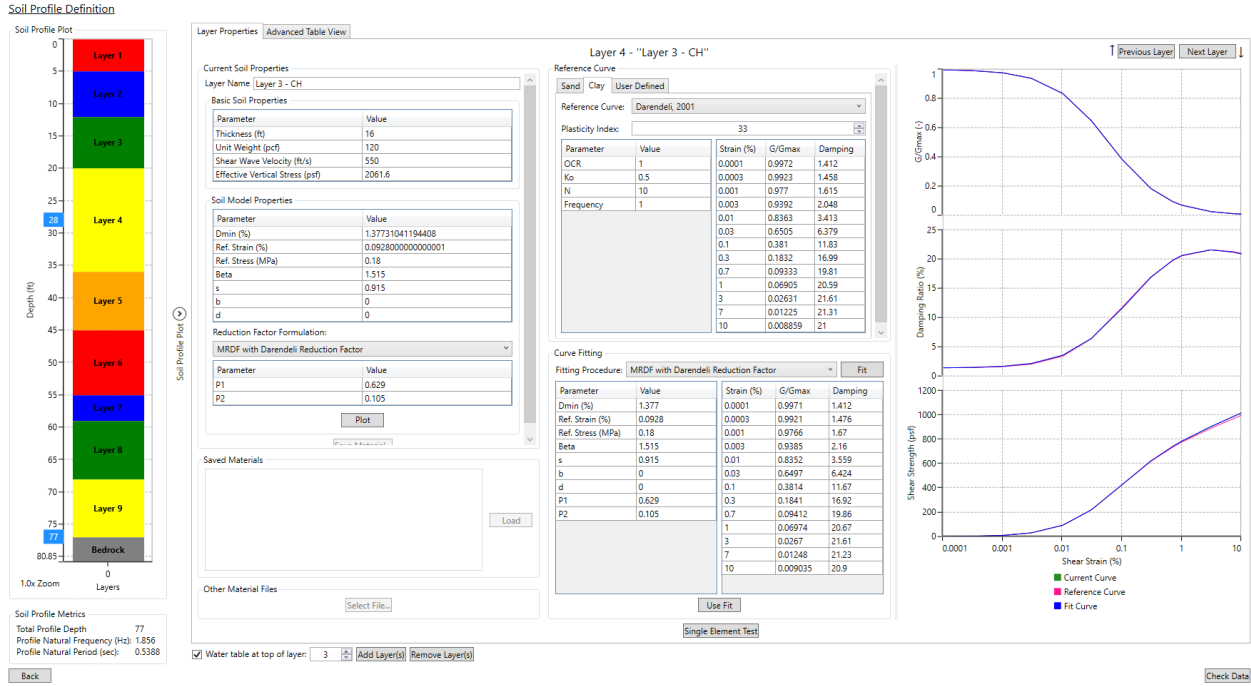


Figure A3-17. Representative Fine-Grained Layer Properties at the Union Island Facility Site

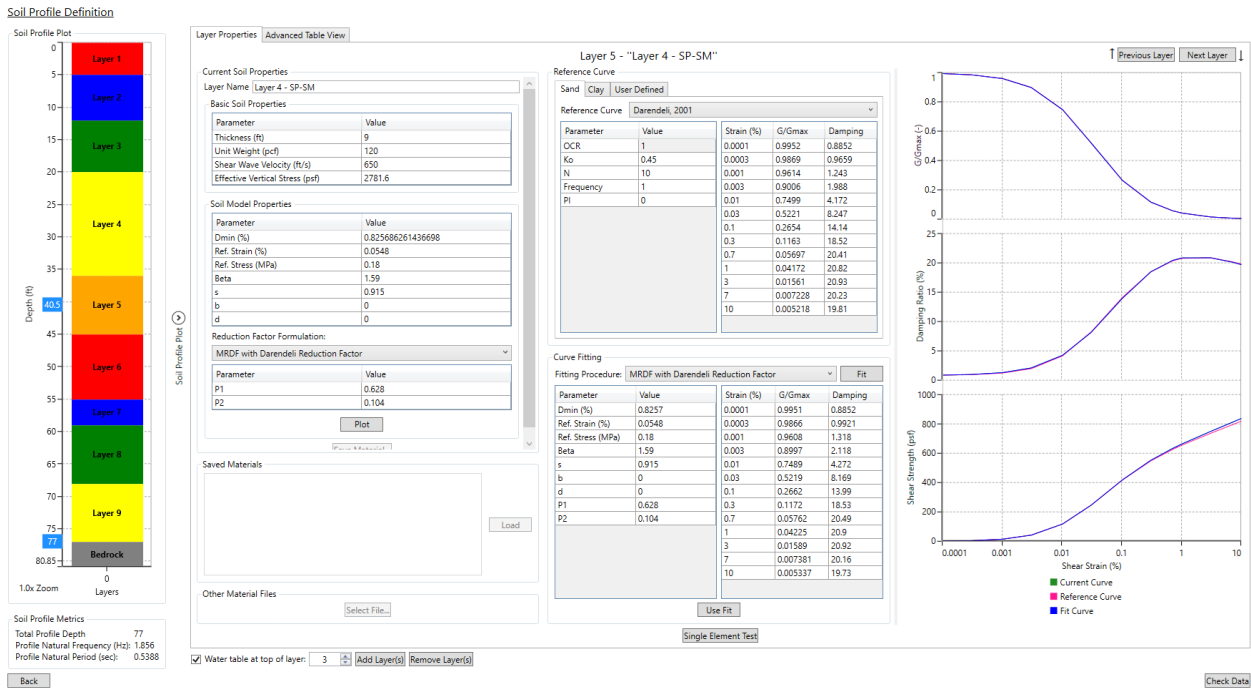


Figure A3-18. Representative Coarse-Grained Layer Properties at the Union Island Facility Site

Attachment 4
Development of Spectrally-Matched Time Histories

DEVELOPMENT OF SPECTRALLY-MATCHED TIME HISTORIES AT 9 SITES

This attachment summarizes the development of spectrally-matched earthquake time histories at the following 5 sites:

- 1) New Hope Tract
- 2) Canal Ranch Tract
- 3) King Island
- 4) Union Island
- 5) Bethany Reservoir Pumping Plant

The acceleration, velocity and displacement plots of the seed and spectrally-matched time histories at each of these 5 sites are presented below. The comparisons of calculated response spectra of the spectrally-matched time histories with the target spectra are shown in Figures 11 through 19 of the main text. Note, for the development of the spectrally-matched time histories at these 9 sites, the time histories already matched to the reference design spectra at the near sites performed by LCI (see Attachment 1) were used as the “seed” time histories.

New Hope Tract

Seed Time Histories (Spectrally-matched time histories for Twin Cities)											
RSN	Year	Earthquake Name	Station Name	Comp	Mag	ClstD (km)	Vs30 (m/s)	PGA (g)	PGV (cm/s)	PGD (cm)	AI (m/s)
187	1979	Imperial Valley-06	Parachute Test Site	225	6.5	12.7	349	0.25	47.6	31.1	1.77
187	1979	Imperial Valley-06	Parachute Test Site	315	6.5	12.7	349	0.44	41.4	28.4	1.65
1277	1999	Chi-Chi, Taiwan	HWA028	E	7.6	53.8	407	0.32	46.0	68.9	2.05
1277	1999	Chi-Chi, Taiwan	HWA028	N	7.6	53.8	407	0.29	35.7	39.7	2.07
4009	2003	San Simeon, CA	Point Buchon – Los Osos	090	6.5	31.9	486	0.37	46.3	37.8	2.07
4009	2003	San Simeon, CA	Point Buchon – Los Osos	360	6.5	31.9	486	0.28	52.2	28.6	1.86
Spectrally-matched Time Histories											
187	1979	Imperial Valley-06	Parachute Test Site	225	6.5	12.7	349	0.32	52.0	34.4	2.68
187	1979	Imperial Valley-06	Parachute Test Site	315	6.5	12.7	349	0.32	38.8	28.6	2.45
1277	1999	Chia-Chia, Taiwan	HWA028	E	7.6	53.8	407	0.36	41.4	102.6	2.63
1277	1999	Chia-Chia, Taiwan	HWA028	N	7.6	53.8	407	0.32	48.7	65.0	3.03
4009	2003	San Simeon, CA	Point Buchon – Los Osos	090	6.5	31.9	486	0.37	45.2	70.0	2.45
4009	2003	San Simeon, CA	Point Buchon – Los Osos	360	6.5	31.9	486	0.31	68.1	126.6	3.83

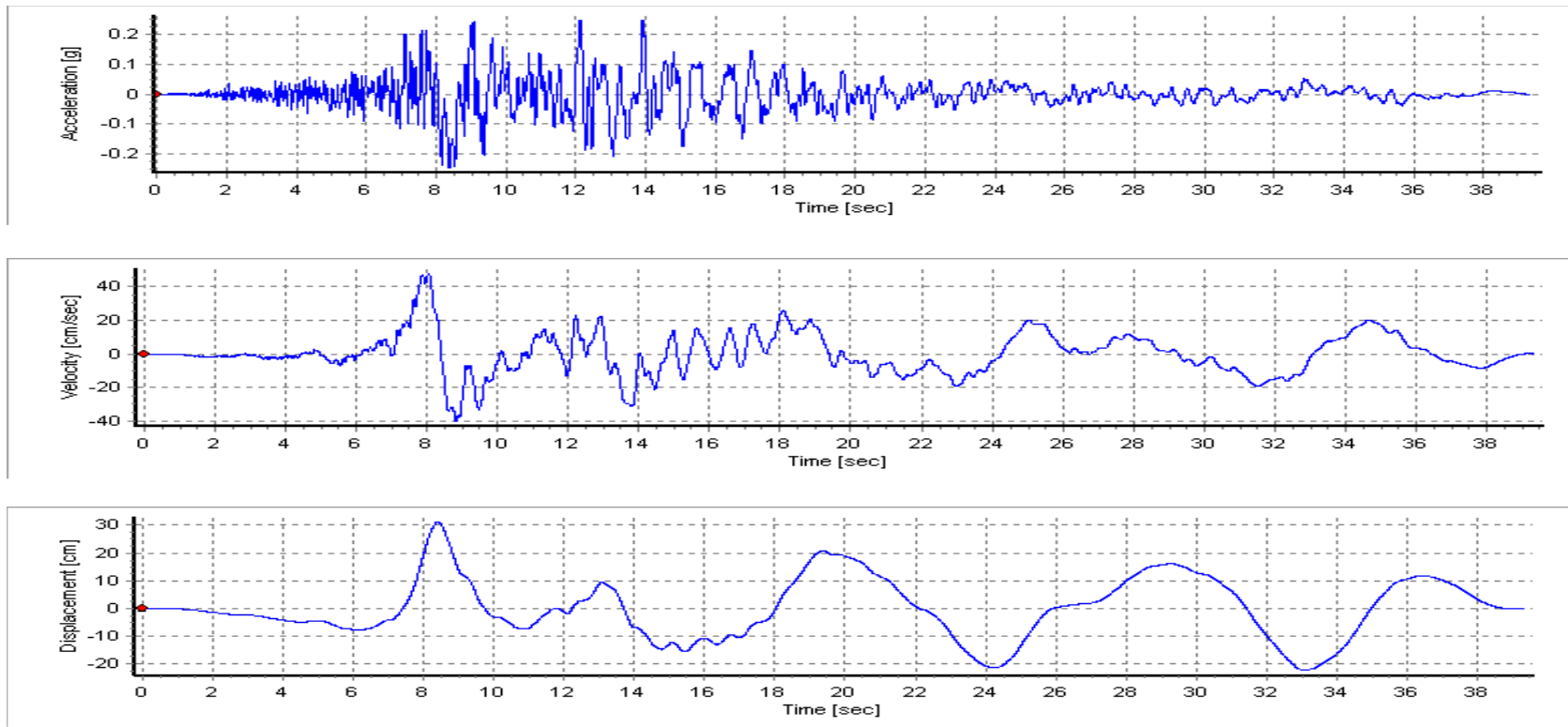


Figure A6-1. Seed Time histories for New Hope Tract – 1970 Imperial Valley Earthquake at Parachute Test Site, 225 deg. Component

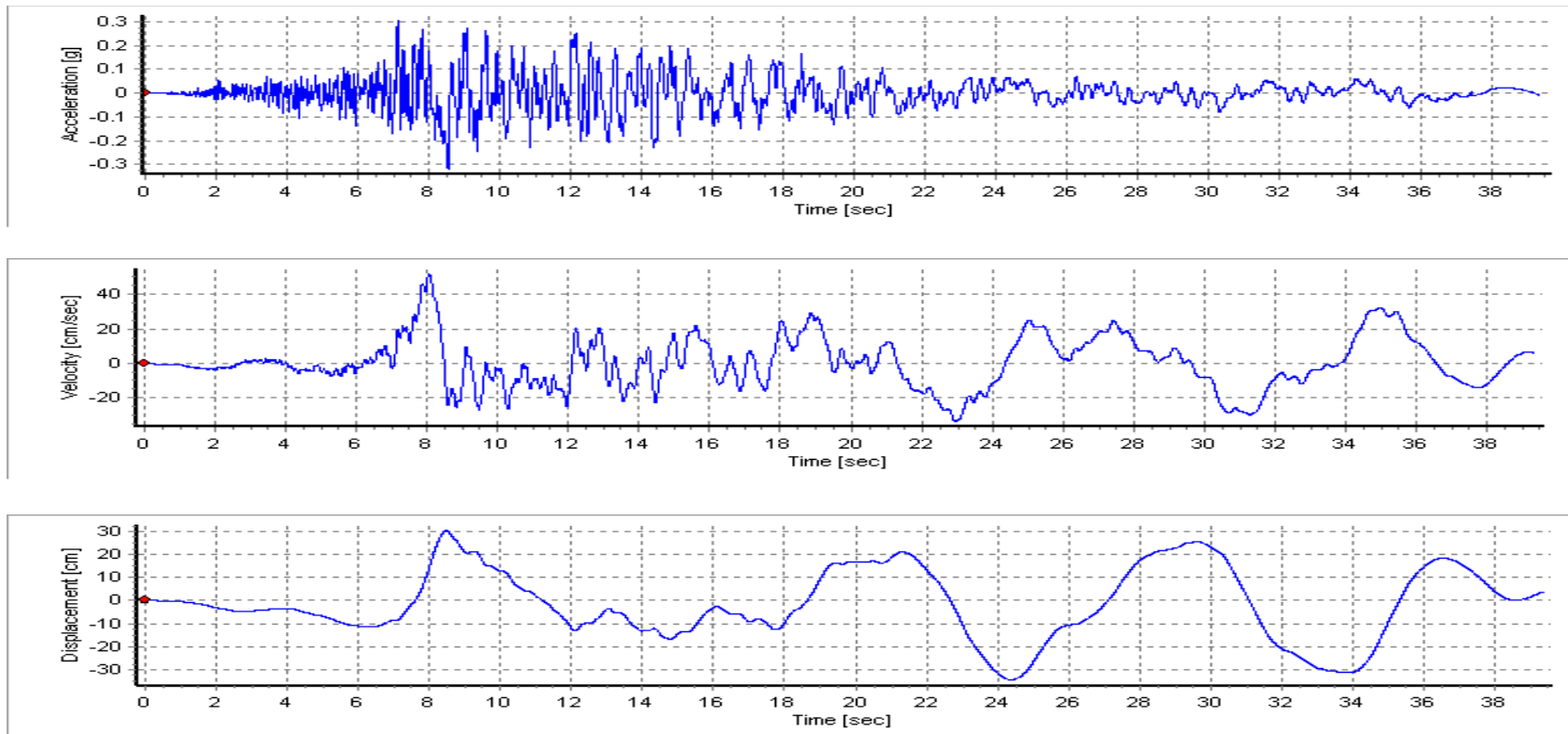


Figure A6-2. Spectrally-matched Time histories for New Hope Tract – 1970 Imperial Valley Earthquake at Parachute Test Site, 225 deg. Component

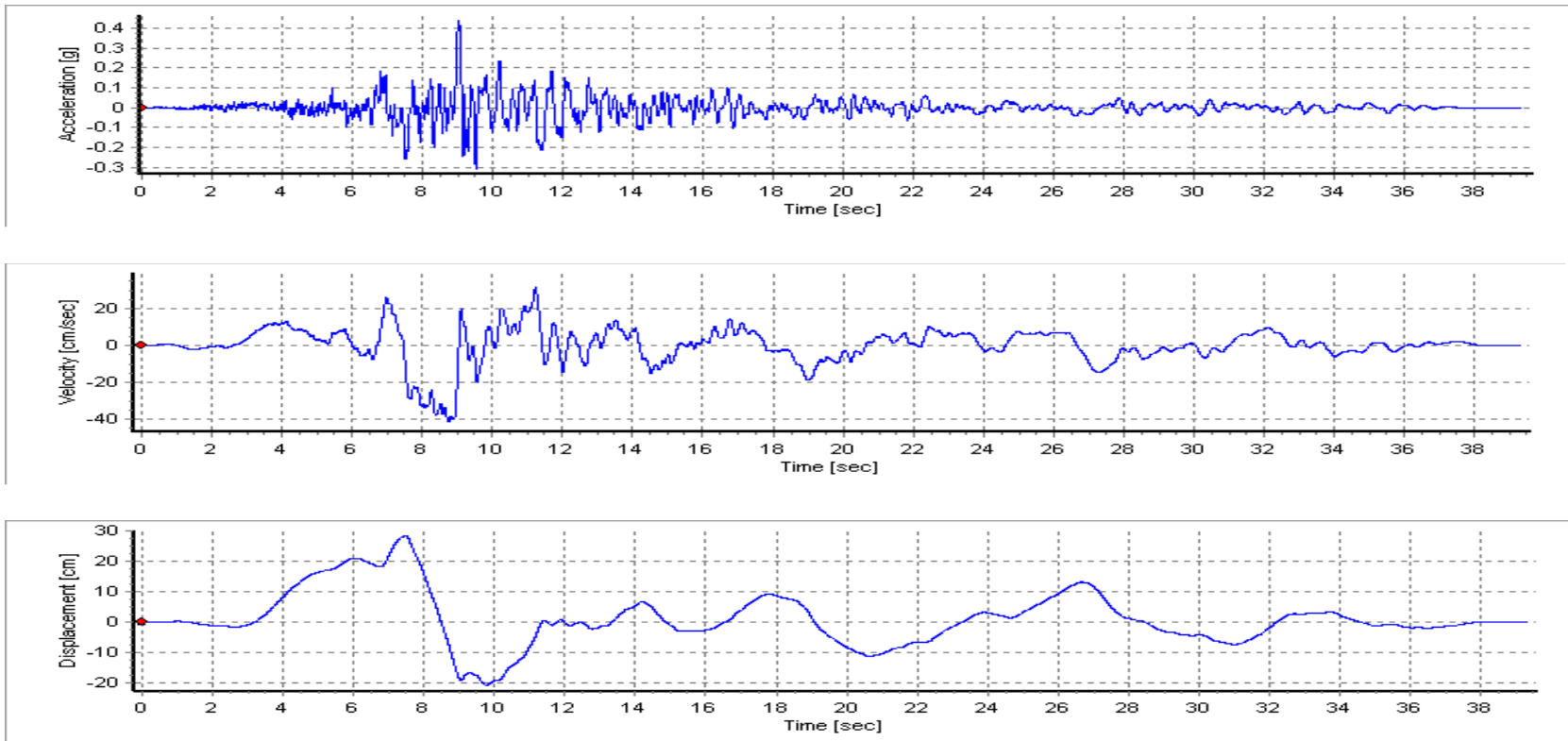


Figure A6-3. Seed Time histories for New Hope Tract – 1970 Imperial Valley Earthquake at Parachute Test Site, 315 deg. Component

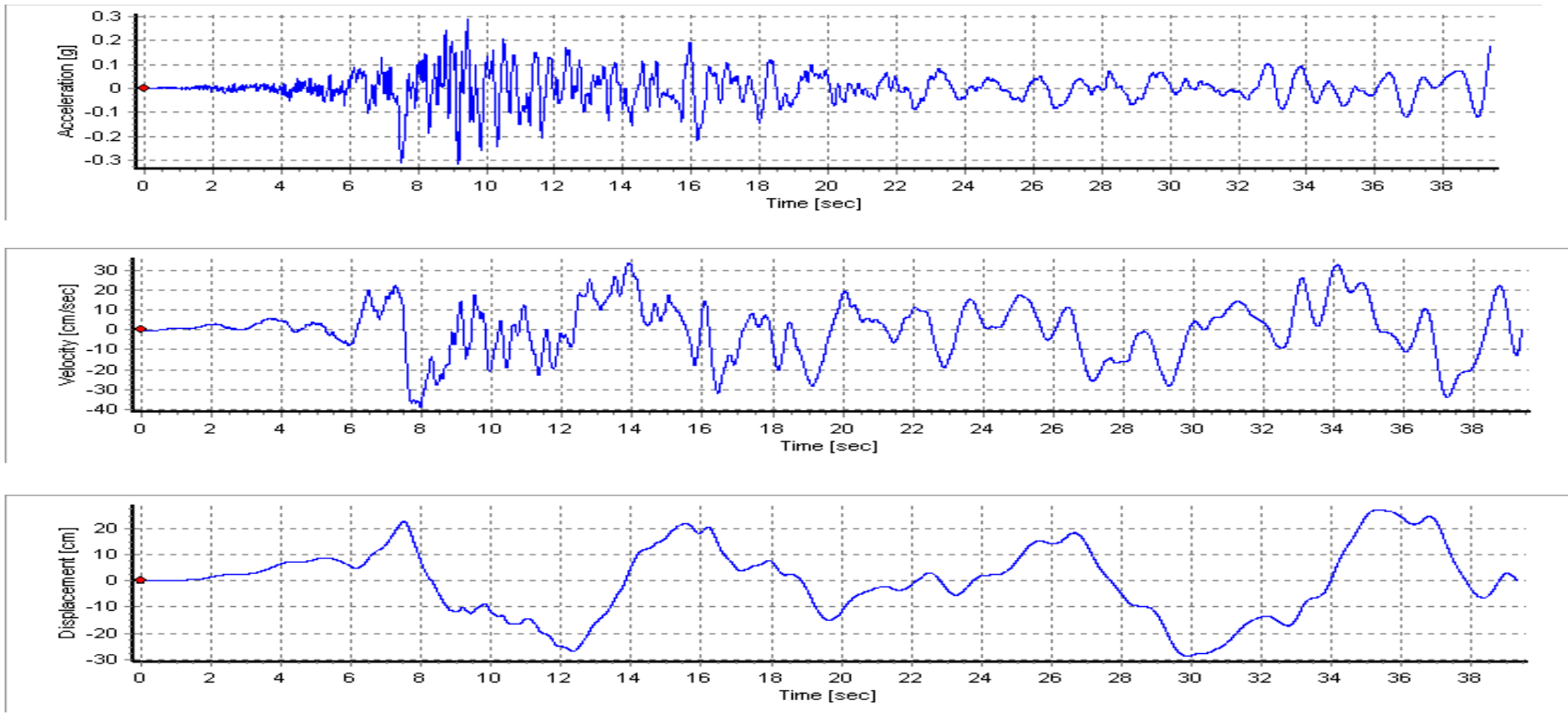


Figure A6-4. Spectrally-matched Time histories for New Hope Tract – 1970 Imperial Valley Earthquake at Parachute Test Site, 315 deg. Component

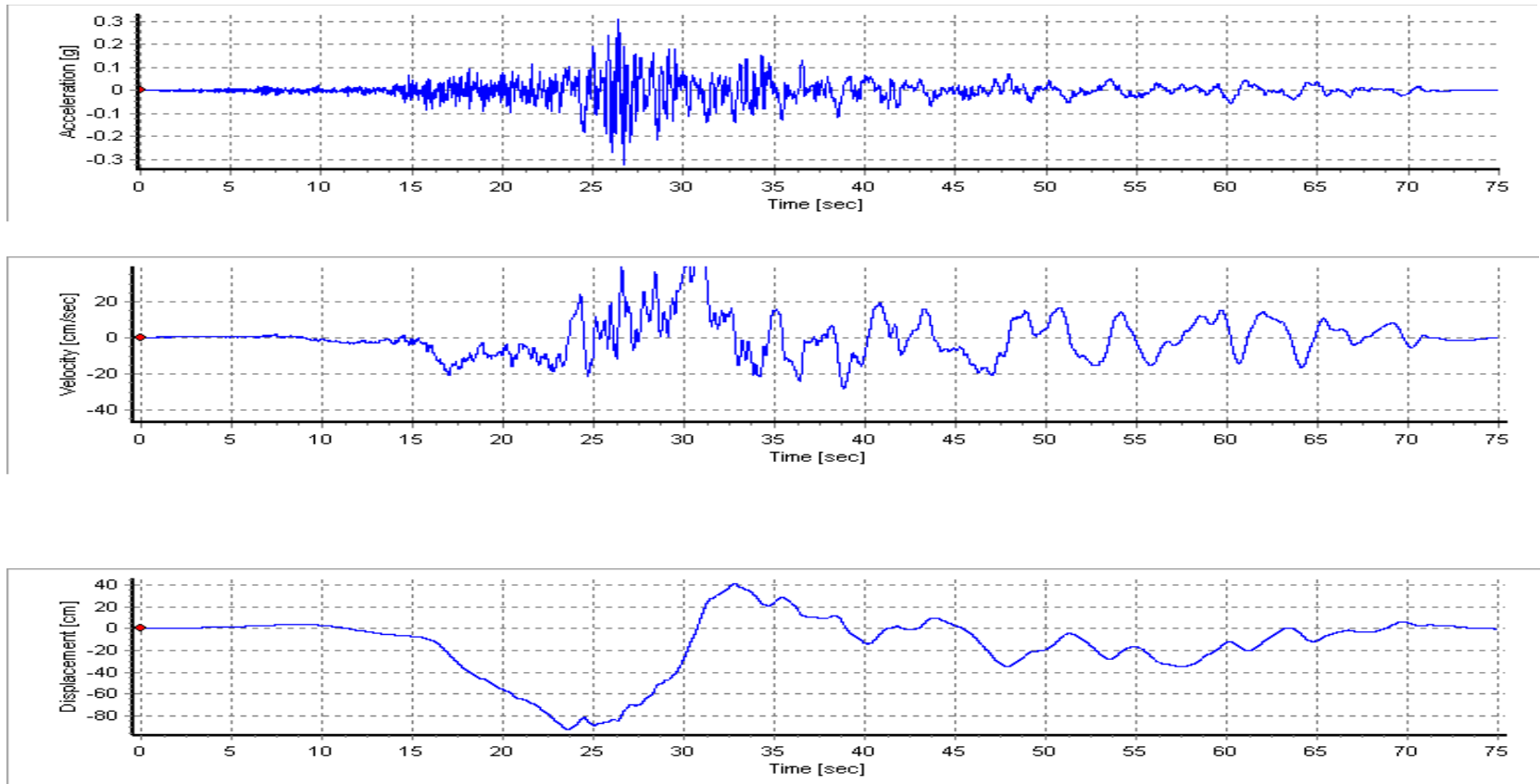


Figure A6-5. Seed Time histories for New Hope Tract – 1999 Chi-Chi, Taiwan Earthquake at HWA028, East Component

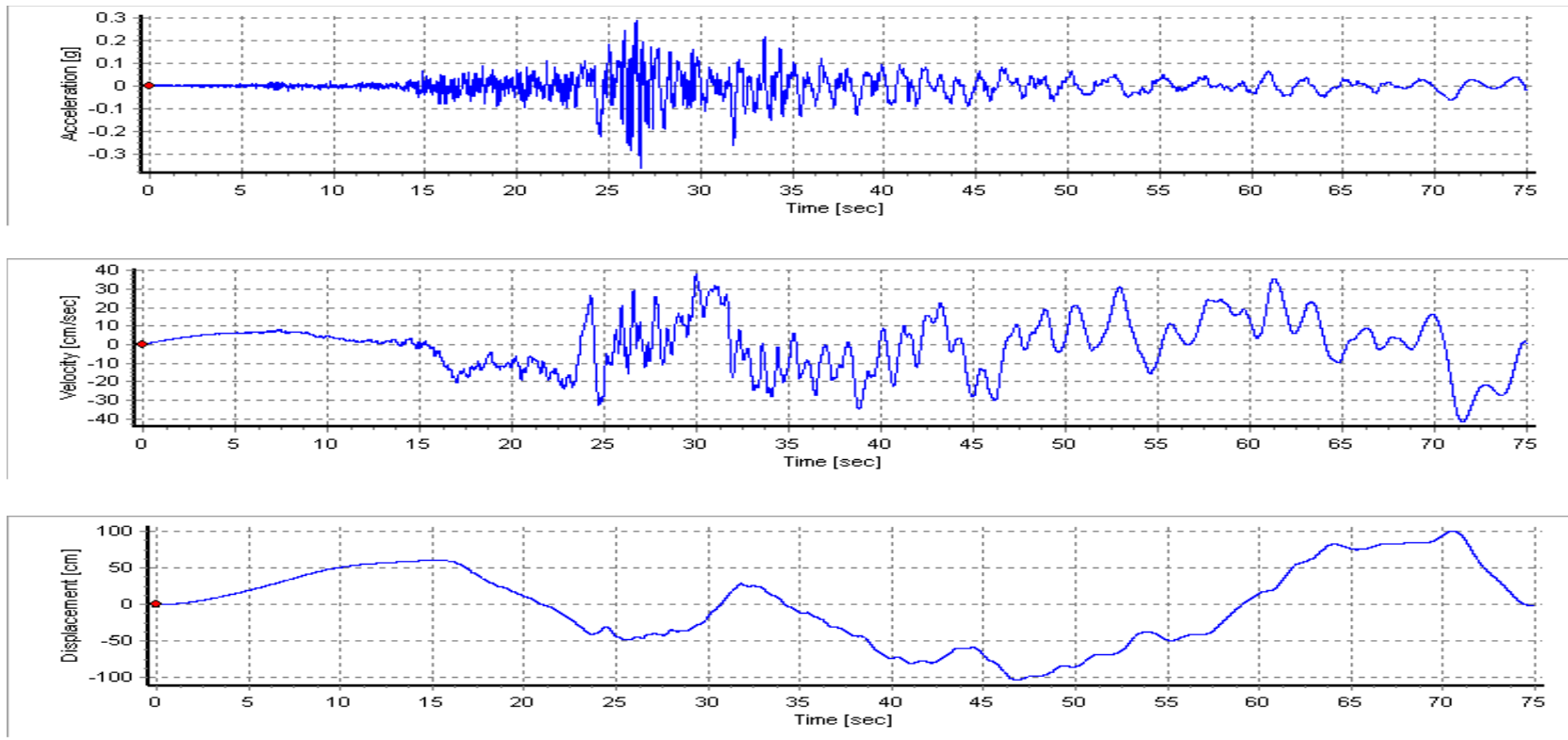


Figure A6-6. Spectrally-matched Time histories for New Hope Tract – 1999 Chi-Chi, Taiwan Earthquake at HWA028, East Component

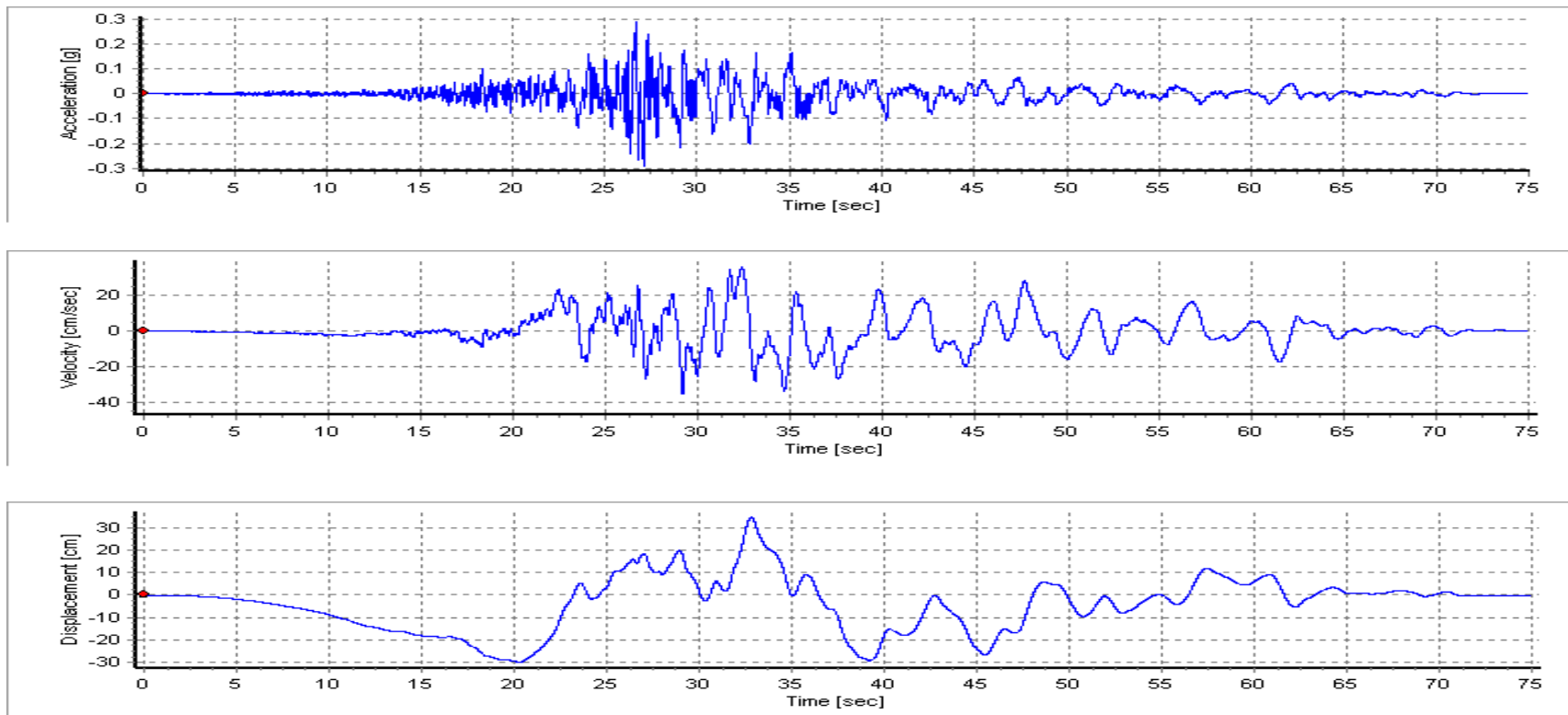


Figure A6-7. Seed Time histories for New Hope Tract – 1999 Chi-Chi, Taiwan Earthquake at HWA028, North Component

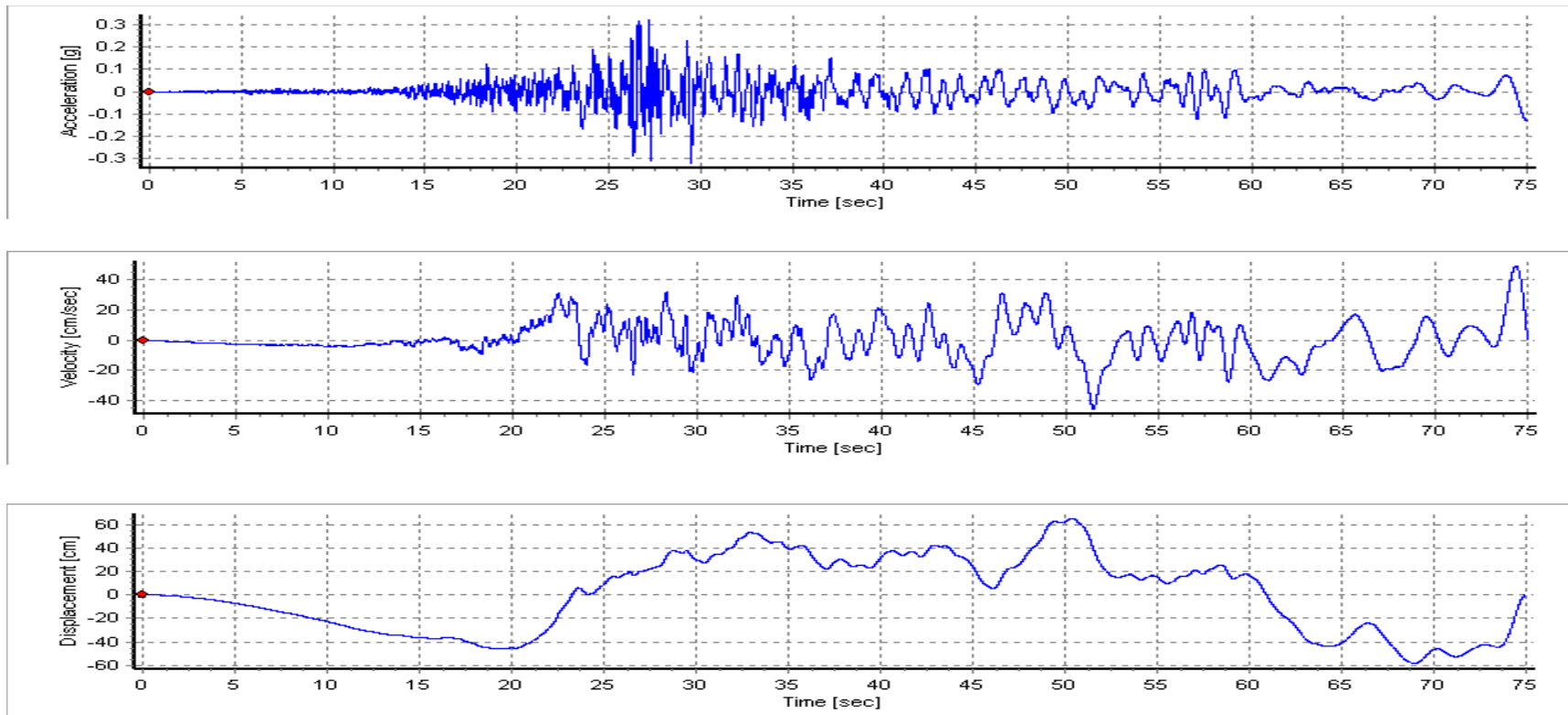


Figure A6-8. Spectrally-matched Time histories for New Hope Tract – 1999 Chi-Chi, Taiwan Earthquake at HWA028, North Component

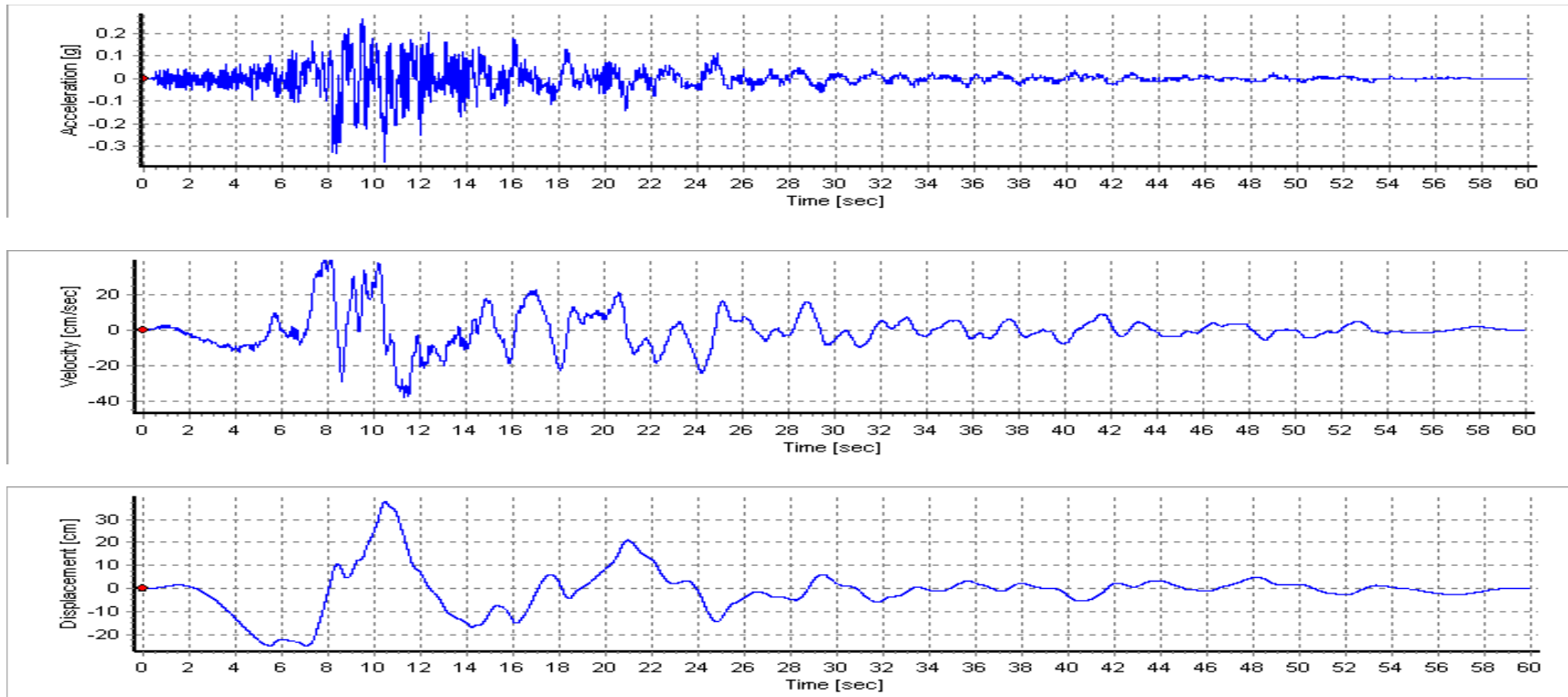


Figure A6-9. Seed Time histories for New Hope Tract – 2003 San Simeon, CA Earthquake at Point Buchon – Los Osos, 090 deg. Component

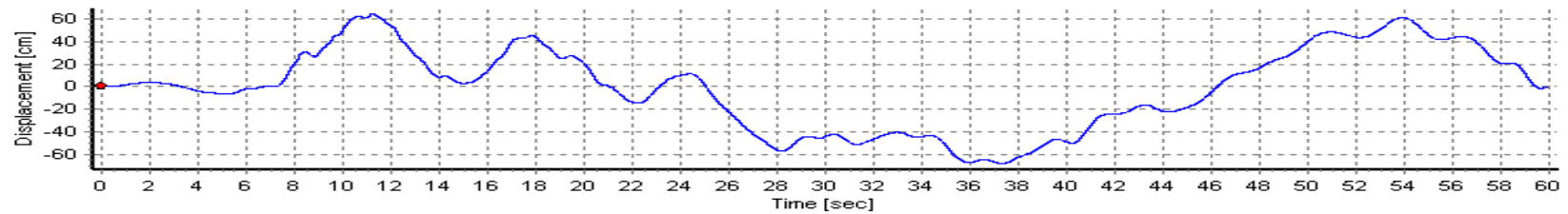
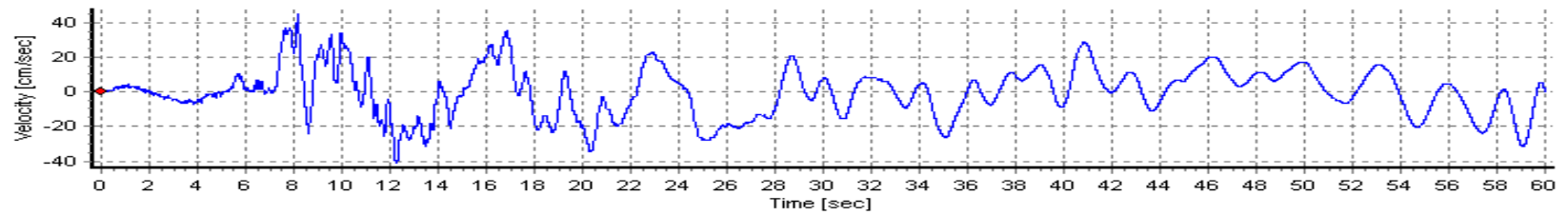
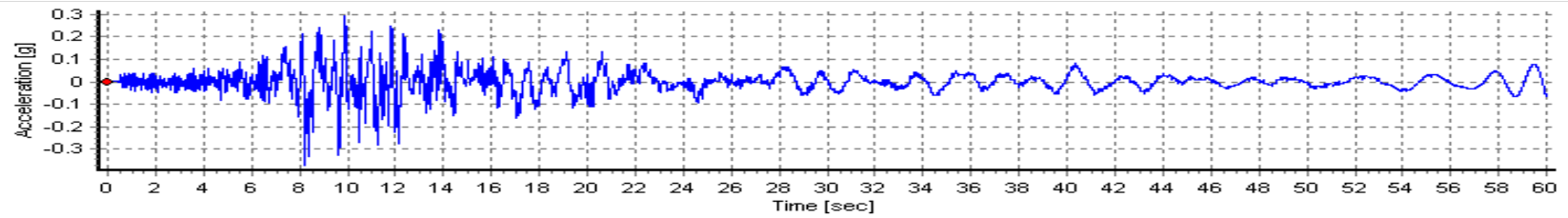


Figure A6-10. Spectrally-matched Time histories for New Hope Tract – 2003 San Simeon, CA Earthquake at Point Buchon – Los Osos, 090 deg. Component

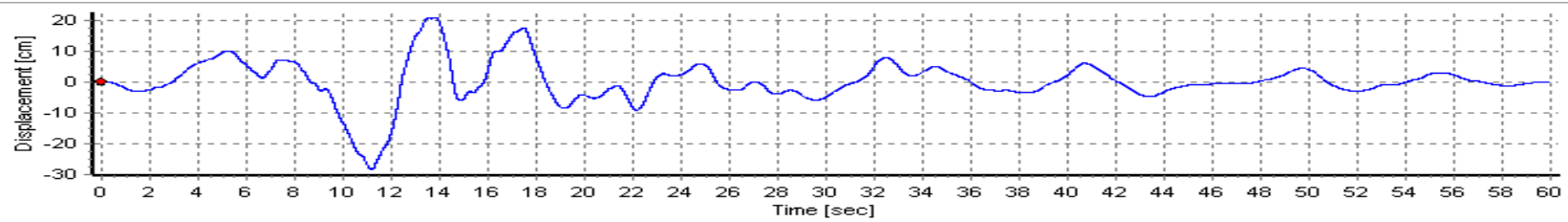
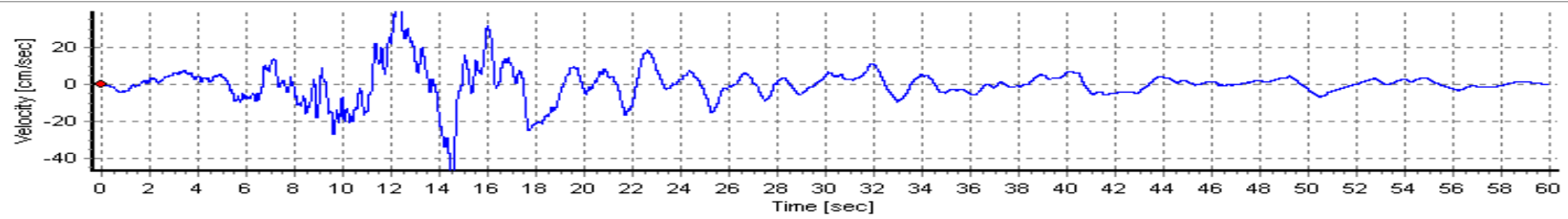
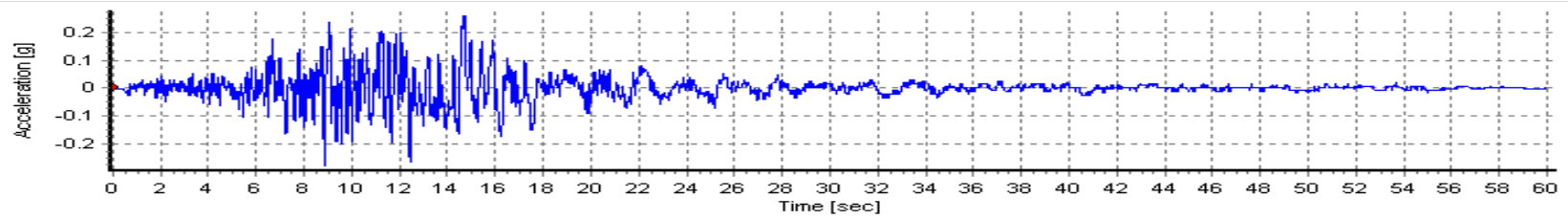


Figure A6-11. Seed Time histories for New Hope Tract – 2003 San Simeon, CA Earthquake at Point Buchon – Los Osos, 360 deg. Component

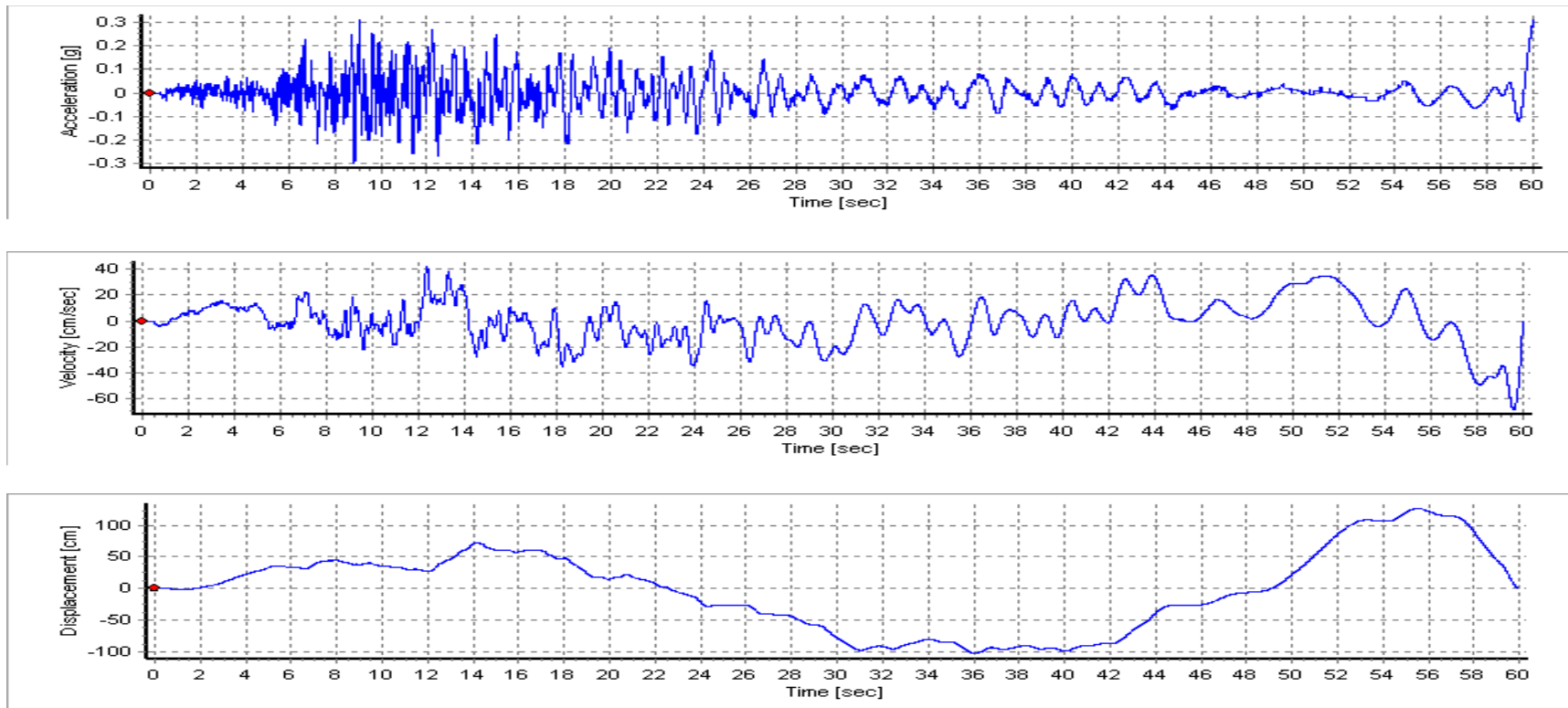


Figure A6-12. Spectrally-matched Time histories for New Hope Tract – 2003 San Simeon, CA Earthquake at Point Buchon – Los Osos, 360 deg. Component

Canal Ranch Tract

Seed Time Histories (Spectrally-matched time histories for Twin Cities)											
RSN	Year	Earthquake Name	Station Name	Comp	Mag	ClstD (km)	Vs30 (m/s)	PGA (g)	PGV (cm/s)	PGD (cm)	AI (m/s)
187	1979	Imperial Valley-06	Parachute Test Site	225	6.5	12.7	349	0.25	47.6	31.1	1.77
187	1979	Imperial Valley-06	Parachute Test Site	315	6.5	12.7	349	0.44	41.4	28.4	1.65
1277	1999	Chi-Chi, Taiwan	HWA028	E	7.6	53.8	407	0.32	46.0	68.9	2.05
1277	1999	Chi-Chi, Taiwan	HWA028	N	7.6	53.8	407	0.29	35.7	39.7	2.07
4009	2003	San Simeon, CA	Point Buchon – Los Osos	090	6.5	31.9	486	0.37	46.3	37.8	2.07
4009	2003	San Simeon, CA	Point Buchon – Los Osos	360	6.5	31.9	486	0.28	52.2	28.6	1.86
Spectrally-matched Time Histories											
187	1979	Imperial Valley-06	Parachute Test Site	225	6.5	12.7	349	0.34	50.3	56.5	2.64
187	1979	Imperial Valley-06	Parachute Test Site	315	6.5	12.7	349	0.30	32.7	43.5	1.56
1277	1999	Chia-Chia, Taiwan	HWA028	E	7.6	53.8	407	0.34	44.9	83.5	2.22
1277	1999	Chia-Chia, Taiwan	HWA028	N	7.6	53.8	407	0.30	30.6	38.8	2.56
4009	2003	San Simeon, CA	Point Buchon – Los Osos	090	6.5	31.9	486	0.35	57.1	59.1	2.29
4009	2003	San Simeon, CA	Point Buchon – Los Osos	360	6.5	31.9	486	0.27	42.0	58.8	2.93

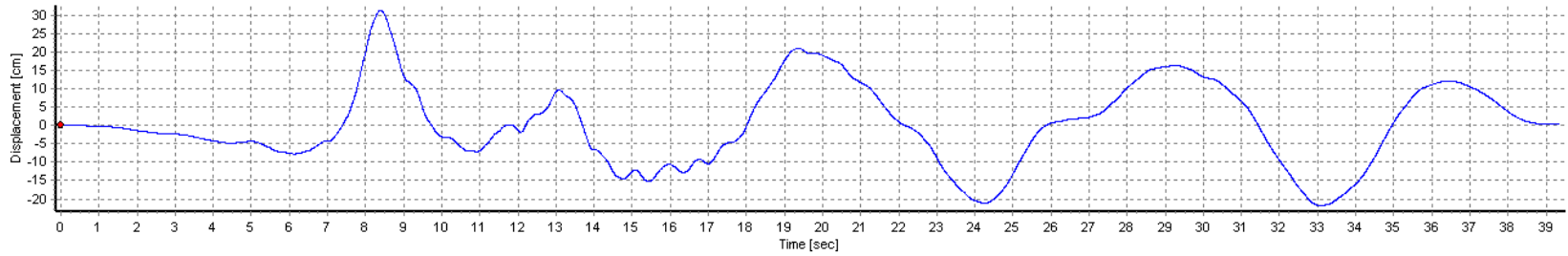
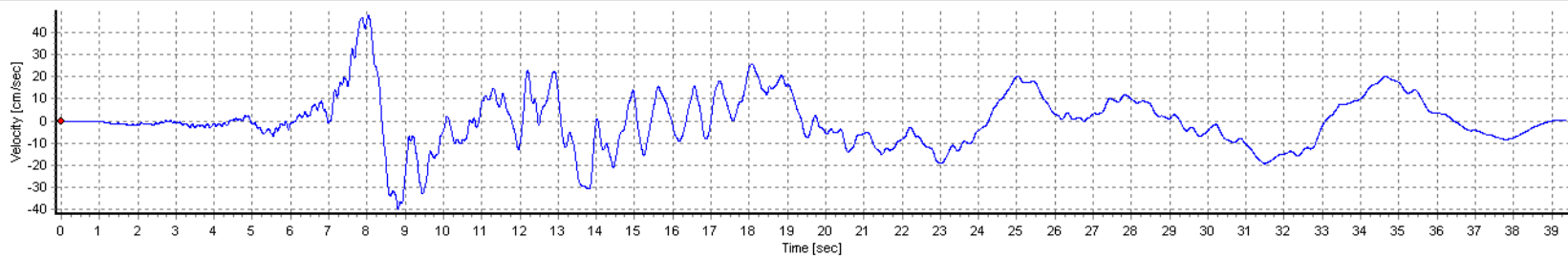
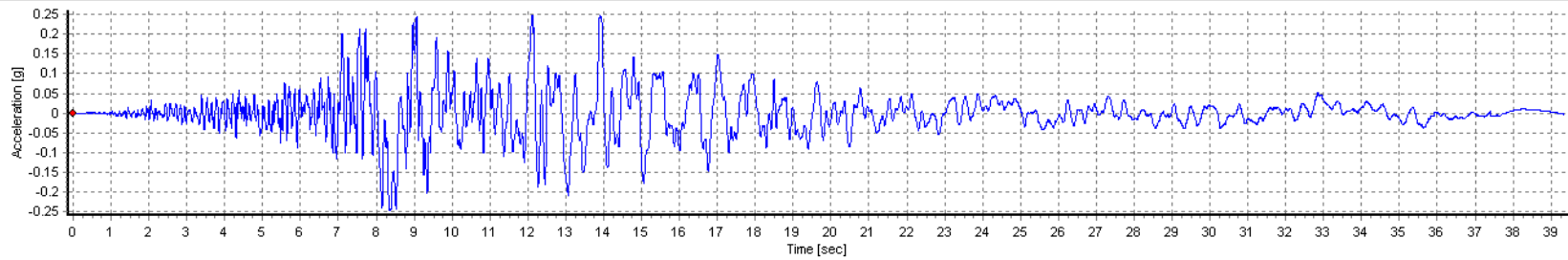


Figure A6-13. Seed Time histories for Canal Ranch Tract – 1970 Imperial Valley Earthquake at Parachute Test Site, 225 deg. Component

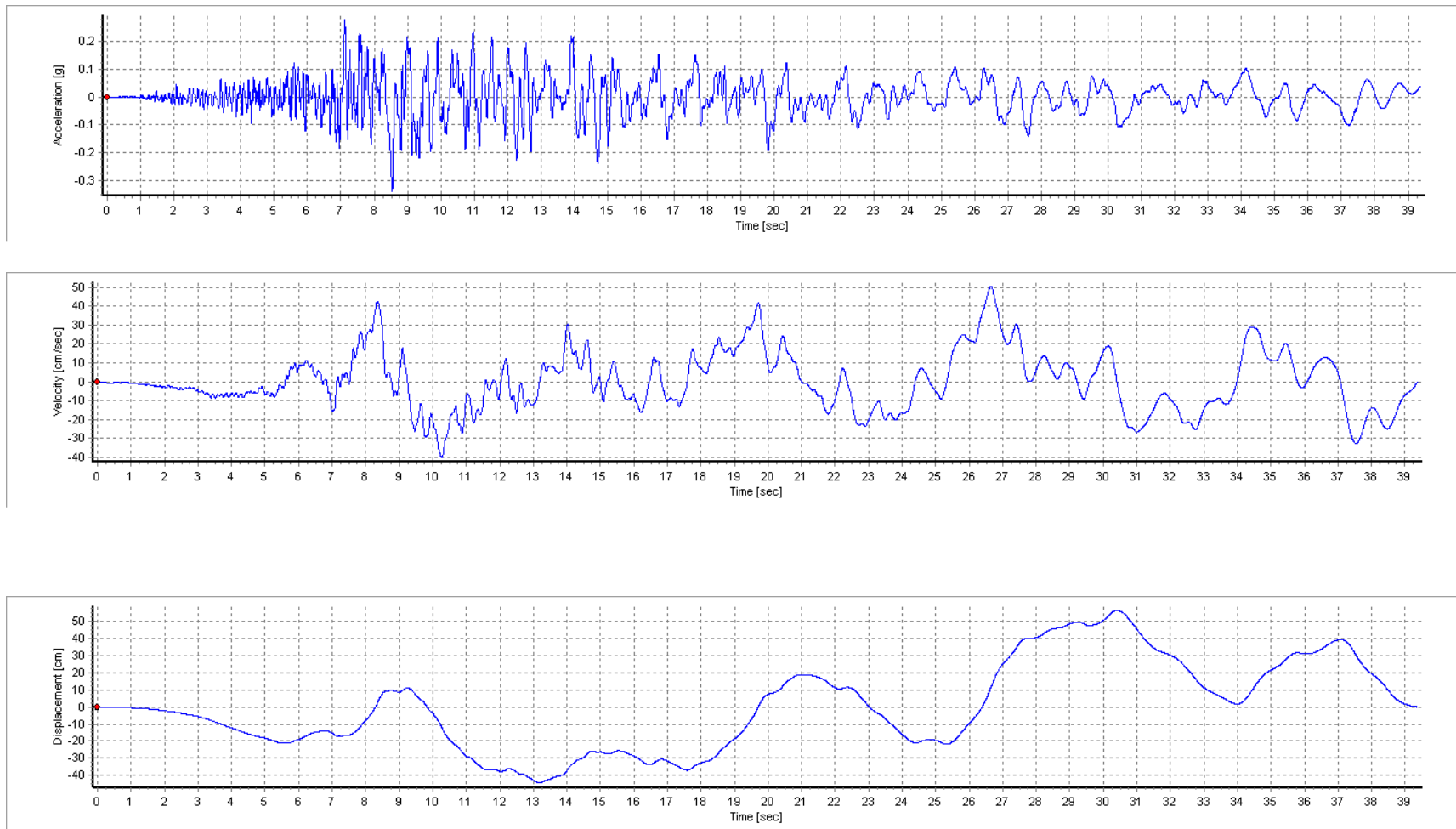


Figure A6-14. Spectrally-matched Time histories for Canal Ranch Tract – 1970 Imperial Valley Earthquake at Parachute Test Site, 225 deg. Component

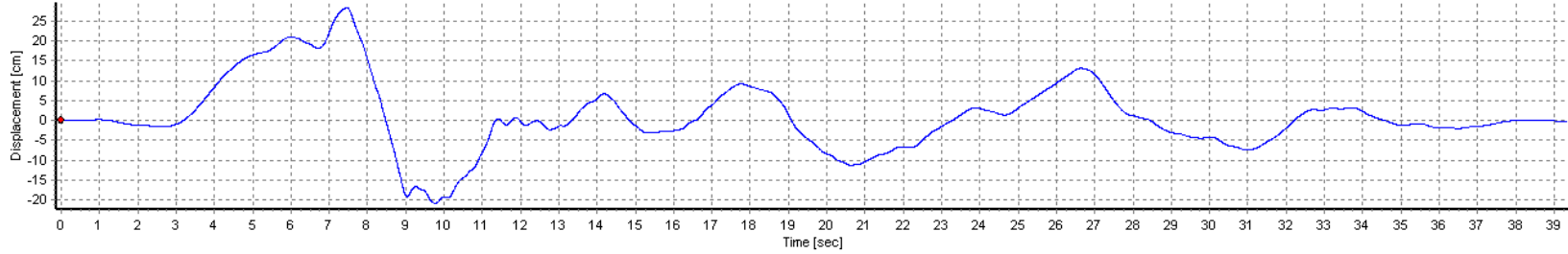
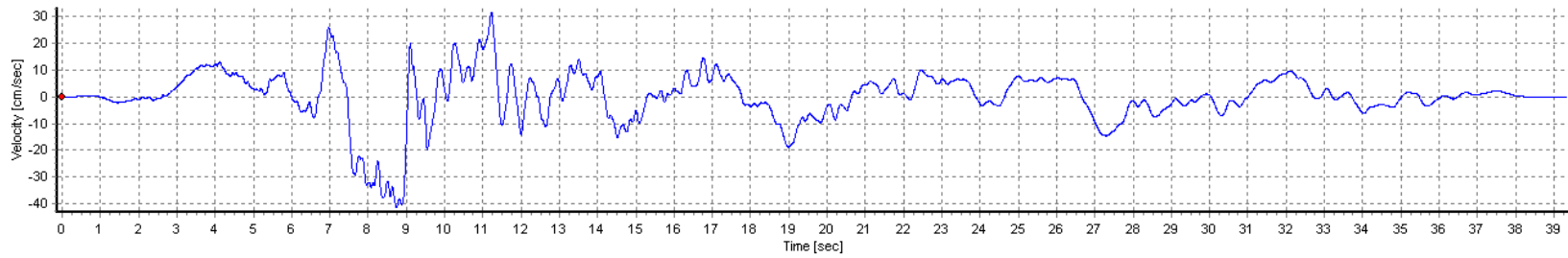
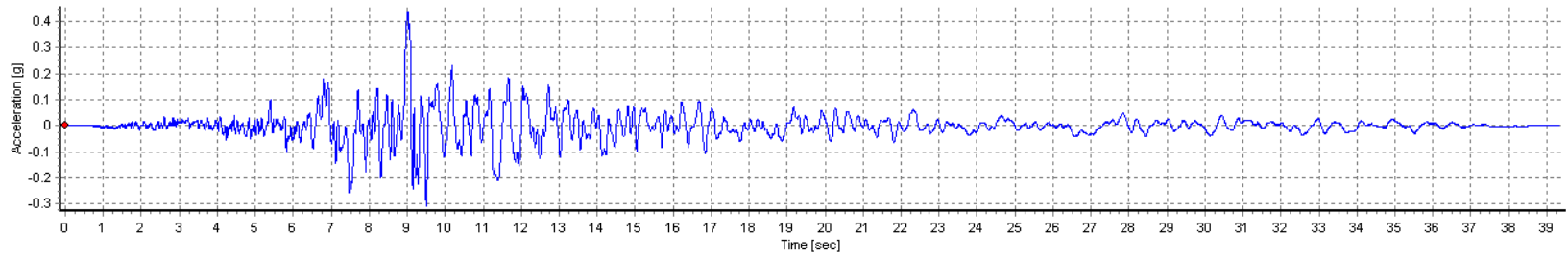


Figure A6-15. Seed Time histories for Canal Ranch Tract – 1970 Imperial Valley Earthquake at Parachute Test Site, 315 deg. Component

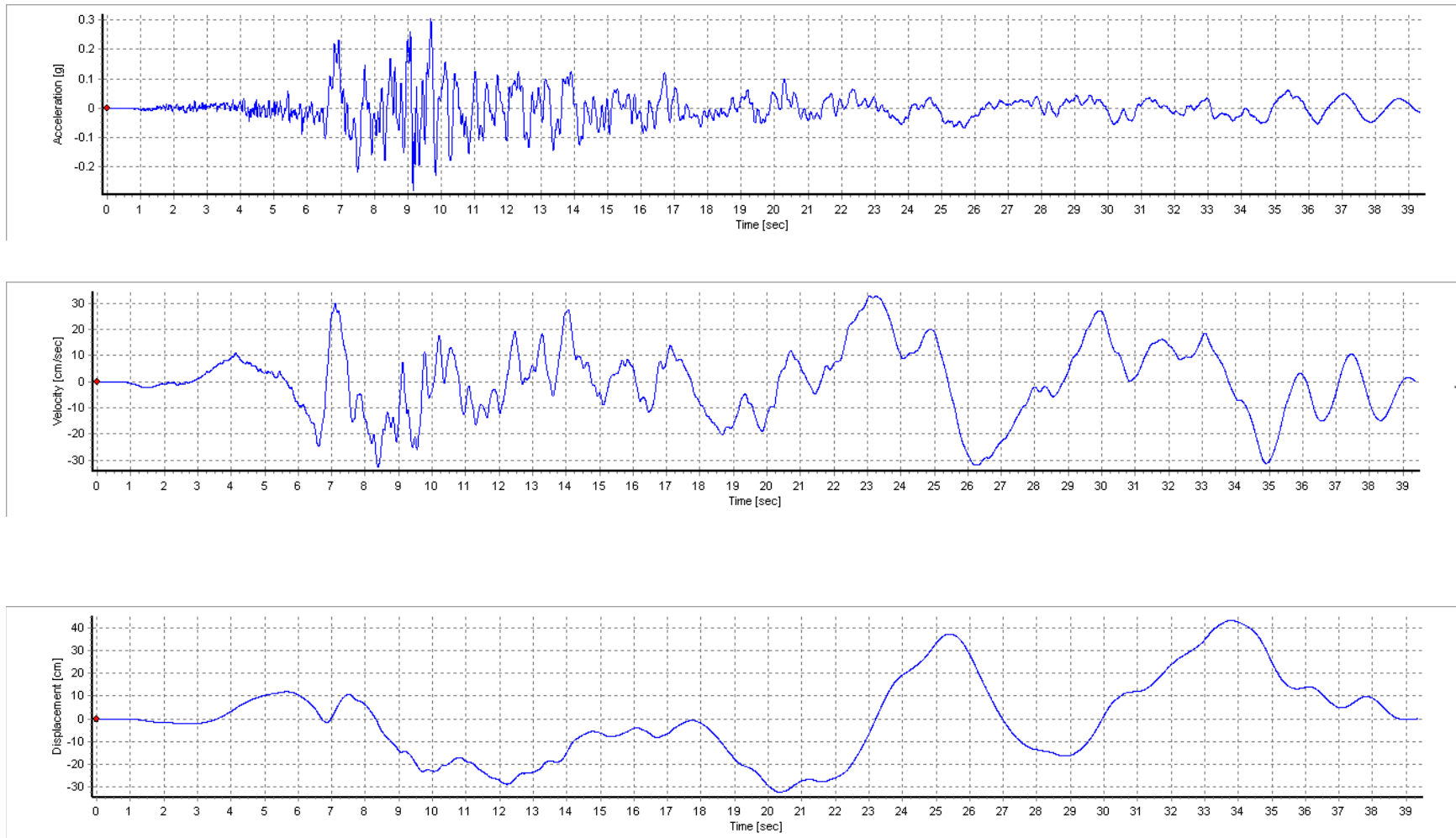


Figure A6-16. Spectrally-matched Time histories for Canal Ranch Tract – 1970 Imperial Valley Earthquake at Parachute Test Site, 315 deg. Component

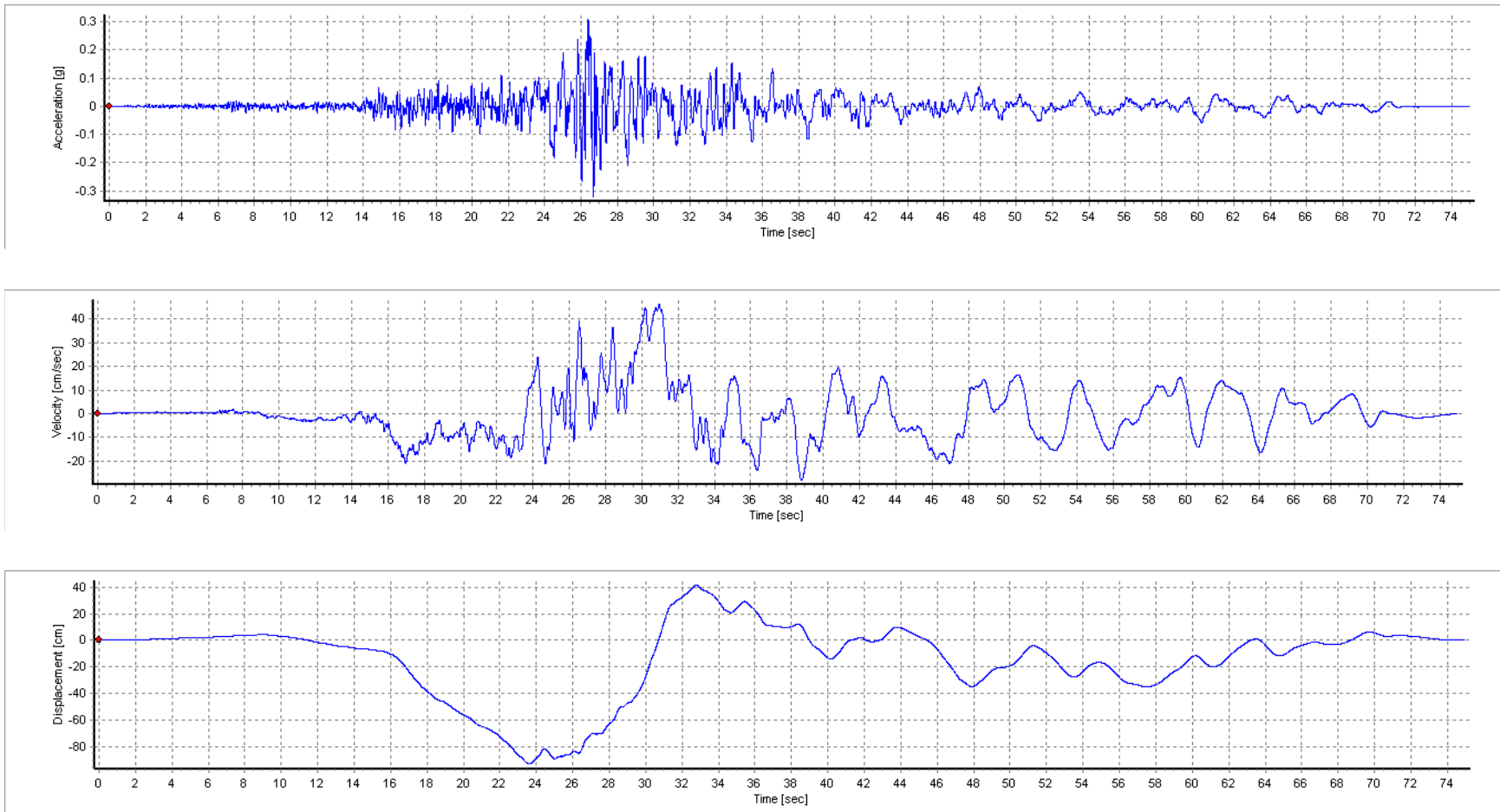


Figure A6-17. Seed Time histories for Canal Ranch Tract – 1999 Chi-Chi, Taiwan Earthquake at HWA028, East Component

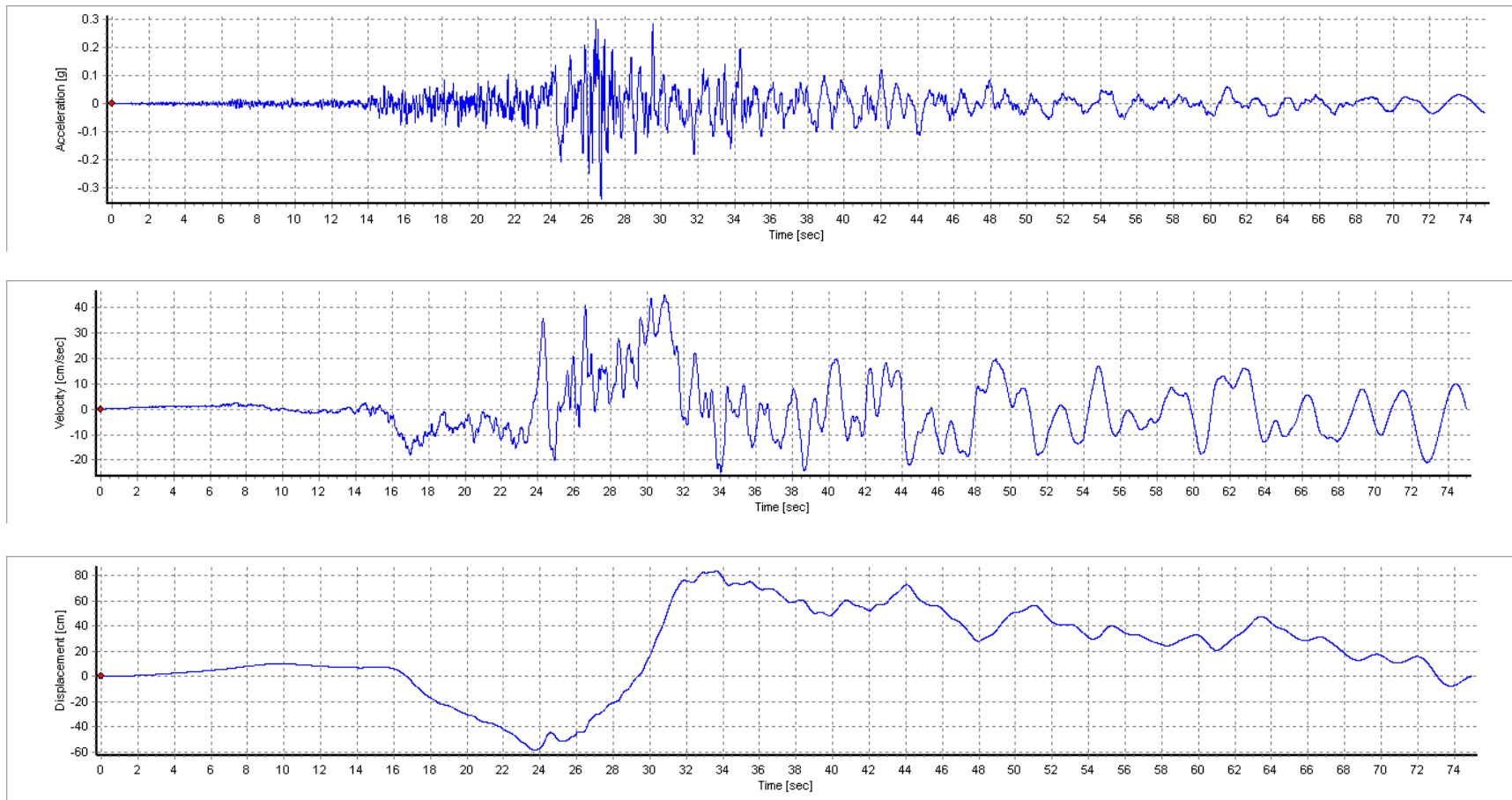


Figure A6-18. Spectrally-matched Time histories for Canal Ranch Tract – 1999 Chi-Chi, Taiwan Earthquake at HWA028, East Component

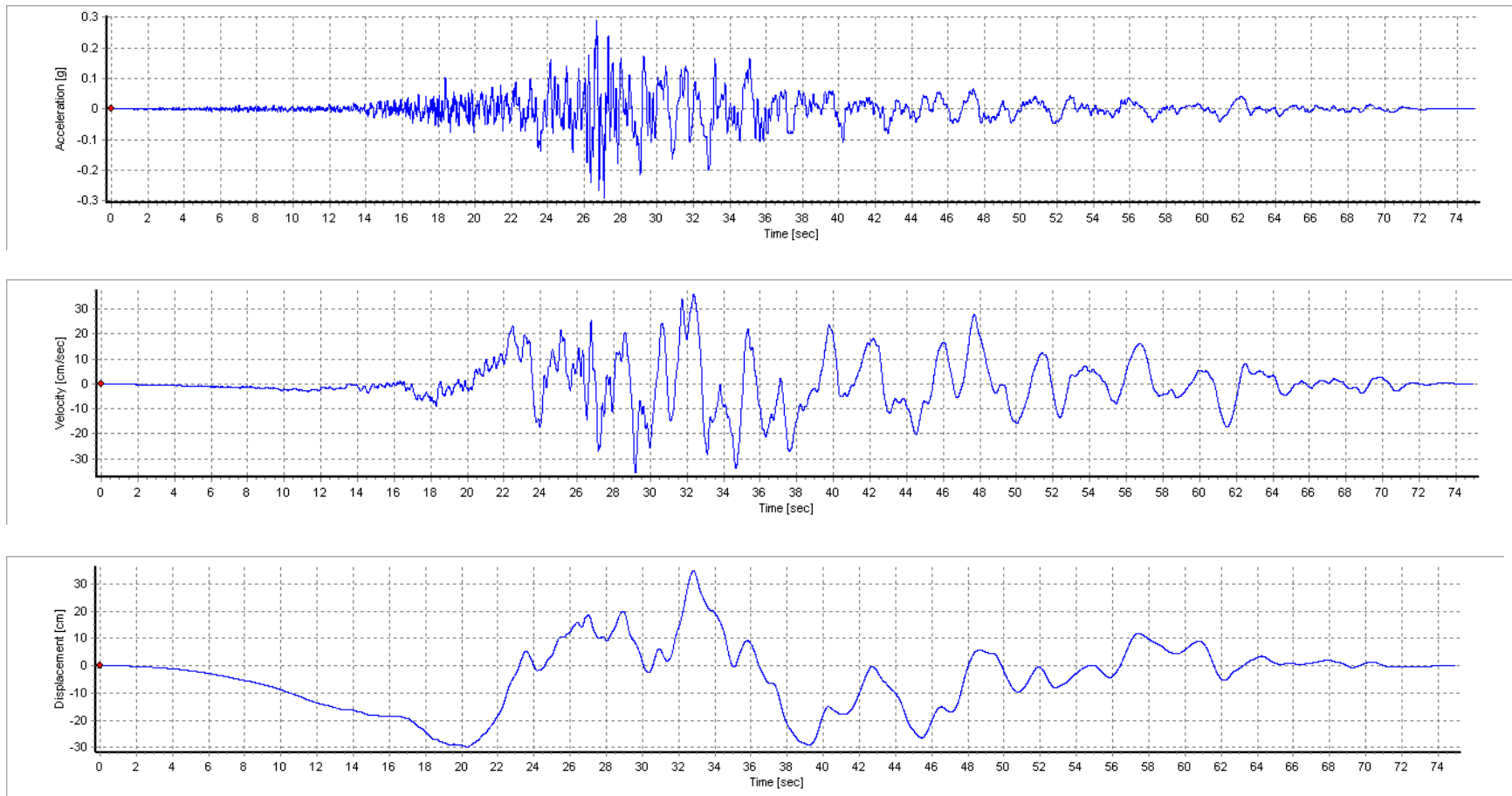


Figure A6-19. Seed Time histories for Canal Ranch Tract – 1999 Chi-Chi, Taiwan Earthquake at HWA028, North Component

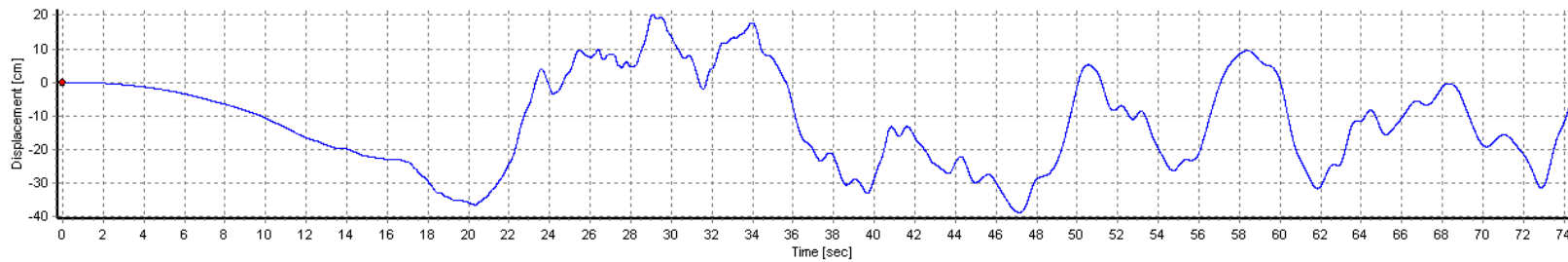
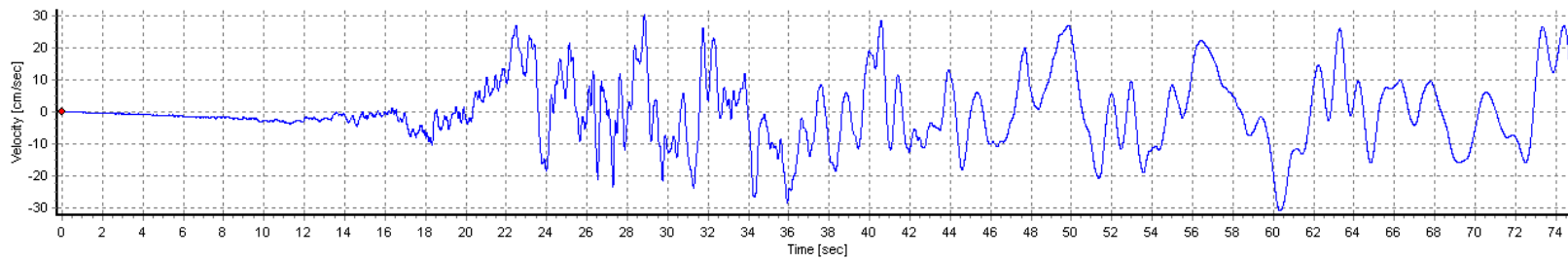
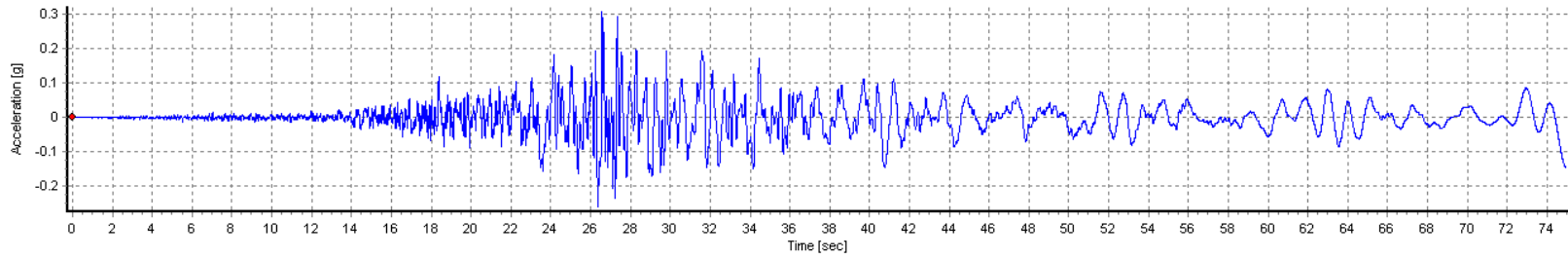


Figure A6-20. Spectrally-matched Time histories for Canal Ranch Tract – 1999 Chi-Chi, Taiwan Earthquake at HWA028, North Component

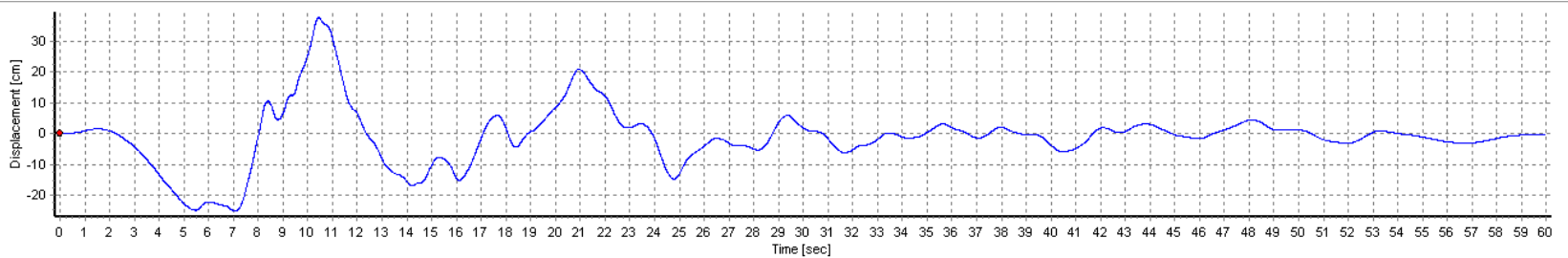
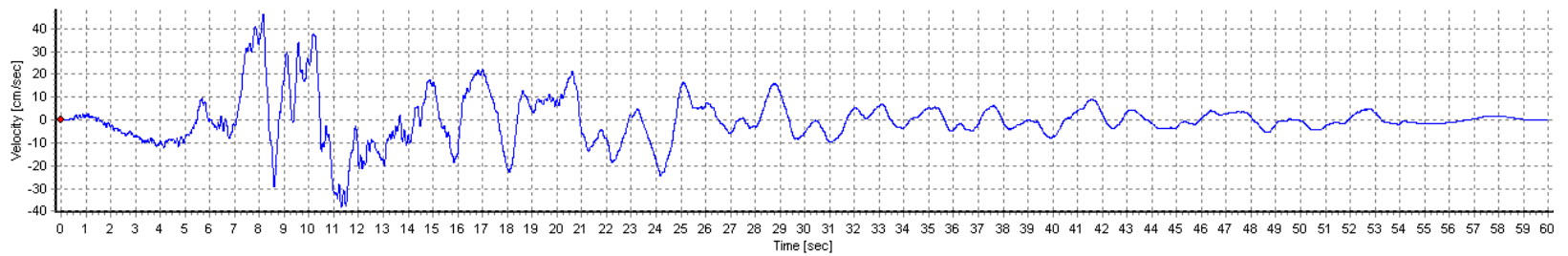
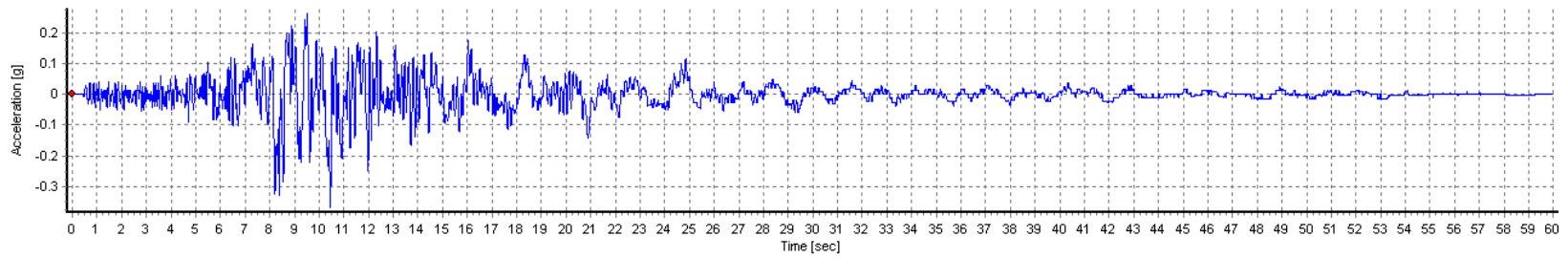


Figure A6-21. Seed Time histories for Canal Ranch Tract – 2003 San Simeon, CA Earthquake at Point Buchon – Los Osos, 090 deg. Component

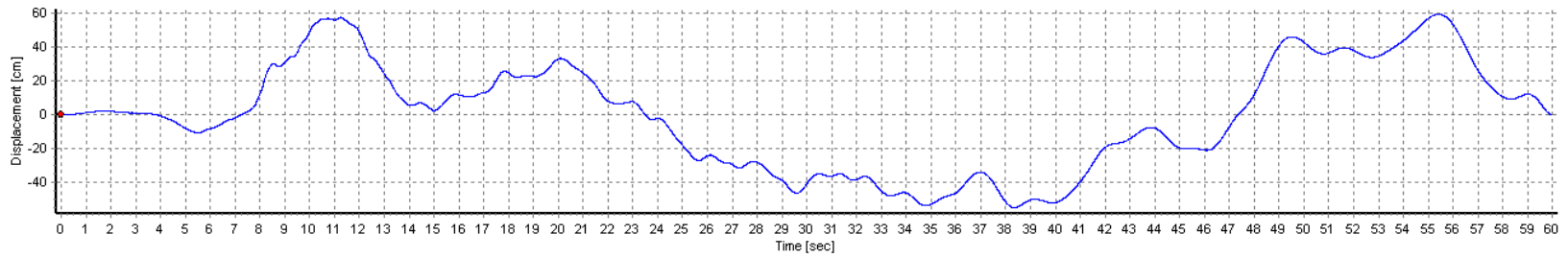
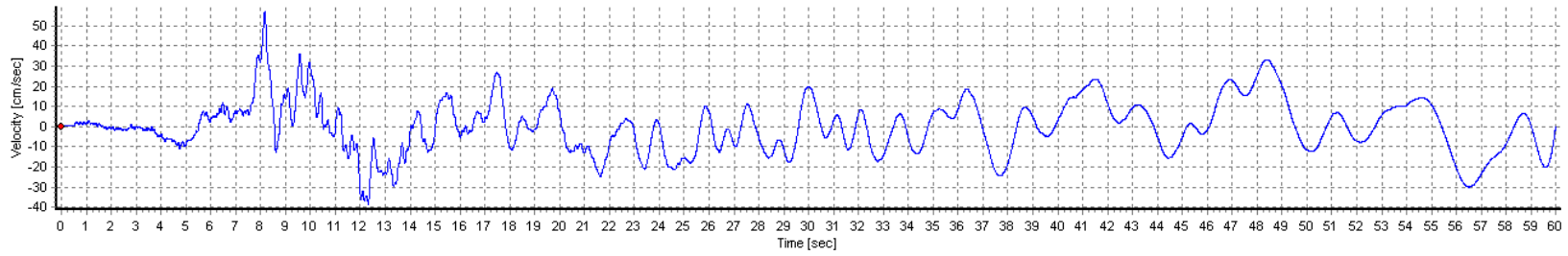
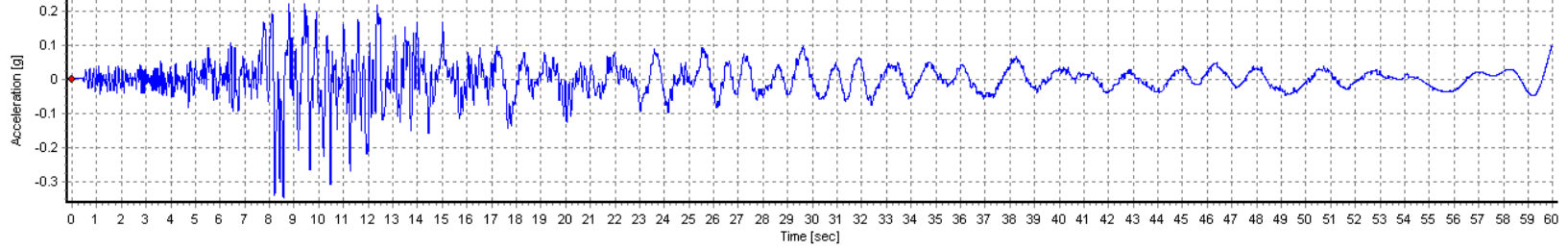


Figure A6-22. Spectrally-matched Time histories for Canal Ranch Tract – 2003 San Simeon, CA Earthquake at Point Buchon – Los Osos, 090 deg. Component

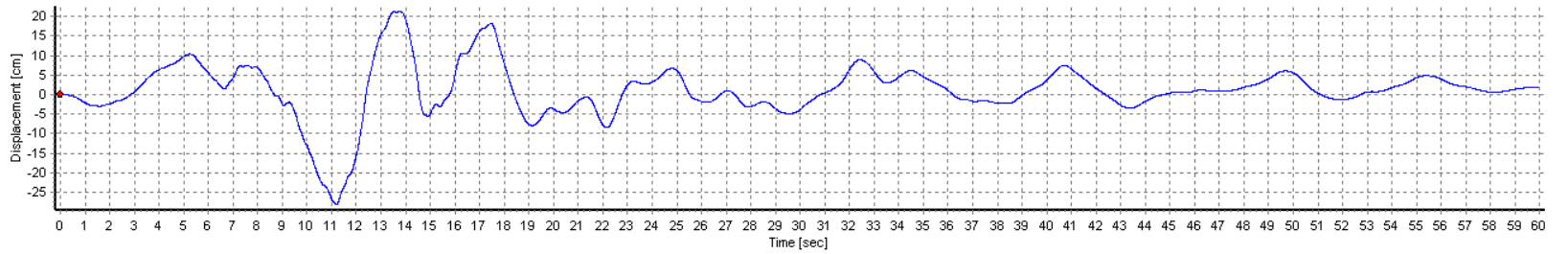
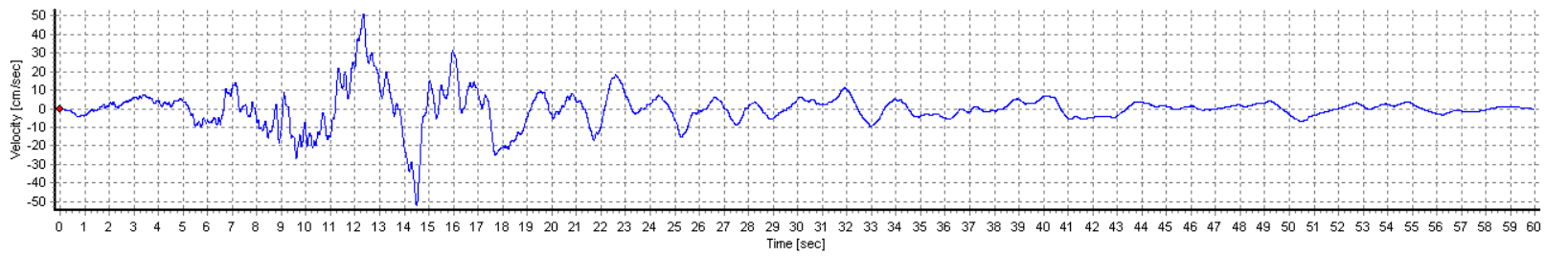
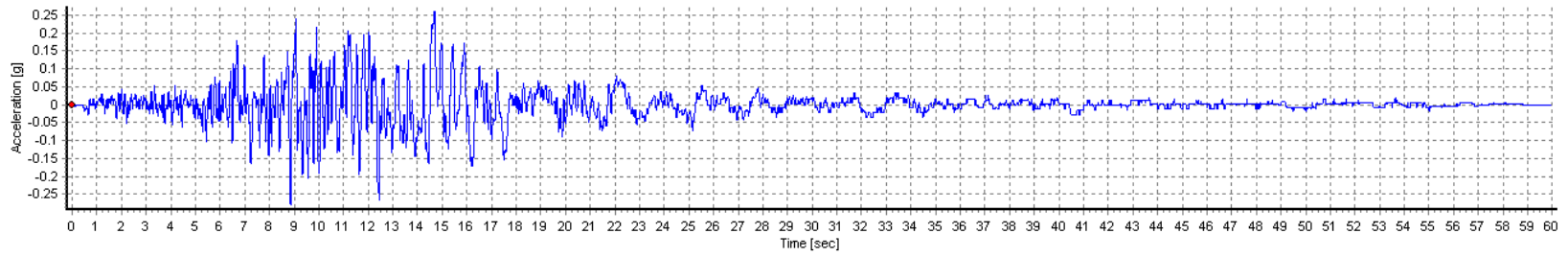


Figure A6-23. Seed Time histories for Canal Ranch Tract – 2003 San Simeon, CA Earthquake at Point Buchon – Los Osos, 360 deg. Component

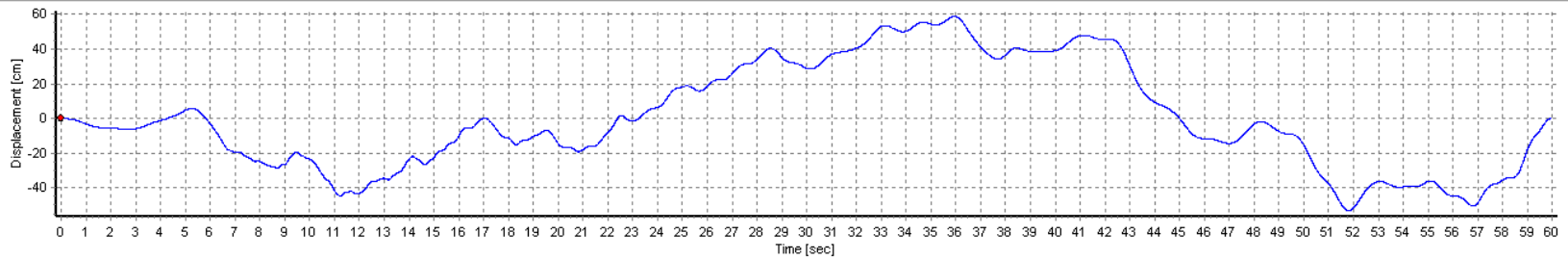
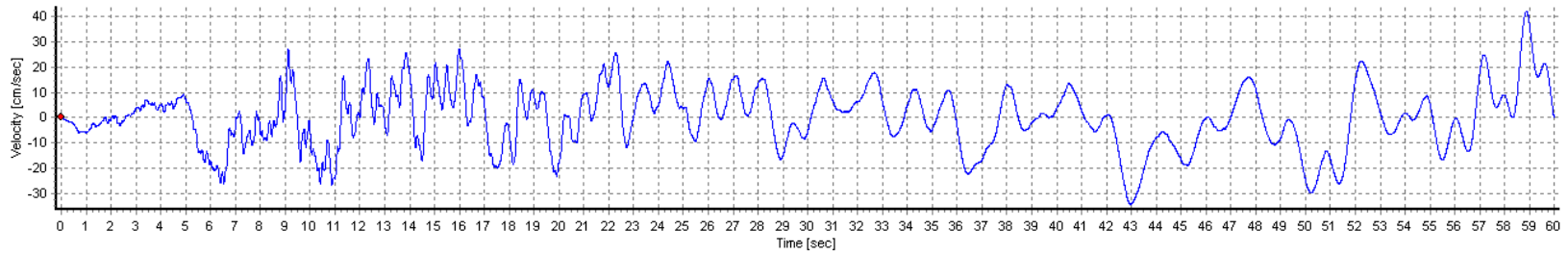
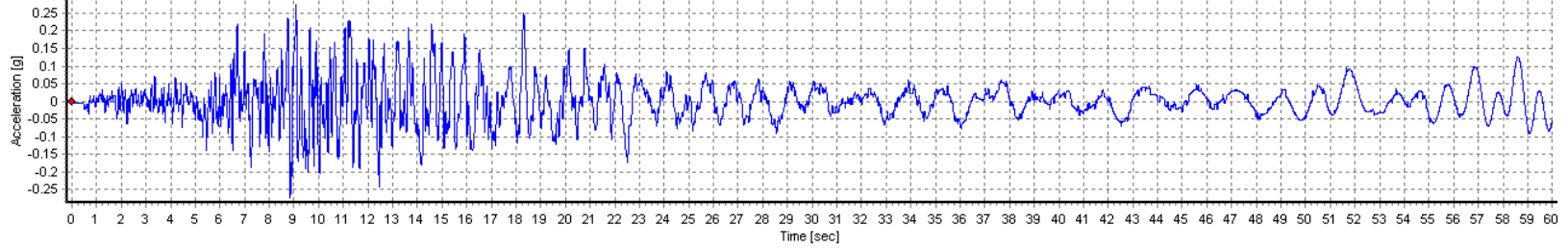


Figure A6-24. Spectrally-matched Time histories for Canal Ranch Tract – 2003 San Simeon, CA Earthquake at Point Buchon – Los Osos, 360 deg. Component

King Island

Seed Time Histories (Spectrally-matched time histories for Lower Roberts)											
RSN	Year	Earthquake Name	Station Name	Comp	Mag	ClstD (km)	Vs30 (m/s)	PGA (g)	PGV (cm/s)	PGD (cm)	AI (m/s)
812	1989	Loma Prieta	Woodside	000	6.9	34.1	454	0.38	53.7	35.6	2.73
812	1989	Loma Prieta	Woodside	090	6.9	34.1	454	0.43	76.9	53.3	2.65
1101	1995	Kobe, Japan	Amagasaki	000	6.9	11.3	256	0.37	51.2	37.7	2.53
1101	1995	Kobe, Japan	Amagasaki	090	6.9	11.3	256	0.46	60.6	41.5	2.91
1277	1999	Chi-Chi, Taiwan	HWA028	E	7.6	53.8	407	0.43	65.8	93.3	3.85
1277	1999	Chi-Chi, Taiwan	HWA028	N	7.6	53.8	407	0.37	51.1	49.4	3.51
Spectrally-matched Time Histories											
812	1989	Loma Prieta	Woodside	000	6.9	34.1	454	0.32	56.5	72.1	3.52
812	1989	Loma Prieta	Woodside	090	6.9	34.1	454	0.33	65.1	67.1	3.42
1101	1995	Kobe, Japan	Amagasaki	000	6.9	11.3	256	0.39	53.8	51.4	2.92
1101	1995	Kobe, Japan	Amagasaki	090	6.9	11.3	256	0.36	76.1	108.5	3.25
1277	1999	Chi-Chi, Taiwan	HWA028	E	7.6	53.8	407	0.36	52.3	69.7	3.64
1277	1999	Chi-Chi, Taiwan	HWA028	N	7.6	53.8	407	0.36	43.2	36.9	3.62

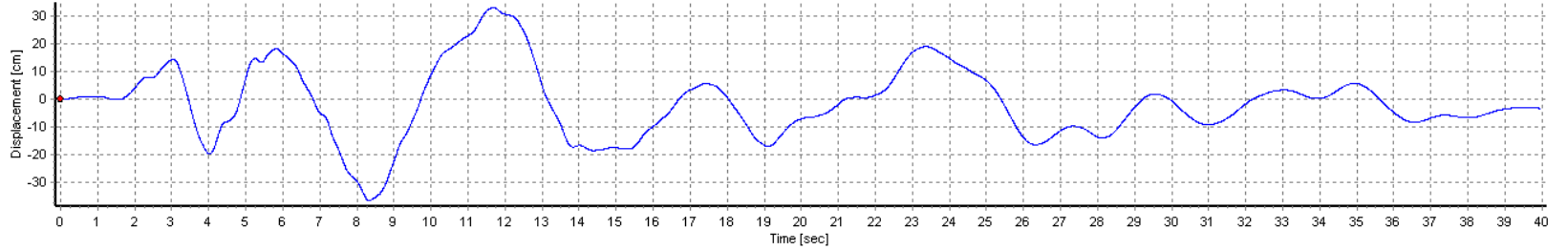
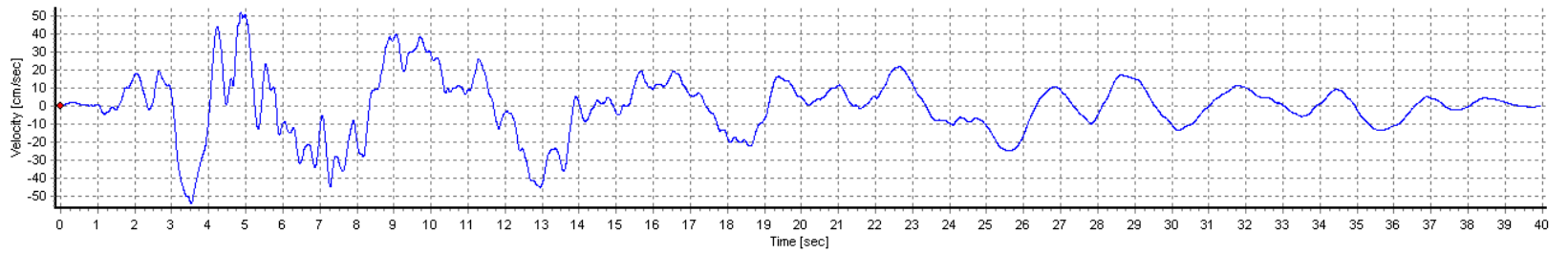
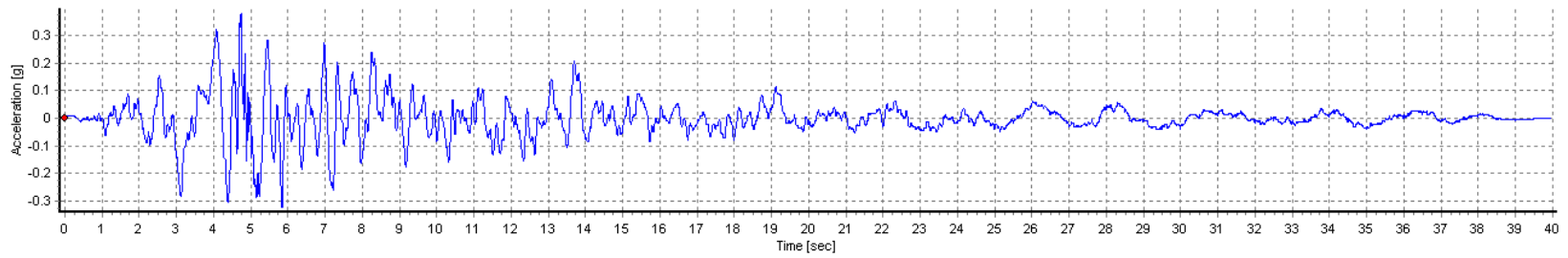


Figure A6-25. Seed Time histories for King Island – 1989 Loma Prieta Earthquake at Woodside, 0 deg. Component

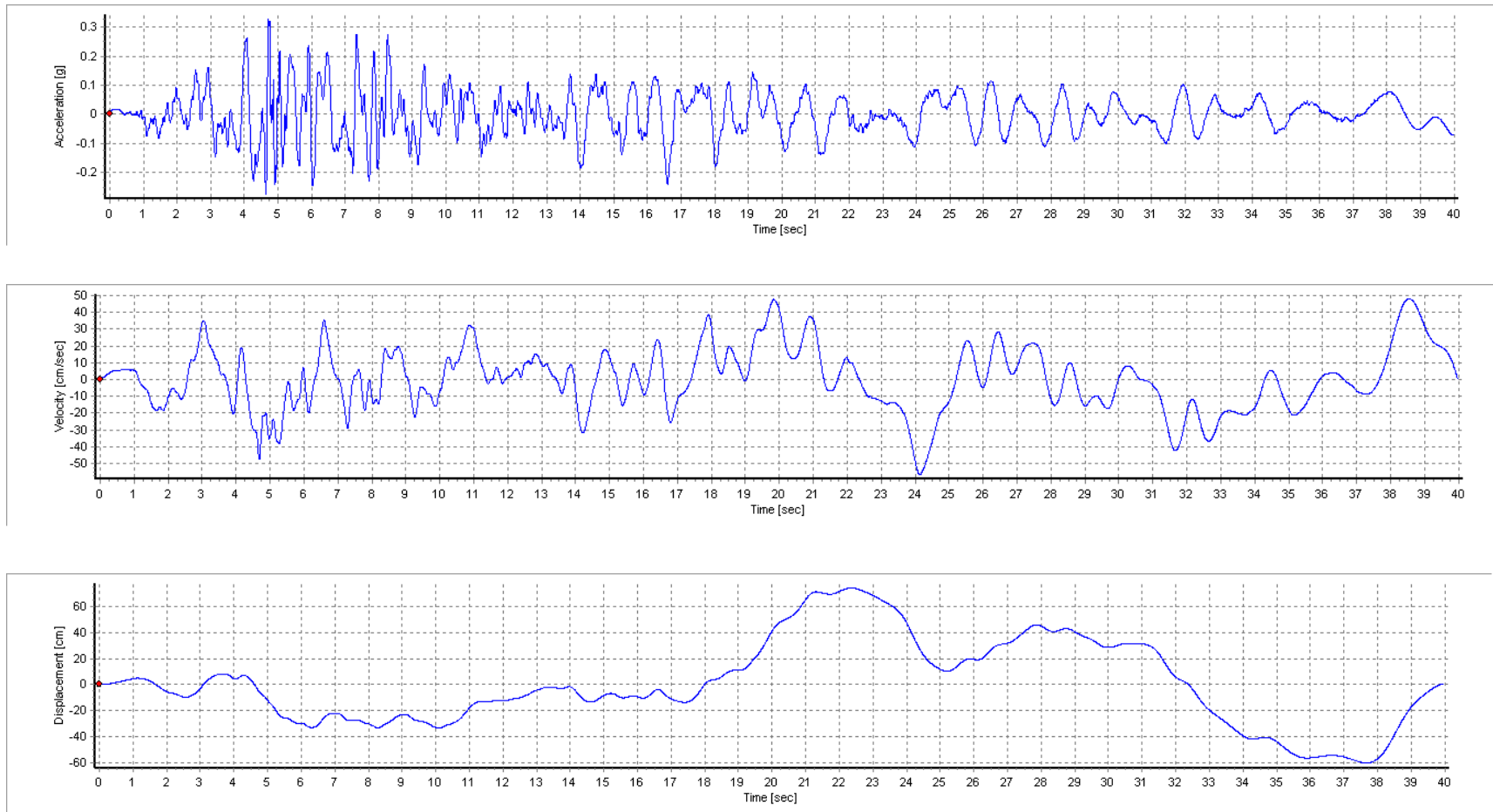


Figure A6-26. Spectrally-matched Time histories for King Island – 1989 Loma Prieta Earthquake at Woodside, 0 deg. Component

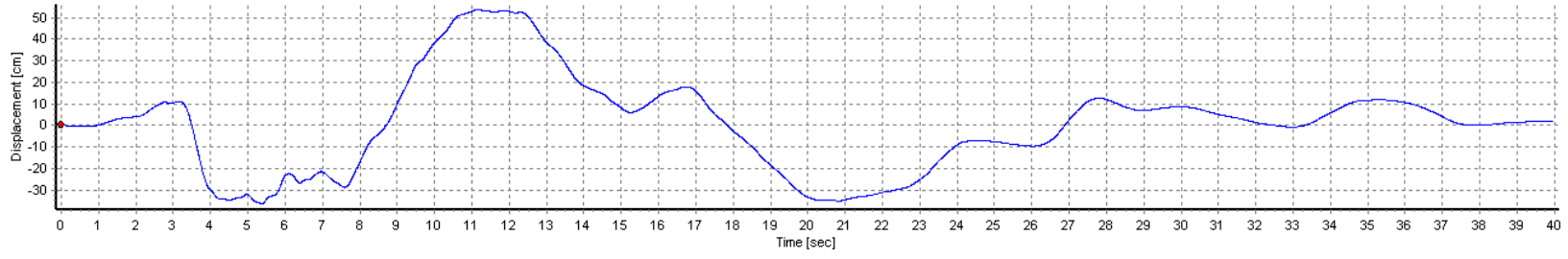
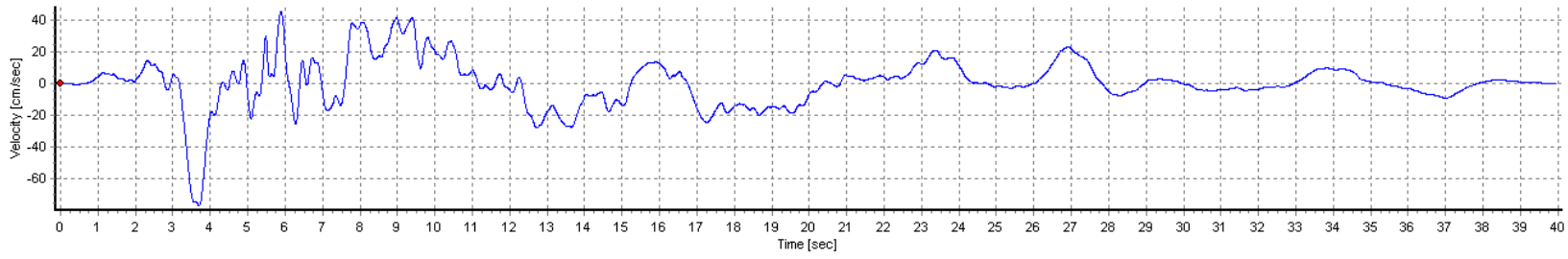
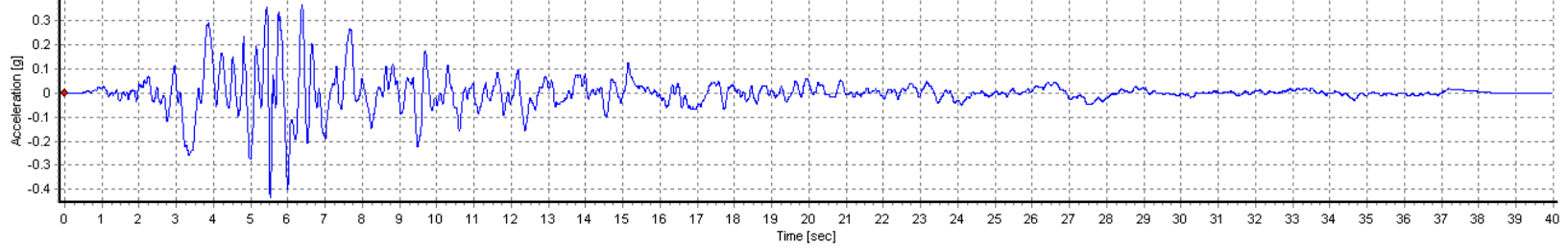


Figure A6-27. Seed Time histories for King Island – 1989 Loma Prieta Earthquake at Woodside, 90 deg. Component

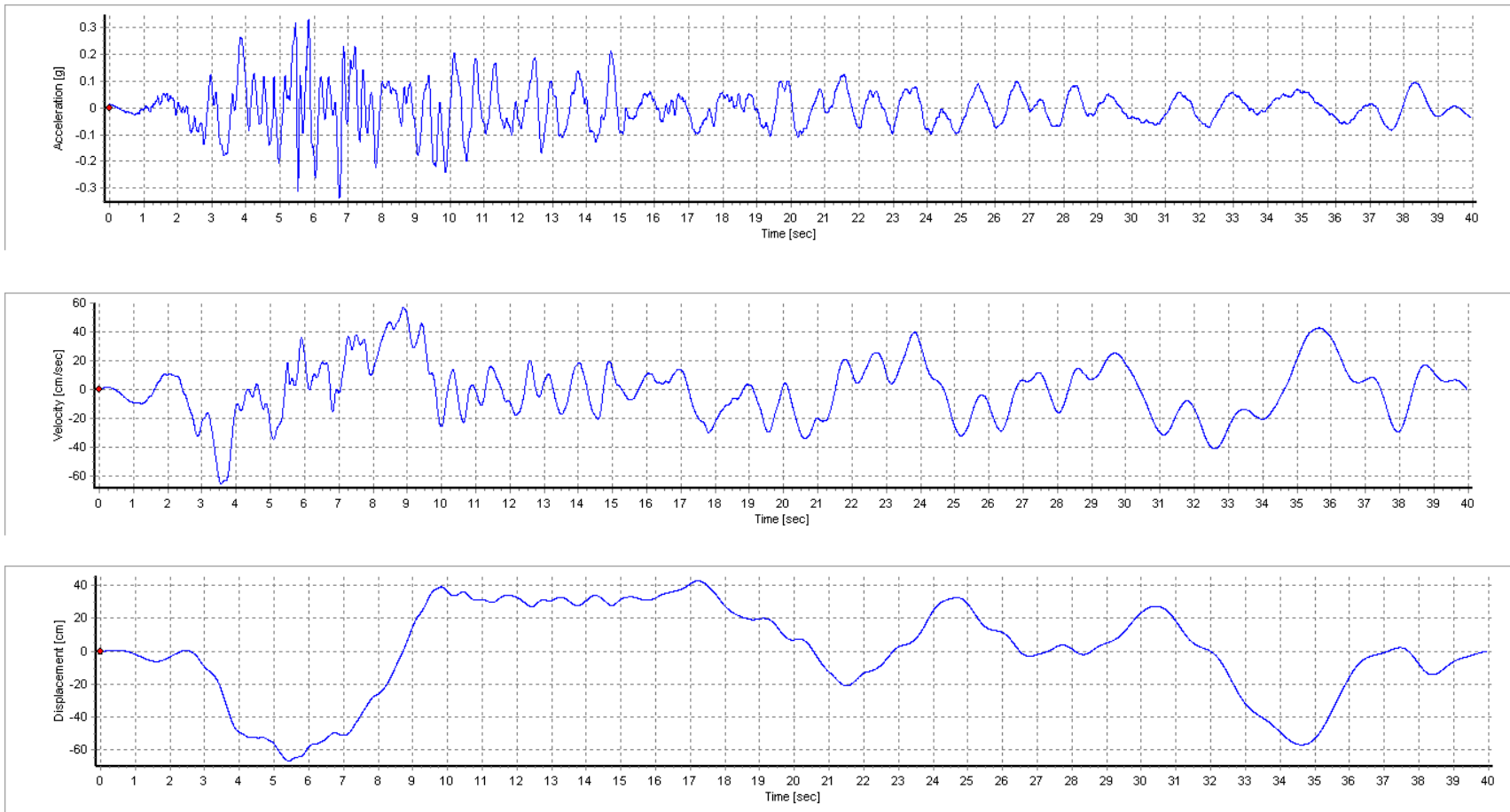


Figure A6-28. Spectrally-matched Time histories for King Island – 1989 Loma Prieta Earthquake at Woodside, 90 deg. Component

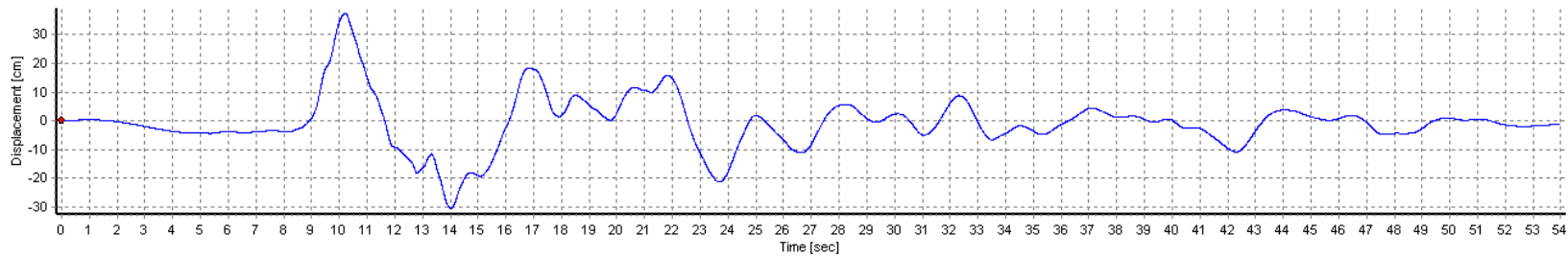
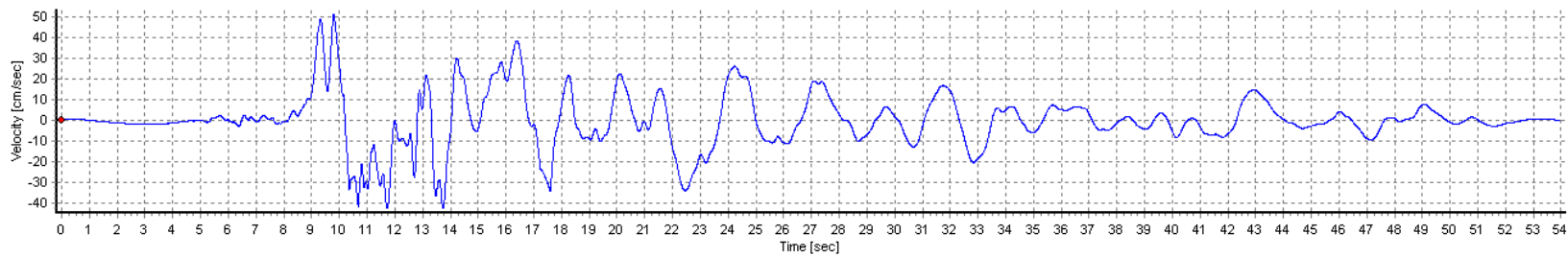
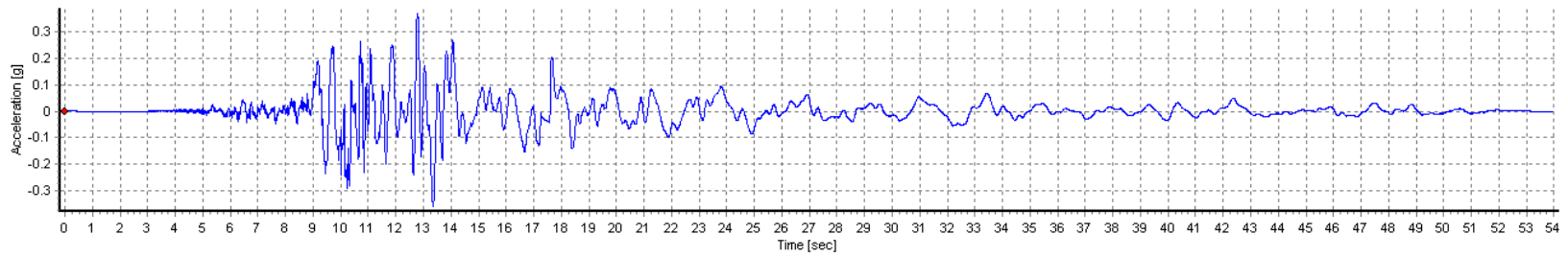


Figure A6-29. Seed Time histories for King Island – 1995 Kobe, Japan Earthquake at Amagasaki, 0 deg. Component

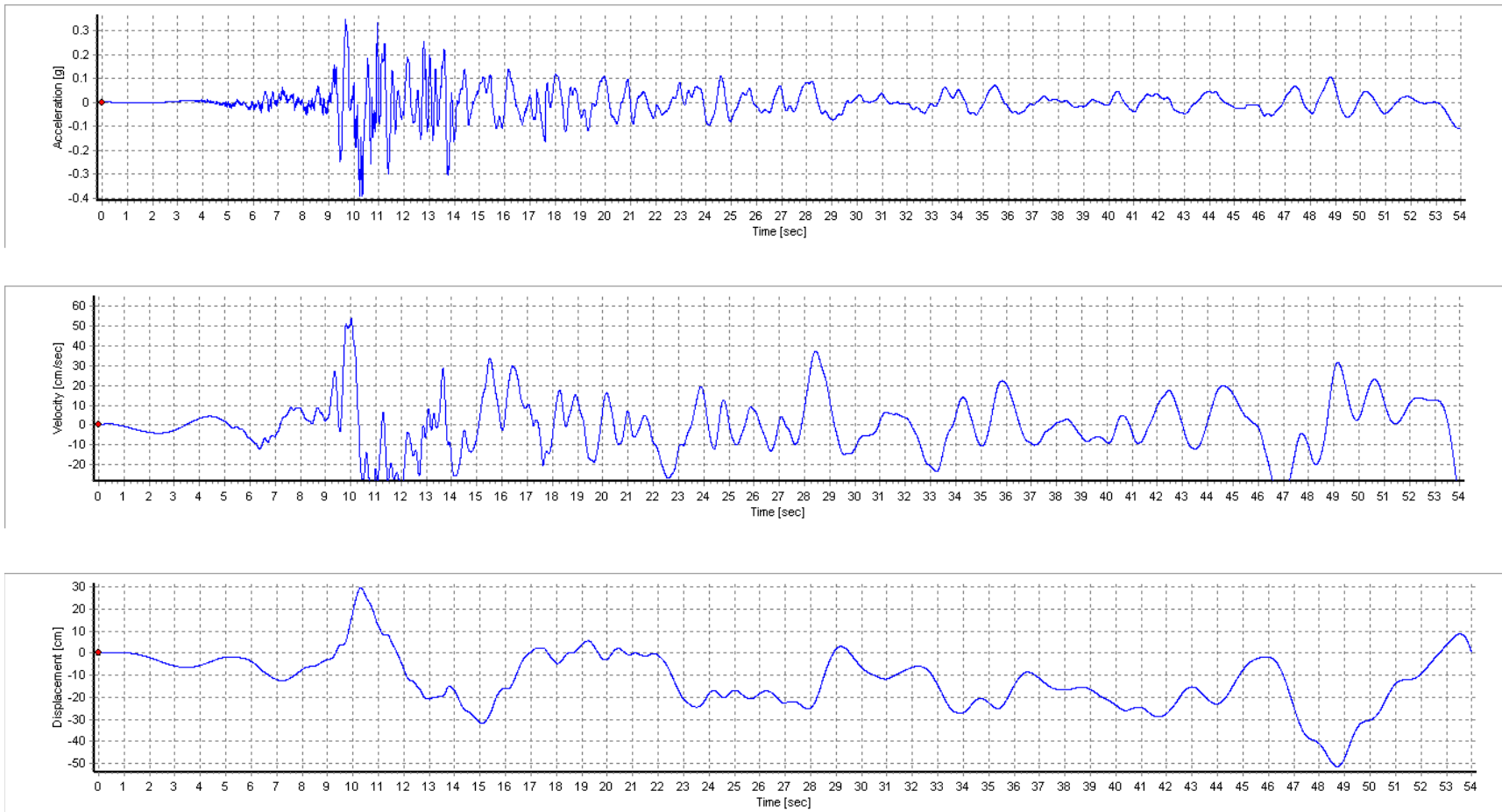


Figure A6-30. Spectrally-matched Time histories for King Island – 1995 Kobe, Japan Earthquake at Amagasaki, 0 deg. Component

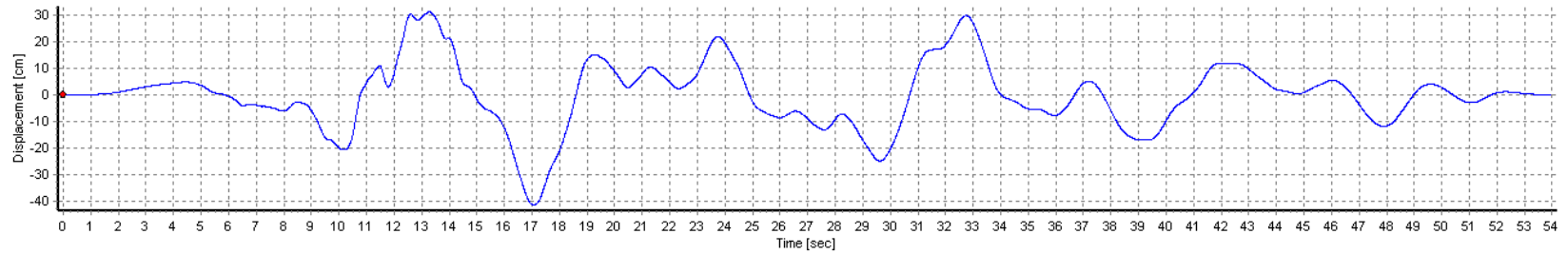
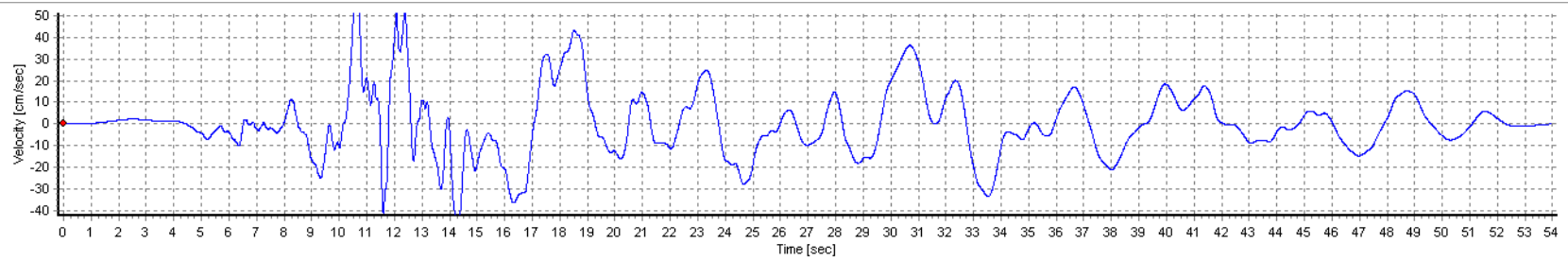
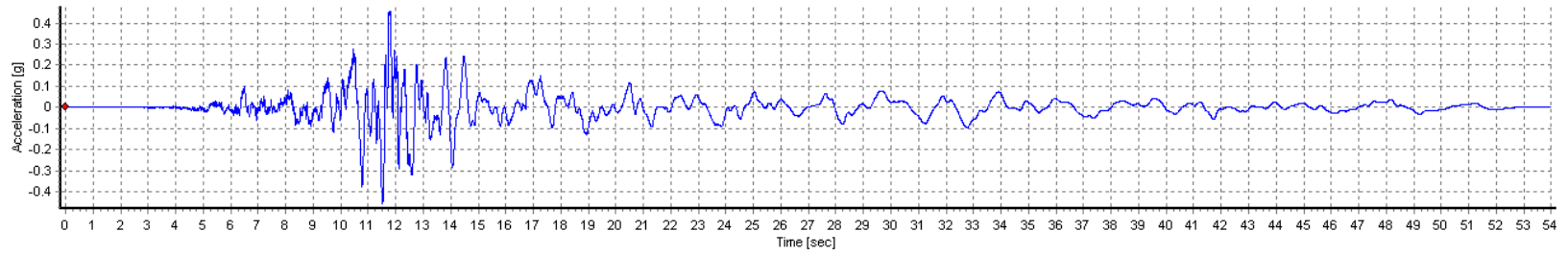


Figure A6-31. Seed Time histories for King Island – 1995 Kobe, Japan Earthquake at Amagasaki, 90 deg. Component

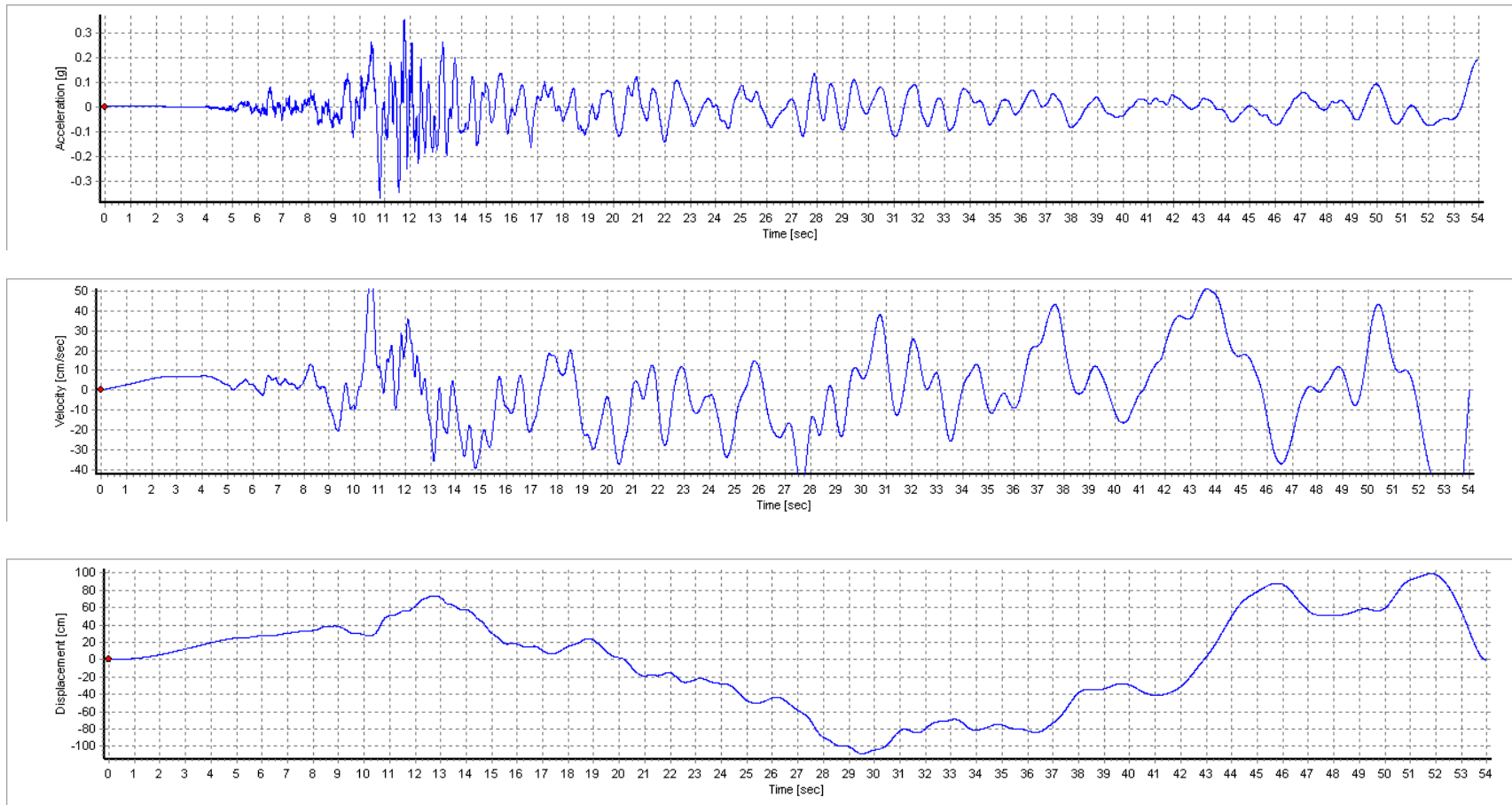


Figure A6-32. Spectrally-matched Time histories for King Island – 1995 Kobe, Japan Earthquake at Amagasaki, 90 deg. Component

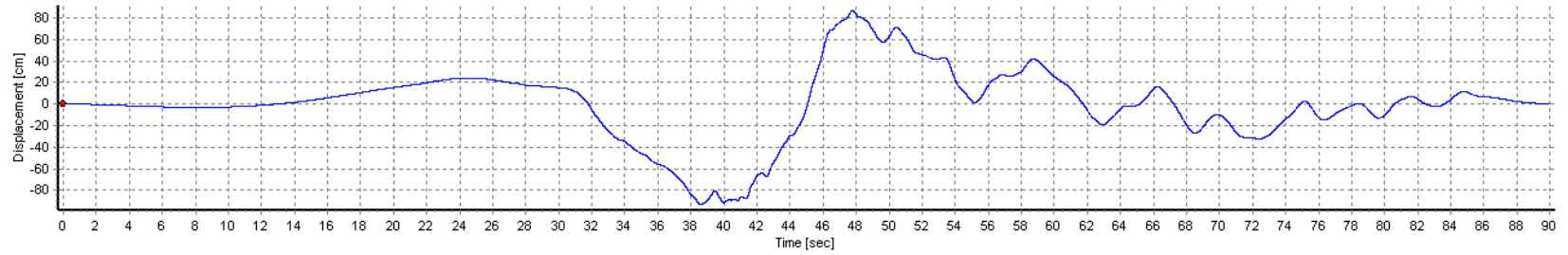
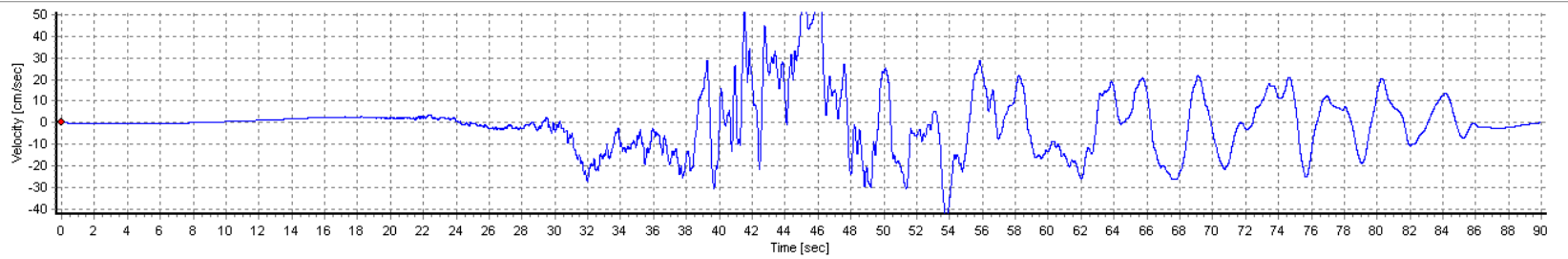
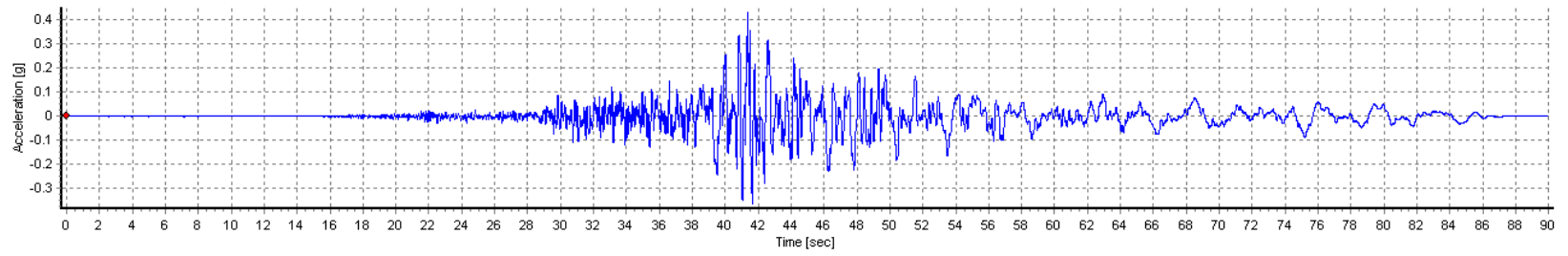


Figure A6-33. Seed Time histories for King Island – 1999 Chi-Chi, Taiwan Earthquake at HWA028, East Component

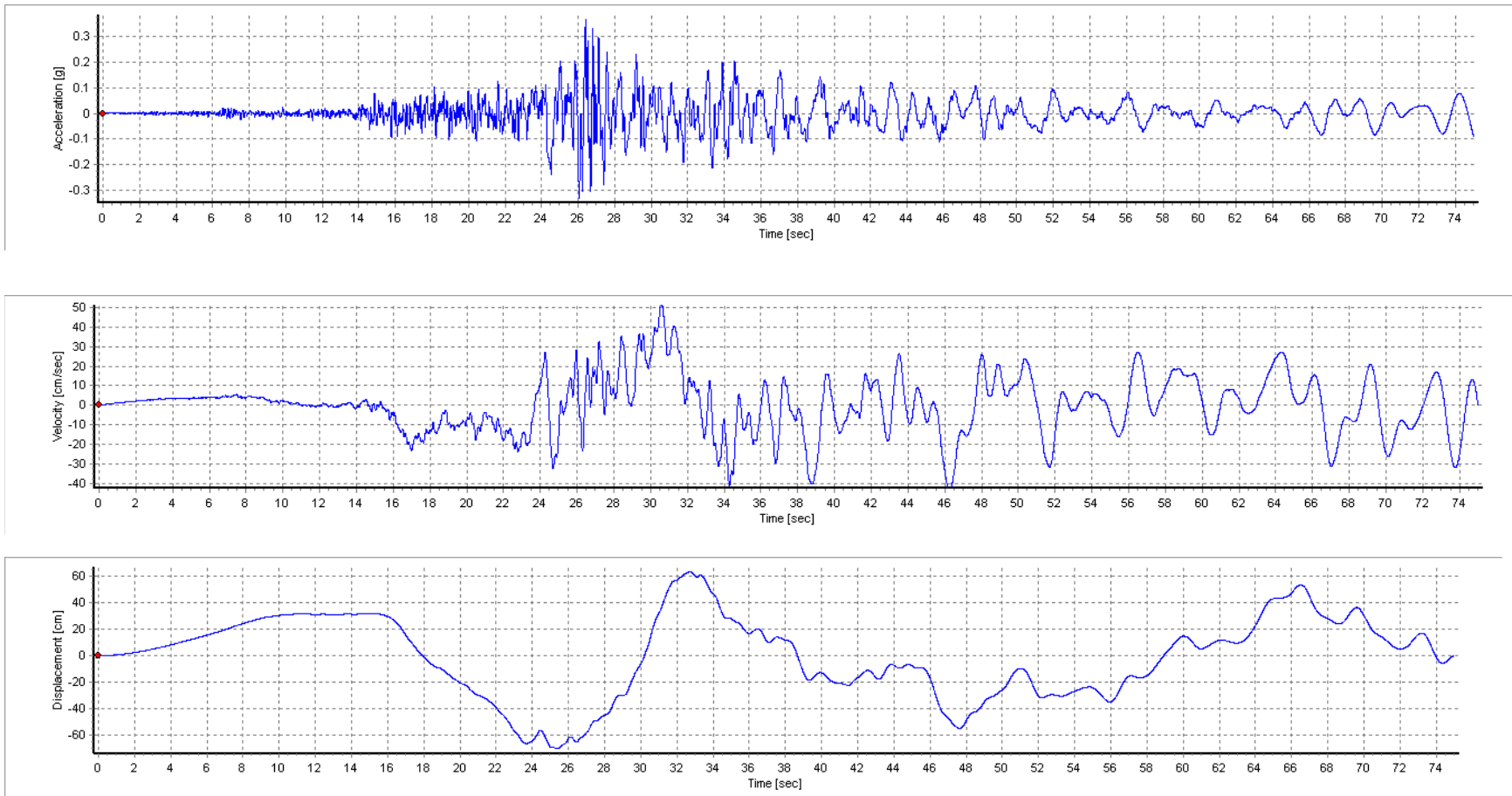


Figure A6-34. Spectrally-matched Time histories for King Island – 1999 Chi-Chi, Taiwan Earthquake at HWA028, East Component

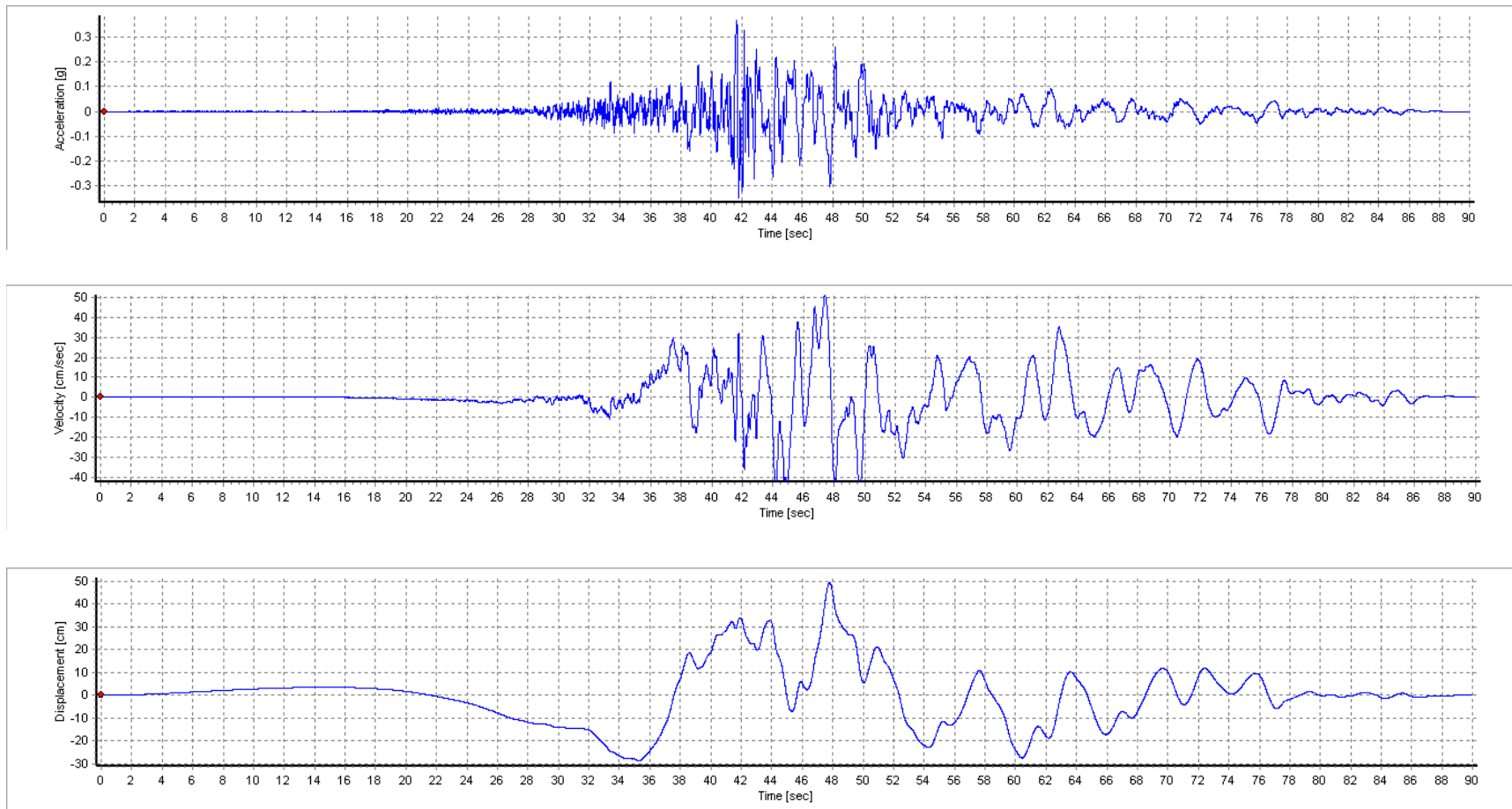


Figure A6-35. Seed Time histories for King Island – 1999 Chi-Chi, Taiwan Earthquake at HWA028, North Component

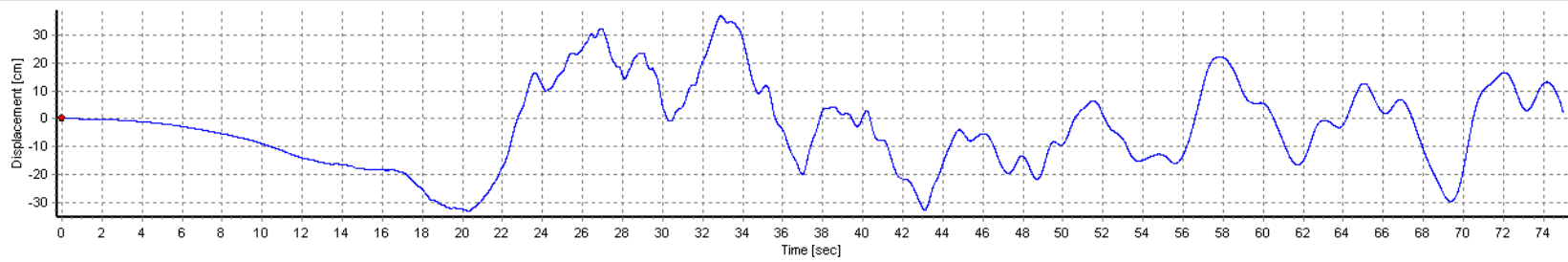
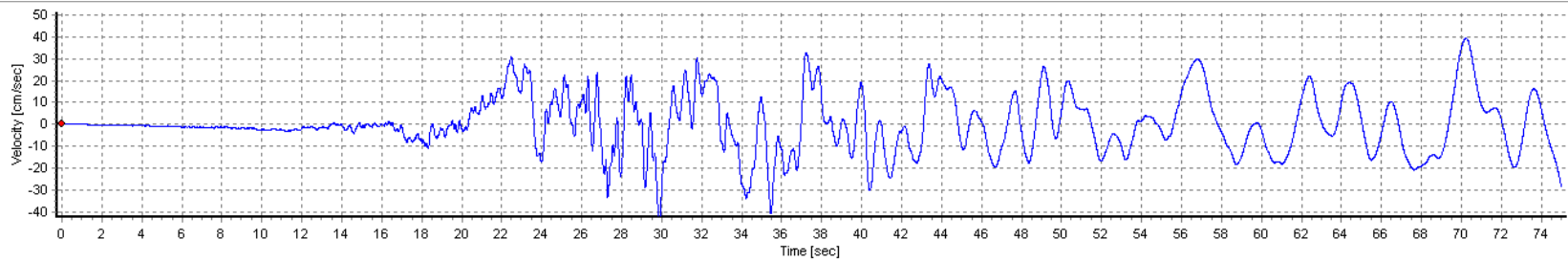
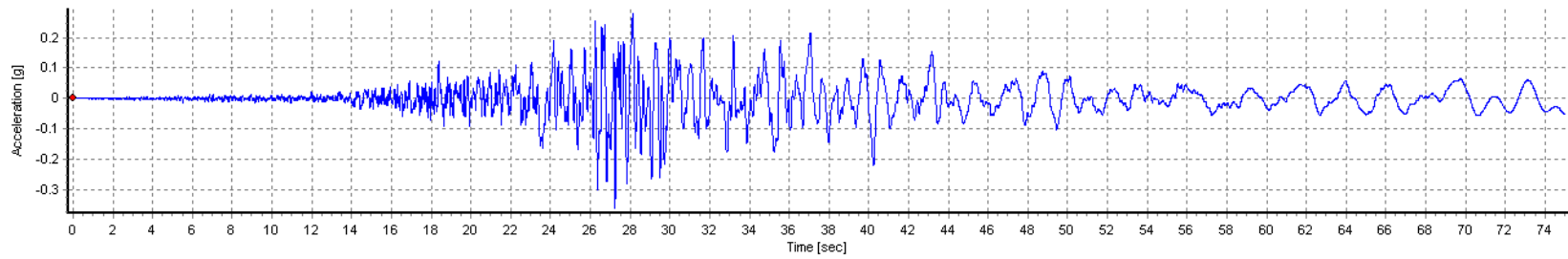


Figure A6-36. Spectrally-matched Time histories for King Island – 1999 Chi-Chi, Taiwan Earthquake at HWA028, North Component

Union Island

Seed Time Histories ((Spectrally-matched time histories for Southern Forebay-North)											
RSN	Year	Earthquake Name	Station Name	Comp	Mag	ClstD (km)	Vs30 (m/s)	PGA (g)	PGV (cm/s)	PGD (cm)	AI (m/s)
778	1989	Loma Prieta	Hollister Differential Array	165	6.9	24.8	216	0.74	159.2	94.1	9.38
778	1989	Loma Prieta	Hollister Differential Array	255	6.9	24.8	216	0.83	128.5	56.8	10.33
821	1992	Erzican, Turkey	Erzincan	NS	6.7	4.4	352	0.74	246.5	94.6	8.45
821	1992	Erzican, Turkey	Erzincan	EW	6.7	4.4	352	0.86	180.3	76.8	8.26
1605	1999	Duzce, Turkey	Duzce	180	7.1	6.6	282	0.63	136.2	69.5	9.99
1605	1999	Duzce, Turkey	Duzce	270	7.1	6.6	282	0.78	171.4	91.9	13.37
Spectrally-matched Time Histories											
778	1989	Loma Prieta	Hollister Differential Array	165	6.9	24.8	216				
778	1989	Loma Prieta	Hollister Differential Array	255	6.9	24.8	216	0.72	105.7	97.1	8.88
821	1992	Erzican, Turkey	Erzincan	NS	6.7	4.4	352	0.77	138.2	63.5	5.79
821	1992	Erzican, Turkey	Erzincan	EW	6.7	4.4	352	0.72	144.0	48.6	5.72
1605	1999	Duzce, Turkey	Duzce	180	7.1	6.6	282	0.71	101.5	109.0	10.8
1605	1999	Duzce, Turkey	Duzce	270	7.1	6.6	282	0.89	92.9	72.2	9.4

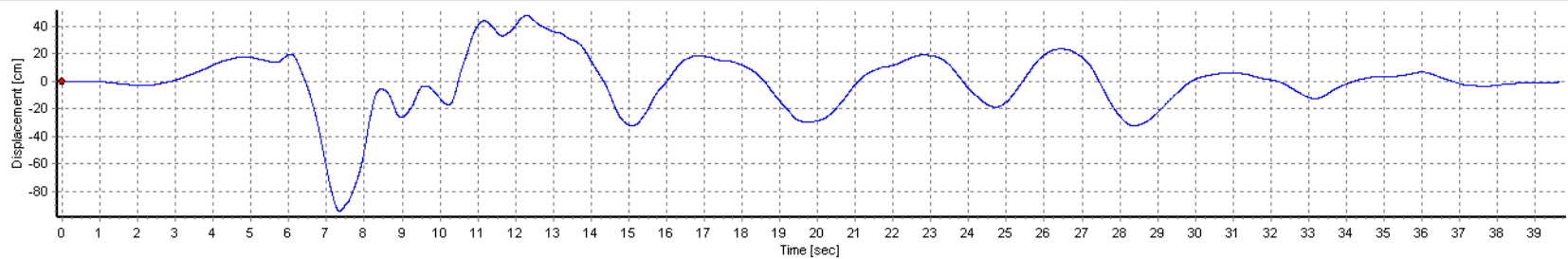
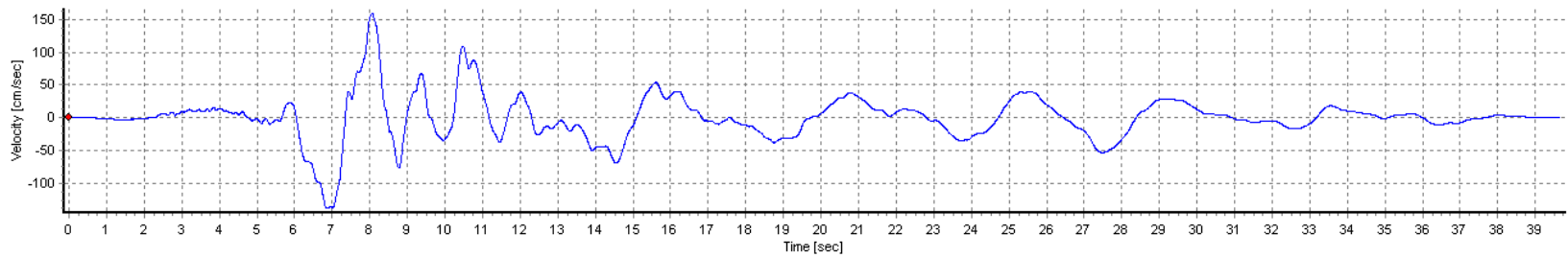
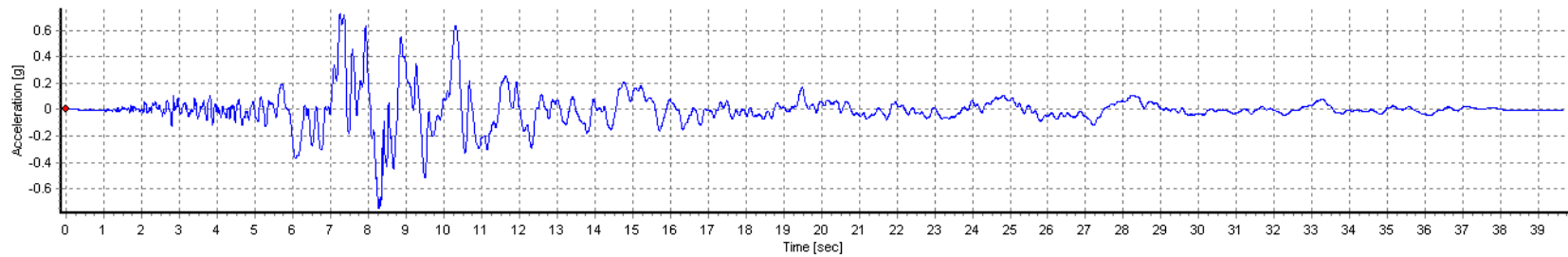


Figure A6-85. Seed Time histories for Union Island – 1989 Loma Prieta Earthquake at Hollister Differential Array, 165 deg. Component

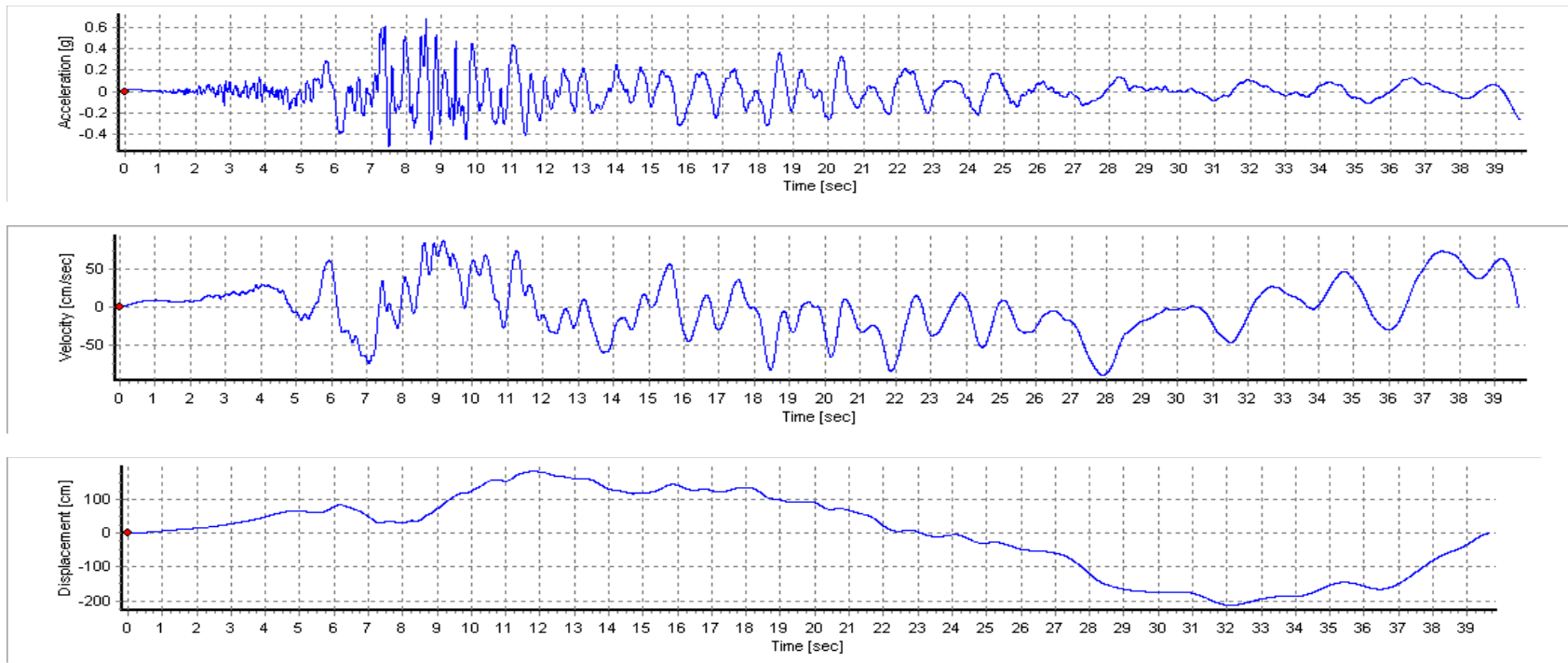


Figure A6-86. Spectrally-matched Time histories for Union Island – 1989 Loma Prieta Earthquake at Hollister Differential Array, 165 deg. Component

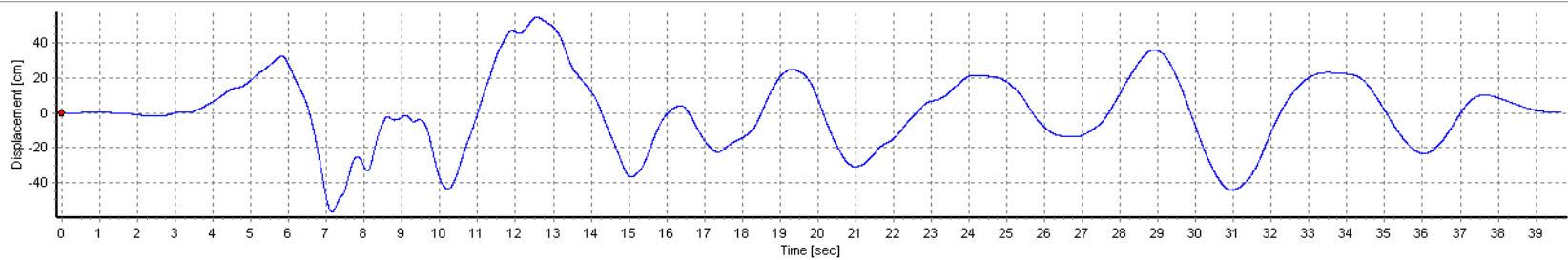
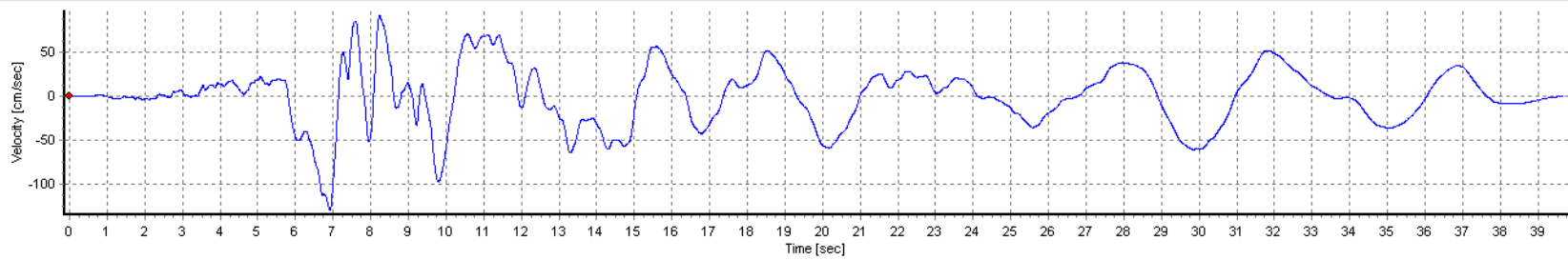
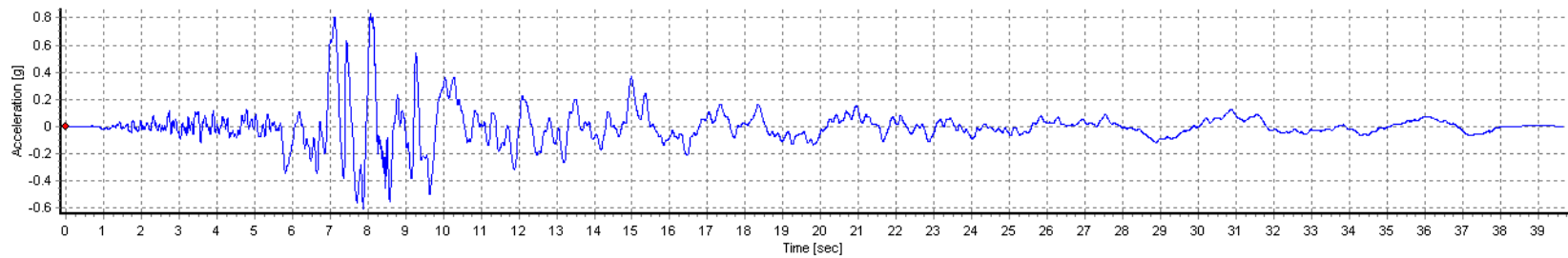


Figure A6-87. Seed Time histories for Union Island – 1989 Loma Prieta Earthquake at Hollister Differential Array, 255 deg. Component

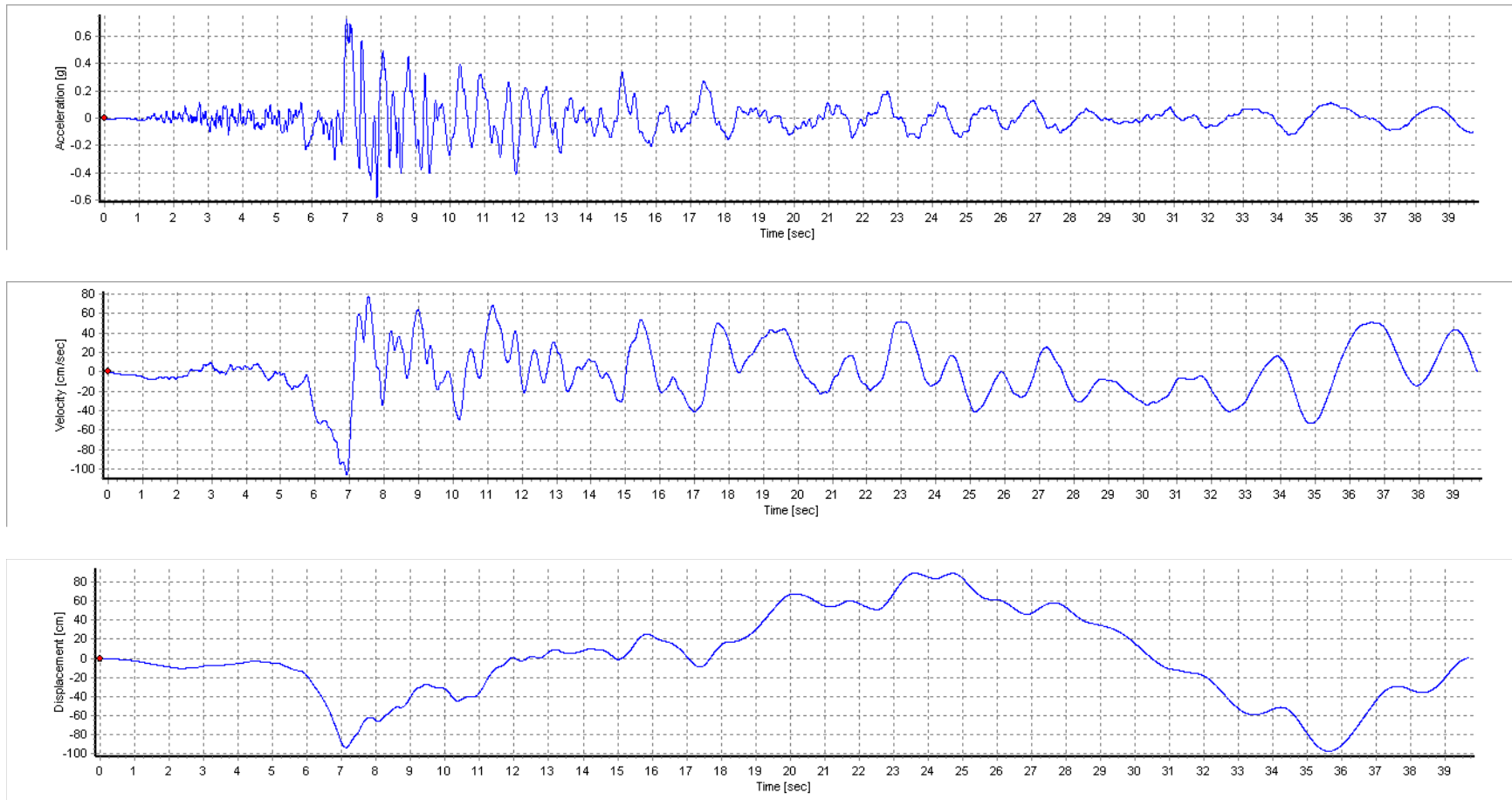


Figure A6-88. Spectrally-matched Time histories for Union Island – 1989 Loma Prieta Earthquake at Hollister Differential Array, 255 deg. Component

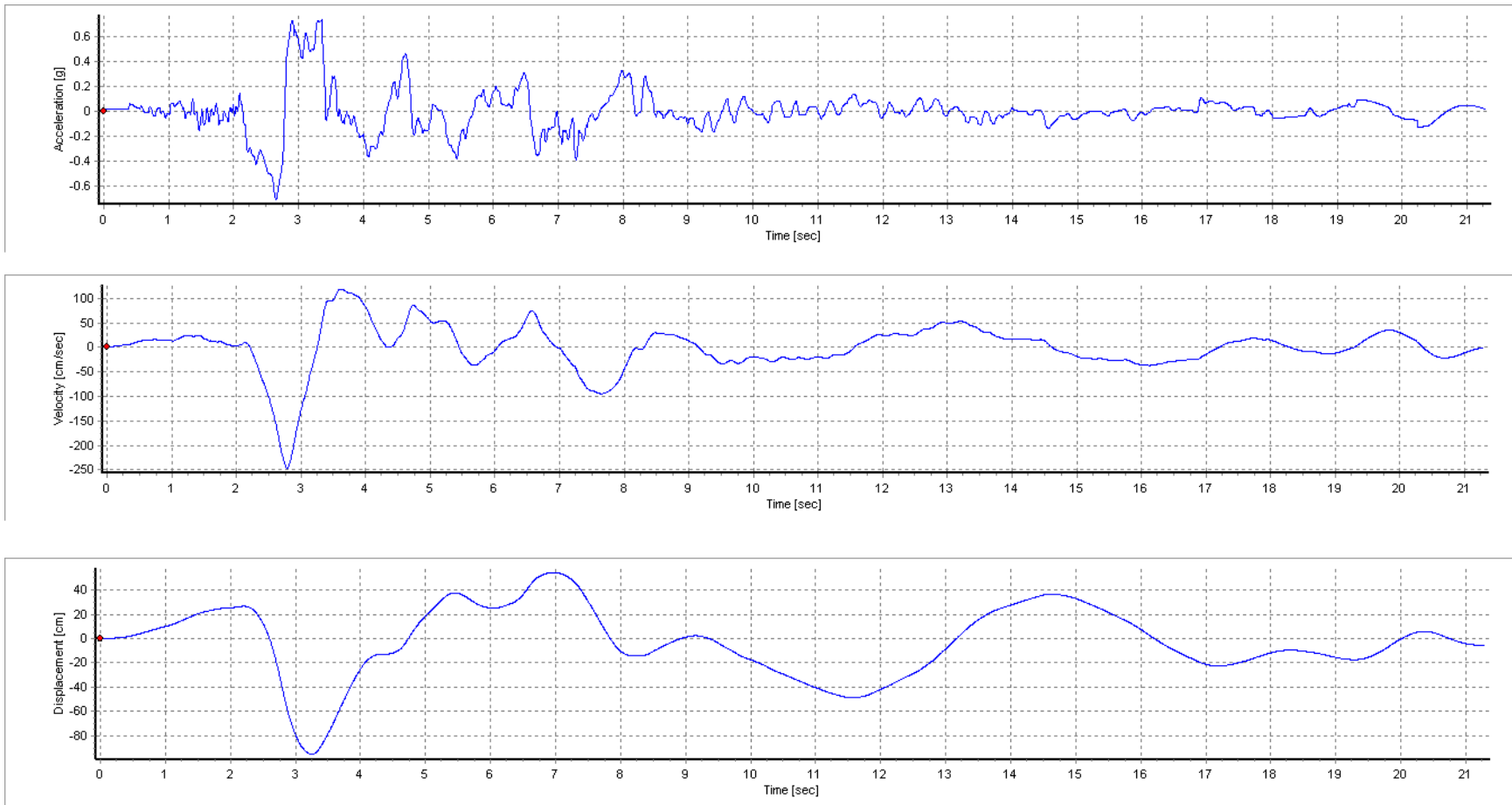


Figure A6-89. Seed Time histories for Union Island– 1992 Erzican, Turkey Earthquake at Erzincan, NS Component

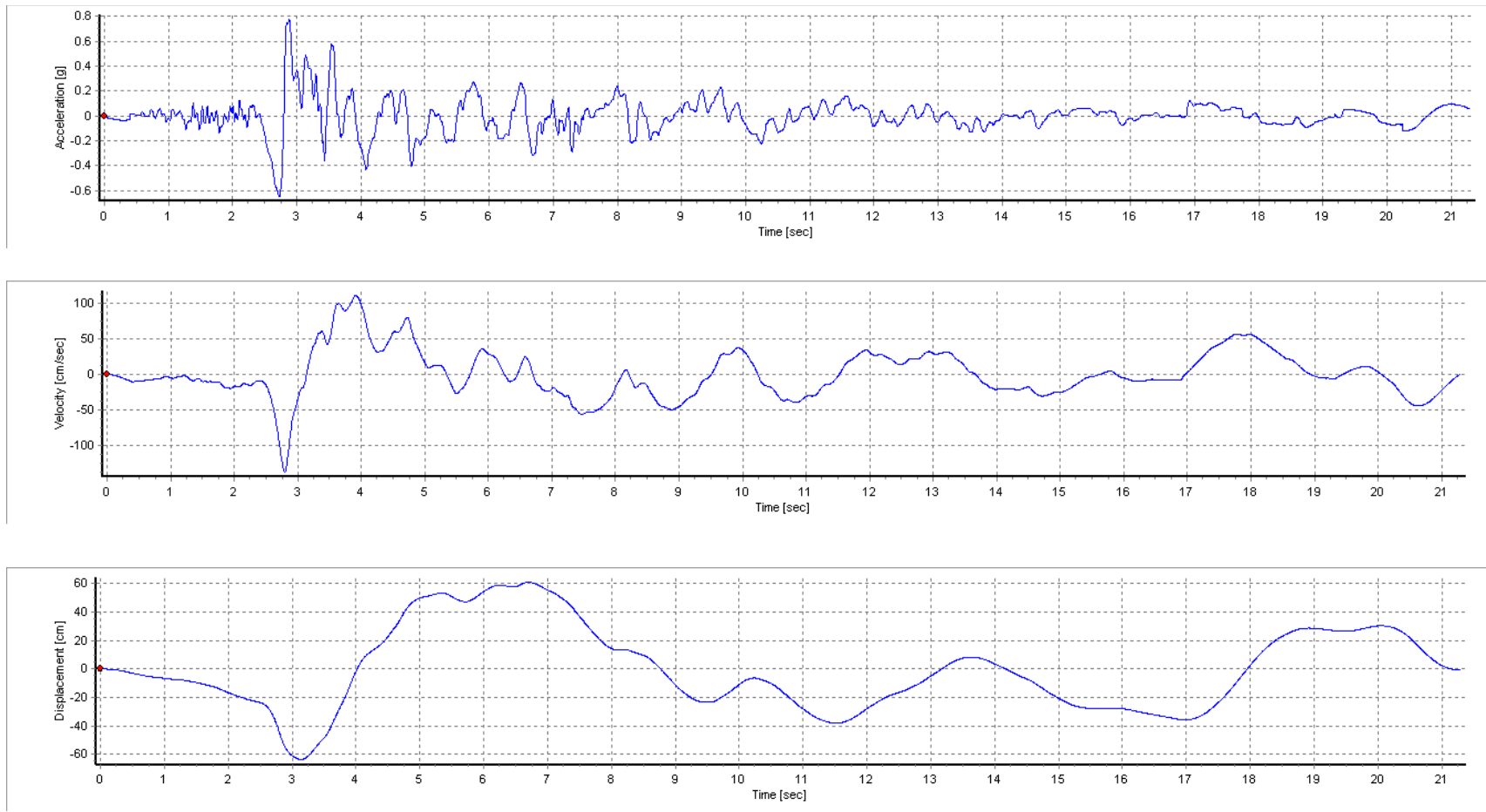


Figure A6-90. Spectrally-matched Time histories for Union Island – 1992 Erzincan, Turkey Earthquake at Erzincan, NS Component

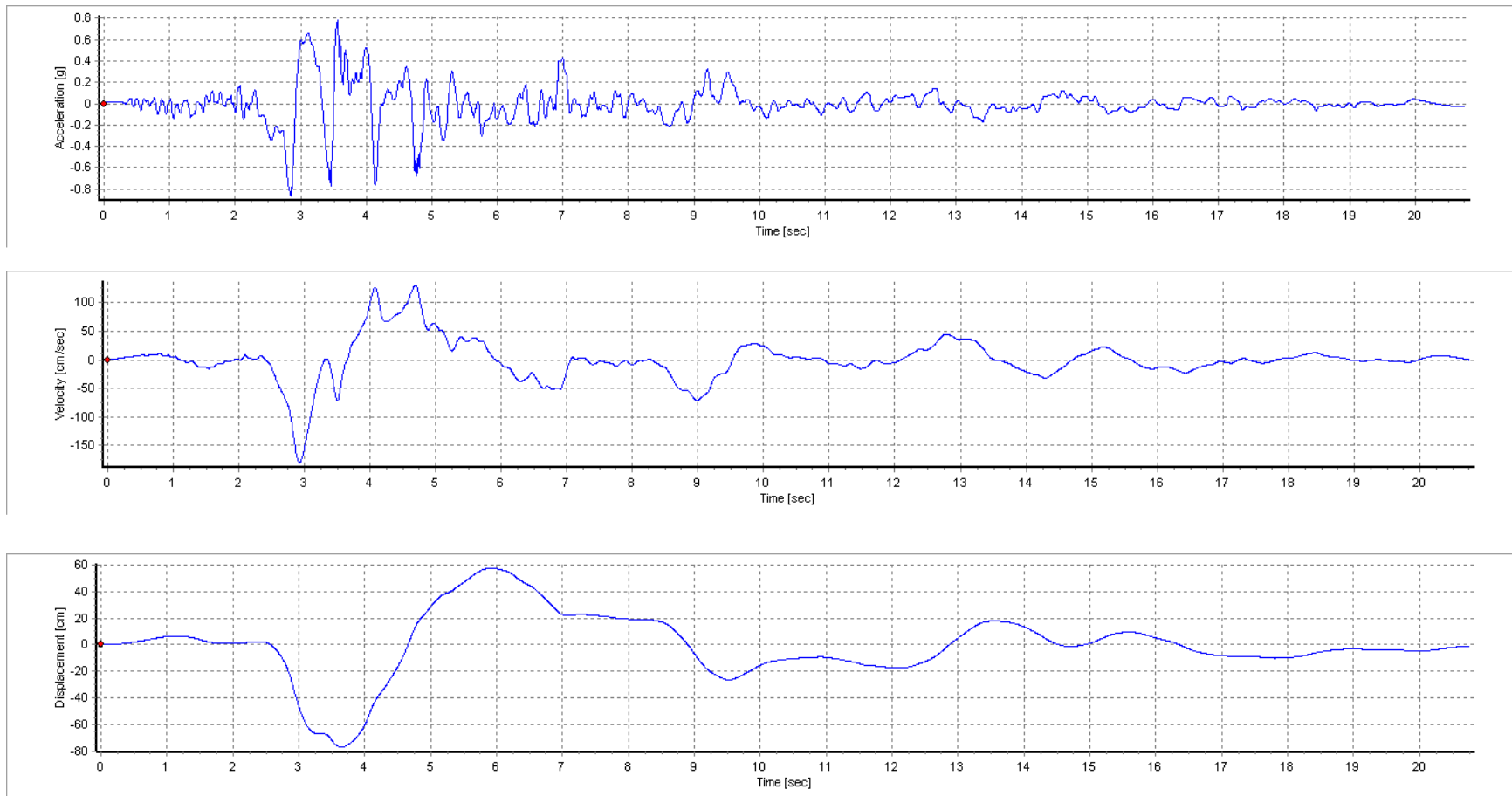


Figure A6-91. Seed Time histories for Union Island – 1992 Erzican, Turkey Earthquake at Erzincan, EW Component

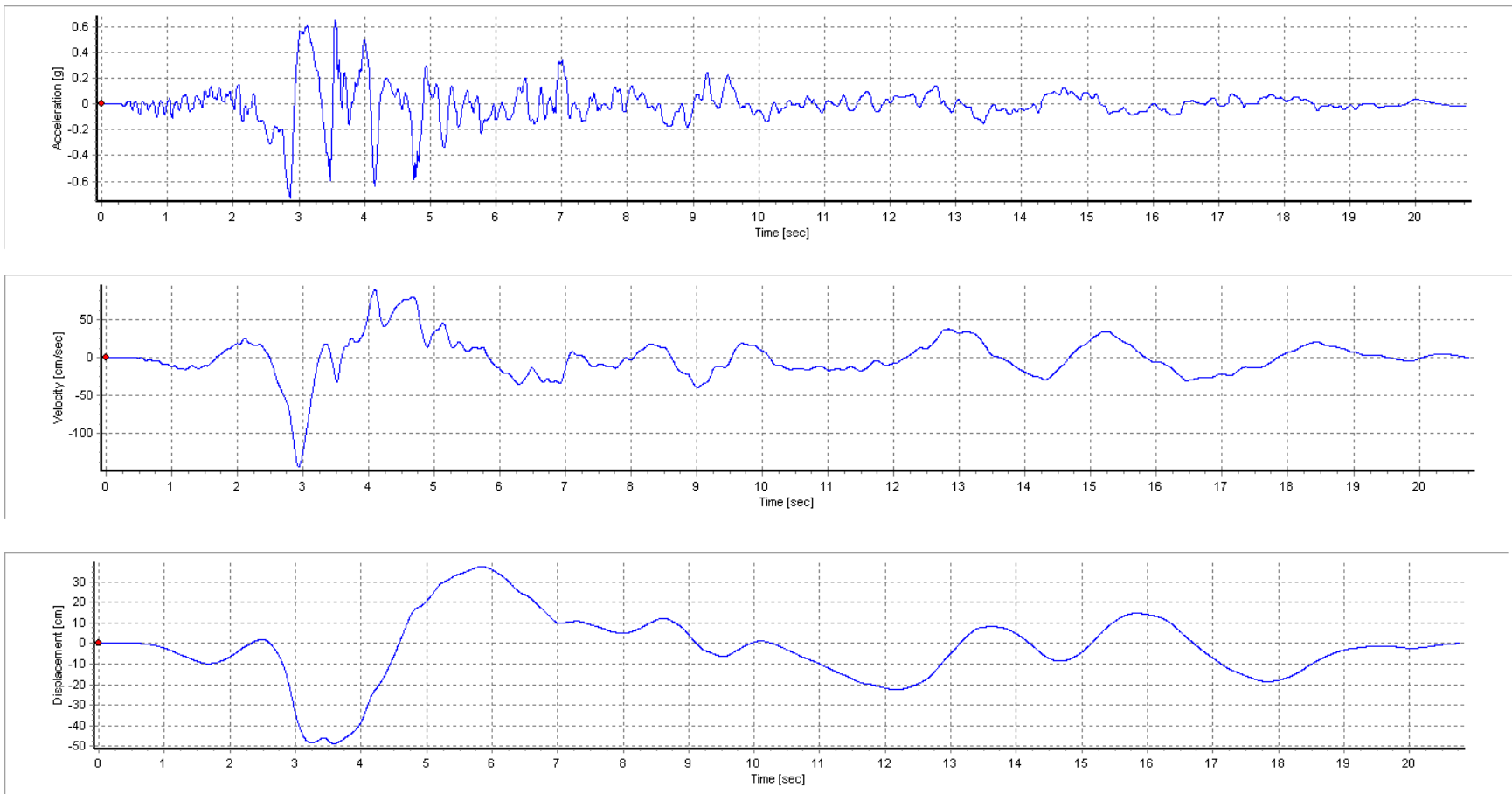


Figure A6-92. Spectrally-matched Time histories for Union Island – 1992 Erzican, Turkey Earthquake at Erzincan, EW Component

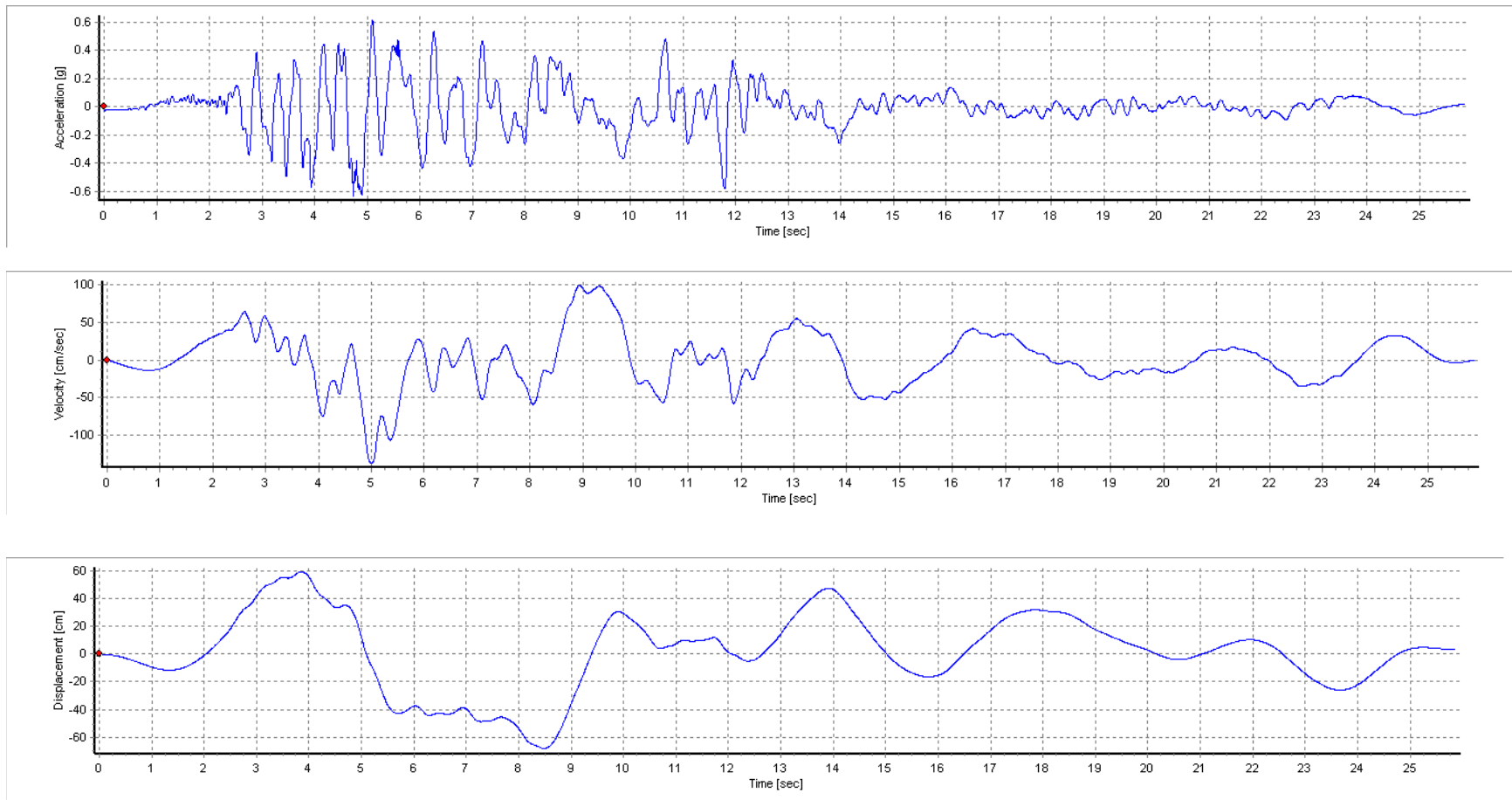


Figure A6-93. Seed Time histories for Union Island – 1999 Duzce, Turkey Earthquake at Duzce, 180 Component

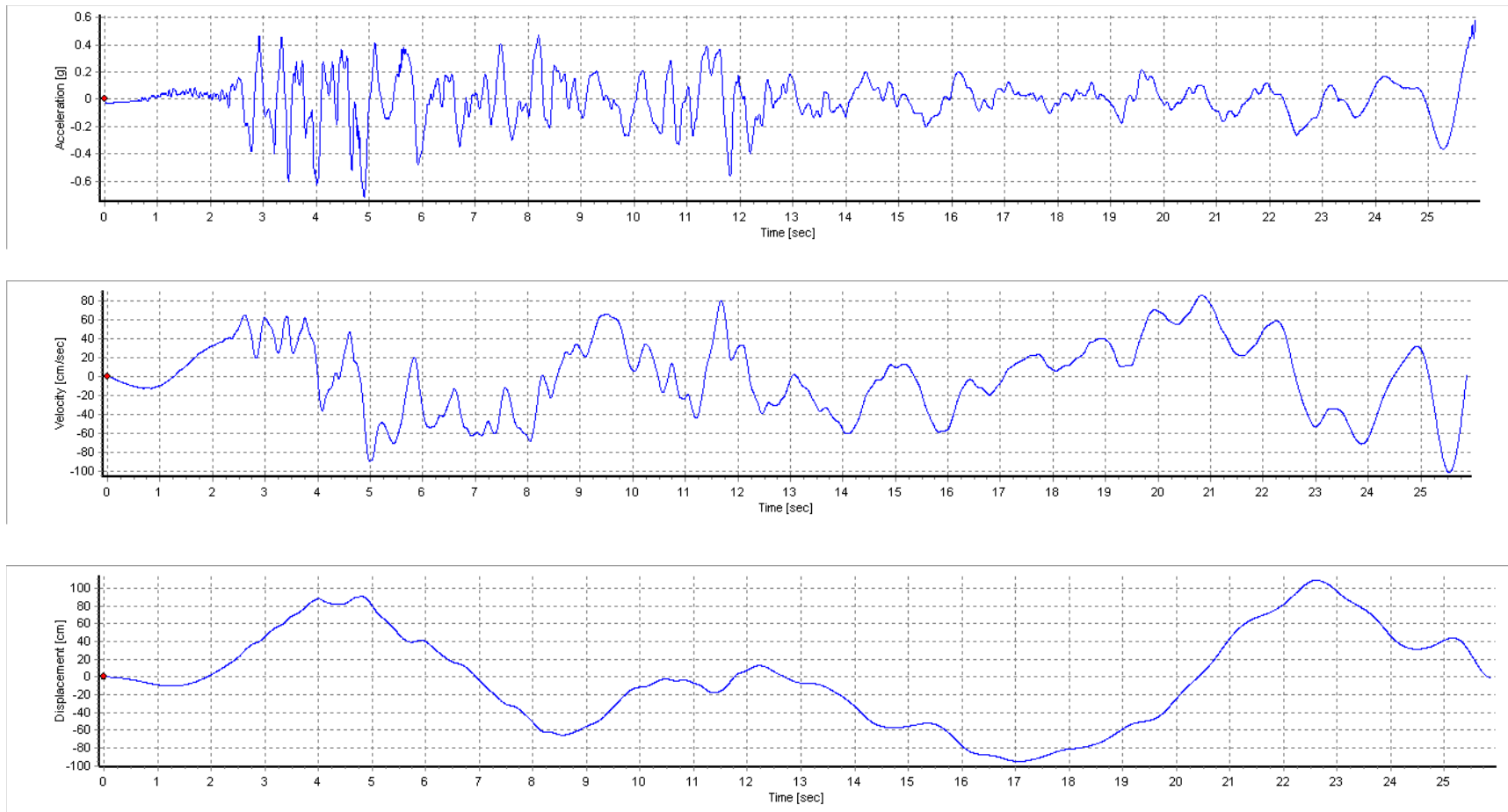


Figure A6-94. Spectrally-matched Time histories for Union Island – 1999 Duzce, Turkey Earthquake at Duzce, 180 Component

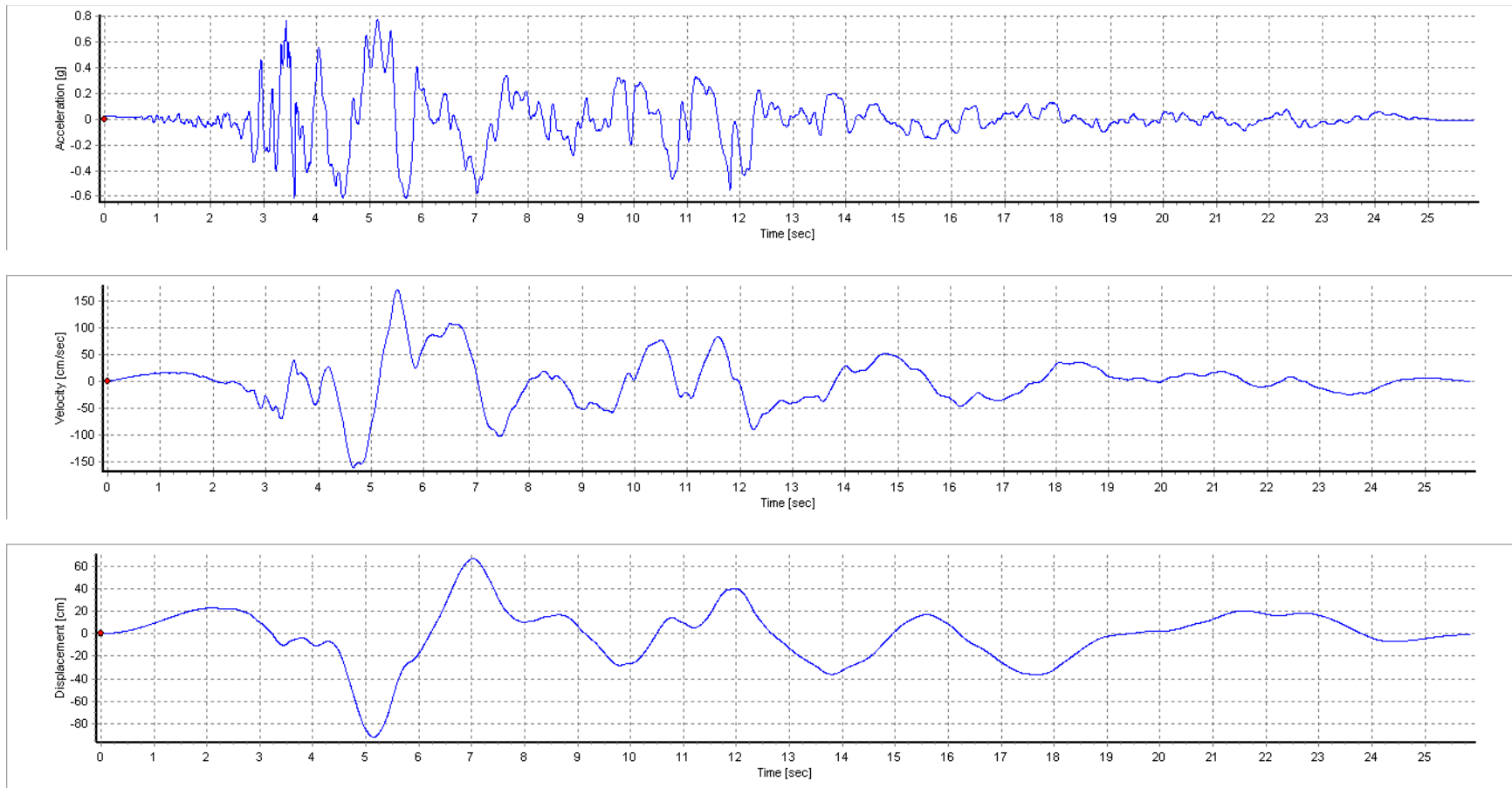


Figure A6-95. Seed Time histories for Union Island – 1999 Durce, Turkey Earthquake at Duzce, 270 Component

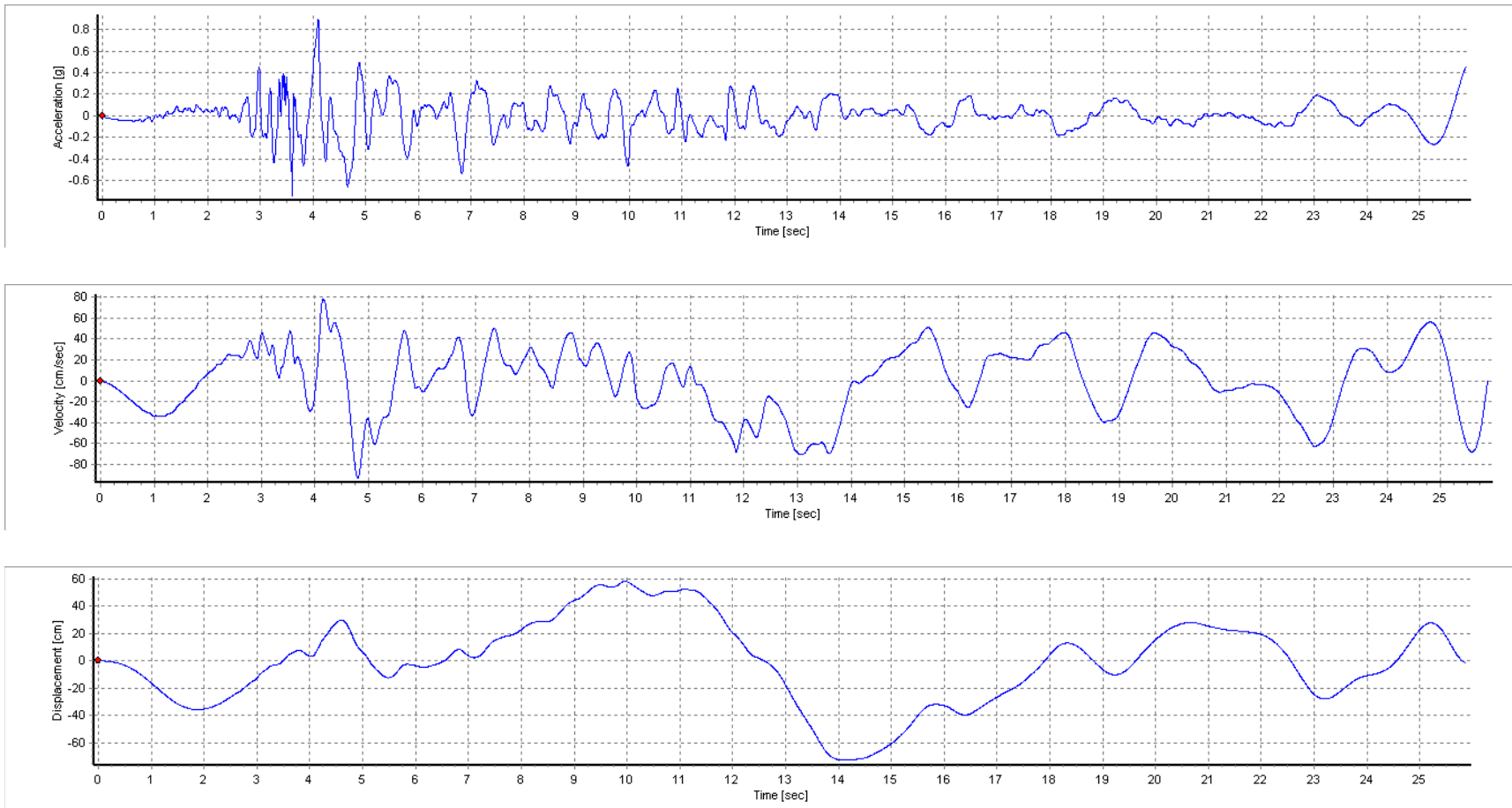


Figure A6-96. Spectrally-matched Time histories for Union Island – 1999 Duzce, Turkey Earthquake at Duzce, 270 Component

Bethany Reservoir Pumping Plant

Seed Time Histories ((Spectrally-matched time histories for Southern Forebay-North)											
RSN	Year	Earthquake Name	Station Name	Comp	Mag	ClstD (km)	Vs30 (m/s)	PGA (g)	PGV (cm/s)	PGD (cm)	AI (m/s)
778	1989	Loma Prieta	Hollister Differential Array	165	6.9	24.8	216	0.74	159.2	94.1	9.38
778	1989	Loma Prieta	Hollister Differential Array	255	6.9	24.8	216	0.83	128.5	56.8	10.33
821	1992	Erzican, Turkey	Erzincan	NS	6.7	4.4	352	0.74	246.5	94.6	8.45
821	1992	Erzican, Turkey	Erzincan	EW	6.7	4.4	352	0.86	180.3	76.8	8.26
1605	1999	Duzce, Turkey	Duzce	180	7.1	6.6	282	0.63	136.2	69.5	9.99
1605	1999	Duzce, Turkey	Duzce	270	7.1	6.6	282	0.78	171.4	91.9	13.37
Spectrally-matched Time Histories											
778	1989	Loma Prieta	Hollister Differential Array	165	6.9	24.8	216	0.72	82.4	108.9	6.39
778	1989	Loma Prieta	Hollister Differential Array	255	6.9	24.8	216	0.62	99.8	72.8	6.00
821	1992	Erzican, Turkey	Erzincan	NS	6.7	4.4	352	0.61	108.2	49.1	3.72
821	1992	Erzican, Turkey	Erzincan	EW	6.7	4.4	352	0.58	109.0	48.5	3.66
1605	1999	Duzce, Turkey	Duzce	180	7.1	6.6	282	0.54	102.8	65.4	6.05
1605	1999	Duzce, Turkey	Duzce	270	7.1	6.6	282	0.54	94.6	50.5	5.96

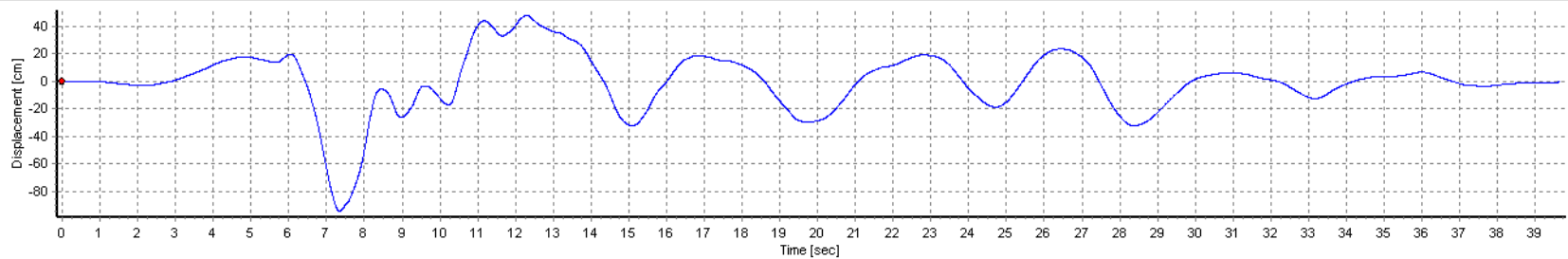
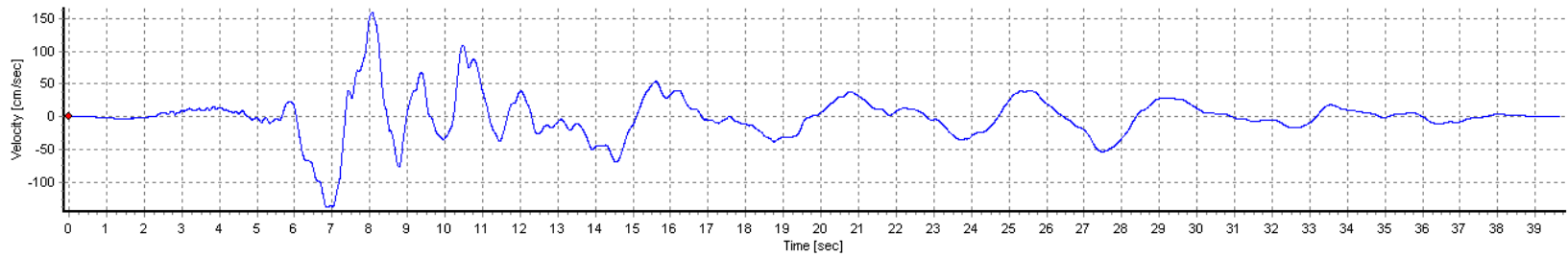
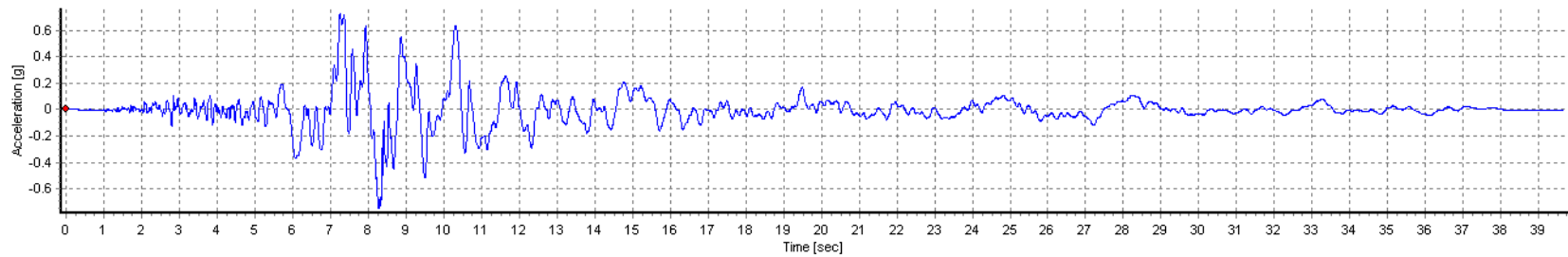


Figure A6-97. Seed Time histories for Union Island – 1989 Loma Prieta Earthquake at Hollister Differential Array, 165 deg. Component

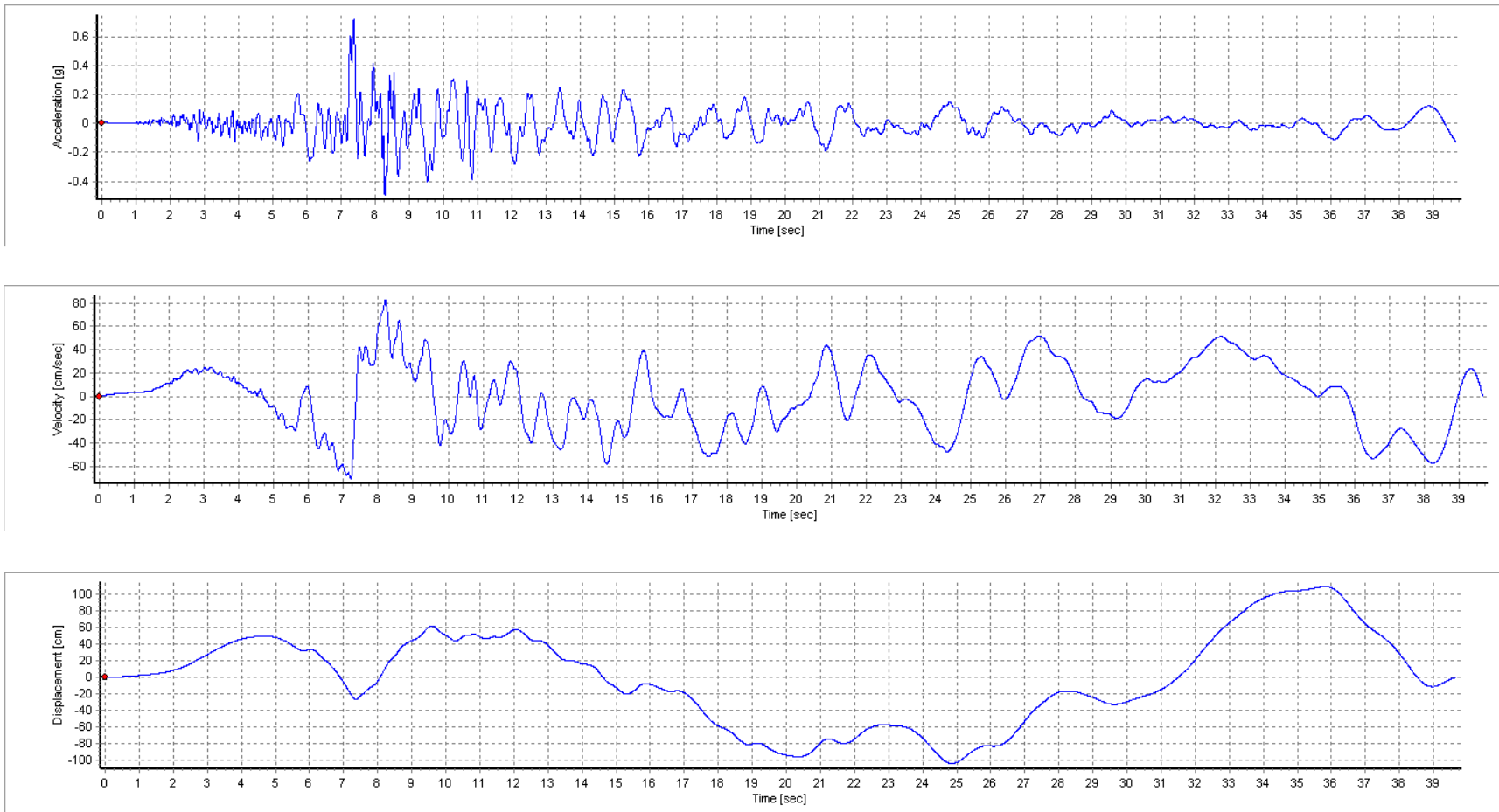


Figure A6-98. Spectrally-matched Time histories for Union Island – 1989 Loma Prieta Earthquake at Hollister Differential Array, 165 deg. Component

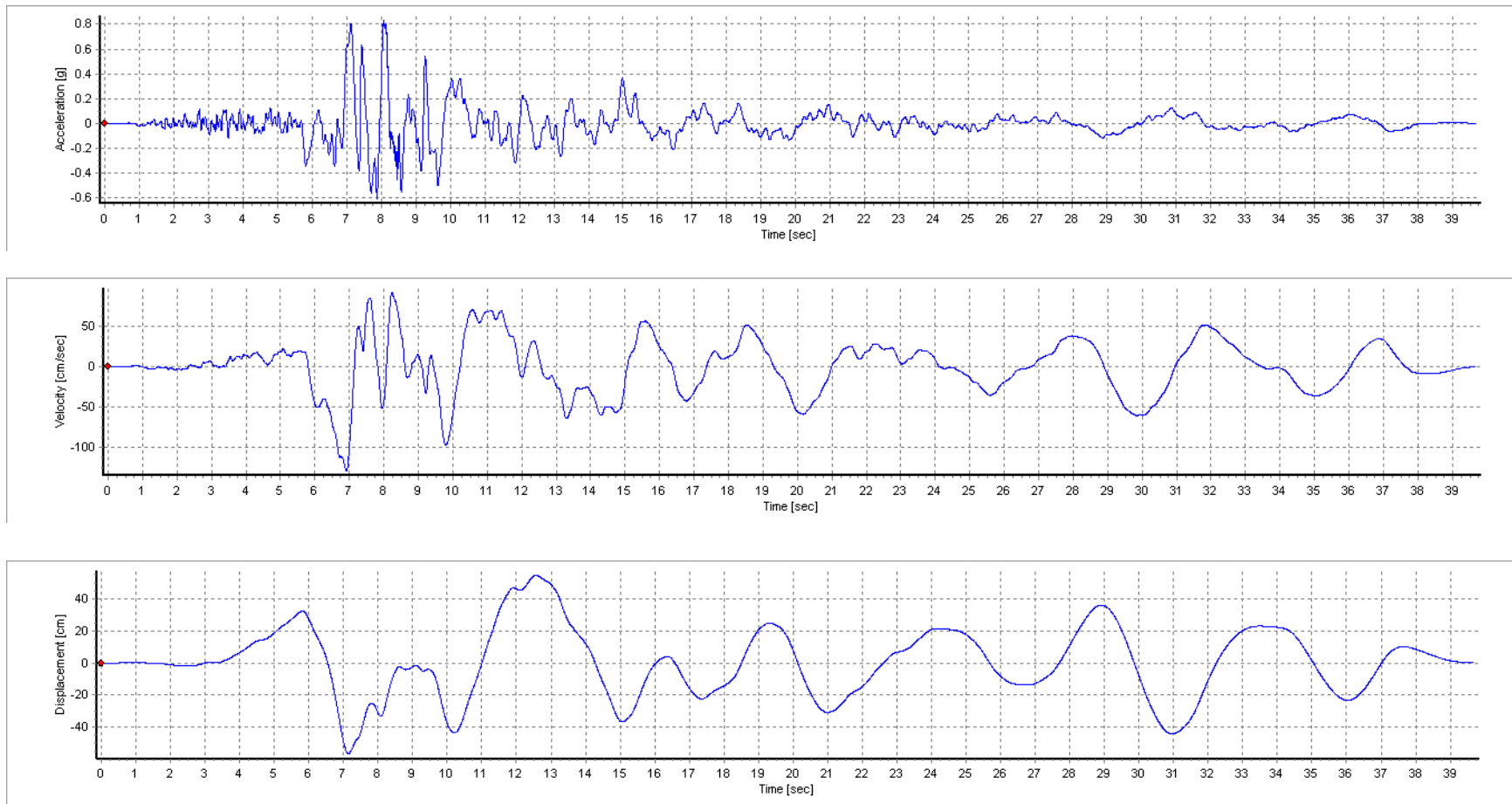


Figure A6-99. Seed Time histories for Union Island – 1989 Loma Prieta Earthquake at Hollister Differential Array, 255 deg. Component

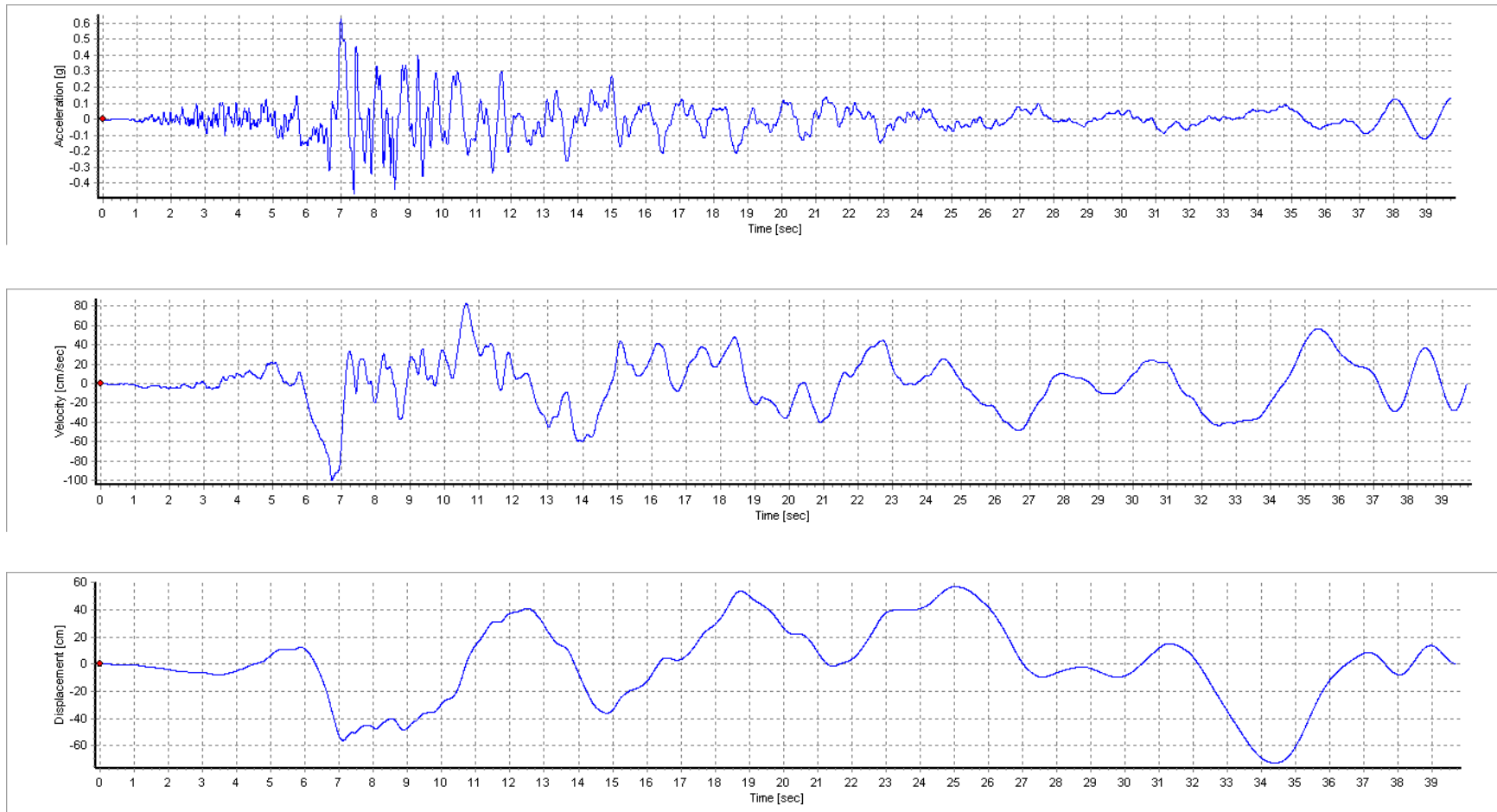


Figure A6-100. Spectrally-matched Time histories for Union Island – 1989 Loma Prieta Earthquake at Hollister Differential Array, 255 deg. Component

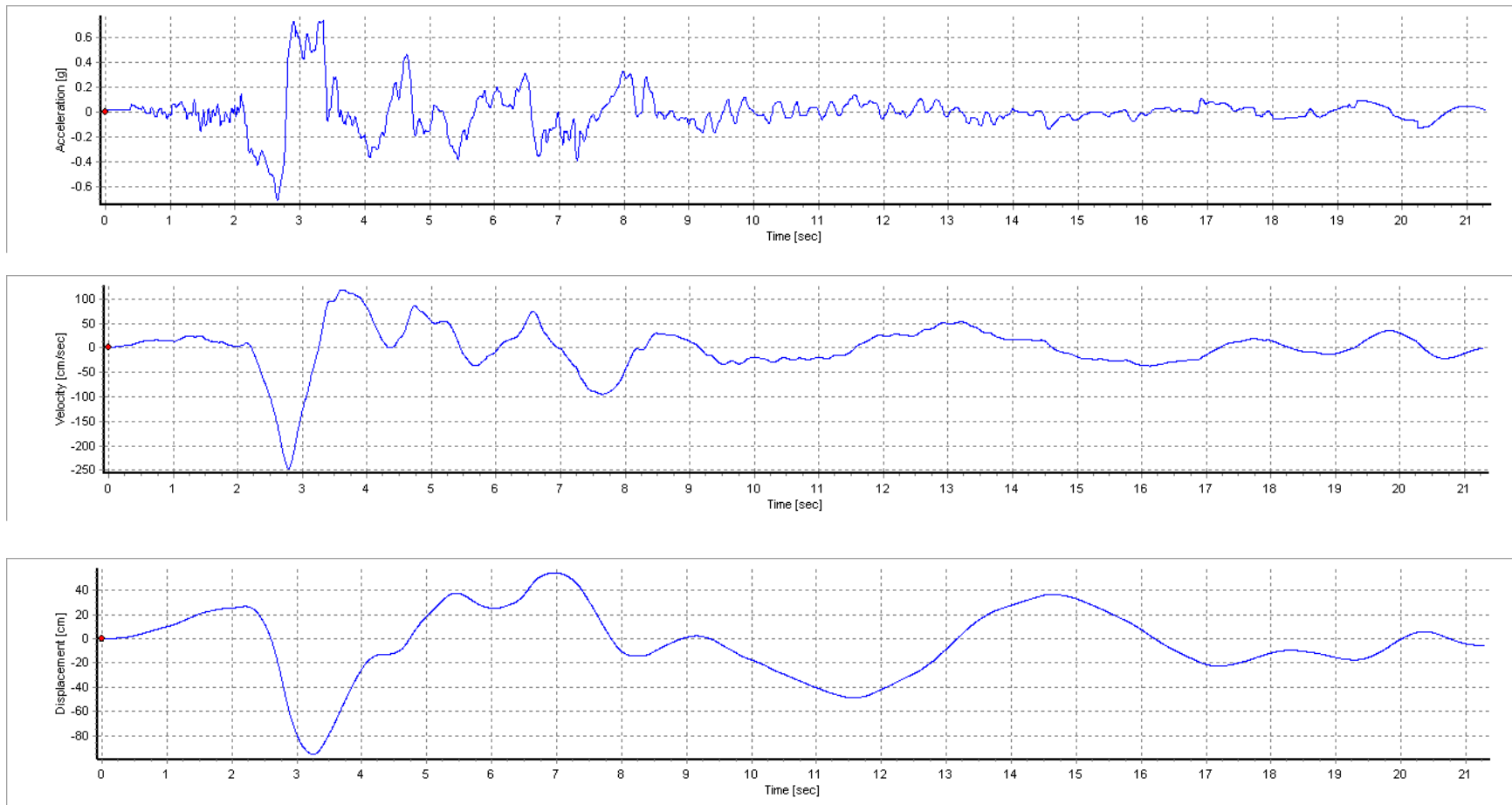


Figure A6-101. Seed Time histories for Union Island– 1992 Erzican, Turkey Earthquake at Erzincan, NS Component

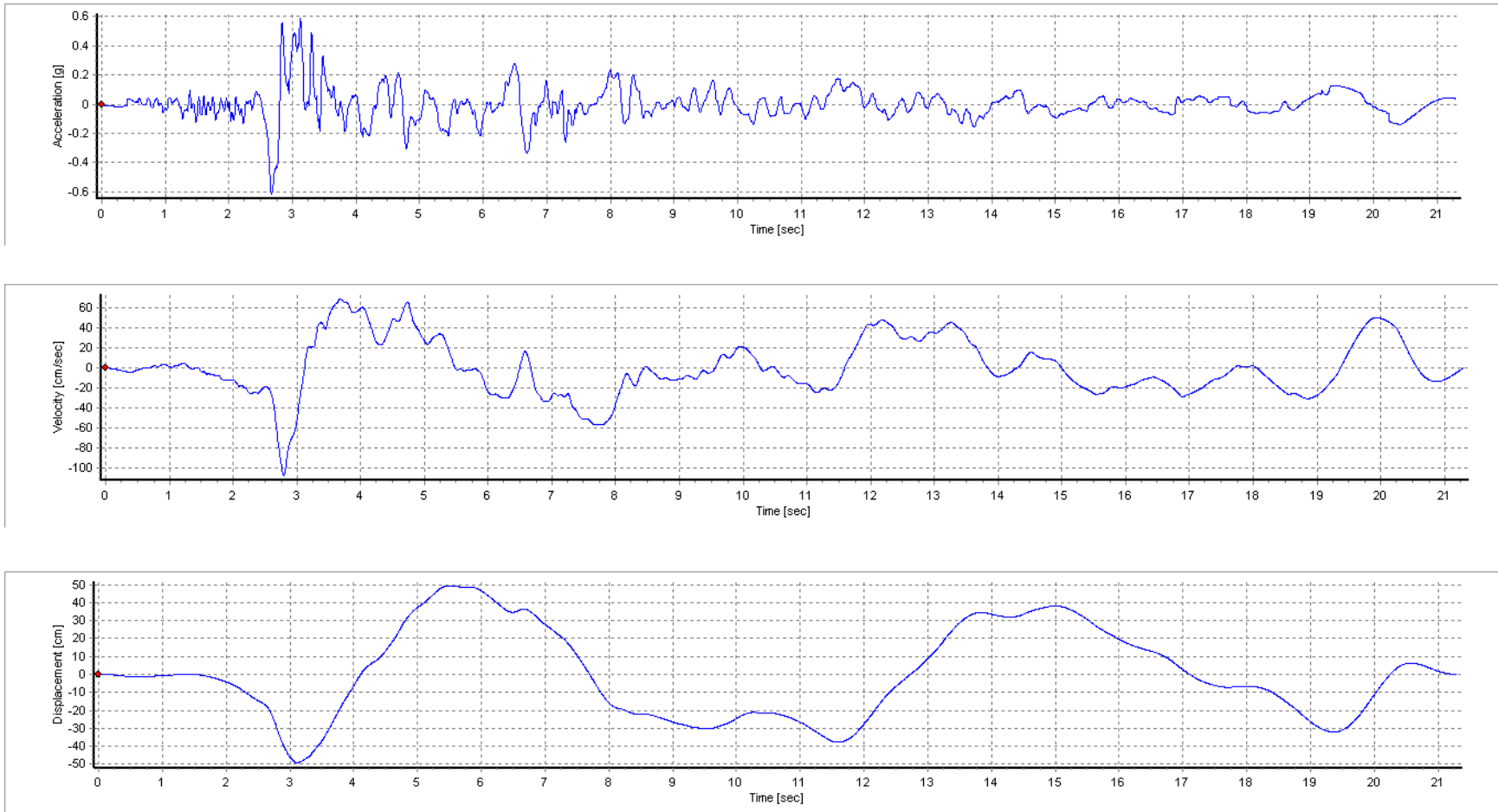


Figure A6-102. Spectrally-matched Time histories for Union Island – 1992 Erzican, Turkey Earthquake at Erzincan, NS Component

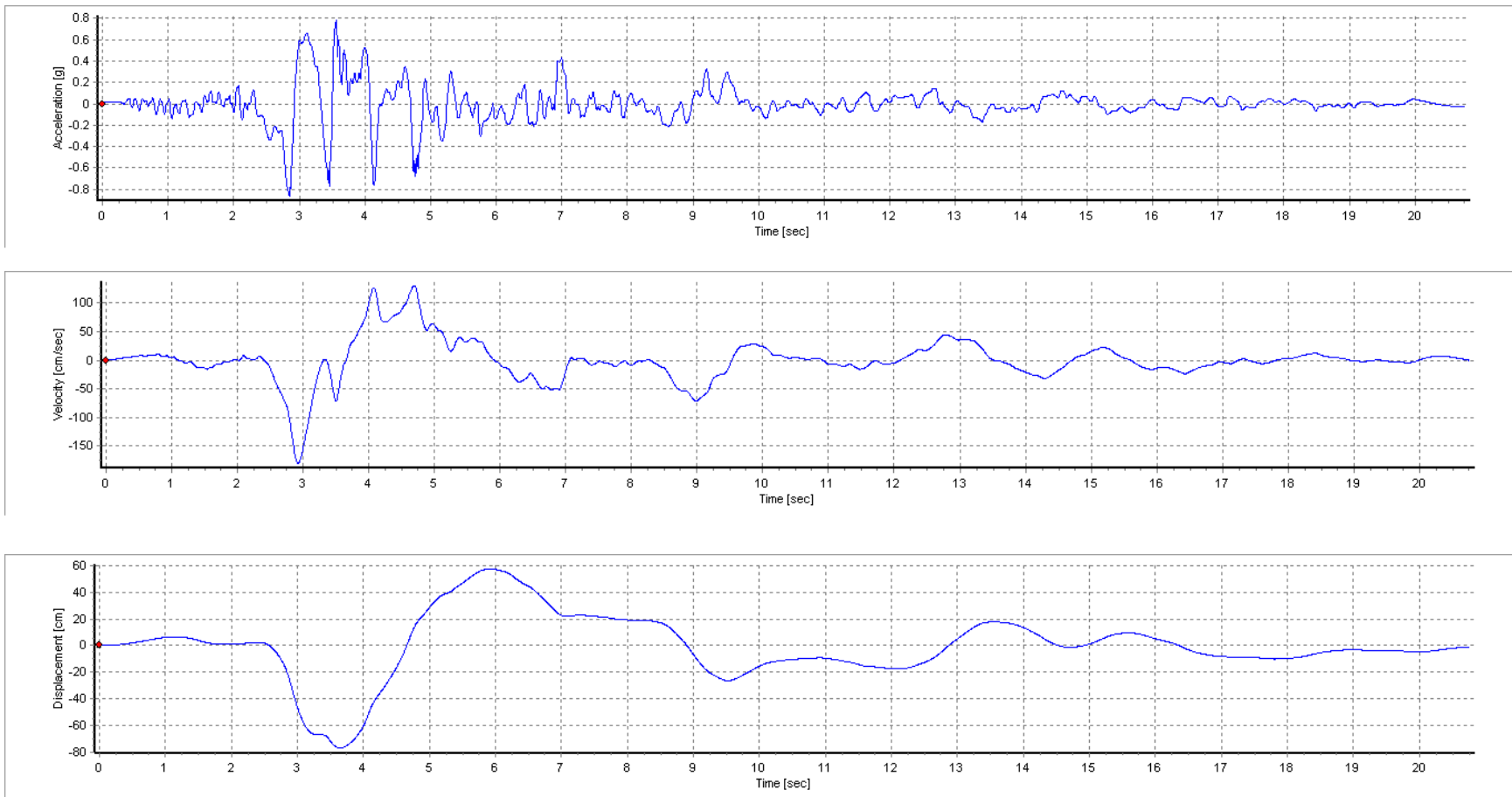


Figure A6-103. Seed Time histories for Union Island – 1992 Erzincan, Turkey Earthquake at Erzincan, EW Component

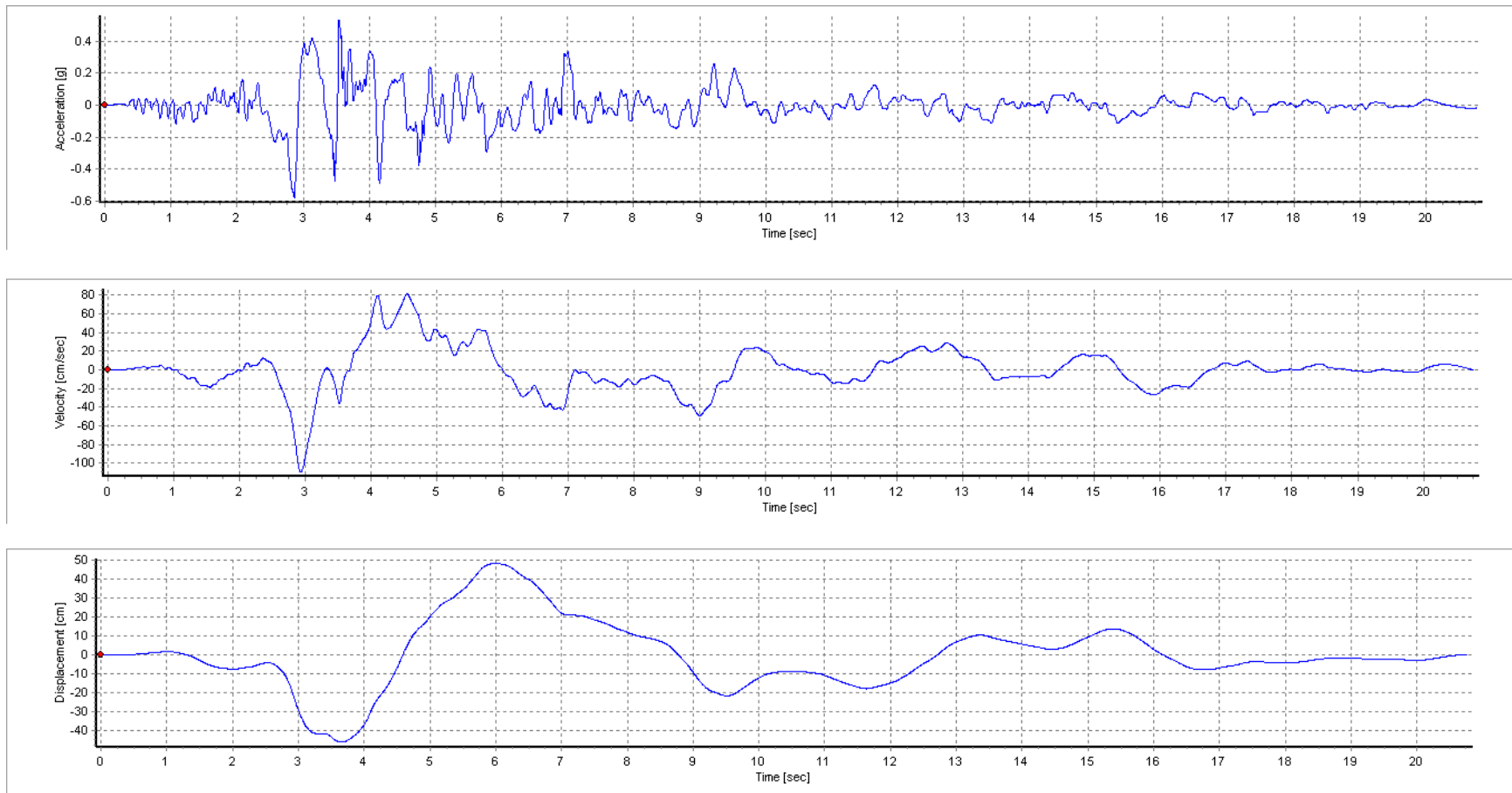


Figure A6-104. Spectrally-matched Time histories for Union Island – 1992 Erzican, Turkey Earthquake at Erzincan, EW Component

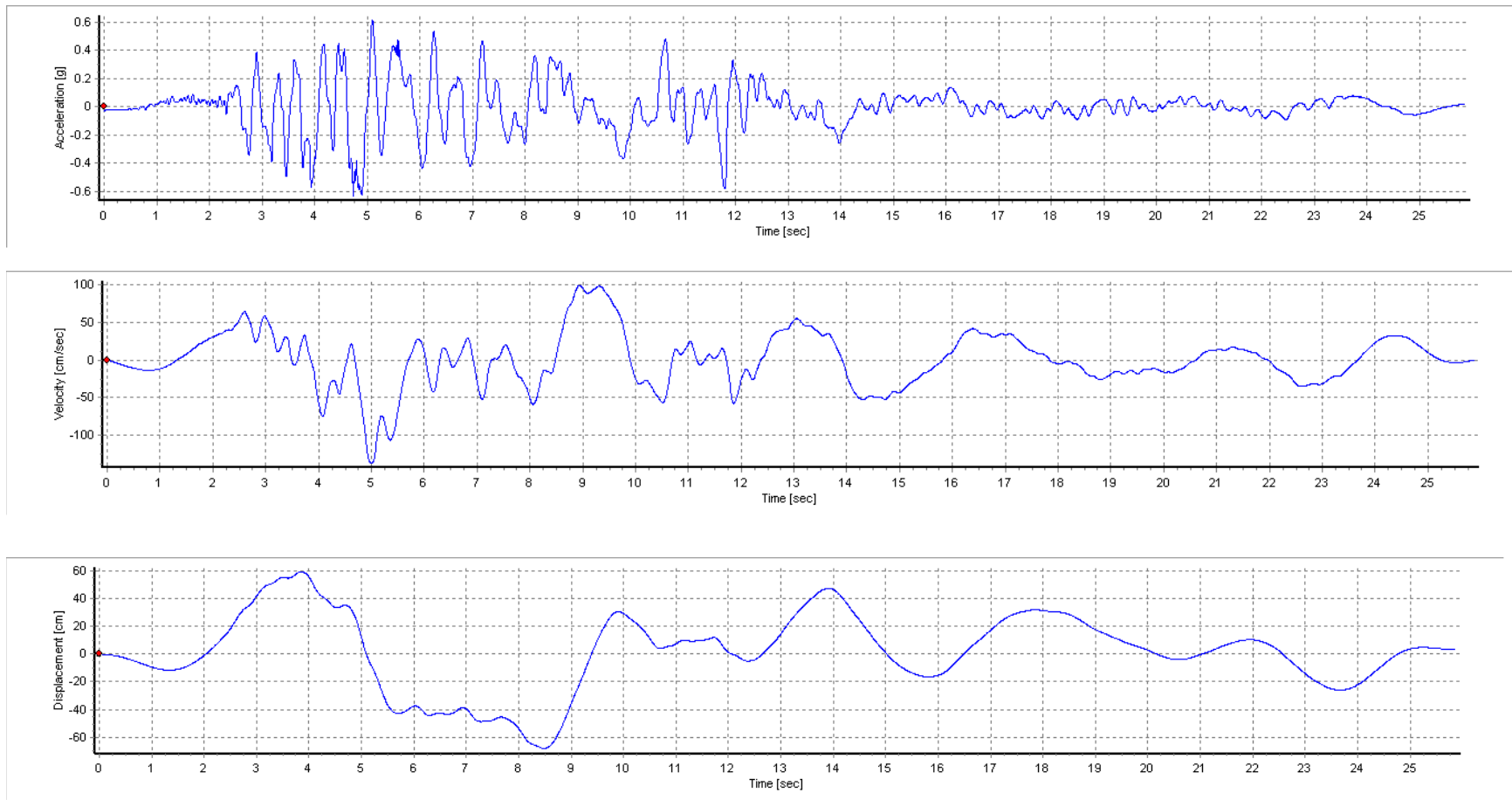


Figure A6-105. Seed Time histories for Union Island – 1999 Duzce, Turkey Earthquake at Duzce, 180 Component

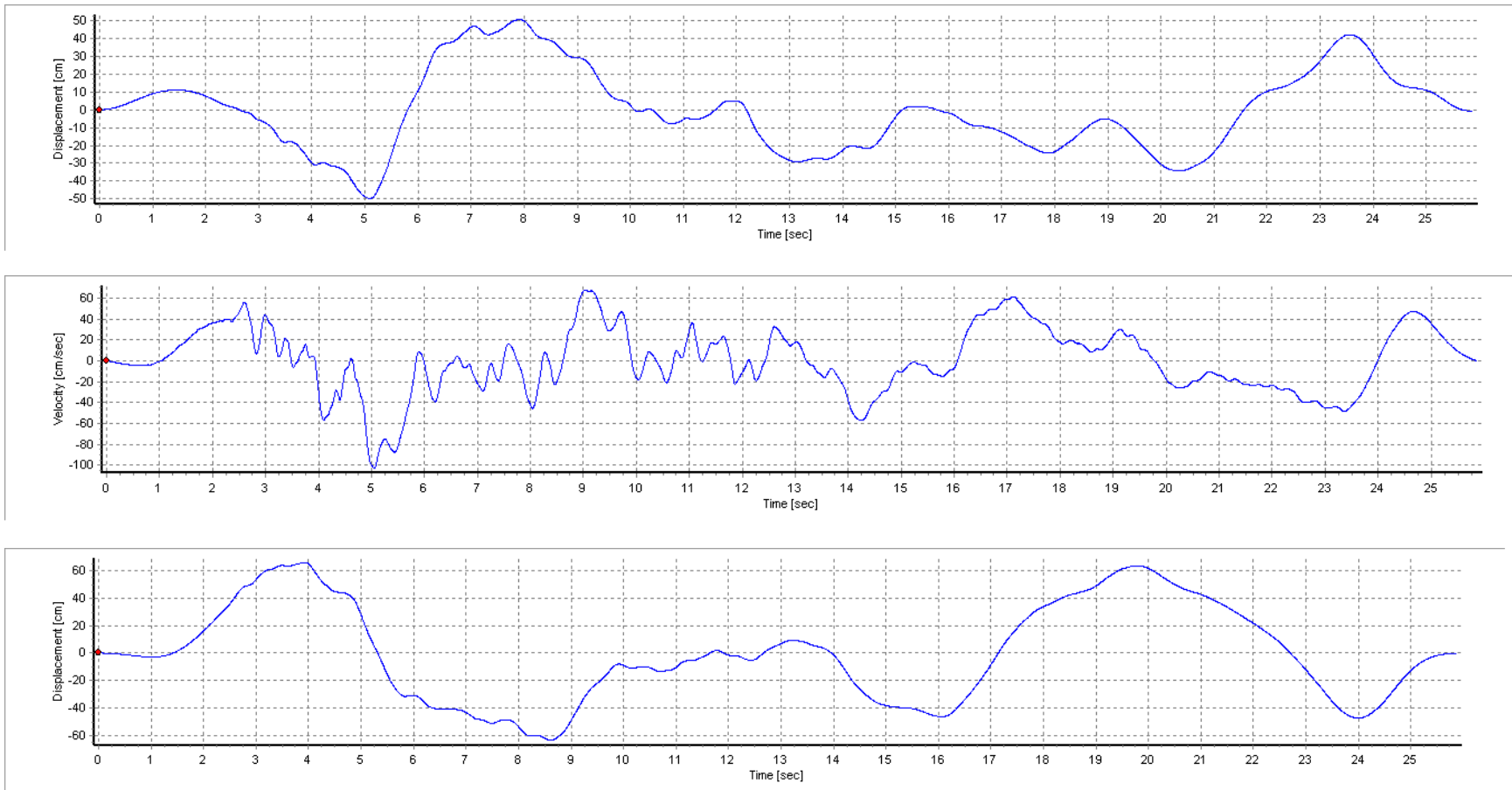


Figure A6-106. Spectrally-matched Time histories for Union Island – 1999 Durce, Turkey Earthquake at Duzce, 180 Component

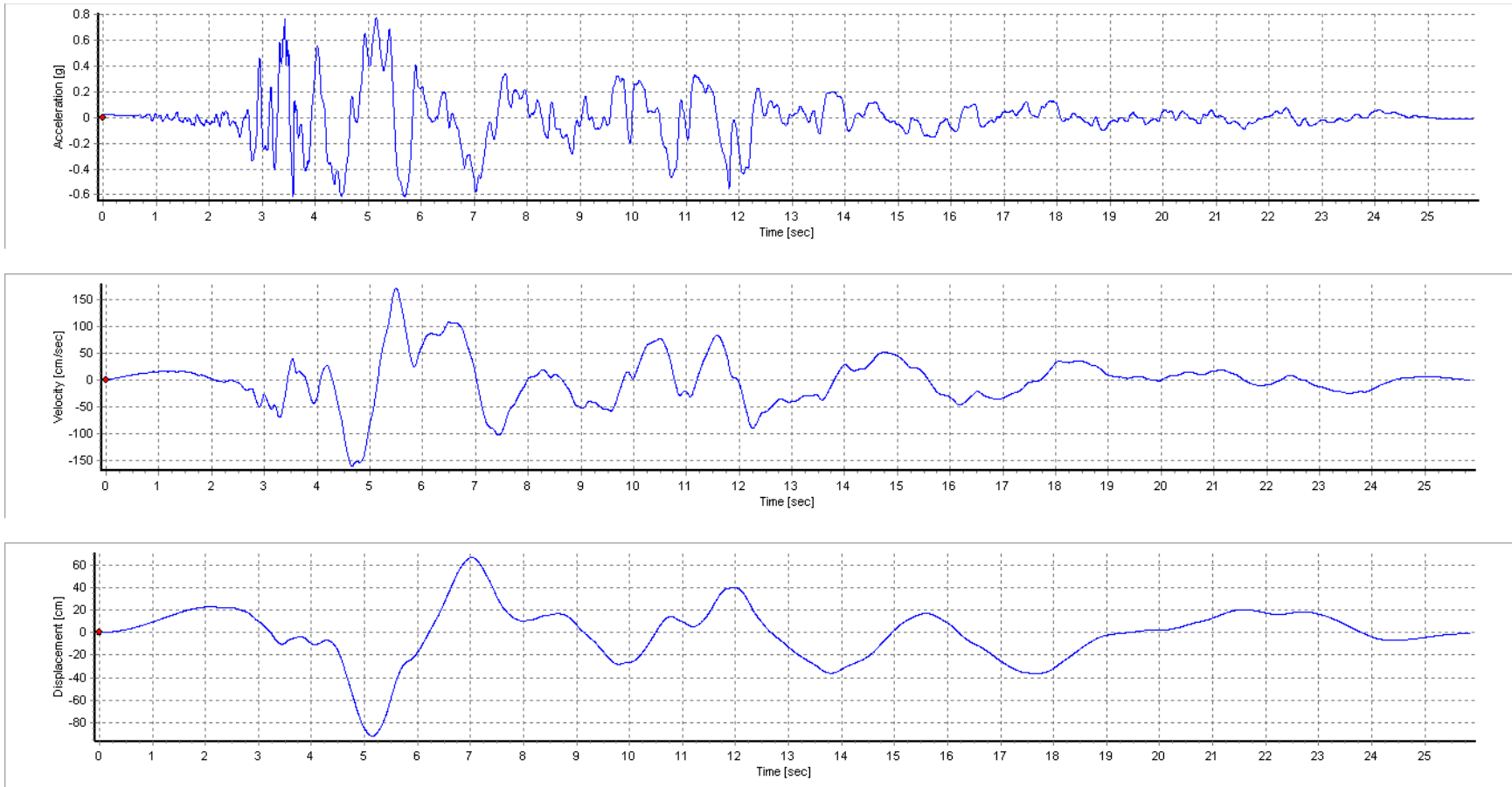


Figure A6-107. Seed Time histories for Union Island – 1999 Duzce, Turkey Earthquake at Duzce, 270 Component

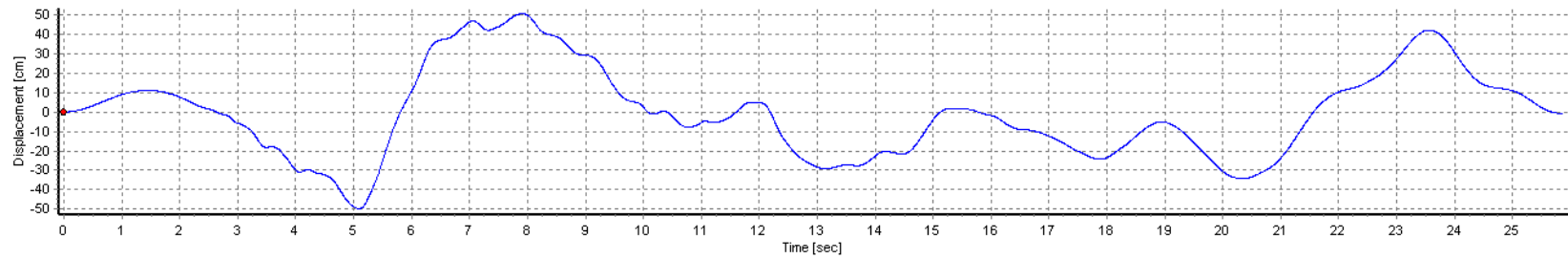
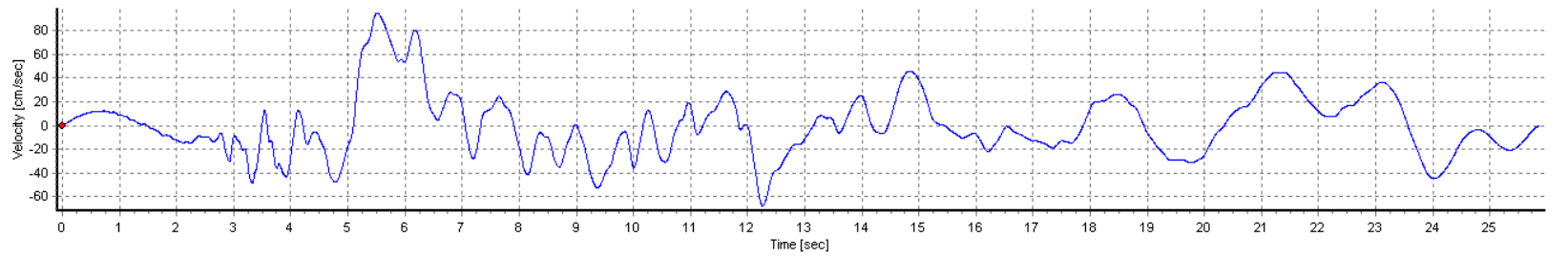
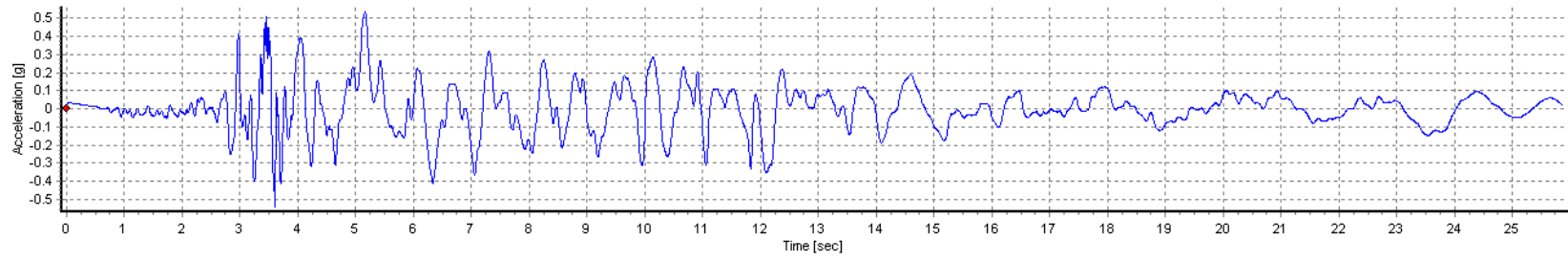


Figure A6-108. Spectrally-matched Time histories for Union Island – 1999 Durce, Turkey Earthquake at Duzce, 270 Component